Chemical and Biological Studies with Nek2 Kinase Inhibitors

This thesis is submitted to Newcastle University for the degree of doctor of philosophy

Christopher J Matheson

September 2012

Declaration

All work described herein was performed between October 2008 and September 2012 in the Medicinal Chemistry Laboratories of the Northern Institute for Cancer Research and Newcastle Cancer Centre, Bedson Building, Newcastle University, Newcastle-upon-Tyne, UK, NE1 7RU. The research was conducted in collaboration with scientists from the CR UK Centre for Cancer Therapeutics, The Institute of Cancer Research, 15 Cotswold Rd, Sutton, Surrey, UK, SM2 5NG and 237 Fulham Road, London, SW3 6JB, and the Department of Biochemistry, Henry Wellcome Building, University of Leicester, Leicester, UK, LE1 9HN.

All research described in this thesis is original material and does not contain any material that has previously been published or disclosed by other authors except where due reference is given.

No part of this thesis has previously been submitted for a degree, diploma or any other qualification at any other university.

Acknowledgements

First and foremost I would like to extend my utmost thanks to my supervisor Professor Roger Griffin and colleagues Dr Celine Cano, Professor Bernard Golding and Dr Ian Hardcastle for their support and guidance throughout my career in research. With their help I have built a strong foundation of knowledge and enthusiasm for a career in scientific research.

I would like to thank all members of the Nek research team past and present, Dr Benoit Carbain, Dr Chris Coxon, Dr Chris Wong, David Turner and Honorine Lebraud, for stimulating and productive discussion, and making the laboratory an enjoyable place to be when the research was not going to plan. In particular I would like to thank Dr Mangalesh Sivaprakasam for such a good introduction to chemical research and for all of his help and guidance. I would like to extend my thanks to Dr Karen Haggerty for HPLC support and keeping the lab working so efficiently, and Carlo Bawn for all NMR related guidance. I appreciate the support of collaborators within the Northern Institute for Cancer Research, Professor Herbie Newell, Lan Zhen-Wang and Huw Thomas for conducting Cdk2 counter screening assays, mouse pharmacokinetic and efficacy analysis, and contributing to my understanding of the biochemistry of Nek2.

I would also like to acknowledge the Medicinal Chemistry team at the Northern Institute for Cancer Research, namely Lauren Barrett, Annalisa Bertoli, Dr Ruth Bawn, Dr Tim Blackburn, Sarah Cully, Dr Suzannah Harnor, Honorine Lebraud, Nick Martin, Dr Elisa Meschini, Duncan Miller, Tristan Reuillon, Dr Charlotte Revill, Andrew Shouksmith, Dr Kate Smith, Dr Andrey Zaytsev and Bian Zhang for their continued contribution to scientific discussion and for making the laboratory such a good place to work. In particular I would like give thanks to Dr Chris Coxon, Dr Tommy Rennison, Dr Stephanie Myers and Dr Sarah Payne for helping me to thouroughly enjoy my time in the laboratory.

I would like to thank the scientists at the CR UK Centre for Cancer Therapeutics, Institute for Cancer Research, Sutton and Chelsea, UK, particularly Dr Swen Hoelder, Dr Richard Bayliss and Dr Corine Mas-Droux for providing medicinal chemistry and structural biology support and advice throughout my research. All X-ray crystal structures disclosed herein were created by Dr Bayliss and Dr Mas-Droux. I would also like to thank the Analytical Technology and Screening Laboratory, including Dr Wynne Aherne, Kathy Boxall and Maura Westlake for conducting all Nek2 biochemical assays throughout the project. I would also like to thank

Professor Andrew Fry, Dr Jo Baxter and Tara Hardy for all their help and support during my placement at the University of Leicester.

My deepest thanks must go to my parent Des and Liz Matheson, my brother Nic and my sister Lucy, for supporting me during my PhD and tolerating me during the stressful times, and to my housemate Andrew Morrison and all of my friends. Thank you for helping to take my mind of chemistry for a few hours each day.

Finally, I would like to thank Cancer Research UK for their generous funding during my research, and Newcastle University for the facilities in which it was conducted.

Abstract

The aim of modern cancer chemotherapy is to develop targeted drugs designed to exploit pharmacological differences between tumour cells and healthy tissues. One focus of this effort has been the identification of protein kinases that are expressed at elevated levels or in mutated forms, indicating a reliance of the tumour on specific kinase function. Nek2 is a human serine/threonine protein kinase related to the fungal protein NIMA, a critical mediator of mitosis. Interestingly, Nek2 is found to be upregulated in a variety of tumour cell lines derived from breast, cervical and prostate carcinomas, as well as lymphomas.

Human Nek2 is implicated in the regulation of the centrosome and formation of a bipolar spindle, a framework that is vital for correct separation of sister chromatids during mitosis. It is proposed that Nek2 may complex with, and phosphorylate, proteins accumulated at the centrosome, possibly playing a role in intercentriolar linker cleavage during the centrosome cycle. Abnormalities in centrosome number and function are common in many cancers, indicating that loss of centrosome cycle regulation may be a major contributing factor in tumour progression. Overexpression of Nek2 may result in premature centrosome disjunction, and deregulation of this tightly controlled mitotic machinery leads to chromatid segregation errors, aneuploidy and chromosomal instability, common genetic abnormalities observed in tumour cells. This indicates a role for abnormal Nek2 function in tumourigenesis, and Nek2 depletion in a number of tumour cell lines has been shown to cause growth suppression and apoptosis.

Nek2 is thus a potentially attractive cancer therapeutic target for small-molecule kinase inhibitors. Previous studies identified substituted purine derivatives as modest inhibitors of Nek2, leading to the discovery of two distinct inhibitor classes, exhibiting ATP-competitive and irreversible inhibition of the kinase, respectively.

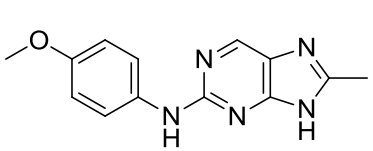

45

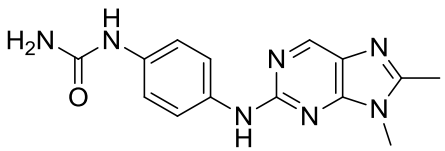

129

Purine-based compounds bearing substituents at the 8-position have emerged as modest competitive inhibitors of Nek2 that occupy the kinase ATP-domain through an unusual

binding orientation (**45**; IC_{50} = 51.8 μM). Additional possible interactions within the ATP-binding site available to inhibitors of this class were explored, with the objective of developing tight-binding type II reversible inhibitors of Nek2. Structure-activity relationship studies resulted in a 10-fold improvement in activity over the initial hit compounds and a substantial improvement in drug-like properties (*e.g.* **129**; IC_{50} = 5.1 μM)). However, all efforts to improve the potency of this series were unsuccessful.

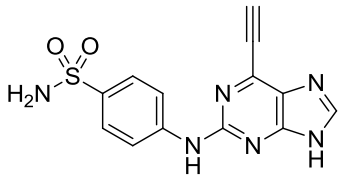

147

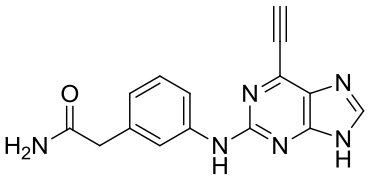

177

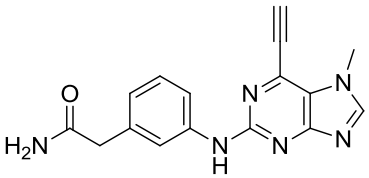

425

6-Ethynylpurines have been identified as irreversible inhibitors of Nek2 through covalent modification of an active-site cysteine residue. The initial hit compound (**147**; IC_{50} = 0.14 μM) was found to be a potent and selective inhibitor of the kinase *in vitro*, but with poor cellular activity attributed to limited permeability. Extensive structural modification of the 2-arylamino side-chain of this series afforded cell permeable analogues with improved potency, both *in vitro* and *in vivo* (*e.g.* **177**; IC_{50} = 0.062 ± 0.01 μM).

Biochemical studies using **177** suggested that inhibition of Nek2 resulted in an increase in mitotic abnormalities and a delay in mitotic progression, despite poor cellular growth inhibition being observed in initial tumour cell lines. Further cellular growth inhibition and cytotoxicity studies with selected compounds identified several sensitive tumour cell lines. However, kinase-inactive control compounds essentially devoid of Nek-inhibitory activity (*e.g.* **425**; IC_{50} > 100 μM) retained growth-inhibitory activity, indicating an alternative locus of activity for the 6-ethynylpurine chemotype.

Abbreviations

A	ADME	Absorption distribution metabolism excretion
	ALL	Acute lymphoblastic leukaemia
	AP	Alkaline phosphatase
	APC/C	Anaphase promoting complex/centrosome
	ATP	Adenosine triphosphate
	AUC	Area under the curve
B	BCR	Breakpoint cluster region
C	Cdc	Cell division control protein
	CDI	1,1'-Carbonyldiimidazole
	Cdk	Cyclin-dependent kinase
	CENPE	Centromere protein E
	Chk	Checkpoint kinase
	CIN	Chromosomal instability
	CML	Chronic myeloid leukaemia
	C-Nap1	Centrosomal Nek2 associated protein 1
D	d	Doublet
	ddH_2O	Double-distilled water
	Dec.	Decomposed
	DHFR	Dihydrofolate reductase
	DLBCL	Diffuse large B-cell lymphoma
	DNA	Deoxyribonucleic acid
	DSB	Double strand breaks
E	ECL	Enhanced chemiluminescence
	ECM	Extracellular matrix
	EGFR	Epidermal growth factor receptor

	EI	Electron impact
F	FACS	Fluorescence-activated cell sorting
	FCS	Foetal calf serum
	FDA	Food and Drug Administration
G	GCP	Gamma-complex protein
	GFP	Green fluorescent protein
	GI_{50}	Half maximal growth inhibitory concentration
	GIN	Genomic instability
	GIST	Gastrointestinal stromal tumour
	GTP	Guanosine triphosphate
	γTuRC	Gamma-tubulin ring complex
H	Hec1	Highly expressed in cancer 1
	hERG	Human ether-a-go-go-gene related product
	HMBC	Heteronuclear multiple bond correlation
	HPLC	High performance liquid chromatography
	HRP	Horseradish peroxidase
	Hz	Hertz
I	IC_{50}	Half maximal inhibitory concentration
	IEM	Immunoelectron microscopy
	IFM	Immunofluorescence microscopy
	Inh2	Inhibitor 2
	IR	Infra-red
K	KD	Kinase dead
L	LC	Liquid chromatography
	LE	Ligand efficiency
	LipE	Lipophilic efficiency

M	m	Multiplet
	MAPK	Mitogen-activated protein kinase
	MBP	Myelin basic protein
	MCC	Mitotic checkpoint complex
	MDR	Multidrug resistance
	mol	Moles
	MS	Mass spectrometry
	MTD	Maximum tolerated dose
	MTOC	Microtubule organising centre
	MW	Microwave irradiation
N	NBD	Nitrobenzoxadiazole
	NBT	Nitro blue tetrazolium chloride
	NEBD	Nuclear envelope breakdown
	Nek	NIMA-related kinase
	NIMA	Never in mitosis gene A
	Nlp	Ninein-like protein
	NMR	Nuclear magnetic resonance
	NSCLC	Non-small cell lung cancer
P	PAGE	Polyacrylamide gel electrophoresis
	PBD	Polo-box domain
	PBS	Phosphate buffered saline
	PCM	Pericentriolar material
	PDGFR	Platelet derived growth factor receptor
	PET	Positron emission tomography
	PK	Pharmacokinetics
	PKD	Polycystic kidney disease

	Plk	Polo-like kinase
	PP1	Protein phosphatase 1
Q	q	Quartet
R	Rb	Retinoblastoma
	RCC	Renal cell carcinoma
	R_f	Retardation factor
	RNA	Ribonucleic acid
	Rsk	Ribosomal s6 kinase
	RT	Room temperature
S	s	Singlet
	SAC	Spindle assembly checkpoint
	SARs	Structure-activity relationships
	SDS	Sodium dodecyl sulfate
	siRNA	Small-interfering ribonucleic acid
	SRRs	Structure-reactivity relationships
T	t	Triplet
	TBAF	Tetra-*n*-butylammonium fluoride
	tetO	Tetracycline operators
	TFA	Trifluoroacetic acid
	TFE	2,2,2-Trifluoroethanol
	TIPS	Triisopropylsilyl
	TLC	Thin layer chromatography
	TRE	Tetracycline response elements
U	UV	Ultraviolet
V	VEGFR	Vascular epidermal growth factor receptor
W	WT	Wild-type

Contents

Chapter 1: Chemotherapy and the Cell Cycle

1.1. The Birth of Modern Chemotherapy

1.1.1. The Discovery of Cellular Toxins as Chemotherapeutic Agents

Despite the recognition of tumour formation in humans for centuries, a clear understanding of the biomolecular processes involved was not apparent until the later stages of the twentieth century. Prior to 1950, the mainstay of cancer treatment was the responsibility of surgeons, until the advent of the linear accelerator brought radiotherapy to the fore. However, the success of both techniques relies on early diagnosis and detection of the tumour, and both are relatively ineffective against metastatic cancers.[1] In order to treat a patient with a liquid or metastatic tumour, a therapeutic effect is required throughout the entire body. It was therefore necessary to identify and develop chemical agents that could be administered systemically to treat a patient whose cancer could be present in any organ.

It was not until the 1940s that such compounds were identified by Louis Goodman and Alfred Gilman, investigating the potential therapeutic value of chemical weapons stockpiled during World War II. It was noted that the autopsies of soldiers killed by exposure to mustard gas revealed high levels of myelosuppression, resulting in a low white blood cell count (leukopenia), underdeveloped (hypoplastic) lymphoid tissues, and ulceration of the gastrointestinal tract;[2] all of these are indications that such compounds were having a cytotoxic effect on rapidly dividing cells.

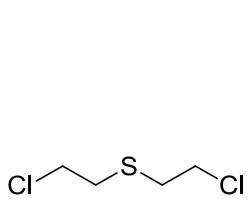

1

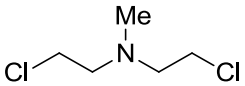

2

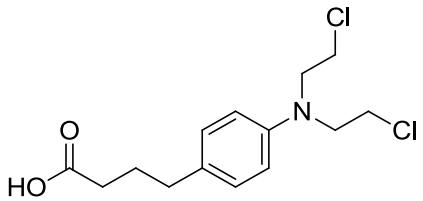

3

The active agent in mustard gas is sulfur mustard (**1**). However, the toxicity of sulfur mustard is too high for systemic use, and thus the structurally similar but less toxic nitrogen mustard (**2**) was investigated. Although limited in success, systemic treatment of a patient with non-Hodgkin's Lymphoma with nitrogen mustard provided the first example of tumour regression observed following administration of a chemical agent,[3, 4] and the age of modern

chemotherapy was born. In the years following their discovery, the identification of more stable nitrogen mustards with electron-rich substituents, allowed the development of orally administered chemotherapeutics, such as chlorambucil (**3**).[1]

The same scientists went on to devolve the now accepted mechanism of action of nitrogen mustards, which is initiated through the formation of a reactive aziridinium ion. This reactive alkylating species forms covalent adducts with DNA bases, in particular the N-7 position of guanine. The ability of nitrogen mustards to form two such species results in cross-linking of DNA strands.[5] This induces DNA miscoding and strand breaks during replication, and triggers the cell to 'self-destruct', or undergo apoptosis.

A further major development in modern cancer chemotherapy followed the observation of the renowned pathologist Sydney Farber, that treatment of patients suffering from leukaemia with the vitamin folic acid was detrimental to the patient's disease, seeming to trigger proliferation of acute lymphoblastic leukaemia (ALL).[6] The cellular substrate of folic acid is dihydrofolate reductase (DHFR), an enzyme that plays a key role in the biosynthesis of thymidylate and purines, essential components for cell viability due to their role in DNA and RNA synthesis.

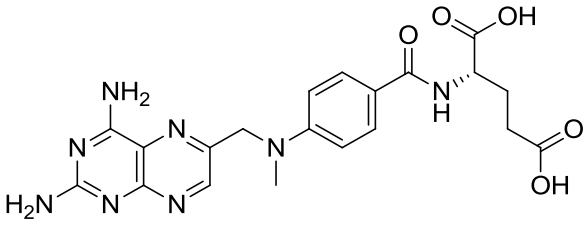

4

Amethopterin, or methotrexate (**4**), was synthesised as an analogue of folic acid, and acts as an inhibitor of DHFR, disrupting the ability of a cell to synthesise components essential for DNA and RNA biosynthesis and cellular growth. Compounds within this class are termed antifolates. Such compounds rely on active transport into the target cell through the reduced-folate transporter 1 (RFT-1), followed by polyglutamation of the drug and subsequent binding to DHFR.[1] Methotrexate (**4**) was successful in the treatment of a range of epithelial malignancies, including remission in patients suffering from cholangiocarcinoma, making it the first drug to successfully cure a solid tumour.[7]

Despite these initial successes, both nitrogen mustards and antifolates soon encountered the rapid onset of resistance in patient populations, a problem that has come to characterise many modern chemotherapeutic therapies. The evolutionary pressure exerted on a tumour cell population through administration of a cytotoxic drug, coupled with the elevated rate of cell proliferation and loss of regulation in cancer, increases the likelihood of the emergence of cells with genetic mutations sufficient to circumvent the desired therapeutic effect.[8]

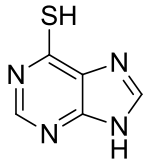

5

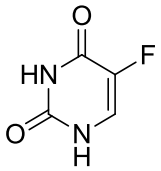

6

Methotrexate (**4**) is an antimetabolite, as it acts to inhibit the natural metabolism of folic acid for the biosynthesis of DNA and RNA. Additional advancements in the field of chemotherapy made during the 1950s included the discovery of further antimetabolites such as 6-mercaptopurine (6-MP, **5**)[9] and 5-fluorouracil (5-FU, **6**).[10] These antimetabolites highlighted the ability of such compounds to disrupt the life cycle of the cell, often through interference in DNA and RNA synthesis. Natural products such as the *Vinca* alkaloids (*e.g.* vincristine, **7**)[11] and taxanes (*e.g.* taxol, **8**),[12] which interfere with microtubule polymerisation, a vital event for the mitotic process (see chapter 2.2.), added to the growing repository of available chemotherapeutic agents. However, the development of resistance to single agent therapy remained, despite the diverse nature of the cellular targets and processes being targeted.

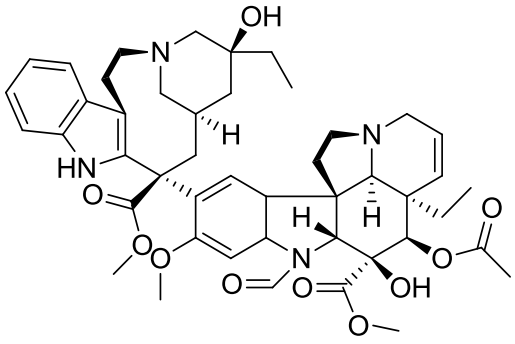

7

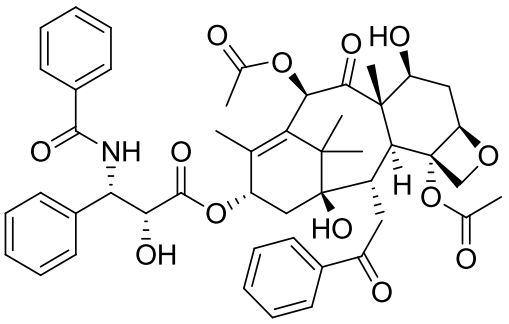

8

In an attempt to address this problem, clinicians have administered chemotherapeutic agents from a variety of classes, with different modes of action, as a single regimen. For example,

the POMP regimen; a combination of prednisone, vincristine, methotrexate and 6-MP, has been commonly used, and shown to induce remissions in children suffering from ALL. Similarly, the MOPP regimen; a combination of a nitrogen mustard, vincristine, prednisone and procarbazine, has been used to successfully treat patients with Hodgkin's and non-Hodgkin's lymphomas.[13, 14]

During the 1970s and 1980s, additions to the arsenal of chemotherapeutic agents continued to be made, including widely used compound classes such as platinum complexes. These agents bind to DNA and cause DNA cross-linking, and include cisplatin (**9**) and its analogues.[15, 16] A number of inhibitors of topoisomerase II, a key enzyme involved in DNA replication and repair, such as the anthracyclins (*e.g.* Daunorubicin, **10**) were also discovered.[17] However, at this time anticancer drug discovery was dominated by government-funded and academic laboratories, with very little representation from industry. This was driven by the high risk nature of the field, with a relatively low success rate of potential drugs passing from the clinic to the market. Progress towards novel treatments for patients was slow, particularly for the treatment of solid tumours, and very few truly novel classes of compounds emerged.[1]

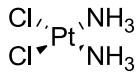

9

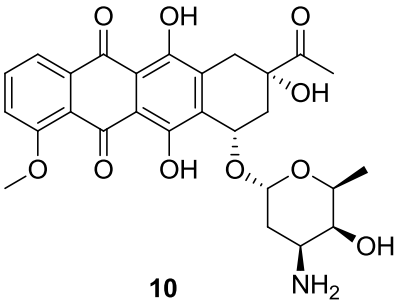

10

Throughout the development of early anticancer drugs, clinicians repeatedly encountered serious toxicities associated with the nature of the compounds used. Such agents inevitably carry with them a serious therapeutic disadvantage due to their lack of selectivity for tumour cells, as the compounds have an effect on all cells undergoing DNA replication and/or mitosis. This results in widespread destruction of tumour and healthy cells alike, and, as such, these compounds are associated with a high toxicity. In order to exert a therapeutic effect, such compounds rely on the fact that tumour cells have an increased rate of proliferation. This is often responsible for the side effects seen in regions of the body associated with rapid cell division, such as loss of hair, gastrointestinal toxicity and myelosuppression.[18] This has long been accepted as the price for controlling a potentially fatal disease, but as treatments

have improved and patient survival increased, the need to eliminate serious long-term damage to off-target tissues and improve patient prognosis has become an important goal.

1.1.2. Understanding the Molecular Pathology of Cancer

It was not until the late 1980s that continuing research into the molecular and genetic composition of cells allowed researchers to gain a deeper understanding of the molecular processes involved in cell growth and division. A highly complex array of cellular processes was elucidated, regulating all aspects of the cell, including proliferation, survival, and apoptosis. The molecular pathology of such processes is now better understood, highlighting the key role of growth factors, signalling molecules, regulators of apoptosis and the cell cycle.[19] Of particular interest to oncologists was the possibility of linking key cellular components to processes vital to the initiation and propagation of a tumour.

All cancers arise by modification of the genome of a single healthy cell, leading to errors in transcription and subsequent modification of gene expression. Such genetic modification can be the result of random errors in DNA replication, or due to the mutagenic effect of exogenous or endogenous agents. The majority of modifications to a cell's genetic material have little effect. However, such alterations can contribute to the development of neoplasia when they cause the mutation of a proto-oncogene, a gene coding for a protein involved in processes such as cell growth or differentiation. The resulting activation of the oncogene causes the transcription of mutated or elevated levels of proteins governing aspects of cell proliferation, driving aberrent cell growth and the development of a tumourigenic phenotype. Mutations may also cause damage to tumour suppressor genes, causing loss or downregulation of proteins involved in regulating cell division or promoting apoptosis.[20]

Over the past two decades, our understanding of the key oncogenes and tumour suppressor genes involved in tumour progression has allowed the identification of a large number of novel targets for anti-cancer drug discovery. There are now understood to be several 'hallmarks of cancer', which are acquired by normal cells as they progress towards a cancerous state (Figure 1).[19, 21]

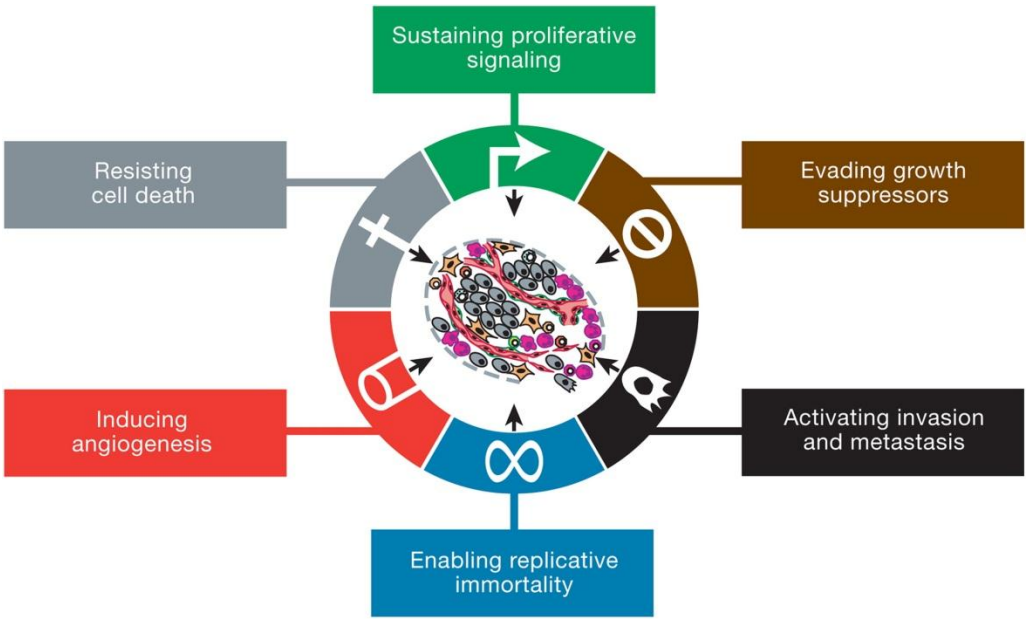

Figure 1: The major characteristics a cell must acquire during the process of tumourigenesis.[19, 21]

In normal cells, the formation and release of growth factors is tightly controlled, ensuring well maintained regulation of the cell's ability to enter growth and division cycles. Cancer cells acquire the ability to circumvent this control and receive sustained proliferative signalling. This is possible either through the increased production of growth factors by the cancer cells, by signalling to the surrounding stroma to stimulate normal cells to release growth factors,[22] or by the overexpression of receptor proteins, such as the epidermal growth factor receptor (EGFR) family, at the cell surface.[23]

There are a number of tumour suppressor genes dedicated to the negative regulation of cell proliferation, by encoding for proteins such as retinoblastoma (Rb) and p53. These proteins interpret extra- and intra-cellular signals relating to the suitability of the cell to undergo growth and division, from both growth-inhibitory signals and indicators of cellular stress and abnormality.[24] If overwhelming signals of the cells unsuitability to divide are received, tumour suppressor proteins can trigger the cell to enter senescence or undergo apoptosis. In order to undergo unrestricted proliferation, despite inherent defects within the tightly controlled cellular machinery, it is necessary for pre-malignant cells to overcome the action of these growth suppressors. Indeed, many tumour suppressor genes have been discovered owing to their inactivation in cancer.[19]

Apoptosis serves as a major obstacle to the development of cancer from a pre-cancerous cell,[25] and is initiated in response to a range of physiological stresses. Many of these are

experienced by the cell during the development of a tumourigenic phenotype, such as DNA damage and the inability to satisfy cell-cycle checkpoint requirements. For a cell to progress to an advanced cancerous state, the ability to resist cell death must be acquired, through mutation or deregulation of apoptotic machinery components.[19] The most common mutation seen in cancer is the loss of p53 function,[26] which compromises the cellular stress sensing component of the apoptotic framework. Another mechanism for resisting apoptosis acquired by cancerous cells is upregulation of antiapoptotic regulators such as Bcl-2 and Bcl-x_L, or downregulation of proapoptotic factors including Bax and Bak.[27]

To sustain the rapid proliferation exhibited by tumour tissue, extensive vasculature is required to provide the tumour with the necessary nutrients and oxygen, as well as to remove metabolic waste products and carbon dioxide. This vascular network is formed *via* the formation of new blood vessels from the existing system, in a process called angiogenesis. In healthy tissue this process is limited to wound healing and certain stages of the female reproductive cycle. However, in cancer, angiogenic signalling is often permanently activated, resulting in formation of the required neovasculature to support the growing tumour.[28] Again, this process is controlled by growth factors and receptors, such as vascular endothelial growth factor (VEGF) and the vascular endothelial growth factor receptor (VEGFR), and upregulation of VEGF can be caused by oncogenic signalling.[29] Indeed, one of the early examples of a targeted cancer therapy was the anti-angiogenic VEGFR inhibitor peptide endostatin.[1]

A further obstacle for cells to overcome on the path to neoplasia is the inherent restriction on the proliferative potential of a cell. In normal cells the number of cycles of cell division through which any given cell can pass is limited by telomere length. These multiple hexanucleotide repeats at the terminus of a chromosome are sequentially removed upon each phase of DNA replication, until there is no protection at the end of chromosomal DNA to prevent end-to-end fusion. Such events terminate cell division and thus either force apoptosis through chromosomal instability (CIN) or cause the cell to enter senescence, or cellular dormancy (G_0, see chapter 1.2.). However, oncogenic activation of telomerase, a DNA polymerase capable of adding telomere repeats to the ends of telomeric DNA, is acquired by many human cancers.[19, 30]

The final major hallmark of cancer is the ability of a tumour to invade local tissue and ultimately metastasise. However, it is known that in healthy epithelial tissue, cells are

prevented from detaching from their parent sheet by adheren junctions, attachments between cells and from cells to the extracellular matrix (ECM). One key regulator of adheren formation is E-cadherin, and loss of this molecule is observed in cancer cells. Frequent down-regulation and occasional mutation of E-cadherin affords human carcinomas the ability to invade local tissue and eventually produce metastatic tumours in other organs.[31]

This complex set of characteristics adds to the difficult task facing the cancer research community, and the still relatively high mortality rate from cancer reinforces the need for continued research into the understanding of the processes behind cancer development and new targets for cancer chemotherapy. However, all of the hallmark traits highlight cellular processes in which the molecular pathology of a cancer cell differs from that of a normal cell. This raises the possibility that potential drug targets exist upon which cancer cells have become dependent for their tumourigenic phenotype. A further understanding of the molecular biology of the cell has helped to identify a wide range of cellular processes for which targeted therapies can be applied.

To date, approximately 300 genes have been identified that are mutated in at least one cancer.[32] Although this does not translate into over 300 druggable targets, protein and lipid kinases have emerged as some of the most suitable targets for the development of small molecule chemotherapeutic agents. This explosion of drug targets, many of which are present at elevated levels or in mutated forms in cancer, provides an opportunity to selectively disrupt processes vital to the survival of cancer, whilst limiting the cytotoxic effect on healthy tissue. The age of 'targeted therapy' has arrived, transforming the field into a multi-billion dollar industry, now led by pharmaceutical companies.[1]

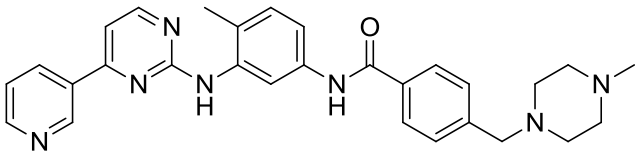

11

A prime example of the new found knowledge of cellular pharmacology generating novel targeted therapies is the discovery of imatinib (**11**), marketed as a mesylate salt under the name *Glivec*. The first specific genetic change associated with a human cancer was the translocation between chromosomes 9 and 22 in chronic myeloid leukaemia (CML). The result is the formation of a fusion gene due to translocation of the Abl1 gene on chromosome

9 to part of the breakpoint cluster region (BCR) on chromosome 22.[33] The BCR-Abl fusion gene, also termed the Philadelphia chromosome, encodes the Bcr-Abl protein, a receptor tyrosine kinase with elevated activity, upregulation of which was shown to induce leukaemia in mice. The Bcr-Abl protein was therefore identified as a highly attractive target for the development of inhibitors,[34] especially due to the absence of the Bcr-Abl kinase in normal tissue.

Drug discovery efforts identified the kinase inhibitor imatinib, which gained Food and Drug Administration (FDA) approval in the United States in 2001, and has been shown to cause remission in approximately 90% of patients with the chronic-phase of CML.[35] Further studies ascertained that imatinib was also an inhibitor of c-Kit, a tyrosine kinase strongly linked to gastrointestinal stromal tumours (GIST). Imatinib has gone on to be highly successful in the treatment of both chronic-stage CML and GIST, acting as 'proof of concept' for the development of targeted kinase inhibitors.[34]

However, despite the success of imatinib, issues identified during the development of single agent cytotoxic therapies persist. In acute-stage CML, imatinib was shown to cause brief remission, although this was often followed by the emergence of drug-resistance. Under the evolutionary pressure of treatment with a chemotherapeutic agent, the genetic diversity within a tumour and the inherent mutability of the cancer cells, may give rise to an outgrowth of drug-resistant cells.[1] This can result from mutation or upregulation of the target protein, modifications to the pathways involved in triggering cell death, or removal of the drug from the cell by means such as the multi-drug resistance (MDR) transporter.[36] This may limit the effectiveness of some targeted therapies when administered as single agents. Fortunately, clinical trials have shown potential synergy between targeted molecules and traditional chemotherapy,[37, 38] potentially reducing the risk of resistance.

Furthermore, it has become apparent that specific groups within a larger patient population may exhibit particular sensitivity or resistance to a targeted therapy based on key genetic variations within a cancer type.[39, 40] It is likely that as more targeted therapies are used, molecular or genomic markers of drug sensitivity will be developed to aid clinicians in the selection of patient populations most likely to benefit from the drug regimen.

1.2. The Eukaryotic Cell Cycle

The phenotypic characteristics of unregulated cell growth and proliferation are present in all cancer types. It is therefore not surprising that a vast amount of research has investigated the misregulation of the cell cycle as a key factor in driving tumourigenesis. In basic terms, the role of the cell cycle is to accurately replicate the genetic information of a cell and precisely separate the resultant copies into two identical daughter cells. This cycle is divided into 4 discrete biochemically defined phases. These are the presynthetic gap/growth phase G_1, the DNA synthesis phase S, the premitotic gap/growth phase G_2, and the mitotic phase M, with an additional quiescent G_0 phase (Figure 2).[41, 42]

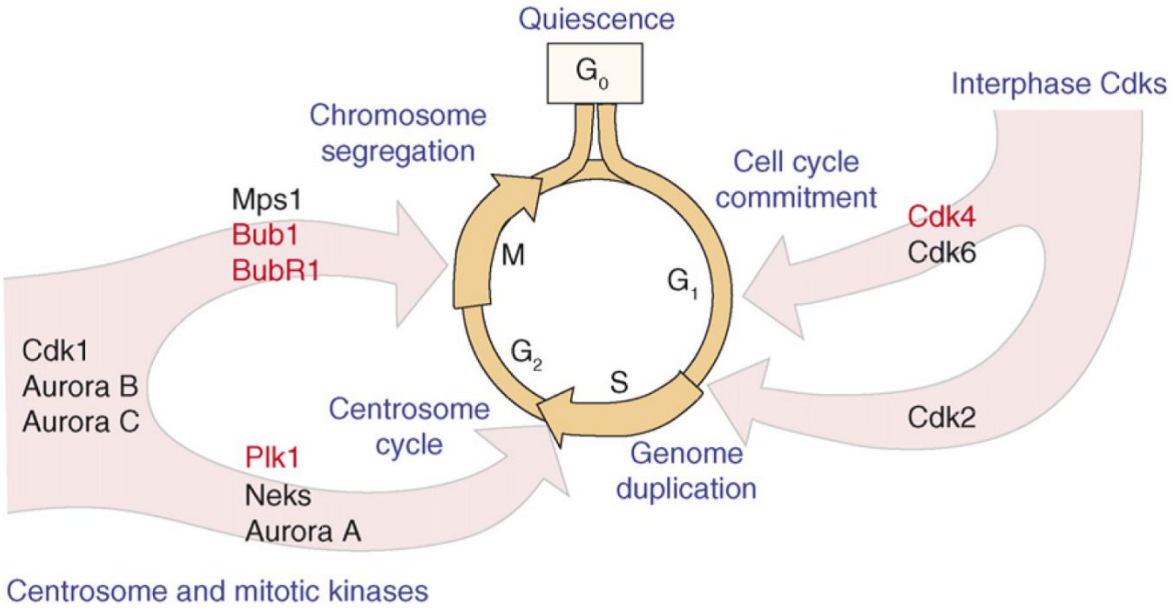

Figure 2: The main cell cycle phases and associated protein kinases.[43]

The cell cycle in rapidly dividing human cells lasts approximately 24 hours. The majority of this time is occupied by interphase (G_1, S, and G_2), with mitosis (M) taking less than 1 hour.[41] Cells in G_1 must initiate the synthesis of proteins and organelles necessary to facilitate chromosomal duplication. During this time the external and internal environment of the cell is monitored to ensure that conditions are suitable for the cell to progress to the S phase. For this reason the length of G_1 may vary, with cells remaining at early G_1 or entering a prolonged period of inactivity, the quiescent or G_0 phase, if the criteria to pass such checkpoints are not met. If checkpoint requirements are satisfied and growth signals are present, the cell passes a restriction point, after which it is committed to entering S phase.[41]

S-phase occurs at the midpoint of interphase and last for approximately 6 hours, a significant proportion of the cell cycle. The chromosomes of eukaryotic cells are large and dynamic structures consisting of DNA and protein packaging. During S phase the chromosomal structure must be dismantled and the DNA quickly and accurately replicated, minimising mutations passed to subsequent cellular generations. Upon completion, the DNA is rewound and the protein packaging must be reformed. The replicated chromosomes now exist as pairs of identical sister chromatids, joined together at multiple points along their length by cohesin, and remain so until the onset of mitosis.[41, 42]

During G_2 phase the cell again undergoes protein synthesis and checkpoint control in preparation for mitosis (see chapter 2). Entry into and progression through all stages of interphase is tightly controlled by a variety of cell cycle kinases (Figure 2).[43] Significant research has been dedicated to an understanding of the roles of cell cycle kinases and their potential in cancer.

1.3. Protein Kinases and Regulation of the Cell Cycle

Protein kinases catalyse the transfer of the γ-phosphate of ATP to the hydroxyl group of a serine, threonine or tyrosine amino acid residue of their substrate (Figure 3). Phosphorylation can cause significant changes to the kinase substrate, such as enzyme activation, enzyme inhibition, alterations to protein conformation affecting recognition properties, or the creation of surfaces with novel binding characteristics. Such changes can trigger a host of downstream cellular events and responses, and in turn, this signal may be removed through dephosphorylation by protein phosphatases.[44] The finely balanced nature of the equilibrium between protein phosphorylation/dephosphorylation, means that misregulation or mutation of a protein kinase or phosphatase may have detrimental consequences for a cell.

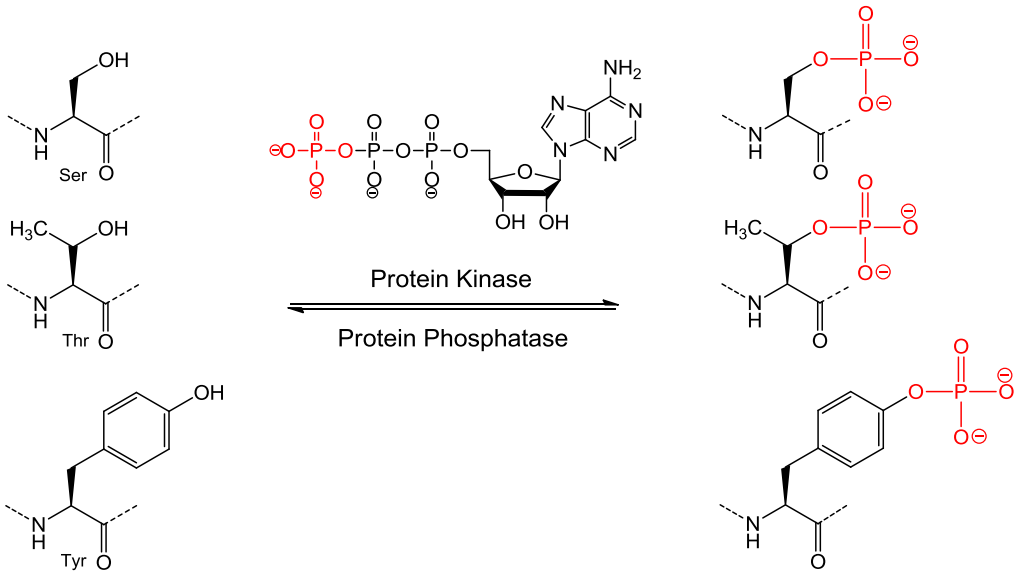

Figure 3: Protein kinase- and phosphatase-mediated phosphorylation/dephosphorylation of amino acid residues.

Kinases are involved in a multitude of cellular processes, such as apoptosis, cell growth and proliferation, metabolism, differentiation, migration, and secretion of proteins including growth factors.[45] However, despite almost 80% of targeted kinase therapeutics residing within the field of oncology, kinases are implicated in a variety of other disease types, such as inflammatory, immunological, metabolic, neurological and infectious diseases.[46] Of the human kinases involved in the progression of a cell through interphase, there are two main families; the cyclin-dependent kinases (Cdks) and the checkpoint kinases (Chks).

1.3.1. Cyclin-Dependent Kinases (Cdks)

Accurate progression through the cell cycle is monitored through the use of checkpoints. These are activated in response to cellular defects such as DNA damage, as a means to allow the cell to repair such damage and prevent the transmission of irregularities to daughter cells. Alternatively, if the damage is too severe the cells may enter senescence or apoptosis. Checkpoint activation induces cell cycle arrest through effects on the activity of cyclin-dependent kinases (Cdks).[47]

The activity of Cdks relies on formation of an active heterodimer between the Cdk and a partner cyclin subunit. In normal cells the expression of specific cyclins is tightly controlled in order to maintain accurate regulation of the processes for which Cdks are responsible. However, in many human cancers mutations are present that contribute to misregulation of Cdk activity. These include overexpression of specific cyclins and inactivation of Cdk

inhibitors, such as members of the Inhibitor Kinase 4 (INK4) and Cip/Kip families.[48] There are 12 members of the Cdk family identified thus far, although only five are directly implicated in cell cycle progression, namely Cdks 1, 2, 3, 4 and 6.[43]

Cdk1, also known as cell division control protein 2 (Cdc2) in yeast, is the only Cdk regarded as a mitotic kinase, and is activated through binding cyclin A at the end of interphase to promote cellular entry into mitosis. Upon completion of nuclear envelope breakdown (NEBD), cyclin A is degraded and Cdk1-cyclin B complexes form, with the effect of driving the cell through mitosis.[47] Cdk1 complexes with A- and B-type cyclins are implicated in a variety of roles, including centrosome duplication, chromosome condensation and assembly of the spindle.[43, 49] These vital roles in mitosis are reflected in experimental outcomes of Cdk1 inhibition. Prior to mitosis, cells subjected to Cdk1 inhibition fail to progress through the G_2/M transition, arresting in G_2. If Cdk1 inhibition occurs during mitosis, cells exit mitosis without undergoing cytokinesis.[43] Indeed, of the Cdk family it is only Cdk1 that is shown to cause cell cycle arrest upon systematic knockdown in healthy tissues, and there is no compensation for Cdk1 activity by other family members.[47] For this reason it is likely that therapeutic modulation of Cdk1 activity may impose serious toxicity, limiting its usefulness as a drug target.

The critical role of Cdk1 in cell cycle progression is similar to that in yeast, with a single Cdk responsible for cell cycle control. The reason for the presence of multiple Cdk members in eukaryotic cells is likely due to the need for mammalian systems to control a large number of distinct cell types. This is highlighted by the fact that systematic knockdown of Cdks 2, 4 and 6 fails to cause cell cycle arrest in the majority of cells.[47] However, detrimental effects are observed in distinct cell subtypes. Cdk2 activity is vital for meiotic division of germ cells,[50] Cdk4 is required for pancreatic β-cell proliferation,[51] and Cdk6 knockdown causes erythroid cell lineage defects.[52]

Despite the apparent lack of effect on cycle cycle arrest following depletion of Cdk2,[50, 53] it is a key kinase in checkpoint control and homeostasis. Passage through the G_1/S transition is reliant on the formation of a Cdk2-cyclin E complex. Subsequent formation of a Cdk2-cyclin A2 complex, which is present during the late stages of DNA replication, facilitates the S/G_2 transition.[54] Further evidence links Cdk2, along with Cdk4, with a role in controlling the proliferative potential of stem and progenitor cells, as Cdk2 deficient progenitor cells are defective in their potential to self-renew and display increase differentiation.[55]

It has been shown that, unlike healthy tissue, a number of tumours have developed a reliance on Cdk2 activity for proliferation.[56] Mutations in Cdk2 have not been found in such cells, but overexpression of E-type cyclins is a common trait of human tumours. Additionally, p21 and p27 inhibitors of Cdk2 are often downregulated, contributing further to misregulation of Cdk2 activity. This, coupled with the lack of effect of Cdk2 downregulation on normal cells, has highlighted Cdk2 as an attractive and highly investigated target for cancer drug discovery.[47]

Cdk3 is inactive in laboratory mouse strains and has therefore been overlooked when compared to other members of the family. It is implicated with a role during interphase in complex with cyclin C.[47] Cdks 4 and 6 are G_1 kinases, playing a part in early cell cycle progression. The onset of mitogenic signals is triggered by expression of D-type cyclins, the regulatory partners of Cdks 4 and 6. Formation of the active complexes of these kinases results in inactivation of pocket proteins Rb, RbL1 and RbL2. This allows E-type cyclins to be expressed and enables eventual G_1/S transition through activation of Cdk2-cyclin E.[57]

Misregulation of Cdks 4 and 6 is common in many tumour types, particularly by effects on expression of D-type cyclins and INK4 family Cdk inhibitors.[47] Cdk4 activity is further modulated through mutation to a form unable to bind INK4 inhibitors, as well as being overexpressed in a variety of epithelial malignancies. No Cdk6 mutation has been identified thus far but overexpression is often observed in leukaemias and sarcomas.[47] This indicates that Cdk4 and Cdk6 appear to be upregulated in a variety of cancers, suggesting potential value for selective inhibitors. Of particular note is the observation that both Cdk4-deficient and cyclin D1-deficient mice are resistant to mammary tumour formation induced by the ERBB2 oncogene, responsible for the human EGFR2 (Her2) protein.[58] This raises the possibility that Cdk4 inhibition may offer a therapeutic advantage in Her2-positive breast cancer patients.

1.3.2. Checkpoint Kinases (Chks)

Two structurally unrelated serine/threonine protein kinases have been identified that are major regulators of cell cycle checkpoints, checkpoint kinase 1 (Chk1) and checkpoint kinase 2 (Chk2). Homozygous knockout of Chk1 results in non-viable mouse embryonic stem cells.[59] However, in adult somatic cells a lack of Chk1 is non-lethal, although cells lack the G_2 arrest of healthy cells upon exposure to ionizing radiation. This indicates a role of Chk1 in

the G_2/M checkpoint. Chk2 shares several substrates with Chk1, including key cell cycle regulators Cdc25A, Cdc25B and Cdc25C. Chk2 has been shown to play a role in both S and G_2 checkpoints in response to double strand breaks (DSBs) in several immortalized human cell lines.[60]

It is thought that genotoxic stress activates ATM/ATR kinases, which phosphorylate and activate Chk1/Chk2. For genotoxic stress requiring S phase arrest, Chk1 and Chk2 target Cdc25A for ubiquitination and degradation, which suppresses Cdk2 activity, resulting in failure of the cell to exit S phase. In a similar manner, agents conferring G_2/M arrest result in degradation of Cdc25A, but also sequestration of Cdc25B and Cdc25C. This results in a lack of Cdk1 activity and subsequent failure to satisfy the G_2/M checkpoint.[60, 61]

A major obstacle to many current DNA-damaging chemotherapeutic agents is the rapid emergence of resistant colonies. Contributing to this is the intricate machinery in the cell that detects DNA damage and arrests cells at different stages of the cell cycle. Due to abrogation of the p53-mediated checkpoint control apparatus in the majority of human tumours, it is likely that such cells are dependent on the checkpoint kinase pathways. Chk1 and Chk2, are therefore of potential interest for inhibition, as a means to confer selective chemosensitization to cancer cells over normal tissue on treatment with DNA-damaging therapies.[60]

Chapter 2: Mitosis and its Regulation by Kinases

2.1. Stages of Eukaryotic Mitosis

The M phase of the cell cycle is made up of two key events. The first event is mitosis, the process by which the sister chromatids generated during the S phase are separated and distributed into two identical daughter nuclei, each with a full copy of the parent genome. This is followed by cytokinesis, where the cell divides in two, giving a pair of cells with a full complement of genetic information with which to undergo a new round of the cell cycle. Alterations in the tightly controlled processes of mitosis can lead to cell death through mitotic catastrophe, or chromosome segregation errors, potentially resulting in unevenly distributed genetic material in daughter cells following cytokinesis. This phenotype is termed aneuploidy, and is a key characteristic of many cancers.

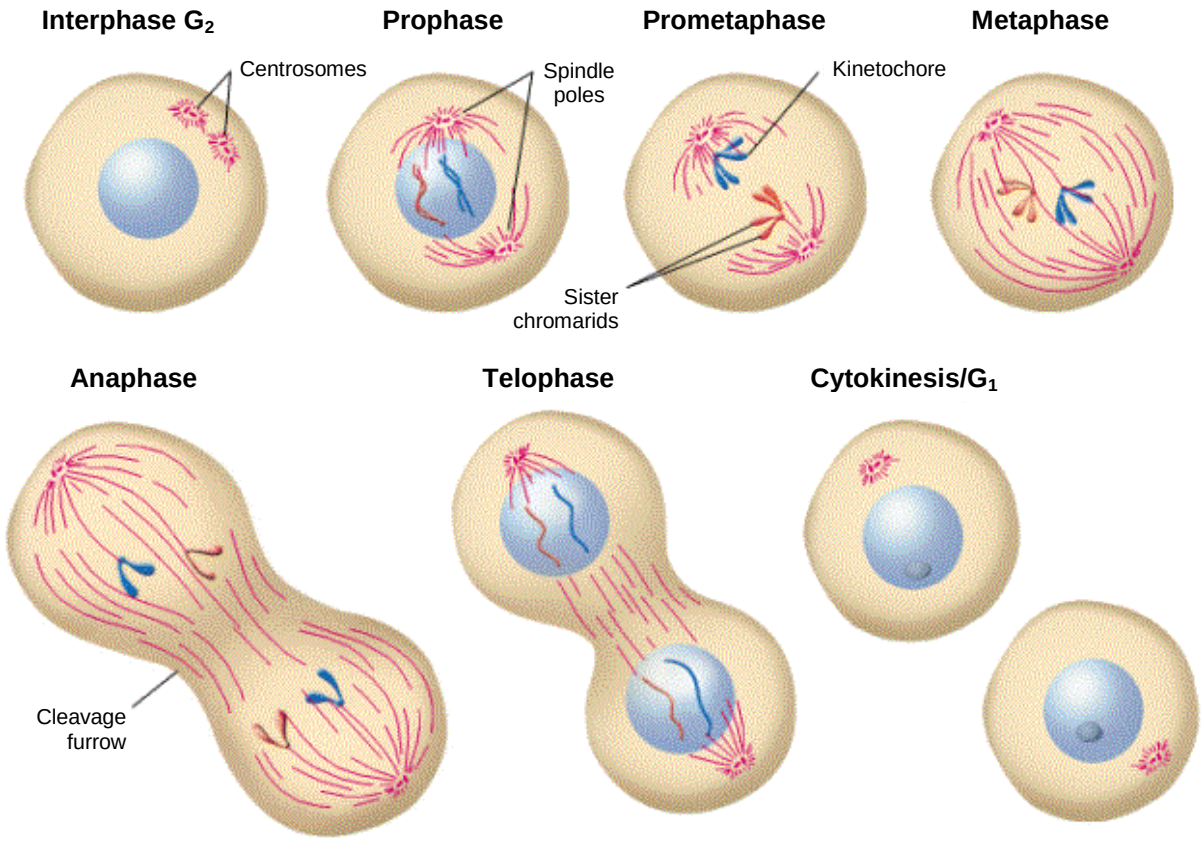

Figure 4: The stages of eukaryotic mitosis.[62]

The frequent occurrence of aneuploidy in cancer has generated considerable interest in the molecular biology of mitosis in both normal and cancer cells, to identify potential targets for

the development of cancer therapeutics. Mitosis is divided into five distinct stages; prophase, prometaphase, metaphase, anaphase and telophase (Figure 4).[62]

During prophase, genetic information replicated during S phase condenses into well-defined sister chromatids. Outside of the nucleus the pair of centrosomes, or microtubule organising centres (MTOC), present at mitotic entry migrate to opposite poles of the cell and the mitotic spindle begins to form (see chapter 2.2.).[41]

Prometaphase starts abruptly with the disappearance of the nucleus through nuclear envelope breakdown (NEBD). The nuclear envelope is composed of inner and outer nuclear membranes surrounding a protein layer called the lamina, punctuated by nuclear pores to allow transfer of components between the cytoplasm and nucleus. Phosphorylation of lamina components results in their disassembly and breakdown.[42] The released sister chromatids are now free to attach to microtubule components of the spindle array, and undergo active movement facilitated by microtubule and kinesin motor proteins.[63]

Cells reach metaphase when all chromosomes are oriented at the spindle equator and sister chromatids have formed kinetochore attachments to opposite poles of the mitotic spindle. Failure to form a proper attachment between a kinetochore and a microtubule results in the kinetochore sending a 'wait-signal' as part of the spindle assembly checkpoint (SAC – see chapter 2.2.1.). Correct attachment of all kinetochores culminates in checkpoint silencing and mitotic progression.[64]

Transition into anaphase is triggered by activation of the anaphase promoting complex/cyclosome (APC/C), a multi-subunit E3 ubiquitin ligase, by the cell division cycle 20 homologue (Cdc20).[65] APC/C causes ubiquitination of key cell cycle regulators which targets them for destruction by the 26S proteasome.[66] One such cell cycle regulator is the separase inhibitor securin, a protease that destroys the cohesin link between sister chromatids. Activation of APC/C results in a surge in separase activity and subsequent cleavage of the link between sister chromatids.[64] This allows the chromatids to be drawn apart *via* spindle elongation, and as anaphase progresses a cleavage furrow forms as the plasma membrane begins to close in around the spindle midpoint.[41]

During telophase the separated sister chromatids arrive at opposite spindle poles and decondense. The nuclear envelope reforms around each new genomic set, generating two new

nuclei and marking the end of mitosis. The M phase is completed when the contracting cleavage furrow divides the cytoplasm; yielding two identical interphase cells.[41]

2.2. Centrosomes and the Mitotic Spindle

Accurate chromatid attachment and separation is mediated by the mitotic spindle, a bipolar framework consisting of microtubules. Microtubules are made up of polymers of α- and β-tubulin subunits, which form protofilaments. The tubule structure is a 25 nm diameter hollow tube, formed *via* the lateral association of 13 such protofilaments.[67] Microtubules possess cytoplasmic 'plus' ends, which grow rapidly, in comparison to 'minus' ends, which grow relatively little. These minus ends are anchored at the centrosomes, which are the primary site of microtubule nucleation in most mammalian cells. In higher animal cells, the polarity of the spindle framework is usually directly related to the number of cellular centrosomes.[68]

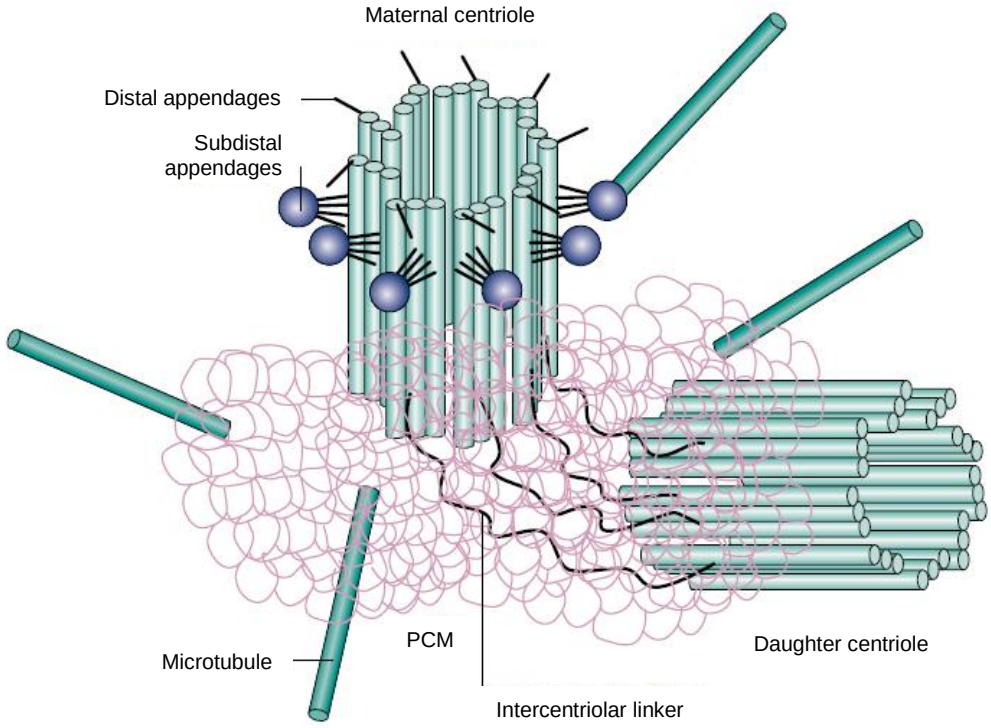

Figure 5: Structural elements of the centrosome.[68]

Centrosomes were first observed in 1888 by Theodor Boveri, who identified small focal points of phase-dense material in the centre of cells.[69] Centrosomes are made up of barrel-shaped centrioles connected by an intercentriolar linker (see chapter 3.7.4.) and surrounded by pericentriolar material (PCM) (Figure 5). The centrioles are barrel-shaped configurations of nine microtubule triplets, giving nine-fold symmetry and lying perpendicularly to one

another. The two centrioles are distinguishable as maternal and daughter centrioles, with the maternal centriole possessing distal and subdistal appendages.[68]

Microtubule nucleation occurs within the fibrillar mass of the PCM and is reliant on a further member of the tubulin family, γ-tubulin. The form of γ-tubulin that triggers microtubule nucleation is the γ-tubulin ring complex (γTuRC), in which γ-tubulin associates with γ-complex proteins (GCPs) 1 and 2 with a ring shaped morphology.[70] These γTuRCs are thought to cap the minus ends of microtubules and cause nucleation within the PCM.[71] However, it is thought that there is a distinction between microtubule nucleation and microtubule anchoring, with the latter being the process by which microtubules are attached to the centrosome during spindle formation. The subdistal appendages of the maternal centriole have been shown to act as further sites capable of capping the minus ends of microtubules, despite lacking the associated microtubule nucleating proteins. Instead, they associate with proteins ninein and centriolin.[68, 72, 73]

Following nucleation and anchoring of microtubules, the mitotic spindle can be formed *via* continuous addition of α- and β-tubulin subunits from the plus end of the microtubule, accompanied by removal from the anchored minus end.[68] The resultant highly dynamic spindle framework is maintained in position through the relatively static nature of the spindle poles. The centrosomes are typically in a 'face-to-face' configuration separated by overlapping pole-to-pole microtubules. Further sets of astral microtubules spread out from either centrosome to the cell cortex and kinetochore microtubules emanate and attach to the kinetochores, such that each sister chromatid in a pair is attached *via* its kinetochore to opposite poles of the mitotic spindle.[49] Kinesin motor proteins are proteins capable of interacting with, and travelling along, the α- and β-tubulin protofilament tracks to aid in the trafficking of cellular components and signals.[63] These proteins, along with inherent dynamics within the spindle framework, facilitate the mitotic spindle to carry out accurate mitotic segregation of the cell's genome.

2.2.1. The Spindle Assembly Checkpoint (SAC)

As with other phases of the cell cycle, the division of sister chromatids is governed by a checkpoint; the spindle assembly checkpoint (SAC).[66] The SAC detects the presence of unattached kinetochores or a lack of tension between sister centromeres in mitosis, and sends a 'wait-anaphase' signal, preventing cleavage of the cohesin link between centromeres.

Several proteins identified in budding yeast have vertebrate homologues that make up components of the SAC complex; Budding uninhibited by benomyl (Bub) proteins 1, 2 and 3, and mitotic arrest deficient (Mad) proteins 1, 2 and 3.[66] In addition, higher eukaryotes also possess Bub-related-1 kinase (BubR1), centromere protein E (CENPE), the ZW10-ROD-Zwilch complex, and mitogen-activated protein kinase (MAPK) as proteins associated with the SAC.[64]

Unattached kinetochores transiently bind the mitotic checkpoint complex (MCC), comprising BubR1, Mad2, Bub3 and Cdc20. This holds Cdc20 within this stable complex, preventing activation of the APC/C and, ultimately, mitotic progression through ubiquitination of securin and chromatid separation.[74] Furthermore, once activated, the APC/C triggers cyclin B1 degradation and subsequent inactivation of Cdk1, driving mitotic exit.[64]

In healthy cells the presence of a single unattached kinetochore is sufficient to trigger mitotic arrest. However, individual unattached kinetochores fail to produce a 'wait signal' strong enough to prevent mitotic progression in several tumour cell lines.[75, 76] Modification to the expression levels of SAC components may lead to an inability to halt mitosis, although results for the misregulation of such protein levels in cancer cells through genetic analysis have been mixed. This highlights the probability that a weakened SAC response can act to facilitate cancer development, but not act as a causative effect of cancer. It has been found that complete inactivation of the SAC response can be lethal, rather than oncogenic, through mitotic crisis.[77] However, incomplete inactivation of the checkpoint through sub-optimal inhibition will carry a serious risk of increasing CIN and driving tumourigenesis.

2.3. The Centrosome Cycle

Errors in the formation of a bipolar mitotic spindle can perpetuate aneuploidy and CIN through defects in chromosome segregation. The centrosome number in mitotic cells is therefore of vital importance. One exception to this requirement is observed with some plant cells, in which spindle formation and cell division can occur independently of the presence of centrosomes.[78] However, in mammalian cells the lack of astral microtubules yields spindle frameworks that are mispositioned, resulting in aberrant cytokinesis.[68] Upon completion of cytokinesis, each daughter cell possesses a single centrosome from opposite poles of the mitotic spindle. At the onset of mitosis a pair of centrosomes is required to form a bipolar

spindle framework. During the cell cycle, the cell replicates each progeny centrosome prior to the G2/M transition *via* the centrosome cycle (Figure 6).

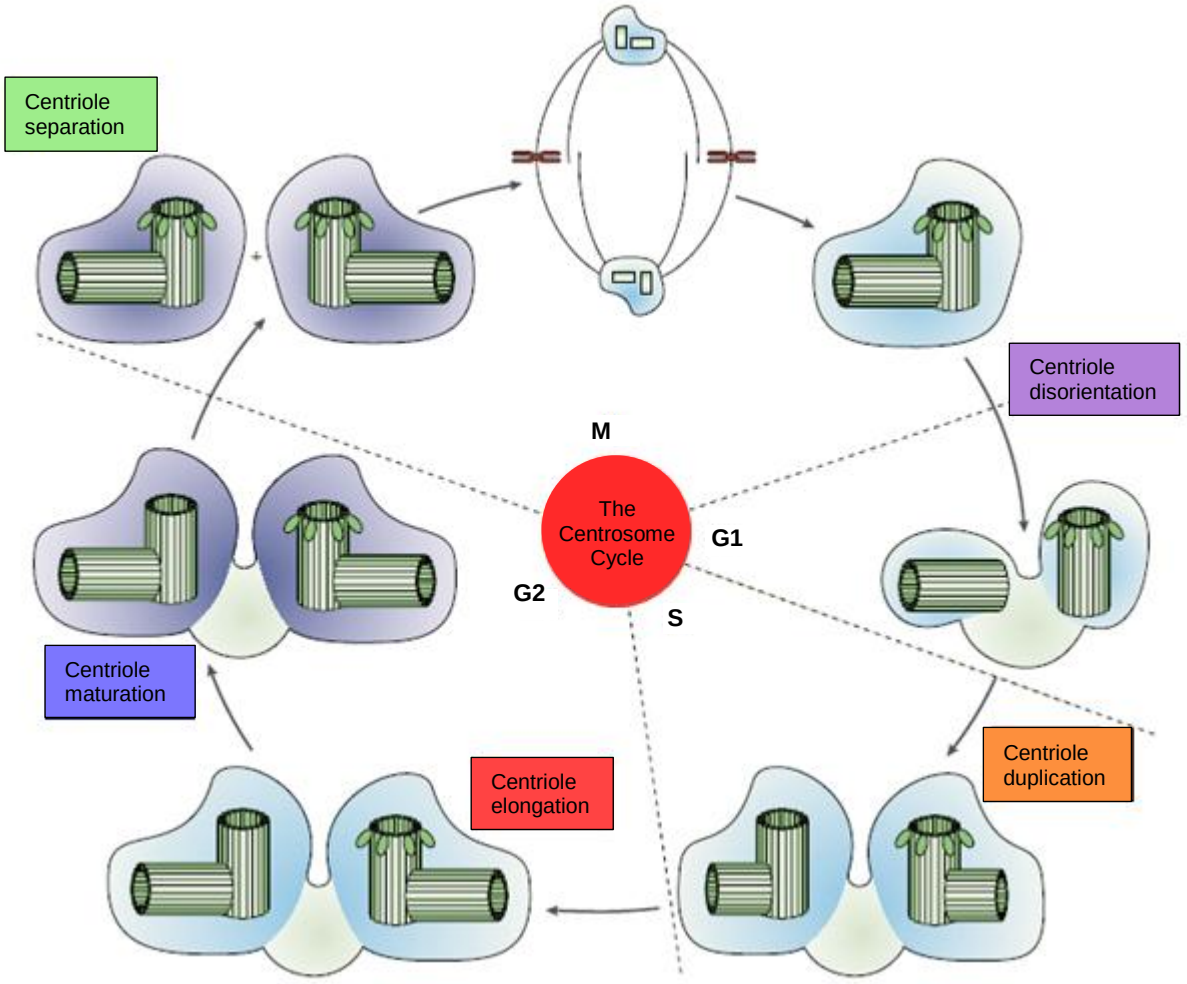

Figure 6: The centrosome cycle.[79]

The precise mechanism(s) triggering the onset of centrosome duplication is not fully understood.[79] However, it is known that during healthy cell cycle transit the centrosome replicates only once. Importantly, this replication must be closely coordinated with DNA replication to ensure all necessary components are acquired by the cell prior to the key events of mitosis, preventing the risk of genomic instability (GIN). One potential source of such coordination is the Rb pathway; both cycles have been shown to require phosphorylation of Rb, and in particular the presence of the transcription factor E2F, the primary downstream effector of Rb. Due to this reliance on both cycles, it is likely that oncogenic mutation of the Rb pathway will lead to loss of cycle coordination and contribution to GIN. The same studies highlighted the key role of cyclin expression, in conjunction with Cdk2, in regulating both cycles. Cdk2-cyclin E appears to be the primary complex responsible for allowing G1/S

transition and triggering DNA synthesis, whereas Cdk2-cyclin A was the favoured complex for inducing centrosome duplication.[80]

The centrosome cycle commences during G_1 as the maternal and daughter centrioles lose their orthogonal relationship. At the start of S phase the centrioles begin to duplicate, with the appearance of procentrioles growing perpendicularly from the proximal ends of both mother and daughter centrioles. By the completion of the S phase the procentrioles have reached maturation, matching the length of their parental centrioles, and the centrosome now has the configuration of two centriolar pairs connected by the flexible intercentriolar linkage. At a variable time prior to the G_2/M transition, centrosomal disjunction occurs, and the PCM divides to form separate mother and daughter centrosomes. The centrosome cycle is completed with maturation of the daughter centrosomes upon acquisition of distal and subdistal appendages.[79, 81]

2.4. Regulatory Kinases in Mitosis

A number of non-targeted antitumour agents exert their cytotoxic activity in mitotic cells. Such compounds often act as spindle poisons, due to a locus of their toxic effect in mitotic spindle formation and dynamics (see Vincristine, Taxol, chapter 1.1.1.).[82] *Vinca* alkaloids, such as vincristine and vinblastine, are cytotoxic through their effect on the ability of a cell undergoing mitosis to form a mitotic spindle. *Vinca* alkaloids bind to tubulin dimers and inhibit their ability to polymerise into the larger tubulin networks required for spindle formation.[83] Taxol, on the other hand, binds to and stabilizes polymerised tubulin, and consequently interferes with the ability of the spindle framework to manipulate and traffic cellular components during mitosis.[84] The effects of both classes of antitumour agents on the dynamics of the mitotic spindle result in apoptosis due to mitotic catastrophe. Such spindle poisons have provided some success as clinical treatments, despite a lack of selectivity for tumour cells over healthy tissue. As the chemotherapeutic effort has moved towards targeted therapy, driven by a deeper understanding of mitosis on a biomolecular level, several key kinases involved in mitosis have attracted attention.[43]

2.4.1. Aurora Kinases

Aurora kinases were first identified during a screen to establish genetic mutations in yeast that correlate with an increase-in-ploidy phenotype. This identified the yeast protein termed Ilp1.[85] Three vertebrate homologues were discovered that shared high sequence homology within the carboxy-terminal catalytic domain, but varied in their functions, all of which were mitotic. They were termed Aurora kinases A, B and C, owing to the observation that Ilp1 was associated to the cellular poles, analogous to the *Aurora borealis* and *Aurora australis* phenomena at the polar regions of our planet.[86] Within the same screen a further pole-associated kinase was identified and termed Polo-like kinase (Plk) – after the Spanish word for pole (see chapter 2.4.2.).[87]

Aurora A activity is dependent upon phosphorylation of a key regulatory threonine residue (T288) on the kinase "activation loop". Negative regulation of kinase activity is achieved through dephosphorylation by protein phosphatase 1 (PP1). Expression levels of Aurora A are tightly controlled, and the kinase is targeted for degradation by the APC/C during late M/early G_1, through a C-terminal D-box (destruction box) and a D-box-activating-domain (DAD).[88, 89]

Aurora A kinase localises in a dynamic equilibrium with separating centrosomes during late S/early G_2 phases. Late in M phase, elevated Aurora A levels are reported at the spindle midzone and midbody.[87] Depletion of Aurora A in a variety of systems has suggested a role for the kinase in centrosome separation.[90, 91] With decreased levels of Aurora A, cells lack the ability to recruit necessary PCM components, including γ-tubulin.[91, 92] In addition, the centrosome's astral array of microtubules is disrupted, potentially due to alterations in the activity of transforming-acidic-coiled-coil containing protein 3 (TACC3), a regulator of microtubule dynamics, and the motor protein Eg5, both of which are substrates of Aurora A.[90, 93] This implicates Aurora A with a role in centrosome maturation.

A role for Aurora A has also been described in spindle assembly in association with the small GTPase Ran-GTP, and its associated protein TPX2.[94] TPX2 activates Aurora A by binding to the kinase and countering the negative regulation of PP1. This complex subsequently associates to and orientates the spindle microtubules during mitosis.[95]

Aurora B kinase is a chromosomal passenger protein, forming a complex with the proteins inner centromere protein (INCENP) and survivin. INCENP is both a substrate for and a

positive regulator of Aurora B, and is a microtubule associated protein (MAP) that targets chromosomes and centromeres.[87, 96] Aurora B localises to centromeres in metaphase cells and associates tightly with central spindle microtubules during anaphase.[97]

Aurora B is implicated with a role in ensuring bipolar kinetochore attachments supplementary to the SAC. Although the exact mechanism is poorly understood, it is proposed that Aurora B recognises the attachment of kinetochores to the same spindle (syntelic attachment) as a function of the reduced centromeric tension with regards to kinetochores attached to opposite centrosomes (amphitelic attachment).[87, 98]

A further function has emerged for Aurora B as a regulator of chromosome bioorientation.[99] Prior to chromosomal segregation, microtubule dynamics orient the sister chromatids at the cellular equator. This bioorientation has been shown to be dependent on inner centromere KinI stimulator (ICIS) and mitotic centromere-associated kinesin (MCAK). ICIS is a substrate of Aurora B, and thus Aurora B has a direct impact on the microtubule-disassembly activity of MCAK.[85, 99]

The role of the final family member, Aurora C, is poorly understood. However, it is thought that the kinase plays a role in mitosis, where it is associated to the centrosome. There is also evidence for Aurora C acting during spermatogenesis.[85, 100]

Aurora A and B kinases are overexpressed in a range of tumours, and are associated with a poor prognosis. Overexpression of Aurora A may result in loss of coordination between the centrosome cycle and cell cycle, leading to centrosomal amplification and subsequent CIN. Interestingly, it has been shown that phenotypic abnormalities that are associated with loss of Aurora A regulation are found to be amplified in cells lacking p53.[101] The common nature of this oncogenic modification, coupled with Aurora A overexpression, may result in a synergistic acceleration of CIN and aneuploidy. Aurora B has also been shown to be overexpressed in tumours, resulting in defects in mitosis and aneuploid progeny.[102] These observations have led to Aurora A and B being thoroughly investigated kinases in the field of anticancer drug discovery.

2.4.2. Polo-like Kinases (Plks)

Polo-like kinases (Plks) are a family of serine/threonine protein kinases of which there are four known members, Plk1, 2, 3 and 4. The Plk members have suggested roles in the mediation of a variety of mitotic events. They share high sequence homology across the family, with all kinases bearing a canonical N-terminal kinase domain and conserved C-terminus polo-box domains (PBDs). Plks are activated through phosphorylation of residues within the activation loop (T-loop) of the catalytic domain.[103, 104]

Regulation of activity is also mediated by the PBDs. These regions act as phosphopeptide-binding domains, recognising and binding to proteins already phosphorylated by a 'primer' kinase.[105] In the absence of a phosphorylated ligand, the PBD is thought to bind to the kinase catalytic domain, inhibiting substrate binding and preventing kinase activation through T-loop phosphorylation. This reliance on substrate phosphorylation to allow kinase activation may aid in the temporal and spatial control of Plk activity.[103, 106]

Of the Plk family, current understanding of the roles of Plk2, 3 and 4 is relatively poor. Plk1 is thought to participate in several events during mitosis. Importantly, Plk1 is implicated in the recruitment of key centrosome components, including γ-TuRCs, through the Plk1 substrate ninein-like-protein (Nlp).[107] A further centrosomal protein with a potential Plk1-mediated action in centrosome maturation is Asp-like microcephaly associated (ASPM), of which the *Drosophila* homologue Asp is phosphorylated by Polo and is needed for microtubule nucleation.[108] However, a role for ASPM in mitosis has yet to be identified, with only activity in neurogenesis being described thus far.[103]

In addition to the spindle poles, Plk1 also associates with kinetochores during mitosis, highlighting possible activity in chromosome segregation.[109] It is thought that Plks may phosphorylate cohesin subunits, aiding the dissociation of sister chromatids.[110] Further effects of Plk activity appear to be APC/C dependent, presenting Plk activity as a regulator of many mitotic processes, including mitotic entry and cytokinesis, as a consequence of APC/C substrate degradation.[111, 112]

Of the other Plk family members, the function of Plk2, also called Snk, is not fully known. Although viable, Plk2-/- mice show retardation of growth and skeletal development.[113] Plk3, also known as Fnk, has been implicated in G_1/S transition *via* the induction of cyclin E

expression.[104] Finally, Plk4 is a key component for the regulation of centriole replication in both *Drosophila* and humans.[114]

Chapter 3: NIMA-Related Kinases (Neks)

A final key family of kinases involved in mitotic regulation are the never in mitosis gene A-related kinases (Neks). In 1976 the genetic analysis of cell cycle mutants in the filamentous fungi *Aspergillus nidulans* was reported.[115] During these studies, screening temperature-sensitive mutant genes, the effect of genetic disruption was noted as either causing the fungal cells to be blocked in mitosis (*bim*) or never in mitosis (*nim*). Members of the bim subset were later found to be genes encoding for key proteins involved in mitotic progression, including components of the APC/C. Amongst several recognised cell cycle regulators, the *nim* subset also contained 4 alleles of an unknown gene, termed *nim*A. The protein encoded by the *nim*A gene is a 79 kDa serine/threonine protein kinase designated NIMA.[116]

Interestingly, NIMA-null mutants were shown to possess an irregular nuclear envelope and lack a bipolar mitotic spindle, when expressed in conjunction with knockdown of *bim*E7, which was later found to encode an APC/C subunit.[117] Induction of NIMA was shown to cause mitotic irregularities, including errors in spindle formation, and chromosome condensation was possible in cells blocked at S phase,[118] related to the fact that overexpression of NIMA has the potential to induce mitosis in cells at any stage of the cell cycle.[118]

3.1. NIMA in *Aspergillus nidulans*

NIMA expression and activity are tightly controlled in a cell cycle-dependent manner through transcriptional means and post-translational modification (Figure 7). Prior to mitosis, NIMA expression and activity levels are low. At the G_2/M transition, NIMA expression levels begin to rise in conjunction with its degree of phosphorylation. The expression and phosphorylation state of NIMA are mirrored by the activity of the cyclin B complex with Cdc2, the human counterpart (Cdk1) which is the so called ‘master regulator’ of mitotic entry.[116]

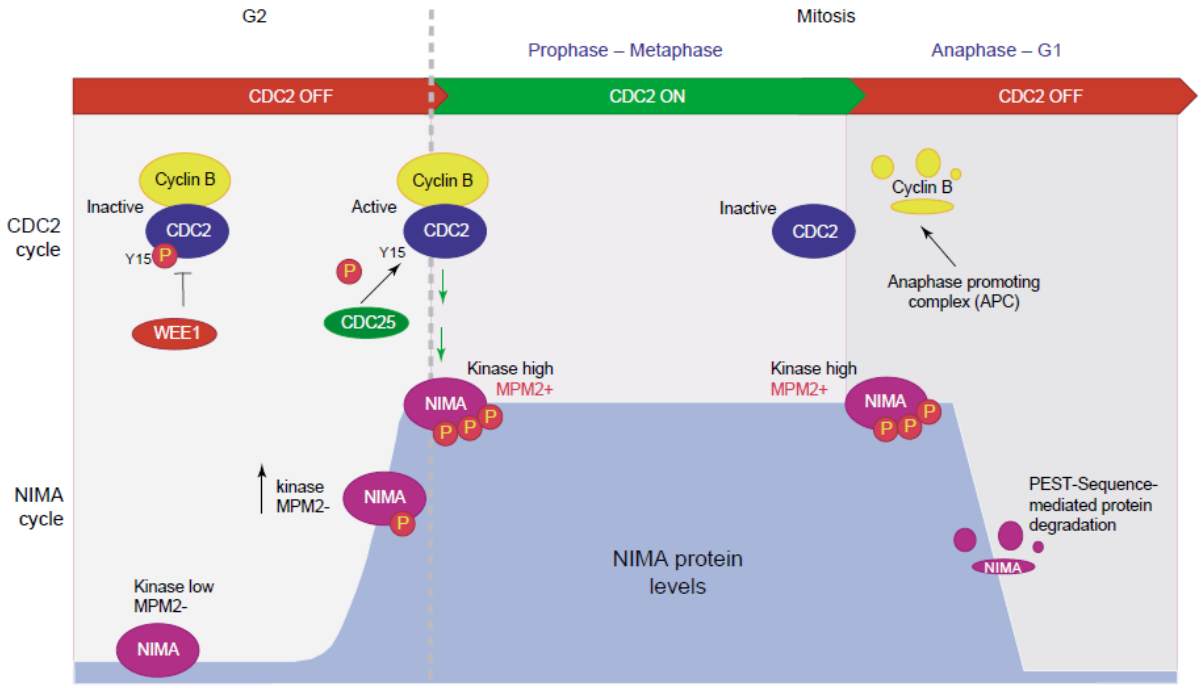

Figure 7: Dual regulation of NIMA and Cdc2 during mitosis in *Aspergillus nidulans*.[116]

During G2, the Cdc2-cyclin B complex is maintained in an inactive state through inhibitory phosphorylation of a key tyrosine residue (Y15) on Cdc2 by the kinase Wee1. At the G_2/M transition, Cdc25-mediated dephosphorylation of Y15 results in activation of Cdc2-cyclin B, with corresponding expression and phosphorylation of NIMA. Further Cdc2-mediated phosphorylation of NIMA occurs during mitosis, possibly by Cdc2 itself, until cells approach anaphase. At this point, the activity of Cdc2-cyclin B is lost though APC/C dependent ubiquitination of B type cyclins, and this coincides with degradation of NIMA *via* an unidentified ubiquitin ligase.[116] Furthermore, destruction of NIMA has been shown to be required for mitotic exit.[119] This tightly controlled expression and activity clearly indicates a role for NIMA during mitosis.

3.2. Members of the Human Nek Family

The critical role of NIMA in mitotic progression raised the possibility that NIMA counterparts may possess similar functions in higher vertebrates. Homologues of NIMA exist in other species, including the functionally related kinase in budding yeast, termed *fin*1, which is involved in spindle formation.[120] Designation of human kinases that are related to NIMA has focussed on sequence homology within the catalytic domain. A family of 11 NIMA-related kinases (Neks) has been identified to date (Figure 8), with varying degrees of

homology to NIMA. Several family members have a higher degree of similarity in their C-terminal motifs than others, and can be classed as true NIMA homologues. Other members, however, have either lost such motifs or gained additional sequences, possibly relating to additional roles outside of mitosis.[116]

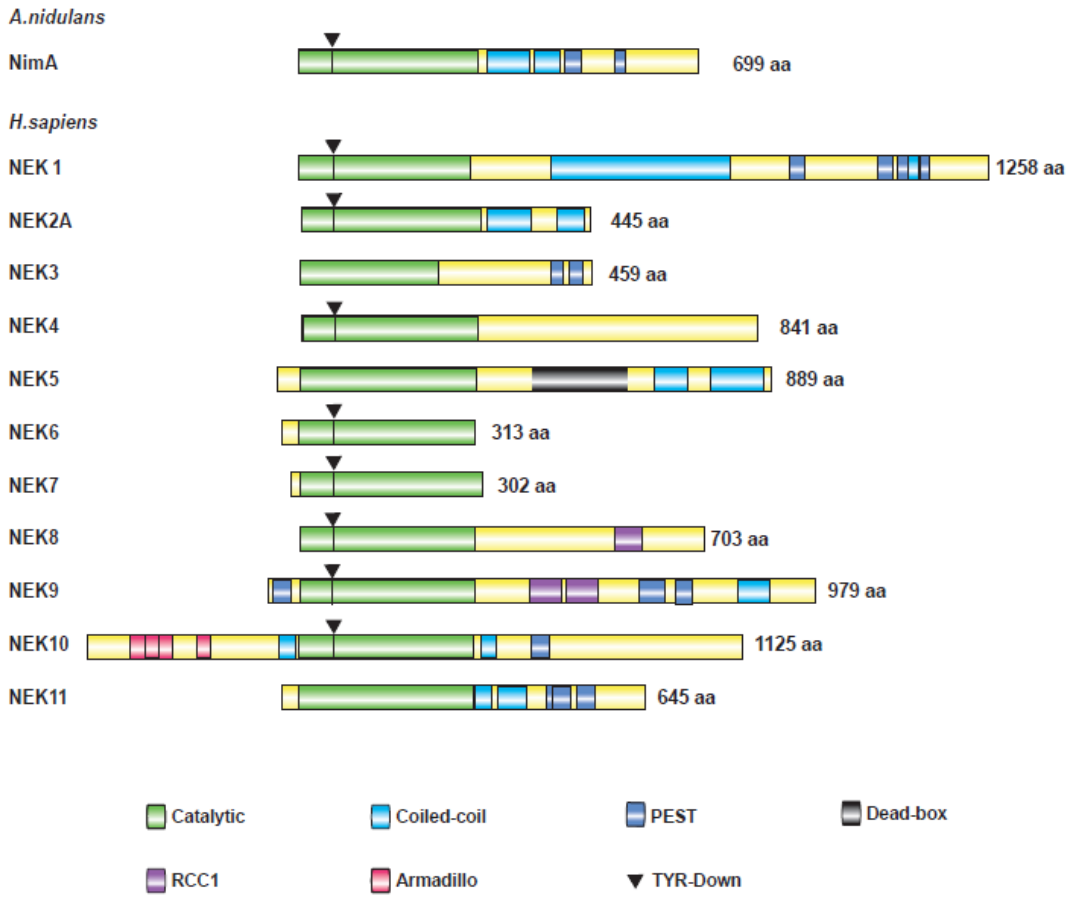

Figure 8: Significant motifs and structural alignments of the 11 human members of the NIMA-related kinase family.[121]

Outside of the catalytic domain, which is at the N-terminus in all members excluding Nek10, the homology of the family is variable.[121] Neks 4, 6 and 7 contain no coiled-coil motif, a region conferring the structural characteristic of multiple coiled α-helices. Just over 50% of the Neks contain PEST sequences, motifs that participate in ubiquitin-dependent proteolysis. Furthermore, additional motifs are observed in selected members, such as regulator of chromosome condensation (RCC1) motifs in Nek8 and 9, which may be responsible for an interaction with the Ran GTPase.[121] Nek5 bears a predicted DEAD-box (Asp-Glu-Ala-Asp), a motif that is conserved in a family of DEAD-box RNA helicases.[122] Nek10 also contains a small region of armadillo repeats, motifs responsible for hairpin pairs of short α-helices, and

yielding α-solenoid protein folds.[123] The majority of Nek family members contain a tyrosine-down autoinhibitory motif within the catalytic domain, which projects a tyrosine residue into the active site maintaining the kinase in an inactive conformation. This motif was first observed in the X-ray crystal structure of Nek7, with autoinhibition being removed by phosphorylation of the kinase activation loop (T-loop).[121]

The currently established roles of Nek members are not limited to the cell cycle and mitosis, with Nek1 and Nek8 in particular having been found to play important roles in ciliogenesis. Cilia are microtubule-based organelles that are organised by maternal centrioles during interphase prior to pre-mitotic disassembly. Motile cilia, such as those found in the trachea, act to move extracellular fluid and particulates. However, primary cilia are ubiquitous in the body and are responsible for detection and coordination of extracellular events with intracellular responses. Importantly, primary cilia mutations are responsible for a variety of genetic disorders, including retinal degradation and polycystic kidney disease (PKD).[121, 124]

Nek1 and Nek 8 mutations are seen to result in PKD in mouse models,[125] and mutations of Nek1 have been shown to be causal in a wide range of further ciliopathies,[126] indicating a vital role for wild-type (WT) Nek1 in healthy ciliogenesis. Nek8 has been shown to associate with primary cilia, and mutations in Nek8 result in loss of cilia localization and increases in cilia length, affecting their function.[127] The importance of Nek1 and Nek8 in cilia formation raises the point that inhibitors designed for other Nek members must exhibit high selectivity over Nek1 and Nek8, so as to avoid ciliopathy related toxicity.

The functions of Nek3, 4 and 5 are poorly understood, with no characterisation of Nek5 being available at this time. However, a putative role for both Nek3 and Nek4 in microtubule dynamics has been suggested, with knockdown of either kinase resulting in spindle formation errors.[121] Neks 6, 7 and 9 have more clearly understood roles in the control of spindle formation and suggested roles in cytokinesis. Nek6 and 7 are structurally very similar, sharing 87% homology within their catalytic domains,[121] of which they are almost completely comprised. Depletion or inactivation of either kinase results in similar phenotypes of weak spindle formation and delays in SAC deactivation, suggesting very similar cellular functions.[128] Nek6 and 7 operate downstream of Nek9, the knockdown of which results in related spindle defects and errors in chromosome alignment.[121] More recently it has been suggested that Nek9 is phosphorylated during mitosis by both Cdk1 and Plk1, resulting in

Nek6/7-mediated phosphorylation of the Eg5 motor protein, activating Eg5 for centrosome disjunction.[129]

The functions of Nek10 and Nek11 remain poorly understood. However, recent studies have suggested that the kinases are involved in cell cycle checkpoint control.[121] The involvement of Nek10 in the process is less well understood, but depletion of Nek10 results in cells that are defective in their ability to arrest at G_2/M in response to UV genotoxic stress.[130] This is reported to be through a loss of Nek10 interaction with, and activation of, Raf1 and MEK1, members of the Erk signalling pathway with indications in checkpoint control.[131] Nek11 has been shown to be a substrate of Chk1, and activation of Nek11 prompts phosphorylation of Cdc25A within the conserved DSG-motif, a region that promotes ubiquitin-mediated proteolysis. In relation to this, inactivation of Nek11 prevents Cdc25A degradation, and results in cells lacking the ability to arrest at G_2/M in response to IR irradiation.[132]

3.3. NIMA-Related Kinase 2 (Nek2)

3.3.1. Nek2 Structure and Regulation

Nek2 is the most closely related human Nek to NimA, sharing 44% homology in the amino acid sequence of the catalytic domain. Nek2A is a 445 amino acid (48 kDa) serine/threonine protein kinase bearing the conserved N-terminal kinase domain, and a C-terminal non-catalytic regulatory domain with 2 coiled-coil regions akin to NIMA.[133] Nek2 is expressed as two splice variants, Nek2A and Nek2B (Figure 9), with Nek2B diverging in sequence from the 8 exon encoded Nek2A at intron 7 shortly after the splice site. Nek2B is therefore a shorter 44 kDa protein, and lacks the second coiled-coil region present in Nek2A, with the initial leucine zipper coiled-coil conserved (see below). Furthermore, Nek2B lacks important motifs responsible for activity (PP1 binding site), ubiquitin proteolysis (KEN-box) and mitotic entry (D-box), indicating that Nek2B has a role distinct from Nek2A.[133] Indeed, Nek2A is the abundant form in adult cells, whereas Nek2B is detected at higher levels during meiotic spermatogenesis and in meiotically active oocytes.[134] This observation correlates with the lack of a KEN destruction box in Nek2B, as maintaining levels of a stable form of Nek2 may facilitate the rapid embryogenic cell cycles. Due to the primary role of Nek2A in mature cells and cancer, further discussions regarding function and regulation will refer to Nek2A unless stated otherwise.

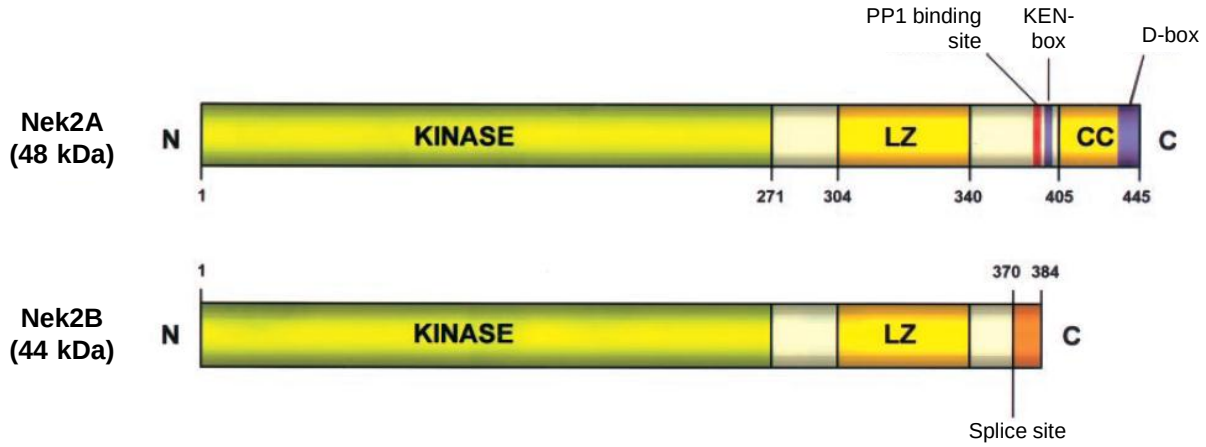

Figure 9: Schematic representation of the Nek2 splice variants Nek2A and Nek2B.[133]

The crystal structure of the mutant kinase domain (T175A) of Nek2A has been solved (Figure 10), giving insights into regulatory motifs and residues within the kinase sequence.[135] Several conserved motifs may be responsible for conformational changes of kinases upon activation. The DFG and HRD motifs both contain catalytically vital aspartic acid residues. The activation loop, which lies at the C-terminus of the DFG motif, acts to organise other motifs and aid in binding of the substrate. The conserved glutamic acid residue present in the C-helix forms a crucial salt bridge with a conserved leucine residue in the ATP binding site.[135]

Autophosphorylation can act as a key regulator of kinase activity on exogenous substrates. The non-catalytic domain of Nek2 has two predicted coiled-coil regions, one of which is at the end of the C-terminus, whilst the other is immediately downstream from the kinase domain. This initial coiled-coil contains six heptad-spaced leucine residues, which indicate the presence of a leucine zipper motif, and this promotes homodimerization between two Nek2 proteins allowing *trans*-autophosphorylation. This may be needed to generate the active conformer of Nek2 *via* disruption of the inhibitory αT helix, formed from the DFG motif and five following residues, in the activation or T-loop. This αT helix is well conserved in Nek family members, but is less common in other kinase families. However, more recently additional crystal structures of Nek2 bound to various inhibitors have been solved, showing that this region is able to adopt several different conformations, depending on the ligand occupying the ATP-binding site.[135] In addition to the required phosphorylation of the Thr-175 residue, autophosphorylation of activation/T-loop residues Thr-170 and/or Ser-171 has been shown to be necessary for kinase activity, and may act to fine-tune the overall activity of Nek2.[136]

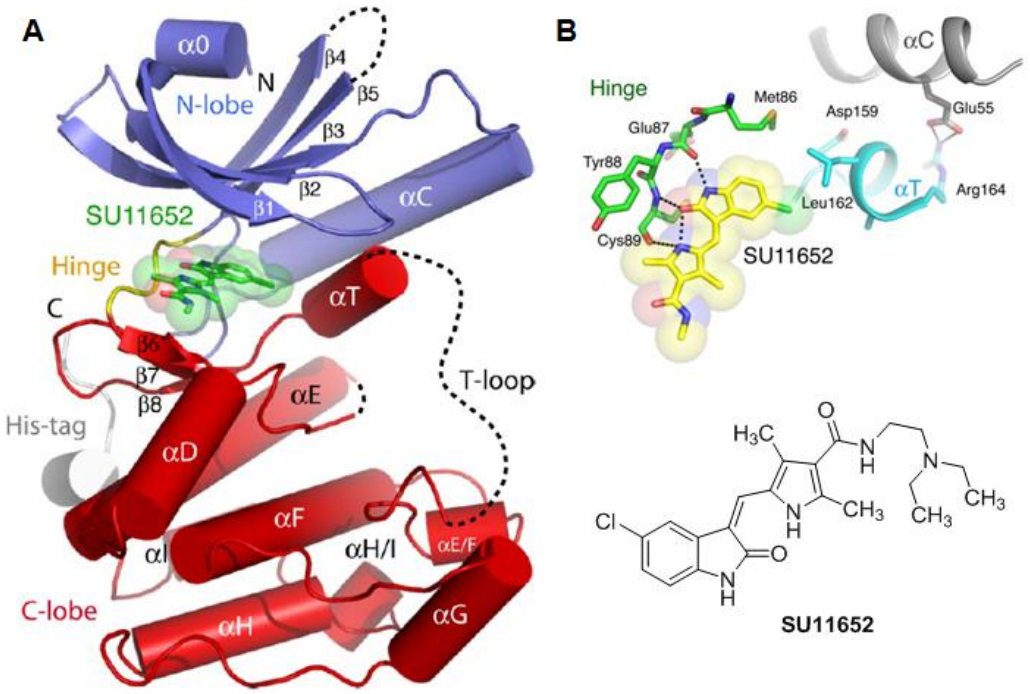

Figure 10: A) X-ray crystal structure of the Nek2A-T175A catalytic domain in complex with SU11652 showing the N-terminal lobe (blue), C-terminal lobe (red), hinge region (yellow) and inhibitor (green); **B)** interactions of SU11652 with the kinase hinge region showing the inhibitory αT-helix.[136]

Autophosphorylation has also been shown to play a possible role in inhibitory regulation of Nek2 activity. The T-loop residue Thr-179 acts as an anchor point for the C-terminus of the T-loop, stabilizing the conformation of key residues involved in phosphoryl transfer. Phosphomimetic mutation of this residue resulted in a marked decrease in kinase catalytic activity.[136] This result is matched by mutation of the C-terminal domain residue Ser-241, located within the αH-helix. This residue is remote from the kinase active-site, but a mechanism for inhibitory autophosphorylation has been proposed to be due to effects on the homodimerization of Nek2. In EGFR kinase domains, the αH helix of one monomer stacks against the αC helix of its partner, disrupting the inhibitory αT helix and allowing the kinase to adopt an active conformation. Due to the importance of the phosphorylation state of the Ser-241 residue within the region, it is likely that a similar system exists in Nek2 dimerization, and that pSer-241 inhibits this interaction, although further studies are required to validate this hypothesis.[136] Further regulation of Nek2 activity is related to the binding of specific substrates and interactions with associated proteins.

3.3.2. Nek2 is a Cell Cycle Regulated Centrosome Associated Protein

The cell cycle-dependent expression of Nek2 strongly indicates a role in mitotic entry. Cell-synchronization studies have determined that Nek2 expression levels are extremely low at G_1, with a steady rise in expression observed through S and G_2.[133] Nek2 protein levels reach a maximum at the G_2/M transition, before rapid D-box targeted degradation mediated by the APC/C results in near undetectable levels during mitosis.[137] This expression is slightly different from that of NIMA, which maintains expression and activity levels through to the onset of G_1, suggesting that the key event that is mediated by Nek2 occurs prior to or very early in mitosis. Evidence suggests that Nek2 mRNA is repressed in G_1 rather than stimulated in S and G_2.[133]

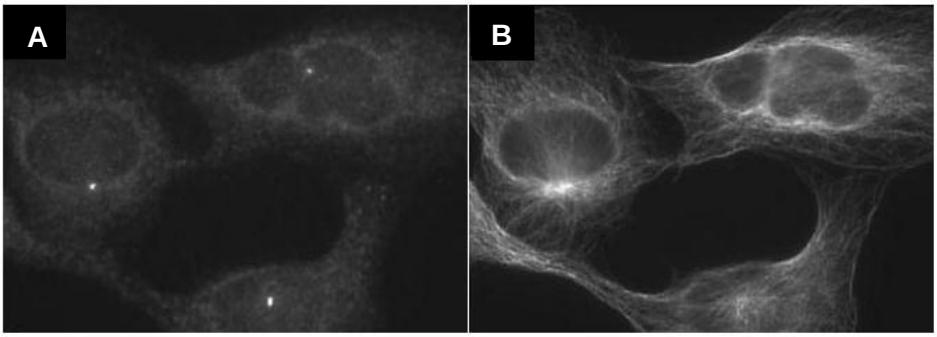

Figure 11: Immunofluorescence microscopy of U2OS cells showing Nek2 localisation to the centrosomes; **A**) Staining for anti-Nek2; **B**) Staining for anti-α-tubulin.[138]

The use of anti-Nek2 antibodies has allowed the cellular localisation of Nek2 to be determined. Immunofluorescence microscopy (IFM), staining for Nek2 with fluorescent secondary antibodies, shows Nek2 to be localised in the cell at two neighbouring points, indicative of centrioles. Co-staining the same cells with α-tubulin allows visualisation of the spindle framework, and the Nek2 spots were observed at the centre of the interphase microtubule array (Figure 11; **A**).[138] To confirm this result, purified human centrosomes were isolated from a variety of cells at different stages of the cell cycle. In all cases the centrosomes were shown to be strongly associated with Nek2 by staining with the anti-Nek2 antibody.[138] These observations confirm Nek2 to be a *bona fide* centrosomal protein. Initial attempts to establish the precise centrosomal location of Nek2 using immunoelectron microscopy (IEM) have shown that Nek2 appears to associate with the proximal ends of the centrioles.[139]

Despite this, the kinase is not exclusively located at the centrosome, with up to 90% of the cellular pool occupying the wider cellular space. It is possible for passive diffusion to be responsible for the association of centrosomal proteins to their site of action. However, endogenous levels of the kinase are of low abundance, and it is likely that active transport mechanisms are involved in its recruitment. The cellular pool of Nek2 is present in small cytoplasmic granules, which have been shown to traverse the cytoplasm in rapid linear trajectories, determined to be due to even distribution of the granules along the lengths of microtubules. A 36 amino acid region (335-370) in the C-terminal domain of the kinase has been shown to be essential for the binding of Nek2 to both microtubules and the centrosome.[140]

The active transport of Nek2 along microtubules and subsequent recruitment to the centrosome has been shown to be dependent on the protein pericentriolar material 1 (PCM1).[140] Similar to Nek2, PCM1 is present in cytoplasmic granules, termed centriolar satellites. PCM1 is known to move towards the centrosome along microtubules *via* the motor protein dynein, mediated by dynactin, the protein that anchors the cellular cargo.[141] However, the precise role of PCM1 in the transport of Nek2 to centrosomes is unclear, as the rate of Nek2 recruitment is distinct from the rate of recruitment of other proteins mediated by PCM1. Interestingly, it seems that localised degradation of Nek2 at the centrosome is required to maintain the cellular dynamics and ensure the recruitment of new Nek2.[140]

3.3.3. Substrates and Regulators of Nek2

In vitro studies were initially carried out to identify substrates of Nek2, with strong phosphorylation being observed in the case of β-casein, myelin basic protein (MBP), and microtubule associated protein 2 (Map2); moderate phosphorylation of histone H1 and phosphovitin was also encountered.[142] However, as it has been determined that Nek2 associates to the centrosomes, identification of centrosomal substrates of Nek2 has aided in the elucidation of a putative role for the kinase in mitosis.

Apart from Nek2 itself, the first physiological substrate of Nek2 was identified as a high molecular weight protein with a predicated molecular mass of 281 kD, which interacted with Nek2 when used as ‘bait’ in a yeast two-hybrid screen. Nek2 was found to phosphorylate the C-terminal domain of the protein of interest both *in vitro* and *in vivo*. The protein was subsequently found not only to associate with Nek2, but also to localize at the centrosome,

and as such it was termed centrosomal Nek2-associated protein 1 (C-Nap1).[139] C-Nap1 was shown to be a core component of the centrosome, which was specifically found at the proximal ends of both the maternal and daughter centrioles (Figure 12).[143] Interestingly, this centriolar localisation of C-Nap1 is markedly reduced in mitotic cells, suggesting that C-Nap1 is associated with centrosomes in a cell cycle-dependent manner.[139]

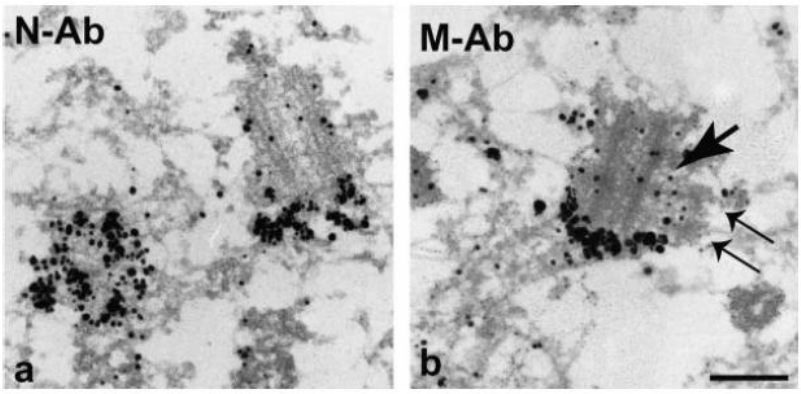

Figure 12: IEM using two antibodies for C-Nap1 (N-Ab and M-Ab, dark spots) at the proximal ends of centrioles (single arrow) and procentrioles (double arrow) in U2OS cells.[143]

The activity of many protein kinases, and hence their cellular effects, is often regulated by dephosphorylation by protein phosphatases. Protein phosphatase 1 (PP1) is a key member of this family that acts to dephosphorylate serine and threonine residues on a diverse range of substrates.[144] The presence of a predicted PP1-binding motif in Nek2A raised the possibility that Nek2A is a substrate for PP1. This was confirmed with the identification of Nek2-PP1 complexes both in cell-free and cell extracts.[145] Nek2 has so far been shown to interact with two isoforms of PP1, namely PP1α and PP1γ. Interestingly, PP1α has been shown to associate to centrosomes during mitosis.[146]

In this complex, PP1 is able to dephosphorylate Nek2 and reverse the effects of Nek2 activity. At higher levels of activity, Nek2 is likely to partially inhibit PP1 through phosphorylation, allowing subsequent phosphorylation of Nek2 substrates. As Nek2 activity subsides and inhibition of PP1 is lost, rapid dephosphorylation of Nek2 would essentially abolish kinase activity on exogenous substrates.[145, 147] This suggests the existence of a dynamic molecular switch for Nek2, allowing kinase activity to be triggered in a highly transient and cell cycle-dependent manner. Importantly, C-Nap1 is known to be a substrate for both Nek2 and the Nek2-PP1 complex, and the three proteins can form a ternary complex *in vitro*.[145] This observation strongly suggests that PP1 acts to regulate the activity of Nek2

on C-Nap1, either by controlling the activity of Nek2 directly, or *via* dephosphorylation of C-Nap1.

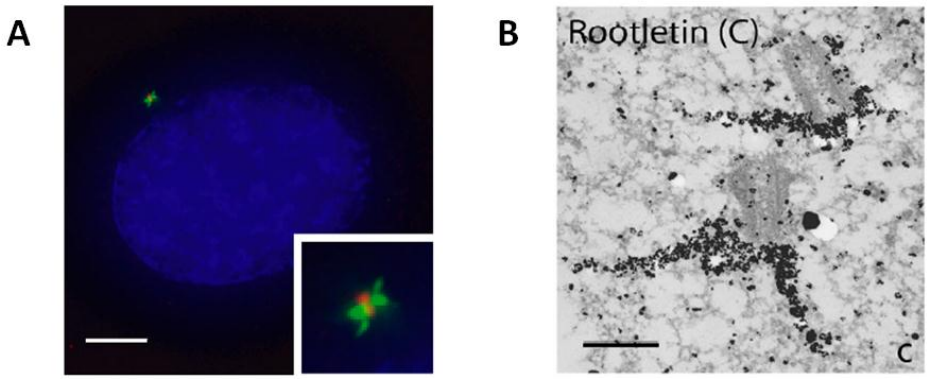

Figure 13: A) IFM of U2OS cells showing staining for centrosomes (red), rootletin (green) and DNA (blue); **B)** IEM of U2OS cells showing localisation of rootletin (dark spots) to centriole proximal ends and formation of filaments.[148]

Rootletin is a 228 kD protein that forms thin fibers protruding from the proximal ends of centrioles (Figure 13). Rootletin has been shown to associate with, and be phosphorylated by, Nek2. Association with C-Nap1 is also observed *in vitro* and *in vivo*, and the interaction between rootletin and C-Nap1 is dependent on the C-terminal domain of C-Nap1. In addition, association of rootletin with the proximal ends of the centrioles is through the N-terminal domain of the protein.[148] Further insight into the relationship between C-Nap1 and rootletin was gained following the observation that localisation of C-Nap1 to the centrioles was not affected by rootletin siRNA, whereas the use of C-Nap1 siRNA clearly disrupted the ability of rootletin to associate with centriole ends.[148]

β-Catenin is a well characterised protein with a variety of roles identified outside of the centrosome. However, more recently β-catenin has been identified as being centrosome associated by the use of IFM and immunoprecipitation techniques.[149] Furthermore, β-catenin was found to be a binding partner and substrate for Nek2 *in vitro* and *in vivo*, and to associate with both C-Nap1 and rootletin at the centrosome. In particular, the protein was found to be in complex with rootletin in the region between the centrioles. In relation to this, a similar result was observed upon depletion of C-Nap1, resulting in initial disorganisation of β-catenin at the centrioles, followed by a complete loss of centriolar association upon abrogation of C-Nap1. In the absence of rootletin, C-Nap1 association with the centrosomes is lost. This, together with studies on the organisation of the other centrosomal proteins,

supports a model in which C-Nap1 acts as an anchoring point for rootletin, which in turn recruits β-catenin to the proximal ends of centrioles.[149]

The Hippo pathway is a signal transduction cascade with a variety of cellular roles, most notably the control of organ size.[150] It was found that several Hippo pathway components localised to centrosomes, although little was known of their function at this site. Subsequently, Hippo components human Salvador 1 (hSav1) and mammalian sterile 20-like kinases 1 and 2 (Mst1 and Mst2) were found to interact with both Nek2 and C-Nap1.[151] Nek2 was shown to be phosphorylated by Mst2 within a hSav1-Mst1/Mst2 complex, with this phosphorylation facilitating recruitment of Nek2 to the centrosomes at the G2/M transition.[151] It is possible that this mechanism is working in conjunction with PCM-1-mediated transport of Nek2.

A further centrosomal protein found to be involved in this system is the Plk1 binding partner Nlp, a substrate of Plk1 (see chapter 2.4.2.) that is associated to interphase centrosomes. However, Nlp is barely detectable at mitotic centrosomes,[107] indicating that an event occurs at the G_2/M transition resulting in protein displacement. As previously described, prior substrate phosphorylation is often required for recognition of Plk1 targets through the PBD. This led researchers to investigate kinases that are active at the G_2/M transition, and the observation that Nlp is a substrate of Nek2 raised the possibility that Nek2 may act as a priming kinase for Plk1.[152] Nlp associates to mother centrioles and is proposed to act as an anchoring site for γ-TuRCs and microtubules. Upon phosphorylation by Nek2 and Plk1 at mitotic entry, Nlp is lost from centrosomes. The precise role of Nlp in mitotic progression is poorly understood, but cells expressing Nlp that lacks N-terminal phosphorylation sites lead to severe defects in mitotic spindle formation.[107] It is possible that phosphorylation of Nlp results in loss of astral microtubules, allowing centrosome dynamics within the cell, an event necessary for bipolar spindle formation.[152]

Highly expressed in cancer 1 (Hec1) is a kinetochore outer layer component involved in the regulation of the spindle assembly checkpoint. Hec1 undergoes interactions with kinetochore components such as Nuf2, Spc25 and Zwint-1, as well as the mitotic kinases Aurora B and Nek2, identified though a yeast two-hybrid screen.[153, 154] Hec1 mediates the correct formation of the spindle lattice between the kinetochores and centrosomes, and is thus responsible for the proper formation of kinetochore bipolar spindle attachments and subsequent symmetrical chromosome separation during mitosis. Although the regulation of Hec1 is not fully

understood, it appears that Nek2 binds and phosphorylates Hec1 in a cell cycle-dependent manner, and may be responsible for modulation of Hec1 activity[155] and hence correct kinetochore attachment to the mitotic spindle. Small molecule antagonists of the Nek2-Hec1 interaction have been developed, and are found to induce changes in cellular morphology indicative of cells undergoing apoptosis due to mitotic catastrophe (see chapter 4.3.).[156]

3.3.4. Role of Nek2 in Centrosome Separation

An understanding of Nek2 substrate specificity, combined with experimental misregulation of Nek2 and these binding partners, has allowed a putative role for Nek2 in mitotic entry to be detailed. During early studies into the action of Nek2, it was shown that upregulation of WT-Nek2 through transfection resulted in a significant increase in interphase cells exhibiting centrosomes seperated by several microns, accompanied by cells found to be lacking centrosomes altogether.[138] This strongly indicated that Nek2 may be involved in centrosome separation, a process which has yet to be fully characterised and understood. In support of this, overexpression of Nek2 results in dissociation of centrosomal proteins including rootletin.[148]

Use of a kinase dead (KD) inactive mutant of Nek2 (K37R) in transfection experiments prevented the centrosome split phenotype, although a loss of centrosomes was still apparent, indicating that these events originate from separate mechanistic events.[138] Interestingly, centrosomes in cells after tetracycline-induced expression of Nek2-KD (see chapter 7) were classed as unsplit, despite being separated on average by 2.1 μm. The corresponding centrosomes in cells treated with inhibitors of the Eg5 motor protein had an intercentriolar distance of less than 2 μm, suggesting the possibility that, following Nek2-KD expression, motor proteins were attempting to separate centrosomes that were still physically connected.[157] Knockdown of Nek2 using siRNA in early mouse embryos, resulted in the majority of embryos reaching the blastocyst stage with a high prevalence of abnormal spindle structures and M phase arrest.[121, 158]

Supporting evidence for a role of Nek2 and associated proteins in centrosome separation is found upon misregulation of Nek2 substrates. Downregulation of C-Nap1 or Rootletin generated cells with a split centrosome phenotype. Disruption of C-Nap1 is also associated with disorganised Rootletin and β-catenin structures at centrosomes.[148, 159] However, this is not the case for the other centrosome-associated proteins Cep170, centrin-2, BBS4, PCM-1 or

ninein, suggesting that the induced centrosome splitting is not as a result of general loss of centrosome proteins, and is specific to C-Nap1 and Rootletin. As would be anticipated, inhibition of PP1 in several cell lines also induced centrosome splitting, accompanied by loss of the centrosomal association of Rootletin.[148]

In contrast to other centrosome-associated proteins, β-catenin acts as a negative regulator of centrosome cohesion. Depletion of β-catenin using siRNA techniques has been shown to generate cells with monopolar spindles consisting of replicated but unseparated centrosomes.[160] In addition, cells expressing stabilised β-catenin, with a low turnover rate, showed increased intercentrosome distance, similar to the effect observed upon upregulating Nek2. Unlike C-Nap1 and Rootletin, β-catenin remains associated with centrosomes during mitosis.[149]

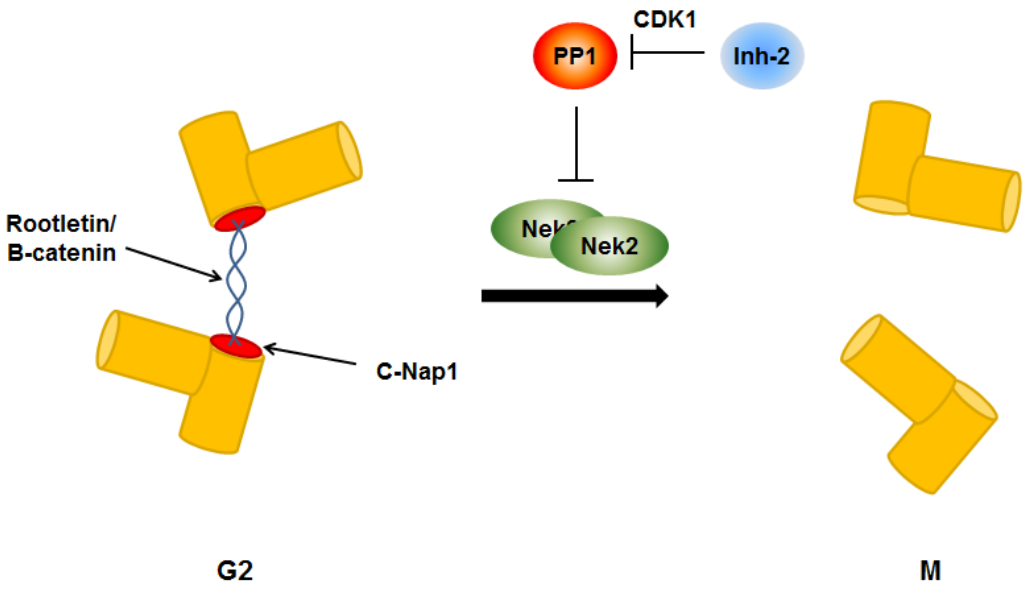

Figure 14: Proposed model for Nek2-mediated centrosome separation at mitotic entry.[161]

The aforementioned evidence allows a model to be proposed that provides potential structural insights into the intercentriolar linker, and the role that Nek2 plays in linker cleavage and ultimately centrosome separation (Figure 14). During interphase the activity of Nek2 is suppressed by PP1 through dephosphorylation of Nek2, and Nek2 substrates C-Nap1 and Rootletin. This highly sensitive molecular switch allows for precise temporal control of formation of the active Nek2 homodimer and phosphorylation of downstream targets. Spatial control of Nek2 activity is further controlled through association with Hippo pathway

components, triggering centrosome association at mitotic onset. At the G2/M transition phosphatase inhibitor 2 (Inh2) is activated, possibly due to activation of Cdk1, the 'master regulator' of mitosis. Activation of Inh2 has been shown to trigger immediate inhibition of PP1 and, ultimately, conformational inactivation.[162] Release from PP1 suppression results in a surge of Nek2 activity and subsequent substrate phosphorylation.[161] This system is analogous to the Cdc2-mediated activation of NIMA in *Aspergillus nidulans*.

Since it was first proposed, owing to the correlated movements of sister centrioles, the exact composition of the intercentriolar linker is yet to be fully elucidated.[163] Localisation and downregulation studies provide strong evidence to suggest that C-Nap1 attaches to the proximal ends of centrioles to act as an anchor for further linker components, consisting of Rootletin, β-catenin and possible additional proteins yet to be identified. The observed flexibility and variability in the distance between parental centrioles, makes the existence of a continuous protein linker unlikely. Instead, it has been proposed that the linker is in fact made up of an entanglement of fibers involving Rootletin and β-catenin anchored to C-Nap1, allowing for a highly dynamic linker.[148]

Upon activation of Nek2, phosphorylation of linker components occurs, triggering a loss of centrosomal cohesion. Phosphorylation of rootletin and C-Nap1 may result in conformational changes or repulsion through surface charge effects. Alternatively, phosphorylation may target intercentriolar components for degradation. A model for the negative regulation of centrosome cohesion by β-catenin has been proposed, in which as yet unidentified rootletin-independent β-catenin binding sites exist on centrosomes, which are required for separation.[149] Prior to G_2/M a pool of β-catenin is reserved at the centrosome but prevented from binding to such sites through interaction with Rootletin. However, upon cleavage of the intercentriolar linker, β-catenin is released and can bind to these sites, facilitating centrosome disjunction.[149]

Following cleavage of the intercentriolar linker, centrosome duplication is complete and motor proteins are able to mediate migration of centrosomes to opposite poles of the cell to form a bipolar mitotic spindle and ensure accurate division of chromosomes during anaphase.

3.3.5. Nek2 as a Cancer Therapeutic Target

Owing to the prevalence of centrosomal abnormalities in the majority of tumour cells, loss of regulation of the tightly controlled machinery dictating centrosome duplication has been

implicated as a major contributor to tumourigenesis. Aberrant centrosome function is also strongly associated with CIN and aneuploidy, two major hallmarks of cancer.

Nek2 was first implicated in cancer following the observation that the gene encoding Nek2 was upregulated in Ewing's osteosarcoma and diffuse large B-cell lymphoma (DLBCL), using a tumour-derived cell line screen for mRNA abundance.[164, 165] Later work identified elevated Nek2 protein expression in cancer cell lines, with an approximate 2-5 fold increase in Nek2 levels detected in a variety of cell types originating from breast, cervical and prostate carcinomas, as well as various lymphomas.[166] Loss of the transcriptional inhibitors p107 and p130 has been proposed as a potential mechanism of amplified gene expression for genes activated by the transcription factor E2F4, such as Nek2.[167]

Nek2 overexpression has been shown to result in multinucleated cells and cells bearing extra-chromosomal material; two potential indicators of aneuploidy. Such cells were found to contain extra centrosomes, likely due to aborted mitosis or failed cytokinesis.[166] Such observations clearly show the potential of elevated Nek2 expression in the development of CIN.

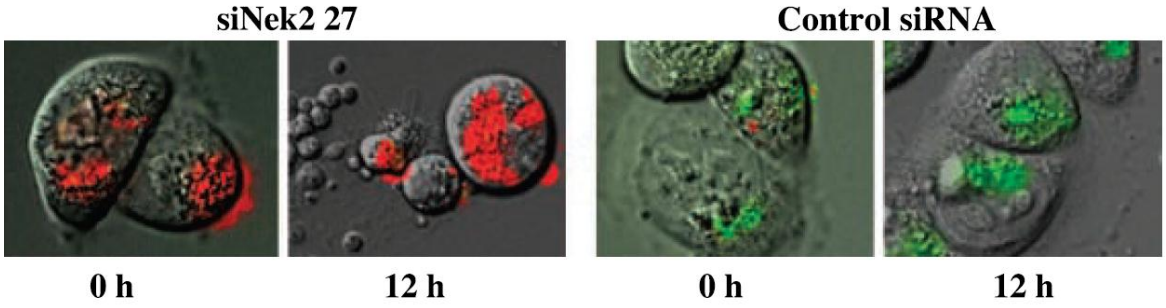

Figure 15: Increased cell death in HuCCT1 cholangiocarcinoma cells upon treatment with Nek2 siRNA, compared to control siRNA.[168]

As a means to validate the disruption of Nek2 activity as a potential chemotherapeutic approach, depletion of Nek2 levels was attempted. Using siRNA in cholangiocarcinoma cell lines, it has been shown that Nek2 siRNA results in growth suppression and cell death *in vitro* (Figure 15), as well as increased survival in mouse models.[168]

As described previously, Nek2 activation is controlled *via* a highly sensitive molecular switch. It is likely that misregulation of components within this system, including Nek2, may lead to gross errors in centrosome separation, bipolar spindle formation and chromosome

segregation, all factors that could drive mitotic errors and hence tumourigenesis. Upregulation of Nek2 in a variety of tumour types implies that such cancer cells may potentially have become dependent on the Nek2-mediated pathway for centrosome separation, possibly as a means to propagate CIN. From an understanding of the role of Nek2 in mitosis, it can be predicted that upregulation of Nek2 may disrupt the finely balanced control system that regulates kinase activity. Deregulation of this control mechanism may result in a loss of cell cycle synchronicity with the centrosome cycle, and premature entry into mitosis. This would propagate abnormal spindle formation and hence chromosome segregation errors. These are all factors that can promote CIN and aneuploidy, driving further errors in progeny cells and facilitating tumourigenesis.

Kinases are important mediators of many cellular processes and signalling events.[46] The development of our understanding of kinase function and biology has introduced an emerging class of biological targets for the treatment of a variety of diseases.[169] Through the clinical success of early inhibitors, targeting kinases has been confirmed as a viable approach for the treatment of disease where kinase activity is misregulated. As such, selective inhibition of Nek2 is an attractive prospect for the validation of this kinase as a chemotherapeutic target, with the potential to develop antitumour agents targeting a Nek2 dependent phenotype.

Chapter 4: Kinases as Targets in the Treatment of Cancer

Upon selection of a suitable kinase target within a disease area of interest, it is important to identify hit compounds, usually simple inhibitors with modest activity against the kinase. To develop the initial hit compounds into more potent and more drug-like lead molecules, it is highly desirable to have insights into the structure of the target, usually through acquisition of a protein crystal structure. Not only can this inform medicinal chemists as to the potential effects of inhibitor modification within the binding site, it can also provide information as to the mechanism of kinase inhibition.

4.1. Reversible Kinase Inhibitors

4.1.1. Classes of Reversible Kinase Inhibitor

The most common class of kinase inhibitors act in a reversible manner, forming a stable equilibrium between a non-bound pool of compound and compound bound to the target enzyme *via* non-covalent interactions. In particular, compounds that compete for binding with the natural ligand within the active-site are termed competitive reversible inhibitors. In kinases this is usually through competition with ATP within the ATP-binding domain. The majority of kinases possess a bi-lobal catalytic structure with a cleft located between the N- and C-terminal domains. This is termed the hinge region, and is the location of ATP binding through hydrogen bonding with the adenine ring and hinge amino acid residues.[45] Despite the conserved nature of the ATP-binding domain, sufficient structural variation is present within the catalytic site and surrounding hydrophobic regions to allow selective inhibition, although selectivity between close family members can be more challenging to achieve.[170]

As mentioned previously, access to the ATP-binding site can be hindered due to the activation loop residing within an inactive conformation. Most inhibitors are designed to mimic ATP, and are identified by the use of enzyme inhibition assays in which the kinase is pre-activated. Consequently, the majority of competitive reversible inhibitors bind to the active conformation of the target kinase.[45] Such compounds are termed type I inhibitors, and generally comprise a heterocyclic core that makes hinge region H-bond interactions. This acts as a central template from which side-chains can be attached to make additional interactions within the kinase ATP-binding domain, to improve inhibitor potency and confer kinase selectivity.[45, 46]

Several early kinase inhibitors, including imatinib (see chapter 1.1.2.), were found to bind to and stabilise the inactive, or 'DFG-out', conformation of their target kinases. These compounds are termed type II inhibitors, and their binding exposes an allosteric hydrophobic pocket adjacent to the ATP-binding site through the positioning of the activation loop. Inhibitor interactions with this hydrophobic pocket often result in tight binding kinetics and potent target inhibition.[45]

A third class of reversible kinase inhibitors bind outside of the ATP-binding site at an allosteric site. Allosteric inhibitors mediate their inhibitory activity through induction of conformational changes in the kinase, reducing the ability of the protein substrate or ATP to interact with the kinase.[5] Allosteric inhibitors generally have an improved selectivity profile when compared to ATP-competitive inhibitors, because the likelihood of kinase allosteric binding sites sharing structural homology is very limited.[45] In addition, the high ATP concentration in cells can restrict cellular activity to only the most potent ATP-competitive inhibitors. The absence of competition with a cellular substrate can improve the cellular profile of allosteric inhibitors.

4.1.2. Examples of Known Reversible Kinase Inhibitors in Cancer Therapy

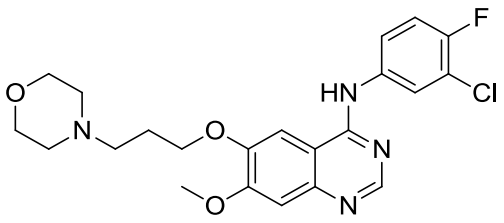

12

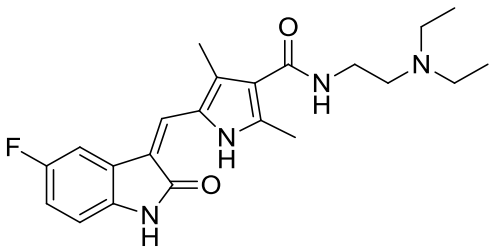

13

As the focus of medicinal chemistry has been brought to bear on kinases, an increasing number of kinase inhibitors are progressing to clinical trials and reaching the market. Examples of type I kinase inhibitors licenced for clinical use include gefitinib (**12**) and sunitinib (**13**). Gefitinib, marketed as *Iressa*, was the first example of a selective inhibitor of the EFGR tyrosine kinase,[171] and was approved in 2003 for use in non-small-cell lung carcinoma (NSCLC).[172] Sunitinib (*Sutent*) is a type I inhibitor of multiple receptor tyrosine kinases,[173] and gained approval for the treatment of renal cell carcinoma (RCC) and imatinib-resistant GIST in 2006.[172]

In addition to imatinib, further type II inhibitors including sorafenib (**14**) and nilotinib (**15**) have been licensed. Sorafenib (*Nexavar*) is an inhibitor of multiple receptor tyrosine kinases including platelet-derived growth factor receptor (PDGFR) and VEGFR, as well as members of the Raf kinase family.[174] Approved in 2005, sorafenib is used to treat both hepatocellular and renal cell carcinoma.[172] Nilotinib (*Tasigna*) is also a multi-targeted kinase inhibitor, with targets including BCR-Abl and c-Kit.[175] The drug was approved in 2007 for the treatment of chronic myeloid leukaemia.[172]

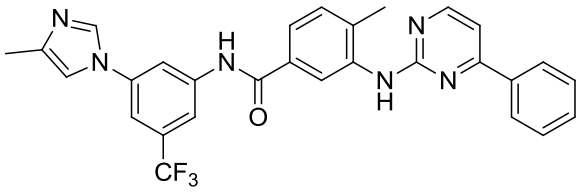

14

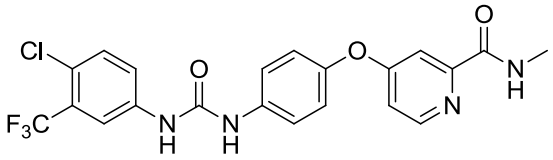

15

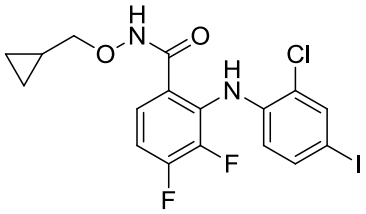

16

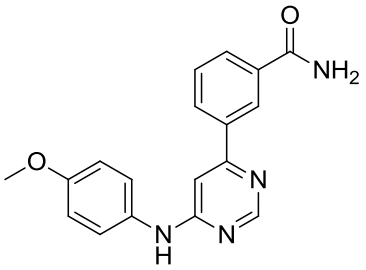

17

The most well characterised allosteric kinase inhibitor is CI-1040 (**16**), an inhibitor of MEK1 and MEK2 that is currently in clinical trials.[176] This compound binds to a unique allosteric pocket adjacent to the ATP-binding site, locking the kinase into a closed catalytically-inactive conformation.[177] Another example of an allosteric inhibitor in early development is GNF-2 (**17**). This compound, and others in its class, interact with BCR-Abl through a myristate-binding site, indirectly inhibiting kinase activity.[178]

4.2. Irreversible Kinase Inhibitors (Inactivators)

An alternative type of kinase inhibitors act through covalent modification of the target. Such irreversible inhibitors can be categorised as affinity labelling, or mechanism-based (Figure 16). Affinity labelling inhibitors compete initially with the substrate to form an enzyme-inhibitor complex (E.I), followed by covalent reaction with an amino acid residue. The formation and dissociation of the E.I complex ($K_i = k_{off}/k_{on}$) is usually rapid when compared to covalent bond formation (k_{inact}), and as such this is the rate determining step.[5] The

incubation time between the drug and target enzyme is important, as the degree to which an enzyme is covalently inactivated is a function of time. When calculating IC_{50} values for irreversible inhibitors it is essential that the incubation time is kept constant. Furthermore, if the incubation time is too long, the enzyme will be saturated with inhibitor, and IC_{50} values will reflect total inhibition. Mechanism-based, or suicide, enzyme inactivators are unreactive species bearing a similarity to the natural substrate. Upon formation of the E.I complex, the normal catalytic activity of the enzyme converts the inhibitor into a reactive species (I'), which can either dissociate from the enzyme or react to form a covalent adduct.[5] Affinity labelling compounds are most common in irreversible kinase inhibitor design, and further discussion will centre on this inhibitor class.

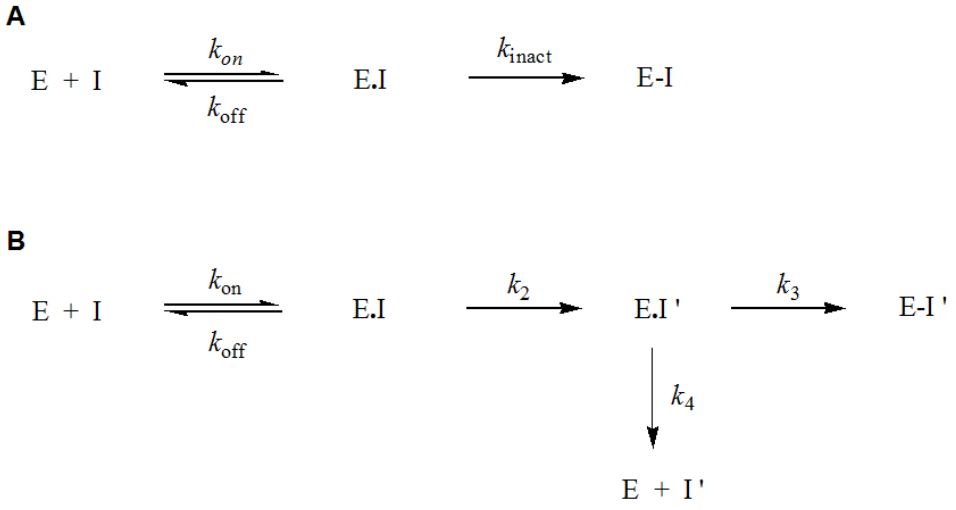

Figure 16: Enzyme inhibition kinetics for affinity labels (**A**) and mechanism-based enzyme inactivators (**B**).[5]

It is interesting to note that providing that formation of the E.I complex is rapid, if the reactive warhead and nucleophilic residue are positioned close to their ideal Bürgi-Dunitz angle,[179] the covalent bond formation essentially becomes unimolecular. The entropic advantage that this endows may result in a reaction rate many orders of magnitude faster than non-specific bimolecular reactions in solution.[5] Once the covalent adduct is formed, these inhibitors are no longer in equilibrium between unbound drug and enzyme-inhibitor complex, and the duration of action is thus a direct function of the stability of the chemical bond or the turnover of the target protein. Turnover times may vary from several hours to days, and a circulating concentration of drug need not be maintained during this time. This has the potential to widen the therapeutic window of the drug and ultimately improves patient outlook.

4.2.1. Design Considerations for Irreversible Inhibitors

In order to generate a covalent species it is necessary to design a compound with a reactive 'warhead' functional group that is presented to a nucleophilic amino acid residue within the kinase. This approach brings with it problems of selectivity and toxicity, as reaction with collateral targets and/or general nucleophilic species (*e.g.* glutathione, DNA) within the body may be a primary source of adverse side-effects. Clearly, within the field of cancer therapy the tolerance for side effects is greater than for many clinical indications. However, as the focus moves towards targeted therapy with improved toxicity profiles, indiscriminant electrophilic compounds do not meet the desired requirements. One drug characteristic that may improve the therapeutic window is a rapid clearance rate, a factor that designers of reversible inhibitors normally endeavour to lower.[180] The development of any irreversible inhibitor should be influenced both by the reversible binding affinity (structure-activity relationships, SARs) and the warhead reactivity (structure-reactivity relationships, SRRs).[180] If SRRs alone direct inhibitor design, the likelihood of poor selectivity and the inevitable toxicity issues are greatly enhanced.

A wide range of reactive functional groups have been used to intercept nucleophilic amino acids (see below), including epoxides, sulfonyl halides, halomethylketones, and ring systems that are subject to nucleophilic ring opening. However, the most common class are Michael acceptors. To date, the majority of irreversible inhibitors react with lysine or cysteine residues within the ATP-binding domain of their kinase targets. No accounts of reactions with other potential residues such as serine or threonine have been reported.[180] Due to its highly conserved nature, and key role in phosphate transfer the lysine residue is not an ideal target for selective irreversible inhibitors. Lysine residues positioned in unique locations within the active site may be suitable targets for covalent adduct formation, but this has been relatively poorly investigated.[180]

By far the most interest has been directed towards covalent modifiers of cysteine residues. A bioinformatics analysis-based approach has been used to identify all kinases that possess cysteine residues amenable to covalent modification.[45, 181] Approximately 200 kinases were found to contain a cysteine residue that could potentially be targeted by an ATP-binding site inhibitor. Analysis of the locations of the cysteine residues has allowed the kinases to be sub-divided into distinct classes (Figure 17).[45, 180]

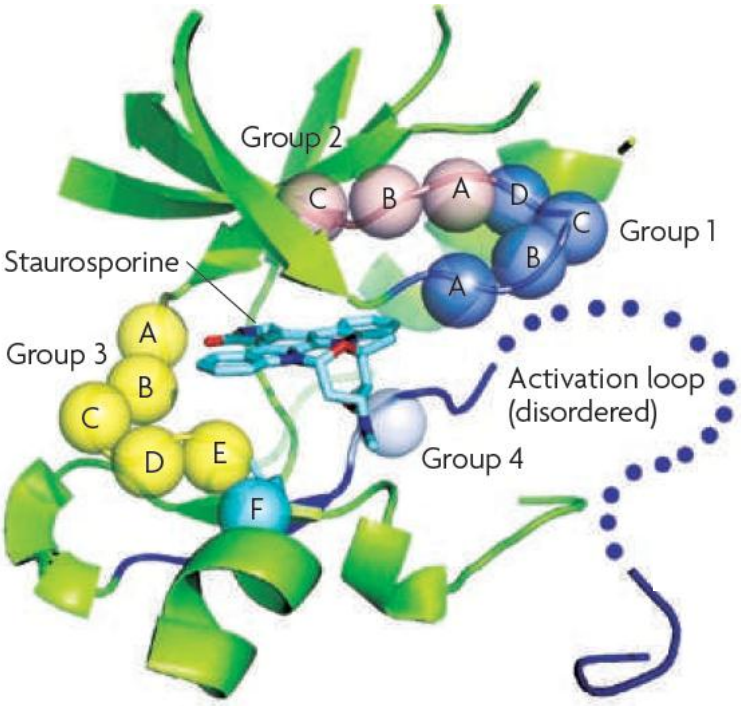

Figure 17: Schematic representation of cysteine locations in different classes of kinases.[45]

Kinases in group 1 contain a cysteine residue within the glycine rich loop (dark blue), whereas group 2 kinases bear a cysteine in the 3 residues immediately following the glycine rich loop (pink). The cysteine in group 3 kinases is present within the amino acid residues constituting the hinge region (yellow). Kinases containing a cysteine residue at a single position adjacent to the DFG-motif, and the start of the activation loop (blue) are classed as group 4.[45] More recently, a further 2 groups have been identified; group 5 kinases contain a cysteine on the flexible activation loop (dotted blue); a further class of miscellaneous cysteines are present in an allosteric pocket that are accessible by type II compounds binding to the DFG-out kinase conformation.[180] Interestingly, Nek2 belongs to the 2B group of cysteine-containing kinases.

4.2.2. Examples of Known Irreversible Kinase Inhibitors in Cancer Therapy

Although relatively little focus has been attributed to inhibitors that covalently modify lysine residues, examples of such compounds do exist (reactive moieties shown in red).[180] As described above, due to the highly conserved nature of the key binding site lysine residue throughout the kinome, such compounds are rarely selective. The ATP analogue 5'-fluorosulfonylbenzoyl adenosine (FBSA, **18**) is a multi-kinase affinity label used as a chemical probe rather than as a therapeutic agent. FBSA irreversibly inhibits kinases by

formation of a sulfonamide upon reaction with a binding site lysine.[180] A class of pyrrolecarboxaldehydes (*e.g.* **19**) have been identified as inhibitors of type 1 insulin-like growth factor receptor (IGF-1R) kinase. These inhibitors are examples where the chemical lifetime of the covalent bond formed dictates the nature of the inhibition, as they are found to be covalent reversible inhibitors through imine formation between the aldehyde and Lys1003 of IGF-1R kinase. This interaction was identified through chemical reduction of the imine, allowing isolation of the inhibitor-kinase complex and analysis by X-ray crystallography.[182] The final example is one in which a slightly unorthodox electrophile has been utilised. Lys802 of phosphoinositide 3-kinase (PI3K) covalently reacts with wortmannin (**20**) *via* nucleophilic attack and subsequent ring opening of the activated furan ring.[183]

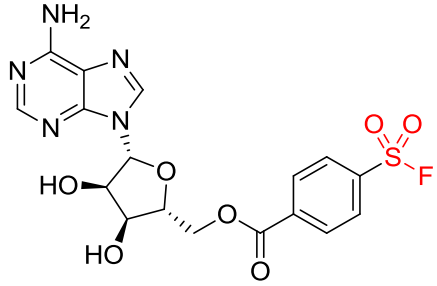

18

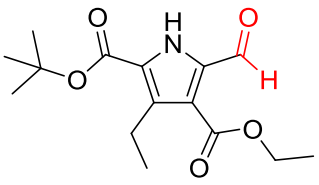

19

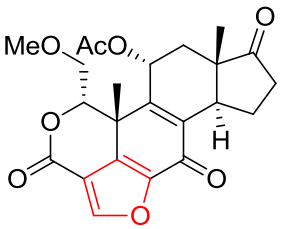

20

By contrast, a large number of irreversible kinase inhibitors are known to react with kinase cysteine residues. Described herein are examples for each class of cysteine-containing kinases detailed previously, with variation in the electrophile used, although this does not reflect the overall abundance or chemical class of inhibitors for each group. Modification of established reversible inhibitors led to the indentification of FIIN-1 (**21**) as a potent irreversible inhibitor of members of the fibroblast growth factor receptor (FGFR) family of group 1 cysteine-containing kinases.[184] Nucleophilic attack of the appropriate residue on the Michael acceptor acrylamide group gives rise to the covalent adduct.

The presence of a conserved cysteine residue in the glycine rich loop of members of the p90 ribosomal protein S6 kinase (Rsk) family identified these as members of the group 2 cysteine containing kinases.[181] Structural biology studies with adenine analogues revealed the opportunity to trap the cysteine residue with electrophilic groups at the purine 8-position. The fluoromethyl ketone **22** was accordingly found to be a potent and selective irreversible inhibitor of Rsk1 and Rsk2.[181]

Detailed investigations have been carried out with the group 3 cysteine kinases, in particular kinases with a cysteine at 3F (Figure 17, cyan). Members of this group include the ErbB (EGFR) family, which has been validated as a target for cancer chemotherapy by the clinical utility of reversible inhibitors such as gefitinib (**12**). Inhibitor design for ErbB members is dominated by quinoline/quinazoline structures, and extensive modification of related compound side-chains has been undertaken in an attempt to capture the 3F cysteine residue. One such compound is the epoxide **23**, a potent irreversible inhibitor of EGFR.[185]

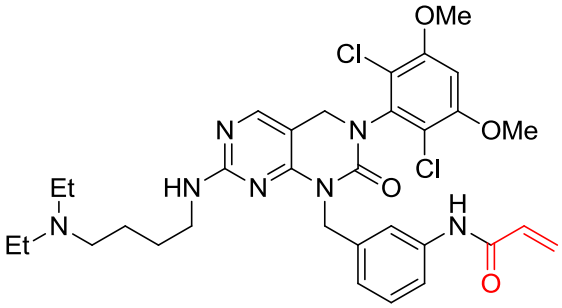

21

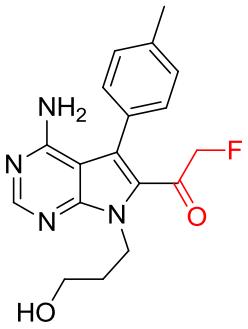

22

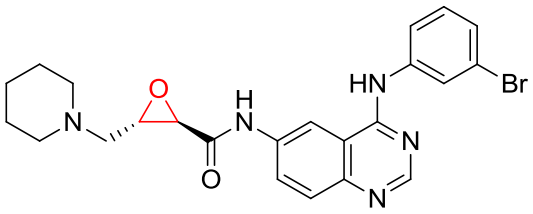

23

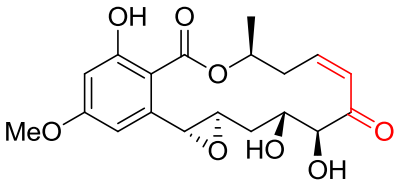

24

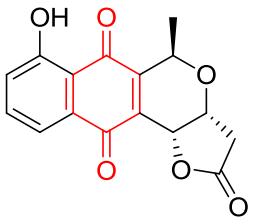

25

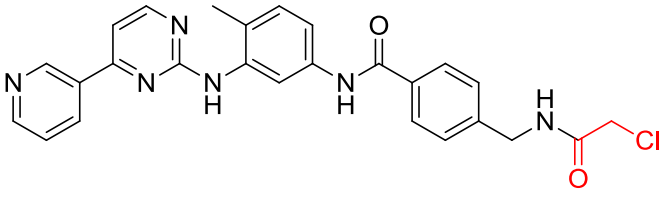

26

Despite the restriction of group 4 cysteine-containing kinases to a single amino acid position, almost 10% of the kinome possesses this highly conserved residue.[180] Resorcyclic acid lactones such as hypothemicin (**24**) are known to irreversibly inactivate group 4 kinases through the *cis*-enone functionality. As would be expected with such a highly conserved amino acid, selectivity across the group 4 members is an issue.[186]

The kinase Akt1 contains two cysteine residues within the activation loop and is thus a member of the recently described group 5 cysteine-containing kinases.[187] Pyranonaphthoquinone analogues, such as frenolicin B (**25**) have been reported to act as irreversible inhibitors of Akt1 through the quinone moiety.[187] Finally, modification of existing type II inhibitors, including imatinib, has allowed the generation of irreversible inhibitors of kinases containing cysteine residues within the allosteric binding pocket (*e.g.* **26**, against cKit/PDGFR).[188]

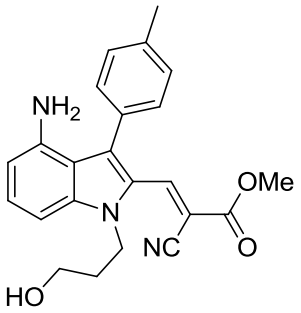

27

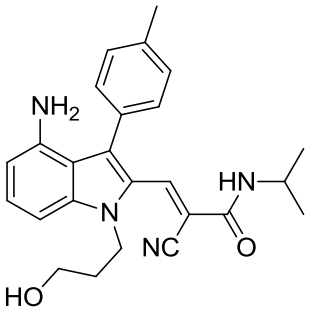

28

It is possible to combine some of the advantages of irreversible kinase inhibition, namely an extended duration of action and a good selectivity profile, whilst minimising the disadvantages of potential off-target reactivity. It has been reported recently that chemical modification of acrylate and acrylamide Michael acceptors can result in covalent, but rapidly reversible reactions with cysteine residues in target kinases.[189] The use of doubly activated Michael acceptors appears to result in rapid exchange between thiol addition and elimination. Substituting acrylate and acrylamide analogues of the Rsk inhibitor **22** with a cyano group at the α-position (**27** and **28**) results in sustained, but reversible inhibition of Rsk2. Through this approach it may be possible to maintain tight-binding kinetics with the target kinase, whilst reducing the formation of covalent adducts of non-target cysteine containing proteins, such as glutathione.

4.3. Inhibitors of Nek2 Kinase

The first compounds to be described that interfered with a biological process involving Nek2 were inhibitors of the Hec1/Nek2 interaction. The work of Qui *et al.*[156] described the identification of hit compounds based upon an *N*-(4-phenylthiazol-2-yl)carboxamide core structure (**29**).

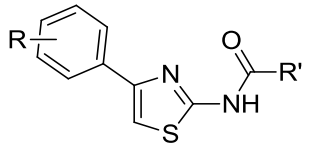

29

Following chemical modification of the initial hit compounds a series of inhibitors was prepared that exhibited effects upon cells similar to that of Hec1/Nek2 antagonism (siRNA or antibody). Thus, cells treated with these compounds exhibited mitotic abnormalities, an increased population of cells with multipolar spindle networks, and an increase in chromosomal misalignment. Furthermore, cells displayed changes in morphology characteristic of apoptosis due to mitotic catastrophe. Although mechanistic studies identified the molecular target of the inhibitors as Hec1 rather than Nek2, the growth-inhibitory activity of the compounds in cellular assays highlighted the potential benefit of disruption of Nek2 function in suppressing tumour cell proliferation.[156, 190]

More recently, several examples of small molecule inhibitors of Nek2 have been disclosed. A class of aminopyrazine-based inhibitors were the result of research at the Institute of Cancer Research (ICR).[191] SAR studies culminated in the identification of the aminopyrazine **30** as a potent ATP-competitive inhibitor of Nek2 (IC_{50} = 0.23 μM). Interestingly, compounds of this class were found to bind to an unusual inactive conformation of Nek2 in which Tyr70 is directed down into the binding site, owing to the presence of a pocket formed by the Met86 'gatekeeper' residue and an active site Leu89. Furthermore, structural biology studies identified a Phe148 residue within the ATP-binding site that exerted a strong influence on the active site and ligands that it can accommodate. A phenylalanine at this position is very rare among kinases, with only Wee1, Plk1 and Braf sharing this homology. These restraints within the ATP-binding site raise the possibility that Nek2 is a challenging target for ATP-competitive inhibitor design. This notwithstanding, compounds within this class displayed good selectivity over Plk1, although selectivity over Nek1 was not achieved.[191]

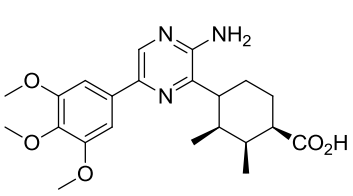

30

Nek2; IC_{50} = 0.23 μM

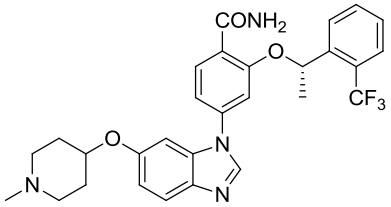

31

Nek2; IC_{50} = 0.36 μM

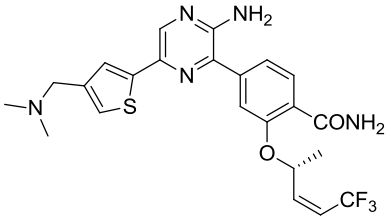

32

Nek2; IC_{50} = 0.022 μM

A parallel class of compounds was identified during a selectivity screen of a series of Plk1 inhibitors. SARs for this benzimidazole-based series eventually removed the original Plk1 inhibitory activity, generating a potent compound with >200-fold selectivity for Nek2 over Plk1 (**31**). Crystallographic studies showed that these compounds were type II, binding to the inactive DFG-out conformation of Nek2 and inhibiting both autophosphorylation and substrate phosphorylation. However, such inhibitors suffered from a modest ligand efficiency (LE), attributed to inefficient binding of the core scaffold.[192]

In order to resolve this problem, a hybrid class of compounds combining the core aminopyrazine moiety of the initial series with the side-chain characteristics of the benzimidazole series was generated. Optimisation of this new class of inhibitors improved potency, LE and kinase selectivity against a panel of cell cycle kinases, and culminated in the identification of **32** (Nek2; IC_{50} = 0.022 μM). The *Z*-configuration of the alkene, as well as the *R*-stereocentre, were found to be necessary for optimum positioning of the trifluoromethyl group into a pocket formed by the glycine rich loop of Nek2.[193]

A series of ATP-competitive reversible Nek2 inhibitors was also identified *via* high-throughput screening (HTS). These viridin/wortmannin-like compounds (*e.g.* **33**) exhibited modest Nek2-inhibitory activity, with reasonable selectivity over other Nek family members. In addition, some activity was observed in cellular growth inhibition and centrosome splitting assays.[194]

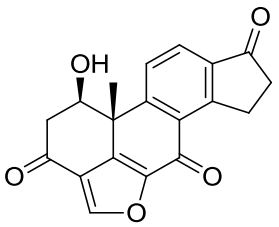

33

Nek2; IC_{50} = 1.9 μM

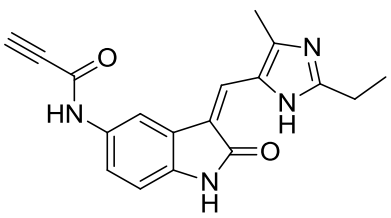

34

Nek2; IC_{50} = 0.77 μM

Finally, a group of compounds based upon the common oxindole core have been identified.[195] Analysis of the crystal structure of Nek2 in complex with these sunitinib-like analogues, including SU11652 (Figure 10)[136], revealed that the 5-position of the indole was positioned within a suitable distance of Cys22 (a group 2B cysteine) such that electrophilic groups might intercept the residue. This was achieved with the addition of a propiolamide moiety at this position. Modification of the initial compounds afforded the irreversible inhibitor **34**, which exhibited sub-micromolar activity and good selectivity over Cdk1 and other mitotic kinases.[195] However, the selectivity results for **34** from a kinase screen (National Centre for Protein Kinase Profiling, Dundee University) revealed that the compound exhibited poor selectivity for Nek2 (see appendix, Table A2).

4.4. Identification of Substituted Purines as Inhibitors of Nek2

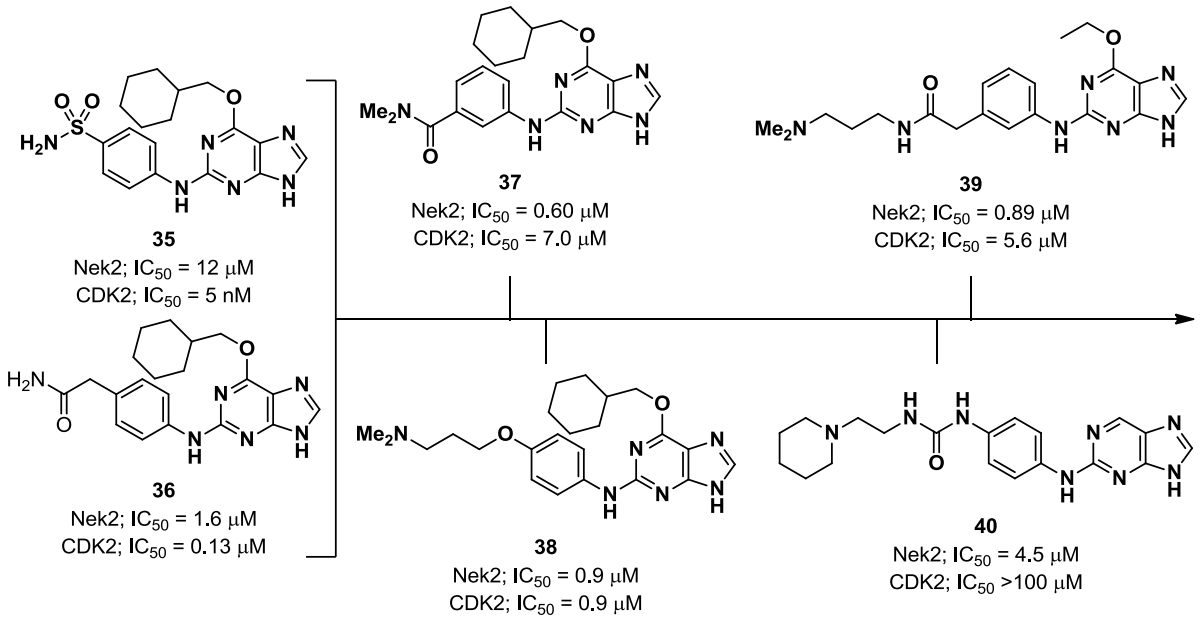

Figure 18: Elaboration of initial purine hit compounds to ATP-competitive inhibitors with improved Nek2 potency and selectivity.

In conjunction with the identification of aminopyrazine and benzimidazole inhibitors, collaborators at the ICR conducted a medium-throughput screen to identify other pharmacophores capable of inhibiting Nek2. The purine scaffold was highlighted as a modest inhibitor of the kinase worthy of further investigation. To validate this result, a range of purine derivatives from Newcastle University were submitted for screening against Nek2. Purines bearing 6-alkoxy substituents (*e.g.* **35**) were found to inhibit Nek2 in the micromolar range. However, such compounds were developed as part of a Cdk2 inhibitor project, and

were also potent Cdk2 inhibitors. Modifications around the purine scaffold were carried out to improve the potency against Nek2, and to design out structural motifs that confer potency against Cdk2. This enabled the elucidation of initial SARs for ATP-competitive Nek2 inhibition (Figure 18).

The 2-arylamino group of the purine was found to be amenable to modification, and in particular *meta*- or *para*-substituted side-chains containing basic functionalities conferred potency against Nek2 (*e.g.* **39**). X-ray crystallographic studies of Nek2 in complex with compounds of the 6-alkoxypurine series have revealed the binding mode of purines within the ATP-binding domain (Figure 19). The results of these studies have guided the design of further purine-based inhibitors of Nek2.

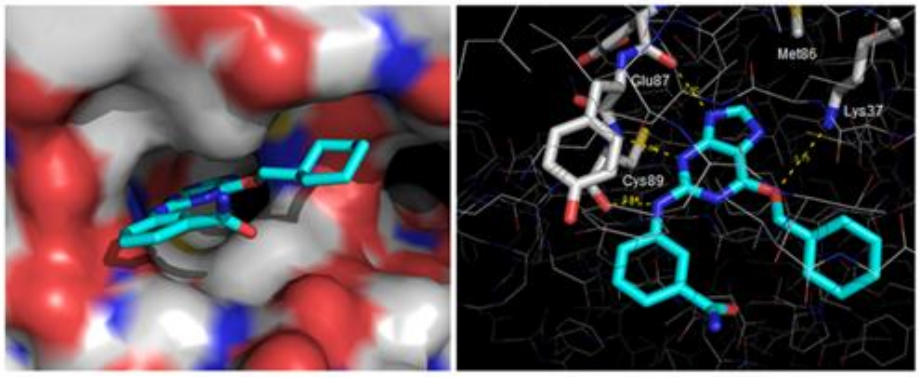

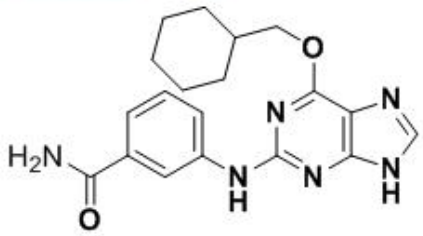

41

Nek2; IC_{50} = 18.6 μM

CDK2; IC_{50} = 0.48 μM

Figure 19: X-ray crystal structure of Nek2 in complex with 6-alkoxypurine inhibitor **41**.

The X-ray crystal structure of **41** in complex with Nek2 revealed that the compound binds *via* a classical hydrogen bonding triplet between the purine N^9-H, N^3 and C^2-NH, and the kinase hinge region residues Cys89 and Glu87. This dictates that alkylation or removal of the participating purine nitrogen atoms will be detrimental to activity. Furthermore, the 6-alkoxy substituent was adjudged to be non-critical for binding affinity, in contrast to Cdk2 inhibition where the 6-cyclohexylmethyl group occupies the ribose-binding pocket and is responsible

for binding affinity. Gratifyingly, removal of the 6-substituent (*e.g.* **40**) was found to essentially abolish Cdk2 activity, although activity against Nek2 was also reduced. Unfortunately, compounds within the most active series against Nek2 (*e.g.* **39**) were found to be poorly selective for Nek2 when tested in a small panel of mitotic kinases. It was therefore necessary to establish alternative points of modification on the purine pharmacophore to improve both potency and selectivity for the target kinase.

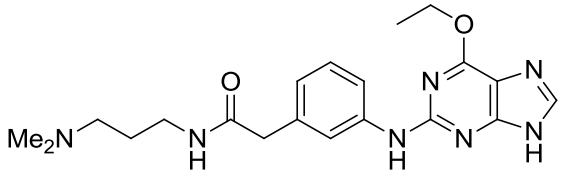

39

Nek2; IC_{50} = 0.89 μM
Cdk2; IC_{50} = 5.6 μM
Chk1; IC_{50} = 0.04 μM
Chk2; IC_{50} = 0.20 μM
AurA; IC_{50} = 0.47 μM

Chapter 5: 8-Alkyl-2-arylaminopurine Nek2 Inhibitors

5.1. 8-Alkylpurines as Selective Nek2 Inhibitors

I was responsible for all further chemical synthesis described, unless stated otherwise. In an attempt to build on the promising improvement in selectivity observed for 6-unsubstituted purines, the crystal structure of Nek2 in complex with purine-based inhibitors was reconsidered. It was noted that the gatekeeper residue of the ATP-binding domain is located in close proximity to the purine C-8 position. For Nek2 this residue is Met86, a less common amino acid present at this location in kinases. Cdk2 contains the larger Phe80 gatekeeper, presenting the possibility that tighter steric constraints may be found within this region of Cdk2 compared with Nek2.

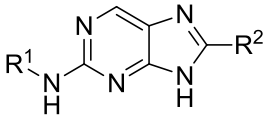

			IC_{50} (µM)	
Compound	**R^1**	**R^2**	**Nek2[a]**	**Cdk2[b]**
42	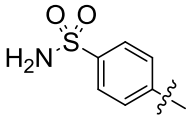	-Me	20.7	3.1
43	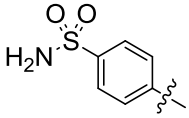	-Et	62.1	3.1
44	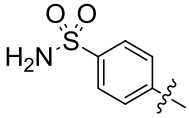	-^{i}Pr	79.9	5.0
45	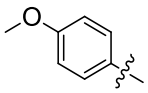	-Me	51.8	18% *
46	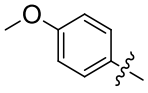	-Et	67.5	39% *

IC_{50} = half maximal inhibitory concentration; [a] Nek2 IC_{50} values determined at 30 µM ATP concentration; [b] Cdk2 IC_{50} values determined at 12.5 µM ATP concentration; * = Percentage inhibition at 50 µM.

Table 1: Inhibitory activity of initial 8-alkyl-2-arylaminopurines against Nek2, and Cdk2.

It was therefore proposed that simple substitution at the purine 8-position may be better tolerated in Nek2, and would serve to probe the binding site in a manner that would be detrimental to Cdk2 activity. As part of an earlier MSc project, a small series of compounds was prepared and evaluated against both Nek2 and Cdk2 (Table 1). Unfortunately, compounds bearing a sulfonamide group (**42**-**44**) were more potent against Cdk2, with only modest Nek2 inhibitory activity observed. This was postulated to be due to the sulfonamide group confering good potency against Cdk2 (*e.g.* **35**), and so the alternative 4-methoxyphenylamino side-chain was employed at the purine 2-position (**45** and **46**). This restored selectivity for Nek2, although the compounds were still considerably less potent than those lacking substitution at the 8-position. These limited results suggested that the largest alky substituent tolerated was a methyl group (*e.g.* **45**).

5.1.1. A Non-classical Binding Mode for 8-Alkyl-2-arylamino-purines

In order to understand the loss in potency against Nek2, compounds **45** and **46** were co-crystallised with the kinase and the resultant X-ray crystal structures analysed. Although crystal structures for both complexes were obtained, the resolution of the structure of **46** in complex with Nek2 (2.0 Å) allowed for the most accurate assessment (Figure 20).

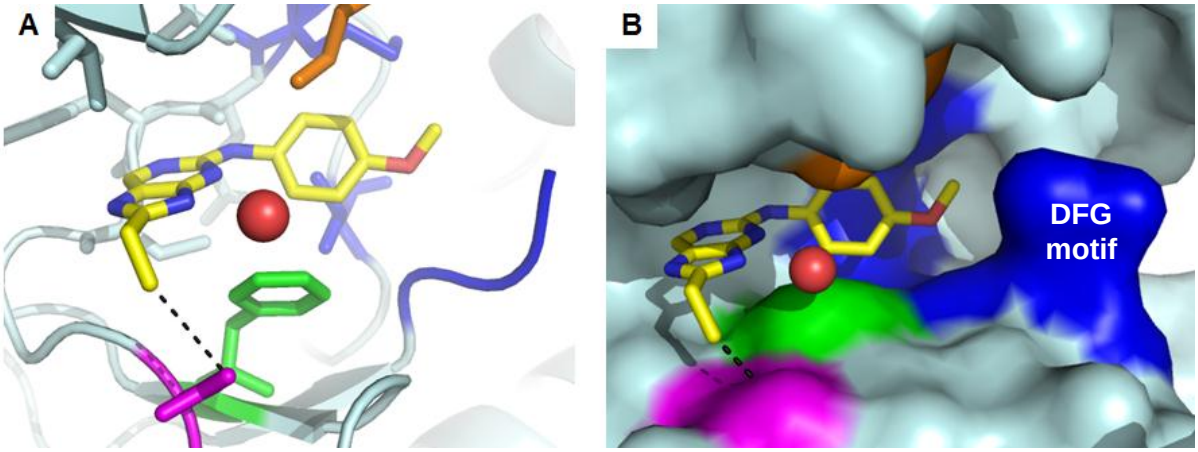

Figure 20: X-ray crystal structure of 8-alkylpurine inhibitor **46** (yellow) in complex with Nek2 at 2.0 Å, shown as stick and ribbon (**A**) and sphere (**B**) representations. Highlighted are Asp93 (purple), a water molecule (red), Phe148 (green), the Met86 gatekeeper residue (orange) and the DFG motif/hydrophobic pocket (blue).

Interestingly, this revealed that compounds **45** and **46** were no longer interacting with the kinase through a triplet of hinge H-bonds. It was clear that even simple alkylation at the purine 8-position is not tolerated in Nek2, and the compounds adopt an unusual 'flipped'

orientation, making hinge region H-bond interactions with the N^1 and C^2-NH of the purine (Figure 21). Fortunately, this presented opportunities to determine SARs for this alternative binding orientation through substitution on the purine previously not possible.

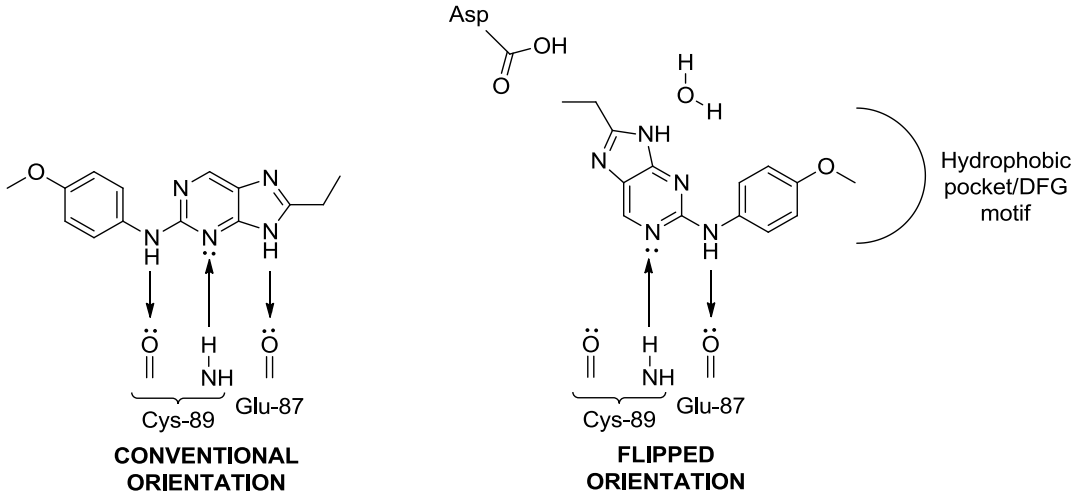

Figure 21: Schematic representation of the conventional and 'flipped' purine binding modes, with the hinge region of the Nek2 ATP-binding domain.

It was noted that the *para*-position of the 2-arylamino ring of **46** was directed towards a large hydrophobic pocket equivalent to the allosteric site occupied by type II kinase inhibitors. Expansion into this region may thus improve binding affinity as expected for type II kinase inhibitors. Furthermore, the DFG motif was now positioned to be probed for interactions from the purine 2-arylamino ring, allowing the potential for Nek2 to be stabilised in the DFG-out inactive kinase conformation. The aromatic ring of the 2-arylamino side-chain also appears to be making an edge-face π-π, or T-stacking, interaction with Phe148 in the ATP-binding site.

A bound water molecule was found to be located adjacent to the purine N^9-position of **46** in the ATP-binding site of Nek2, offering opportunities for expansion into this region, particularly given that this position no longer makes a hinge-binding interaction. Thus, it was likely that alkylation at the N^9-position would be tolerated and may improve inhibitor potency through water molecule displacement. Finally, the 8-position of the purine was observed to occupy a region in the vicinity of an aspartate residue (Asp93). A potential improvement in binding affinity may thus be achieved by interaction with basic functional groups at the purine-C^8 position. The identification of these possible points of interaction required the synthesis of several new 8-alkylpurines to test these hypotheses (Figure 22).

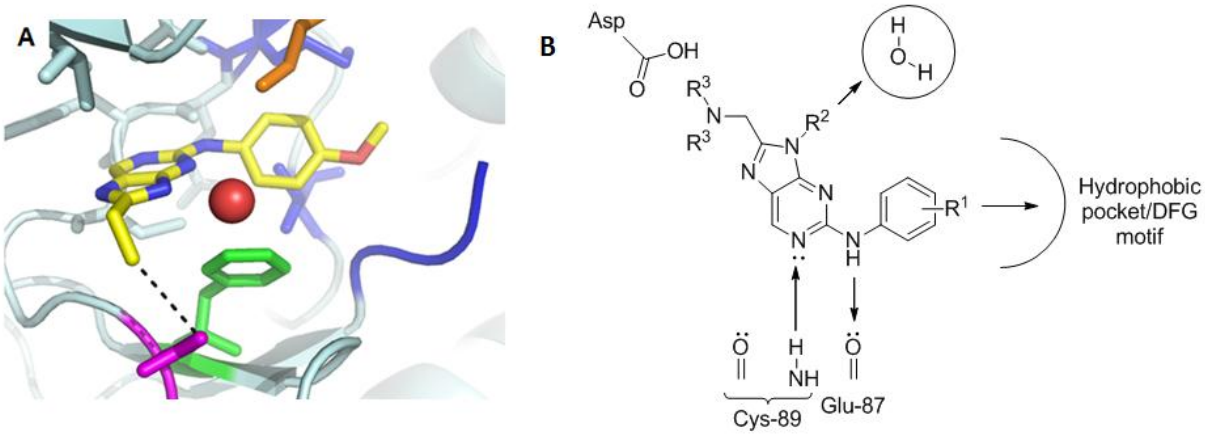

Figure 22: A) X-ray crystal structure of 8-alkylpurine inhibitor **46** (yellow) in complex with Nek2 at 2.0 Å; **B)** Possible points of interaction to determine SARs for the 8-alkyl-2-arylaminopurine chemotype.

5.2. Probing the Proposed Hydrophobic Pocket at R^1

5.2.1. Target Compound Selection and Synthesis

Compounds within the 8-alkylpurine series were initially synthesised such that modification of the 8-position could be carried out at the final stage, in order to utilise common intermediates as extensively as possible. This involved the synthesis of a diaminopyrimidine with the desired substituted 2-arylamino side-chain, followed by a 2-step purine synthesis utilising the appropriate acyl chloride to acylate the 5-amino group, with subsequent base-mediated cyclisation (Scheme 1).

Scheme 1: Initial synthesis of 8-alkyl-2-arylaminopurines.

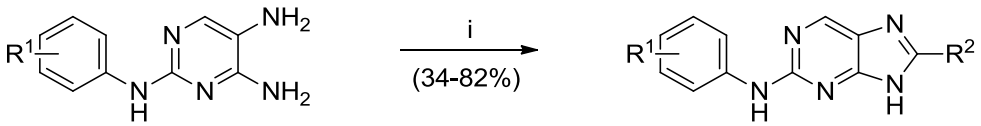

Reagents and conditions: i) a) R^2COCl, pyridine, DCM, RT, 3 h, b) NaOH, H_2O, reflux, 2 h.

Unfortunately, this cyclisation procedure was unsatisfactory for the generation of multiple analogues or for scale-up, as the yields obtained were highly variable and product isolation difficult. An alternative procedure was thus required to allow the synthesis of sufficient quantities of an intermediate suitable for the preparation of a series of 2-substituted purine derivatives. Due to the low tolerance for substitution at the C^8-position previously observed,

it was decided that a methyl group would be employed from the outset, solely to induce binding *via* the alternative conformation and allow access to the putative hydrophobic pocket.

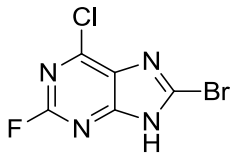

47

An approach that had not previously been attempted within the group was halogenation at the purine 8-position. It was envisaged that a trihalogenated purine (**47**) would serve as a versatile intermediate for the stepwise functionalization of the purine. This would particularly be the case if different halogens were introduced at each position, allowing the inherent reactivity differences to be exploited for regioselective functionalisation.

Initial studies established that when using classical bromination conditions of NBS in acidic media, the nature of the N^9-substituent was important. With no protecting group at the N^9-position the reaction did not proceed. A common group utilised for purine N^9-protection is THP, but the acid lability of this group meant that it was not suitable. A successful C^8-bromination was achieved employing an N^9-benzylpurine, but all subsequent efforts to remove the benzyl moiety failed.

To allow use of the more labile THP group, the method of bromination was revised. Following protection of the N^9-position, C^8-deprotonation was investigated to allow reaction of the resulting anion with an electrophilic bromine source. A synthetic strategy was designed (Scheme 2), which would allow the synthesis of the first compound to be prepared in this series, bearing a 4-phenoxyanilino substituent (**48**). This would enable validation of the strategy and initial assessment of the effect of probing the hydrophobic pocket with bulky substituents.

Starting from the commercially available 2-amino-6-chloropurine (**49**), the 2-fluoropurine **50** was prepared in moderate yield (61%) *via* a Balz-Schiemann reaction. Protection of the purine N^9-position with THP gave the required substrate (**51**) for the base-mediated bromination reaction.

Scheme 2: Synthesis of 8-methylpurine **48**.

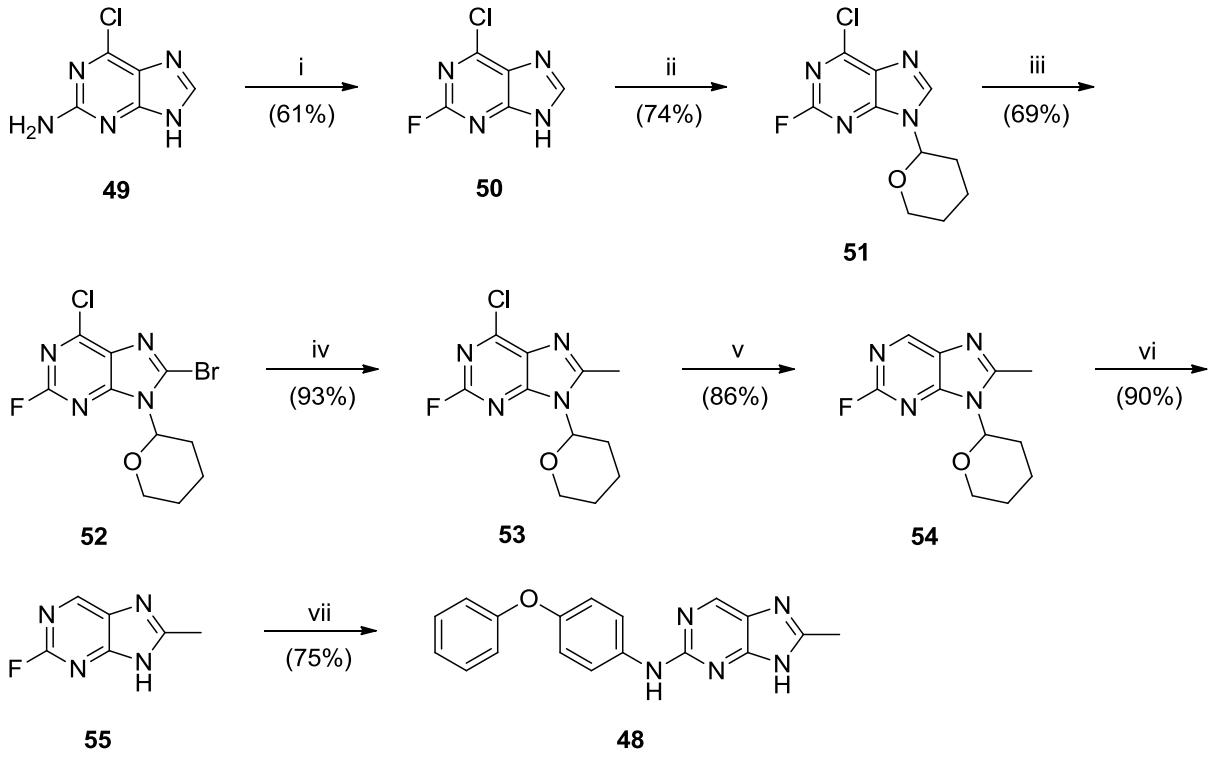

Reagents and conditions: i) $NaNO_2$, HBF_4, 0 °C to RT, 70 min; ii) DHP, CSA, EtOAc, reflux, 18 h; iii) a) nBuLi, DIPA, THF, -78 °C, 25 min, b) $(CCl_2Br)_2$, THF, -78 °C to RT, 3 h; iv) a) nBuLi, THF, -78 °C, 20 min, b) MeI, -78 °C to RT, 3 h; v) $Pd(OH)_2$, NH_4HCOO, MeOH, reflux, 2 h; vi) TFA, iPrOH, H_2O, MW 130 °C, 15 min; vii) 4-Phenoxyaniline, TFA, TFE, reflux, 24 h.

Direct lithiation of the purine C-8 position has been reported previously as a route to 8-functionalised nucleosides,[196] and this approach was investigated with **51**, using LDA as the base. Under these conditions it is possible to deprotonate both the 8-position and effect lithium-halogen exchange of the 6-chloro group. However, formation of the carbanion at the 6-position has been reported to be the kinetically favoured product, with reaction at the 8-position the thermodynamically favoured product. At reaction temperatures below -130 °C the principal product arises through reaction at the 6-position. However, at the higher temperature of -78 °C the desired 8-functionalised product prevails.[197] Therefore, this higher temperature was used during the lithiation step.

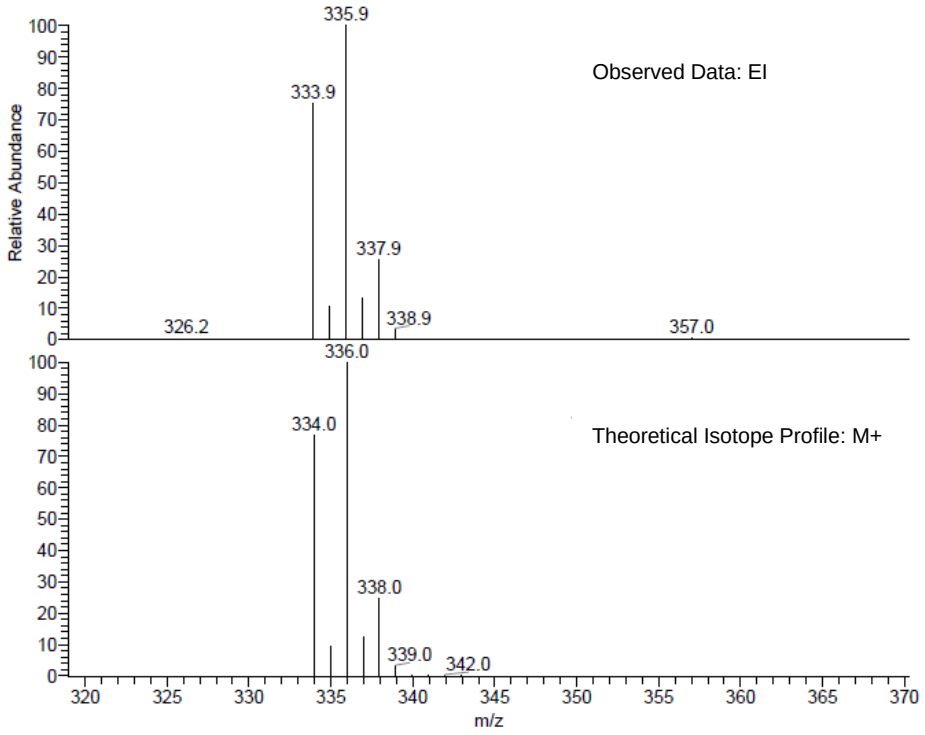

Figure 23: Predicted and observed MS isotope profiles for **52**.

It was found that the lithiated species derived from **51** was very sensitive to the bromide source, with classical electrophilic bromine sources failing to afford the desired product (**52**). 1,2-Dibromotetrachloroethane has been reported to brominate the purine 8-position under similar conditions,[198] and clean conversion to the desired compound (**52**) was achieved in reasonable yield (69%) utilising this reagent. Spectroscopic analysis of **52** by ^{1}H and ^{13}C NMR did not give definitive confirmation of the structure of the product. However, EI mass spectrometry revealed the characteristic isotope profile expected for compound **52** (Figure 23).

Introduction of a methyl group at the 8-position was attempted using a palladium-mediated Suzuki coupling reaction between **52** and trimethylboroxine. However, it was found to be difficult to establish conditions in which selectivity was achieved for reaction at the 8-position over the 6-position. It was therefore decided to generate the C^{8}-lithiated species through lithium-bromine exchange and react with methyl iodide. Although this approach could be used on **51** at the previous step, the generation of the trihalogenated purine **52** was desirable as a reagent for polyfunctionalisation of the purine scaffold.

After introduction of the 8-methyl group, the 6-chloro group of **53** was removed *via* a palladium-mediated reductive dehalogenation to give **54**, from which the N^{9}-THP protecting

group was cleaved (**55**). Due to electrostatic repulsion from the purine nitrogen lone pairs,[199] S_NAr reactions at the 2-position of a purine or pyrimidine are very slow under neutral conditions. Previous work within the group has identified a combination of TFA in TFE as an effective system for facilitation of S_NAr reactions between an aniline and the 2-position of a purine.[200] The stoichiometric ratio of aniline to TFA is important to minimise protonation of the aniline, whilst activating the purine to nucleophilic attack through N^1/N^3 protonation. The use of 2 equivalents of aniline and 2.5-5.0 equivalents of TFA was found to result in a significantly improved reaction rate for the coupling reaction. 4-Phenoxyaniline was coupled to the 2-fluoropurine intermediate **55** under these reaction conditions to give the target compound **48**.

Despite the successful synthesis of compound **48** using this synthetic strategy, the route was lengthy, and several steps, particularly the lithiation reactions, were poorly reproducible and not amenable to a larger scale. In order to generate a series of analogues it was necessary to redesign the synthesis to require fewer steps and more reproducible chemistry. In addition, to determine the effect of displacement of the water molecule adjacent to the purine N^9-position in the kinase binding site, a strategy was needed by which the analogous N^9-methyl purine (**56**) could be prepared. This was not desirable through direct alkylation of the purine, as the problem of N^7/N^9 regioselectivity, and separation of such regioisomers may arise.

Scheme 3: Synthesis of 2-arylamino-8-methylpurines.

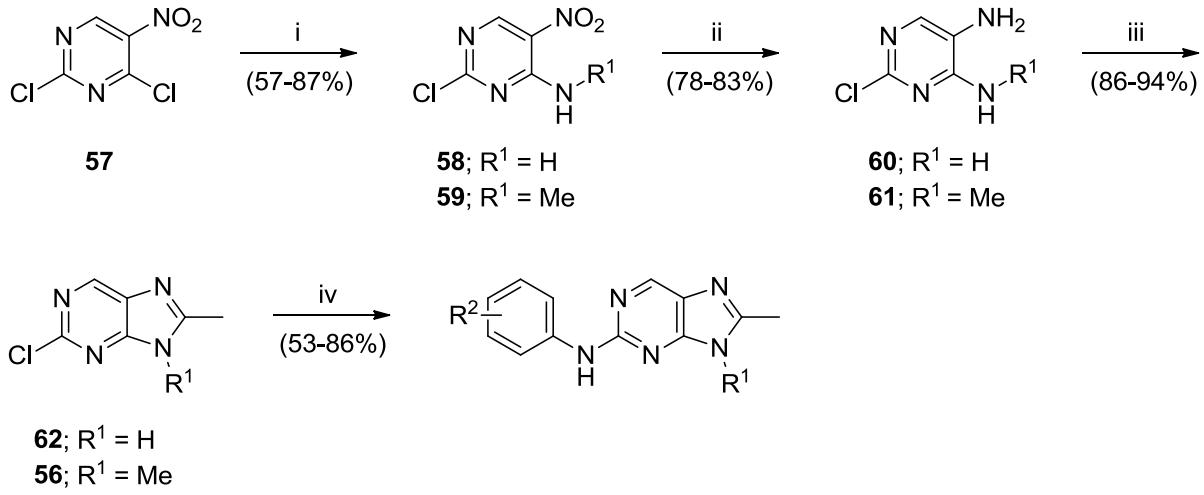

Reagents and Conditions: i) RNH_2, THF, 0 °C, 30 min; ii) $SnCl_2$, EtOH, 80 °C, 1.5 h; iii) $(EtO)_3CCH_3$, TFA, TFE, MW 140 °C, 90 min; iv) $ArNH_2$, TFA, TFE, MW 160 °C, 1 h.

A synthetic strategy was employed using simple, scalable reactions that would also allow the unequivocal assignment of the location of the N^9-methyl group (Scheme 3). Due to electrostatic repulsion of the pyrimidine nitrogen lone pairs, it is possible to selectively displace the 4-chloro group of 2,4-dichloro-5-nitropyrimidine (**57**) with a variety of amines through S_NAr reactions. Using ammonia and methylamine it was possible to prepare pyrimidines **58** and **59**, respectively, under these conditions.

The required purine was prepared by reduction of the 5-nitro group of **58** and **59** using stannous chloride in refluxing ethanol to give the diaminopyrimidines **60** and **61**. This was followed by acid-catalysed cyclisation with triethyl orthoacetate to give purines **62** and **56**. In order to further facilitate the cyclisation reaction, microwave heating was utilised; when using conventional heating, reactions of this type were found to proceed over several hours. However, under microwave irradiation conditions full conversion to the products was achieved in 90 minutes, giving the required purine intermediates **62** and **56** in good yields (86% and 94%, respectively).

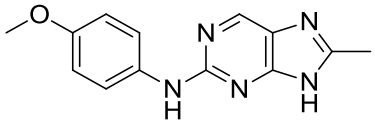

45

IC_{50}; Nek2 = 51.8 μM
Cdk2 = 18% at 50 μM

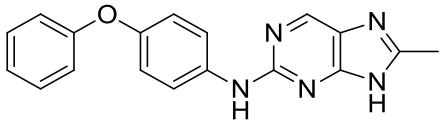

48

IC_{50}; Nek2 = 70.5 μM
Cdk2 = 17% at 100 μM

Unfortunately, incorporation of the 4-phenoxy substituent to give compound **48** did not translate to an improvement in potency over the 4-methoxy analogue **45**. As a consequence the effect of simple alkyl and alkoxy substituents at the 4-position of the 2-arylamino ring was assessed to determine the steric constraints at this position. In addition, all compounds were synthesised as both the N^9-unsubstituted and N^9-methyl analogues, to validate the proposed improvement in binding affinity achieved by displacement of the bound water molecule in the Nek2 ATP-binding site. A small series of compounds was proposed (**63**-**74**).

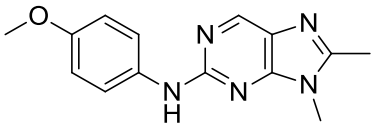

63

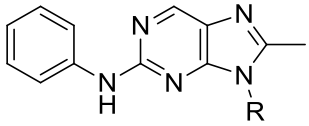

64; R = H
65; R = Me

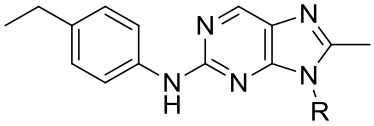

66; R = H
67; R = Me

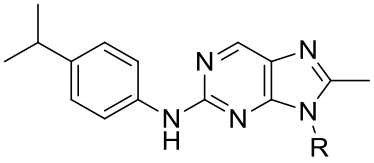

68; R = H
69; R = Me

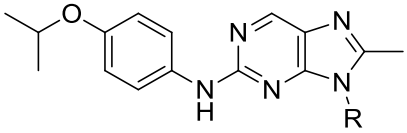

70; R = H
71; R = Me

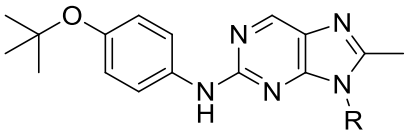

72; R = H
73; R = Me

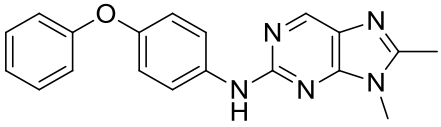

74

It was intended to synthesise the corresponding 4-*tert*-butoxyarylamino analogues (**72** and **73**) in addition to the isopropoxyanilines **70** and **71**. However, the required aniline reagent proved unstable to the TFA/TFE mediated coupling conditions, and it was decided to determine the Nek2 inhibitory activity of the initial set of compounds prior to preparing further target compounds. For the synthesis of compounds **70** and **71** it was necessary to prepare 4-isopropoxyaniline (**75**). This was achieved through reaction of 4-fluoronitrobenzene (**76**) with sodium isopropoxide to give **77**, followed by reduction of the aromatic nitro group through a palladium-mediated transfer hydrogenation to afford the aniline **75** (Scheme 4).

Scheme 4: Synthesis of aniline **75**.

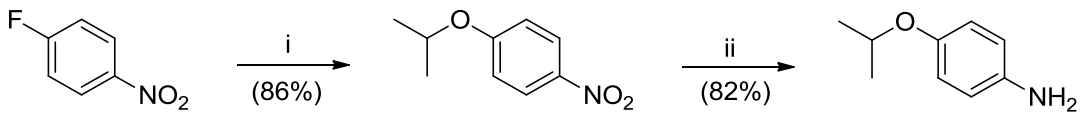

76 **77** **75**

Reagents and conditions: i) NaH, ^{i}PrOH, 0 °C to RT, 18 h; ii) Pd/C, NH_4HCOO, MeOH, RT, 18 h.

Reaction times for the TFA/TFE mediated S_NAr coupling were improved by the use of microwave heating, with near complete consumption of starting material observed after 1 hour at 160 °C (Scheme 5). The required anilines were coupled with intermediates **62** and **56** to afford the desired target purines (**63-71** and **74**) in moderate to good yields (Table 2).

Scheme 5: Coupling of required anilines to 2-chloropurines **62** and **56**.

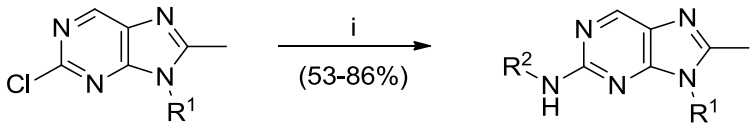

62; R^1 = H
56; R^1 = Me

Reagents and conditions: i) $ArNH_2$, TFA, TFE, MW 160 °C, 1 h.

Compound	R^1	R^2	Yield (%)
63	Me	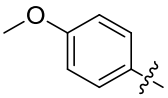	61
74	Me	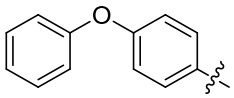	78
64	H	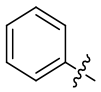	83
65	Me	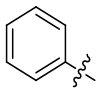	57
66	H	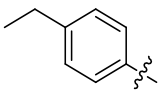	76

Compound	R^1	R^2	Yield (%)
67	Me	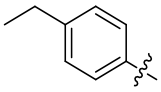	57
68	H	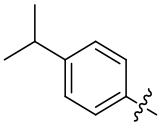	53
69	Me	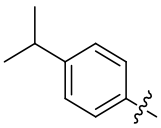	58
70	H	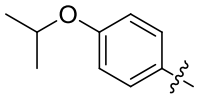	70
71	Me	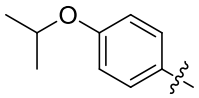	86

Table 2: Isolated yields for the coupling of anilines to the 2-chloropurine intermediates **62** and **56** under microwave assisted TFA/TFE mediated conditions.

For the N^9-unsubstituted inhibitors (**64**, **66**, **68** and **70**) a potential trend was observed in improved potency against Nek2, with the size of the alkyl substituent at the 4-position of the 2-arylamino ring (*e.g.* **70**; IC_{50} = 9.6 μM). Within the compound series with N^9-methylation (**63**, **65**, **67**, **69**, **71** and **74**) there was limited SARs, with 4-methoxyarylamino compound **63** being one of the most potent compounds. However, all compounds bearing methyl groups at the purine N^9-position (**63**, **65**, **67**, **69**, **71** and **74**) exhibited increased potency when compared with their N^9-unsubstituted counterparts (**45**, **48**, **64**, **66**, **68** and **70**). In the case of compounds **45** and **63** a 10-fold increase in potency was observed.

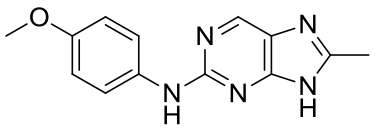

45

IC_{50}; Nek2 = 51.8 μM

Cdk2 = 18% at 50 μM

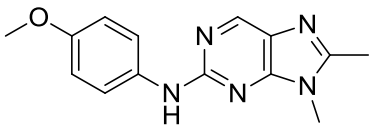

63

IC_{50}; Nek2 = 5.23 μM

Cdk2 = 21% at 100 μM

To confirm whether the observed enhanced Nek2 inhibition was due to displacement of the binding site water molecule, compound **63** was co-crystallised with Nek2 and the crystal structure determined. When compared with that of **46** it was apparent that both **45** and **63**

adopt a similar binding orientation, and that the water molecule is no longer present at the N^9-position when **63** is bound to Nek2 (Figure 24).

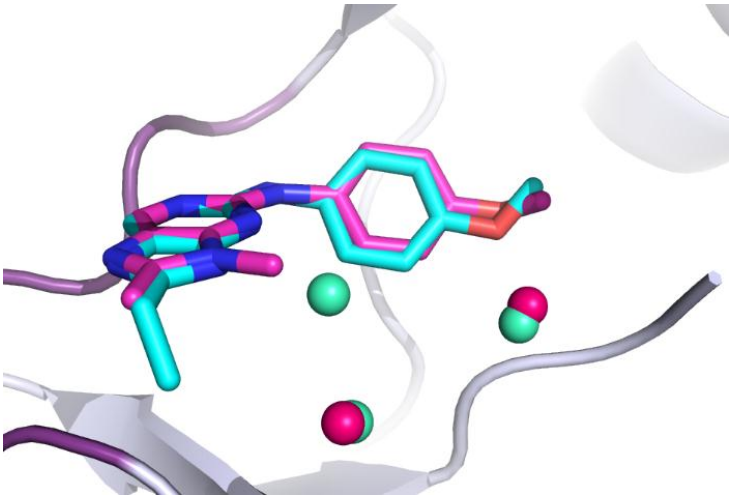

Figure 24: Overlay of **46** (cyan) and **63** (magenta) within the ATP-binding domain of Nek2. Water molecules shown are either present with **46** bound (cyan) or with both inhibitors bound (cyan/magenta).

As a result of this observation, it was decided that all subsequent inhibitors in this series would bear the N^9-methyl group. It is possible that the lack of potency observed for the 4-phenoxyarylamino compounds **48** and **74** was a result of the phenoxy substituent failing to occupy the hydrophobic pocket. It may be necessary to extend lipophilic groups further into this region to participate in potential interactions favourable to kinase binding affinity. To this end, the 4-benzyloxyarylamino analogue (**78**) was prepared. Attempts to couple 4-benzyloxyaniline directly to the 2-chloropurine **56** resulted in formation of the *ortho*-benzyl phenol **79** in poor yield, owing to the inherent instability of this side-chain to acidic conditions, followed by electrophilic aromatic substitution between the phenol (**80**) and the resultant benzyltrifluoroacetate (Scheme 6).[201]

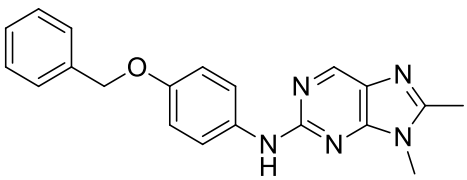

78

Scheme 6: Synthesis of the undesired *ortho*-benzyl phenol **79**.

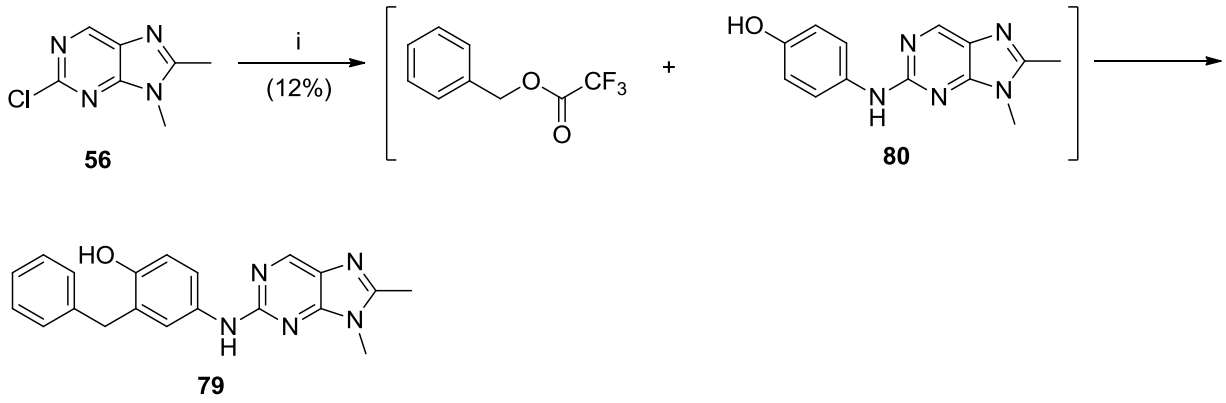

Reagents and conditions: i) 4-Benzyloxyaniline, TFA, TFE, MW 160 °C, 1 h.

To avoid this problem, and to facilitate the synthesis of further analogues, a route utilising a common phenol intermediate (**80**) followed by alkylation was employed (Scheme 7). A small series of 4-benzyloxyanilino purines (**78** and **81**-**83**) was readily prepared using this approach.

Scheme 7: Alkylation of phenol **80** with substituted benzyl chlorides.

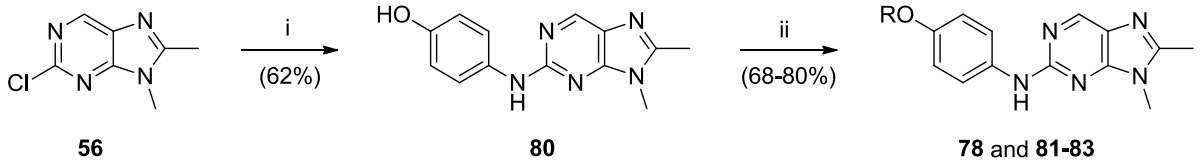

Reagents and conditions: i) 4-Aminophenol, TFA, TFE, MW 160 °C, 1 h; ii) RCl, K_2CO_3, DMF, 60 °C, 18 h.

In an attempt to probe further into the hydrophobic pocket, the benzyl group of **78** was homologated. The required aniline (**85**) was prepared in good yield (84%) through reaction of 4-fluoronitrobenzene (**76**) with sodium 2-phenylethoxide, followed by reduction of the aromatic nitro group by catalytic transfer hydrogenation. Final coupling of the aniline **85** under the established conditions afforded the target purine **86** (Scheme 8).

Scheme 8: Synthesis of purine **86**.

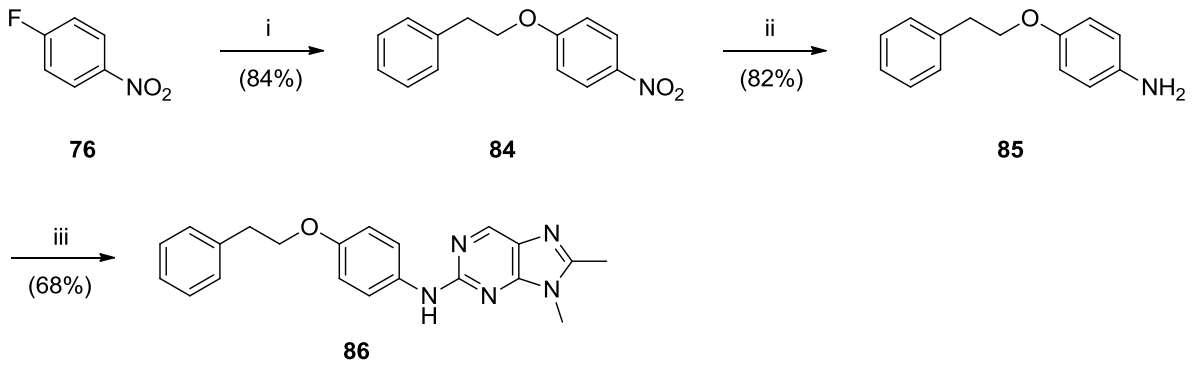

76 **84** **85** **86**

Reagents and conditions: i) NaH, 2-phenylethanol, 0 °C to RT, 18 h; ii) Pd/C, NH_4HCOO, MeOH, RT, 18 h; iii) **56**, TFA, TFE, MW 160 °C, 1 h.

The loss of potency for the 4-phenoxyaryl compound **74** (Nek2; IC_{50} = 32.9 µM) compared with the 4-methoxyaryl analogue **63** (Nek2; IC_{50} = 5.2 µM), may indicate steric limitations within the hydrophobic pocket. To access the target pocket it may thus be necessary to direct substituents in such a way as to avoid binding site clashes. To investigate this, a small set of derivatives bearing alkyne groups at the 2-arylamino position was proposed. The target compounds (**87**-**89**) were prepared by coupling 4-bromoaniline with the 2-chloropurine intermediate **56** under microwave assisted TFA/TFE coupling conditions. The bromo group of the resultant compound (**90**) was substituted with the required functionalised alkynes using a palladium-mediated (Buchwald) coupling procedure (Scheme 9).

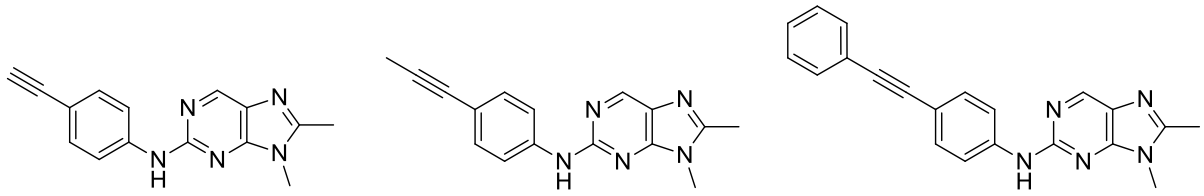

87 **88** **89**

Difficulties were encountered when attempting to isolate compounds **88** and **89** due to their co-elution with the starting material (**90**) under a variety of chromatography conditions. Compound **91** was prepared by coupling (triisopropylsilyl)acetylene with **90**, followed by removal of the TIPS-protecting group using TBAF. Evaluation of the potency of **87** (Nek2; IC_{50} = 12.5 µM) suggested that it was not necessary to attempt to purify compounds **88** and **89** further, as no significant improvement in binding affinity was observed.

Scheme 9: Synthesis of compound **87**.

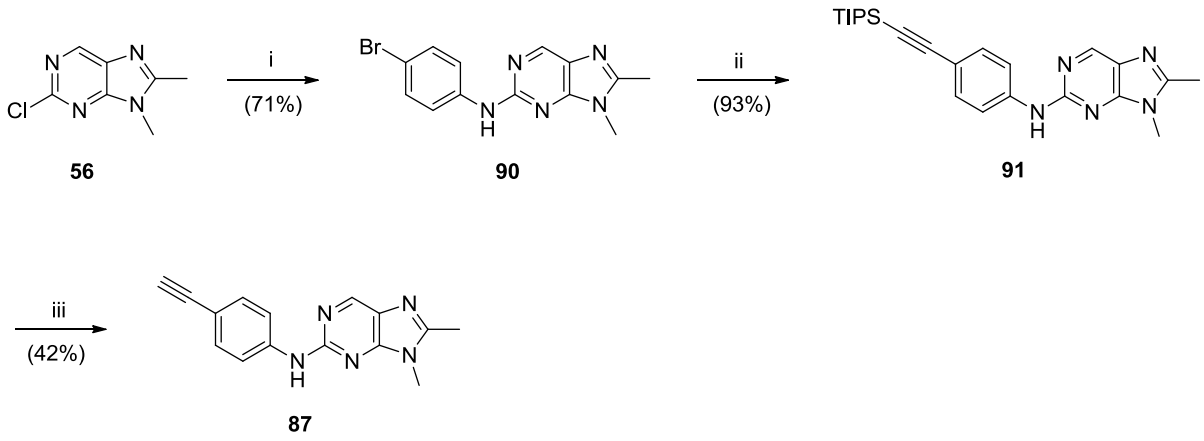

Reagents and conditions: i) 4-Bromoaniline, TFA, TFE, MW 160 °C, 1 h; ii) TIPS-acetylene, $PdCl_2(MeCN)_2$, XPhos, Cs_2CO_3, MeCN, 80 °C, 2 h; iii) TBAF, THF, RT, 5 min.

It has been reported that the binding energy for edge-face π-π interactions can be lowered by introducing fluorine atoms at the *ortho*- and *para*-positions to the ring hydrogen involved in the interaction.[202] To this end, fluoro groups were introduced onto the 2-arylamino ring of **63** by TFA/TFE mediated coupling of the required anilines to the 2-chloropurine intermediate **56**, to give compounds **92** and **93**. 3-Fluoro-4-methoxyaniline **94**, required for the synthesis of **93**, was easily synthesised from 2-fluoro-4-nitroanisole (**95**) *via* catalytic transfer hydrogenation in good yield (89%) (Scheme 10).

Scheme 10: Synthesis of fluorinated 2-arylamino-8-methylpurines **92** and **93**.

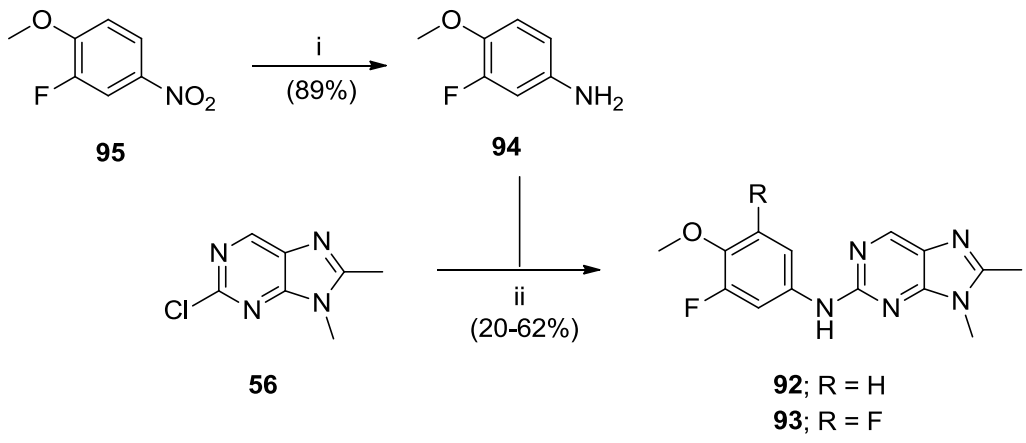

Reagents and conditions: i) Pd/C, NH_4HCOO, MeOH, RT, 18 h; ii) **94** or 3,5-difluoro-4-methoxyaniline, TFA, TFE, MW 160 °C, 1 h.

5.2.2. Biological Results

All compounds prepared were tested for inhibitory activity against both Nek2 and Cdk2. (Table 3).

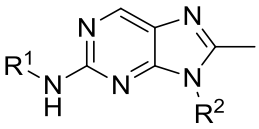

Compound	R^1	R^2	IC_{50} (μM) Nek2[a]	Cdk2[b]	LE[c]	LipE[d]
45	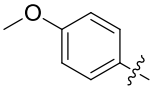	H	51.8	18%*	0.32	2.15
63	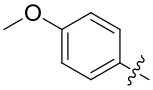	Me	5.2	21%*	0.37	2.90
48	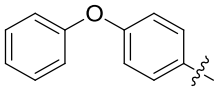	H	70.5	17%*	0.24	0.35
74	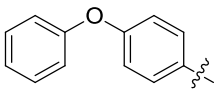	Me	32.9	17%*	0.25	0.44
64		H	30.7	32%*	0.37	2.24
65		Me	11.2	30%*	0.39	2.45
66	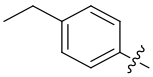	H	17.4	26%*	0.35	1.59
67	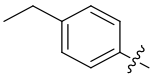	Me	12.3	34%*	0.34	1.50
68	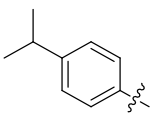	H	16.9	28%*	0.33	1.27
69	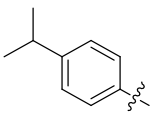	Me	11.9	15%*	0.33	1.18

Compound	R^1	R^2	IC_{50} (μM) Nek2[a]	Cdk2[b]	LE[c]	LipE[d]

70	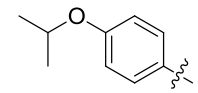	H	9.6	22%*	0.33	2.22
71	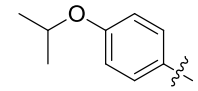	Me	4.7	14%*	0.34	2.30
78	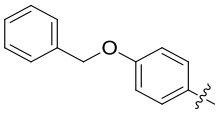	Me	40%*	13%*	N/A	N/A
81	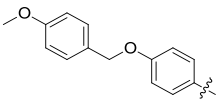	Me	24%*	16%*	N/A	N/A
82	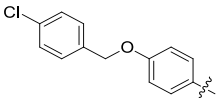	Me	27%*	13%*	N/A	N/A
83	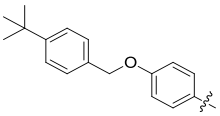	Me	16%*	2%*	N/A	N/A
86	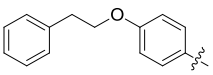	Me	34%*	14%*	N/A	N/A
87	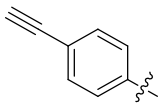	Me	12.5	44%*	0.34	2.24
92	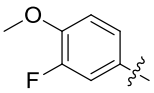	Me	8.40	-	0.34	2.55
93	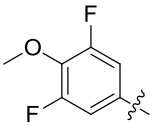	Me	7.10	-	0.33	2.46
79	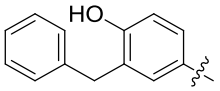	Me	7.30	45.8	0.28	0.93

[a] Nek2 IC_{50} values determined at 30 µM ATP concentration; [b] Cdk2 IC_{50} values determined at 12.5 µM ATP concentration; [c] Ligand efficiency = ΔG/HA (where HA = number of heavy atoms); [d] Lipophilic efficiency = pIC_{50} – ClogP; * = Percentage inhibition at 100 µM.

Table 3: Inhibitory activity of 8-alkyl-2-arylaminopurines against Nek2 and Cdk2.

Compounds bearing a substituted benzyloxyarylamino group at the purine 2-position suffered a loss of Nek2 inhibitory activity with respect to **63**, with inhibitors (**78**, **81**-**83** and **86**) exhibiting an IC_{50} of greater than 100 µM. This indicates that there is limited tolerance for

substitution at the 4-position of the 2-arylamino ring, and that simple alkyl (**66**-**69**) and alkoxy (**70** and **71**) are the largest groups that can be accommodated. As such it was decided that targeting the hydrophobic pocket was not useful as a means to improve the potency of this compound class. It is possible that the compounds in this series are unable to stabilise the DFG motif in the DFG-out conformation necessary for the allosteric site to be accessed. Although modest Nek2 inhibitory activity was retained for compounds **87**, **92** and **93**, the lack of a marked improvement in potency lead to the conclusion that significant interactions were not being made within the kinase ATP-binding domain. Interestingly, the unexpected product resulting from the rearrangement of **78** (**79**; IC_{50} = 7.30 μM) was a modest inhibitor of Nek2. It is possible that the phenol group of **79** is able to form interactions with the DFG motif of Nek2, allowing the benzyl group to access the hydrophobic pocket. However, the modest activity of **79** was accompanied by a detrimental effect on both ligand efficiency (LE) and lipophilic efficiency (LipE). To investigate this result further a series of compounds was designed to incorporate functional groups capable of interacting with the DFG motif, whilst reducing CLogP with the intention of improving LipE (see chapter 5.4.).

The compounds detailed in Table 3 retained selectivity for Nek2 over Cdk2 as observed for **45**. However, it was unnecessary to profile the selectivity of such compounds in a wider panel of kinases, or to evaluate their effect in cellular assays, owing to the general lack of Nek2 inhibitory potency. The synthesis of 8-alkypurines bearing lipophilic groups at the 4-position of the 2-arylamino ring was thus seen as an inappropriate method for the improvement of such compounds as inhibitors of Nek2.

5.3. Investigating Interactions at the Purine N^9-Position

5.3.1. Target Compound Selection and Synthesis

In addition to the bound water molecule observed adjacent to the N^9-position of **46** within the Nek2 ATP-binding domain, it was proposed that it may be possible to make additional interactions with the kinase through further substitution at this position of the purine. This was highlighted by a comparison of the X-ray crystal structures of the 8-alkypurine **63** and the benzimidazole inhibitor **31**[192] in complex with Nek2 (Figure 25).

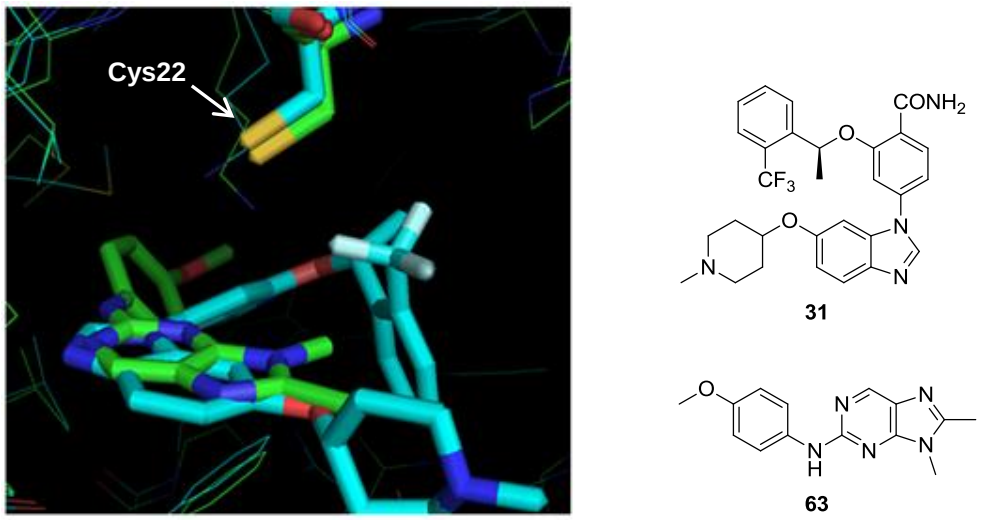

Figure 25: Overlay of **63** (green) and **31** (cyan) within the ATP-binding domain of Nek2 with Cys22 shown.

The trifluoromethyl group of **31** is known to be important for binding affinity, as a result of its location within a pocket formed by the glycine rich loop adjacent to Cys22. When the X-ray crystal structure of **63** was compared with that of **31** (Figure 25) it was apparent that the purine N^9-methyl group of **63** is positioned close to the pocket occupied by the trifluoromethyl moiety of **31**. It was proposed that incorporation of hydrophobic groups at this position, including trifluoroalkyl moieties, may improve potency. A small series of compounds was to be prepared with groups introduced at the purine N^9-position, to probe the hydrophobic pocket. To allow a direct comparison between inhibitor series the target compounds (**96**–**101**) were also designed bearing the 4-methoxyarylamino side-chain present in **63**.

Scheme 11: Synthesis of 2-arylamino-8-methyl-N^9-alkylpurines **96**-**101**.

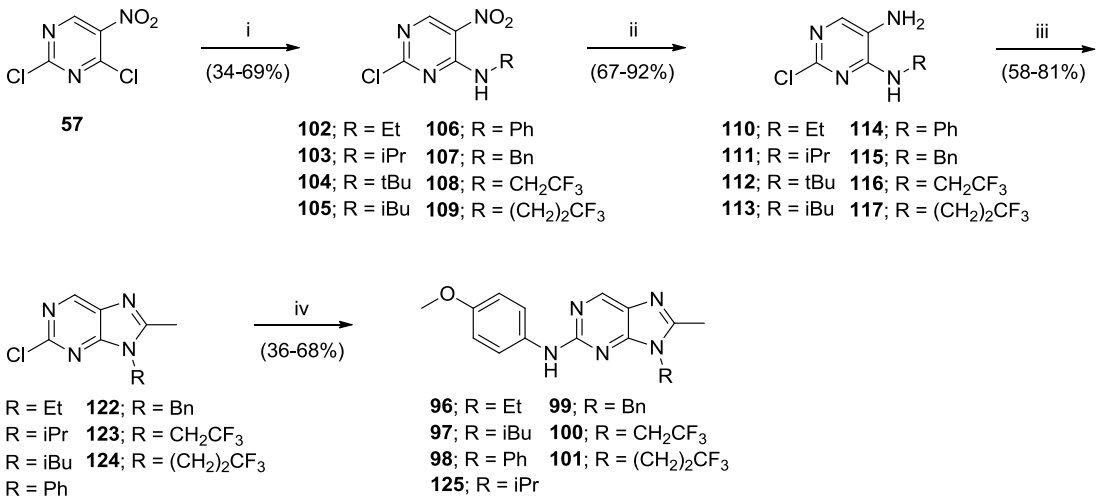

Reagents and Conditions: i) RNH_2, THF, 0 °C, 30 min; ii) $SnCl_2$, EtOH, 80 °C, 1.5 h; iii) $(EtO)_3CCH_3$, TFA, TFE, MW 140 °C, 1.5-2.5 h; iv) $ArNH_2$, TFA, TFE, MW 160 °C, 1 h.

	Step in Scheme 11			
R	**i**	**ii**	**iii**	**iv**
Et	57%	70%	78%	49%
^{i}Pr	69%	85%	58%	-
^{t}Bu	63%	86%	-	-
^{i}Bu	35%	67%	63%	47%
Ph	34%	92%	81%*	36%
Bn	36%	78%	73%	42%
CH_2CF_3	62%	84%	76%	68%
$CH_2CH_2CF_3$	65%	88%	74%	62%

* = Reaction time extended by 1 h

Table 4: Isolated yields for reaction steps as shown in Scheme 11, for the synthesis of N^9-functionalised purines.

The synthetic strategy used previously was employed for the preparation of this series (Scheme 11). 2,4-Dichloro-5-nitropyrimidine (**57**) was treated with the appropriate amines to give pyrimidines **102**-**109**. Reduction of the 5-nitro group of **102**-**109** was performed using tin(II) chloride in refluxing ethanol to give diaminopyrimidines **110**-**117**, which were reacted with triethyl orthoacetate in the presence of TFA to give the required purine scaffold.

However, yields for this this cyclisation step varied with the substitution at the pyrimidine C^4-position. As the steric bulk of the amine increased, conversion to the purine decreased (Table 4), to the point that there was no reaction for *tert*-butylamine analogue **112**. In order to achieve a satisfactory conversion for the *N*-phenyl analogue **114** the reaction was carried out over 2.5 hours. Final coupling of 4-methoxyaniline to the purine intermediates (**118-124**) was accomplished in satisfactory yields. However, purification of the *iso*-propyl analogue **125** to sufficient purity for biological testing (≥95%) proved difficult.

5.3.2. Biological Results

All compounds were evaluated for inhibitory activity against Nek2 and Cdk2, and LE and LipE values were calculated (Table 5).

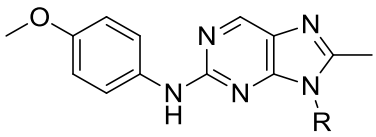

		IC_{50} (µM)			
Compound	**R**	**Nek2[a]**	**Cdk2[b]**	**LE[c]**	**LipE[d]**
63	Me	5.23	21%*	0.37	2.90
96	Et	21.3	49%*	0.31	1.96
97	iBu	43%*	17.3	N/A	N/A
98	Ph	13%*	28%*	N/A	N/A
99	Bn	>100	23%*	N/A	N/A
100	CH_2CF_3	51.4	91.8	0.25	0.94
101	$(CH_2)_2CF_3$	53.6	74.1	0.24	0.43

[a] Nek2 IC_{50} values determined at 30 µM ATP concentration; [b] Cdk2 IC_{50} values determined at 12.5 µM ATP concentration; [c] Ligand efficiency = ΔG/HA (where HA = number of heavy atoms); [d] Lipophilic efficiency = pIC_{50} – ClogP; * = Percentage inhibition at 100 µM; N/A = not applicable as no IC_{50}.

Table 5: Inhibitory activity of N^9-substituted 8-alkyl-2-arylaminopurines against Nek2 and Cdk2.

All attempts to increase the size of the substituent at the N^9-position resulted in a significant loss in inhibitor potency against Nek2. Based on the X-ray crystal structure, it is surprising that such steric constraints exist, but it appears that a methyl group is the largest tolerated substituent at this position. The observed loss in potency against Nek2 was also reflected by changes in the degree of selectivity over Cdk2, with compound **97** reversing the desired selectivity trend. For these reasons, no further work was conducted at the purine N^9-position, and subsequent compounds were synthesised with an N^9-methyl group.

5.4. Attempts to Make Additional Interactions with the DFG Motif at the 2-Arylamino Ring

5.4.1. Target Compound Selection and Synthesis

Previous attempts to probe the hydrophobic allosteric site of Nek2 in the vicinity of the purine 2-arylamino ring resulted in limited SARs and no appreciable improvement in activity. This may be a result of limited access to the hydrophobic pocket owing to the conformation of the DFG motif. It is known for classical type II ATP-competitive inhibitors that their ability to occupy the allosteric site is dependent on the compound's ability to stabilise the kinase in the inactive DFG-out conformation. To achieve this, interactions must arise between the inhibitor and the aspartate of the DFG motif. A small series of 2-arylaminopurines substituted with carboxamides and ureas (**126**-**131**) was proposed, to assess the hypothesis of interacting with the DFG motif, and hence to probe the allosteric site.

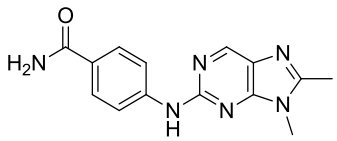

126

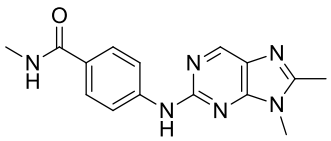

127

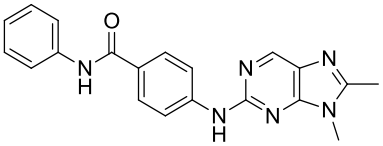

128

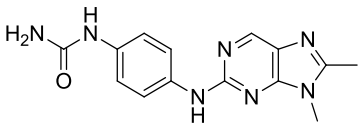

129

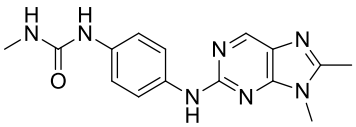

130

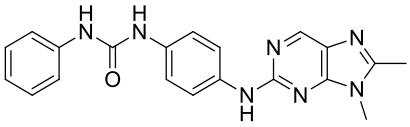

131

The synthesis of the required carboxamides entailed treatment of a common carboxylic acid intermediate (**132**) with carbonyldiimidazole (CDI) to activate the acid, followed by treatment with the appropriate amines. Previous work had reported that the coupling of anilines bearing carboxylic acids using TFA/TFE conditions resulted in formation of a trifluoroethyl ester, which required saponification to the acid. The S_NAr reactions also generally give rise to multiple products and contaminants, and isolation of a polar acid from this mixture can be challenging.

Scheme 12: Synthesis of carboxamide derivates **126**-**128**.

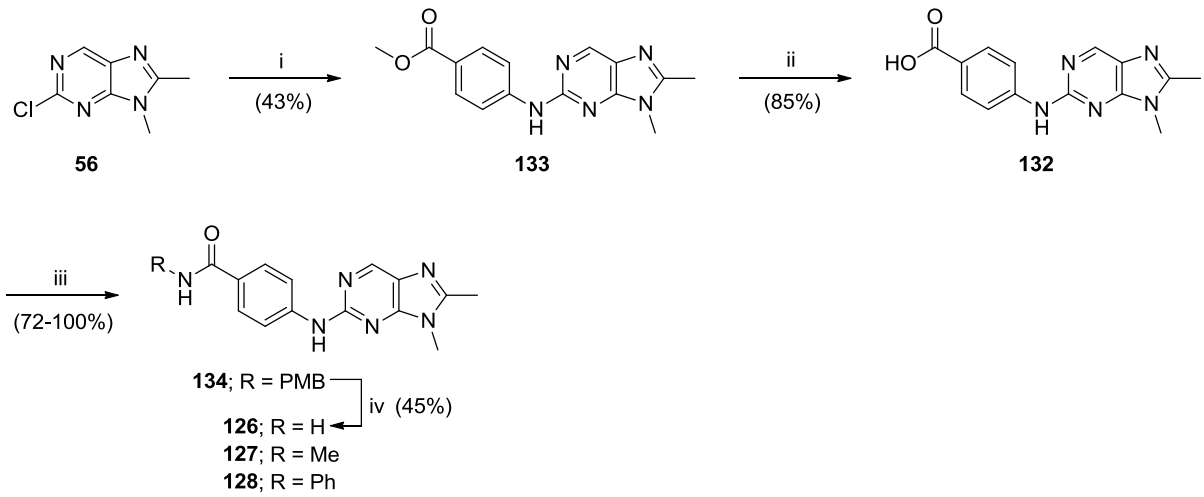

Reagents and conditions: i) Methyl-4-aminobenzoate, TFA, TFE, MW 160 °C, 1 h; ii) LiOH, THF, H_2O, 65 °C, 2 h; iii) RNH_2, CDI, DIPEA, DMF, RT, 18 h; iv) TFA, reflux, 18 h.

A synthetic strategy was developed whereby methyl-4-aminobenzoate was coupled to the purine (**56**), enabling isolation of the product (**133**) in high purity. Subsequent ester hydrolysis proceeded cleanly, allowing isolation of the intermediate (**132**). The CDI-mediated coupling of **132** with methylamine and aniline proceeded in good yields (72% and 77%, respectively). The primary carboxamide (**126**) was prepared by coupling with 4-methoxybenzylamine in quantitative yield. Subsequent cleavage of the PMB group of **134** afforded the primary carboxamide **126** in a modest overall yield (45%) (Scheme 12).

Synthesis of the target ureas also proceeded through a common intermediate (**135**). In this case the required intermediate was prepared by coupling 4-nitroaniline with the purine **56** to give the nitro purine **136**, followed by reduction of the nitro group to furnish **135**. The poorly nucleophilic nature of 4-nitroaniline hampered the coupling reaction, with prolonged heating required and giving rise to side products. This was reflected in the poor yield for this reaction (30%). Intermediate **135** could subsequently be functionalised to the desired ureas through reaction with suitable reagents. Reaction of the aniline group of **135** with cyanic acid and phenyl isocyanate proceeded smoothly to afford the urea (**129**) and *N*-phenyl urea (**131**) derivatives in 44% and 73% yield, respectively (Scheme 13). Synthesis of the target *N*-methylurea (**130**) was attempted by treating **135** with triphosgene, followed by reaction of the resultant isocyanate with methylamine. Although a product with the correct mass was

observed by LC-MS analysis, repeated attempts failed to improve the reaction sufficiently to afford the target compound **130** in suitable yield following purification.

Scheme 13: Synthesis of ureas **129** and **131**.

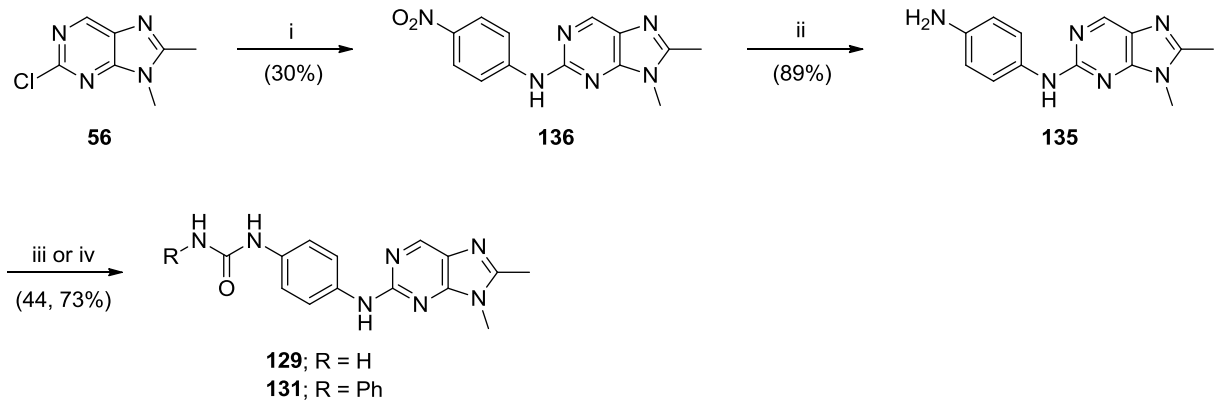

Reagents and conditions: i) 4-Nitroaniline, TFA, TFE, MW 160 °C, 6 h; ii) Pd/C, NH_4HCOO, MeOH, RT, 18 h; iii) Sodium cyanate, AcOH, H_2O, RT, 30 min; iv) Phenyl isocyanate, THF, RT, 18 h.

To avoid resynthesis of intermediate **134**, a synthetic approach to the *N*-methylurea **130** was employed in which formation of the urea moiety was carried out prior to coupling to the purine (**56**). Boc-protection of *para*-phenylenediamine (**137**) gave compound **138**, which when treated with *N*-succinimidyl *N*-methyl carbamate furnished the required *N*-methylurea (**139**). Removal of the Boc-protecting group gave aniline **140** required for coupling to purine **56**. It is interesting to note that TFA/TFE coupling conditions failed to yield any product (**130**) with aniline **140**. It is unlikely that this is due to the electron-withdrawing nature of the urea moiety of **140**, as it has been shown that it is possible to couple electron-poor anilines such as 4-nitroaniline under these condition, albeit with extended reaction times and in poor yields. One possibility is that **140** is unstable to the reaction conditions, as it was no longer detectable by LC-MS analysis of the reaction mixture.

Scheme 14: Synthesis of N-methylurea **130**.

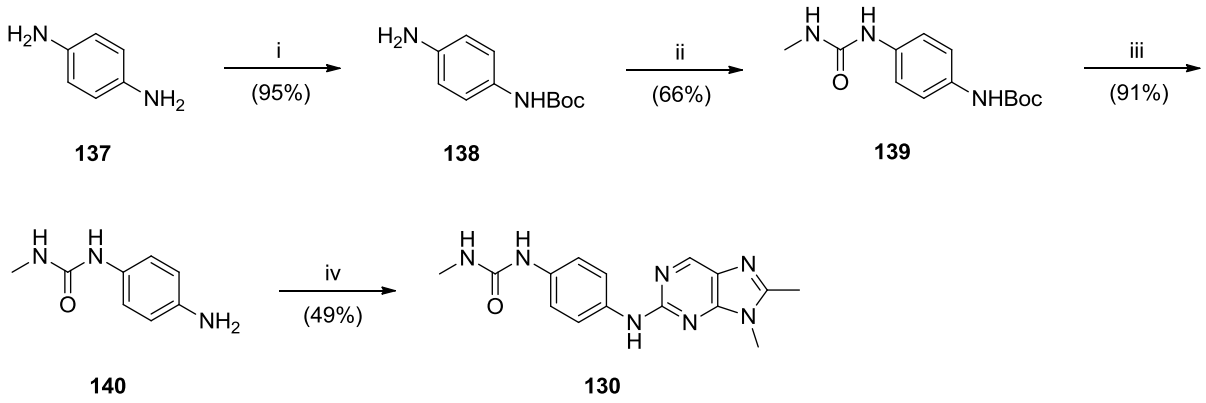

Reagents and conditions: i) Boc_2O, K_2CO_3, THF, DMF, H_2O, RT, 4 h; ii) *N*-succinimidyl *N*-methyl carbamate, DIPEA, DMF, 70 °C, 18 h; iii) TFA, DCM, RT, 18 h; iv) **56**, $Pd_2(dba)_3$, XPhos, K_2CO_3, MeCN, 100 °C, 2 h.

A Buchwald amination approach was employed as an alternative to TFA/TFE aniline coupling. A wide variety of conditions are available for such reactions.[203] Work elsewhere within the group established optimised conditions comprising tris(dibenzylideneacetone) dipalladium(0) ($Pd_2(dba)_3$), 2-dicyclohexylphosphino-2′,4′,6′-triisopropylbiphenyl (XPhos) and potassium carbonate in acetonitrile, as suitable for coupling of a variety of anilines to the purine (**56**). These reaction conditions were used successfully to couple aniline **140** to **56** in moderate yield (49%) (Scheme 14).

Scheme 15: Buchwald amination approach to the synthesis of **141**.

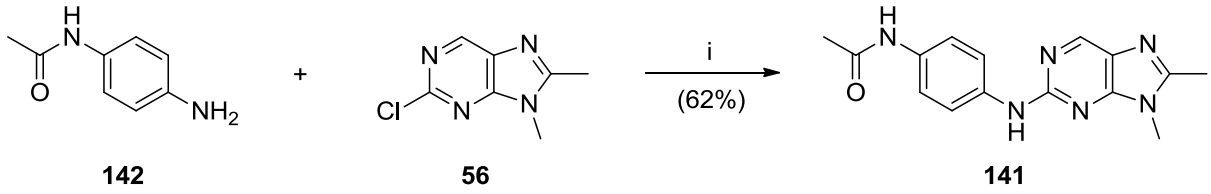

Reagents and conditions: i) $Pd_2(dba)_3$, XPhos, K_2CO_3, MeCN, 100 °C, 2 h.

A further functional group capable of forming interactions with the DFG motif is the *N*-acetyl amine **141**. The required aniline, 4-aminoacetanilide (**142**), failed to yield the desired product (**141**) under TFA/TFE coupling conditions, and was again synthesised using the Buchwald approach, affording target compound **141** in moderate yield (62%) (Scheme 15).

5.4.2. Biological Results

All target compounds (**126**-**131** and **141**) and the carboxylic acid intermediate **132** were evaluated for inhibitory activity against Nek2 and Cdk2, and LE and LipE values were calculated (Table 6).

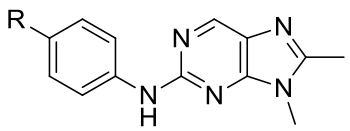

		IC_{50} (µM)			
Compound	**R**	**Nek2[a]**	**Cdk2[b]**	**LE[c]**	**LipE[d]**
63	OMe	5.23	21%*	0.37	2.90
132	CO_2H	8.3	43%*	0.34	3.02
126	$CONH_2$	4.3	40.0	0.36	3.96
127	CONHMe	5.8	34%*	0.33	3.60
128	CONHPh	11.3	39%*	0.26	1.64
129	$NHCONH_2$	5.1	31%*	0.34	4.21
130	NHCONHMe	11.1	32%*	0.30	3.63
131	NHCONHPh	3.4	26%*	0.27	2.49
141	NHCOMe	8.2	23%*	0.32	3.68

[a] Nek2 IC_{50} values determined at 30 µM ATP concentration; [b] Cdk2 IC_{50} values determined at 12.5 µM ATP concentration; [c] Ligand efficiency = ΔG/HA (where HA = number of heavy atoms); [d] Lipophilic efficiency = pIC_{50} – ClogP; * = Percentage inhibition at 100 µM.

Table 6: Kinase inhibitory activity of 2-arylamino-8-methylpurines **126**-**132** and **141** against Nek2 and Cdk2.

The inhibitory activities of compounds **126**-**132** and **141** against Nek2 indicate that all modifications made are tolerated at the 4-position of the purine 2-arylamino ring. When compared with the unsubstituted 2-phenyl analogue (**65**, Nek2; IC_{50} = 11.2 μM) it is clear that interactions are being made in the ATP-binding domain of Nek2, conferring improved potency. Furthermore, the polar nature of inhibitors in this series, in particular ureas **129**-**131**, equates to substantially improved lipophilic efficiency. However, despite tolerance of the substitutions made with respect to Nek2 inhibition, significant improvements in potency were not observed over the 4-methoxyaryl compound **63** (Nek2; IC_{50} = 5.23 μM). This suggests that although interactions with the DFG motif may occur, this approach is not adequate for achieving significant improvements in the binding affinity of 8-alkyl-2-arylaminopurines to Nek2.

5.5. Establishing Interactions with Asp93 at the C-8 of 2-Arylaminopurines

5.5.1. Target Compound Selection and Synthesis

Work within the group has attempted to establish an interaction between basic functional groups at the 8-position of 2-arylaminopurines and Asp93 of Nek2, observed to be close to this position when **46** is in complex with the ATP-binding site of Nek2 (see chapter 5.1.1.). To this end, a range of 2-arylamino-8-aminomethylpurines was synthesised, with variation of the basic group at the purine 8-position, culminating in the identification of **143**.

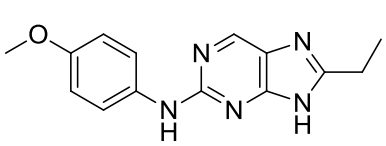

46
IC_{50}; Nek2 = 67.5 μM
Cdk2 = 39% at 100 μM

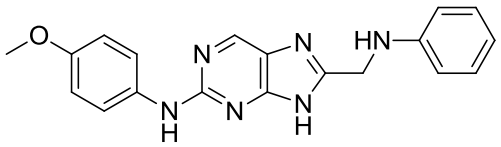

143
IC_{50}; Nek2 = 9.2 μM
Cdk2 = 27% at 100 μM

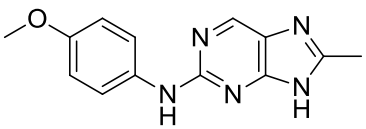

45
IC_{50}; Nek2 = 51.8 μM
Cdk2 = 18% at 100 μM

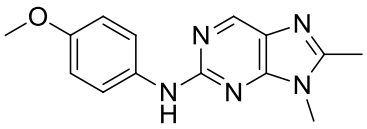

63
IC_{50}; Nek2 = 5.23 μM
Cdk2 = 21% at 100 μM

A comparison between the Nek2 inhibitory activities of **143** and **46** suggests that an interaction is being made within the kinase ATP-binding domain resulting in the observed

increase in potency. Previously it had been shown that when methylated at the purine N^9-position (*e.g.* **63**, Nek2; IC_{50} = 5.23 μM), compounds within the 8-alkyl-2-arylaminopurine series have improved binding affinity for Nek2 compared with their N^9-unsubstituted analogues (*e.g.* **45**, Nek2; IC_{50} = 51.8 μM). Although the degree to which the potency of such compounds is improved is variable, synthesis of the N^9-methylated analogue of **143** (**144**) is a potential approach to improve the activity of compounds within the 2-arylamino-8-aminomethylpurine series.

Intermediate **145**, previously prepared within the group, was deprotonated at the purine 8-position by treatment with LDA, and reaction with DMF afforded the 8-formylpurine **146**, as observed by LC-MS analysis and TLC. In previous studies, reactions of this type were performed using an N^9-THP protected purine, and were typically high yielding (81-91%). It is possible that the THP protecting group acts to coordinate the lithium base and facilitate deprotonation of the purine C^8-carbon. In this case, the target compound **144** was prepared by reductive amination of the aldehyde group of crude **146** with aniline and sodium borohydride in relatively poor yield (36% over 2 steps) (Scheme 16).

Scheme 16: Synthesis of 2-arylamino-8-aminomethylpurine **144**.

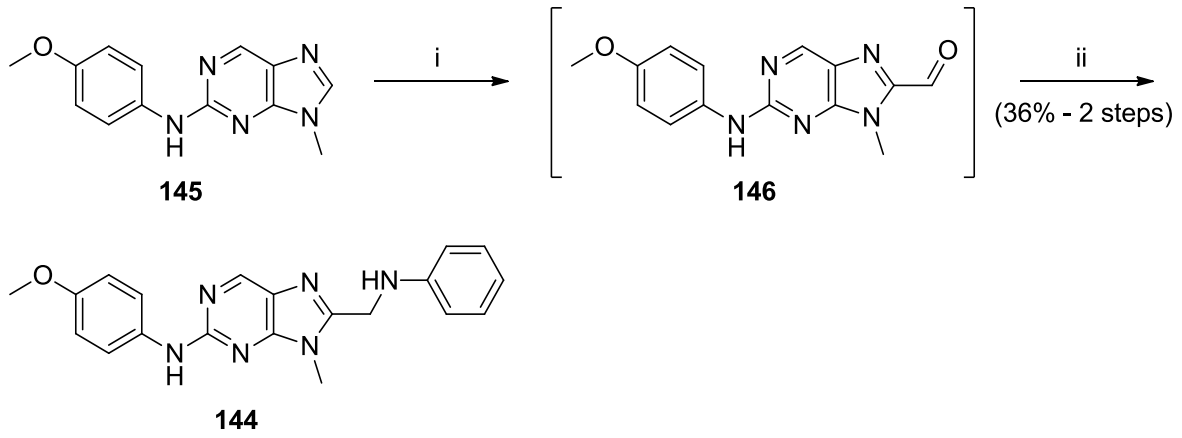

Reagents and conditions: i) a) LDA, THF, -90 °C, 15 min, b) DMF, -90 °C to RT, 2 h; ii) a) Aniline, Mg_2SO_4, DCM, RT, 2 h, b) $NaBH_4$, DCM, RT, 6 h.

5.5.2. Biological Results

Compound **144** was tested for inhibitory activity against Nek2 and Cdk2:

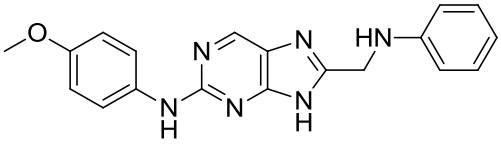

143
IC_{50}; Nek2 = 9.2 μM
Cdk2 = 27% at 100 μM

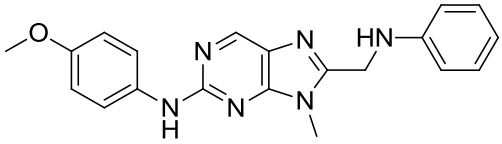

144
IC_{50}; Nek2 = 34% at 100 μM
Cdk2 = 40% at 100 μM

The significant reduction in inhibitory potency for **144** with respect to **143** suggests that it is unlikely that these compounds occupy the ATP-binding site of Nek2 in the same orientation as **46**. To investigate this, attempts were made to obtain an X-ray crystal structure of **144** in complex with Nek2. However, it was not possible to obtain such a structure as the electron density observed suggested that **144** binds to the ATP-binding site of Nek2 in more than one orientation. It is likely that compound **143** also resides within the kinase in a binding conformation distinct from that of **46**, as previous SARs have indicated that methyl is the largest group tolerated at the purine C^8-position (*e.g.* **45**, Nek2; IC_{50} = 51.8 μM).

5.6. Conclusions and Further Work

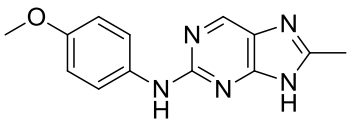

45
IC_{50}; Nek2 = 51.8 μM

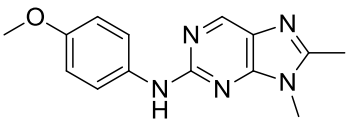

63
IC_{50}; Nek2 = 5.2 μM

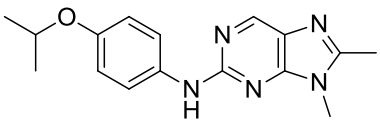

71
IC_{50}; Nek2 = 4.7 μM

To improve the selectivity of 2-arylaminopurines for Nek2 over Cdk2, a series of 8-alkypurines was synthesised to take advantage of the disparity in gatekeeper residues between the two kinases. Such compounds (*e.g.* **45**, Nek2; IC_{50} = 51.8 μM) were found to occupy the ATP-binding domain of Nek2 in an unusual conformation, presenting opportunities to substitute the purine scaffold at positions not previously viable. Efforts were made to improve the binding affinity of 8-alkyl-2-arylaminopurines by probing putative hydrophobic pockets at the 4-position of the 2-arylamino ring (*e.g.* **71**; R = ^{i}PrO, Nek2; IC_{50} = 4.7 μM) and at the purine N^9-position (*e.g.* **63**; R = Me, Nek2; IC_{50} = 5.2 μM), culminating in low micromolar inhibition of Nek2.

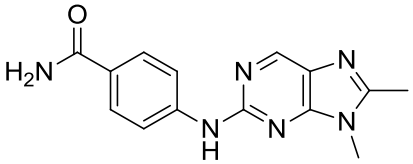

126

IC_{50}; Nek2 = 4.3 μM

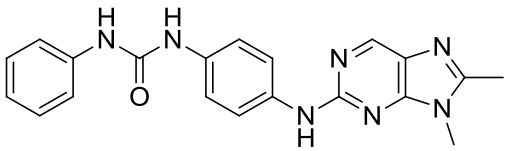

131

IC_{50}; Nek2 = 3.4 μM

X-ray crystallographic analysis of 8-alkyl-2-arylaminopurines (*e.g.* **63**) in complex with the ATP-binding domain of Nek2 indicated that interactions were possible with the DFG motif of Nek2 through substitution at the 2-arylamino ring. A series of 8-alkyl-2-arylaminopurines, bearing substituted carboxamides (*e.g.* **126**, Nek2; IC_{50} = 4.3 μM) and ureas (*e.g.* **131**, Nek2; IC_{50} = 3.4 μM) at the 4-position of the 2-arylamino ring, was prepared. Despite limited improvements in inhibitor potency, such compounds possessed enhanced ligand efficiency and lipophilic efficiency. The improved drug like properties and low molecular weight of such compounds indicated that they may serve as suitable starting points for the development of further inhibitors. However, at this stage in the project the focus of research was turned to a compound series with potency surpassing that achieved thus far.

Chapter 6: Synthesis of 6-Ethynylpurines

6.1. Identification of 6-Ethynylpurines as Irreversible Inhibitors of Nek2

As an additional area of research, with the intention of improving inhibitor potency and selectivity, SARs were conducted at the purine 6-position. These studies identified the 6-ethynylpurine **147**, which displayed significantly improved Nek2 inhibitory activity compared with **35** and moderate selectivity over Cdk2.

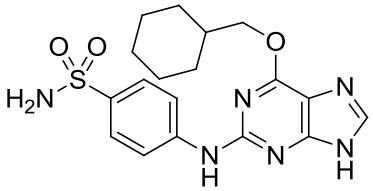

35
IC_{50}; Nek2 = 12 μM
Cdk2 = 5 nM

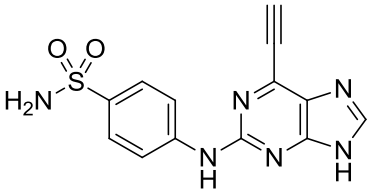

147
IC_{50}; Nek2 = 0.14 μM
Cdk2 = 0.84 μM

The 6-ethynylpurine pharmacophore possesses a non-classical Michael acceptor motif, as the alkyne moiety is activated through the electron-withdrawing effect of the purine ring nitrogens. Interest in such compounds was heightened when it was noted that compound **147** exhibited a kinetic profile characteristic of an irreversible inhibitor in a kinase inhibition reversibility assay (Figure 26). The assay evaluated the ability of an enzyme, pre-incubated with an inhibitor, to recover activity upon rapid dilution of the enzyme-inhibitor complex with a solution containing the natural cofactor of the enzyme (*e.g.* ATP) and a substrate peptide. Analysis of the kinetics of the recovery of enzyme activity can aid in determining the mechanism of action of an inhibitor when compared to inhibitors of known mechanism. Following a 30 minute pre-incubation with **147** at a concentration 10-fold in excess of its IC_{50}, the enzymatic activity of Nek2 was slow to recover when the Nek2-**147** complex was diluted with a solution containing ATP and a substrate 'peptide-11'. 1 hour post-dilution the enzymatic activity of Nek2 had recovered to approximately 3%. When the assay was conducted with a known ATP-competitive inhibitor of Nek2, the enzyme activity had recovered to approximately 11% 1 hour post-dilution. This suggests that **147** is making significant interactions within the ATP-binding domain of Nek2 such that it is acting as a tight-binding reversible inhibitor, or as an irreversible inhibitor of Nek2.

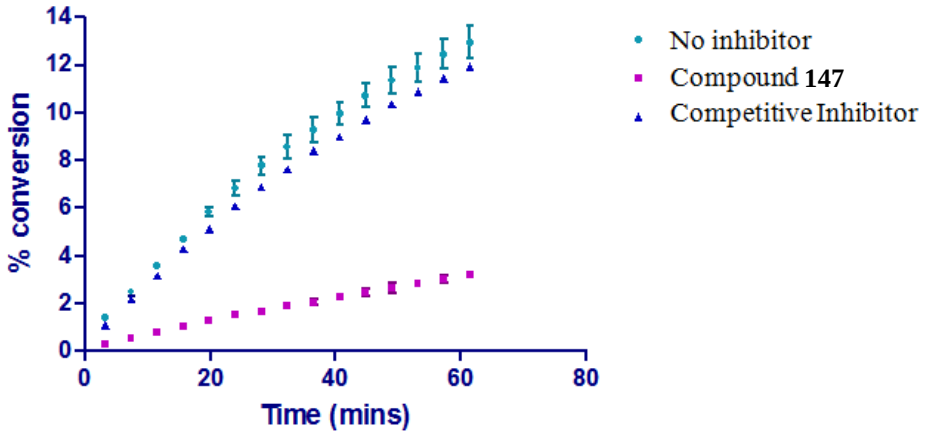

Figure 26: Recovery of enzyme activity of Nek2 following dilution of the enzyme-inhibitor complex with ATP for **147** and a known ATP-competitive inhibitor of Nek2.

Through our understanding of the binding mode of 8-unsubstituted purines, it was known that the terminal moiety of the alkyne of **147** would be presented towards the region of the Nek2 ATP-domain containing the glycine rich loop. As previously mentioned, Nek2 is a group 2B cysteine containing kinase, with a cysteine (Cys22) occupying the second amino acid position following the glycine rich loop. To determine whether the tight-binding enzyme kinetics observed between **147** and Nek2 are due to nucleophilic attack of Cys22 at the Michael acceptor alkyne group, the X-ray crystal structure of the ATP-binding domain of Nek2 in complex with **147** was determined at 2.0 Å (Figure 27). Compound **147** was found to interact with the hinge region of Nek2 through a triplet of hydrogen bonds as previously described for purine based inhibitors. The formation of a thioenol ether bond between the Cys22 residue of the protein and the purine 6-position was also observed, confirming that the purine acts as a Michael acceptor for the Cys22.

The effect of **147** on the growth of U2OS (osteosarcoma) and HeLa (cervical) cancer cell lines was determined. Unfortunately, the activity of **147** was outside of the range of the assay (GI_{50}; U2OS = >100 µM, HeLa = >100 µM), and this poor cellular activity was attributed to limited cell permeability. The sulfonamide moiety likely contributes to the highly polar nature of the compound (CLogP = 0.92), and this group is also known to confer potency towards Cdk2. It was therefore desirable to remove the sulfonamide to improve both cell permeability and selectivity.

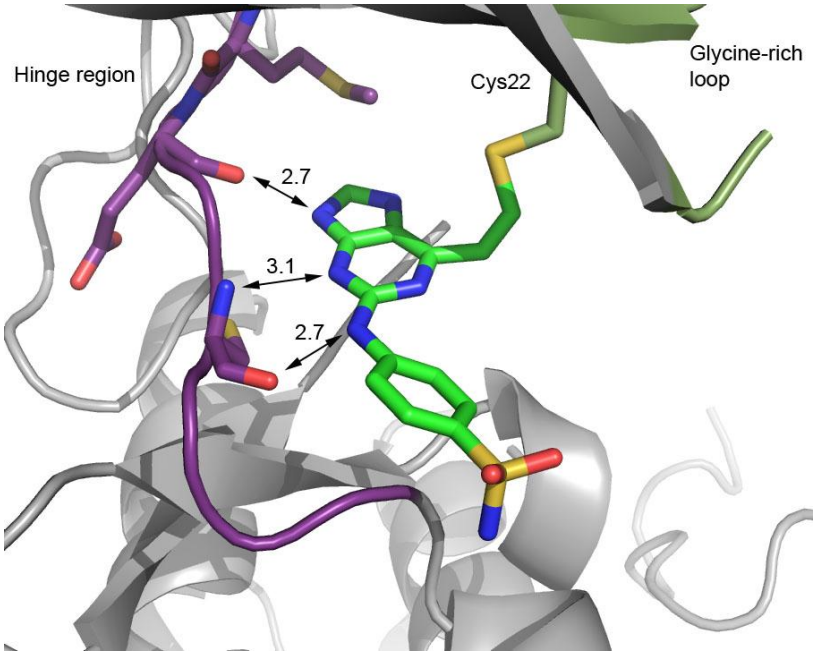

Figure 27: X-ray crystal structure of **147** in complex with Nek2 showing interactions with the hinge region and covalent modification of Cys22.

6.2. Identification of Cell Permeable 6-Ethynylpurines

6.2.1. Target Compound Selection and Synthesis

In addition to removal of the sulfonamide moiety from **147**, investigation of initial SARs for the 6-ethynylpurine series was undertaken. It was known that the H-bond motif (C^2-NH/N^3/N^9-H) is important for interactions with the kinase hinge region, which in turn positions the electrophilic 6-alkyne group towards Cys22. Observations from the 8-alkylpurine series suggested that substitution at the 8-position would be unfavourable for compounds of this class. Other work within the group was focussed on alternative electrophiles at the purine 6-position, and as such the effect of modifying the 2-arylamino ring on inhibitor potency remained to be evaluated.

To establish preliminary SARs at the 2-position, a defined series of compounds, bearing small alkyl and other simple substituents on the 2-arylamino ring, intended to probe this region of the kinase, was designed (**148**-**158**). Trends within previous series had suggested that *ortho*-substitution of the 2-arylamino ring is poorly tolerated. For this new inhibitor class it was necessary to corroborate these finding, and the *ortho*-methoxy (**155**) and *ortho*-chloro (**158**) analogues were included for this purpose.

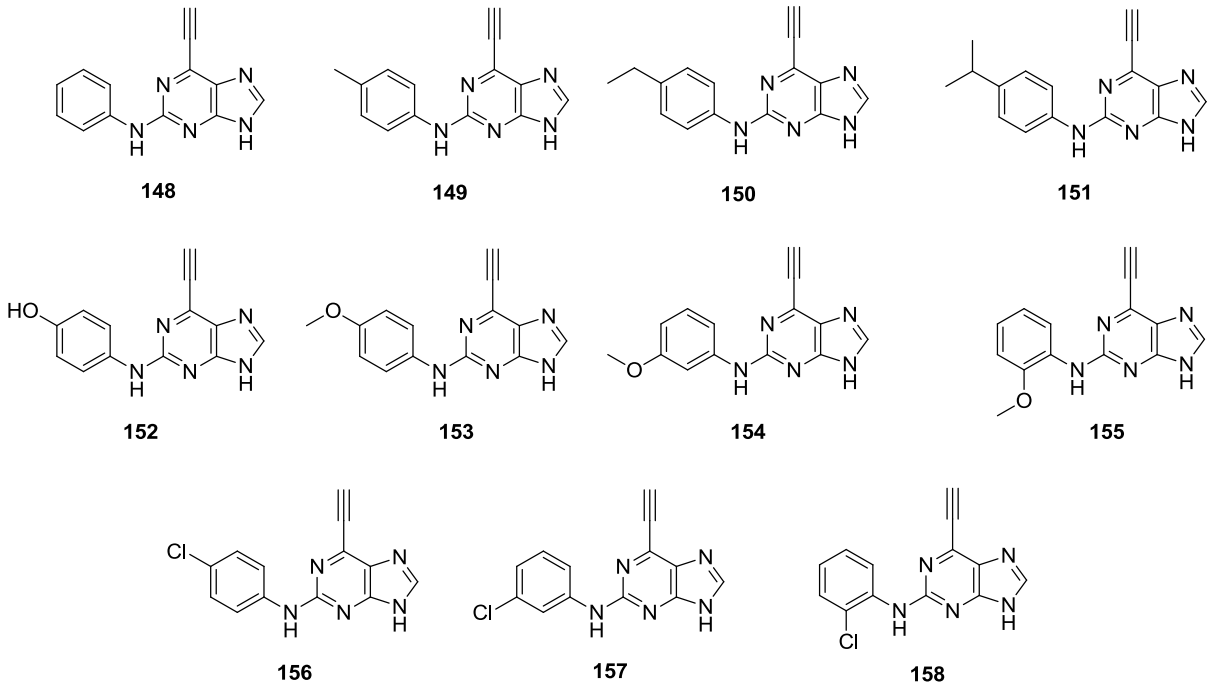

Previous work within the group had established a viable synthetic route for the synthesis of 6-ethynylpurines (Scheme 17).[204] Synthesis of the THP-protected 2-fluoro-6-chloropurine (**51**) was achieved using a Balz-Schiemann reaction on 2-amino-6-chloropurine (**49**) followed by THP-protection of the purine N^9-position of the resulting 2-fluoro-6-chloropurine (**50**). The ethynyl function was introduced selectively at the purine 6-position of **51** using Sonogashira methodology to give intermediate **159** in excellent yield (96%). Removal of the N^9-THP protecting group from **159** under acidic conditions afforded the key 2-fluoropurine intermediate **160**. Coupling of the appropriate anilines was carried out under the TFA/TFE conditions previously described, with variable yields attained. The reaction between intermediate **160** and 4-aminophenol was attempted for the synthesis of the 4-hydroxylphenyl analogue **152**. However, this resulted in a complex mixture of products with only a trace amount of the desired compound evident by LC-MS, and it was thus deemed necessary to protect the phenol hydroxyl group. Treatment of 4-nitrophenol (**161**) with triisopropylsilyl chloride gave the TIPS-protected compound **162**, and the aromatic nitro group was reduced with zinc powder in acetic acid to give the required aniline **163** (Scheme 18).

Scheme 17: Synthesis of 2-arylamino-6-ethynylpurines.

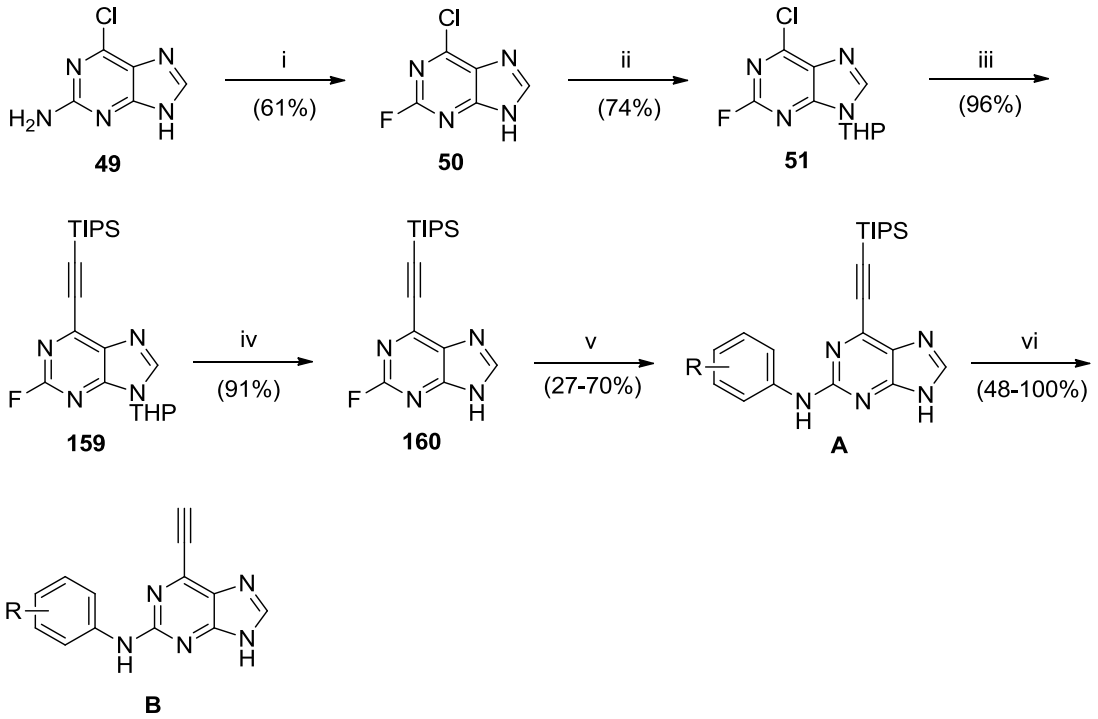

Reagents and conditions: i) $NaNO_2$, HBF_4, 0 °C to RT, 70 min; ii) DHP, CSA, EtOAc, reflux, 18 h; iii) TIPS-acetylene, $Pd_2Cl_2(PPh_3)_2$, CuI, Et_3N, THF, RT, 18 h; iv) TFA, IPA, H_2O, reflux, 2h; v) $ArNH_2$, TFA, TFE, reflux, 24 h; vi) TBAF, THF, RT, 5 min.

	Compound number	
R	**A**	**B**
H	**164**	**148**
p-Me	**165**	**149**
p-Et	**166**	**150**
p-iPr	**167**	**151**
p-OTIPS	**168**	-
p-OH	-	**152**
m-MeO	**169**	**154**
o-MeO	**170**	**155**
p-Cl	**171**	**156**
m-Cl	**172**	**157**

Table 7: 6-Ethynylpurines prepared according to Scheme 17.

Scheme 18: Synthesis of aniline **163**.

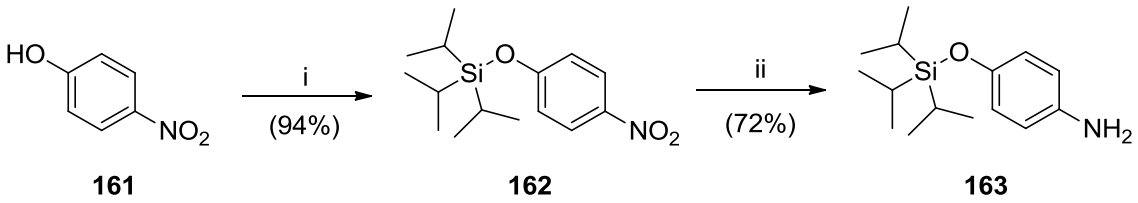

161 **162** **163**

Reagents and conditions: i) TIPSCl, imidazole, DCM, RT, 2 h; ii) Zn, AcOH, RT, 2.5 h.

Coupling of aniline **163** with the 2-fluoropurine intermediate **160** gave **168** in poor yield (27%), suggesting that the silyl ether was unstable under the reaction conditions used. Despite this, the quantity of product isolated was sufficient to furnish the target inhibitor **152** on treatment of **168** with TBAF. No product was observed when attempting to couple *ortho*-chloroaniline with **160** under the standard conditions. Efforts to identify alternative conditions in order to obtain this compound were postponed pending the results for the inhibitory activity of the *ortho*-methoxyphenyl compound **155**, and the *para*-methoxyphenyl analogue **153** was prepared by a colleague within the group. The TIPS-protecting groups were removed from all compounds (**164**-**172**) with TBAF to afford the target inhibitors (**148**-**157**) following purification. Unfortunately, it was not possible to isolate the *ortho*-methoxyarylamino analogue **155** in sufficient purity for biological testing, and other results mitigated against further efforts to synthesise this compound.

6.2.2. Biological Results

The substituted 2-arylaminopurines (**148**-**154**, **156** and **157**) were tested for inhibitory activity against Nek2 and Cdk2. For quoted IC_{50} values (Table 8) the incubation time of inhibitor with kinase was 30 minutes.

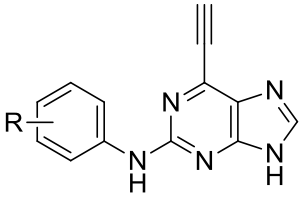

		IC_{50} (µM)	
Compound	**R**	**Nek2**[a]	**Cdk2**[b]
148 (NCL-00016727)	H	0.14 ± 0.1	22.9
149	*p*-Me	0.26	30.2
150	*p*-Et	0.18	40.6
151	*p*-^{i}Pr	0.40	54.7
152	*p*-OH	0.50	-
153	*p*-OMe	0.16	-
154	*m*-OMe	0.09	14.6
156	*p*-Cl	0.16	-
157	*m*-Cl	0.21	9.0

[a] Nek2 IC_{50} values determined at 30 µM ATP concentration; [b] Cdk2 IC_{50} values determined at 12.5 µM ATP concentration.

Table 8: Kinase inhibitory activity of substituted 2-arylamino-6-ethynylpurines against Nek2 and Cdk2.

Compounds within this series (**148**-**154**, **156** and **157**) combined good inhibitory potency against Nek2, with at least 40-fold selectivity over Cdk2. As was perhaps expected with time-dependent inhibitors, SARs were difficult to evaluate. All compounds appear to exhibit the necessary initial competitive reversible binding to Nek2, allowing subsequent covalent

reaction between Cys22 and the alkyne moiety to take place. Therefore, if the initial binding affinity is relatively uniform across the compound series, it would perhaps be expected that the final IC_{50} values following 30 minutes incubation with the kinase may show little variation, giving the observed values within a relatively confined potency range (~0.10-0.50 µM). This limits the conclusions that can be drawn from these data, apart from the fact that substitution on the 2-arylamino ring is generally well tolerated. It is possible that compounds **151** and **152** undergo slower initial competitive binding, accounting for the modest loss of potency, although more detailed kinetic studies, for all compounds over short incubation times, would be required to confirm this.

Enzyme	Nek2	Nek1	Cdk1	Cdk2	Cdk4	Cdk7	Cdk9	Plk1	P70S6K
IC_{50} (µM)	0.15	20.8	40.4	22.9	17%*	76.7	25%	15.0	16.0
Enzyme	Chk1	Chk2	Aur A	PKCz	Rsk1	PRAK	Erk1	PKD2	CK1d
IC_{50} (µM)	12.0	4.4	1.3	21.8%*	22.8	29%*	26.4	47%*	40.2
Enzyme	ABL	FYN	LYN	MET	LCK	SRC	GSK3b	Erk2	PKA
IC_{50} (µM)	13.1	20.9	24.8	86.8	14.4	11.2	7.4	22.2	46%*
Enzyme	AKT2	INSR	P38a	AKT1	Msk1				
IC_{50} (µM)	55.4	25%*	9%*	33%*	16%*				

* = Percentage inhibition at 100 µM.

Table 9: Inhibitory activity of **148** (NCL-00016727) against selected kinases.

The 2-phenylaminopurine **148**, designated NCL-00016727, was selected for further studies to investigate initial cellular effects of inhibitors within this class. To improve the confidence that Nek2 inhibition was responsible for any observed cellular activity, **148** was tested against a small panel of in-house kinases to establish preliminary selectivity data (Table 9). Despite evidence of modest Aurora A and Chk2 inhibition, at least 10-fold selectivity for Nek2 was maintained. Interestingly, **148** was poorly active against Nek1 (IC_{50} = 20.8 µM), which shares a high sequence homology with Nek2 within the active site, but lacks the corresponding cysteine residue necessary for covalent modification to occur. Furthermore, selectivity was maintained over Rsk1, Plk1 and Msk1, kinases that contain active-site cysteine residues capable of reacting with **148**.

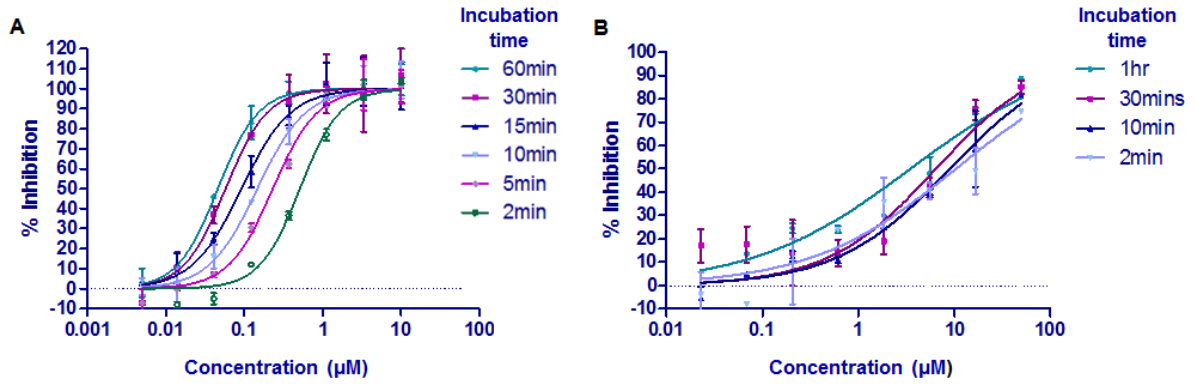

Figure 28: Dose-response curves as a function of incubation time between **148** and Nek2-WT (**A**), and Nek2-C22A (**B**).

Further evidence for the irreversible mechanism by which compounds within this class inhibit Nek2 was obtained through the observation of a time-dependent inhibition profile when the duration of incubation of Nek2 with **148** was varied prior to measurement of an IC_{50} value (Figure 28; **A**). To confirm whether time-dependent inhibition was mediated through Cys22, site-directed mutagenesis of the Cys22 residue to an alanine (Nek2-C22A) was performed, resulting in only weak competitive inhibition by **148** (IC_{50}, Nek2-C22A = 3.5 µM), with no increase in the degree of inhibition being observed with time of incubation (Figure 28; **B**).

	GI_{50} (µM) [a]			
Compound	**U2OS** (Osteosarcoma)	**HeLa** (Cervical)	**MDA-MB-231** (Breast)	**HEK293** (Kidney)
147 (NCL-00016066)	>100	>100	N.D.[b]	N.D.
148 (NCL-00016727)	1.8	1.2	1.1	0.1

[a] Half maximal growth inhibitory concentration; [b] Not determined.

Table 10: Growth-inhibitory activity of **147** and **148** in selected tumour cell lines.

The effect of **148** on the growth of three tumour cell lines, as well as the 'normal' HEK293 cells, was determined (Table 10). When compared to the **147**, compound **148** showed markedly increased growth inhibitory activity in the cell lines studied. This indicated that removal of the polar sulfonamide group improved the cellular permeability of the 6-

ethynylpurine. Activity in the HEK293 cell line raises the possibility of non-specific toxicity, although this cell line is of limited value as a surrogate for normal tissue.

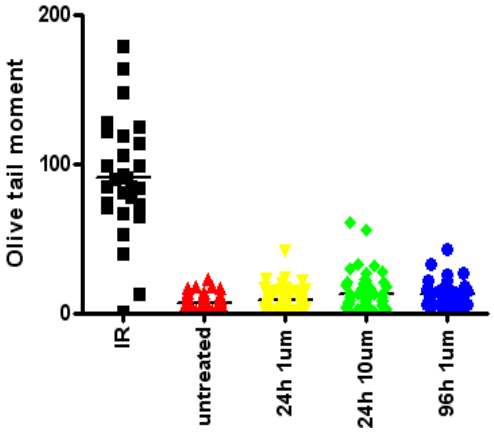

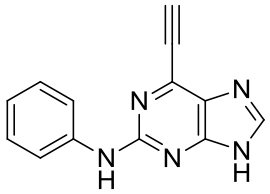

148

Figure 29: Comet assay results for cells treated with **148**.

There is literature evidence to implicate 6-vinylpurines as DNA damaging agents, thought to occur through covalent conjugate addition between the DNA bases and the vinyl substituent.[205] Given the mechanism of the 6-ethynylpurine inhibitors, it was suggested that they could act as DNA alkylators *via* a similar mechanism. This could be an alternative locus of action for the cellular activity of **148**. In order to determine the effect of treatment with the inhibitor on cellular DNA damage, a Comet assay[206] was performed (Figure 29). MDA-MB-231 breast cancer cells were treated with **148** for up to 96 hours before being embedded in agarose, lysed, and treated with alkali to denature and unwind the DNA. Gel electrophoresis causes any damaged DNA fragments to move with the electric field out of the nucleoid. Undamaged DNA migrates more slowly under the electric field, and so remains within the nucleoid. Damaged DNA fragments are observed to streak from the nucleoid in the shape of an olive when stained with a DNA-specific dye, and DNA damage is measured as an 'Olive tail moment' and compared to an IR positive control. Cells treated with **148** displayed minor olive tail moments when compared to the IR control, and were similar to untreated cells, confirming that DNA damage is not a major effect of inhibitor treatment.

To confirm that cellular Nek2 is inhibited upon treatment with **148**, a cellular biomarker was required. The phosphorylation state of C-Nap1 localised to the centrosomes was used. As C-Nap1 is a substrate only for Nek2, this can be used as a direct measure of cellular Nek2 activity. Staining of cells with an antibody specific for phosphorylated C-Nap1 (pC-Nap1, see chapter 7.3) allows for the percentage of cells containing pC-Nap1 at the centrosomes to be

determined by immunofluorescence microscopy (IFM). Treatment of U2OS cells with a dose range of inhibitor, followed by staining with the pC-Nap1 antibody, showed a dose-dependent decrease in phosphorylated C-Nap1, analogous to inhibition of Nek2 activity, with increasing concentration of **148** (Figure 30). This indicated that not only does this compound enter cells and elicit growth inhibition, it also inhibits cellular Nek2 in a dose-dependent manner.

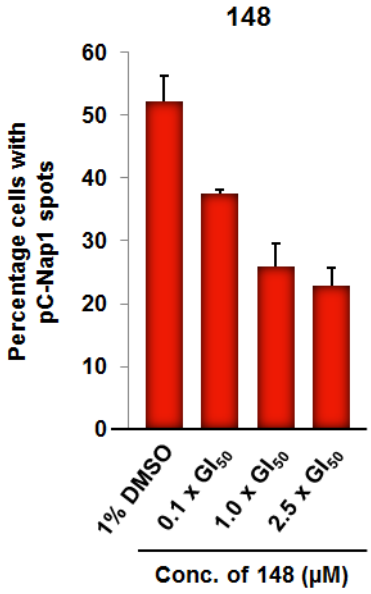

Figure 30: Dose response of pC-Nap1 levels in U2OS cells following **148** treatment.

The series of compounds synthesised exhibited good inhibitory activity against Nek2, with a small range of structural modifications at the 2-arylamino ring, confirming that this position is amenable to modification and worthy of further investigation. Limited SARs were apparent, owing to the irreversible action of compounds within this class. It is likely that significant differences in potency between compounds will be observed only when there is a large difference in the initial competitive binding affinity, or for compounds that do not react covalently with Nek2. **148** has been shown to be a cell permeable 6-ethynylpurine, exhibiting potent growth inhibition in all cell lines tested. Furthermore, the use of a pC-Nap1 biomarker confirmed inhibition of cellular Nek2 levels upon treatment with inhibitor. 6-Ethynylpurine **148** was therefore a suitable starting point from which to conduct modification to further improve inhibitor potency.

6.3. Designing 6-Ethynylpurines with Improved Potency

6.3.1. Target Compound Selection and Synthesis

As a means to achieve improved activity for compounds within the 6-ethynylpurine class, it was proposed that 2-arylamino side-chains that had been shown to confer good potency against Nek2 when incorporated into Nek2 competitive inhibitors based on 6-alkoxypurines should be investigated. A common feature of potent compounds within previous purine classes was a 2-arylamino ring bearing a basic group. Several examples were selected to be incorporated onto the 6-ethynylpurine, based on the inhibitory activity of the corresponding 2-arylamino-O^6-cyclohexylmethoxypurines (Table 11). In doing so, it was proposed that improvement in the initial competitive binding component of inhibitors would translate into enhanced potency for the irreversible inhibitor.

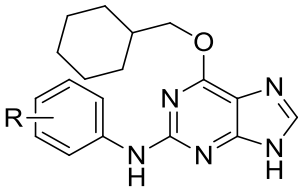

R	Position	Compound	Nek2 IC_{50} (μM)
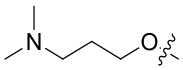	*para*	**173**	0.93
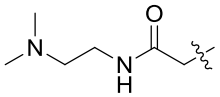	*meta*	**174**	1.00
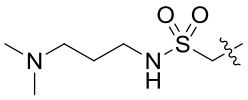	*meta*	**175**	0.89
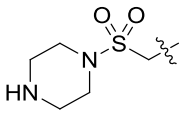	*meta*	**176**	1.70

Table 11: Nek2 inhibitory activity of compounds bearing 2-arylamino side-chain groups known to confer favourable potency against Nek2 when incorporated into the 2-arylamino-O^6-cyclohexylmethoxy purine scaffold.

Owing to their ease of synthesis from common intermediates, it was also decided to prepare the primary carboxamide (**177**) and sulfonamide (**178**) to further establish potential SARs at this position. This generated a small series of target compounds (**177**-**182**).

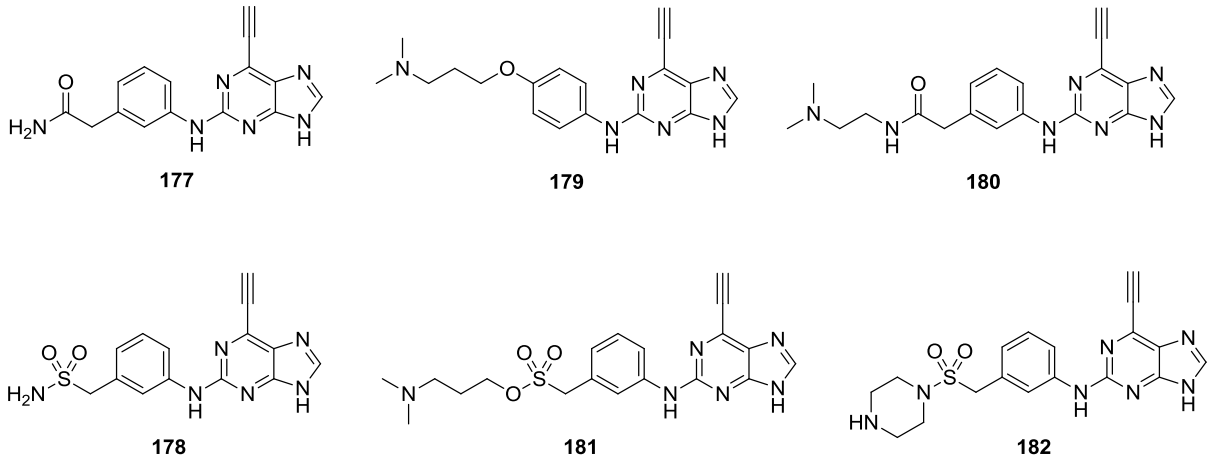

Synthesis of the requisite aniline to prepare **179** involved a reaction between 4-nitrophenol (**161**) and 3-dimethylaminopropyl chloride to give **183**. The nitro group of **183** was reduced by palladium-mediated hydrogenation to give aniline **184** in good yield (91%). Coupling of **184** to the 2-fluoropurine intermediate **160** gave the TIPS-protected precursor (**185**) of the desired compound in moderate yield (41%) (Scheme 19).

Scheme 19: Synthesis of the TIPS-protected purine **185**.

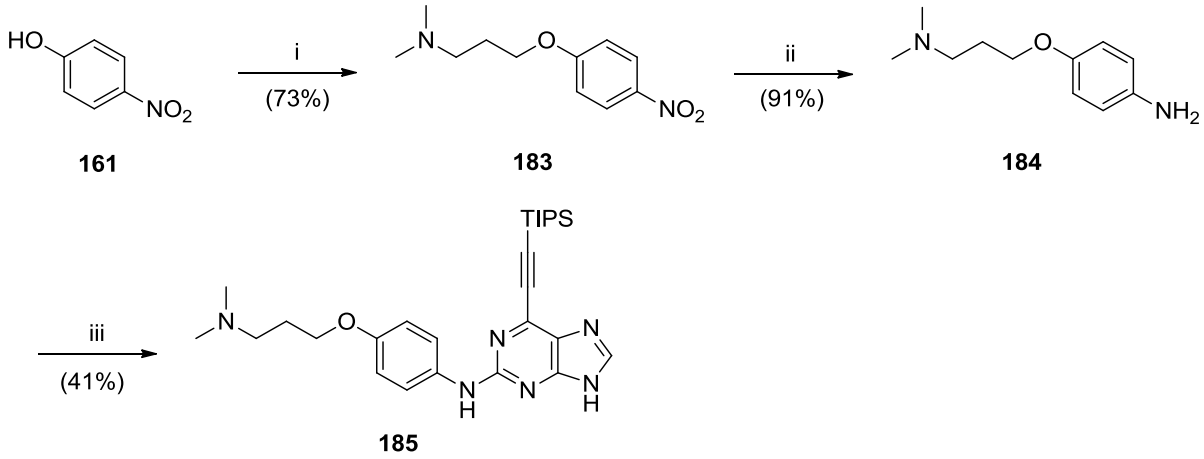

Reagents and conditions: i) $(CH_3)N(CH_2)_3Cl.HCl$, K_2CO_3, DMF, 80 °C, 2 h; ii) H_2, Pd/C, EtOH, RT, 18 h; iii) **160**, TFA, TFE, reflux, 24 h.

In order to synthesise the desired carboxamides (**177** and **180**), a common intermediate coupled to the purine scaffold was required. This was generated through coupling of 3-aminophenylacetic acid to 2-fluoropurine intermediate **160** under TFA/TFE mediated conditions. As previously mentioned, this resulted in the formation of a trifluoroethyl ester, which was hydrolysed to the required acid **186** without isolation. Carboxamide formation

reactions were performed using CDI coupling conditions with 4-methoxybenzylamine and *N*,*N*-dimethylethylenediamine to give **187** and **188** in excellent yields (99% and 100%, respectively). Acidic deprotection of the PMB-carboxamide **187** proceeded very slowly to give the desired primary carboxamide **189** in good yield (90%) (Scheme 20).

Scheme 20: Synthesis of carboxamides **188** and **189**.

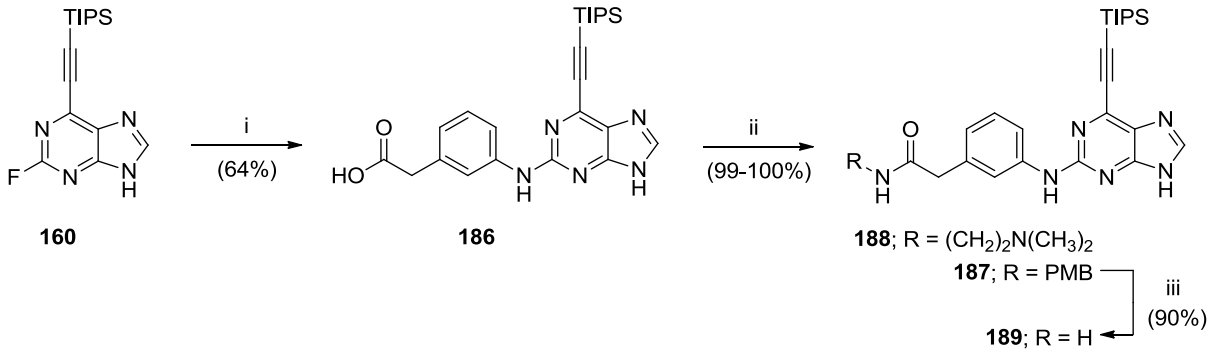

Reagents and conditions: i) a) 3-Aminophenylacetic acid, TFA, TFE, reflux, 24 h, b) 1M NaOH, THF, RT, 18 h; ii) RNH_2, CDI, DIPEA, DMF, RT, 18 h; iii) TFA, reflux, 72 h.

It was demonstrated previously that fluorinated sulfonate esters are useful intermediates for the synthesis of substituted sulfonamides.[207] To this end, the trifluoroethylsulfonate ester **190** was prepared by treatment of 3-nitro-α-toluenesulfonyl chloride (**191**) with TFE in the presence of DMAP. Reduction of the nitro group of **190** and coupling with 2-fluoropurine **160** gave **193** (Scheme 21). Conversion into the target sulfonamides was performed under microwave irradiation conditions in the presence of DBU. The reaction between sulfonate ester **193** and 4-methoxybenzylamine gave the PMB-protected sulfonamide **194**, which was converted into the primary sulfonamide **195** on treatment with refluxing TFA. *N*,*N*-Dimethylpropane-1,3-diamine was coupled with **193** to give sulfonamide **196**. The piperazinyl analogue (**197**) was prepared from **193** and Boc-protected piperazine to give **198**, which gave **197** on treatment with TFA in DCM.

Scheme 21: Synthesis of sulfonamides **195**, **196** and **197**.

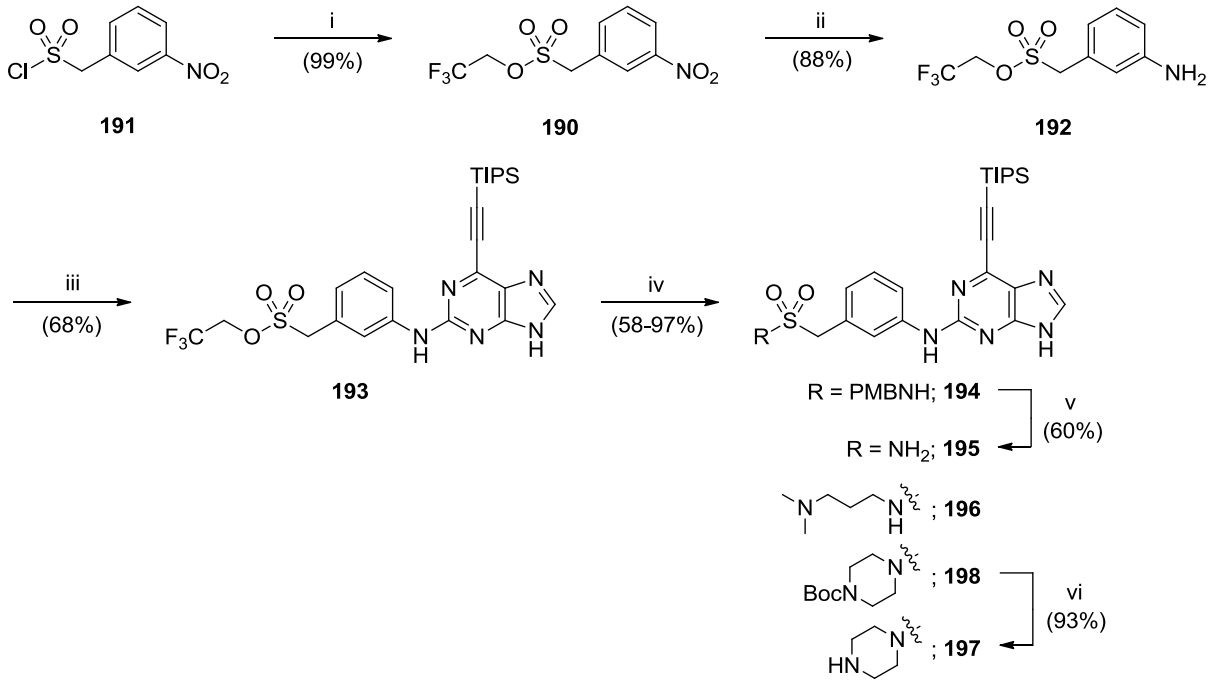

Reagents and conditions: i) TFE, DMAP, NEt_3, RT, 3 h; ii) H_2, Pd/C, TFE, EtOAc, RT, 18 h; iii) **160**, TFA, TFE, reflux, 24 h; iv) R_2NH, DBU, THF, MW 160 °C, 15 min; v) TFA, 70 C, 3 h; vi) TFA, DCM, RT, 18 h.

Final treatment of the TIPS-protected purines with TBAF was required to give the 6-ethynylpurines **177**-**182** (Scheme 22). However, only the carboxamide **177** and sulfonamide **178** derivatives were isolated. Although evidence of product formation was observed by LC-MS and TLC analysis, it was not possible to isolate any product for compounds **179**-**182** after purification, and degradation was observed in reaction mixtures when monitored by LC-MS over time. It became apparent that compounds with basic groups in the 2-arylamino side-chain were subject to decomposition in solution following removal of the TIPS protecting group, implicating the 6-ethynyl substituent as the site of degradation. However, to date no explanation for the observed instability has been established. It was clear that subsequent compounds should lack strongly basic groups, and an alternative strategy for side-chain design was considered.

Scheme 22: Synthesis of 6-ethynylpurines **177**-**182**.

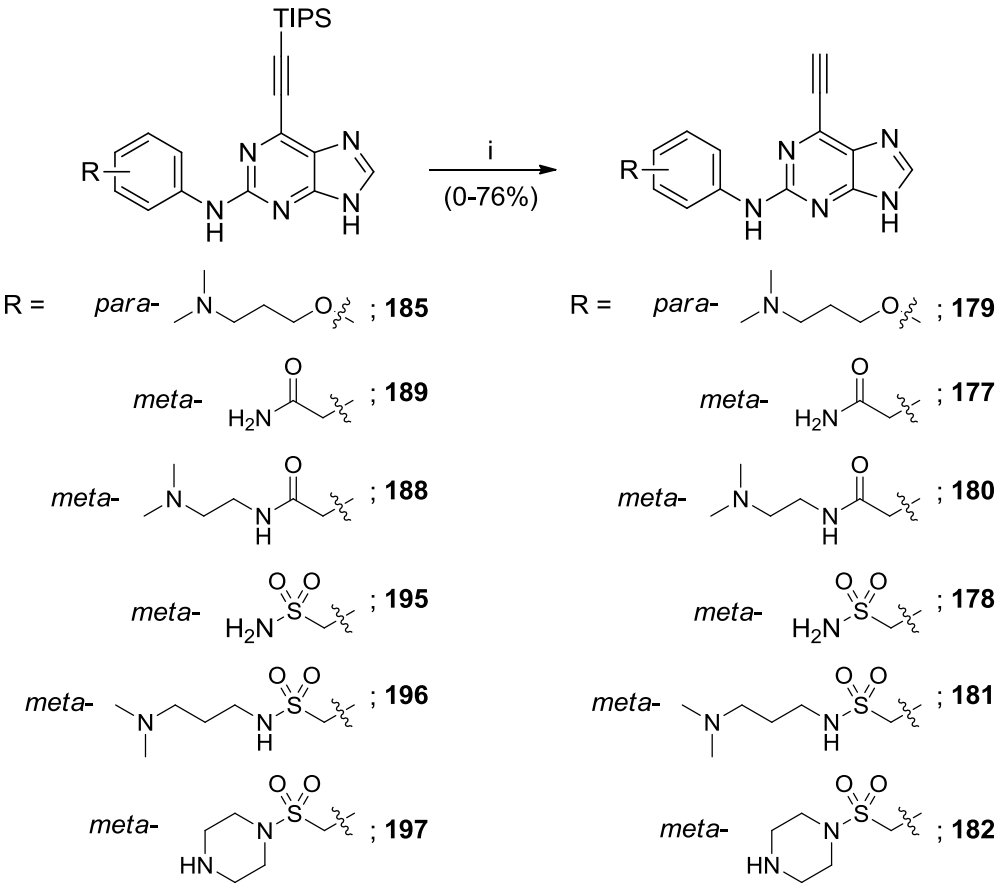

Reagents and conditions: i) TBAF, THF, RT, 5 min.

6.3.2. Identification of NCL-00017509 (177)

Compounds **177** and **178** were tested for inhibitory activity against Nek2 and Cdk2. In addition, growth inhibition of **177** against U2OS and HeLa cell lines was evaluated (Table 12).

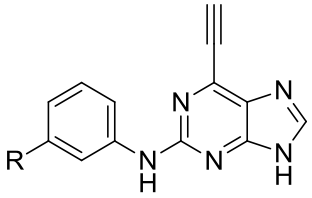

		IC_{50} (µM)		GI_{50} (µM)	
Compound	**R**	**Nek2[a]**	**Cdk2[b]**	**U2OS**	**HeLa**
148	H	0.14 ± 0.1	22.9	2.1 ± 1.0	1.2 ± 0.5
177	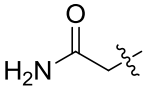	0.062 ± 0.01	11.8	71.0	47.1 ± 2.1
178	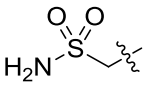	0.13	14.0	N.D.	N.D.

[a] Nek2 IC_{50} values determined at 30 µM ATP concentration; [b] Cdk2 IC_{50} values determined at 12.5 µM ATP concentration; N.D. not determined.

Table 12: Biological evaluation of **177** and **178**.

The carboxamide derivative **177**, designated NCL-00017509, proved the most potent inhibitor in this class to date. However, this improvement in kinase inhibitory activity did not correlate with the cellular activity observed. It was possible that this was again a consequence of the more polar nature of the 2-arylamino side-chain limiting cellular permeability. However, when **177** was evaluated in the pC-Nap1 assay, it was evident that the purine was entering cells and inhibiting cellular Nek2 activity (Figure 31).

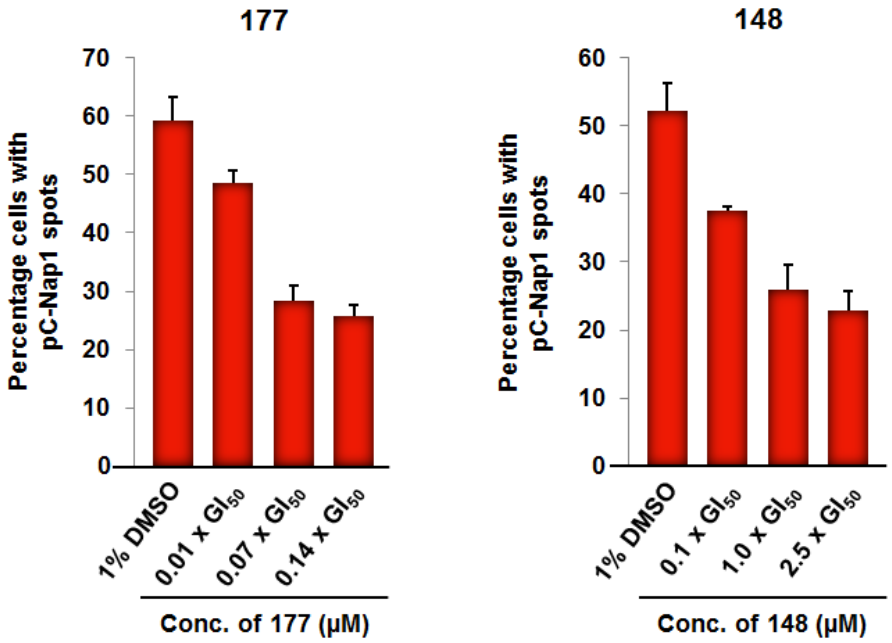

Figure 31: Inhibition of C-Nap1 phosphorylation in U2OS cells by **177** compared with **148**.

Cells treated with **148** display inhibition of pC-Nap1 levels to approximately 20% of control at doses of 1 x GI_{50} (1.8 µM). Despite showing negligible inhibition of cell growth, cells treated with **177** have pC-Nap1 levels reduced to a comparable degree at 0.07-0.14 x GI_{50} (5.0-10.0 µM). This strongly suggests that growth inhibition observed in U2OS cells following exposure to **148** arises *via* an alternative target. Cellular growth inhibition was not evident for **177**, presumably owing to improved compound selectivity. X-ray crystallographic analysis confirmed that **177** is bound to the Nek2 ATP-binding site in the expected manner, with covalent modification of Cys22 evident (Figure 32). Potential interactions between the carboxamide side-chain and Ser96 were identified, although poor electron density within this region of the structure limited a more detailed analysis.

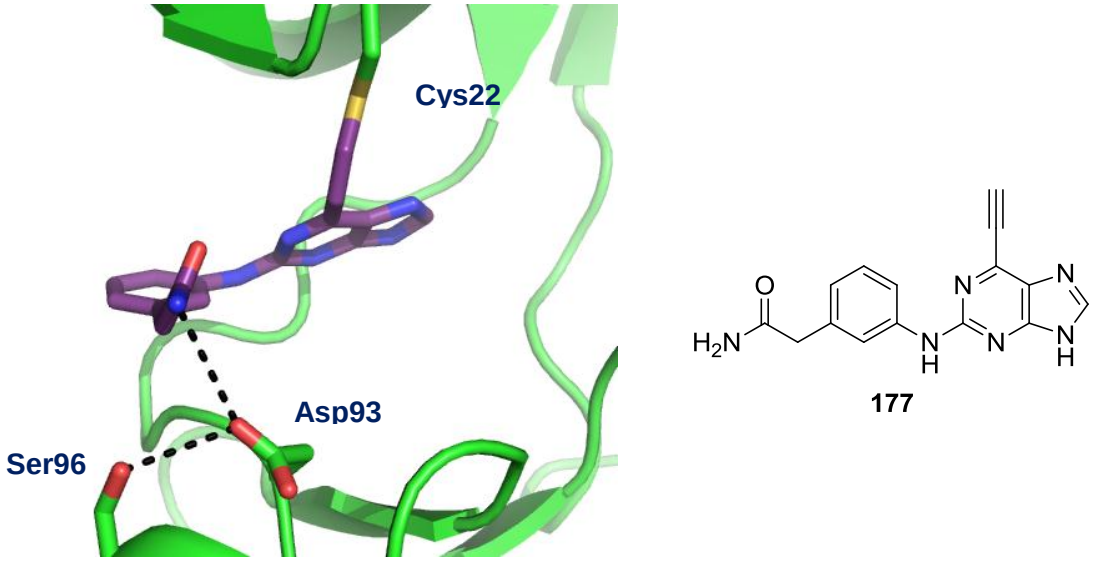

Figure 32: X-ray crystal structure of **177** in complex with Nek2.

Although the initial kinase selectivity of **148** was good, further profiling studies were required for both **148** and **177**. In addition, it is possible that the alternative locus of cellular activity may not be a kinase, and if this were the case, identification of the target would be more challenging. The inhibitory activity of **177** against a panel of 48 kinases selected from commercially available ProfilerPro® plates was determined at 1 μM inhibitor concentration (see appendix, Table A1). Only two kinases other than Nek2 were inhibited by greater than 50%, and IC_{50} values were determined for these; Aurora A (IC_{50} = 0.08 μM) and BMX (IC_{50} = 0.83 μM). However, efforts to confirm the IC_{50} value for Aurora A using a cell-based assay at the Institute for Cancer Research, indicated no inhibitory activity against the kinase. It is notable that BMX kinase, a member of the EGFR tyrosine kinase family, possesses a cysteine residue within the ATP-binding domain that has been identified as a potential target in the design of irreversible inhibitors.[208]

In addition, both **148** and **177** were screened against 121 kinases (National Centre for Protein Kinase Profiling, Dundee University) at a single concentration of 1 μM (see appendix, Table A2). Greater than 50% inhibition of activity was observed for nine of the kinases tested by **177**, including Nek2, and IC_{50} values were determined (Table 13). Encouragingly, the IC_{50} of **177** against Nek2 was 18 nM in this assay, giving the compound at least 5-10-fold selectivity for Nek2 over other kinases, and AurA was only weakly inhibited by **177** in this screen. For **148**, an additional 10 kinases were included owing to the screen being conducted at a later date. Interestingly, this inhibitor displayed a better overall selectivity profile for Nek2 compared with **177**. In addition to Nek2, only 2 other kinases (MLK3 and TAK1) were

inhibited by greater than 50%. It is possible that the alternative target responsible for the cellular activity of **148** is not included in the screen, as it is only a fraction of the human kinome. Alternatively, the locus of cellular activity for **148** may not be a kinase.

Kinase	MKK1	MLK1	MLK3	NUAK1	TBK1	TAK1	JAK2	Chk1
IC_{50} (µM)	0.55	0.27	0.32	0.12	0.74	0.24	0.22	0.56

Table 13: IC_{50} values for kinases inhibited by **177** by greater than 50% in the National Centre for Protein Kinase Profiling screen.

It is possible that the lack of growth inhibition observed for **177** in U2OS and HeLa cells is a result of these cell lines possessing mechanisms by which to facilitate centrosome separation and bipolar spindle formation independently of Nek2 activity. In keeping with the objective of developing targeted therapy, it was necessary to screen a panel of cell lines to identify specific tumour types where depletion of Nek2 activity is growth inhibitory. Collaborators at the ICR had previously conducted a similar screen, and indicated a potential sensitivity of cell lines derived from breast tumours and leukaemias to treatment with **177**. To validate these observations, the inhibitor was tested against a panel of available tumour cell lines, including those derived from breast and leukaemia. Cell lines were evaluated for growth inhibition upon incubation at a 10 µM concentration of NCL-00017509 over 72 hours (Figure 33; A, B and C).

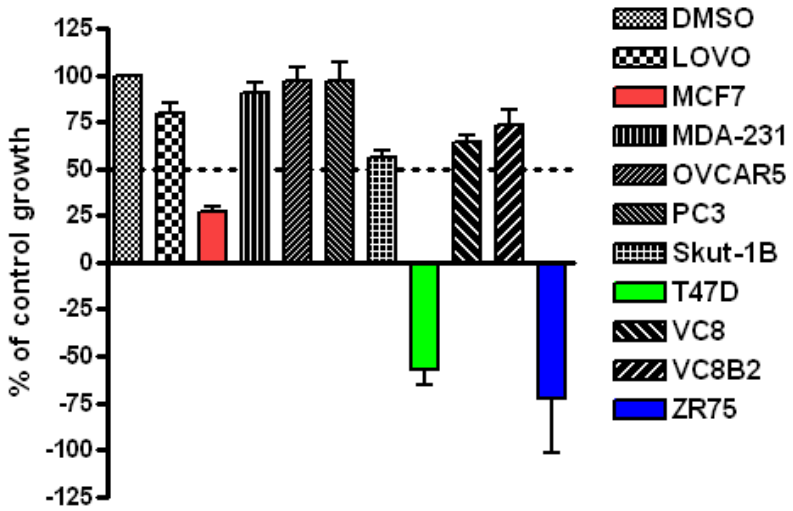

Figure 33: A) Growth inhibition of solid tumour cell lines treated with 10 µM **177** (NCL-00017509) for 72 hours.

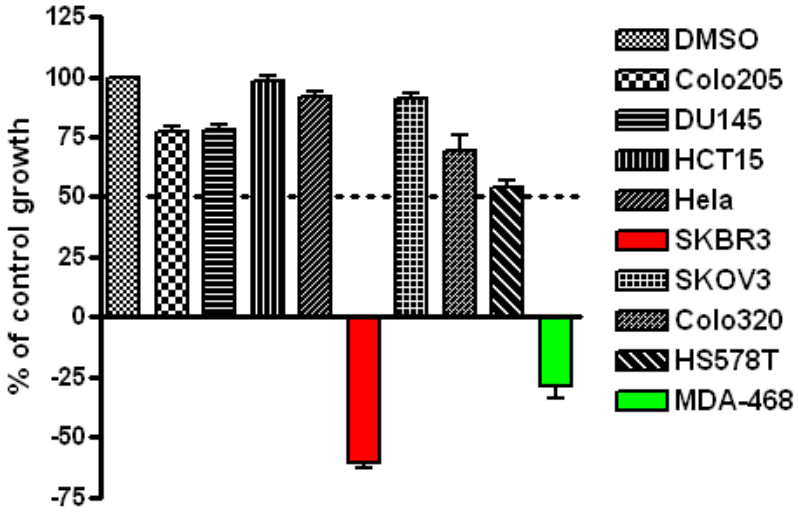

Figure 33: B) Growth inhibition of solid tumour cell lines treated with 10 µM **177** (NCL-00017509) for 72 hours.

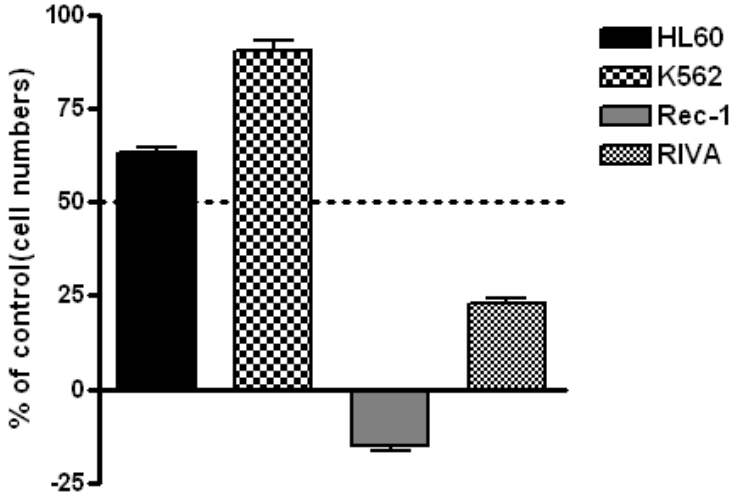

Figure 33: C) Growth inhibition of leukaemia cell lines treated with 10 µM **177** (NCL-00017509) for 72 hours.

As was observed previously, the tumour cell lines most sensitive to inhibitor treatment were those derived from breast (MCF7, T47D, ZR75, SKBR3 and MDA-468) and leukaemia (Rec-1 and RIVA), with all of these cell lines exhibiting greater than 50% growth inhibition at a dose of 10 µM **177**. GI_{50} values were determined for these cell lines, along with HeLa and HCT116 (Figure 34), with the lymphoma Rec-1 (GI_{50} = 1.6 ± 0.1 µM) and breast cancer SKBR3 (GI_{50} = 2.2 ± 0.4 µM) cell lines being identified as particularly sensitive to **177** treatment.

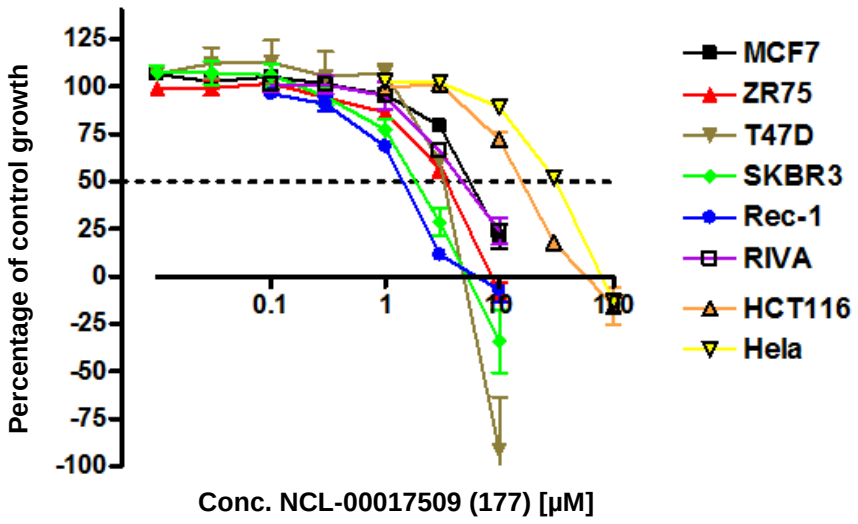

Cell Line	MCF7	ZR75	T47D	SKBR3	Rec-1	RIVA	HCT116	HeLa
GI_{50} (µM)	6.6 ± 0.9	3.7 ± 0.8	3.6 ± 0.5	2.2 ± 0.4	1.6 ± 0.1	5.8 ± 1.4	18.1 ± 1.6	32.2 ± 3.9

Figure 34: Growth inhibition of cell lines identified as being sensitive to **177** (NCL-00017509) following 72 h exposure to inhibitor (n = 3).

Furthermore, **177** was also found to be cytotoxic in SKBR3 cells; clonogenic assays with this cell line gave LC_{50} values in the low micromolar range following pre-incubation for as little as 3 hours prior to subculture (Figure 35).

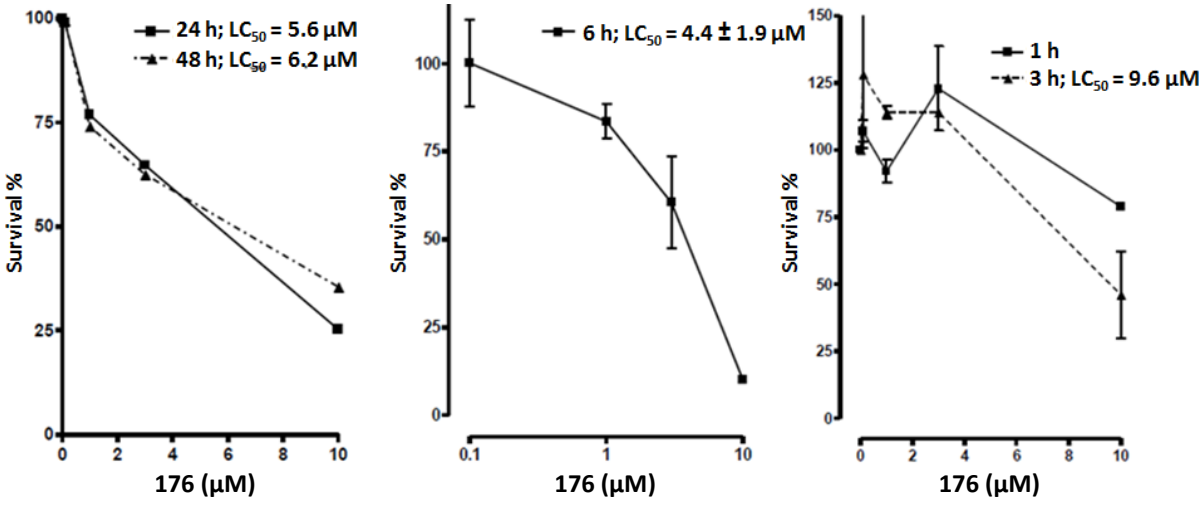

Figure 35: Cytotoxicity of **177** (NCL-00017509) in SKBR3 cells following incubation for a range of times.

Crucially, during such short incubation times, a significant fraction of the cell population would be expected to be outside of the phase of the cell cycle in which active Nek2 is

present. This observation is consistent with, but not conclusive, that the observed cytotoxicity is not due to inhibition of Nek2 alone.

6.4. Synthesis of Analogues of NCL-00017509 (177)

6.4.1. Target Compound Selection and Synthesis

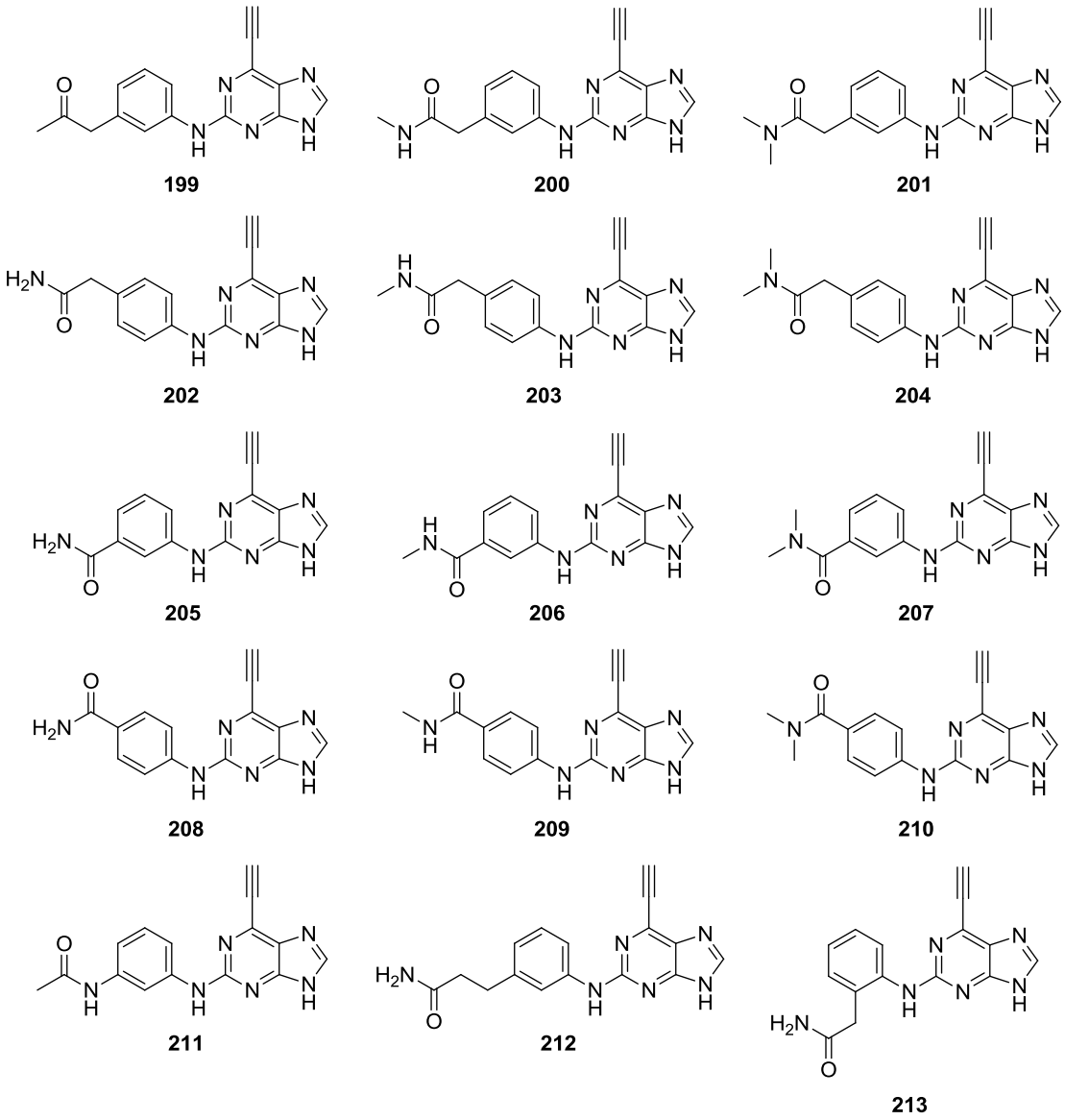

In order to identify components of the carboxamide associated with the improved potency of **177** compared with **148**, a range of analogues was proposed. Systematic modification of potential carboxamide binding interactions may allow the activity of this compound to be further understood, in light of the poor resolution of the X-ray crystal structure in this region of the ATP-binding domain. In addition, further modifications in the positioning of the carboxamide within the binding domain may reveal additional SARs and facilitate improved

inhibitor binding. A series of compounds was thus designed to investigate the binding requirements and spatial optimization of the carboxamide moiety (**199**-**213**).

Of the desired analogues, the synthesis of **201** was conducted initially, owing to the availability of the common acid intermediate **186** from the preparation of **177**. A CDI-mediated coupling between **186** and dimethylamine gave the TIPS-protected precursor of the desired compound (**214**) (Scheme 23).

Scheme 23: Synthesis of carboxamide **214**.

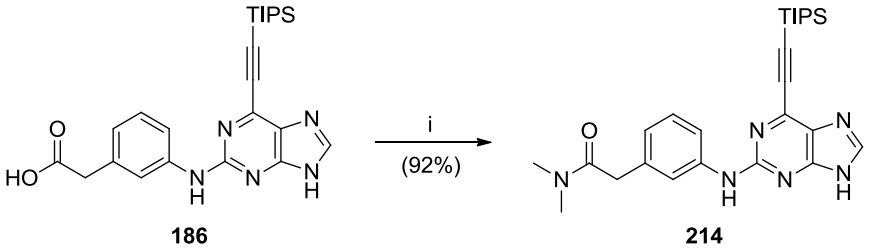

186 **214**

Reagents and conditions: i) $Me_2NH.HCl$, CDI, DIPEA, DMF, RT, 18 h.

A similar approach was utilised for the synthesis of the 4-substituted analogue **202**. 4-Aminophenylacetic acid was coupled to the 2-fluoropurine intermediate **160**, with subsequent base-catalysed hydrolysis of the resultant trifluoroethyl ester. The required acid (**215**) was obtained in moderate yield (53%), to which 4-methoxybenzylamine was coupled under CDI-mediated conditions. The PMB-protected carboxamide (**216**) was converted into the TIPS-protected precursor (**217**) in refluxing TFA (Scheme 24). Owing to the number of analogues required, and the lengthy process of hydrolysing the resultant trifluoroethyl ester, it was decided that subsequent compounds would not be prepared *via* this route. To preserve intermediate **160**, the side-chain groups were synthesised prior to their addition to the purine scaffold. As such, a new synthetic approach was designed for the synthesis of the homologated and truncated analogues of **177** (**212** and **205**).

Scheme 24: Synthesis of the 4-substituted analogue **217**.

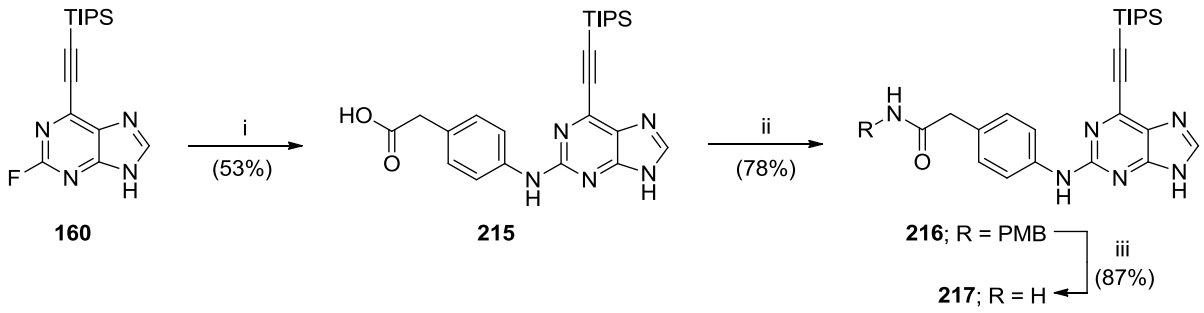

Reagents and conditions: i) a) 4-Aminophenylacetic acid, TFA, TFE, reflux, 24 h, b) 1M NaOH, THF, RT, 18 h; ii) PMB-NH_2, CDI, DIPEA, DMF, RT, 18 h; iii) TFA, reflux, 18 h.

The appropriate anilines, 3-(aminophenyl)propionic acid (**218**) and 3-aminobenzoic acid (**219**), were Boc-protected and CDI-mediated coupling of acids **220** and **221** with 4-methoxybenzylamine gave the protected carboxamides **222** and **223**. Removal of the Boc-protecting group gave anilines **224** and **225**, which were coupled to the 2-fluoropurine (**160**) in moderate to poor yields (41% and 9%, respectively). Removal of the PMB-group from the protected carboxamides (**226** and **227**) under acid conditions gave the target TIPS-protected purines **228** and **229** (Scheme 25).

Scheme 25: Synthesis of carboxamides **228** and **229**.

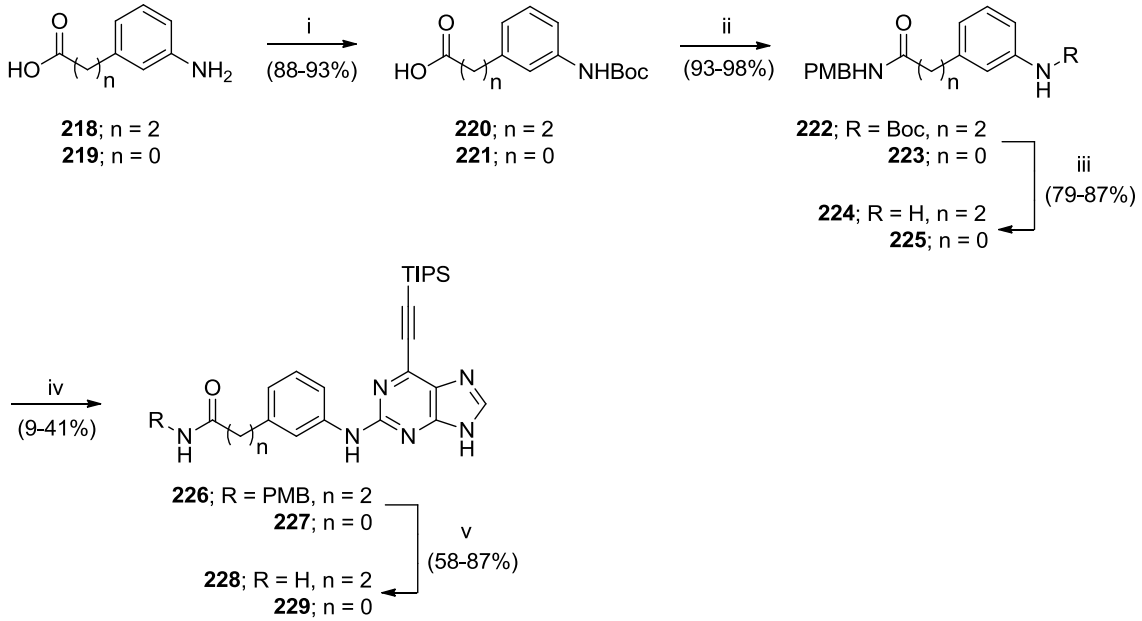

Reagents and conditions: i) Boc_2O, 1,4-dioxane, NaOH, H_2O, RT, 18 h; ii) PMB-NH_2, CDI, DIPEA, DMF, RT, 18 h; iii) TFA, DCM, RT, 18 h; iv) **160**, TFA, TFE, reflux, 24 h; v) TFA, reflux, 18 h.

The TIPS-protected purines **214**, **217** and **228** were deprotected as described previously (Scheme 26). However, although compound **201** was isolated cleanly in 87% yield, a persistent impurity was present in both **202** and **212** following chromatography. Despite being shown to be greater than 95% pure by analytical HPLC, the ^{1}H NMR spectra for each compound showed four multiplet signals in the aliphatic region (Figure 36).

Scheme 26: Removal of TIPS-protecting groups with TBAF.

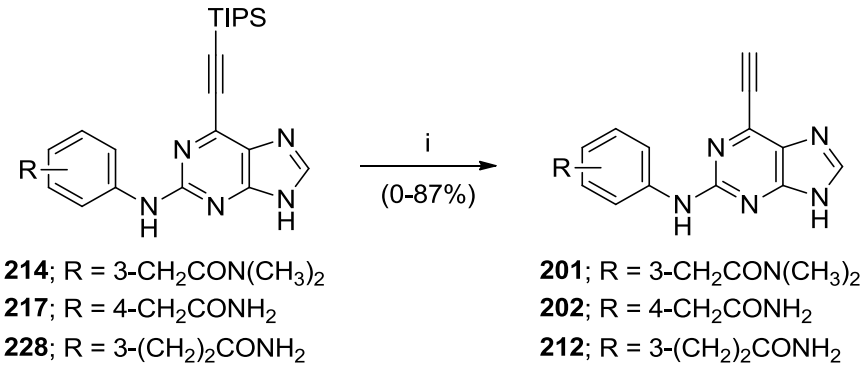

Reagents and conditions: i) TBAF, THF, RT, 5 min.

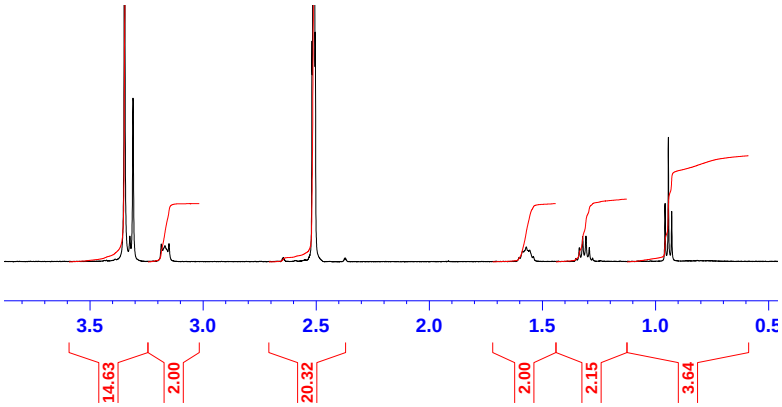

Figure 36: Contaminant signals observed in ^{1}H NMR (DMSO-d_6) spectra of compounds (**202** and **212**) treated with TBAF.

The additional ^{1}H NMR signals were attributed to the *n*-butyl groups of TBAF, although the precise nature of this contaminant remains unclear. Repeated attempts to purify the purines by chromatography failed to remove the contaminant. Compounds within this class had previously been seen to decompose upon heating, and hence recrystallization of the products was not an option. The absence of such contamination in previous compounds led to the proposal that the carboxamide may be involved. However, reports of similar contamination

problems by colleagues within the research group, following the use of TBAF, suggested that this problem is more widespread.

Scheme 27: Removal of TBAF from solution using a sulfonic acid resin **231**.

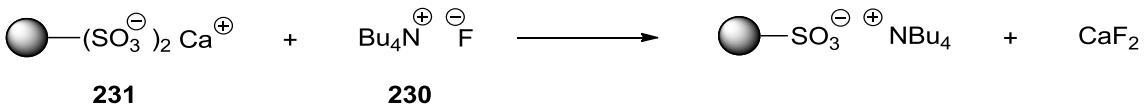

231 **230**

It has been reported that a modified resin system can be used to sequester TBAF (**230**) from reaction mixtures generated in high-throughput syntheses.[209] Treatment of the sulfonic acid-based Amberlite 15 Ion exchange resin with calcium hydroxide gave the solid supported sulfonate calcium salt (**231**). This serves to scavenge TBAF from the reaction mixture in THF, with calcium fluoride precipitating from solution (Scheme 27). A solution of the crude products **202** and **212** in THF were agitated with the resin at room temperature overnight. Removal of the resin and calcium fluoride by simple filtration afforded **202** and **212** free from the TBAF derived contaminant.

However, an alternative method was required for the deprotection of TIPS-protecting groups from subsequent compounds to avoid contamination with TBAF derived species. Potassium fluoride was a suitable fluoride source for the reaction, although it was necessary to conduct the deprotection of 6-ethynylpurines in relatively low boiling solvents due to the observed thermal sensitivity of this compound class. KF is poorly soluble in non-polar solvents, including THF; however, by adding catalytic amounts of 18-crown-6, it was possible to generate soluble fluoride and facilitate the deprotection of **229** to give the required 6-ethynylpurine **205** in excellent yield (94%) (Scheme 28).

Scheme 28: Removal of the TIPS-protecting group of **229** using KF and 18-crown-6.

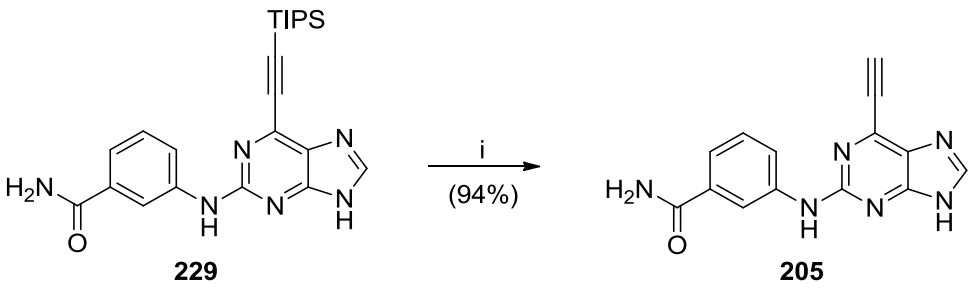

229 **205**

Reagents and conditions: i) KF, 18-crown-6, THF, RT, 24 h.

The synthesis of **228** and **229** detailed in Scheme 25 was further improved, as it was found that the protecting group strategy was unnecessary. Thus, the primary and *N*-methylcarboxamides were prepared directly by reaction of the methyl ester with the appropriate amine, and this strategy was used to prepare compounds **200**, **208** and **209**. Addition of thionyl chloride to a solution of 3-aminophenylacetic acid (**232**) or 4-aminobenzoic acid (**233**) in methanol afforded methyl esters **234** (85%) and **235** (94%), respectively, in good yields, and these were converted into the carboxamidoanilines **236**, **237** and **238** on treatment with the appropriate amine. Anilines **236**, **237** and **238** were coupled to 2-fluoropurine intermediate **160** in the presence of TFA to give TIPS-protected purines **239**, **240** and **241**. The TIPS-protecting groups were removed from all compounds using KF in the presence of 18-crown-6 to yield the target inhibitors **200**, **208** and **209** in good yields (74%, 74% and 69%, respectively) (Scheme 29).

Scheme 29: Synthesis of 6-ethynylpurines **200**, **208** and **209**.

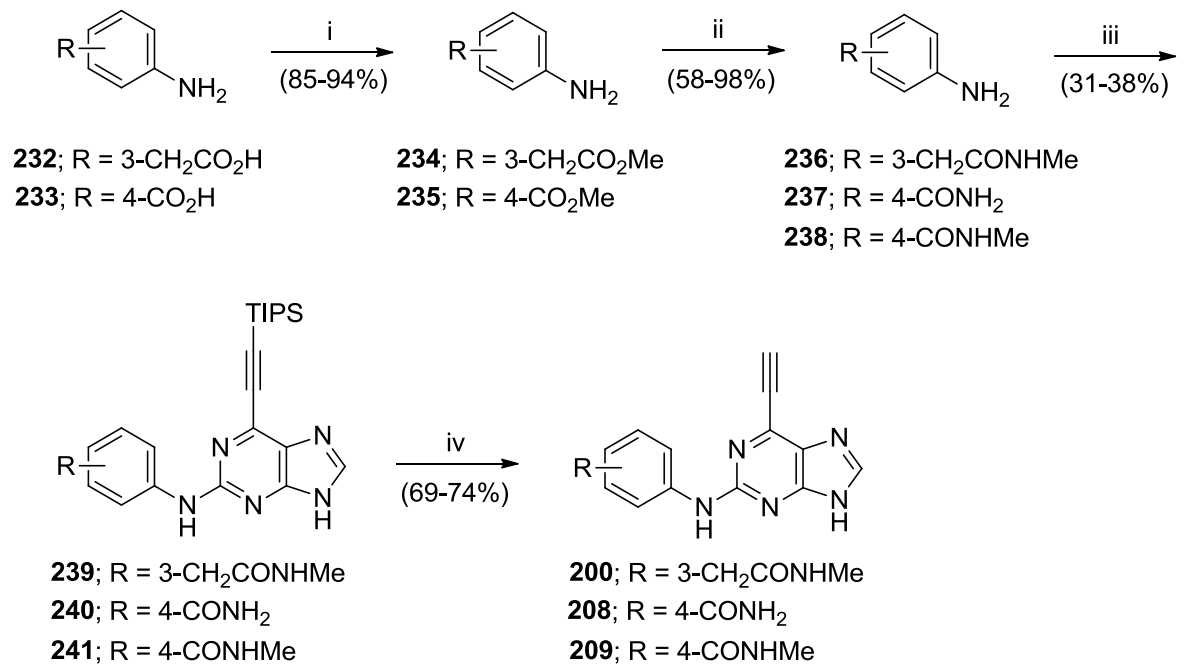

Reagents and conditions: i) $SOCl_2$, MeOH, reflux, 1 h; ii) Aq. RNH_2, RT to 60 °C, 18 h; iii) **160**, TFA, TFE, reflux, 24 h; iv) KF, 18-crown-6, THF, RT, 24 h.

Treatment of methyl ester **235** with dimethylamine resulted in ester hydrolysis, with only trace amounts of the desired product identified by LC-MS analysis. As an alternative approach for the synthesis of **210**, 4-aminobenzoic acid (**233**) was converted into the acid chloride **242** on treatment with thionyl chloride, which was treated with dimethylamine to

give the carboxamidoaniline **243**. This aniline was coupled to purine **160** as before to give the TIPS-protected purine **244**. Removal of the TIPS-protecting group by treatment with KF/18-crown-6 afforded **210** (Scheme 30). Despite the success of this reaction in avoiding the contamination associated with TBAF treatment, deprotection using KF generally proceeded less efficiently than that using TBAF. To obtain compounds in sufficient purity for biological testing (>95%) often required multiple chromatographic separations. The successful removal of tetra-*n*-butylammonium contamination from **202** and **212** with the scavenger beads, and the ease with which these compounds were isolated in high purity, highlighted the value of this approach for the synthesis of future compounds.

Scheme 30: Synthesis of the 6-ethynylpurine **210**.

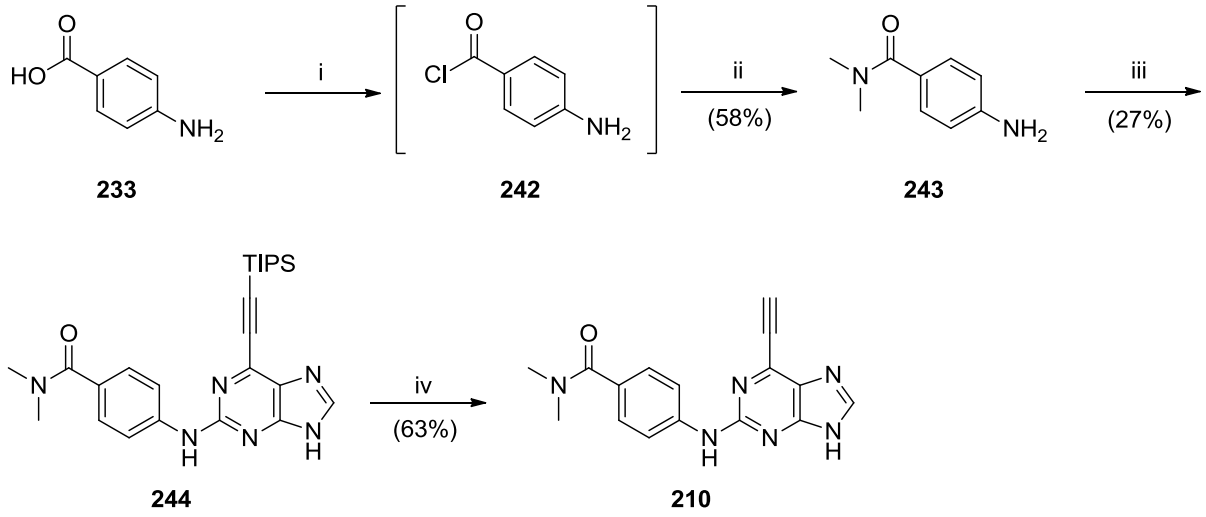

Reagents and conditions: i) $SOCl_2$, DMF, reflux, 1 h; ii) Me_2NH, NEt_3, THF, RT, 18 h; iii) **160**, TFA, TFE, reflux, 24 h; iv) KF, 18-crown-6, THF, RT, 24 h.

The lack of reaction between methyl ester **235** and dimethylamine prompted the use of a different method for the synthesis of the *N*,*N*-dimethylcarboxamide **204**. Preparation of the aniline derivatives required for the synthesis of *N*-methylcarboxamide **203** and *N*,*N*-dimethylcarboxamide **204** was attempted using CDI coupling reactions between 4-nitrophenylacetic acid (**245**) and the appropriate amine (Scheme 31). However, treatment of acid **245** with CDI and DIPEA resulted in a pale purple colour change of the reaction mixture, and following addition of methylamine the required product (**246**) was not observed by LC-MS analysis. In contrast, the synthesis of *N*,*N*-dimethylcarboxamide **247** proceeded cleanly to the desired product, albeit in poor yield (30%).

Scheme 31: Attempted synthesis of carboxamides **246** and **247** using CDI/DIPEA.

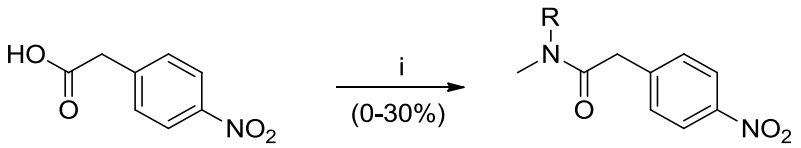

245 **246**; R = H
247; R = Me

Reagents and conditions: i) a) CDI, DIPEA, DMF, RT, 1.5 h, b) MeRNH, THF, RT, 18 h.

Analysis of both the MS and ^{1}H NMR spectrum of the product isolated from the attempted synthesis of **247** indicated that a malonamide derivative (**248**) had been formed. A mechanism for the formation of **248** is proposed in Scheme 32; an acidic proton in the activated acid intermediate (**249**) may be deprotonated to give the charged intermediate **250**, perhaps responsible for the observed purple colouration. Reaction of **250** with a further equivalent of CDI (**251**) to give the activated malonamide **252**, may explain the formation of the observed malonamide **248** upon addition of methylamine.

Scheme 32: Proposed mechanism for the formation of malonamide **248**.

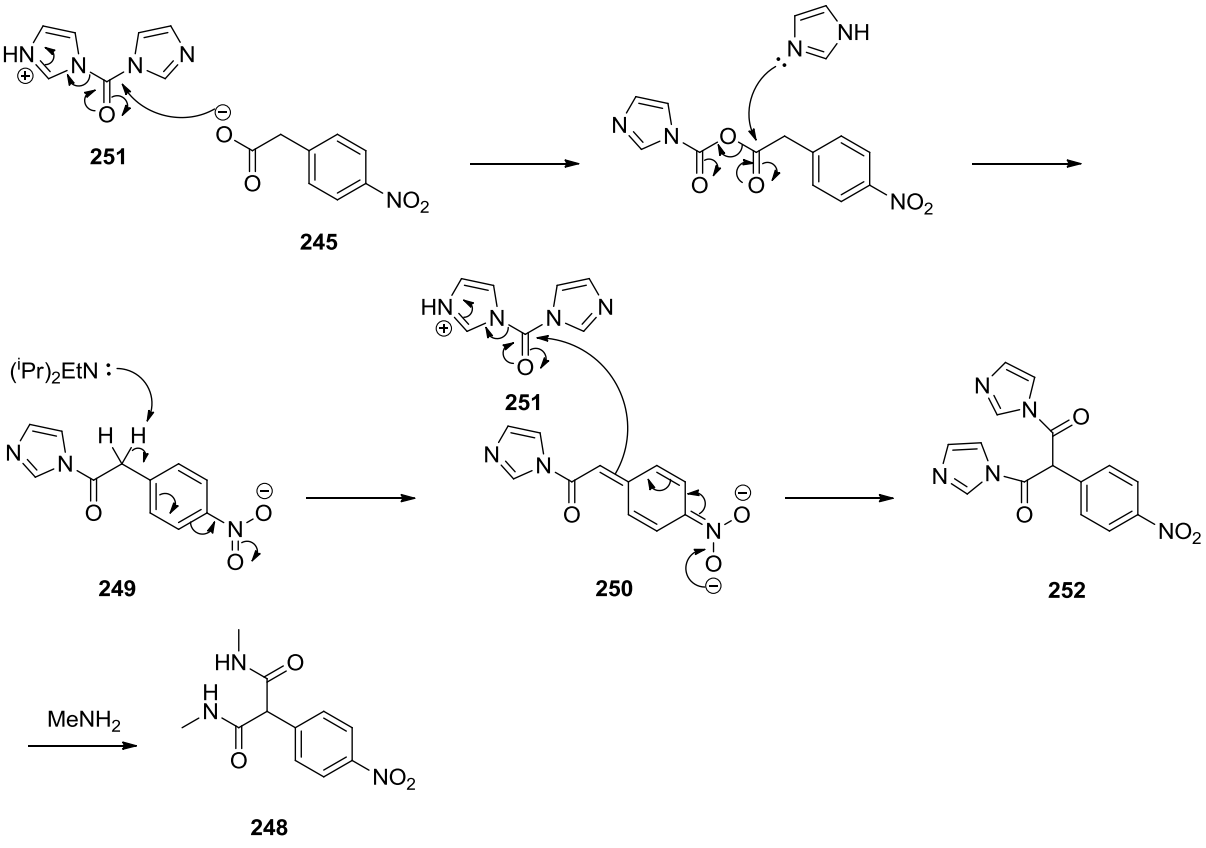

It is unclear as to why the reaction outlined in Scheme 32 did not also occur during the synthesis of **247**, as the proposed mechanism indicates that reaction at the benzylic carbon takes place prior to the addition of an amine, this being the only difference between reaction conditions for the synthesis of **247** and **248**. The low yield of **247** may indicate that intermediate **252** was formed to some degree, but that the additional steric bulk of dimethylamine suppressed the reaction with **252**. Despite formation of the undesired malonamide (**248**), it was decided to couple this compound with the purine scaffold to further investigate SARs at the 2-arylamino ring. Nitroaromatic compounds **247** and **248** were reduced to anilines **253** and **254**, respectively. As an alternative to the conditions using palladium-catalysed transfer hydrogenation utilised previously, iron powder in warm acetic acid was employed for this conversion owing to the rapid reaction times and good yields achieved. Coupling of anilines **253** and **254** to the 2-fluoropurine intermediate **160** was carried out under microwave heating conditions, allowing the reaction time to be reduced from 24 hours to 2 hours, and affording the TIPS-protected purines **255** and **256**, respectively (Scheme 33).

Scheme 33: Synthesis of the 6-ethynylpurines **204** and **257**.

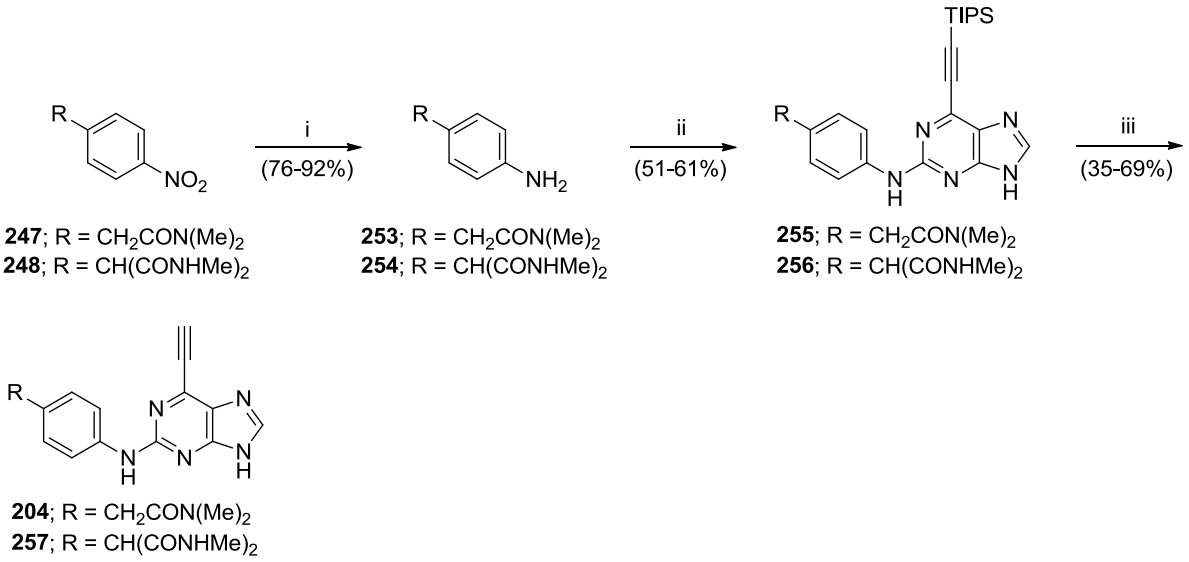

Reagents and conditions: i) Fe, AcOH, 50 °C, 15 min; ii) **160**, TFA, TFE, MW 140 °C, 2 h; iii) a) TBAF, THF, RT, 5 min, b) **231**, THF, RT, 48 h.

Removal of the TIPS-protecting group from **255** and **256** was carried out using TBAF under the conditions previously used. However, the reaction mixture was diluted with THF to solubilise any material that had precipitated from solution and to provide sufficient volume to

utilise the TBAF scavenger beads **231**. By varying the volume of beads added to the reaction mixture for **204**, it was found that an approximate 10-fold w/w excess of **231** completely removed any trace of tetra-*n*-butylammonium contamination after 2 days, as confirmed by ^{1}H NMR analysis. This method was then used for the deprotection of **255** and **256**, to afford the target inhibitors **204** and **257** with no contamination. The success of this procedure prompted its use in all further TIPS-deprotection reactions.

Synthesis of the target *N*-methylcarboxamide **203** was adapted to prevent formation of the undesired malonamide **248**. The required aniline **258** was prepared from the methyl ester (**259**), which was converted into the *N*-methylcarboxamide **258** on treatment with aqueous methylamine analogously to that for **236**. However, in this case the intermediate methyl ester **259** was not isolated and amide formation was carried out as a single reaction. The aniline **258** was coupled to the 2-fluoropurine **160** to give the TIPS-protected purine **260**. Removal of the TIPS-protecting group from **260** using TBAF, followed by treatment of the reaction mixture with the TBAF scavenger **231**, gave the target compound **203** in moderate yield (58%) (Scheme 34).

Scheme 34: Synthesis of the 6-ethynylpurine **203**.

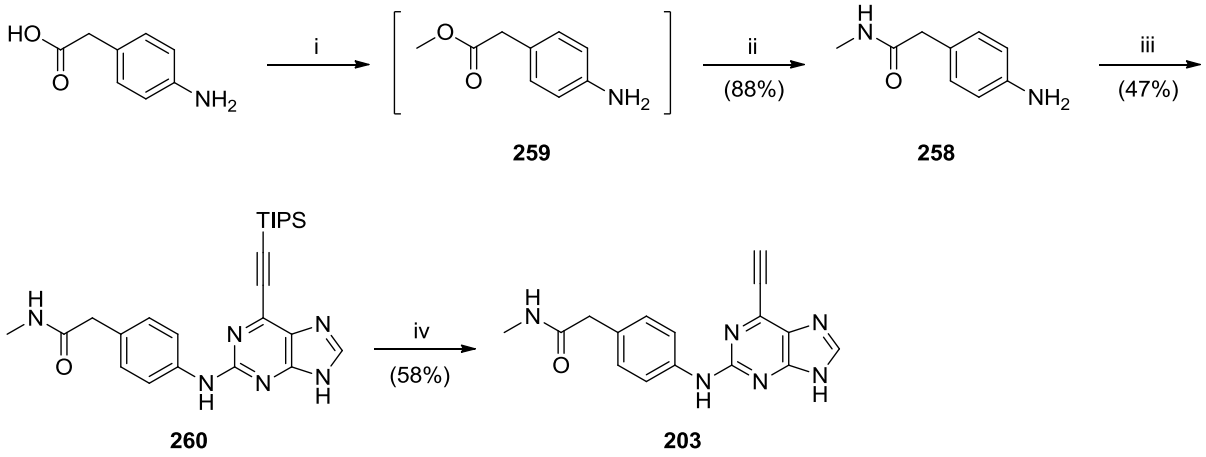

Reagents and conditions: i) $SOCl_2$, MeOH, reflux, 1 h; ii) Aq. $MeNH_2$, RT, 18 h; iii) **160**, TFA, TFE, MW 140 °C, 2 h; iv) a) TBAF, THF, RT, 5 min, b) **231**, THF, RT, 48 h.

As an alternative method for the synthesis of carboxamides, the use of phosphorus trichloride under microwave heating conditions allowed short reaction times to be achieved.[210] Carboxamides **261** and **262** were prepared in this way from 3-nitrobenzoic acid (**263**). Anilines **264** and **265** were synthesised through aromatic nitro group reduction, as previously

described, and subsequently coupled with **160** to give the TIPS-protected purines **266** and **267**. Removal of the TIPS-protecting groups as before gave the target inhibitors **206** and **207** (Scheme 35).

Scheme 35: Synthesis of 6-ethynylpurines **206** and **207**.

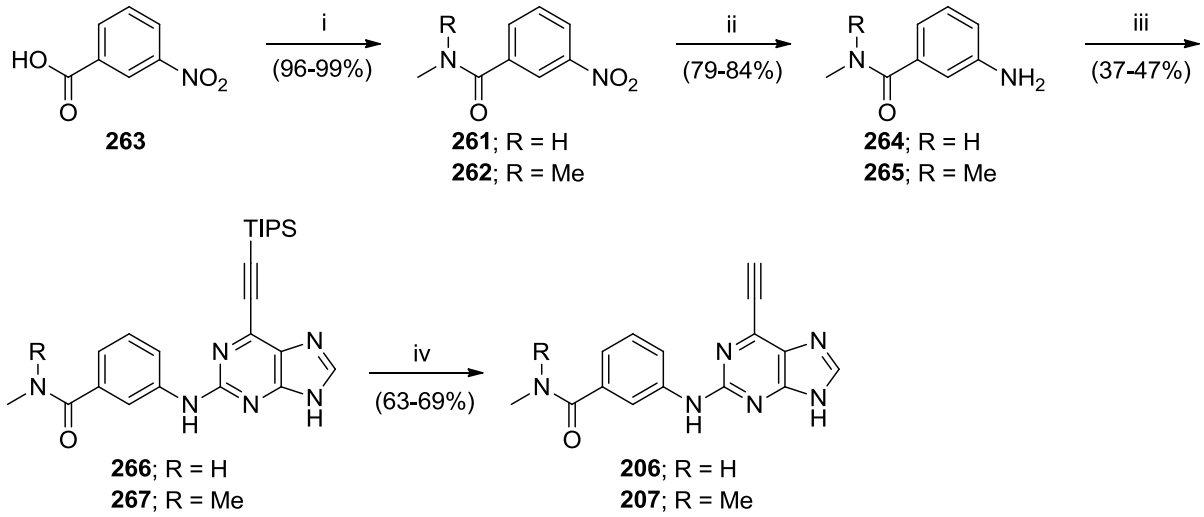

Reagents and conditions: i) R_2-NH, PCl_3, MeCN, MW 150 °C, 5 min; ii) Fe, AcOH, 50 °C, 15 min; iii) **160**, TFA, TFE, MW 140 °C, 3 h; iv) a) TBAF, THF, RT, 5 min, b) **231**, THF, RT, 48 h.

To prepare the 'reverse carboxamide' **211**, 3-nitroaniline (**268**) was acetylated with acetic anhydride to give *N*-acetylaniline **269**. Reduction of the aromatic nitro group of **269** gave aniline **270** in good yield (91%), which was coupled to the 2-fluoropurine **160** under microwave assisted conditions to afford the TIPS-protected purine **271**. Deprotection of **271** with TBAF, as described above, gave the target purine **211** in moderate yield (48%) (Scheme 36). The *ortho*-substituted carboxamide required for the preparation of **213** was synthesised in an analogous manner to that of **258**. However, due to availability, the synthesis commenced from 2-nitrophenylacetic acid (**272**), which was converted into methyl ester **273** with thionyl chloride/methanol, and treated with aqueous ammonia to give the carboxamide **274** in good yield (84%).

Scheme 36: Synthesis of the 6-ethynylpurine **211**.

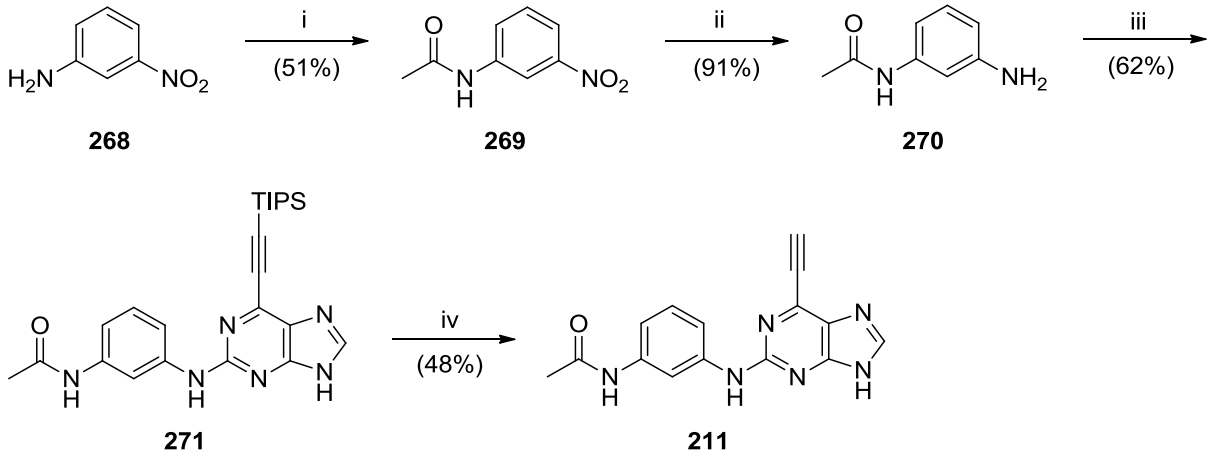

Reagents and conditions: i) Ac_2O, RT, 30 min; ii) Fe, AcOH, 50 °C, 15 min; iii) **160**, TFA, TFE, MW 140 °C, 2 h; iv) a) TBAF, RT, 5 min, b) **231**, THF, RT, 48 h.

Interestingly, reduction of the nitro group of **274** with iron-acetic acid gave only the indolinone **275**, with none of the desired aniline product **276** being observed by LC-MS analysis. It was proposed that the acidic conditions used were responsible for the formation of **275** (Scheme 37), and hence nitro group reduction was performed under neutral conditions using palladium-catalysed transfer hydrogenation to give the requisite aniline **276** (Scheme 38).

Scheme 38: Preparation of 2-aminophenylacetamide **276**.

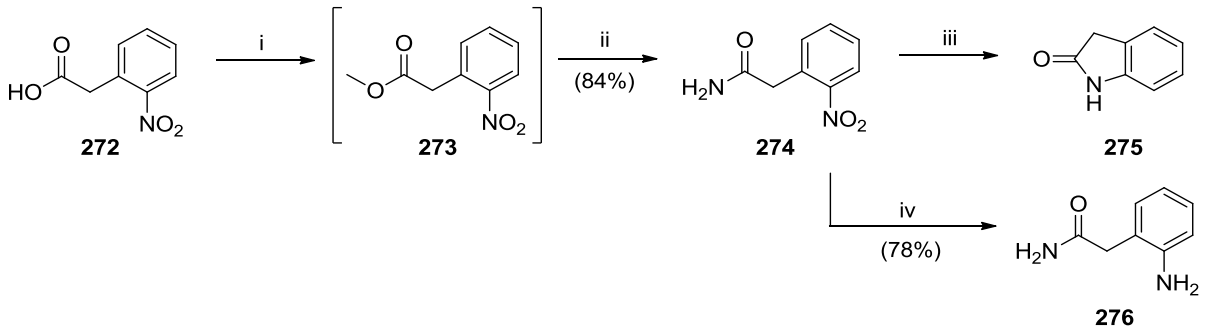

Reagents and conditions: i) $SOCl_2$, MeOH, reflux, 1 h; ii) Aq. NH_3, RT, 18 h; iii) Fe, AcOH, 50 °C, 15 min; iv) Pd/C, NH_4HCOO, MeOH, RT, 3 h.

Scheme 37: Proposed mechanism for the formation of indolinone **275**.

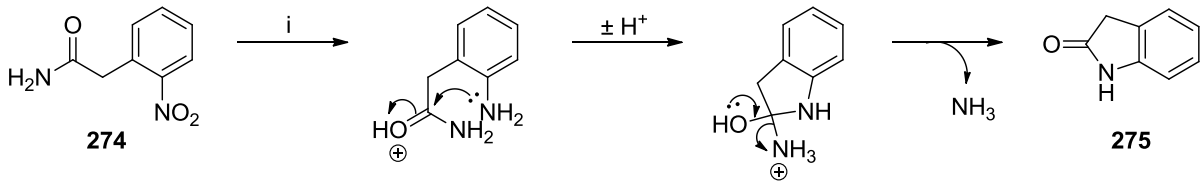

Reagents and conditions: i) Fe, AcOH, 50 °C, 15 min.

Coupling of aniline **276** to purine **160** under standard conditions failed to yield any of the target product (**277**), likely as the indolinone **275** forms from the aniline under the TFA/TFE conditions. It was thus necessary to devise an alternative method for coupling **276** to the purine. It has previously been reported that palladium-catalysed (Buchwald) amination reactions are a suitable alternative to S_NAr methods for the coupling of anilines to the purine scaffold (see chapter 5.4). However, the 2-fluoropurine intermediate **160** utilised thus far is unsuitable for such reactions, owing to the low rate of palladium insertion into the C-F bond. As such, the 2-iodopurine intermediate (**278**) was prepared using Sandmeyer reaction conditions (Scheme 39).

Scheme 39: Synthesis of the 6-ethynylpurine **213** using a palladium-catalysed amination.

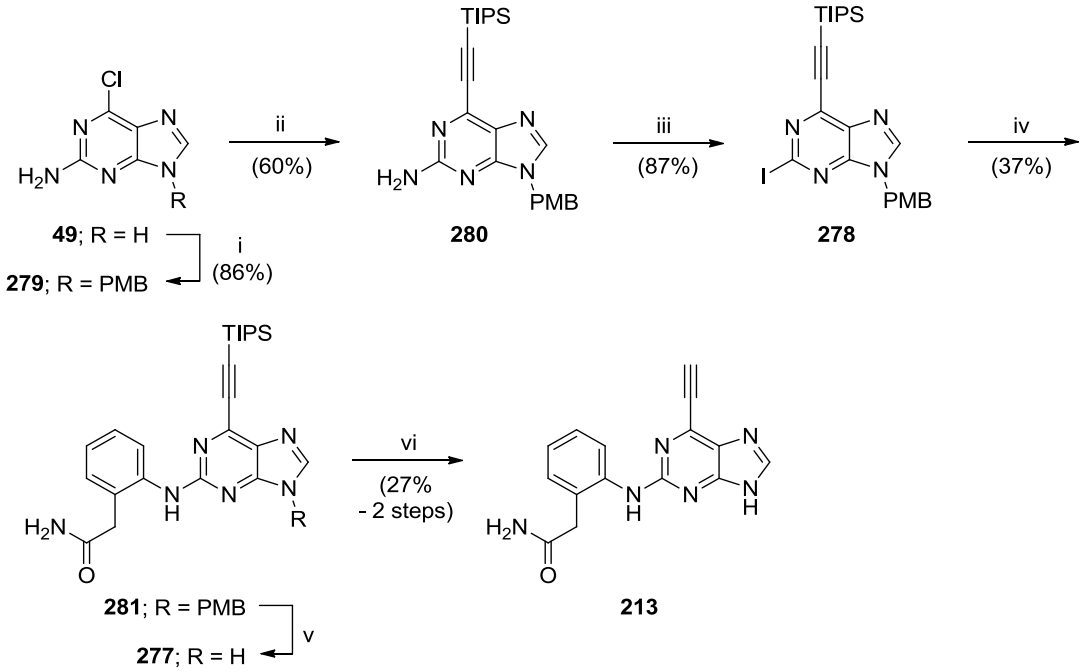

Reagents and conditions: i) PMB-Cl, K_2CO_3, DMF, 60 °C, 18 h; ii) TIPS-acetylene, $Pd_2Cl_2(PPh_3)_2$, CuI, Et_3N, DMF, RT, 18 h; iii) isoamyl nitrite, CuI, CH_2I_2, THF, reflux, 1 h; iv) **276**, $Pd_2(dba)_3$, XPhos, K_2CO_3, MeCN, 100 °C, 2 h; v) TFA, reflux, 18 h; vi) a) TBAF, THF, RT, 5 min, b) **231**, THF, RT, 48 h.

Prior to conducting palladium-mediated amine coupling reactions on the purine scaffold it had previously been found within the research group that protection of the N^9-position was required. This is possibly due to coordination of palladium to the purine N^9-H and N^3 positions. At the outset of the synthesis, it was not known which reaction conditions would be employed to introduce an iodo group at the purine 2-position. As such, it was desirable to introduce a protecting group at the N^9-position that was stable to a wide range of conditions compared with the THP group used previously. Furthermore, treatment of 2-amino-6-chloropurine (**49**) with 4-methoxybenzyl chloride in the presence of base allowed selective N^9/N^7-protection to give compound **279**, whereas the analogous reaction with DHP would result in additional reaction at the purine 2-amino position. However, unlike THP-protection of the purine (*e.g.* **51**), PMB-protection (**279**) gives a mixture of N^9/N^7 regioisomers. Literature precedence reports the discrimination of purine N^9/N^7 regioisomers by observation of the H-8 ^{1}H NMR signal.[211] Accordingly, the ratio of N^9 to N^7 PMB-protection was found to be approximately 7:3 (Figure 37).

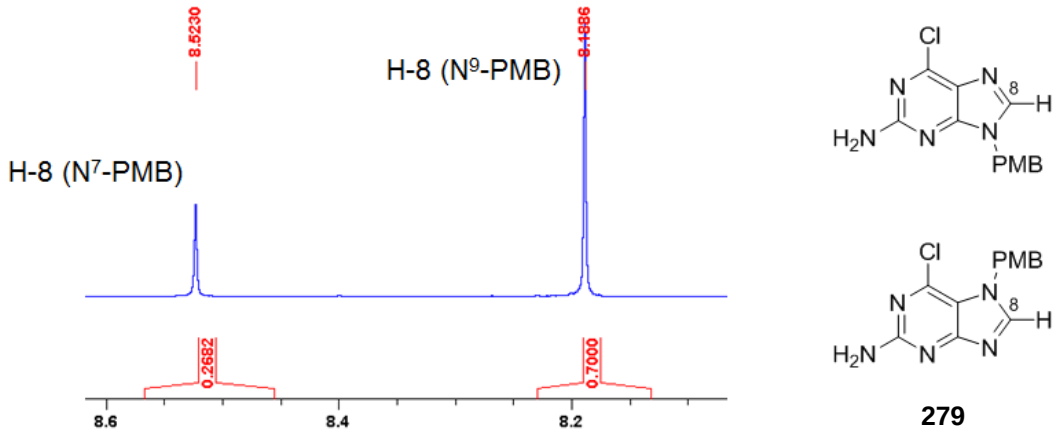

Figure 37: Comparison of the purine H-8 ^{1}H NMR signals for the N^9- and N^7-PMB regioisomers of **279**.

The ethynyl moiety was introduced at the 6-position of **279** employing a Sonogashira reaction with (triisopropylsilyl)acetylene to give the 6-ethynylpurine **280**. Interestingly, this reaction only took place with the N^9-PMB regioisomer of **279**, possibly due to steric constraints encountered at the purine 6-position when the N^7-position was protected by the PMB group. Despite a modest overall yield (69%) based on consumption of starting material, this equated to near quantitative yield with respect to the N^9-PMB regioisomer of **279**. Conversion of the purine 2-amino group of **280** into an iodo substituent was achieved by diazotisation of the amine with isoamyl nitrite under Sandmeyer conditions, with iodine in

the presence of copper iodide and diiodomethane.[212] This afforded the 2-iodopurine intermediate **278** in good yield (87%).

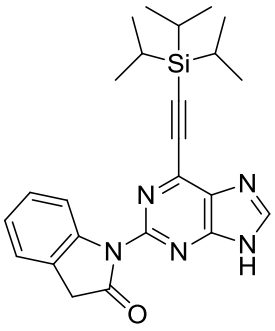

282

Aniline **276** was successfully coupled to the 2-iodopurine **278** by a palladium-catalysed amination under the general conditions previously described (see **141**) to give compound **281**, and PMB-deprotection was achieved in refluxing TFA. The isolated yield of the deprotected purine **277** was relatively poor for this type of reaction (~35%), with some difficulties encountered during purification. In addition, evidence of isoindolinone **282** formation was observed by LC-MS analysis, indicating that the acid-catalysed isoindolinone formation observed during the preparation of **275** was taking place, albeit to a lesser degree. Due to the poor yield of **277** it was decided to remove the TIPS-protecting group from this compound directly without further characterisation to ensure sufficient material for biological studies. Treatment of **277** with TBAF, followed by incubation with the TBAF scavenger beads **231**, afforded the desired inhibitor **280** (Scheme 39). Unfortunately, evidence of tetra-*n*-butylammonium contamination was present in the ^{1}H NMR spectrum of this material, indicating that the scavenger beads had failed to remove all of the contaminant, and the compound was purified by semi-preparative HPLC. Following purification, however, the sample of **280** was seen to darken in colour over the course of 2 weeks, after which ^{1}H NMR and LC-MS analysis revealed that the purine had been subject to decomposition to a complex mixture of degradation products. Insufficient research time remained to investigate compound **280** further.

To establish the role of the carboxamide amino group of **177**, the ketone analogue **199** was synthesised. An efficient method for the conversion of an amino-acid into a ketoamide is the Dakin-West reaction,[213] and a modification of this reaction can be used to convert a carboxylic acid with an enolisable carbon at the α-position into a methyl ketone.[214] This method was employed to convert 3-nitrophenylacetic acid (**283**) into the ketone **284** on

treatment with acetic anhydride in the presence of pyridine. To prevent self-condensation, the ketone carbonyl group of **284** was protected by conversion into the dithiane **285** with 1,3-propanedithiol (Scheme 40).

Scheme 40: Synthesis of the ketone **199** using a modified Dakin-West reaction.

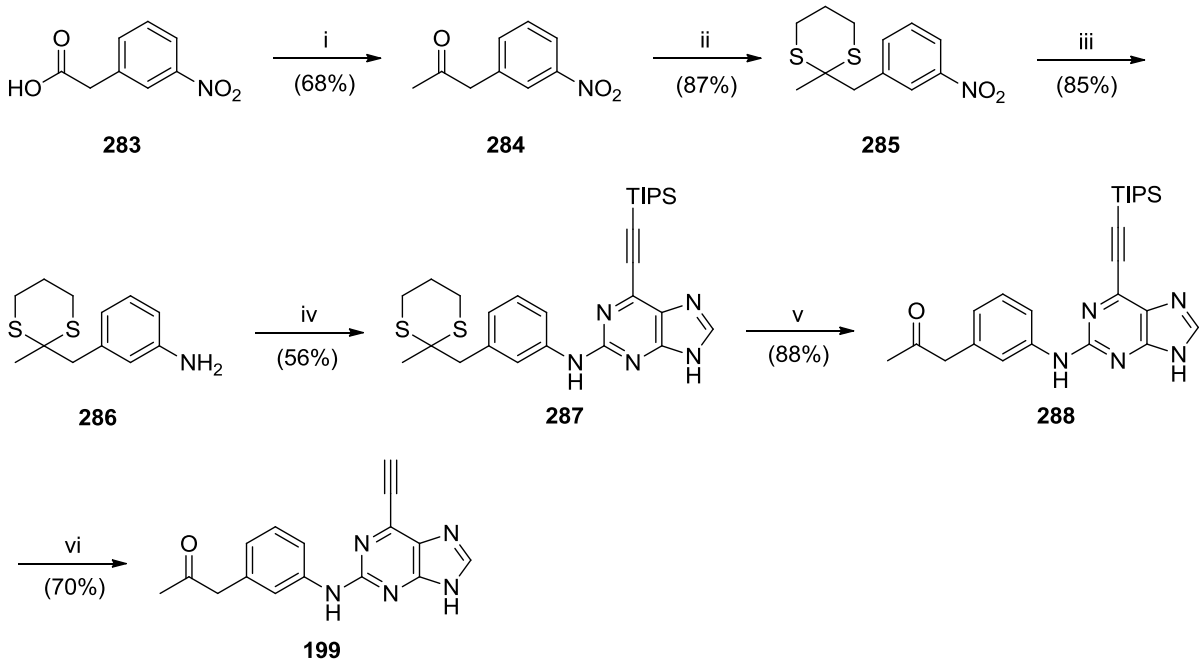

Reagents and conditions: i) Ac_2O, pyridine, reflux, 4 h; ii) 1,3-propanedithiol, $BF_3.Et_2O$, DCM, RT, 18 h; iii) $SnCl_2.H_2O$, EtOH, reflux, 1.5 h; iv) **160**, TFA, TFE, MW 140 °C, 2 h; v) [bis(trifluoroacetoxy)iodo]benzene, MeOH, H_2O, RT, 10 min; vi) a) TBAF, THF, RT 5 min, b) **231**, THF, RT, 48 h.

Attempts to reduce the aromatic nitro group of **285** using iron-acetic acid gave a complex mixture, suggesting that the dithiane moiety was unstable under these conditions. Palladium-catalysed hydrogenation also failed, due perhaps to the metal-coordinating nature of the sulfur atoms. Reduction was finally achieved on treatment with stannous chloride in refluxing ethanol, to give the aniline **286** in good yield (85%), and coupling to the 2-fluoropurine **160**, as detailed previously, gave purine **287**. Removal of the dithiane protecting group was achieved on treatment of **287** with [bis(trifluoroacetoxy)iodo] benzene to give the TIPS-protected purine **288**. Final deprotection of the 6-ethynyl group of **288** with TBAF, in conjunction with scavenger beads (**231**) furnished the target inhibitor (**199**).

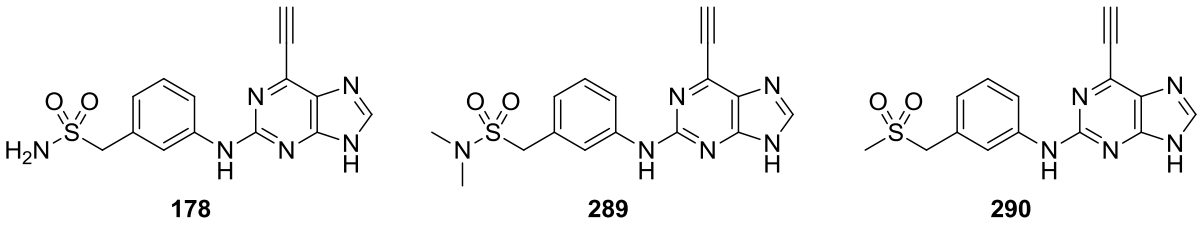

178 **289** **290**

To undertake further SAR studies around the purine 2-arylamino ring, additional derivatives analogous to the sulfonamide **178** were desired. Removal of the H-bond donor properties of the sulfonamide was to be investigated through the synthesis of the *N*,*N*-dimethylsulfonamide **289** and sulfone **290**. For the synthesis of sulfonamide **289**, methodology previously used was employed to prepare the protected *N*,*N*-dimethylsulfonamide **291** in quantitative yield by treatment of trifluoroethylsulfonate ester **193** with dimethylamine in the presence of DBU. Removal of the TIPS-protecting group of **291** under the optimised conditions described above gave the target 6-ethynylpurine **289** (Scheme 41).

Scheme 41: Synthesis of the 6-ethynylpurine **289**.

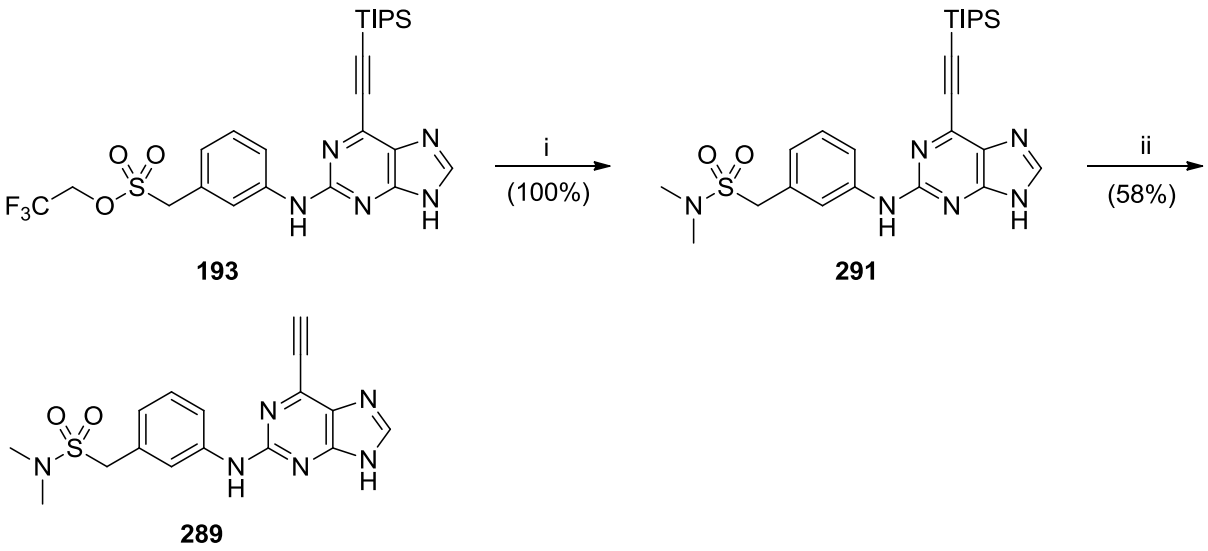

193 **291** **289**

Reagents and conditions: i) Dimethylamine, DBU, THF, MW 160 °C, 15 min; ii) a) TBAF, THF, RT, 5 min, b) **231**, THF, RT, 48 h.

The aniline derivative required for sulfone **290** was prepared by heating 3-nitrobenzyl bromide (**292**) in the presence of sodium methanesulfinate to give the benzylsulfone **293** in excellent yield (94%). Reduction with iron in acetic acid gave aniline **294**, which was coupled with **160** to afford the TIPS-protected purine **295**. Final removal of the TIPS-protecting group gave the target inhibitor **290** (Scheme 42).

Scheme 42: Synthesis of compound **290**.

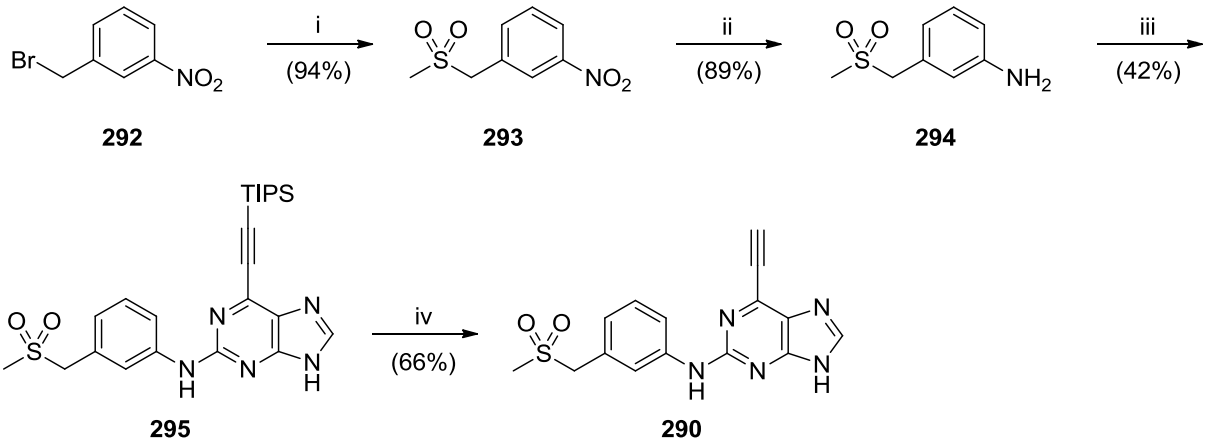

Reagents and conditions: i) $NaSO_2CH_3$, EtOH, reflux, 2 h; ii) Fe, AcOH, 50 °C, 15 min; iii) **160**, TFA, TFE, MW 140 °C, 2 h; iv) a) TBAF, THF, RT, 5 min, b) **231**, THF, RT, 48 h.

To assess the degree to which irreversible inhibition by 6-ethynylpurines contributes to their observed potency in inhibiting Nek2, it was desirable to synthesise a structurally similar analogue of **177** that would act as only a competitive reversible inhibitor of Nek2. The design of such a compound focussed on an isosteric replacement of the 6-ethynyl moiety of **177**, as this had been shown by X-ray crystallography to be responsible for the covalent modification of Cys22 in Nek2. A potential isosteric replacement for the ethynyl moiety is a cyano group, which cannot act as a Michael acceptor when present at the purine 6-position. Therefore, the 6-cyanopurine analogue **296** was proposed as a suitable compound to serve as an equivalent reversible competitive inhibitor of Nek2.

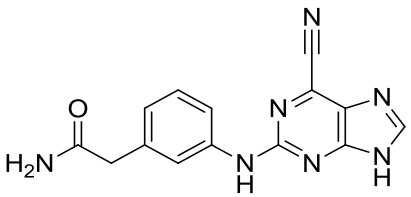

296

The required aniline **297** was synthesised in good yield by treatment of methyl ester **234** with concentrated ammonium hydroxide (77%) (Scheme 43). Previous work within the research group employed a reliable method to introduce a cyano group at the purine 6-position.[215] Thus, addition of tetra-*n*-butylammonium cyanide and DABCO to the PMB-protected purine **279** resulted in the initial activation of the purine 6-position through formation of the

'DABCO-purine' salt (**298**). This species has previously been isolated and characterised.[204] The DABCO group was subsequently displaced by cyanide to give the 6-cyanopurine **299**, and removal of the PMB-protecting group with TFA gave compound **300** as a TFA salt, confirmed by ^{19}F NMR spectroscopy. The purine 2-amino group was converted into a fluoro substituent under Balz-Schiemann conditions, to give the 2-fluoropurine **301**. The poor yield for this reaction indicated the potential instability of the cyano group to aqueous acid, although no evidence of the amide or acid hydrolysis products of **301** were observed by LC-MS analysis.

Scheme 43: Synthesis of aniline **297**.

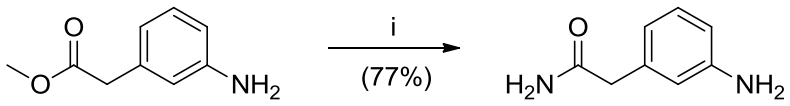

234 **297**

Reagents and conditions: i) Conc. NH_4OH, RT, 18 h.

Despite the stability of the cyano group to the strongly acidic PMB-deprotection conditions, it was thought that an S_NAr reaction at the purine 2-position mediated by TFA/TFE may result in degradation of the nitrile moiety. For this reason, neutral conditions were required for the coupling of aniline **297** to 2-fluoropurine **301**. It is necessary to use TFA when reacting anilines with the 2-fluoro-6-(TIPS-ethynyl)purine **160**, as the purine 2-position is insufficiently electrophilic. However, owing to the electron-withdrawing effect of the 6-cyano group, it was possible to couple the aniline **297** directly to the 2-fluoro-6-cyanopurine **301** by heating in DMSO, although a protracted reaction time (72 h) was required for the reaction to proceed to completion. The target 6-cyanopurine **296** was obtained in moderate overall yield (50%) (Scheme 44).

Scheme 44: Synthesis of the 2-arylamino-6-cyanopurine **296**.

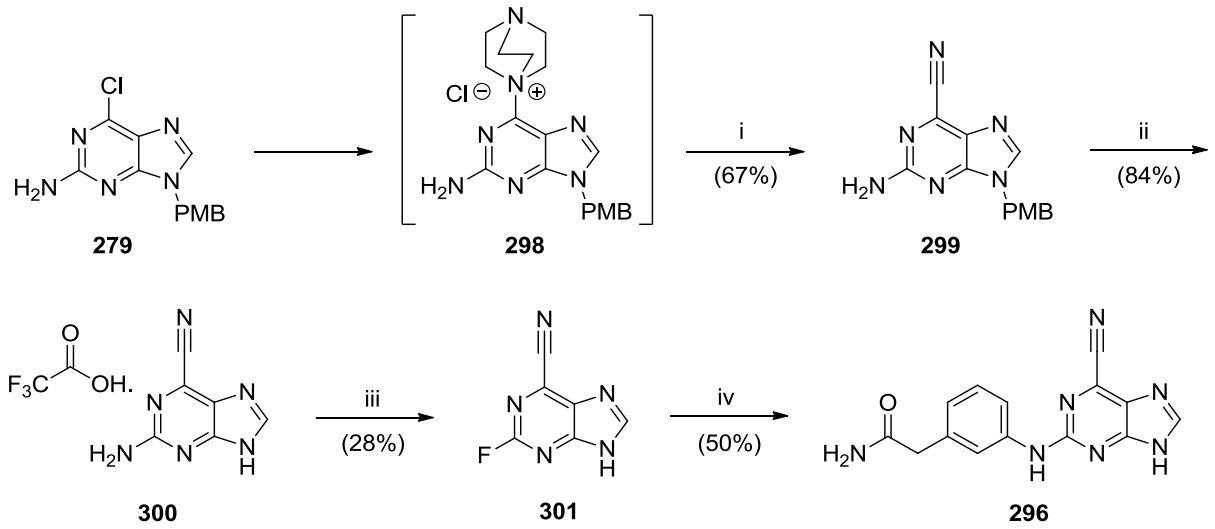

Reagents and conditions: i) ($^{n}Bu_4N$)CN, DABCO, MeCN, RT, 18 h; ii) TFA, 70 °C, 5 h; iii) $NaNO_2$, HBF_4, H_2O, 0 °C to RT, 70 min; iv) **297**, DMSO, 100 °C, 72 h.

6.4.2. Restricting the Conformational Flexibility of the Carboxamide Group of 2-Arylamino-6-ethynylpurines

To investigate the relationship between the carboxamide conformation and biological activity of 6-ethynylpurine **177** (NCL-00017509), efforts to impart conformational restriction on the carboxamide group were undertaken. A common method for reducing the conformational flexibility of functional groups with a methylene group is the preparation of a geminal dimethyl analogue. Accordingly the dimethyl derivative **302** was synthesised (Scheme 45). 3-Nitrophenylacetic acid (**283**) was converted into methyl ester **303** as detailed previously. It was now possible to dimethylate the benzylic position by deprotonation of the enolisable methylene in the presence of methyl iodide. The use of an excess of both sodium hydride and methyl iodide gave the *gem*-dimethyl compound **304** in moderate yield (55%). Attempted conversion of **304** into the carboxamide (**305**) by treatment with concentrated ammonium hydroxide was unsuccessful at room temperature, presumably as a consequence of additional steric hindrance at the ester carbonyl conferred by the *gem*-dimethyl groups. The reaction proceeded on heating at 60 °C, although a significant proportion of the methyl ester **304** was hydrolysed to the carboxylic acid **306**. The crude mixture of **305** and **306** was treated directly with thionyl chloride, before being added to concentrated ammonium hydroxide, giving an increased yield of the required carboxamide **305**.

Scheme 45: Synthesis of the *gem*-dimethyl carboxamide **302**.

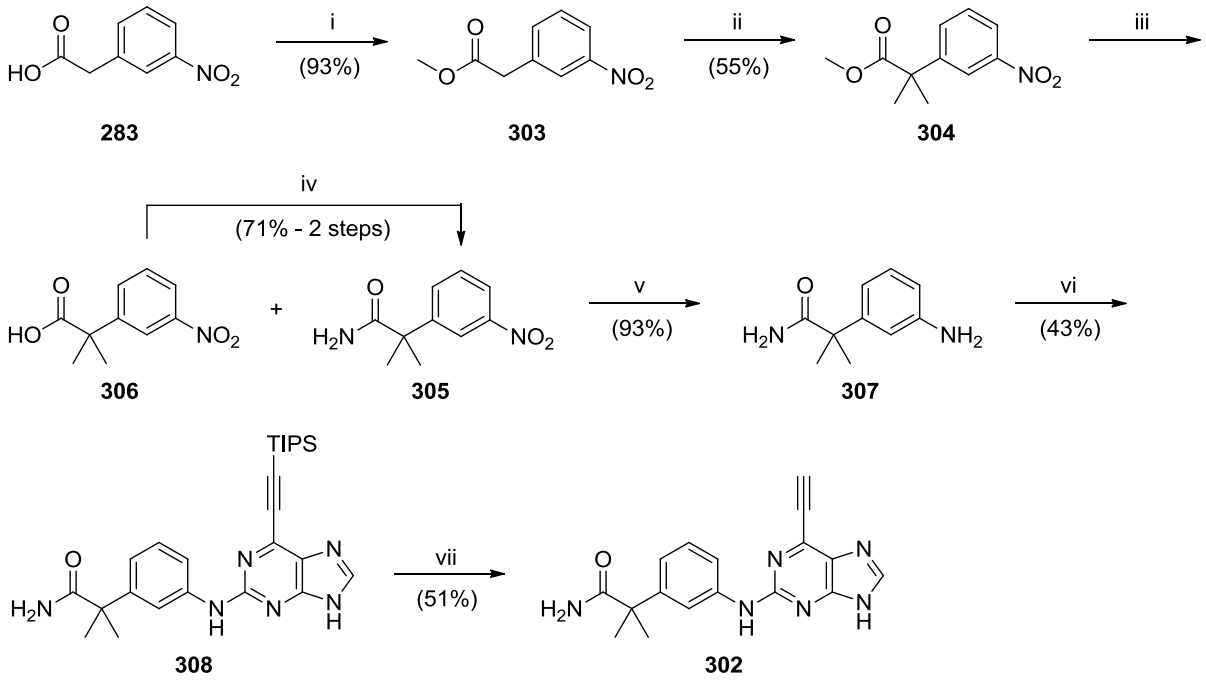

Reagents and conditions: i) $SOCl_2$, MeOH, reflux, 1 h; ii) NaH, MeI, THF, 0 °C to RT, 18 h; iii) Conc. NH_4OH, 60 °C, 18 h; iv) a) $SOCl_2$, DMF, DCM, RT, 15 min, b) Conc. NH_4OH, THF, RT, 18 h; v) Pd/C, NH_4HCOO, MeOH, RT, 18 h; vi) **160**, TFA, TFE, reflux, 24 h; vii) KF, 18-crown-6, THF, RT, 24 h.

Reduction of the nitro group of **305** was carried out *via* catalytic transfer hydrogenation, and the resultant aniline (**307**) was coupled to the 2-fluoropurine intermediate **160** in the presence of TFA, under conventional heating conditions, to give the TIPS-protected purine **308**. Removal of the TIPS-protecting group of **308** was performed as previously using KF/18-crown-6, to yield the target inhibitor **302**.

Further conformational restriction of the carboxamide substituent of **177** was possible by incorporation into a ring system. Thus, a small series of purines was designed bearing lactam groups at the 2-position, to give a number of possible carboxamide conformations (**309**-**316**).

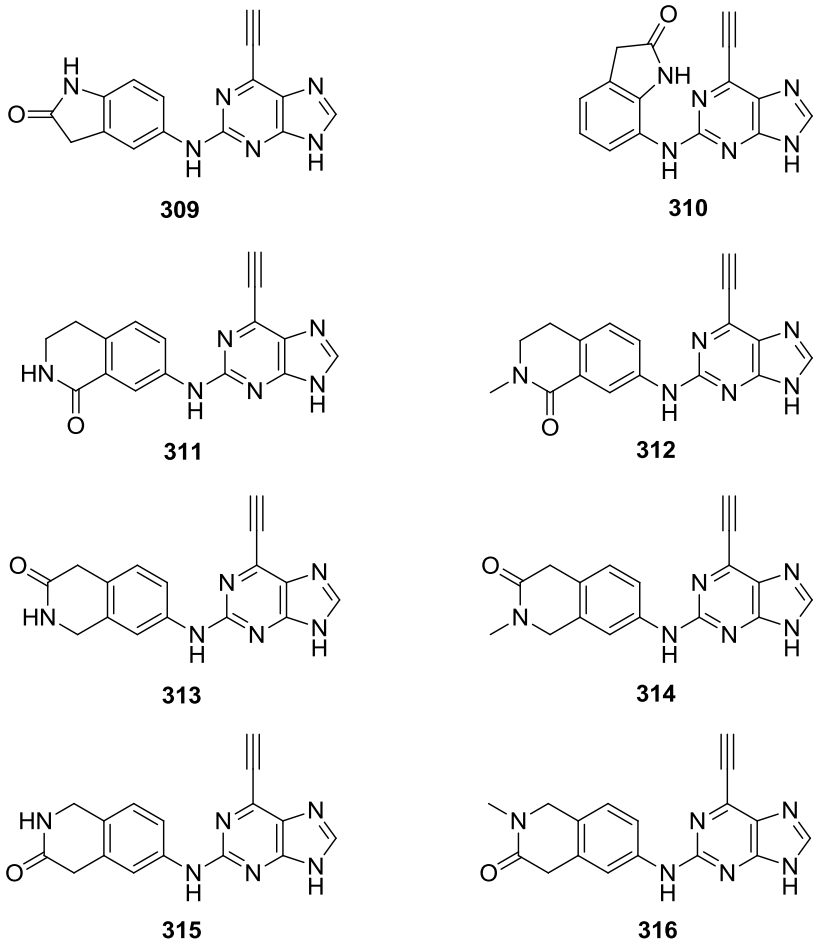

The aniline (5-amino-1,3-dihydro-2H-indol-2-one, **318**) required for the synthesis of the 5-membered ring lactam **309** was commercially available, and was coupled to the 2-fluoropurine **160** under standard conditions to give the TIPS-protected purine **319**. Deprotection of the alkyne moiety under the previously optimised conditions gave the target inhibitor **309** (Scheme 46).

Scheme 46: Synthesis of the 6-ethynylpurine **309** bearing a lactam at the purine 2-position.

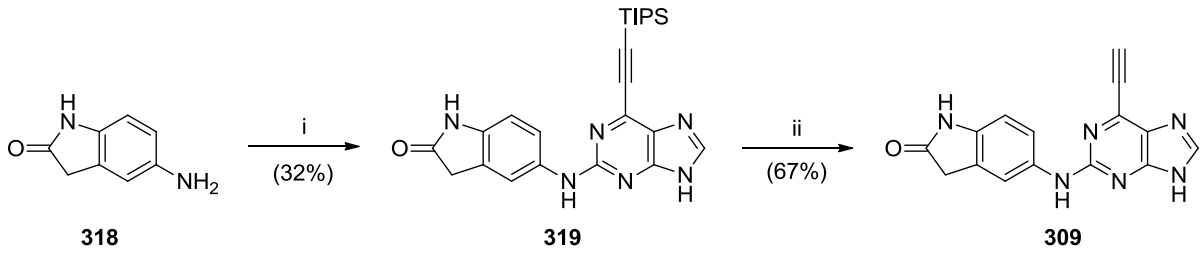

Reagents and conditions: i) **160**, TFA, TFE, reflux, 24 h; ii) a) TBAF, THF, RT, 5 min, b) **231**, THF, RT, 48 h.

The aminoindolinone required for the preparation of compound **310** was prepared following a modified literature procedure for lactam synthesis.[216] 2,6-Difluoronitrobenzene (**320**) was reacted with di-*tert*-butyl malonate to give compound **321**. It was intended to perform a lactam ring forming reaction by reduction of the nitro group of **321** in the presence of acid, followed by nucleophilic attack of the resultant aniline on a malonate carbonyl group. To achieve this, the remaining fluoro group was substituted by 4-methoxybenzylamine to give **322**. It was important that di-*tert*-butyl malonate was used for this reaction sequence, as preliminary studies using dimethyl malonate failed owing to side-reactions between 4-methoxybenzylamine and the diester, resulting in amide formation.

Scheme 47: Synthesis of the 2-aminolactam-6-ethynylpurine **310**.

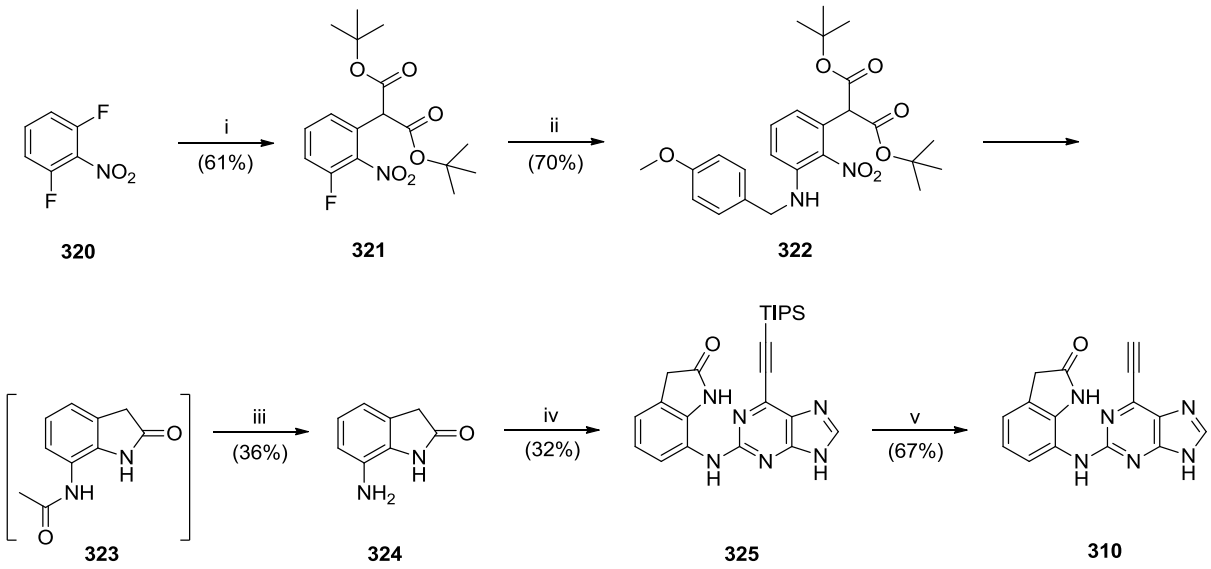

Reagents and conditions: i) Di-*tert*-butylmalonate, K_2CO_3, DMF, 60 °C, 18 h; ii) PMB-NH_2, THF, 80 °C, 18 h; iii) a) Pd/C, NH_4HCOO, AcOH, MW 100 °C, 80 min, b) AcCl, MeOH, RT, 1 h; iv) **160**, TFA, TFE, reflux, 24 h; v) a) TBAF, THF, RT, 5 min, b) **231**, THF, RT, 48 h.

Malonate derivative **322** was subjected to palladium-catalysed transfer hydrogenation in acetic acid with microwave assisted heating, whereby lactam formation occured in conjunction with removal of the PMB group. However, the use of acetic acid as solvent resulted in acetylation of the aniline (**323**), and it was necessary to treat the crude product with methanolic HCl prior to purification to deacetylate the aniline. The required aminolactam **324** was obtained in poor yield (36%), although sufficient material was isolated to proceed with the synthesis of the target purine (**310**). Coupling of **324** with the 2-fluoropurine **160** under microwave heating gave the TIPS-protected purine **325**, with removal

of the TIPS-protecting group proceeding in moderate yield (67%) on treatment with TBAF as before (Scheme 47).

Scheme 48: Synthesis of the 2-aminoisoquinolone-6-ethynylpurine **313**.

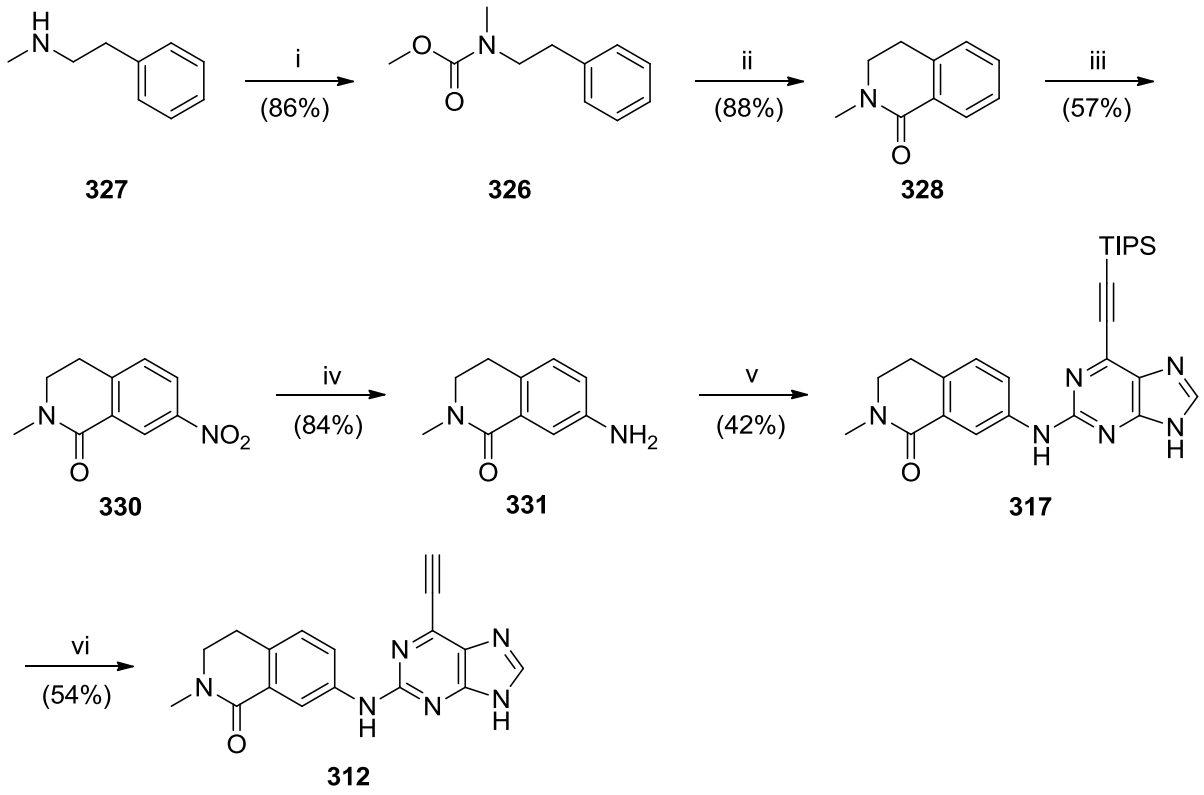

Reagents and conditions: i) $MeCO_2Cl$, K_2CO_3, Et_2O, H_2O, RT, 1 h; ii) Eaton's reagent, MW 120 °C, 15 min; iii) HNO_3, H_2SO_4, 0 °C, 30 min; iv) Fe, AcOH, 50 °C, 15 min; v) **160**, TFA, TFE, MW 140 °C, 2 h; vi) a) TBAF, THF, RT, 5 min, b) **231**, THF, RT, 48 h.

The synthesis of lactam **312** commenced with the preparation of carbamate **326** by treatment of *N*-methyl-phenethylamine (**327**) with methyl chloroformate. Cyclisations employing a Bischler-Napieralski reaction are often performed in polyphosphoric acid (PPA). However, owing to the viscosity of PPA, it was desirable to use an alternative reagent for the cyclisation of carbamate **326** to the tetrahydroisoquinolone **328**. A literature procedure for the synthesis of lactam **333** utilised Eaton's reagent (7.7% w/w phosphorus pentoxide in methanesulfonic acid) as an alternative to PPA with greatly improved ease of handling.[217] Carbamate **326** was heated in Eaton's reagent under microwave conditions to afford the lactam **328** in good yield (88%), and nitration using fuming nitric acid in sulfuric acid gave the nitroisoquinolone **330**. Heteronuclear multiple bond correlation (HMBC) two-dimensional NMR analysis of **330** confirmed the expected regioselectivity of this reaction.

Reduction of the nitro group of **330** using iron-acetic acid gave aniline **331**, which was coupled to the 2-fluoropurine **160** under TFA catalysis. Final removal of the TIPS group under standard conditions afforded the target purine **312** (Scheme 48). The N-unsubstituted analogue **311** was successfully prepared employing a similar synthetic approach, and starting from phenethylamine.

A literature procedure was available for the synthesis of the methyltetrahydroisoquinolone in **314**, utilising the Pictet-Spengler reaction between *N*-methylcarboxamide **332** and paraformaldehyde in the presence of Eaton's reagent.[217] It was proposed that this methodology would also be used for the synthesis of compounds **313- 316**. The first compound investigated was the literature example (**333**) as a means to validate the procedure. 4-Nitrophenylacetic acid (**245**) was converted into the *N*-methylcarboxamide **332** under conditions previously discussed. Although successful, this reaction required 72 hours reaction time, possibly as a consequence of deprotonation of the acidic benzylic proton by excess methylamine, hindering the reaction. Compound **332** and paraformaldehyde were reacted in Eaton's reagent, under microwave conditions, to afford the tetrahydroisoquinolone **333**, in good yield (75%). Reduction of the nitro group and coupling of the resultant aniline (**334**) to **160** afford the TIPS-protected purine **335**. Removal of the TIPS group under the optimised conditions gave the target purine **314** (Scheme 49).

Scheme 49: Preparation of the 2-aminoisoquinolone-6-ethynylpurine **314**.

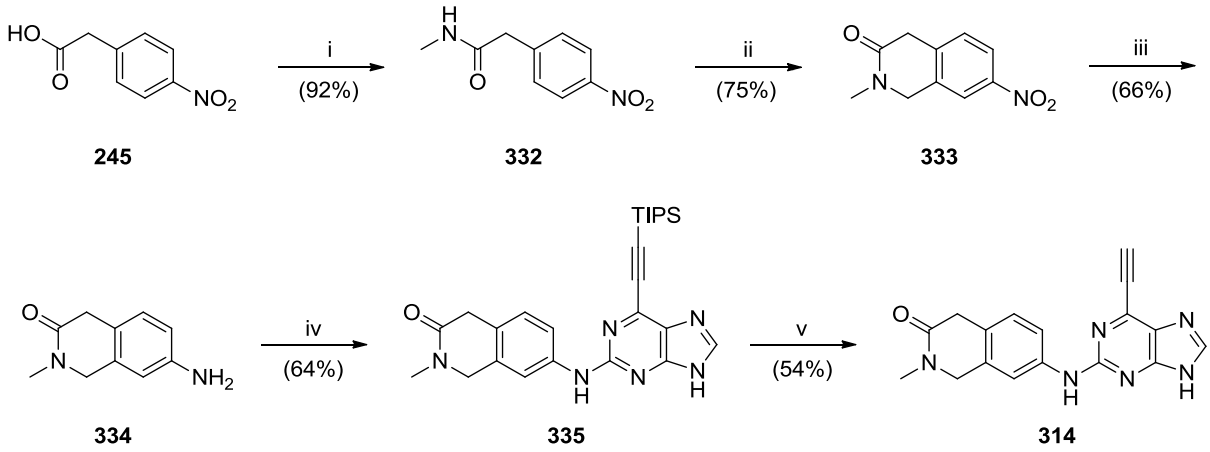

Reagents and conditions: i) a) $SOCl_2$, MeOH, reflux, 1 h, b) Aq. $MeNH_2$, RT, 72 h; ii) $(CH_2O)n$, Eaton's reagent, 80 °C, 6 h; iii) Fe, AcOH, 50 °C, 15 min; iv) **160**, TFA, TFE, MW 140 °C, 2 h; v) a) TBAF, THF, RT, 5 min, b) **231**, THF, RT, 48 h.

However, when this approach was applied to the synthesis of compounds **313**, **315** and **316**, significant problems were encountered. For the synthesis of **313**, an initial attempt was made to prepare lactam **336** by a Pictet-Spengler reaction between carboxamide **337** (synthesis not shown) and paraformaldehyde, resulting in a complex mixture of unidentified products by LC-MS analysis. It was thought that this may be due to side-reactions between the free NH of the carboxamide and reactive imine species in the reaction mixture following the initial cyclisation. It was therefore deemed necessary to identify a protecting group that could be used to prevent such non-specific reactions. However, selection of a protecting group that would be stable under the harsh reaction conditions, whilst being readily removable after the reaction, proved challenging. The cyclisation was attempted using both *N*-allylcarboxamide (**338**) and *N*-benzylcarboxamide (**339**) protection, despite concerns over the ease with which a benzyl group could be removed from the product **340**. In any event, complete compound degradation was observed in both cases, with no product formation detectable by LC-MS analysis (Scheme 50). Owing to time constraints, this work was not pursued further.

Scheme 50: Attempted Pictet-Spengler cyclisation reactions towards the synthesis of **313**.

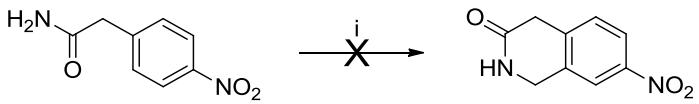

337; R = H
338; R = Allyl
339; R = Benzyl

336; R = H
329; R = Allyl
340; R = Benzyl

Reagents and conditions: i) $(CH_2O)_n$, Eaton's reagent, 80 °C, 3 h.

The synthesis of compound **315** *via* the Pictet-Spengler approach was not attempted in light of the difficulties encountered as outlined in Scheme 50. For the preparation of **316** it was anticipated that formation of the *N*-methyllactam **341** under the conditions used for the synthesis of **333** would be challenging, as the aromatic carbon nucleophile of **342** is deactivated by the *para*-nitro group. However, it was proposed that microwave assisted heating conditions might enable the reaction to proceed. *N*-Methylcarboxamide **342** and paraformaldehyde were heated under microwave irradiation in Eaton's reagent to 150 °C. After 4 hours, some starting material remained, evident by TLC analysis, although the reaction was deemed to have progressed sufficiently to warrant isolation of the target lactam **341**. Upon isolation of the major product of the reaction, ^{1}H NMR analysis indicated the presence of two products, proposed to be the desired lactam **341** and the regioisomeric

compound **343** (Scheme 51). This was despite it being believed that formation of **343** would be sterically disfavoured due to the neighbouring nitro group. The regioisomers **341** and **343** were separable by chromatography and characterised as approximately a 1:1 mixture of regioisomers. The yield of product recovered from the reaction (30%), however, suggested that this approach was unsuitable for the synthesis of the single regioisomer **341**. No further efforts were made to synthesise compound **316** as alternative targets were pursued.

Scheme 51: Synthesis of regioisomeric tetrahydroisoquinolones **341** and **343**.

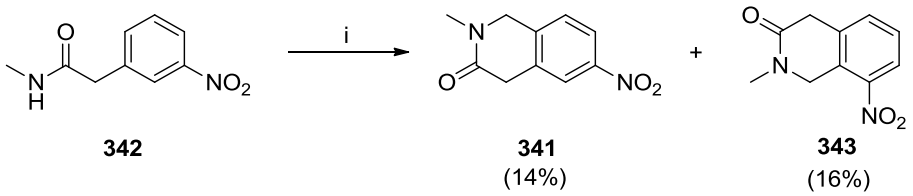

342 **341** (14%) **343** (16%)

Reagents and conditions: $(CH_2O)_n$, Eaton's reagent, MW 150 °C, 4 h.

6.4.3. Analogues of NCL00017509 (177) as Prospective Biochemical Probes

The potent and irreversible inhibition observed for 6-ethynylpurine Nek2 inhibitors offered the possibility of such compounds being used as cellular probes of Nek2 localisation. Incorporation of a fluorescent group into the structure of such compounds may enable a better understanding of the cellular localisation of both drug and protein target through the use of IFM, in conjunction with protein specific fluorescent antibodies. It was desirable to develop an inhibitor based upon **177** (NCL-00017509) with a fluorophore attached to the structure such that Nek2 inhibitory activity was not compromised. From an understanding of the binding mode of **177** within the ATP domain of Nek2 (Figure 32), it was evident that the carboxamide moiety in the 2-arylamino side-chain is directed towards solvent. This indicated that substitution on the carboxamide group would be a viable approach by which to introduce a fluorescent tag.

Nitrobenzoxadiazole (NBD) was considered to be a suitable fluorophore, as NBD is known to exhibit higher intensity fluorescence bound to a kinase compared to in free solution,[218] and this fluorophore may easily be incorporated into the inhibitor. The NBD group is non-fluorescent in the absence of an amino group at the 4-position, and it was therefore designed to be attached to the carboxamide of **177** *via* an alkylamino spacer group (**344**). It was also necessary to design a control compound lacking the NBD group in order to assess the

contribution of this structural modification on Nek2 inhibitory activity. Prior experience indicated that compounds bearing basic groups in the 2-arylamino side-chain were subject to decomposition upon removal of the TIPS-protecting group from the 6-ethynyl substituent (see chapter 6.3.1.). Hence, it was inappropriate to simply remove the NBD group to leave a primary amine, and it was decided to prepare the N-acetylated compound **345** in parallel with **344**.

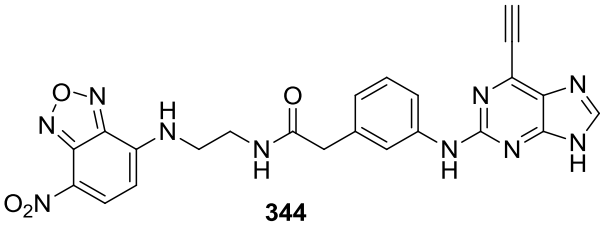

344

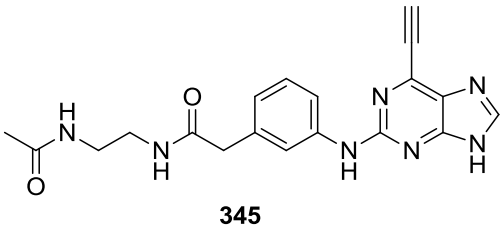

345

A synthetic approach was identified for the preparation of both compounds **344** and **345** (Scheme 52). The amino group of 3-aminophenylacetic acid (**346**) was Boc-protected (**347**), and the requisite alkylamino linker was introduced through a CDI-mediated coupling reaction between carboxylic acid **347** and 1,2-diaminoethane to give intermediate **348**. Subsequent reaction with NBD-chloride or acetic anhydride gave compounds **349** and **350**, respectively. The Boc-protecting group was removed from **349** and **350** with TFA to give anilines **351** and **352**, which were coupled to the 2-fluoropurine **160** to yield the TIPS-protected purines **353** and **354**, respectively. It was not clear why the coupling reactions for both anilines **351** and **352** proceeded at a significantly slower rate (96 hours and 72 hours, respectively) compared with previous reactions of this type, and in low yield (14%) for **353**. There was, however, sufficient material to proceed to the final step, and removal of the TIPS-protecting groups of compounds **353** and **354** as described previously afforded the target inhibitors **344** and **345**.

Scheme 52: Synthesis of 6-ethynylpurines **344** and **345**.

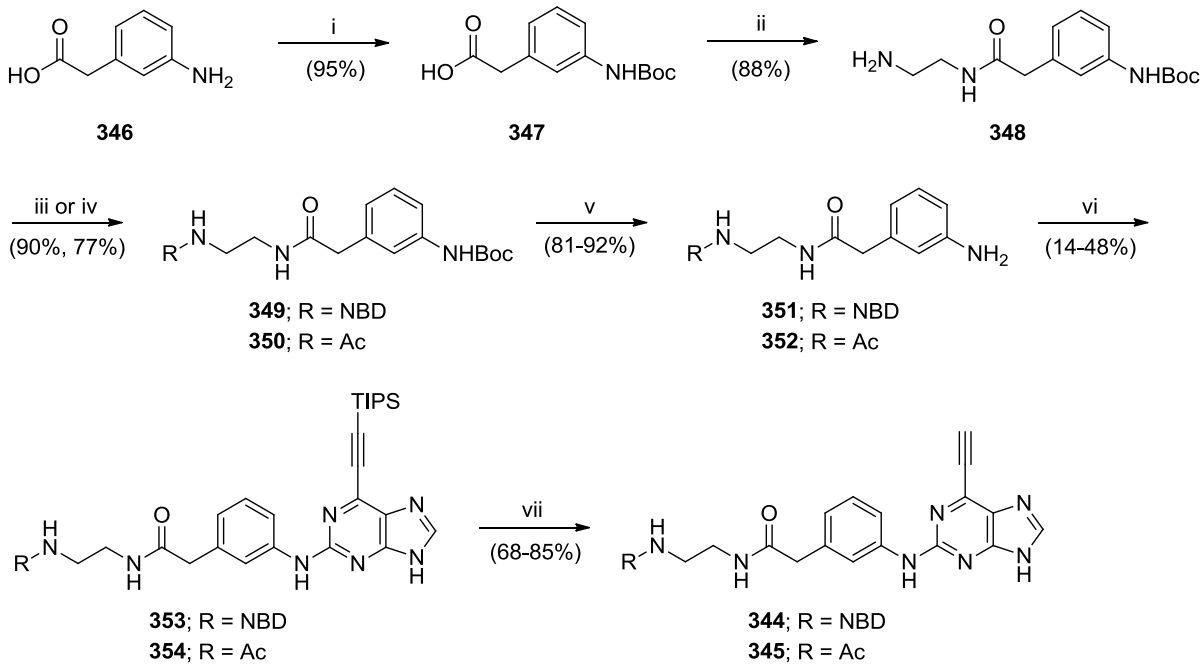

Reagents and conditions: i) Boc_2O, 1,4-dioxane, NaOH, H_2O, RT, 18 h; ii) $H_2N(CH_2)_2NH_2$, CDI, DIPEA, THF, RT, 18 h; iii) NBD-Cl, NEt_3, DMF, RT, 18 h; iv) Ac_2O, pyridine, RT, 18 h; v) TFA, DCM, RT, 18 h; vi) **160**, TFA, TFE, reflux, 72-96 h; vii) KF, 18-crown-6, THF, RT, 18 h.

Positron emission tomography (PET) is a useful imaging technique that can be used to monitor the distribution and localisation of drug molecules and their metabolites *in vivo*.[219] Briefly, a PET scanner detects radiation in the form of gamma-rays, arising from the decay of positrons emitted from a positron-emitting radioisotope. Incorporation of such a radiolabel into a drug molecule may enable a 3-dimensional image to be generated showing drug distribution *in vivo*. A common radioisotope used for such studies is fluorine-18 (^{18}F), owing to its reasonable half-life (109.7 minutes), and the ease with which it can often be incorporated into small molecules. The possibility of using this technique to determine the biological fate of 6-ethynylpurine Nek2 inhibitors was investigated.

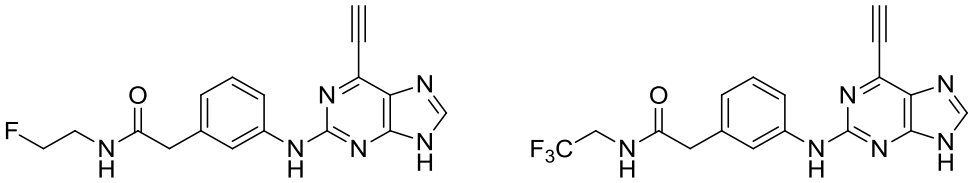

Following discussions with Dr Michael Carroll (Radiopharmacology Group, Newcastle University) it was proposed that incorporation of ^{18}F into the 2-arylamino side-chain of **177** may be a suitable approach for this purpose. The manner by which ^{18}F is generated indicated that 2-fluoroethylamine would be a suitable reagent, leading to the design of compound **355**. Prior to the synthesis of a radiolabelled inhibitor, it was necessary to synthesise the corresponding ^{19}F-analogue of **355** to establish that the Nek2 inhibitory activity of this compound is retained. As an additional compound to further investigate SARs on the carboxamide group of **177**, the trifluoroethyl analogue (**356**) was also synthesised.

Scheme 53: Synthesis of compound **356**.

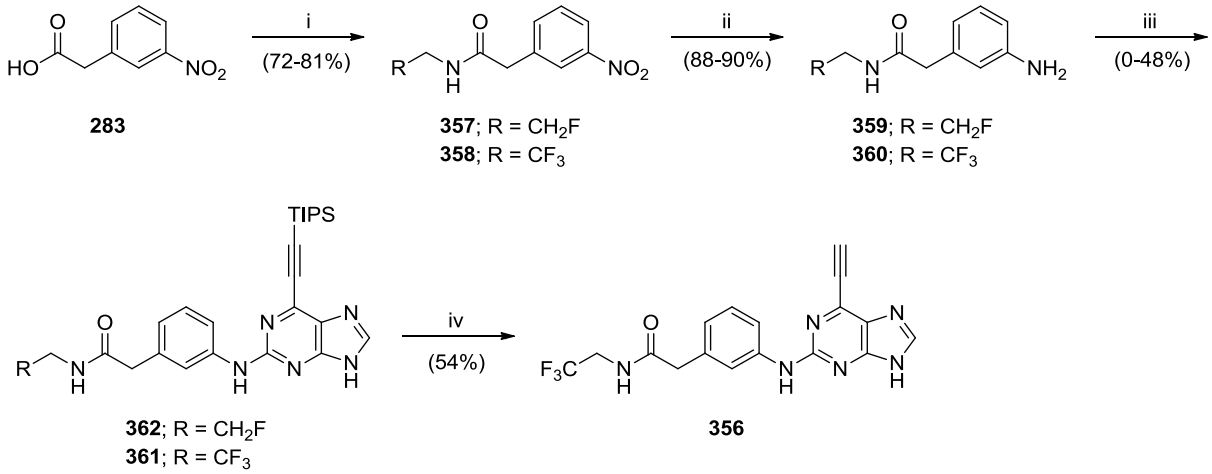

Reagents and conditions: i) RCH_2NH_2, PCl_3, MeCN, MW 150 °C, 5 min; ii) Pd/C, NH_4HCOO, MeOH, RT, 18 h; iii) **160**, TFA, TFE, reflux, 48 h; iv) a) TBAF, THF, RT, 5 min, b) **231**, THF, RT, 48 h.

3-Nitrophenylacetic acid (**283**) was coupled with 2-fluoroethylamine or 2,2,2-trifluoroethylamine using phosphorus trichloride as previously described, to generate fluoroethylcarboxamide **357** and trifluoroethylcarboxamide **358**, respectively. Nitro group reduction of **357** and **358**, gave anilines **359** and **360**, respectively, which were reacted with the 2-fluoropurine **160** under standard conditions. However, whereas aniline **360** coupled to the purine, as expected, to afford **361**, the reaction with **359** failed to yield any of the required product (**362**), although the aniline was consumed. It was proposed that the fluoroethylcarboxamide **359** may be subject to polymerisation under these reaction conditions, to give **363**, by virtue of an S_N2 reaction between the amino function and fluoro substituent (Scheme 54).

Scheme 54: Proposed mechanism for degradation of aniline **359**.

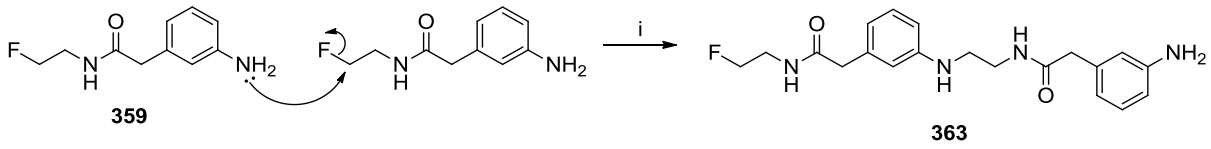

Reagents and conditions: i) TFA, TFE, reflux, 48 h.

The TIPS-protecting group was removed from purine **361** with TBAF under established conditions to give the target compound **356** (Scheme 53). The instability of aniline **359** under the usual coupling conditions prompted an alternative approach to be employed for the synthesis of **355**. Using carboxylic acid **186**, it was possible to prepare the TIPS-protected purine **362** through a CDI-mediated amide coupling with 2-fluoroethylamine. Final removal of the TIPS-protecting group gave the required product **355** (Scheme 55).

Scheme 55: Synthesis of the 6-ethynylpurine **355**.

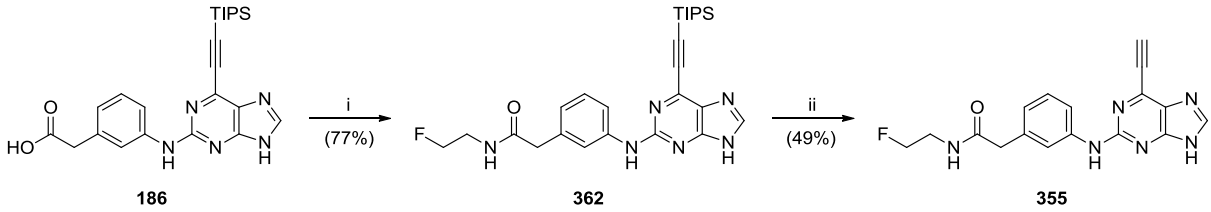

Reagents and conditions: i) $F(CH_2)_2NH_2$, CDI, DIPEA, THF, RT, 18 h; ii) a) TBAF, THF, RT, 5 min, b) **231**, THF, RT, 48 h.

6.4.4. Biological Results

All compounds synthesised were screened for inhibitory activity against both Nek2 and Cdk2. In addition, due to the observation that the SKBR3 cell line is sensitive to 6-ethynylpurine Nek2 inhibitors, the purines were evaluated for growth inhibitory activity *in vitro* against this tumour cell line (Table 14).

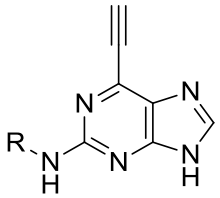

		IC_{50} (μM)		GI_{50} (μM)
Compound	**R**	**Nek2[a]**	**Cdk2[b]**	**SKBR3**
177	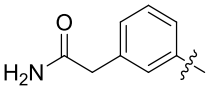	0.062 ± 0.01	11.8	2.2 ± 0.4
200	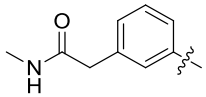	0.076	24.4	2.4 ± 0.1
201	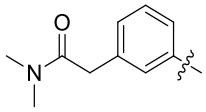	0.088	17.0	0.4 ± 0.2
202	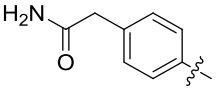	0.093	9.9	8.8 ± 1.8
203	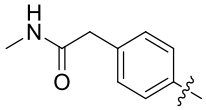	0.072	20.0	4.9 ± 2.4
204	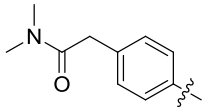	0.057	39.0	1.2 ± 0.6
257	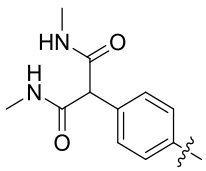	0.071	18.0	87.8
212	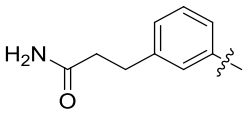	0.079	32.8	3.9 ± 1.3
205	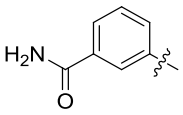	0.116	13.2	0.7 ± 0.1

Compound	R	IC_{50} (µM)		GI_{50} (µM)
		Nek2[a]	Cdk2[b]	SKBR3
206	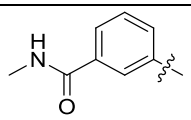	0.026	26.5	0.9 ± 0.1
207	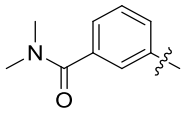	0.050	86.0	0.9 ± 0.1
208	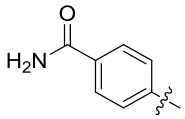	0.110	8.8	7.4 ± 0.1
209	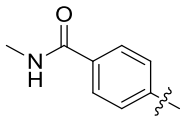	0.110	15.3	4.1 ± 0.5
210	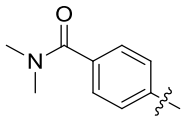	0.064	24.8	1.4 ± 0.4
211	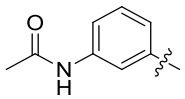	0.039	22.9	0.8 ± 0.5
302	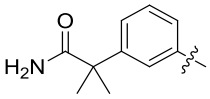	0.210	46.0	1.4 ± 0.6
344	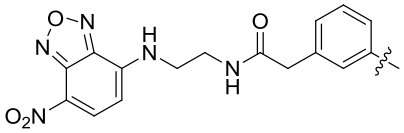	0.220	>100	>30
345	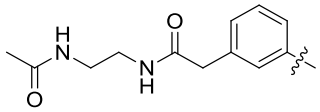	0.190	82.0	>30
355	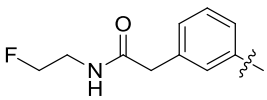	0.056	26.4	2.6 ± 0.3
356	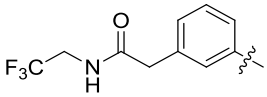	0.078	41.3	1.5 ± 0.1

[a] Nek2 IC_{50} values determined at 30 µM ATP concentration; [b] Cdk2 IC_{50} values determined at 12.5 µM ATP concentration.

Table 14: A) Biological evaluation of carboxamide based analogues of **177** (NCL-00017509).

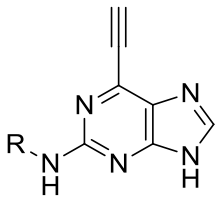

Compound	R	IC_{50} (μM) Nek2[a]	IC_{50} (μM) Cdk2[b]	GI_{50} (μM) SKBR3
199	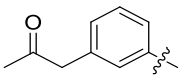	0.076	21.6	0.4 ± 0.1
178	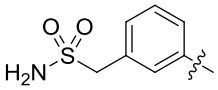	0.130	14.0	4.1 ± 2.2
289	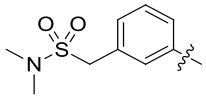	0.010	20.0	0.8 ± 0.1
290	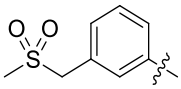	0.057	12.7	1.3 ± 0.0
309	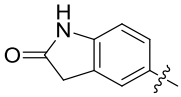	0.100	10.9	10.3
310	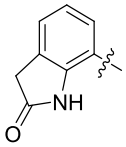	0.820	62.3	1.3 ± 0.2
311	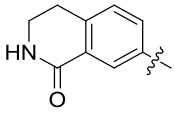	0.830	12.6	0.6 ± 0.1
312	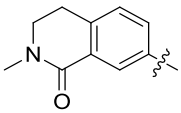	0.010	19.2	0.3 ± 0.1
314	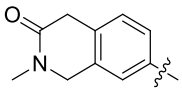	0.042	8.3	0.8 ± 0.1

[a] Nek2 IC_{50} values determined at 30 μM ATP concentration; [b] Cdk2 IC_{50} values determined at 12.5 μM ATP concentration.

Table 14: B) Biological evaluation of non-carboxamide analogues of **177** (NCL-00017509).

All purine derivatives tested exhibited inhibitory activity against Nek2 with all but two compounds (**310** and **311**) possessing an IC_{50} of less than 0.25 μM. It is evident that the activity of **177** (IC_{50} = 0.062 ± 0.01 μM) is not affected by truncation (**205**; IC_{50} = 0.116 μM) or homologation (**212**; IC_{50} = 0.079 μM) of the methylene spacer group. The ability of the carboxamide group to act as an H-bond donor does not appear to be a significant contributory factor to the potency of **177**, as sequential removal of the carboxamide amino hydrogen

atoms with the *N*-methylcarboxamide (**200**; IC_{50} = 0.076 μM) and *N*,*N*-dimethylcarboxamide (**201**; IC_{50} = 0.088 μM) analogues of **177** had little effect on Nek2 inhibitory activity. Interestingly, for the *N*,*N*-dimethylsulfonamide analogue (**289**; IC_{50} = 0.010 μM) the lack of an H-bond donor atom conferred a significantly improved potency when compared with the primary sulfonamide (**178**; IC_{50} = 0.130 μM). Furthermore, the position at which the acetamide substituent is attached to the 2-arylamino ring has limited influence on the potency of inhibitors, as was observed for the 4-substituted analogue (**202**; IC_{50} = 0.093 μM). Unfortunately, it was not possible to synthesise the 2-substituted analogue (**213**) to further validate this observation. However, for compound **310** (IC_{50} = 0.82 μM) it is likely that the conformational restriction imposed by the bicyclic 2-arylamino system forces steric clashes with the binding site of Nek2. This suggests that the optimal 2-arylamino side-chain characteristics are more linear with respect to the purine scaffold, as indicated by comparison of the activity of **310** with that of the regioisomeric analogue **309** (IC_{50} = 0.10 μM). This does not, however, explain the disparity in activity between lactams **311** (IC_{50} = 0.83 μM) and **312** (IC_{50} = 0.01 μM). As previously seen for compounds of this class, only very limited SARs are evident, with no discernible trend observed between the activity of compounds against Nek2 and the degree of modification of the carboxamide group. Presumably, all compounds excluding **310** and **311** exhibit sufficient initial competitive binding affinity for Nek2 to allow the purine to occupy the ATP-binding domain of the kinase and enable subsequent covalent modification of Cys22 to occur. The weaker activity observed for **310** and **311** does suggest that it is possible to elucidate SARs for this compound class and that potent activity is not common to all of the 6-ethynylpurines. Nevertheless, it is likely that both compounds **310** and **311** exhibit a particularly weak initial competitive binding affinity for the kinase, as the diverse range of functionalities tolerated at the 2-arylamino position suggest that subtle changes in competitive binding for an irreversible binding series will be undetectable within this assay format. What these data do reveal, however, is that for irreversible inhibitors in the 6-ethynylpurine class, there is a large degree of tolerance for substitution on the 2-arylamino ring. This is particularly relevant for the synthesis of compounds designed to act as biochemical tools for the study of cellular Nek2 activity (*e.g.* **344**; IC_{50} = 0.22 μM, see chapter 6.4.3.).

During the biochemical evaluation of **177** and related compounds in cellular systems (see chapter 7), U2OS cells overexpressing Nek2 were incubated with the fluorescently tagged irreversible inhibitor **344**. Unfortunately, it was not possible to detect any significant

fluorescence signal, either at the centrosomes or within the cell as a whole by fluorescence microscopy. It is possible that the high CLogP of **344** (3.8) conferred poor cell permeability to this purine, thus limiting the suitability of this compound as a biochemical probe. This is also reflected by the lack of cellular growth inhibitory activity observed for the fluorescent inhibitor **344** and the control compound **345** (SKBR3; GI_{50} > 30 µM).

All analogues of **177** maintained selectivity for Nek2 over Cdk2. Due to the expense and resource required, no further selectivity data were obtained for individual compounds. In addition, all compounds detailed in Tables 14 A and B exhibited growth inhibitory activity in the SKBR3 cell line. It was surprising to find that there appeared to be a poor correlation between the IC_{50} of compounds in the Nek2 kinase assay and their activity in the SKBR3 cellular GI_{50} assay. In particular, compound **311** (Nek2; IC_{50} = 0.83 µM, SKBR3; GI_{50} = 0.6 ± 0.1 µM) was the least active inhibitor in the Nek2 assay, but proved one of the most potent growth inhibitors in SKBR3 cells.

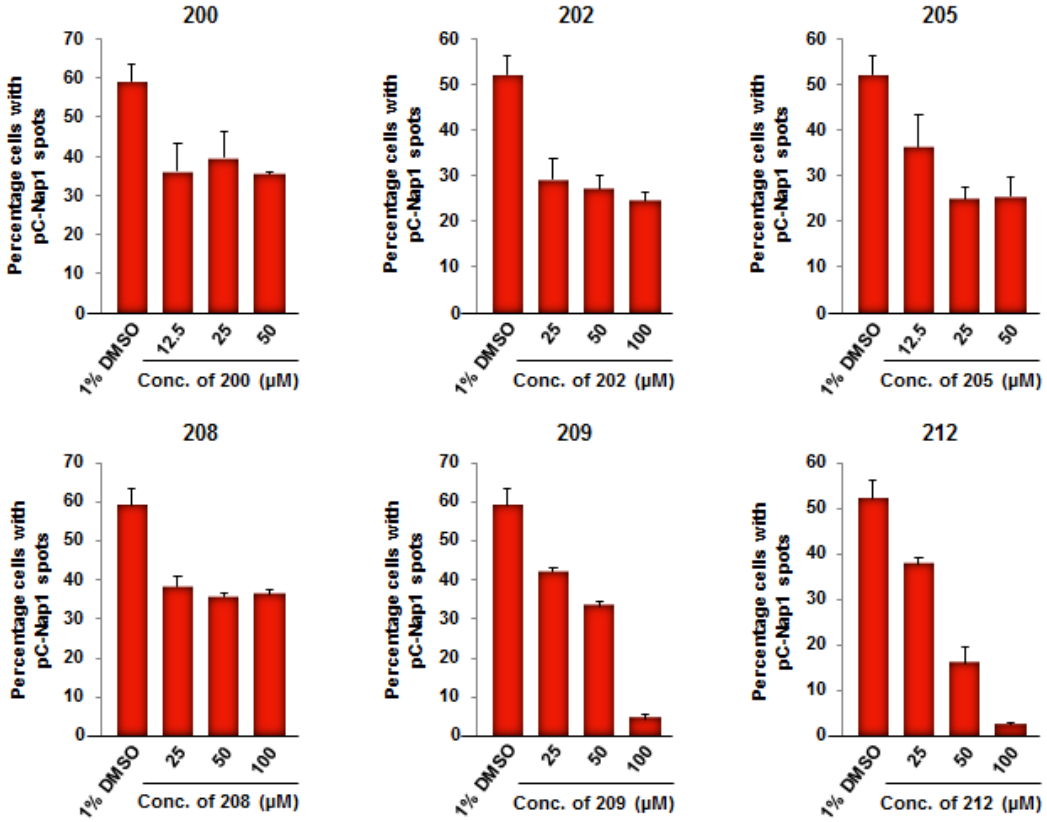

Figure 38: Dose-dependent reduction of pC-Nap1 levels for selected compounds within the 6-ethynylpurine series.

Selected purines were evaluated for inhibition of cellular pC-Nap1 levels (Figure 38). The majority of compounds reduced pC-Nap1 levels in a dose-dependent manner, although to varying degrees. However, the levels of pC-Nap1 inhibition did not correlate with the Nek2 IC_{50} or the growth inhibitory activity of compounds in the SKBR3 cell line. A more comprehensive selection of the inhibitors synthesised would need to be evaluated in this assay to further investigate this observation. A possible reason for the disparity between cellular growth activity and Nek2 inhibitory activity may be the cellular permeability of compounds. Although values from the pC-Nap1 assay are not quantitative, it may be possible to correlate cellular activity with cellular permeability by relating the GI_{50} of compounds in the SKBR3 cell line to their CLogP values (Figure 39; corrected to remove compounds with a GI_{50} greater than 10 µM). Unfortunately, there was no clear correlation, and without evaluation of all synthesised inhibitors in the pC-Nap1 assay it is not possible to draw further conclusions from these results.

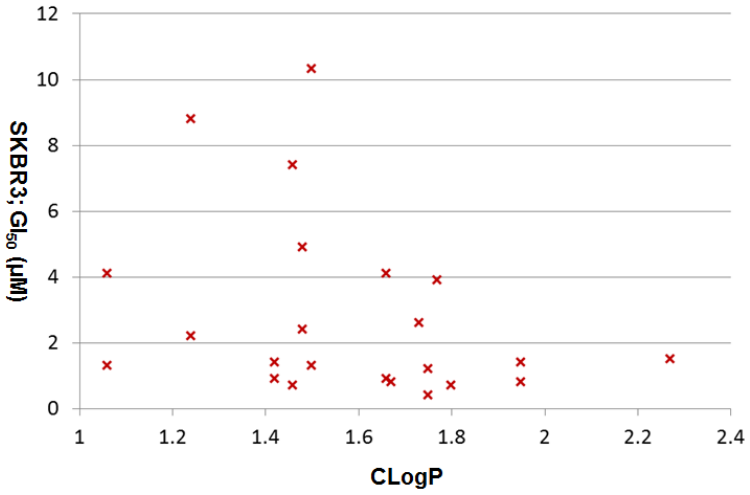

Figure 39: Relationship between the cellular growth inhibitory activity of 6-ethynylpurines in the SKBR3 cell line and their CLogP values for compounds with a GI_{50} <10 µM.

In addition to the 6-ethynylpurine analogues within the series, the 6-cyano derivative (**296**) was synthesised as a purely competitive control compound of **177**. As expected, **296** was much less active against Nek2 when compared with compounds in the 6-ethynylpurine series, highlighting the requirement for the Michael acceptor motif for potent kinase inhibition. The 6-cyanopurine retains low micromolar potency against Nek2, perhaps reflecting the competitive binding component of **177**, and suggests that without covalent modification, the purine template remains a moderately potent competitive Nek2 inhibitor. Furthermore, **296** was significantly less growth inhibitory in the SKBR3 cell line than **177**, likely due to the

modest potency of the compound towards Nek2. However, it must also be noted that **296** (CLogP = 0.64) is more polar than **177** (CLogP = 1.24) and the weak growth inhibition in cells may be a result of poor cellular permeability.

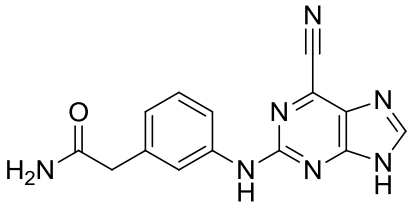

296

IC_{50}; Nek2 = 4.13 μM

Cdk2 = 70.8 μM

GI_{50}; SKBR3 = 80.7 ± 16.0 μM

6.4.5. Further Studies with NCL-00017509 (177)

The 6-ethynylpurine **177** (NCL-00017509) was an attractive early stage lead inhibitor of Nek2, with good potency and kinase selectivity. Cell lines have been identified in which the compound is not only growth inhibitory, but also cytotoxic (SKBR3 and Rec-1). As such, further studies to characterise **177** as a lead compound were undertaken, including preliminary *in vitro* ADME testing (Cyprotex Discovery, Macclesfield) (Table 15). These studies suggested that **177** possessed the attributes of a drug-like compound. The purine was found to combine an excellent plasma protein binding profile (<80%) with good aqueous solubility within the constraints of the assay. No inhibition of hERG (human Ether-a-go-go-Related Gene product) was observed at 25 μM, and **177** exhibited a good stability profile in both human and mouse liver microsomes, despite the electrophilic 6-ethynyl group.

Studies employing the Caco-2 cell line allowed an estimation of compound permeability and efflux to be determined. The direction [A → B] equates to compound passing from the gastrointestinal tract into the blood, with [B → A] relating to drug efflux in the reverse direction. The inhibitor showed low permeability and high efflux, suggesting that the oral bioavailablility of **177** may be poor. It is possible, however, that the inherent permeability of the compound is good, but that it is also a substrate for drug efflux transporters.

Plasma Protein Binding:

Fraction Unbound		Mean Fraction Unbound	Standard deviation (n = 2)	Mean recovery %
Replicate 1	**Replicate 2**			
0.219	0.228	0.223	0.00668	86.3

Microsomal Stability:

Microsomal Stability (Human)				Microsomal Stability (Mouse)			
CLint (µl/min/mg)	**S.E. CLint**	**$T_{1/2}$ (min)**	**n**	**CLint (µl/min/mg)**	**S.E. CLint**	**$T_{1/2}$ (min)**	**n**
6.21	0.681	223	5	10.2	1.82	136	5

Solubility:

Estimated Precipitation Range (µM)		
Lower Bound	**Upper Bound**	**Calculated mid-range**
100	>100	>100

Caco-2 Permeability:

	Papp (x 10^{-6} cm^{-1})		Mean Papp (x 10^{-6} cm^{-1})			Mean recovery (%)
Direction	**1**	**2**		**SD**	**n**	
A → B	0.0534	0.0421	0.0477	0.00799	2	57.6
B → A	4.88	5.29	5.08	0.293	2	64.0

Table 15: *in vitro* ADME properties for **177** (NCL-00017509) at Cyprotex Discovery, Macclesfield.

The promising *in vitro* results prompted the evaluation of **177** in *in vivo* models for both pharmacokinetics (PK) and antitumour efficacy, by collaborators within the NICR. For preliminary PK evaluation **177** was administered at a single dose (10 mg/kg) to female CD1 mice (n = 24). Three routes of administration were used; intravenous (i.v.) *via* the tail vein, intraperitoneal (i.p.), or orally (p.o.) by gavage. The purine was administered in a vehicle comprising 10% (w/w) PEG_{400} and sterile 0.9% w/v saline. Blood samples were taken (n = 3 mice) at selected time points post treatment, HPLC analysis was used to determine inhibitor concentrations at each time point, and PK parameters were calculated (Figure 40).

The compound was rapidly cleared from the blood following i.v. administration, with a low area under the curve (AUC), high clearance and a short half-life ($t_{1/2}$). No inhibitor was detected in blood samples for animals treated p.o., indicating that **177** has poor oral bioavailability, either due to poor absorption, or, as implied by the Caco-2 permeability assay, active efflux. It has been proposed that dosing **177** i.p. may increase exposure and hence the AUC due to prolonged absorption of the compound from the peritoneal cavity.

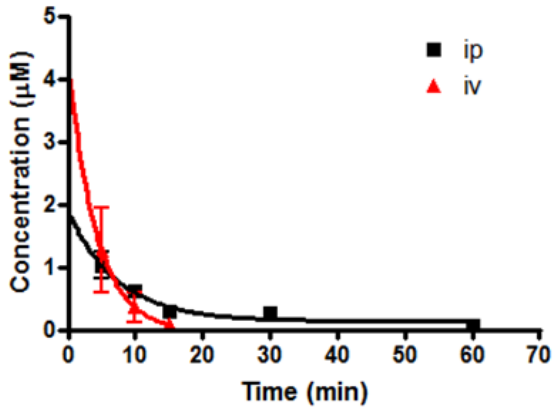

	AUC (µg/ml.min)	Clearance (ml/min/kg)	$t_{1/2}$ (min)	C_{max} (µg/ml)	T_{max} (min)	Time > 1 µM (min)	Vdss (L/kg)	Bioavail.
i.v.	2.52	3965	2.52	0.37 ± 0.34	5	< 10	24.2	-
i.p.	5.93	1687	16.46	0.30 ± 0.11	5	< 10	29.3	235%
p.o.	N/A	N/A	N/A	< 0.05	N/A	N/A	N/A	0

Figure 40: Preliminary PK parameters for **177** (NCL-00017509) administered i.v., i.p. or orally to mice (n = 24) over 6 h (undetectable after 2 h).

To understand the rapid clearance of **177**, stability studies were performed for the compound in buffered solutions at pH 2, 7.4 and 10, and in a solution containing 5 mM glutathione (GSH), which approximates to intracellular concentrations. Samples of **177** in the three solutions were incubated at 37 °C and the concentration of **177** determined by HPLC at time points over 18 hours (Figure 41). It is likely that **177** is poorly soluble in solutions at higher pH, and therefore the concentration only becomes consistent once the sample is incubated at 37 °C for 10 minutes. It was evident that under the assay conditions, **177** is degraded in a

time dependent manner in the presence of glutathione. This suggests that reaction with glutathione may contribute to the rapid clearance observed for **177** in Figure 40.

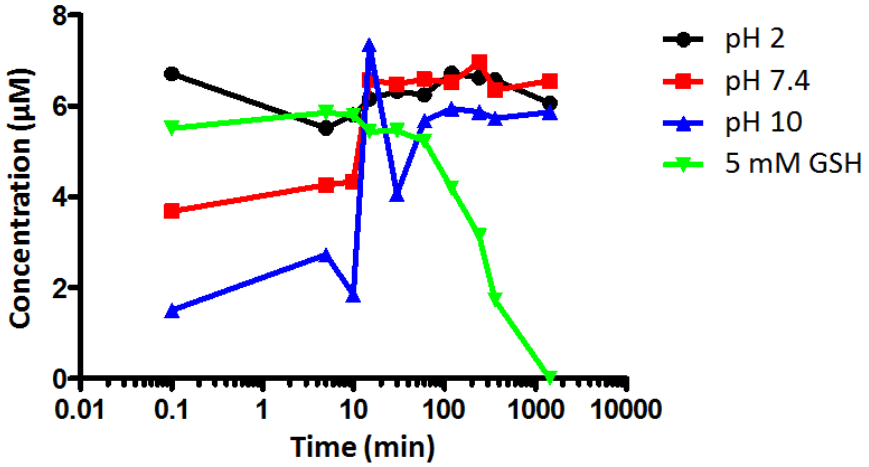

Figure 41: Stability of **177** at pH 2, 7.4 and 10 (37 °C), and in a phosphate buffered saline solution (ph 7.4) containing 5 mM GSH (n = 1); concentration determined by HPLC.

For efficacy studies, i.p. administration of **177** was selected, and it was first necessary to determine the maximum tolerated dose (MTD) of the purine in i.p. treated mice. Female CD1 mice (n = 12) were treated with 50, 100 or 200 mg/kg **177** i.p. and clinical signs and body temperature were monitored over 6 hours, with body weight also being recorded daily for 18 days, as a measure of toxicity (Figure 42).

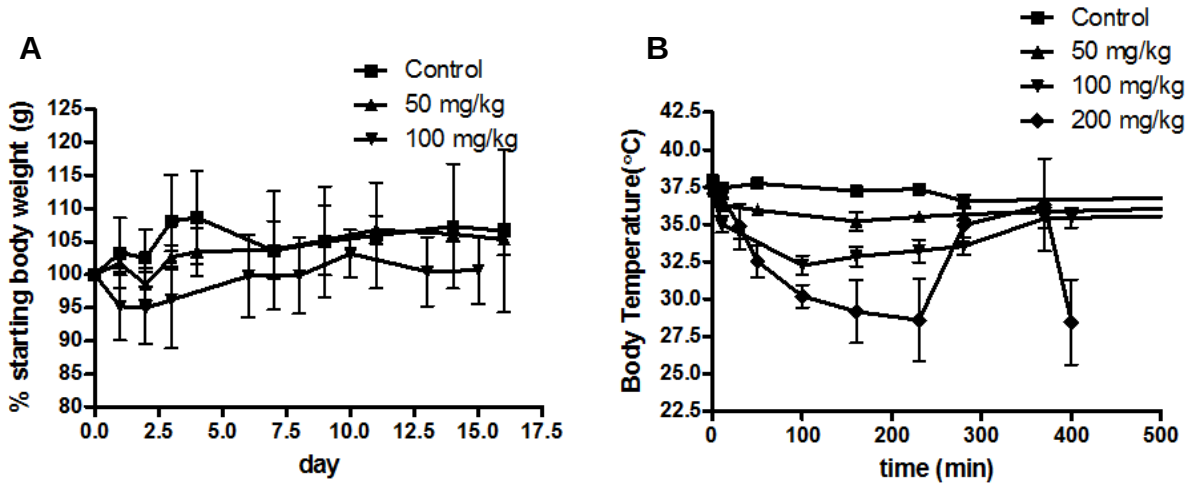

Figure 42: Determination of MTD for mice (n = 12; 3 per group) treated i.p. with **177** (NCL-00017509); **A)** Body temperature measurements recorded over 6 hours post-treatment; **B)** Calculated variations in starting body weight over 18 days post-treatment.

The mice were able to tolerate 100 mg/kg **177** acutely, whereas animals treated with 200 mg/kg inhibitor exhibited a marked hypothermia that normalised slowly over time. Over 24 hours, mice treated with 100 mg/kg inhibitor showed moderate signs of toxicity, including some weight loss, and appeared ungroomed; however, all signs of toxicity disappeared by 48 hours post-treatment. Apart from some evidence of bloating on close inspection no further clinical toxicity was observed over the 18 day period, after which the mice were monitored for a further 10 days. However, under post-mortem examination 28 days post-treatment, signs of severe reaction in the peritoneum manifesting as adhesion of the gut and abdominal organs was observed, attributed to the local toxicity of the compound.

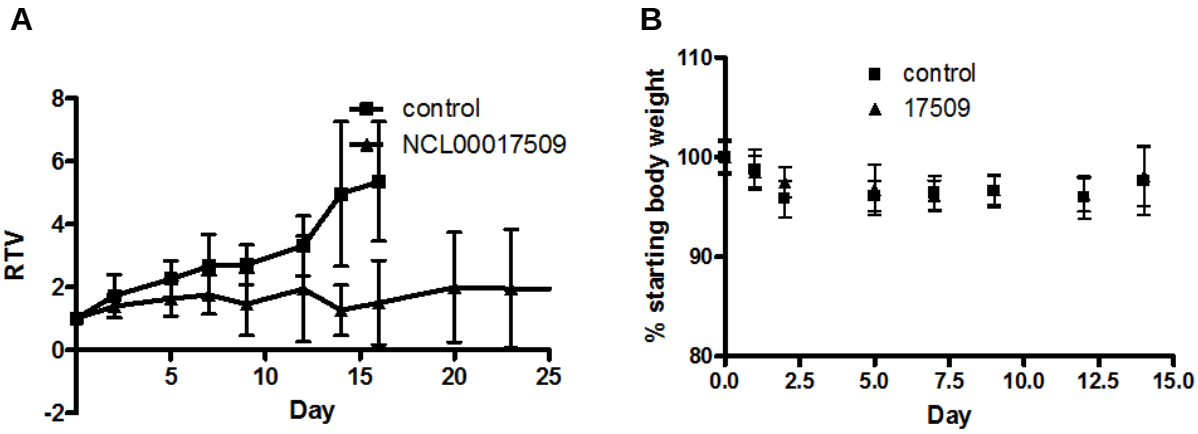

	Time to RTV 4 (d)				
Control	13	16	10	13	7
+ 177	N/A	>100	23	>100	11

Figure 43: Efficacy study for mice with RIVA B-cell lymphoma xenograft treated with **177** (n = 5) at 50 mg/kg hourly i.v. injections (≤ 6 per mouse); **A)** relative tumour volume measurements over the course of the study; **B)** Percentage body weight variations for both study populations.

To circumvent this local toxicity is was necessary to attempt i.v. dosing for the efficacy studies. For this study, 20 mice were transplanted with subcutaneous RIVA tumours, and 10 were randomised and selected for trial. Owing to the rapid clearance of **177** following i.v. administration, six hourly dosing at 50 mg/kg was required to achieve potentially active exposures (AUC), with a total dose of 300 mg/kg. This regimen had previously been shown to cause no appreciable toxicity (data not shown). For both control and **177** treated groups, the tumour volume was monitored over a time period required to allow a 4-fold increase in

relative tumour volume (RTV 4) in the control group. In addition, body weights were recorded to reflect potential compound toxicity (Figure 43).

One mouse within the treated group was killed prior to reaching RTV 4 owing to tumour burden. The initial efficacy results obtained for the remaining mice were promising, with two mice failing to reach RTV 4 within the study period. However, this study would need to be expanded to establish the statistical significance of the results, and subsequent concerns over the selectivity of the inhibitor precluded further studies with **177**.

6.5. 6-Ethynylpurines with Heterocycles at the 2-Position

6.5.1. Target Compound Selection and Synthesis

Although it was apparent that structural variation of the substituent on the 2-arylamino side-chain was tolerated with respect to Nek2-inhibitory activity for the 6-ethynylpurine pharmacophore, little was known about the effect of modifying the 2-aryl ring. To investigate this, a small series of compounds containing six-membered ring nitrogen heterocycles (**364**-**369**) was selected for synthesis.

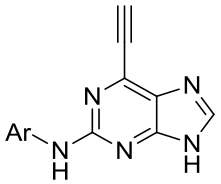

Ar =

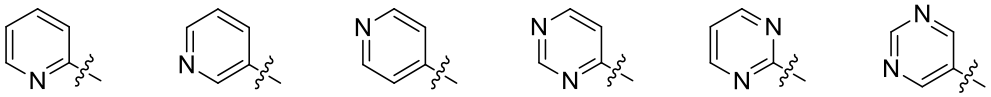

364 **365** **366** **367** **368** **369**

Initial efforts to couple 2-, 3-, and 4-aminopyridine to the 2-fluoropurine intermediate **160** suggested that the usual acid-catalysed S_NAr approach was unsuitable. Under microwave conditions using TFA, only very low conversion into the desired products was observed by LC-MS analysis for the three aminopyridines. It is likely that, when using a weakly basic heterocycle, the quantity of TFA required for optimum reaction conditions is different to that necessary when using anilines. To study this, the reaction between 4-aminopyridine and 2-fluoropurine **160** was carried out in TFE, whilst varying the number of equivalents of TFA added. In each case the reaction was performed at 140 °C with microwave irradiation for 2

hours, after which the percentage conversion to the product (**380**) was estimated by LC-MS analysis (Scheme 56). The reaction mixture using 3 equivalents of TFA was worked-up and the product isolated. Analysis by ^{1}H NMR spectroscopy revealed that, in fact, the product was the zwitterionic pyridinium species **371**.

Scheme 56: Attempted coupling of 4-aminopyridine with **160** using acid-catalysis.

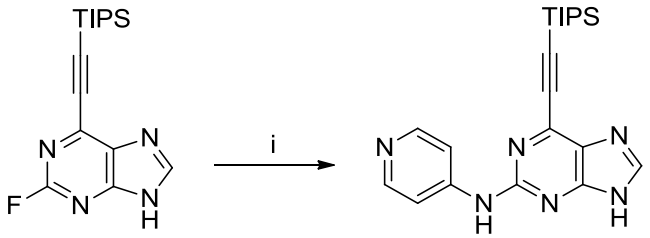

160 **380**

Reagents and conditions: i) 4-Aminopyridine, TFA, TFE, MW 140 °C, 2 h.

Equiv. TFA	Yield of 380 (%)*	Comments
0	0	Degradation
1	0	Degradation
2	4	Degradation
3	24	Clean conversion
4	21	Clean conversion
5	22	Clean conversion

* = Estimated by LC-MS

Table 16: Estimated yields for the coupling of 4-aminopyridine with **160** with varying equivalents of TFA.

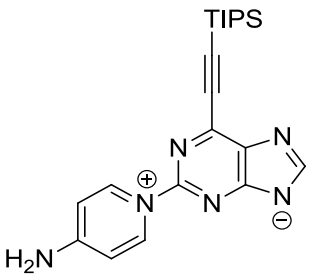

371

In light of this, it was apparent that this approach was not suitable for the coupling of aminoheterocycles to the purine scaffold. For this reason, a palladium-mediated amination was preferred for the key step by which the two heterocycles were to be coupled. The 2-iodopurine intermediate **278** coupled successfully with 2-, 3-, and 4-aminopyridine, as well as 2-, 4- and 5-aminopyrimidine, to give PMB-protected purines **372**-**377**, which were converted into the TIPS-protected purines (**378**-**383**) on heating in TFA. Final deprotection with TBAF gave the target 2-arylaminopurines **364**-**369** (Scheme 57). Unfortunately, it was not possible to isolate **367** in sufficient purity for biological testing, but the Nek2 inhibitory activity of the other compounds was determined (Table 17). 5-Aminopyrimidine (**384**) required for the preparation of compound **369** was prepared by the reductive dehalogenation of 2,4-dichloro-5-aminopyrimidine.

Scheme 57: Synthesis of 2-arylamino-6-ethynylpurines **364**-**369**.

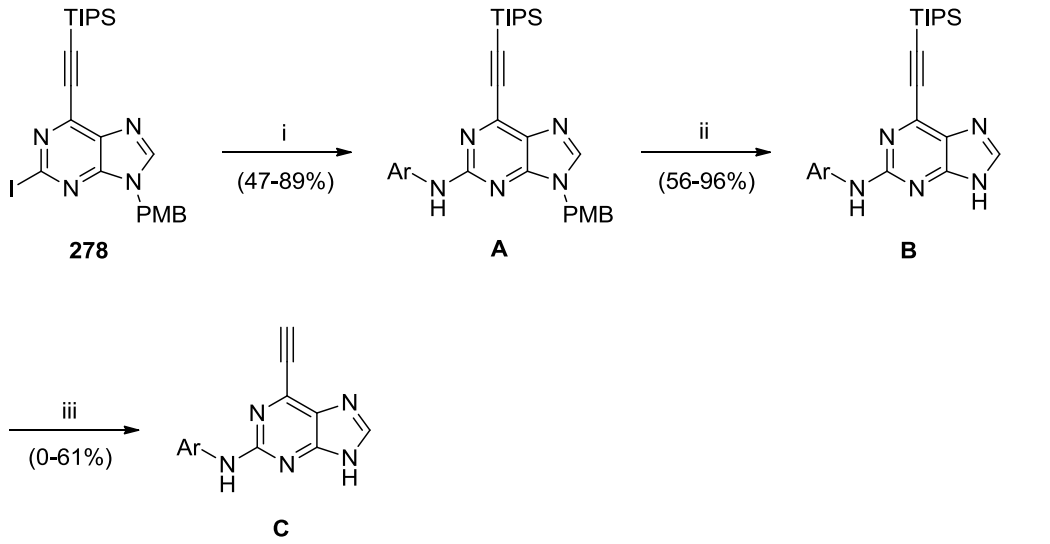

R =						
A	**372**	**373**	**374**	**375**	**376**	**377**
B	**378**	**379**	**380**	**381**	**382**	**383**
C	**364**	**365**	**366**	**367**	**368**	**369**

Reagents and conditions: i) Ar-NH_2, $Pd_2(dba)_3$, XPhos, K_2CO_3, MeCN, 100 °C, 1 h; ii) TFA, reflux, 18 h; iii) a) TBAF, THF, RT, 5 min, b) **231**, THF, RT, 48 h.

6.5.2. Biological Results

Compounds (**364**-**366**, **368** and **369**) were evaluated for inhibitory activity (IC_{50}) against both Nek2 and Cdk2. In addition, growth inhibition in SKBR3 cells was determined (Table 17).

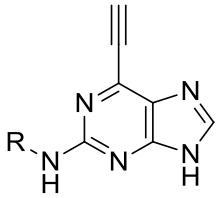

		IC_{50} (µM)		GI_{50} (µM)
Compound	**R**	**Nek2[a]**	**Cdk2[b]**	**SKBR3**
148 (NCL-00016727)		0.14 ± 0.1	22.9	0.3 ± 0.04
364		2.0	20%**	0.2 ± 0.01
365	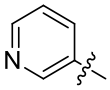	0.6	18.4	0.6 ± 0.06
366	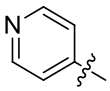	0.1	7.5	0.6 ± 0.4
368		19%*	10%**	2.4 ± 0.8
369	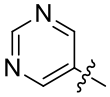	0.2	49.1	0.4 ± 0.1

[a] Nek2 IC_{50} values determined at 30 µM ATP concentration; [b] Cdk2 IC_{50} values determined at 12.5 µM ATP concentration; * = Percentage inhibition at 10 µM; ** = Percentage inhibition at 100 µM

Table 17: Biological evaluation of 6-ethynylpurines bearing heterocyclic groups at the purine 2-position.

The IC_{50} values obtained for compounds **364** and **368** suggest that there is a poor tolerance of both Nek2 and Cdk2 to inhibitors containing a heterocyclic nitrogen at the *ortho*-position on the 2-arylamino ring. It is possible that this is as a consequence of electrostatic clash between the ring nitrogen electron lone pair and amino acids of the kinase hinge region. Of the compounds retaining potency against Nek2 (**365**, **366** and **369**) there appears to be little advantage in terms of potency from incorporating heterocyclic rings at the purine 2-position when compared with the parent phenyl derivative (**148**, NCL-00016727) In addition, the

synthesised heterocyclic compounds strengthen the observation that there appears to be poor correlation between the Nek2 kinase inhibitory activity of 6-ethynylpurines and their corresponding growth inhibitory activity in the SKBR3 cell line (*e.g.* **364**, Nek2; IC_{50} = 2.0 µM, SKBR3; GI_{50} = 0.2 µM).

6.6. Purines Bearing Disubstituted 2-Arylamino Groups

6.6.1. Target Compound Selection and Synthesis

From modification of the 2-arylamino ring of 6-ethynylpurines, it was apparent that there is a high degree of tolerance with respect to activity against Nek2. This has limited the extent to which such modifications have generated meaningful SARs. However, it may be possible to exploit the tolerance to functional group modification at the 2-arylamino ring to fine-tune the reactivity of the 6-ethynyl Michael acceptor group of the purine. Thus, it was proposed that introducing electron-withdrawing or electron-donating groups at the *para*-position of the 2-arylamino group may influence the reactivity of the ethynyl group and, hence modulate potency against Nek2. In addition, varying the electron-withdrawing nature of the group on the 2-arylamino ring may also influence the H-bond donor properties of the 2-NH, and thus affect initial competitive binding affinity.

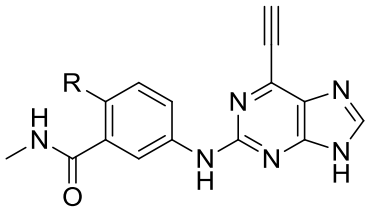

206; R = H **387**; R = MeO
385; R = F **388**; R = CF_3
386; R = Cl **389**; R = CN

A small series of compounds (**385**-**389**) was proposed based upon the *N*-methylbenzamide derivative **206**. This purine combined potent Nek2 inhibitory activity (Nek2; IC_{50} = 26 nM) with synthetic tractability of the required disubstituted aromatic groups. The majority of target purines contain an electron-withdrawing group on the 2-arylamino ring as a means to increase the reactivity of the 6-ethynyl group. The compound bearing an electron-donating methoxy group (**387**) was included to aid in the understanding of any observed effects on activity.

Scheme 58: Synthesis of the disubstituted 2-arylaminopurine **385**.

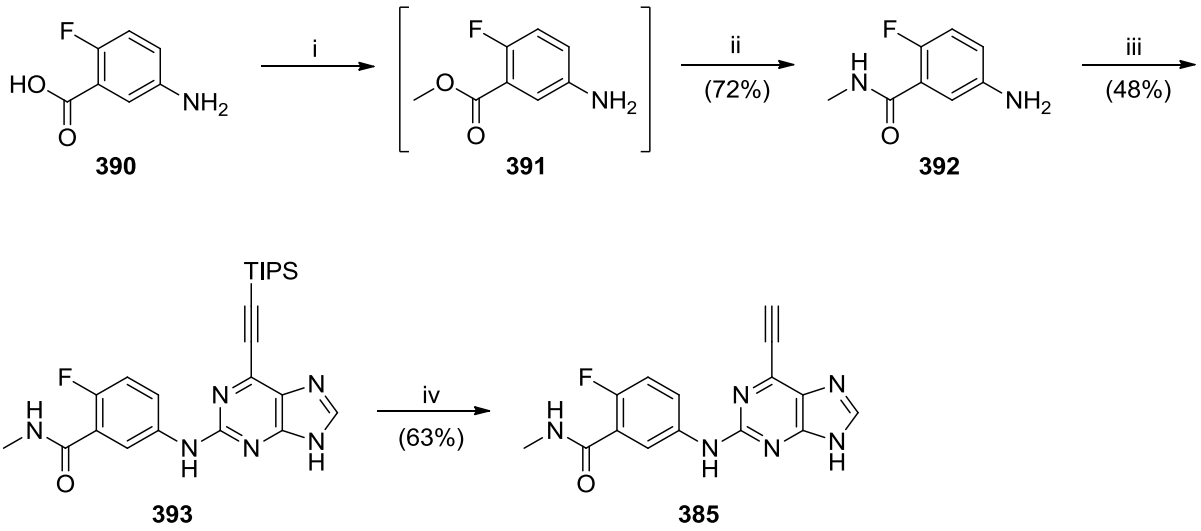

Reagents and conditions: i) $SOCl_2$, MeOH, reflux, 1 h; ii) Aq. $MeNH_2$, RT, 18 h; iii) **160**, TFA, TFE, MW 140 °C, 2 h; iv) a) TBAF, TF, RT, 5 min, b) **231**, THF, RT, 48 h.

Synthesis of the *para*-fluoro analogue (**385**) utilised the commercially available 5-amino-2-fluorobenzoic acid (**390**), which was converted into the methyl ester **391** on treatment with thionyl chloride in methanol and reacted directly with aqueous methylamine to afford the *N*-methylcarboxamide **392**. Compound **392** was coupled to the 2-fluoropurine **160** under microwave conditions as before, to give the TIPS-protected purine **393**. TIPS-deprotection using the established conditions gave the target inhibitor **385** (Scheme 58).

For the preparation of the *para*-chloro analogue (**386**), the commercially available methyl 2-chloro-5-nitrobenzoate (**394**) was reduced to the aniline **395** using iron-acetic acid. Treatment of **395** with aqueous methylamine gave the *N*-methylcarboxamide (**396**), which was coupled to the 2-fluoropurine **160**. The TIPS-protected purine **397** was treated with TBAF to give the target inhibitor **386** (Scheme 59).

Scheme 59: Synthesis of the disubstituted 2-arylaminopurine **386**.

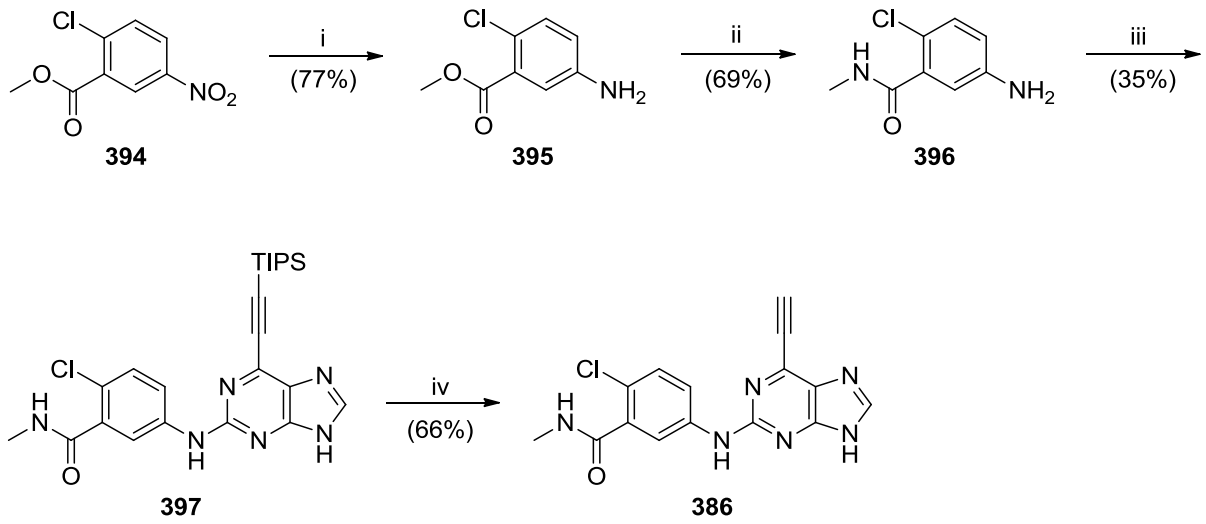

Reagents and conditions: i) Fe, AcOH, 50 °C, 15 min; ii) Aq. $MeNH_2$, RT, 18 h; iii) **160**, TFA, TFE, MW 140 °C, 2 h; iv) a) TBAF, THF, RT, 5 min, b) **231**, THF, RT, 48 h.

The initial attempted synthesis of the trifluoromethyl compound **398** by treatment of commercially available 5-chloro-2-(trifluoromethyl)benzoic acid (**399**) with thionyl chloride was unsuccessful. Attempts to prepare **398** by reaction of the acid chloride of **399** with methanol also failed. However, the use of *O*-methyl-*N*,*N*'-diisopropylisourea,[220] under microwave heating gave the desired methyl ester **398** from **399**. Subsequent attempts to substitute the chloro group of **398** by an amine through S_NAr reactions proved unsuccesful. In an alternative approach, the chloro group of **398** was substituted by 4-methoxybenzylamine, in a palladium-mediated amination, to give compound **400**. Removal of the PMB-group from **400**, with refluxing TFA, gave aniline **401**, which was treated with aqueous methylamine to yield the *N*-methylcarboxamide **402**. The lengthy reaction time (48 hours) required perhaps reflects the steric hindrance imposed on the ester of **401** by the neighbouring trifluoromethyl group. Coupling of aniline **402** with the 2-fluoropurine **160** was attempted under standard reaction conditions. Unfortunately, no reaction was observed, presumably as a consequence of the electron-withdrawing effect of the *para*-trifluoromethyl group reducing the nucleophilicity of the aniline. However, aniline **402** was coupled successfully to the 2-iodopurine **278** using a palladium-mediated amination to give the purine **403**. Removal of the PMB-protecting group at N-9 of **403** with TFA gave compound **404**, from which the TIPS-protecting group was removed under the established conditions (Scheme 60).

Scheme 60: Synthesis of the disubstituted 2-arylaminopurine **388**.

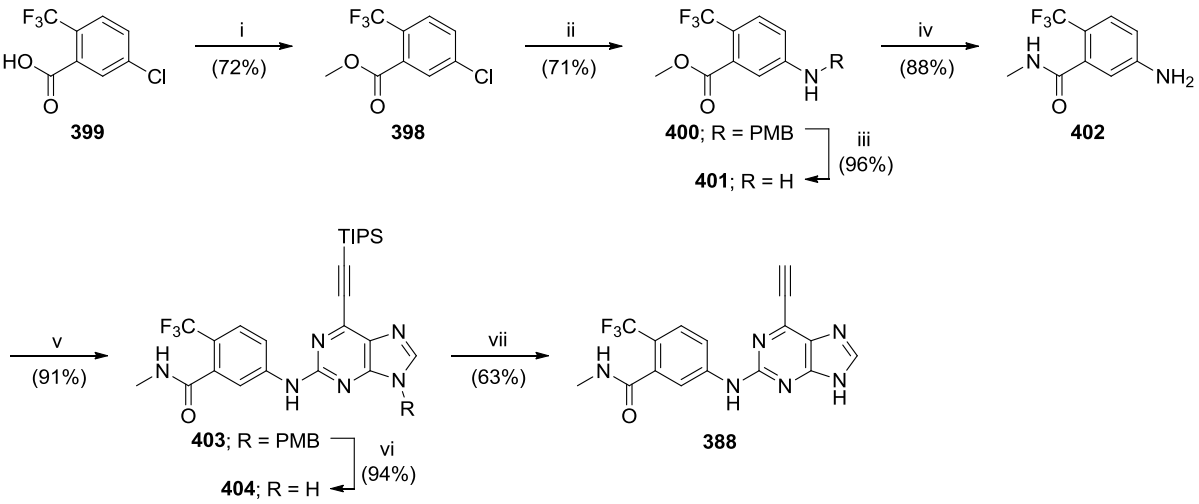

Reagents and conditions: i) ^{i}PrNC(OCH$_3$)NH^{i}Pr, MeCN, MW 120 °C, 5 min; ii) PMB-NH$_2$, Pd(OAc)$_2$, BrettPhos, Cs$_2$CO$_3$, THF, 90 °C, 1 h; iii) TFA, reflux, 18 h; iv) Aq. MeNH$_2$, RT, 18 h; v) **278**, Pd$_2$(dba)$_3$, XPhos, K$_2$CO$_3$, MeCN, 100 °C, 1 h; vi) TFA, reflux, 18 h; vii) a) TBAF, THF, RT, 5 min, b) **231**, THF, RT, 48 h.

Methyl 2-chloro-5-nitrobenzoate (**394**) was treated with sodium methoxide to give the nitroanisole **405**. Nitro group reduction and conversion into *N*-methylcarboxamide **407** was achieved as previously, after which the aniline group of **407** was coupled with the 2-fluoropurine **160**. The TIPS-protecting group was removed from the resultant compound (**408**) to yield the target purine **387** (Scheme 61).

For the synthesis of the *para*-cyano analogue **389**, a palladium-mediated Negishi cyanation reaction was used.[221] Reaction of methyl 2-chloro-5-nitrobenzoate (**394**) with zinc cyanide in the presence of bis(tri-*tert*-butylphosphino)palladium(0) resulted in clean conversion to the aromatic nitrile **409** in excellent yield (96%), and nitro group reduction gave the aniline **410**. Conversion of the methyl ester of **410** into the *N*-methylcarboxamide (**411**) was attempted using methylamine (40% aqueous solution) as for the previous reactions.

Scheme 61: Synthesis of the disubstituted 2-arylaminopurine **387**.

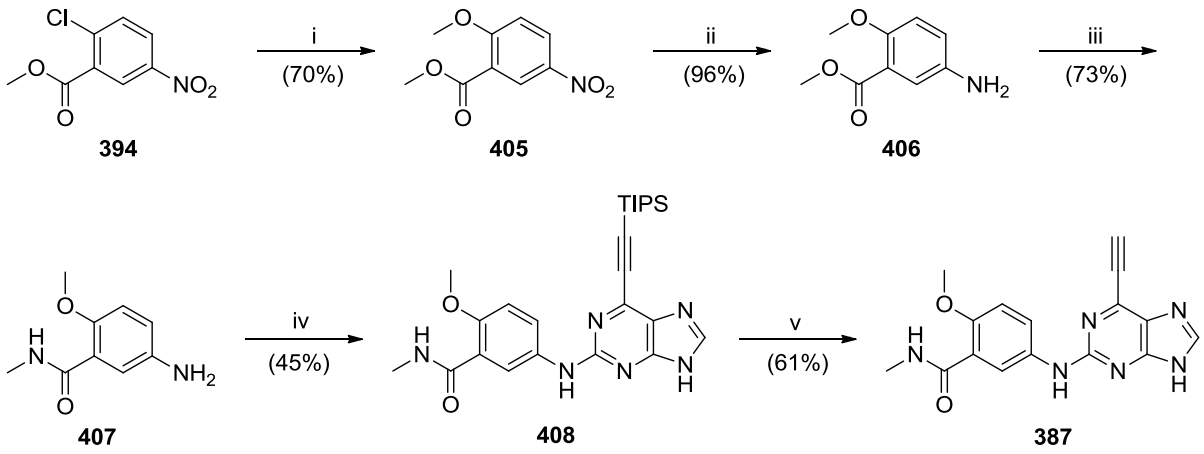

Reagents and conditions: i) NaOMe, MeOH, 50 °C, 4 h; ii) Fe, AcOH, 50 °C, 15 min; iii) Aq. $MeNH_2$, RT, 18 h; iv) **160**, TFA, TFE, MW 140 °C, 2 h; v) a) TBAF, THF, RT, 5 min, b) **231**, THF, RT, 48 h.

However, LC-MS analysis of the reaction mixture indicated that a single product was formed with a mass corresponding to the *N*,*N*-dimethylcarboxamide derivative **412** ([ES+] *m*/*z* = 190). Indeed, upon product isolation, the ^{1}H NMR spectrum was consistent with the *N*,*N*-dimethylcarboxamide **412**. It was initially assumed that dimethylamine had been used erroneously instead of methylamine, despite previous observations indicating that this reaction was unsuccessful using aqueous dimethylamine. Moreover, the reaction between **410** and aqueous methylamine was repeated, and the same result was observed. A literature review revealed that there is a literature precedent for aromatic *ortho*-cyano methyl esters to undergo spontaneous cyclisations to imidines (*e.g.* **413**).[222-224] In an excess of aqueous methylamine, as was used in the reaction of compound **410**, a mechanism was proposed for the formation of imidine **413** (Scheme 62).

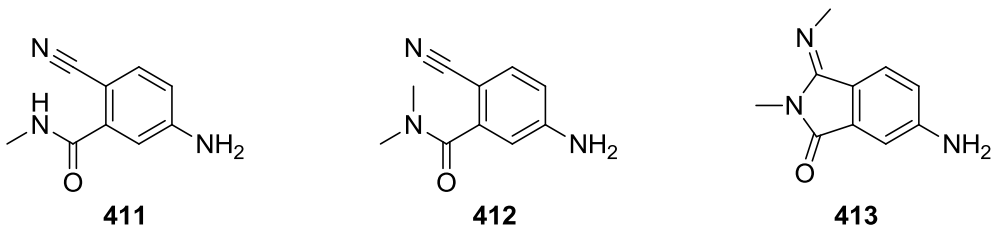

Scheme 62: Proposed mechanism for the formation of imidine **413**.

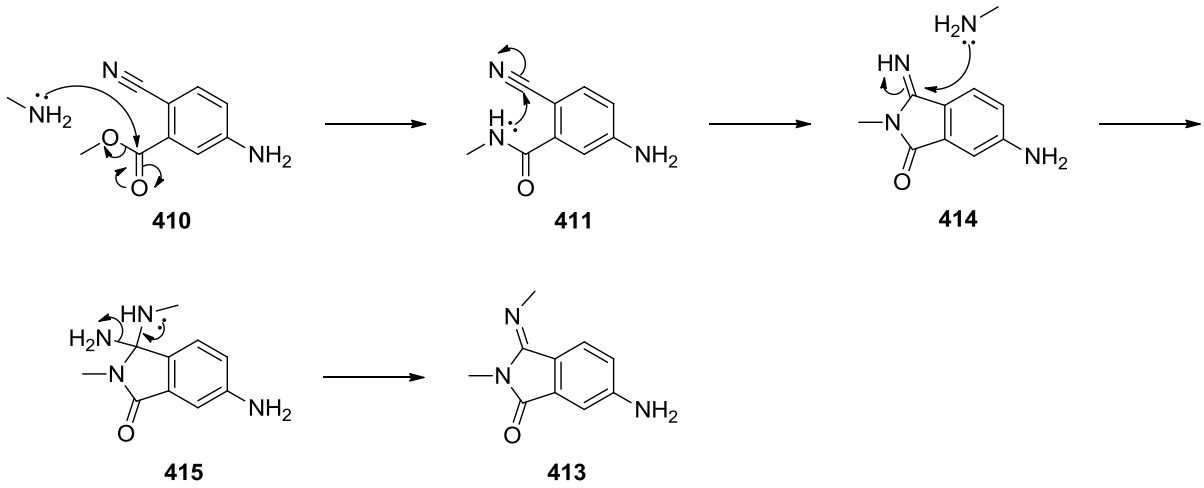

Treatment of **410** with methylamine generates the desired *N*-methylcarboxamide **411**, which undergoes a cyclisation with the nitrile moiety to give the imine **414**. A second equivalent of methylamine attacks the imine, to form the aminal **415**, which eliminates ammonia to give the imidine **413**. Confirmation of the structure of **413**, and assignment of the (*E*)-geometry about the imine, was provided by an X-ray crystal structure determination of **413** (Figure 44). This is counter to literature reports that the (*Z*)-isomer predominates due to steric effects.[223]

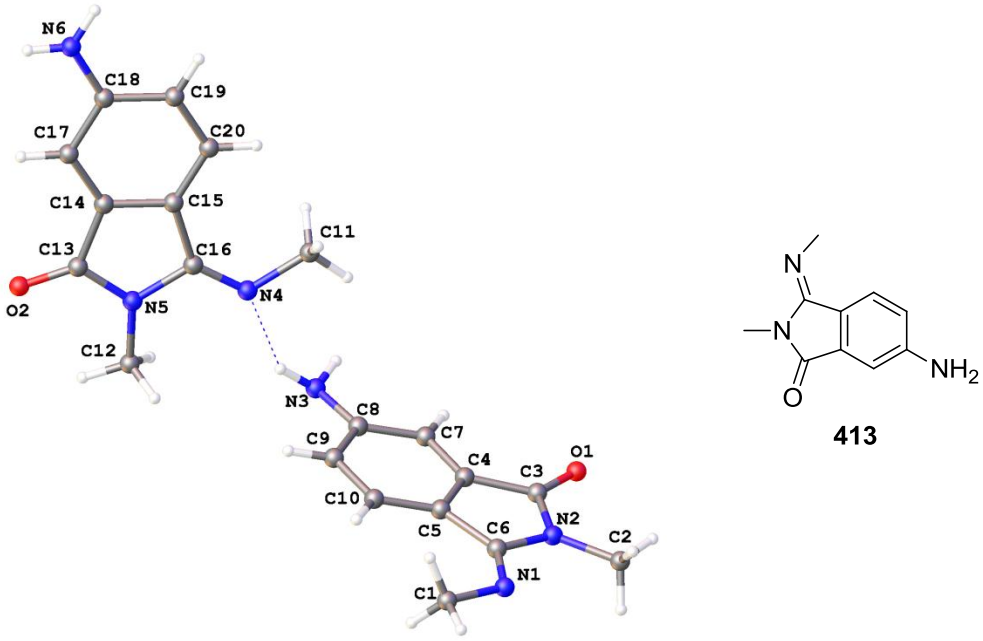

Figure 44: X-ray crystal structure of **413** indicating the (*E*)-geometry of the imine.

Coupling of aniline **413** to the 2-fluoropurine **160** was attempted but proved unsuccessful under TFA-mediated conditions. As such **413** was coupled to the 2-iodopurine **278** employing the Buchwald amination approach to give purine **416**. Removal of the PMB group at N-9 and subsequent deprotection of the 6-ethynyl group as previously described, yielded the target purine **418** (Scheme 63).

Scheme 63: Synthesis of the target purine **418**.

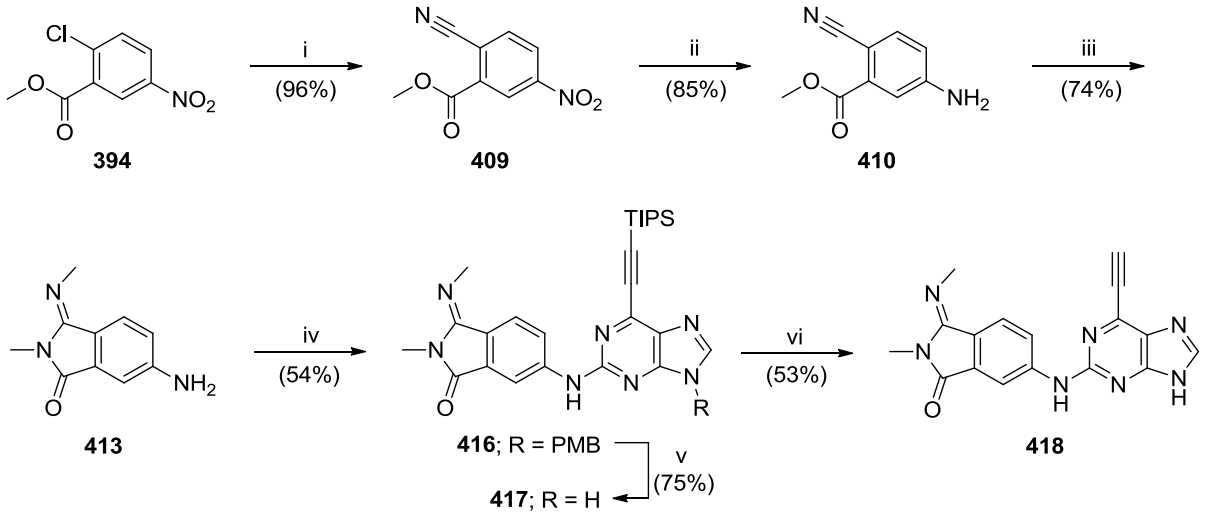

Reagents and conditions: i) $Zn(CN)_2$, Zn, $Pd^0(P^tBu_3)_2$, DMA, 95 °C, 1 h; ii) Fe, AcOH, 50 C, 15 min; iii) Aq. $MeNH_2$, RT, 18 h; iv) **278**, $Pd_2(dba)_3$, XPhos, K_2CO_3, MeCN, 100 °C, 1 h; v) TFA, reflux, 18 h; vi) a) TBAF, THF, RT, 5 min, b) **231**, THF, RT, 48 h.

It was evident that *ortho*-cyanocarboxamides were subject to cyclisation under very mild conditions. As such it was anticipated that formation of **413** would be likely to occur during the synthesis of **389** by alternative routes. For this reason, it was decided to prepare the *N*,*N*-dimethylcarboxamide **416**, where imidine formation cannot occur. The methyl ester of compound **409** was saponified by treatment with aqueous sodium hydroxide, to give carboxylic acid **420** without detriment to the nitrile group. As an alternative to CDI, 1-ethyl-3-(3-dimethylaminopropyl)carbodiimide hydrochloride (EDC.HCl) was used in conjunction with hydroxybenzotriazole (HOBt) to couple dimethylamine to the acid **420** in excellent yield (92%). Nitro group reduction gave aniline **422**, which was coupled to the 2-iodopurine **278** under the established conditions. However, attempted removal of the PMB-protecting group from the purine **423** using TFA resulted in compound degradation after only 2 hours at 60 °C, and none of the expected product (**424**) was observed in the reaction mixture by LC-MS analysis (Scheme 64).

Scheme 64: Attempted synthesis of the target purine **419**.

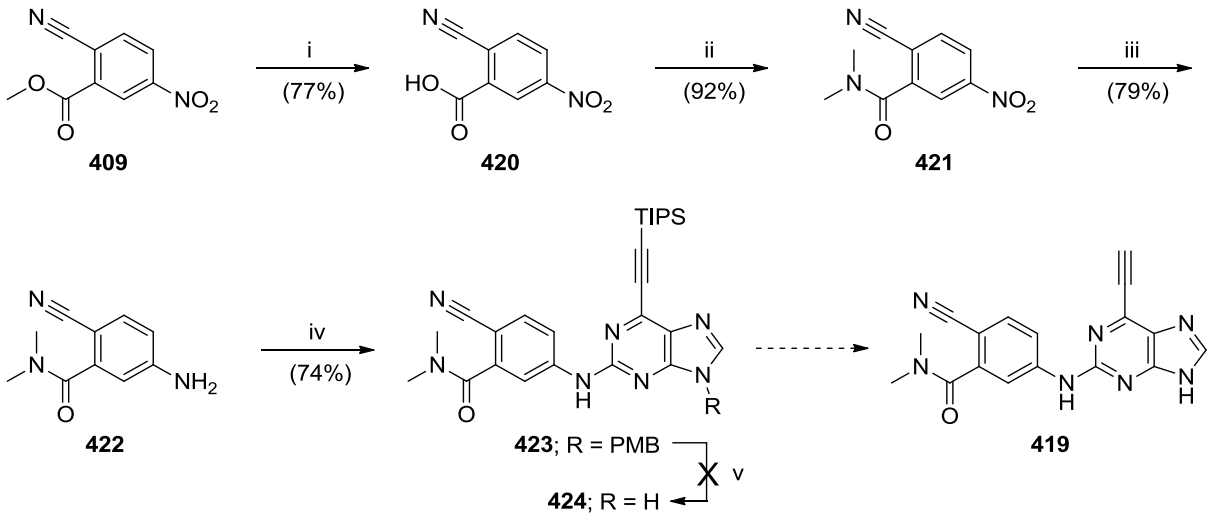

Reagents and conditions: i) NaOH, H_2O, MeOH, RT, 30 min; ii) $Me_2NH.HCl$, EDC.HCl, HOBt, DIPEA, DMF, RT, 18 h; iii) Fe, AcOH, 50 °C, 15 min; iv) **278**, $Pd_2(dba)_3$, XPhos, K_2CO_3, MeCN, 100 °C, 1 h; v) TFA, 60 °C, 2 h.Despite the general applicability of the TFA-mediated PMB-deprotection reaction, it was clear that the cyano substituent was unstable under these conditions and hence responsible for the observed decomposition. An alternative synthetic strategy was required, utilizing a protecting group that could be removed under different conditions. However, owing to time constraints no further efforts were made towards the synthesis of **429**.

As a preliminary measure of the electronic effect of groups at the *para*-position of the 2-arylamino ring of the purine on both the purine C^2-NH and 6-ethynyl terminal CH, the relative ^{1}H NMR chemical shifts of these substituents were compared for compounds **385**-**388** (Figure 45). The trend in ^{1}H NMR chemical shift, as a measure of proton deshielding, for both proton environments, generally mirrored the relative electron-withdrawing and electron-donating potential of the substituents, with the possible exception of the chloro (**386**) and fluoro (**385**) analogues. However, an aromatic fluorine group may be less electron withdrawing than an aromatic chloro group, despite being more electronegative. This is due to fluorine possessing greater resonance-stabilisation characteristics than other halogens as a result of improved orbital overlap between the fluorine 2p orbital and the π-system.[225]

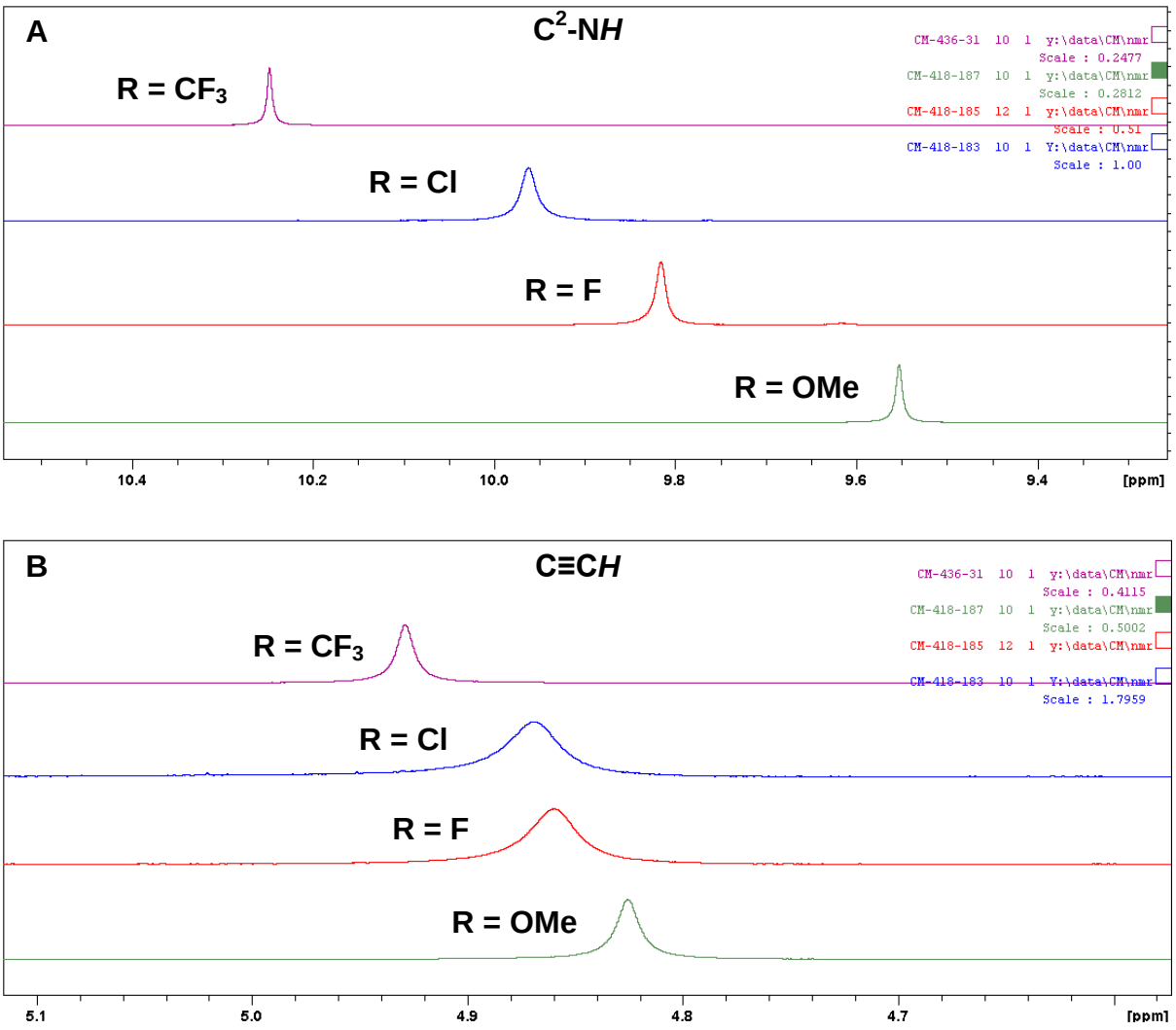

Figure 45: ^{1}H NMR chemical shifts for the C^{2}-NH (**A**) and terminal alkyne (**B**) protons for compounds **385-388**.

The observed effect is much more pronounced in the case of the C^{2}-NH proton, due possibly to the greater distance over which the electron-withdrawing/donating groups must act in order to modulate the electron density of the alkyne group. Despite the initial results being as expected, testing of additional analogues with a wider range of substituents at the 2-arylamino ring is warranted to improve the statistical significance of the results.

6.6.2. Biological Results

Disubstituted 2-arylaminopurines of sufficient purity for biological evaluation were tested for inhibitory activity against both Nek2 and Cdk2. In addition, the effect of cellular growth inhibition in SKBR3 cells was determined (Table 18).

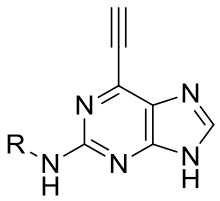

Compound	R	IC_{50} (µM) Nek2[a]	IC_{50} (µM) Cdk2[b]	GI_{50} (µM) SKBR3
385	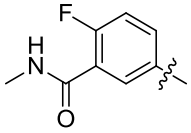	0.16	13.2	0.3 ± 0.2
386	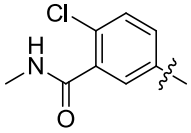	0.08	22.9	0.4 ± 0.2
388	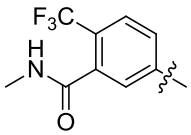	0.14	29.3	0.8 ± 0.3
387	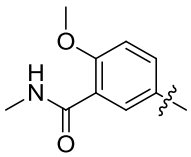	0.44	49.1	0.5 ± 0.1
418	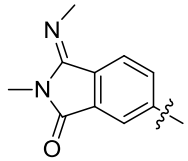	0.33	25%*	2.3 ± 0.6

[a] Nek2 IC_{50} values determined at 30 µM ATP concentration; [b] Cdk2 IC_{50} values determined at 12.5 µM ATP concentration; * = percentage inhibition at 100 µM.

Table 18: Biological evaluation of disubstituted 2-arylamino-6-ethynylpurines.

All of the purines within this series were active as Nek2 inhibitors. Although only limited SARs can be ascribed to inhibitors **385**-**386** and **388**, which all have electron-withdrawing groups, it is interesting that the *para*-methoxy analogue **387** is the least active of the derivatives. This may support the approach of positioning electron-withdrawing groups on the 2-arylamino ring as a means of activating the 6-ethynyl group. It would be necessary to synthesise additional compounds within this series to verify this observation, and strengthen the conclusions that can be drawn from these results. It is clear, however, that there is a high degree of tolerance within the Nek2 ATP-binding domain for inhibitors with diverse functionality at the 2-arylamino ring. As has been seen previously, there appears to be no

clear correlation between the activity of 6-ethnylpurine inhibitors in the Nek2 kinase assay and growth inhibition of SKBR3 cells.

6.7. Conclusions and Further Work

Through modification of the 6-position of purine-based inhibitors of Nek2 kinase it has been possible to identify 6-ethynylpurines as potent, irreversible inhibitors of Nek2. Such compounds act as covalent modifiers of Cys22, a residue immediately following the glycine rich loop in Nek2, by virtue of their ability to act as Michael acceptors. For this inhibitor class it is evident that there is a large degree of tolerance within the Nek2 ATP-binding pocket for substituents on the purine 2-arylamino ring. In addition, it has been found that inhibitors with adequate initial competitive binding affinity for the kinase, result in potent inhibition of Nek2 upon irreversible inactivation. This has limited the extent to which SARs have been determined.

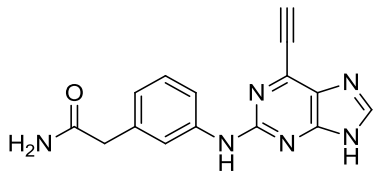

177

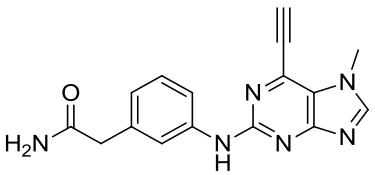

425

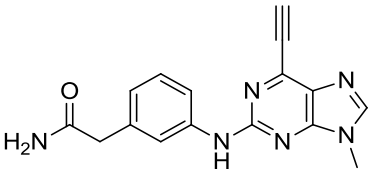

426

	IC_{50} (µM)		GI_{50} (µM)
Compound	**Nek2[a]**	**Cdk2[b]**	**SKBR3**
177	0.062 ± 0.01	11.8	2.2 ± 0.4
425	50%*	25%*	2.9
426	4.0	22%*	1.1

[a] Nek2 IC_{50} values determined at 30 µM ATP concentration; [b] Cdk2 IC_{50} values determined at 12.5 µM ATP concentration; * = Percentage inhibition at 100 µM.

Table 19: Comparison of the biological activity of **177** with control compounds **425** and **426**.

From studies with the benchmark inhibitor, **177** (NCL-00017509), it was possible to identify tumour cell lines sensitive to treatment *in vitro* with inhibitors of this class. However, it was subsequently found that there was a poor correlation between Nek2 kinase inhibitory activity and growth inhibition of SKBR3 cells, with several purines that are weak kinase inhibitors

proving highly growth inhibitory (*e.g.* **364**). This raised that possibility that the observed growth inhibition in SKBR3 cells was unrelated to Nek2 inhibition.

The essential H-bonding interactions between the purine and kinase hinge region were exploited in the synthesis of the N^7-methyl and N^9-methyl analogues of **177** (**425** and **426**) as control compounds. Both compounds are only very weak Nek2 kinase inhibitors but exhibit potent growth-inhibitory activity in the SKBR3 cell line. This strongly suggests that compounds within the 6-ethynylpurine class possess an alternative locus of activity to Nek2 kinase. It may thus be necessary to revisit the known SARs for this chemotype for the identification of truly selective Nek2 inhibitors. Moreover, once a truly selective Nek2 inhibitor is found, it will be necessary for additional screening of tumour cell lines to be performed, to identify cell lines that are sensitive to Nek2 inhibition. However, the findings of this series may suggest that Nek2 function is not essential for cancer cell survival, and it is possible that Nek2 is not a valid cancer therapeutic target.

Chapter 7: Investigating the Cellular Effects of Nek2 Inhibition using NCL-00017509 (177)

7.1. Development of a Nek2 Inducible Cell Line

Tetracycline-inducible gene expression is a common tool used to artificially induce or repress the translation of desired genes in cells stably expressing the relevant DNA construct. Such systems exploit the natural *Escherichia coli* bacterial promoter protein P_{tet}, which expresses the TetR repressor protein. Fusion of TetR with an activation domain, VP16, creates a tetracycline-controlled transactivator (tTA) protein, that upon binding of tetracycline response elements (TREs) triggers the transcription of genes directly downstream of tetracycline operator (tetO) sequences.[226] Generation of constructs bearing the tetO sequence directly upstream of the gene coding for a protein of interest allows the induction of gene expression upon treatment with tetracycline in a system known as TET-ON.

Through the use of tetracycline-inducible gene expression, a U2OS cell line was developed to express myc-tagged Nek2 upon treatment with tetracycline, or the more stable analogue doxycycline. Myc-tagging allows a determination of the level of induced Nek2 as opposed to endogenous Nek2, through the use of myc antibodies in both Western blotting and immunofluorescence microscopy. Due to the low levels of active endogenous Nek2 throughout most of the cell cycle, it is necessary to up-regulate Nek2 gene expression, and therefore activity, in order to observe effects of inhibitor treatment in a population of non-synchronised cells.

The effect of doxycycline on the myc-Nek2 inducible cell line was investigated by the administration of doxycycline at 1 μg/ml to the cell media for varying times. After inhibitor treatment, the cells were fixed and lysed, and the protein expression levels visualised by Western blotting (Figure 46; **A**). It was apparent from the results that expression of induced myc-Nek2 reaches a maximum level after 8 hours.

Induction of myc-Nek2 was further observed by the probing of cells, treated with and without doxycycline at 1 μg/ml for 16 hours, with myc and C-Nap1 antibodies. Cellular staining with fluorescently tagged secondary antibodies allows the presence and localisation of induced myc-Nek2 to be observed (Figure 46; **B**). Both assays confirmed that treatment of the Tet-ON

myc-Nek2 cell line with doxycycline results in upregulated expression of Nek2, enabling the cell line to be used in further studies.

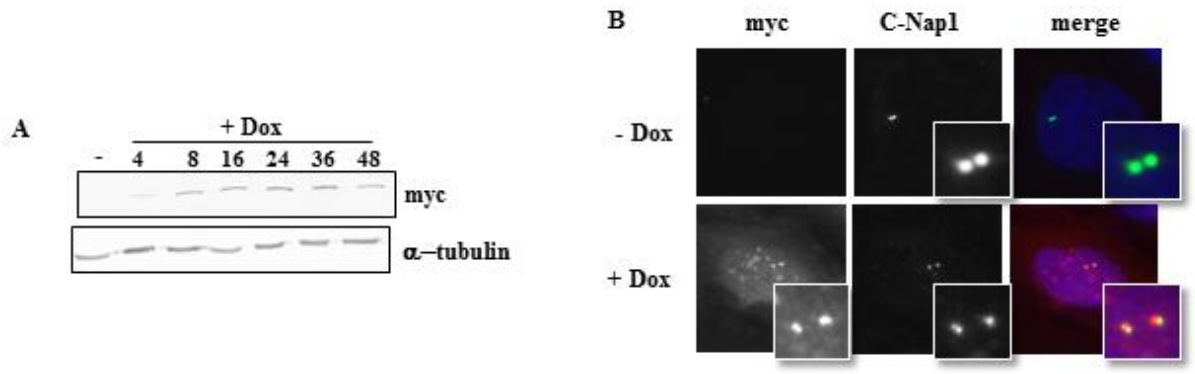

Figure 46: Induction of myc-Nek2 in a U2OS cell line; **A)** Total protein from U2OS myc-Nek2 TET-ON cells treated with doxycycline at 1 µg/ml for varying times separated by SDS-PAGE, immunoblotting with myc and α-tubulin antibodies; **B)** Representative U2OS myc-Nek2 TET-ON cells treated with or without doxycycline at 1 µg/ml for 16 hours, and visualised using anti-mouse myc and anti-rabbit C-Nap1. DNA was visualised with Hoescht dye.

7.2. Effect of Nek2 Inhibition on Centrosome Splitting

It was proposed that as a consequence of the key role of Nek2 in centrosome splitting, upregulation of active Nek2 with doxycycline induction would cause an increased percentage of cells displaying split centrosomes in interphase. Subsequent treatment with varying concentrations of the Nek2 inhibitor **177** (NCL-00017509), will enable an evaluation of the effect of Nek2 inhibition on cellular centrosome splitting.

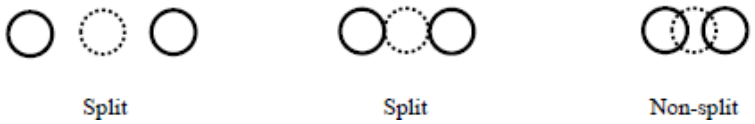

Figure 47: Classification of centrosomes as split or non-split.

Populations of U2OS myc-Nek2 inducible cells grown on microscope coverslips were treated both with and without doxycycline at 1 µg/ml for 16 hours, followed by 4 hours of treatment with **177** at doses of 5 µM, 500 nM and 50 nM. The cells were fixed and probed with a myc antibody to observe induction of myc-Nek2, and a γ-tubulin antibody to allow visualisation of the centrosomes, upon secondary incubation with fluorescently tagged antibodies.

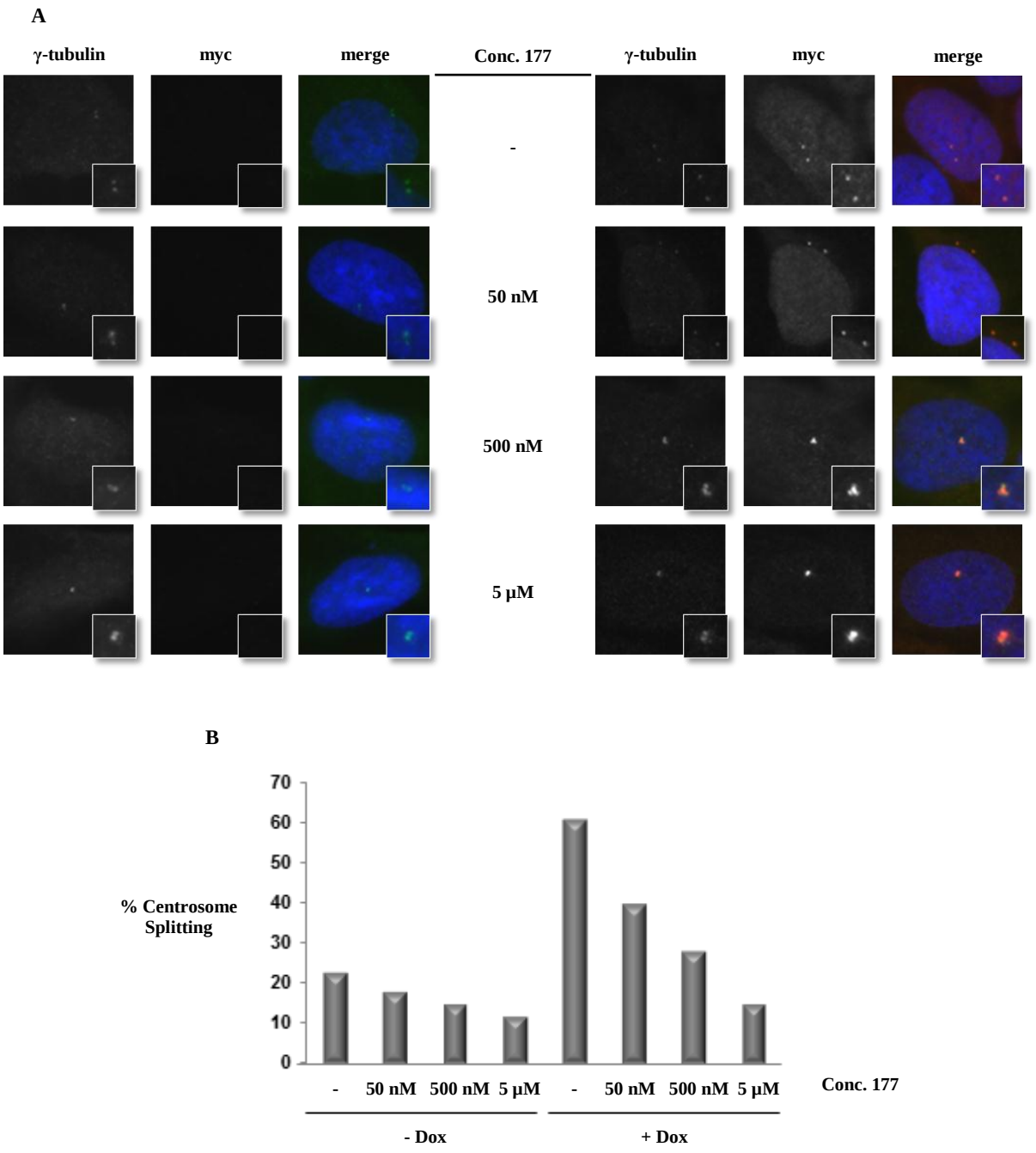

Figure 48: Treatment with NCL-00017509 (**177**) decreases the percentage of cells possessing split centrosomes; **A)** Representative U2OS myc-Nek2 TET-ON cells treated with or with doxycycline at 1 µg/ml for 16 hours, followed by inhibitor treatment for 4 hours. Cells were visualised using immunofluorescence microscopy, staining with anti-rabbit γ-tubulin, anti-mouse myc and Hoescht dye; **B)** Percentage of cells possessing split centrosomes for – Dox/+ Dox populations against inhibitor concentration.

Immunofluorescence microscopy was used to give a qualitative determination of whether centrosomes are split or non-split in 100 cells per population, repeated in triplicate. Visual judgement was used to classify centrosomes to be split if they were separated by equal to or

greater than the diameter of 1 centrosome (Figure 47). Quantitative measurement of the distance of centrosome separation was not carried out to increase the rapid throughput of the assay with an understanding that upon cleavage of the intercentriolar linkage, the distance of separation would be a dynamic process. As anticipated, induction of myc-Nek2 expression with doxycycline treatment resulted in a large increase in the percentage of interphase cells possessing split centrosomes. For both induced and non-induced populations, a dose-dependent decrease in the number of split centrosomes was observed with increasing concentration of Nek2 inhibitor (**177**), with 5 μM compound decreasing centrosome splitting to the level of that in the non-induced population (Figure 48). This observation highlights a potentially interesting aspect of the nature of centrosome splitting, as this appears to be a reversible process. It has previously been assumed that protein components of the intercentriolar linkage connecting the centrosomes were phosphorylated by Nek2, resulting in dissociation and centrosomal separation.[161] Under these conditions, it would be anticipated that, once cleaved, the intercentriolar linkage would remain so. However, as Nek2 expression, and therefore centrosomal disjunction, is activated prior to inhibitor treatment, it is clear that the dose response observed is due to the reversibility of this process.

7.3. Cellular Inhibition of C-Nap1 Phosphorylation

The processes by which centrosomal separation is mediated remains to be fully elucidated, and additional cellular biomarkers of Nek2 activity are required to validate the results obtained in the centrosome splitting assay. One such biomarker in use is the level of phosphorylated C-Nap1 present in cell populations. At present, C-Nap1 is thought to be exclusively phosphorylated by Nek2, allowing the levels of phosphorylated C-Nap1 to be used as a direct measure of Nek2 activity. Work within the laboratory of Professor Andrew Fry (University of Leicester) has enabled the development of antibodies raised against four phosphorylation sites on C-Nap1. The antibodies were generated using peptides prepared with phosphate groups attached to the serine or threonine of interest. These peptides were injected into rabbits and purified from serum. Antibodies were separated into phospho- and non-phospho antibodies by elution on a phosphate column. Such antibodies make it possible to measure Nek2 activity using immunofluorescence microscopy. One antibody is raised against the phosphorylation site Ser2164, named pAQDL. Antibody nomenclature uses the start of the amino acid sequence upstream of the site in question.

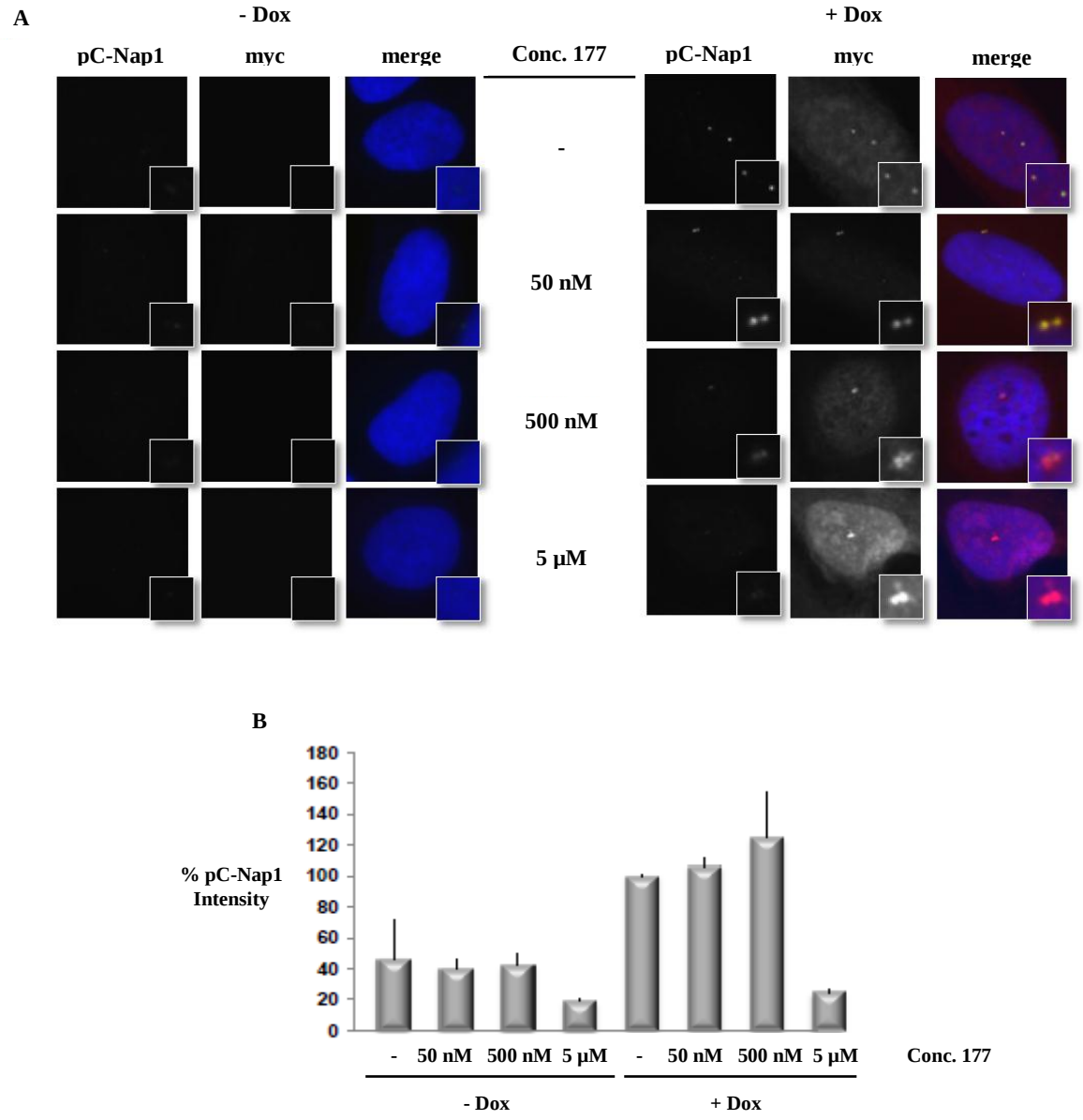

Figure 49: Treatment with NCL-00017509 (**177**) decreases the intensity of pC-Nap1 staining in cells; **A)** Representative U2OS myc-Nek2 TET-ON cells treated with or with doxycycline at 1 µg/ml for 16 hours, followed by inhibitor treatment for 4 hours. Cells were visualised using IFM, staining with anti-rabbit pAQDL, anti-mouse myc and Hoescht dye; **B)** Percentage pC-Nap1 intensity with respect to **177** treatment for - Dox/+ Dox populations.

The cell treatment protocol utilised in the centrosome splitting assay was repeated, and the resulting coverslips were probed with a myc antibody and the pAQDL antibody. The use of Velocity (PerkinElmer) software allowed a quantitative determination of fluorescence intensity for pC-Nap1, enabling a determination of pC-Nap1 levels and therefore Nek2 activity. For each cell population, fluorescence intensity was measured for 20 centrosomes, and average intensity with respect to background determined. Measurements were carried out

in triplicate for induced cells, and average intensities with respect to induced cells with no inhibitor treatment calculated (Figure 49). However, measurements were only made in duplicate for uninduced cells, as it was not possible to reliably identify centrosomes without a myc co-stain when their intensities were very low. This was observed in the first assay, and hence all subsequent uninduced cells were co-stained with a γ-tubulin rather than a myc antibody, so that centrosomes could be easily identified.

Under these assay conditions, pC-Nap1 intensity did not give the same dose-response relationship as observed in the centrosome splitting assay. However, as can be seen from the high degree of error, the reliability of this assay is questionable. There are many variables during the experimental procedure that may result in variable antibody binding from one experiment to another. There was observed to be a sharp decrease in pC-Nap1 intensity to that of the level of uninduced cells between 500 nM and 5 μM **177**. Due to limitations in time, it was not possible to investigate this result further, but it would be important to repeat this assay at dose ranges between 500 nM and 5 μM in an attempt to observe a dose-response between pC-Nap1 intensity and Nek2 inhibitor concentration.

Although C-Nap1 is known to localise to the terminal ends of centrioles and is proposed to be a key component of the intercentriolar linkage, these results may indicate that phosphorylation of C-Nap1 is not the key process in cleavage of this linker. At present, C-Nap1 is thought to be a substrate only of Nek2, but it is possible that another kinase is performing this phosphorylation in the absence of active Nek2. It may be that the phosphorylation site of C-Nap1 targeted by Nek2 is not that which is responsible for centrosomal disjunction. In order to investigate this further, it was necessary to determine the selectivity of Nek2 for the phosphorylation sites of C-Nap1.

There are 22 *in vitro* phosphorylation sites on C-Nap1 identified to date,[227] but at present antibodies have been developed within the group for only four of these sites; Ser2064 (pLLEK), Thr2102 (pRELQ), Ser2164 (pAQDL) and Ser2417 (pRRLD). U2OS myc-Nek2 inducible cells were grown on coverslips, and all cells were induced with doxycycline for 16 hours. Pairs of coverslips were selected for staining by each phospho-specific antibody, as well as total C-Nap1, and one coverslip was treated with **177** at 5 μM for 4 hours. Following incubation with primary and secondary antibodies, immunofluorescence microscopy was used to determine fluorescence intensity for both untreated and **177** treated cells ascribed to each phosphorylation site (Figure 50 and Figure 51).

In order to relate all intensities to one another, the exposure of the camera used to capture the cellular images was fixed such that the most intense fluorescence staining did not overexpose the camera. As such, differences in the overall fluorescence intensity, possibly due to variable antibody affinity, did not allow the results for each phospho-specific antibody to be directly compared. It was necessary to adjust measurements for **177** treated cells to give a percentage of the intensity of untreated cells. It was apparent that once this had been performed, all phosphorylation sites excluding pRELQ were sensitive to Nek2 inhibition.

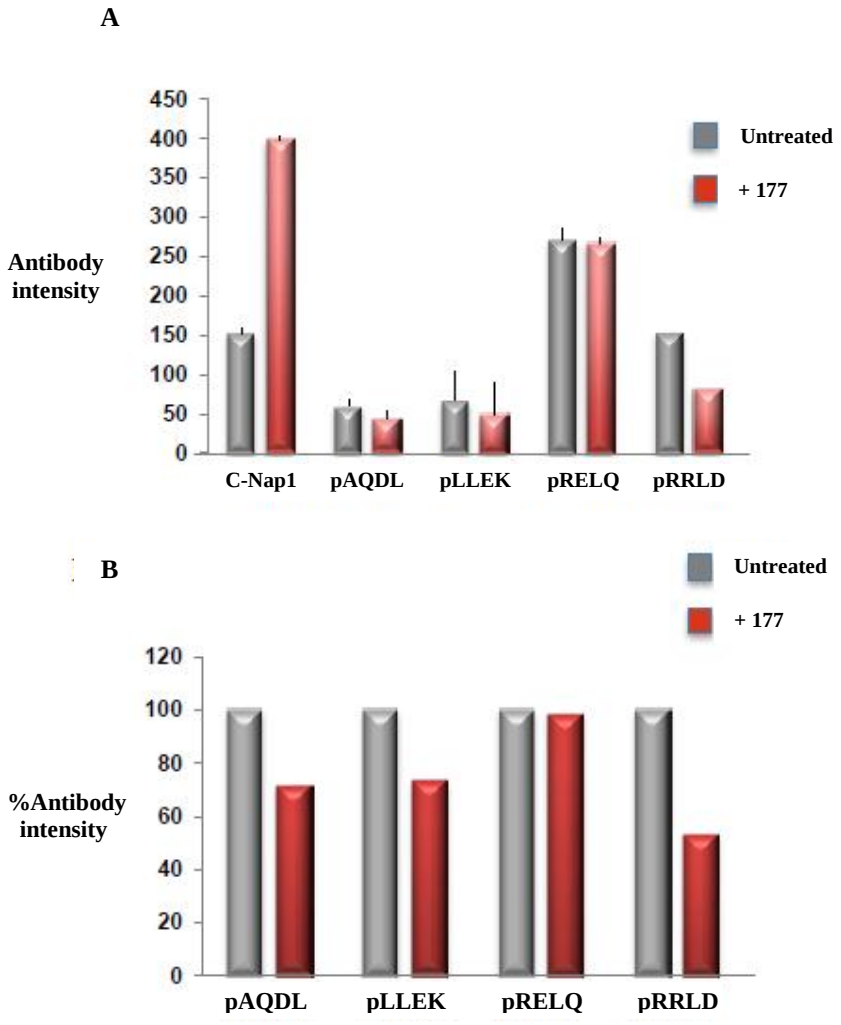

Figure 50: NCL-00017509 (**177**) inhibits phosphorylation of three known sites of C-Nap1 in U2OS myc-Nek2 TET-ON cells; **A)** Phospho-specific antibody fluorescence intensity for untreated and **177** treated cells, at 5 µM inhibitor concentration; **B)** Phospho-specific antibody fluorescence intensity as a percentage of untreated level for each antibody.

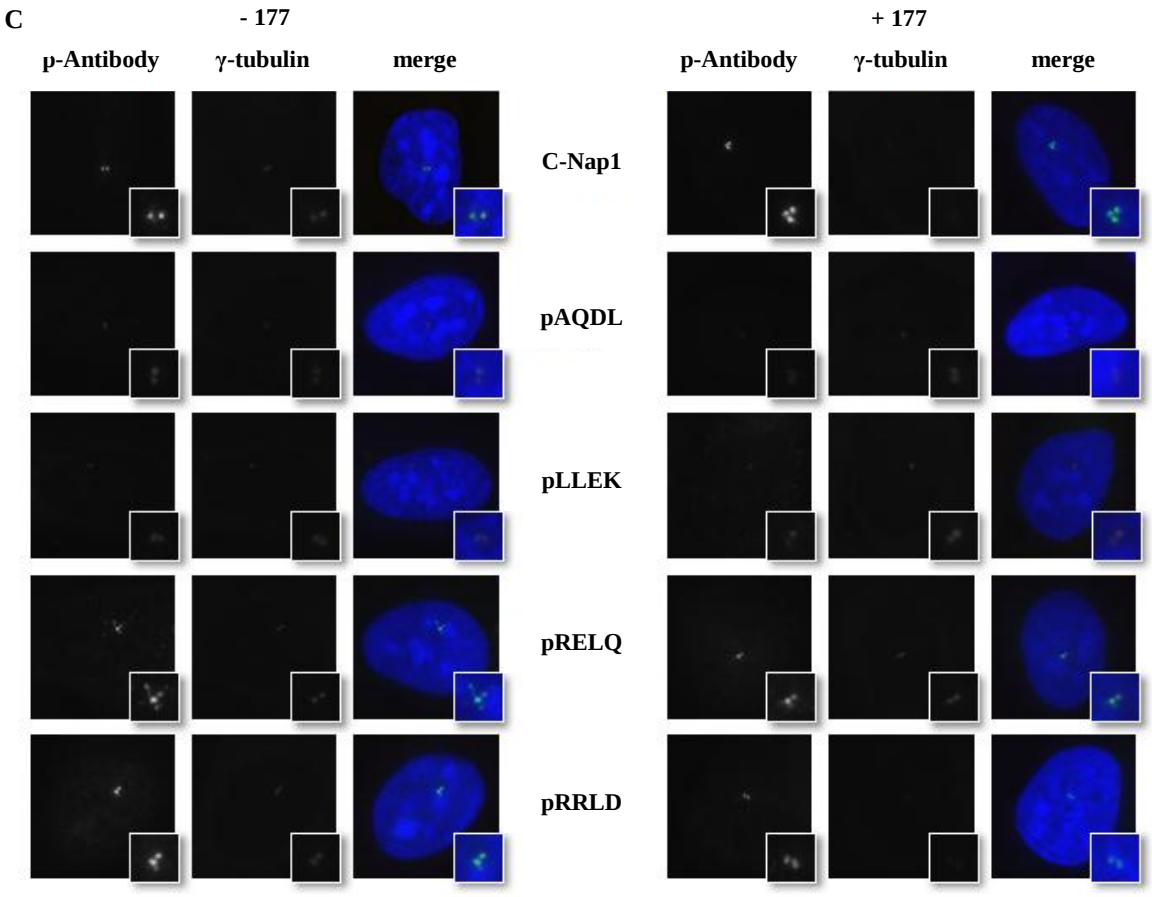

Figure 51: NCL-00017509 (**177**) inhibits phosphorylation of three known sites of C-Nap1; **C)** Representative U2OS myc-Nek2 TET-ON cells treated with doxycycline at 1 µg/ml for 16 hours, followed by **177** treatment for 4 hours. Cells were visualised using immunofluorescence microscopy, staining with anti-rabbit pC-Nap1, anti-mouse myc and Hoescht dye.

Owing to the relatively low intensities of pAQDL and pLLEK fluorescence, it was not possible to use these results to evaluate degrees of sensitivity between each site. In order to do this, the assay would need to be repeated over a dose range with camera exposure calibrated for each antibody individually. It may be noted that due to Nek2 inhibition, and therefore inhibition of C-Nap1 phosphorylation, there was a greater quantity of C-Nap1 at the centrosomes, as seen by the increase in intensity for total C-Nap1. Monitoring of pC-Nap1 was therefore from a larger protein sample, and hence the true inhibition of pC-Nap1 may be more pronounced than is shown in Figure 50.

7.4. Evaluating Mitotic Progression Using Live Cell Imaging

By the use of confocal microscopy, it is possible to clearly image structures, such as cells, that are thicker than the focal plane. This allows for 3-dimensional images to be reconstructed

by layering of multiple planes through a structure, allowing the detailed visualisation of cellular components and, hence, processes. Collating images taken at regular intervals throughout the growth cycle of a cellular population, allows in-depth analysis of the success and duration of such processes, and hence can be used in conjunction with NCL-00017509 (**177**) to evaluate the effect of Nek2 inhibition on mitotic progression and spindle assembly.

A HeLa cell line has been developed within the research group at the University of Leicester, to stably express fluorescent tags on key cellular structures, with green fluorescent protein (GFP, λ_{ex} = 482 nm, λ_{em} = 502 nm) tagged α-tubulin, and mCherry (λ_{ex} = 587 nm, λ_{em} = 610 nm) tagged histone, a protein involved in DNA ordering and nucleosome formation. This cell line allows an observation of a cell's mitotic spindle and DNA to be carried out under live cell conditions using confocal microscopy.

GFP-α-tubulin/mCherry-histone HeLa cells were grown to ~80% confluency and divided into two populations, one of which was treated with **177** at 5 μM for 4 hours. At this point, live cell imaging was initiated, with cells imaged at 5 minute intervals for 15 hours, both with and without inhibitor treatment. The images were used to analyse the progression of cells through mitosis, starting with mitotic duration. At the onset of mitosis, cells lose their flattened morphology and adopt a spherical structure.

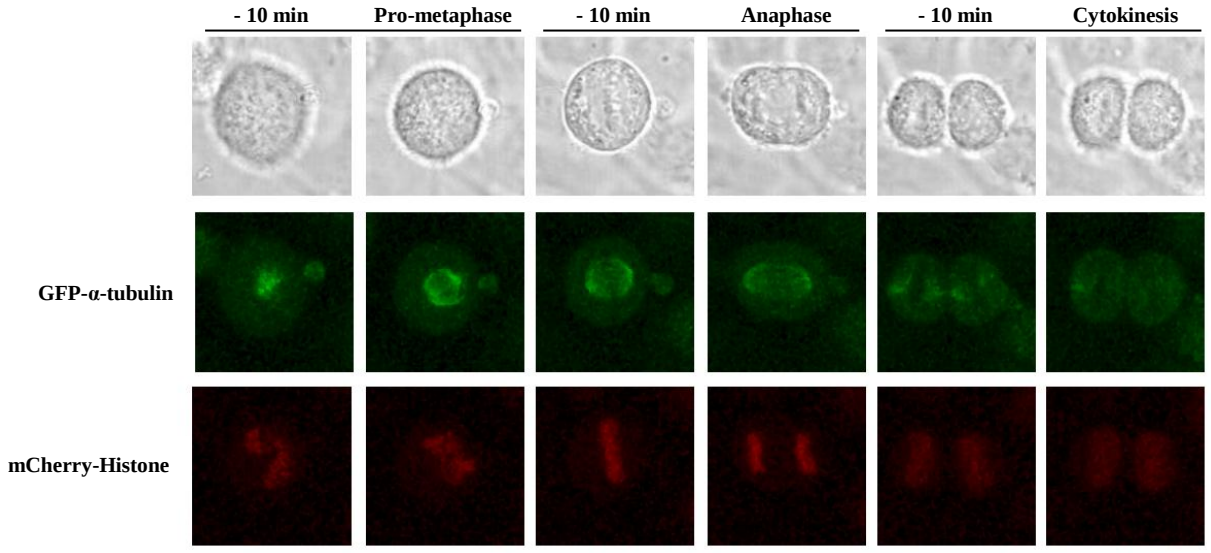

Figure 52: Representative images of cells, highlighting the events used to time mitotic progression.

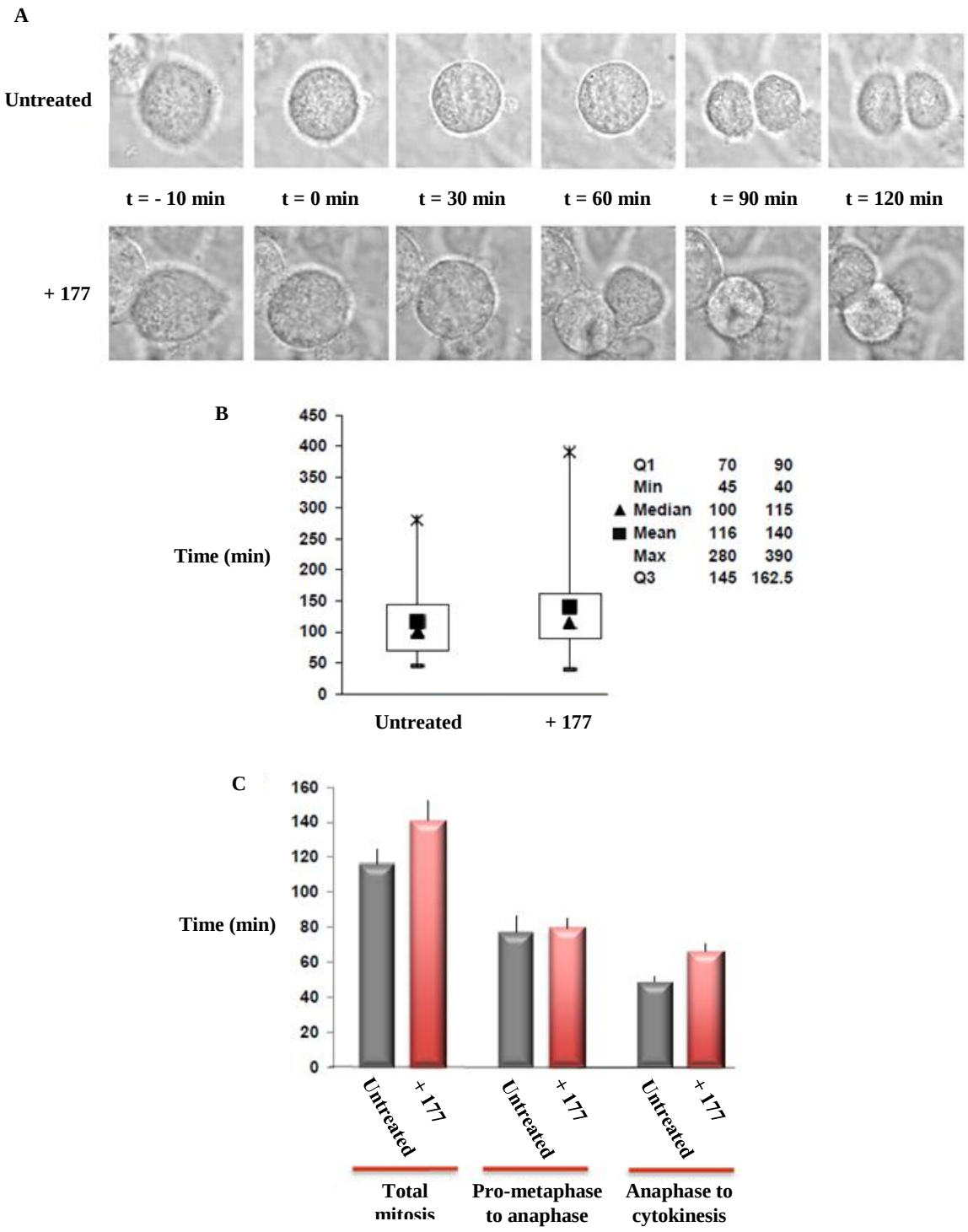

Figure 53: Treatment with NCL-00017509 (**177**) causes a delay in mitotic progression; **A)** Representative HeLa GFP-α-tubulin/mCherry-Histone cells treated without and with inhibitor for 4 hours and observed over 15 hours using confocal laser scanning microscopy; **B)** Box-whisker plot showing minimum value, lowest quartile (Q1), median, mean, upper quartile (Q3) and maximum values for untreated cells and cells treated with inhibitor; **C)** Total time for mitosis for untreated cells and cells treated with inhibitor divided into observable stages of mitosis.

The point at which the cells reached their maximum spherical shape during prophase was classed as t = 0 min, and all timings of mitosis were calculated from this point forward. Timings were made from prophase to anaphase, the first point at which the DNA was seen to be divided from its alignment along the spindle meridian, and from anaphase to cytokinesis, the point at which the cell is fully divided and all spindle networks between cells are disconnected (Figure 52). By measuring these times for 268 cells from 6 distinct populations, it was possible to determine the average times for cells to complete mitosis, to enter anaphase, and to pass between anaphase and cytokinesis, for cells treated both with and without Nek2 inhibitor (Figure 53). From these results, it was apparent that cells treated with NCL-00017509 (**177**) experience a mean delay in mitotic completion of 24 minutes. When this delay was divided into the two defined cell cycle stages, prophase to anaphase and anaphase to cytokinesis, it is clear that the delay is a consequence of the cells requiring greater time to exit mitosis after anaphase. The hypothesised role of Nek2 is in centrosome separation, which would suggest that Nek2 inhibition would result in a delay in bipolar spindle formation, and therefore an increase in the time taken from mitotic entry to anaphase. However, the specific dynamics of this process and the exact role of Nek2 is yet to be fully elucidated, and disruption of Nek2 activity may thus have unexpected effects on spindle assembly and function.

Upon detailed examination of the image sequences, it became apparent that there was an increased occurrence of cells with an irregular mitotic phenotype. These included cells undergoing apoptosis following mitotic entry, those forming a monopolar mitotic spindle with a delay in bipolar spindle formation, and cells with irregular spindle movement and shape. To establish the relevance of these observations, all cells entering mitosis were assessed for successful or failed mitosis, and for the presence of a bipolar or abnormal spindle. Once tabulated, there was seen to be an increase from 7% to 15% in cells failing to complete mitosis upon treatment with the Nek2 inhibitor. Furthermore, the number of cells developing a regular mitotic spindle fell from 86% to 58%, and the number of cells proceeding through an abnormal mitotic division increased from 14% to 42% (Figure 54). This supports the proposed effect of Nek2 inhibition, whereby centrosomal separation is delayed or adversely affected, which may result in the observed abnormalities and delay in bipolar spindle formation.

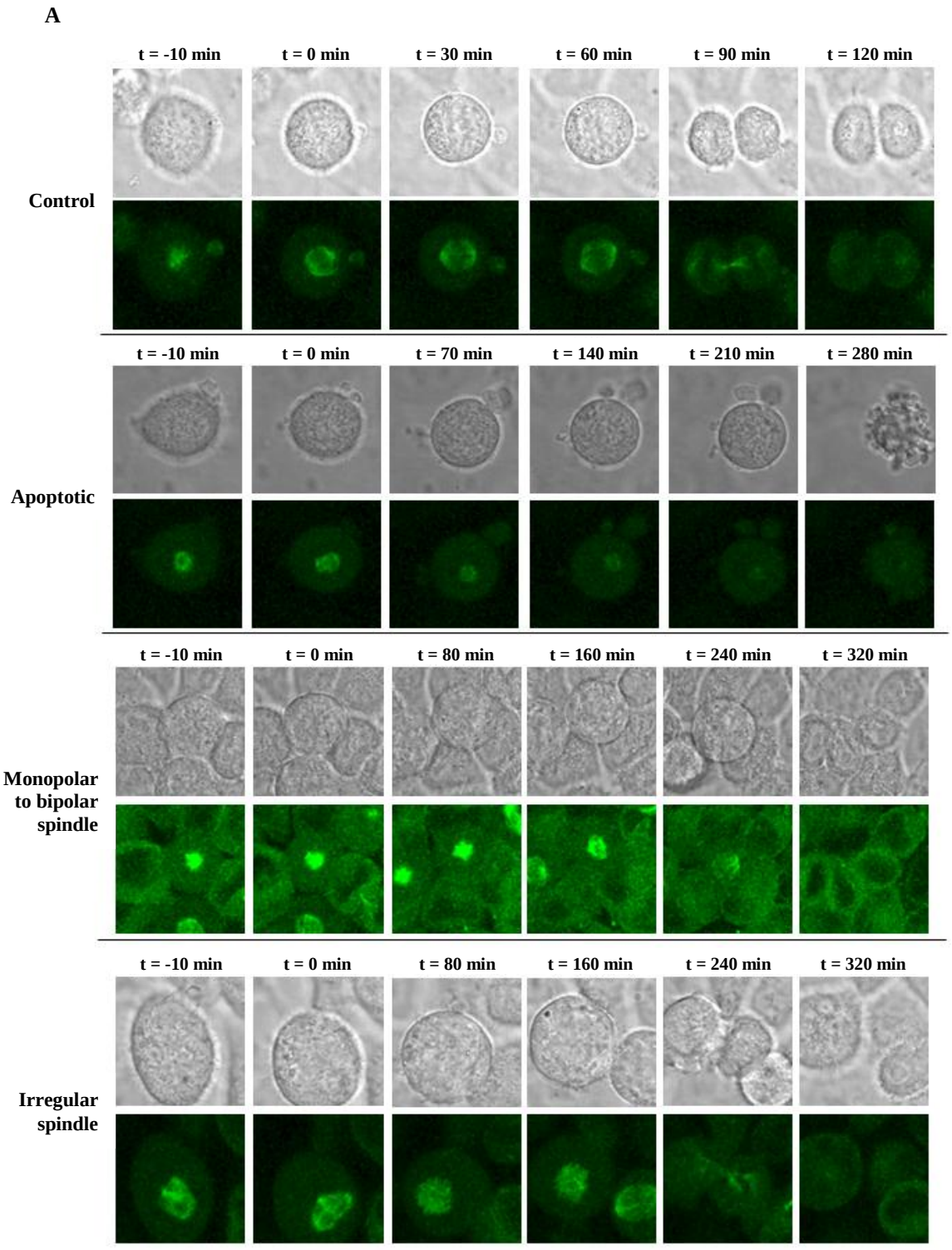

Figure 54: Treatment with NCL-00017509 (**177**) causes an increase in mitotic abnormalities and failure; **A)** Representative HeLa GFP-α-tubulin/mCherry-Histone cells showing mitotic abnormalities and mitosis with respect to control cells.

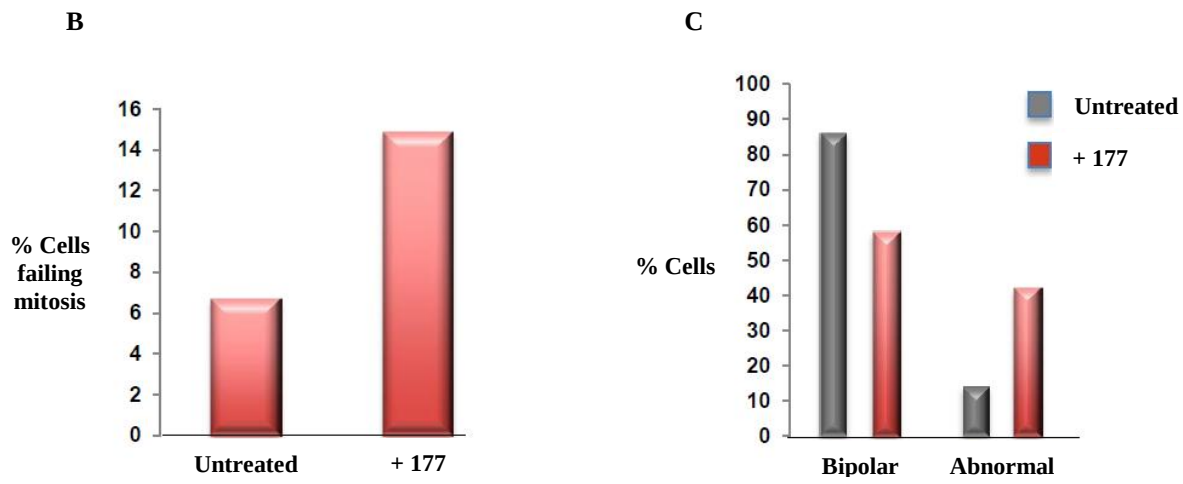

Figure 54: Treatment with NCL-00017509 (**177**) causes an increase in mitotic abnormalities and failure; **B)** Total percentage of cells failing during mitosis for untreated and **177** treated cell populations; **C)** Total percentage of cells possessing bipolar and abnormal spindles for untreated and **177** treated cell populations.

7.5. Confirmation of Mitotic Delay by Flow Cytometry

Flow cytometry is a technique used to analyse a characteristic of individual cells, or similar biological structures, in solution, using an electronic detector. Of particular interest when investigating the cell cycle is fluorescence-activated cell sorting (FACS), a technique that utilises a fluorescent DNA dye to allow the quantification of cellular DNA content, and therefore determine the stage of the cell cycle in which the cell resides. FACS analysis relies on the principle of hydrodynamic focussing to generate a single stream of particles, such as cells, which can subsequently be analysed, allowing highly accurate cell counting to be carried out. After staining with the fluorescent DNA intercalator propidium iodide (PI) a sample profile is acquired, which separates cells depending on fluorescence intensity, and therefore DNA content. Analysis of this profile can provide information of the relative distribution of cells in the cell cycle (Figure 55).[228]

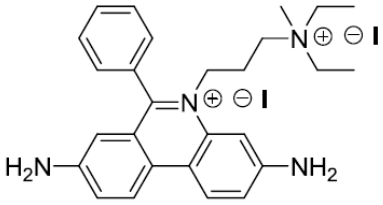

Propidium Iodide

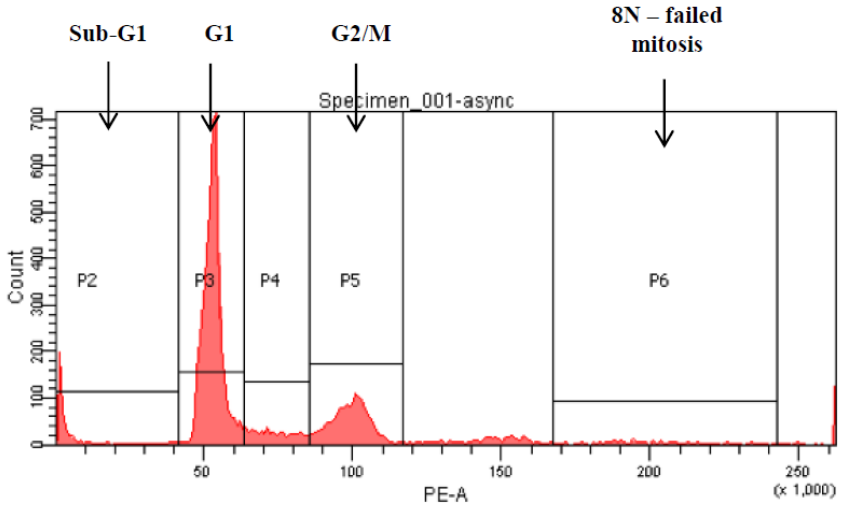

Figure 55: Example profile from PI FACS analysis indicating regions relating to cell cycle stages.

To determine the effect of Nek2 inhibition on cellular outcome over longer treatment durations than those used in live-cell imaging, it was decided to treat uninduced U2OS myc-Nek2 inducible cells with NCL-00017509 (**177**) for times of up to 72 hours, with the cell cycle distribution of the population being analysed by FACS. To do this, cells were treated with **177** at 72, 48, 24, and 4 hours prior to fixing, and an asynchronous sample was grown alongside those selected for treatment. In order to ensure that cells were subject to the same conditions excluding treatment duration, all populations had their growth media changed at 24 hour intervals, with fresh aliquots of **177** administered at each point. This was to prevent pressures on growth through a lack of fresh media, and to replace any Nek2 inhibitor removed on changing media, or that which is lost in kinase degradation.

After staining the cells and applying FACS analysis, the DNA content was quantified and hence the cell cycle stage determined for each condition (Figure 56). The results support the findings of live cell imaging, with a delay in mitotic exit resulting in an increase in the cell population in G2/M and a decrease in cells in G1 with increasing duration of inhibitor treatment. However, due to time constraints, this experiment was only conducted once, and validation of these results would require the experiment in triplicate.

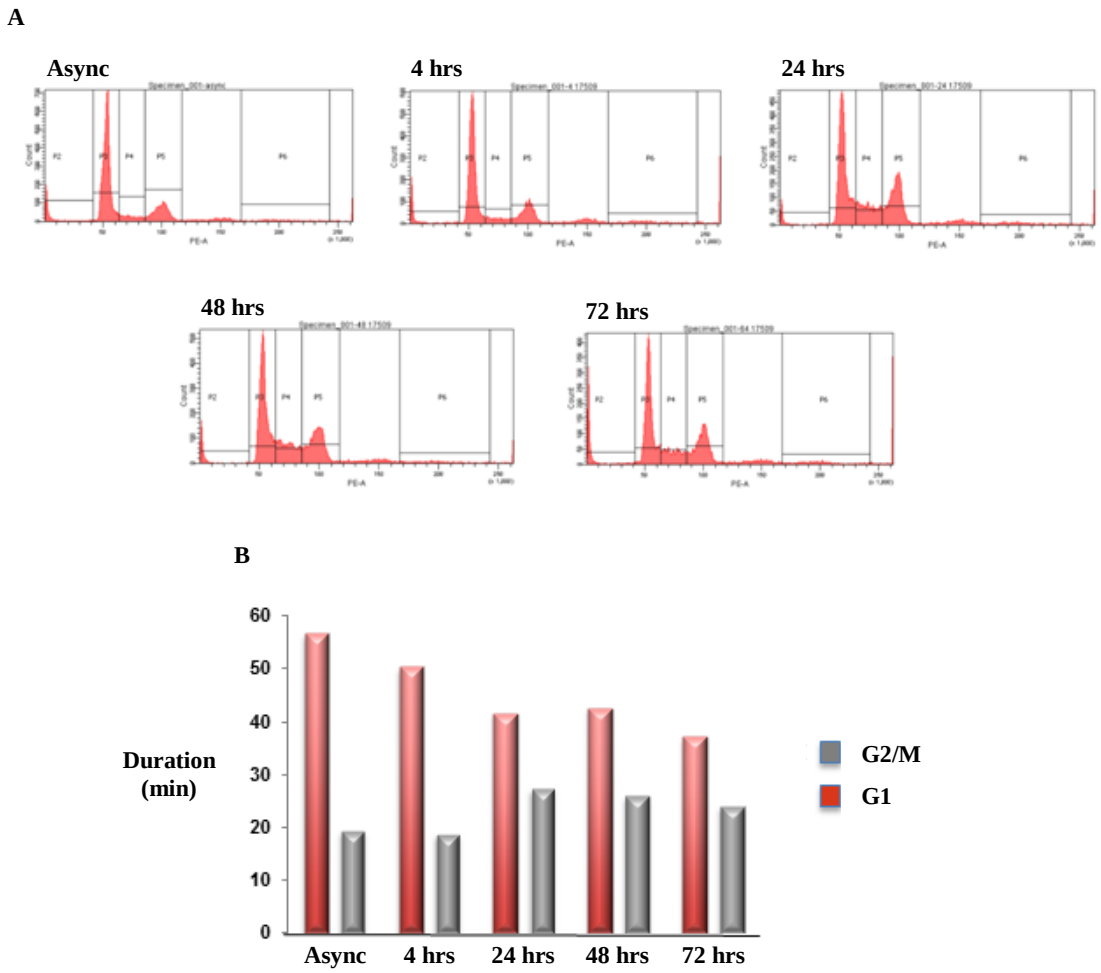

Figure 56: Treatment with NCL-00017509 (**177**) causes cells to delay in mitosis; **A)** FACS profiles for HeLa GFP-α-tubulin/mCherry-Histone cells treated with inhibitor at 5 μM for times up to 72 hours, DNA staining using propidium iodide; **B)** Total percentage of cells in G1 and G2/M stages of the cell cycle for each treatment duration.

7.6. Assessing the Selectivity of NCL-00017509 Against Nek and Mitotic Kinases

Selectivity testing of NCL-00017509 (**177**) provided some evidence of inhibitory activity against Aurora A kinase, although studies by collaborators at the Institute for Cancer Research suggested that this may have been a false positive result. However, it is known that the cellular phenotype of Aurora A inhibition is an increase in monopolar spindles and a delay in mitotic progression.[229] Due to the similarity in phenotypes observed, it was necessary to further investigate the selectivity of **177** against Aurora A. In conjunction with this work, the inhibitory activity of **177** in a panel of Nek kinases and the mitotic kinases Plk1 and Cdk1 was determined.

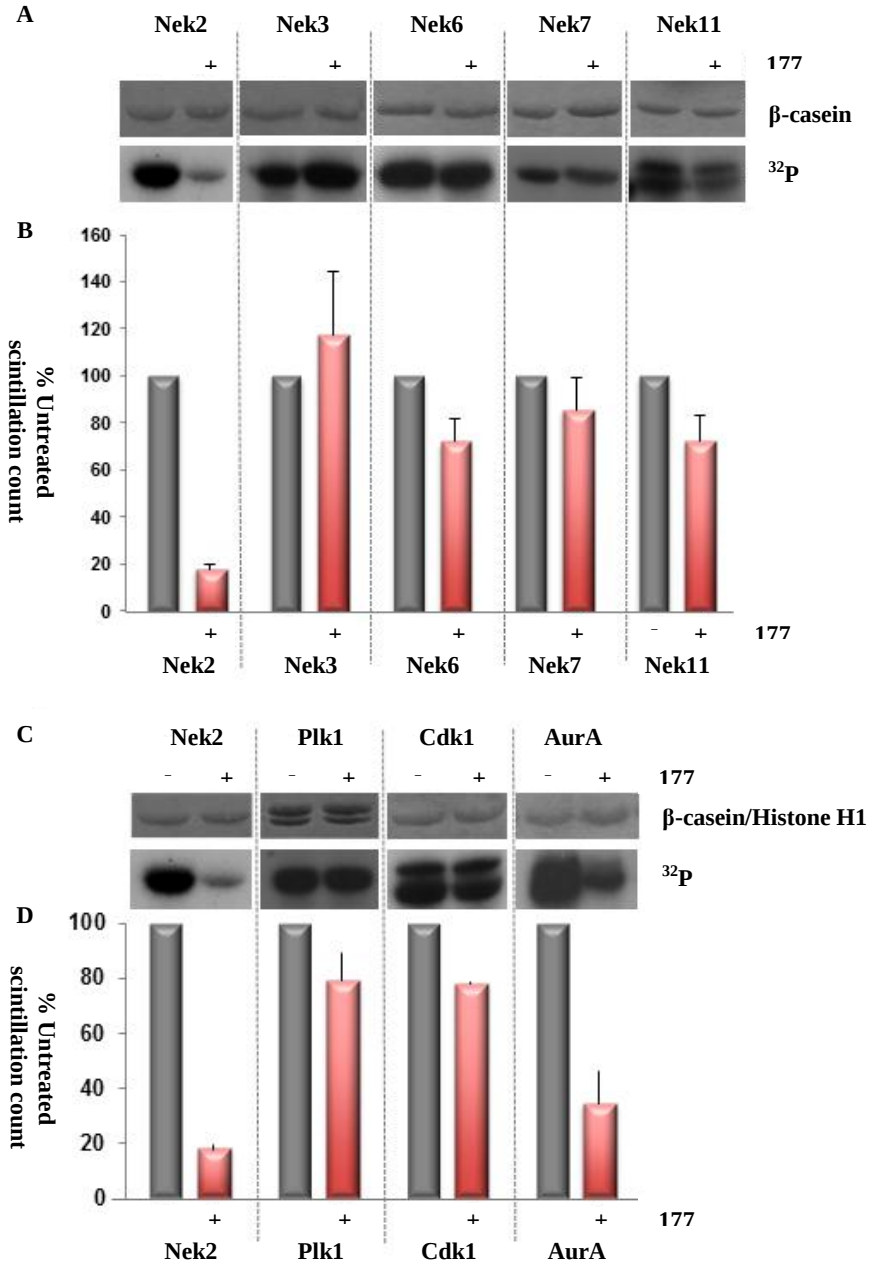

Figure 57: NCL-00017509 (**177**) is selective for Nek2 over other members of the Nek family and mitotic kinases in a recombinant kinase assay; **A** & **C)** Substrate Coumassie staining from SDS-PAGE and X-ray development of ^{32}P labelled substrate; **B** & **D)** Scintillation counts for substrate bands removed from SDS-PAGE gel for untreated and **177** treated kinase.

Using recombinant kinases, inhibition values were measured at a single inhibitor concentration of 1 μM, with the assay conducted in triplicate. Kinases were incubated with the appropriate substrate, Nek2 inhibitor and ^{32}P-ATP in kinase buffer at 30 °C for 30 minutes, followed by boiling in sample buffer, resulting in differing quantities of ^{32}P-radiolabelled substrate depending on kinase activity. Sample mixtures were subjected to SDS-PAGE electrophoresis and the gels stained with Coumassie blue to visualise substrate

bands. Gels were dried and developed on X-ray film to give a visual representation of kinase activity, and the substrate bands were removed and relative radioactivity determined using a scintillation counter (Figure 57). As seen previously, **177** displays good selectivity for Nek2 over other members of the Nek family, with only weak inhibition of Nek6 and Nek11 activity being observed. However, although the compound exhibited only modest potency against Plk1 and Cdk1, under these conditions significant inhibition of Aurora A was observed. To further quantify the extent of this inhibition, it would be necessary to repeat the assay over a range of inhibitor concentrations, allowing the calculation of an IC_{50} value.

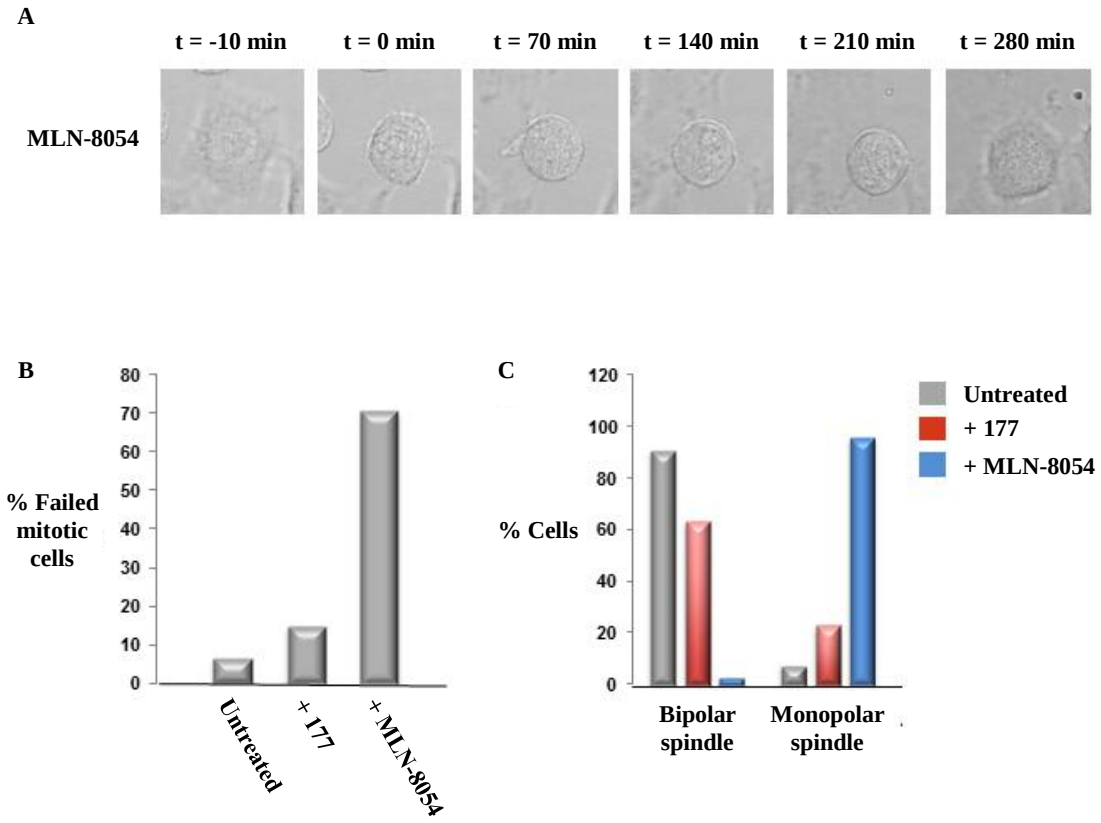

Figure 58: Cells treated with the Aurora A inhibitor MLN-8054 present a different phenotype to NCL-00017509 (**177**) treated cells; **A)** Representative HeLa GFP-α-tubulin/mCherry-Histone cells treated with MLN-8054 for 4 hours observed over 15 hours, showing mitotic failure; **B)** Total percentage of cells failing during mitosis for untreated cells and cells treated with **177** and MLN-8054; **C)** Total percentage of cells with bipolar and monopolar spindles for untreated cells and cells treated with **177** and MLN-8054.

In an attempt to determine whether the effect observed in cells from live cell imaging and FACS analysis was due to the inhibition of Nek2 or Aurora A, the known Aurora A inhibitor MLN-8054 was evaluated.[230] Live cell imaging was repeated under the same conditions

previously used, with MLN-8054 administered at 5 μM. Upon imaging of cells undergoing mitosis after treatment with MLN-8054, it became apparent that Aurora A inhibition presented as a previously unseen phenotype (Figure 58; **A**). Cells entered mitosis and remained in prophase with monopolar spindles before returning to a flattened interphase state without dividing. This was quantified by counting the percentage of cells failing to complete mitosis (Figure 58; **B**). Although cells treated with **177** showed a small increase in failed mitosis with respect to untreated cells (15%) all failed mitotic events were due to apoptosis. In contrast, there was a large increase in cells failing to complete mitosis with MLN-8054 treatment (71%), although the majority of these cells were not apoptotic and instead re-entered interphase.

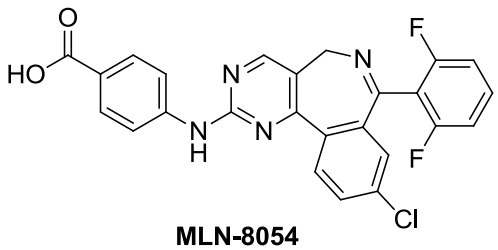

MLN-8054

Furthermore, there was a significant difference in the number of cells possessing bipolar and monopolar spindles between each treatment condition (Figure 58; **C**), with just 3% of cells treated with MLN-8054 bearing a bipolar spindle, and 96% exhibiting monopolar spindles. These findings strongly indicated that the phenotypes observed for treatment with each inhibitor were due to inhibition of different cellular processes; although **177** was shown to inhibit Aurora A *in vitro*, it appears that *in vivo* this does not predominate.

To further support this proposal, FACS analysis of cells treated with MLN-8054, as described previously, was carried out (Figure 59). Due to the observation during live cell imaging that cells return to an interphase state without dividing, it would be anticipated that cellular DNA content would continue to double beyond that seen for G2/M cells, a so called 8N number. Indeed, it was found that over increasing treatment times for cells incubated with MLN-8054 there was a build-up of cells displaying a DNA content profile indicative of 8N cells. The lack of cells showing 8N DNA from those treated with **177** provides further evidence that any cellular effect observed for Nek2 inhibitor treatment is not solely due to off-target inhibition of Aurora A. In order to further strengthen these data, the assays would need to be repeated at higher concentrations of **177**, to establish the level at which an Aurora A inhibition phenotype becomes apparent.

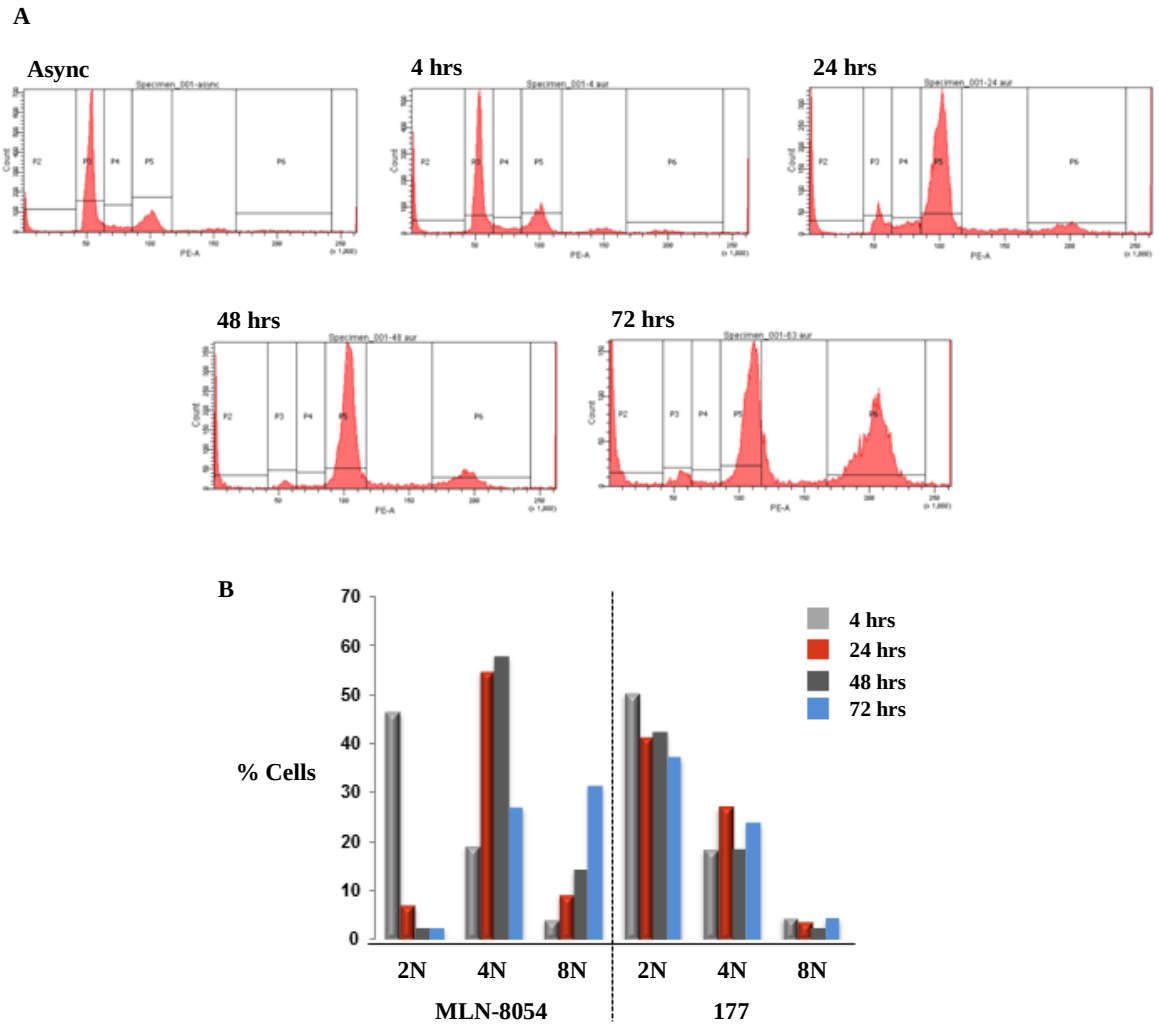

Figure 59: Cells treated with MLN-8054 show an increase in 8N DNA number, indicating failed mitosis; **A)** FACS profiles for HeLa GFP-α-tubulin/mCherry-Histone cells treated with MLN-8054 at 5 µM for times up to 72 hours, DNA staining using propidium iodide; **B)** Total percentage of cells with 2N, 4N and 8N DNA number for cells treated with MLN-8054 and NCL-00017509 (**177**).

7.7. Conclusions and Further Work

The irreversible Nek2 inhibitor NCL-00017509 (**177**) was evaluated in several assays for its effects on cellular Nek2 activity and mitotic outcome. Through an observation of the percentage of cells displaying split centrosomes, a biomarker proposed to be indicative of Nek2 activity, a clear dose-response with increasing inhibitor concentration has been shown. A more accurate cellular biomarker of Nek2 activity is the level of phosphorylated C-Nap1. However, when cells dosed with inhibitor were assayed for antibodies for pC-Nap1, this dose response was lost, with a decrease in pC-Nap1 levels only being seen between 500 nM and 5 µM. This may be as a consequence of phosphorylation of C-Nap1 not being a critical factor in centrosome separation as hypothesised. The results from this assay must be considered

with some caution, as the variability of intensity measurements obtained for each condition introduced a large degree of error in values, and highlights the limitations of this technique. Further work should be carried out on reaction standardisation, together with experiments over dose ranges between 500 nM and 5 μM to validate the results obtained thus far.

To understand the effect of **177** treatment on cellular Nek2 activity in greater detail, further experimental techniques were undertaken. During the course of these studies, it was attempted to extract cellular Nek2 from treated cells and perform ^{32}P-kinase assays. This was investigated using immunoprecipitation with myc antibodies on cell lysates. Unfortunately, during the time of the study this technique was not successful in effectively isolating active Nek2 kinase from cells, as extracts from induced cells lacking inhibitor treatment were inactive in kinase assays. In spite of this, western blot analysis of the extracts with a myc antibody did indeed show that myc-Nek2 had been retrieved from the cells. However, the protein appeared either to be in an inactive form, or a component of the kinase assay was ineffective. Further investigation of this result, and the development of a reliable immunoprecipitation-kinase assay procedure, is needed to obtain conclusive results from this assay and to further evaluate the effect of inhibitor treatment of cellular Nek2 activity.

Live cell imaging using confocal microscopy was used to show that cells treated with inhibitor are delayed in mitosis with respect to untreated cells, particularly between anaphase and cytokinesis. An increase in the prevalence of abnormal mitotic phenotypes was also observed, indicating that treatment with **177** has a detrimental effect on the tightly controlled mitotic machinery. In conjunction with this, FACS analysis supported these findings by indicating that cells treated with inhibitor stall in mitosis with increasing incubation time, albeit that this assay was performed only once, and would need to be repeated to improve the reliability of the data. Interestingly, both the live cell imaging and FACS analysis were performed on cells that have previously been shown to have low sensitivity to **177** in classical growth inhibition assays. It would be informative to develop cell lines that are sensitive to inhibitor, such as SKBR3 or Rec-1, that stably express both the myc-Nek2 TET-ON system and GFP-α-tubulin/mCherry-Histone tags. This would allow the assays to be repeated on sensitive cell lines, where one may anticipate an enhanced effect with respect to U2OS/HeLa cells.

With only limited success being achieved in assays designed to directly examine Nek2 activity in cells, it is not possible to determine whether the effects of **177** on mitotic delay or

the phenotypes observed in cells are due to Nek2 inhibition alone. Thorough kinase selectivity testing has been carried out previously on **177** (see appendix, Table A2), indicating good selectivity, with greater than 10-fold selectivity seen for all kinases tested, and greater than 100-fold selectivity observed for all but 9 kinases. To further support these data, determinations of **177** inhibition at single concentrations of 1 μM were carried out on Neks 2, 3, 6, 7 and 11, and mitotic kinases Plk1, Cdk1 and Aurora A. As observed previously, good selectivity was seen for Nek2 over these kinases, with the exception of Aurora A. To fully investigate the activity seen against Aurora A it would be necessary to repeat the kinase assay over a wider range of inhibitor concentrations for the determination of an IC_{50} value.

Evidence that **177** does not elicit significant inhibition of cellular Aurora A was adduced from a comparison of the inhibition phenotypes observed in live cell imaging and FACS analysis with **177** and the known Aurora A inhibitor MLN-8054. However, questions as to whether the cellular effects seen for **177** are due to Nek2 inhibition alone remain. Preventing the covalent inactivation of Nek2 by such inhibitors may allow this question to be addressed. This may be possible through modification of the 6-ethynyl position into a non-electrophilic isostere, such as the 6-cyanopurine **296**.

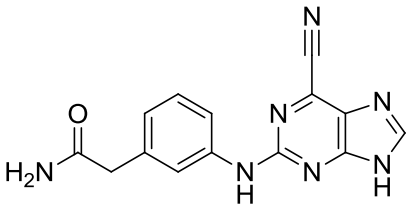

296

However, initial cellular studies with **296** indicated that the increased polarity of the 6-cyanopurine compared with **177**, compromised cellular permeability and reduced effective intercellular compound concentrations to levels that prevented direct comparison. The alternative modification that can be made is to the Cys22 residue. If cells containing a tetracycline-inducible Nek2 Cys22 mutant display the same growth inhibitory response to **177** as Nek2-WT, this would suggest that off-target effects are responsible for any observed growth inhibition. Site directed mutagenesis of WT Nek2 followed by polymerase chain reaction gave Cys22Val/Ala mutant constructs. Unfortunately, during the time of the study, all attempted transient transfections of the constructs into HeLa cells gave insufficient transfection efficiency to be suitable for the available assays. However, evaluation of

analogues of **177** has suggested that additional efforts to address this question are unneccessary. The poor correlation between the Nek2 kinase IC_{50} and SKBR3 cellular GI_{50} for these inhibitors, in conjunction with the identification of analogues of **177** that combine potent cellular growth inhibition with only modest Nek2 kinase potency, strongly indicates that the cellular potency of **177** is independent of Nek2 activity.

7.8. Materials and Methods

7.8.1. Tissue Culture

7.8.1.1. Cell Maintenance

U2OS myc-Nek2 cells were grown as adherent colonies on tissue culture dishes in Dulbecco's Modified Eagle Medium (DMEM) tissue culture medium (Gibco®, Invitrogen), with G418 (Gibco®, 500 µg/ml), puromycin (3 µg/ml), foetal calf serum (FCS, 10%) and penicillin (100 µg/ml)/streptomycin (100 µg/ml) as additives. G418 and puromycin, which are toxic to both prokaryotic and eukaryotic cells, act as selectivity reagents, ensuring the cell population is predominantly made up of cells possessing the desired mutation, in this case the myc-Nek2 TET-ON system. This is due to the construct encoding for the tetracycline-inducible gene expression system bearing G418 and puromycin resistance factors. Penicillin and streptomycin are added to act as antibacterial agents, reducing the likelihood of bacterial infection of cell culture colonies. FCS acts as a serum supplement, as it contains many growth factors that are advantageous to eukaryotic cell growth.

GFP-α-tubulin/mCherry-Histone HeLa cells were grown as adherent colonies on tissue culture dishes in Minimum Essential Media (MEM) tissue culture medium (Gibco®, Invitrogen) containing FCS (10%) and penicillin (100 µg/ml)/streptomycin (100 µg/ml).

7.8.1.2. Lifting of Adherent Cell Colonies

In order to maintain optimal colony sizes on plates, cells must be regularly passaged, or split. In order to do this, and to harvest cells for use in assays, adherent cells must be lifted from tissue culture dishes. Cell media was removed *via* aspiration, and the cells monolayer was washed with phosphate buffered saline (PBS) solution, which was subsequently aspirated. The cells were lifted from the plate through incubation with a solution of ethylenediaminetetraacetic acid (EDTA, 5 mM) in PBS for 15 minutes.

Phosphate Buffered Saline (10x): NaCl (4% w/v), KCl (0.1% w/v), $Na_2HPO_4.7H_2O$ (0.6% w/v), KH_2PO_4 (0.1% w/v), NaN_3 (0.01% w/v).

7.8.1.3. Harvesting and Lysis of Cell Suspension

The suspended cells in PBS/EDTA were centrifuged at 1,100 rpm for 5 minutes, before the supernatant was removed through aspiration, leaving a cell pellet. The pellet was washed with PBS solution and centrifuged for a further 5 minutes at 1,100 rpm. The supernatant liquid was again removed, leaving a cleaned pellet of cells which was kept on ice.

Lysis of the cell wall will result in cell lysate containing proteins of interest. However, this will also result in loss of the cells metabolic regulation, and enzymes such as proteases may result in sample degradation prior to analysis. In addition to cooling of the cell sample, inhibitors are added to the lysis buffer to inhibit these processes.

NebA buffer: (for 5 ml) 4-(2-hydroxyethyl)-1-piperazineethanesulfonic acid (HEPES, 0.5M, 0.5 ml), MnCl2 (0.5M, 50 µl), MgCl2 (0.5M, 100 µl), ethylene glycol tetraacetic acid (EGTA, 0.5M, 100 µl), EDTA (0.5M, 20 µl), NaCl (5M, 100 µl), KCl (1M, 25 µl) and Nonident (10%, 50 µl) in ddH_2O (3.915 ml).

Inhibitors: (to 1 ml NebA) RNAse A (10 mg/ml, 3 µl), DNAse I (10 mg/ml, 3 µl), Protease inhibitor cocktail (PIC, Sigma) containing 4-(2-aminoethyl)benzenesulfonyl fluoride, pepstatin A, trans-epoxysuccinyl -L-leucylamido(4-guanido)butane, bestatin, leupeptin and aprotinin in DMSO (10 mg/ml, 1 µl), phenylmethylsulfonyl fluoride (PMSF, 1M, 1 µl), NaF (0.5M, 10 µl) and β-glycerophosphate (0.5M, 10 µl).

Cell pellets were suspended in NebA lysis buffer (50-250 µL, based on pellet size) and kept on ice for 30 minutes. The samples were subsequently passed through a 27 gauge needle 10

times to mechanically break up the cell membrane, before being centrifuged for 10 minutes at 4 °C and 13,000 rpm. The supernatant liquid was removed, affording a pellet of lysed cellular material, which can be carried forward for further experimentation.

7.8.2. Gel Electrophoresis

7.8.2.1. Principle

In order to study proteins from cell lysate or immunoprecipitation, it is necessary to separate the proteins using gel electrophoresis, using an electric field and separating the proteins based on molecular weight. In order for molecular weight to be the only factor in their separation, the proteins must be denatured from their original tertiary structure and given an overall net negative charge to negate the intrinsic variable charge of proteins. This is achieved by heating the protein samples to 100 °C in sample buffer, containing the anionic detergent sodium dodecyl sulfate (SDS), 2-mercaptoethanol for the cleavage of disulfide bonds, and bromophenol blue to act as a marker dye running in front of the protein samples.

Polyacrylamide gel is utilised as the support medium due to its active participation in the separation process, as it has pores in the same order of magnitude as the peptide units, allowing it to act as a molecular 'sieve'. Furthermore, it is chemically inert, stable to temperature and pH, and is transparent which allows the progress of marker proteins to be monitored during electrophoresis. Gel density can be adjusted depending on the molecular weight of the proteins of interest; increasing density by using a higher percentage of acrylamide will decrease pore size, allowing separation of smaller molecular weight peptide units. This process is known as sodium dodecyl sulfate polyacrylamide gel electrophoresis (SDS-PAGE).

7.8.2.2. General Reagents

SDS Sample Buffer: Tris(hydroxymethyl)aminomethane hydrochloride pH 6.8 (Tris.HCl, 63 mM), SDS (2% w/v), 2-mercaptoethanol (5% w/v), glycerol (20% v/v) and bromophenol blue (0.005% w/v) in ddH_2O.

Tris-Glycine-SDS Running Buffer: Tris (0.025 M), glycine (0.20 M) and SDS (3.5 mM) in ddH_2O.

Stacking Polyacrylamide Gel: (1 gel) 30% ProtoGel® (37.5:1 Acrylamide:Bisacrylamide, 0.65 ml), ddH_2O (3.0 ml), stacking buffer (0.5M Tris pH 6.8, 0.4% SDS, 1.25 ml), 10% ammonium persulfate (APS, 75 µl), tetramethylethylenediamine (TEMED, 5 µl).

Resolving Polyacrylamide Gel (10%): (1 gel) 30% ProtoGel® (2.0 ml), ddH_2O (2.5 ml), resolving buffer (1.5M Tris pH 6.8, 0.4% SDS, 1.5 ml), 10% APS (75 µl), TEMED (5 µl).

7.8.2.3. General Procedure

Cell lysate pellets are suspended in SDS sample buffer (10-100 µl, based on pellet size) and boiled at 100 °C for 5 minutes. Samples (10-30 µl) are added along with a protein size ladder to the stacking layer of a polyacrylamide gel, and sample wells filled with Tris-Glycine-SDS running buffer. The gel is run in Tris-Glycine-SDS running buffer at 180 volts until the bromophenol blue reaches the bottom of the resolving gel (approx. 1 hour). The gel is removed from the buffer, the stacking layer is cut away and the resolving layer is washed with water.

7.8.3. Western Blotting and Immunodetection

7.8.3.1. Principle

It is necessary to identify and analyse proteins separated by SDS-PAGE, which is not possible when the proteins remain on the gel. In order to transfer the proteins to a suitable medium and detect proteins of interest, the techniques of Western blotting and immunodetection may be used. In order to probe for proteins of interest using antibodies, the proteins residing on the acrylamide gel are first transferred to a thin membrane, such as nitrocellulose.

Nitrocellulose membrane is a thin film of nitrocellulose, generated through the exposure of cellulose to nitric acid, which has a high affinity for proteins and nucleic acids. This allows proteins transferred to the membrane to be immobilised on its surface for detection using immuno-antibodies. The net negative charge given to the proteins during SDS-PAGE can be used to transfer proteins from the gel to nitrocellulose through the application of an electric current perpendicular to the plane of the gel.

Due to the high affinity of nitrocellulose membrane to proteins, prior to treating the membrane with antibodies, it is necessary to block all unoccupied sites on the membrane.

This can be achieved using both bovine serum albumin (BSA) or milk, in buffer containing the polysorbate surfactant Tween-20, which further aids in non-specific antibody binding.

After blocking the membrane, the membrane can be probed with primary antibodies, which have been specifically raised against the protein of interest, resulting in specific binding of the antibody to regions of the membrane at which the protein is present. Following primary antibody incubation, the membrane can be probed with secondary antibodies, which are targeted for the species specific immunoglobulin heavy chain of the primary antibody. This allows membranes to be probed with antibodies for alternative proteins raised in different species, and these proteins to be identified using species specific secondary antibodies. The secondary antibodies can be used to visually detect proteins due to the fact that they can bear enzymes that can be used to catalyse reactions that illicit a visual response. The two most common types of reporter assay utilise alkaline phosphatase (AP) and horseradish peroxidase (HRP) secondary conjugates.

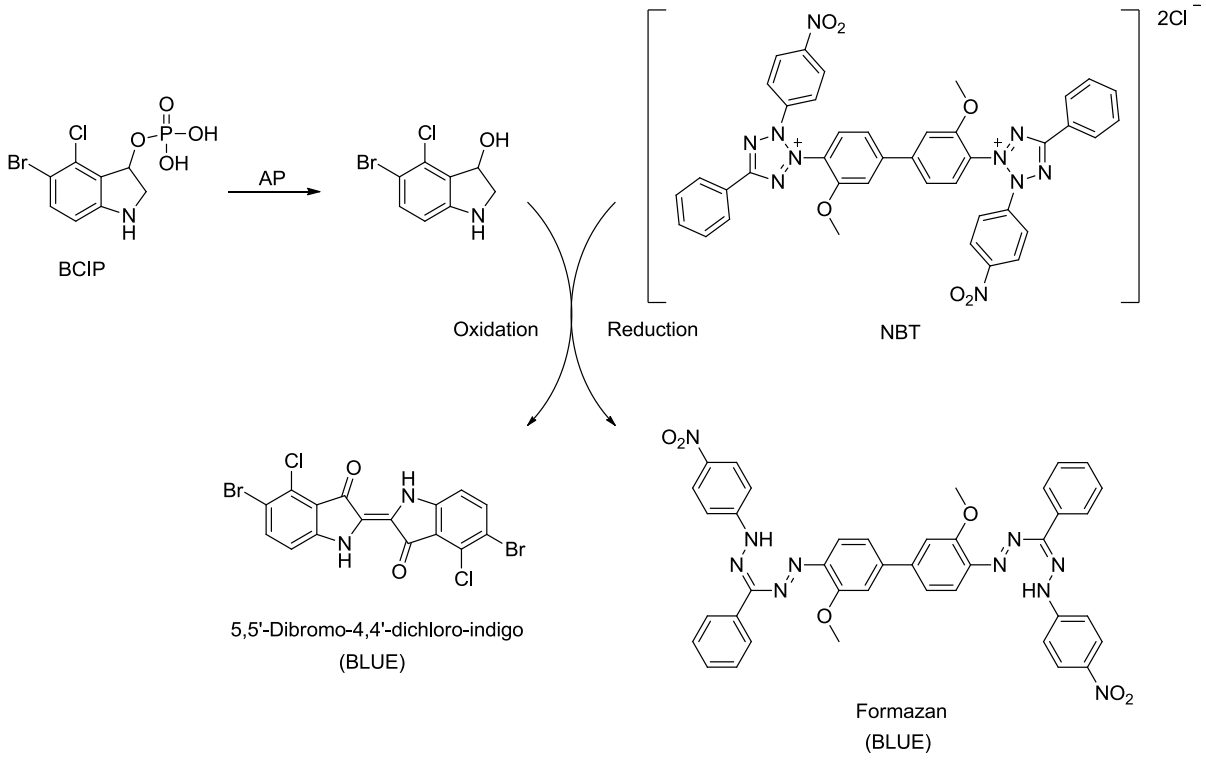

Figure 60: Mechanism of colour generation using AP conjugate secondary antibodies.

Alkaline phosphatase is used to generate a colourimetric assay, through the use of the developing agents 5-bromo-4-chloroindolyl phosphate (BCIP) and nitro blue tetrazolium chloride (NBT). AP catalyses the dephosphorylation of BCIP to 5-bromo-4-chloroindolin-3-

ol, which undergoes a redox reaction with NBT to generate the strongly blue coloured precipitates 5,5'-dibromo-4,4'-dichloro-indigo and formazan (Figure 60).

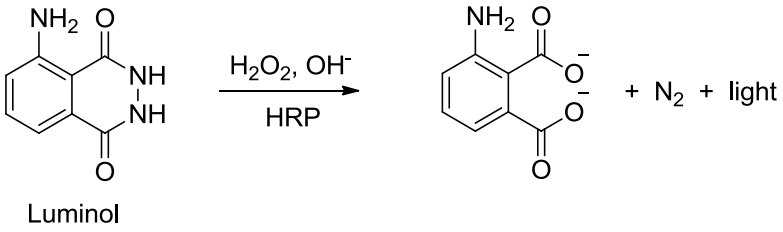

Figure 61: Mechanism of light generation using ECL conjugate secondary antibodies.

Horseradish peroxidase is used in enhanced chemiluminescence (ECL) systems, in which HRP in the presence of hydrogen peroxide and an enhancer,usually in the form of a substituted phenol, catalyses the conversion of luminol to an aminophthalate, with the production of light (Figure 61). This light can be detected through the development of photographic films exposed to membranes after treatment with ECL systems. Bleaching of the photographic film not only provides information as to the presence of protein, but also the relative abundance.

7.8.3.2. General Reagents

Transfer Buffer: Tris (0.025M), glycine (0.20M), and methanol (10% v/v) in ddH_2O.

Ponceau Stain: Ponceau S (0.2% w/v), trichloroacetic acid (3% w/v) and sulfosalicylic acid (3% w/v) in ddH_2O.

Blocking Solution: Milk powder (5% w/v), Tween20 (0.1% v/v) in PBS.

AP Buffer pH 9.5: Tris.HCl (100mM), NaCl (100mM), $MgCl_2$ (5mM) and Tween20 (0.1% v/v) in ddH_2O).

AP Developing Solution: BCIP (0.02% w/v) and NBT (0.03% w/v) in AP buffer pH 9.5.

7.8.3.3. General Procedure

A film of nitrocellulose membrane is soaked in transfer buffer and placed on 3 sheets of blotting paper, also soaked in buffer, in a blotting unit. A polyacrylamide gel from SDS-PAGE is carefully soaked in transfer buffer and placed on top of the membrane, followed by a further 3 soaked sheets of blotting paper. The resulting layers are gently rolled to remove

any air bubbles and further transfer buffer is poured over them. The lid of the blotting unit is closed and a current of 70 mA/gel is passed through the system for 1-2 hours depending on protein size. Upon completion, the membrane is removed and stained with ponceau stain for 5 minutes, after which water is used to destain the membrane so only protein locations can be seen. At this point, the location of the channels and marker ladder can be marked with pencil, and the membrane can be imaged to record relative protein levels in each channel.

The unoccupied sites of the membrane are subsequently blocked by covering the membrane in blocking solution and placing the membrane on an agitator for 10 minutes. The blocking solution is changed and the process repeated a further 2 times. The primary antibody is prepared as a dilution, according to suppliers instructions, in blocking solution (3-5 ml, depending on membrane size), and the membrane is incubated in this solution for 1 hour at room temperature, or for 18 hours at 4 °C. The primary antibody solution is removed and the membrane is washed with PBS-Tween (10 ml) for 10 minutes, 3 times.

The requisite secondary antibody conjugate solution is prepared as for the primary solution in blocking solution (3-5 ml, depending on membrane size), and the membrane is incubated in this solution for a further 1 hour at room temperature. This is followed by a further course of washes with PBS-Tween (10 ml) for 10 minutes, 3 times.

For the development of blots incubated with AP conjugate secondary antibodies, the developing solution (3-5 ml) is prepared and added to the membrane. The membrane is incubated with the developing solution until protein bands have developed to the desired level (5-30 minutes), at which point the developing solution is removed and the membrane is washed with PBS-Tween (10 ml). The membrane can now be imaged to record the resultant band pattern.

For the development of blots incubated with ECL conjugate secondary antibodies, the developing solution (ThermoScientific, Pierce ECL WB substrate, 32106) is prepared as per suppliers instructions and added to the dry membrane for 60 seconds. The developing solution is removed by blotting with paper towel and the membrane is loaded into a film cassette and exposed to photographic film (<1 min – 1 hour, depending on protein abundance). Development of the photographic film reveals the band pattern, which can be imaged.

7.8.4. Immunofluorescence Microscopy

7.8.4.1. Principle

When working with cellular populations, it is desirable to determine the location and abundance of target proteins within the cell. One such technique that allows this is immunofluorescence microscopy. Similar to immunodetection of proteins on membranes, this technique relies on the specificity of antibodies for target proteins to allow this information to be acquired from whole cell populations. When working with adherent cell lines, it is possible to grow cell colonies on microscope cover slips that have been etched using acetic acid, followed by sterilization in an autoclave.

Upon completion of a desired cell treatment protocol, it is possible to fix cells in their present state using cold methanol, preventing any further cell growth or death. This allows the cells to be probed with antibodies, and detailed information about the location and abundance of proteins at the time of fixation to be ascertained. The coverslips that are removed from cell culture dishes possess large areas of glass that are free of cells, and glass has a latent affinity for proteins. It is therefore necessary to block the vacant sites of the coverslips in a similar manner to nitrocellulose membrane, to limit non-specific antibody binding. This is done using BSA. The coverslips can subsequently be probed with antibodies raised against the proteins of interest. It is common when conducting immunofluorescence microscopy to probe cells with more than one antibody at a time, relying on the differing species specific immunoglobulin heavy chain of the primary antibodies to ensure these proteins can be differentiated once imaged.

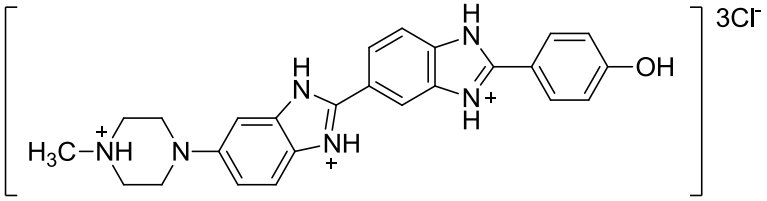

Hoechst 33258

A secondary antibody mix can now be applied to the cover slips, containing antibodies targeting the species specific immunoglobulin heavy chain, bearing fluorescent reporter proteins. It is also common for the secondary antibody mix to contain a fluorescent DNA minor groove binder of the Hoechst family, to allow the visualisation of DNA within the cell. During the course of this work Hoechst33258 was used, displaying blue fluorescence.

The coverslips now bear cells within which proteins of interest are tagged with fluorescent reporter proteins, and microscopy utilising laser excitation of the relevant wavelength can be used for detection.

7.8.4.2. General Reagents

Blocking Solution: BSA (3% w/v) in PBS.

Incubation Solution: BSA (1% w/v) in PBS.

7.8.4.3. General Procedure

Upon completion of the desired cell treatment regimen, the cell media is removed by aspiration, and the coverslips are transferred to clean wells. The remaining cells in the cell culture dish may be used for further assay techniques. The coverslips are fixed using methanol (-20 °C, 2-5 ml, depending on size of cover slip) at -20 °C for 15 minutes. The methanol is removed from the cover slips and they are washed with PBS (2-5 ml) for 5 minutes, 3 times. Each cover slip is blocked with blocking solution (1-3 ml) for 10 minutes, before the solution is removed. The primary antibody mix is prepared in incubation solution at concentrations as per supplier's instructions, and the solution (100-200 µl) is pipetted directly onto each cover slip, ensuring that the entire surface is covered. The cover slips are incubated with primary antibody in the dark for 1 hour, before being washed with PBS (2-5 ml) for 5 minutes, 3 times. The secondary antibody mix is prepared in incubation solution and pipetted directly onto the cover slips. Incubation is repeated for a further 1 hour in the dark. The cover slips are washed with PBS (2-5 ml) for 5 minutes, 3 times, before being mounted onto microscope slides. At this point, the slides can be stored at 4 °C in the dark prior to microscopy.

7.8.5. Fluorescence-Activated Cell Sorting (FACS)

7.8.5.1. Principle

When subjecting cells to a treatment regimen that is proposed to affect progression through the cell cycle, it is desirable to determine the relative distribution of a cell population through the cell cycle. Due to the complexity of this process, it can be very challenging to do this. However, one factor that can be used as a measure of cell cycle progression is DNA content in cells. In a given asynchronous cell population, the majority of cells will be in a quiescent,

or resting, state, or in G1. Thus, DNA content will be equal to that which is resultant from the previous cycle of mitosis, and hence will be 1 copy of the cells genetic information. Once the cell cycle has entered the S-phase, the cells genetic information is replicated, resulting in a doubling of DNA content. From this point, the cell cycle progresses relatively quickly through to mitosis, yielding new daughter cells with a DNA content equal to that of G1.

It is possible to utilise this disparity in DNA content of cells in G1 with respect to those at G2/M to gauge the cells progression through mitosis, and in particular identify cell populations experiencing mitotic delay, through an increase in cells with a DNA indicative of a G2/M profile. Once such method used to determine this distribution is fluorescence-activated cell sorting (FACS).

FACS uses the techniques of flow cytometry, and in particular hydrodynamic focussing, to allow samples of particles, such as cells, to be analysed individually. Under hydrodynamic focussing conditions, a sample flow may be passed down a capillary into the flow of a separate fluid, known as the sheath. If the velocities of the two media differ sufficiently, essentially no mixing occurs, and through narrowing of the chamber through which the sample and sheath fluids flow, a very narrow sample flow can be achieved (Figure 62).[231]

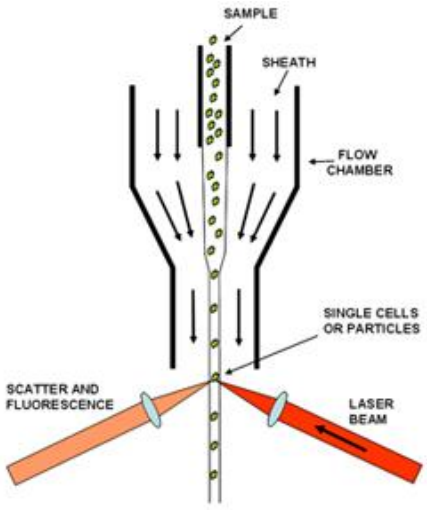

Figure 62: Hydrodynamic focussing used in flow cytometry.[231]

In FACS, fluorescence spectroscopy of the resultant flow allows the determination of the relative DNA content in individual cells of an entire cell population. In order to do this, the DNA must be labelled in a quantitative manner with a fluorescent marker molecule. For this purpose, the fluorescent DNA intercalating agent propidium iodide is used. Incubation of cell

samples with propidium iodide, followed by FACS analysis results in a fluorescence readout which reflects the abundance of DNA in cells with respect to their cumulative abundance.

7.8.5.2. General Reagents

Staining Solution: RNAse A (100 µg/ml), propidium iodide (50 µg/ml) in PBS.

7.8.5.3. General Procedure

For asynchronous and G1/S cells, cell culture media is removed *via* aspiration, and the cell monolayer is washed with PBS (5 ml). The PBS is removed and the cells are incubated with PBS/EDTA (1-3 ml). Cells are collected and transferred to centrifuge tubes. Due to the fact that G2/M cells have rounded up and partially detached from the cell culture dish, for these cells the cell culture media is removed and added to a centrifuge tube. Any remaining cell monolayer is harvested as per G1/S cells. All cell harvests are subsequently centrifuged at room temperature for 5 minutes at 1,000 rpm.

Once centrifuged, the supernatant is removed from all cells *via* aspiration, and the cell pellet is resuspended in PBS (5 ml), followed by a further centrifugation at room temperature for 5 minutes at 1,000 rpm. Again, the supernatant is removed, and the cell pellets are resuspended in PBS (200 µl). In order to fix the cells, 70% ice-cold ethanol (2.0 ml) is added drop-wise, whilst the cells are gently vortexed to prevent aggregation. At this point, the fixed cells can be stored at 4 °C.

The fixed cells are now centrifuged at 4 °C for 5 minutes at 3,000 rpm, and the supernatant removed *via* aspiration. The cell pellets are washed with PBS (5 ml) twice, with centrifugation and aspiration, to remove all ethanol. The resulting pellets are resuspended in staining solution (1 ml) and incubated at 4 °C in the dark for 18 hours. The resulting samples are subjected to FACS analysis, with the use of asynchronous, mitotic and S-phase control samples used to control the calibration of cell counting population restrictions.

7.8.6. *In Vitro* ^{32}P Kinase Assay

7.8.6.1. Principle

It is often necessary to determine the catalytic activity of kinases, either purchased as recombinant kinases, or as purified kinases from immunoprecipitation. One method to

achieve this is the use of ^{32}P in a kinase assay. ^{32}P is one of 23 known isotopes of phosphorus, and long with ^{33}P is a β-emitting radioisotope. It is possible to take advantage of this β-emission to monitor kinase activity through incorporation of ^{32}P into kinase substrates. Incubation of a kinase of interest with its substrate in the presence of ^{32}P-ATP will result in radiolabelling of the substrate through phosphorylation. When compared to a control kinase assay, the relative level of radioactivity will give a direct measure of kinase activity.

Boiling of assay samples in SDS sample buffer will halt any further reaction through denaturing of the proteins, and the samples can be subjected to SDS-PAGE. This results in a gel with bands of radiolabelled substrate. There are two ways in which kinase activity can be determined from this gel. Exposure of the radioactive gel to X-ray film will result in bleaching of the film, which when developed can be analysed by densitometry, to give the integrated optical density (IOD) of each band. However, this technique has a relatively large error associated, and as such can only be used to give semi-quantitative analysis. A much more accurate measure of activity can be acquired by drying the gel and manually removing each substrate band. The substrate can now be subjected to scintillation counting, allowing an accurate numerical figure for the relative kinase activity to be determined.

7.8.6.2. General Reagents

Kinase Buffer: (for 10 reactions) HEPES (0.5M, 50 µl), NaF (0.5M, 5 µl), β-glycerophosphate (0.5M, 5 µl), $MnCl_2$ (0.5M, 5 µl), ATP (100µM, 20 µl), dithiothrietol (DTT, 1M, 0.5 µl) and ^{32}P-γ-ATP (~100 µCi, 10 µl) in ddH_2O (404.5 µl).

Coumassie Blue: Coumassie brilliant blue (2.25% w/v), methanol (45% v/v), acetic acid (10% v/v) and ddH_2O (45% v/v).

Coumassie Destain: Methanol (20% v/v), acetic acid (10% v/v) and ddH_2O (70% v/v).

7.8.6.3. General Procedure

The kinase of interest (0.1 µg/µl, 5 µl) is added to the side of two eppendorf tubes, followed by substrate (5 mg/ml, 5 µl), and inhibitor at a desired concentration to 1 tube, ensuring all reagents do not mix. All tubes are stored on ice, and kinase buffer (50 µl) is added to each, with gently vortexing to mix. Samples are incubated at 30 °C for 30 minutes, after which point SDS sample buffer (50 µl) is added and samples are boiled at 100 °C for 5 minutes.

Samples are subjected to SDS-PAGE and the resultant gel is washed with water, covered with Coumassie blue stain (10-20 ml), and left on a shaker for 1-2 hours at room temperature. The Coumassie blue stain is removed and any excess washed with water, after which the gel is washed with Coumassie destain (10-20 ml) until the substrate bands are visible. It may be necessary during this time to change the destain solution.

The gel is removed from the destain solution, with any excess removed with water, and dried under vacuum at 40 °C for 1-2 hours. At this point the gel can be imaged to record substrate bands to confirm substrate loading is equal in comparative lanes. The gel is then exposed to X-ray film (<5 min – 24 h, depending on kinase activity), after which the developed film can be recorded *via* densitometry. However, in the work described herein, all kinase activity measurements were determined using scintillation counting. The substrate bands are cut from the gel and added to scintillation fluid (2 ml) in scintillation vials. Kinase activity in each sample is determined using a scintillation counter, and the relative activity between the control and inhibitor treated samples can be used to determine kinase inhibition.

7.9. Experimental and Results

7.9.1. Monitoring Induction of myc-Nek2 in U2OS Cell Line

7.9.1.1. Antibodies

Primary: Myc-mouse (Cell Signalling, 2276), α-tubulin-mouse (Sigma, T5168), pAQDL-rabbit (500 µg/ml).

Secondary: Anti-mouse AP conjugate (Promega, S3721), Goat-anti-mouse 488 (Invitrogen, A11001), Goat-anti-rabbit 594 (Invitrogen, A11012).

7.9.1.2. Procedure

U2OS myc-Nek2 inducible cells were grown in 7 x 10 cm cell culture dishes in 10 ml DMEM until ~80% confluent. Doxycycline (1 µg/ml) was added at time points of 48, 36, 24, 26, 8 and 4 hours, in addition to a population lacking doxycycline treatment. All cell populations were lifted from the dish, lysed, and subjected to SDS-PAGE. Western blotting of the resultant gels with myc-mouse (1/1000) and α-tubulin-mouse (1/2000) antibodies, followed by development of the membrane with anti-mouse AP conjugate (1/7500) allowed the observation of protein bands by colourimetric analysis.

Immunofluorescence observation of myc-Nek2 induction was carried out using 2 populations of U2OS myc-Nek2 cells grown on cover slips, one treated with doxycycline (1 µg/ml) for 18 hours, and one with no treatment. Upon completion of the treatment regimen, the cover slips were removed from media, fixed with cold methanol, and stained primary antibodies myc-mouse (1/1000) and pAQDL-rabbit (1/500). Fluorescent tagging of the primary antibodies with goart-anti-mouse 488 (1/200) and goat-anti-rabbit 594 (1/200), in conjunction with Hoechst (1/1000) allowed visualisation of proteins *via* immunofluorescence microscopy and hence confirmation of myc-Nek2 induction.

7.9.2. Evaluating the Effect of NCL-00017509 (177) on Centrosome Splitting

7.9.2.1. Antibodies

Primary: Myc-mouse (Cell Signalling, 2276), γ-tubulin-rabbit (Sigma, T3559).

Secondary: Goat-anti-mouse 594 (Invitrogen, A11005), goat-anti-rabbit 488 (Invitrogen, A11008).

7.9.2.2. Procedure

U2OS myc-Nek2 cells were grown on 8 x 6 cm cell culture dishes in 5 ml DMEM containing cover slips until ~80% confluent. The cell populations on 4 of the pleates were treated with doxycycline (1 µg/ml) for 16 hours, after which both +Dox and -Dox sets of cells were treatment with NCL-00017509 at doses of 50nM, 500nM and 5µM. All cover slips were lifted from the media and fixed with cold methanol, followed by immunofluorescence staining.

Myc-mouse (1/1000) primary antibody was used to confirm induction, and γ-tubulin-rabbit (1/2000) primary antibody was used to stain the centrosomes to score for splitting. A seconday antibody mixture of goat-anti-mouse 594 (1/200), goat-anti-rabbit 488 (1/200) and Hoechst (1/1000) was applied to the cover slips, and the cells were imaged using fluorescence microscopy. Cells were scored for splitting (see Figure 48), and $\geq$100 cells were counted on each cover slip. The assay was carried out in triplicate, with fresh cell colonies used in each case.

7.9.2.3. Results

Condition (Dox/Inhibitor)	Centrosomes split	Centrosomes non-split	% Split centrosomes
- / -	73	241	23
- / 50nM	55	253	18
- / 500nM	49	275	15
- / 5µM	38	275	12
+ / -	187	120	61
+ / 50nM	128	191	40
+ / 500nM	85	217	28
+ / 5µM	47	268	15

Table 20: Percentage of centrosomes split for tetracycline induced and non-induced cells treated with NCL-00017509 (**177**) (n = 3).

7.9.3. Evaluating the Effect of NCL-00017509 (177) on pC-Nap1 Intensity

7.9.3.1. Antibodies

Primary: pAQDL-rabbit (500 µg/ml), myc-mouse (Cell Signalling, 2276), γ-tubulin-mouse (Sigma, T6557), C-Nap1-rabbit (500 µg/ml), pLLEK-rabbit (500 µg/ml), pRELQ-rabbit (500 µg/ml), pRRLD-rabbit (500 µg/ml).

Secondary: Goat-anti-mouse 594 (Invitrogen, A11005), goat-anti-rabbit 488 (Invitrogen, A11008).

7.9.3.2. Procedure

Cells were grown as detailed above (3.2.2.), and the cover slips incubated with the primary antibodies pAQDL-rabbit (1/500) and myc-mouse (1/1000). However, after the first completion of this assay, it became apparent that a clear indicator of centrosome location was necessary for uninduced cells, as pC-Nap1 intensity was sufficiently low to make identification difficult. In subsequent repeats of this assay, uninduced cells were incubated with γ-tubulin-mouse (1/2000) in place of myc-mouse. The seconday antibody mixture of goat-anti-mouse 594 (1/200), goat-anti-rabbit 488 (1/200) and Hoechst (1/1000) was applied

to the cover slips, and the cells were imaged using fluorescence microscopy. The average intensity of 20 centrosomes under each condition were calculated and given as a percentage of the intensity for induced cells lacking inhibitor treatment, as this is expected to give the most intense reading. This assay was repeated in triplicate.

In order to determine the selectivity of Nek2 inhibition over the 4 phosphorylation sites of C-Nap1 to which antibodies are available, the assay was repeated on 10 x 6 cm cell culture plates with DMEM (5 ml). All cells were induced with doxycycline (1 µg/ml) for 16 hours, after which 5 cell populations were treated with NCL-00017509 at 5µM. Cover slips were removed and fixed, and the cover slips were divided into 5 pairs of untreated and inhibitor treated cells. The primary antibody mixture were prepared consisting γ-tubulin-mouse (1/2000) and a C-Nap1 antibody; total C-Nap1-rabbit (1/500), pAQDL-rabbit (1/500), pLLEK-rabbit (1/500), pRELQ-rabbit (1/500) and pRRLD-rabbit (1/500). Following incubation, treatment with the secondary antibody mixture of goat-anti-mouse 594 (1/200), goat-anti-rabbit 488 (1/200) and Hoechst (1/1000) was applied. Cells were imaged and 20 centrosome intensity measurements made under each condition. During the course of this study, it was not possible to repeat this assay.

7.9.3.3. Results

	pAQDL Percentage Intensity							
Condition	**+ / -**	**+ / 50nM**	**+ / 500nM**	**+ / 5µM**	**- / -**	**- / 50nM**	**- / 500nM**	**- / 5µM**
1	100	106.9	76.4	21.2	20.8	34.8	34.1	20.9
2	100	114.8	177.5	27.5	71.8	45.5	50.3	16.8
3	100	96.6	120.5	27.3				
Average	100	106.1	124.8	25.3	46.3	40.2	42.2	18.9
Std. dev.	-	9.13	50.7	3.58	36.1	7.57	11.5	2.90
Std. error	-	5.27	29.3	2.07	25.5	5.35	8.10	2.05

Table 21: Percentage pAQDL intensity with respect to untreated cells for tetracycline induced and non-induced cells treated with NCL-00017509 (**177**) (n = 3).

Antibody	C-Nap1		pAQDL		pLLEK		pRELQ		pRRLD	
177	-	+	-	+	-	+	-	+	-	+
Average	152.3	399.1	60.4	43.0	67.4	49.5	271.0	267.0	153.4	81.5
Percent	100	262.1	100	71.2	100	73.5	100	98.5	100	53.1
Std. dev.	68.1	130	29.8	18.8	32.3	42.6	164	183	63.5	31.7
Std. err.	15.2	29.3	6.66	4.21	7.23	9.52	36.7	41.0	14.2	7.09

Table 22: C-Nap1 phospo-specific antibody intensity values for tetracycline induced cells both treated and untreated with NCL-00017509 (**177**) (n = 1).

7.9.4. Monitoring Mitotic Progression Using Live Cell Imaging

7.9.4.1. Reagents

Opti-MEM® I (Gibco®, Invitrogen): Reduced serum Eagle's Minimum Essential Medium – reduced serum media gives improved performance in microscopic analysis.

7.9.4.2. Procedure

HeLa GFP-α-tubulin/mCherry-Histone cells grown in a 10 cm plate in 10 ml MEM were passaged into a 4 chamber microscope dish in MEM (1 ml) and incubated for 16 hours to adhere to the dish. The media was aspirated and Opti-MEM® I (1 ml) was added to each chamber, and 2 chambers were treated with either **177** (5μM), or MLN-8054 (5μM) for 4 hours. The cells were loaded into a Leica TCS SP5 confocal laser scanning microscope, with the chamber maintained at 38 °C and 5.0% CO_2, and the cells were visualised. 2 fields of view for each treatment condition were acquired, where mitotic cells were present with surrounding free space for further division, and the maximum and minimum focal planes of a mitotic cell were defined. This focal field was divided into 5 μm planes (~20-25), and an image was taken at each focal plane for all positions every 5 minutes for 15 hours.

Compression of focal planes allows a representative image of the cell to be acquired, and all positions were viewed and cells scored for time from prometaphase to anaphase, and time from anaphase to mitosis. Further analysis made note of the presence cells with spindle abnormalities, and cells entering but failing to complete mitosis. This process was repeated 6 times, using distinct cell populations on each occasion.

7.9.4.3. Results

177	Average Time (min)		
	Total mitosis	**Prometaphase to anaphase**	**Anaphase to cytokinesis**
-	116.2	77.2	48.8
+	140.8	79.8	66.1

Table 23: Duration of mitosis for cells treated with NCL-00017509 (**177**) compared with untreated cells.

	Total cells		
	Untreated	**177**	**MLN-8054**
Division	70	101	2
Apoptosis/failure	6	22	67
Bipolar spindle	82	94	3
Monopolar spindle	7	34	91
Bipolar spindle delay	1	15	1
Other defects	5	18	9

Table 24: Number of cells exhibiting specific mitotic characteristics for untreated cells and cells treated with NCL-00017509 (**177**) and MLN-8054.

7.9.5. Confirming Mitotic Delay Using FACS Analysis

7.9.5.1. Procedure

U2OS myc-Nek2 cells were plated into 10 x 6 cm cell culture dishes in DMEM (5 ml) at low confluency (~30%). Both NCL-00017509 and MLN-8054 were administered to separate dishes at 5µM, and further dishes were treated with inhibitor at 24, 48, 68 and 72 hours point. This resulted in cell populations treated with either inhibitor for 4, 24, 28 and 72 hours. Of the remaining dishes, 1 was maintained as an untreated sample, and the other was treated with Nocodazole (0.5 µg/.ml) to generate a mitotic block control sample. This was used to calibrate the analysis software to ensure the correct counting of mitotic cells.

In order to maintain fresh media, every 24 hours the media was aspirated from all cells and replaced with fresh DMEM (5 ml). Furthermore, in order to maintain compound concentration in media, which may be lost due to chemical degradation and kinase turnover, inhibitor was readministered to all previously treated cells during the change of media.

Upon completion of the treatment regimen, all cell populations were lifted and prepared for FACS analysis as detailed above (2.5.3.). FACS counting of populations afforded quantitative data on relative population distribution between G1 (2N DNA), G2/M (4N DNA) and failed mitosis (8N DNA).

7.9.5.2. Results

		+ 177				**+ MLN-8054**			
	Async.	**4 h**	**24 h**	**48 h**	**72 h**	**4 h**	**24 h**	**48 h**	**72 h**
2N	56.6	50.3	41.5	42.4	37.1	46.4	7.1	2.6	2.6
4N	19.4	18.6	27.2	18.6	23.9	19.3	54.8	57.7	27.1
8N	3.0	4.6	3.7	2.6	4.4	4.2	9.3	14.4	31.5

Table 25: DNA number assigned by FACS analysis for cells treated with NCL-00017509 (**177**) and MLN-8054 for times up to 72 h.

7.9.6. Testing Selectivity of NCL-00017509 (177) using *In Vitro* ^{32}P Kinase Assay

7.9.6.1. Reagents

Kinases: Nek2A (Upstate, 14-545), Nek3 (Upstate, 14-694), Nek6 (Upstate, 14-578), Nek7 (Upstate, 14-567), Nek11 (Upstate, 14-700), Cdk1/Cyclin A2 (Sigma, C0244), Aurora A (Upstate, 14-511), Plk1 (Cell Sciences, CSI10299).

Substrates: β-casein (5 mg/ml), Histone H1 (5 mg/ml).

7.9.6.2. Procedure

All kinases (0.1 mg/ml, 1 µl) were subjected to ^{32}P kinase assay conditions as described above (2.6.) with β-casein (5 mg/ml, 5 µl) as substrate, excluding Plk1, with which Histone H1 (5 mg/ml, 5 µl) was used as substrate. Inhibitor concentration was 1µM in all cases. Prior to assay execution, it was necessary to pre-activate Nek11. This was achieved through incubation of Nek11 kinase in kinase buffer (50 µl) lacking ^{32}P-γ-ATP at 30 °C for 30 minutes, followed by addition of substrate, inhibitor and ^{32}P-γ-ATP. All assays were repeated in triplicate.

Kinase activity was determined *via* scintillation counting, with average activity with respect to untreated kinase calculated to give a single point indicator of kinase inhibition at 1µM **177**.

7.9.6.3. Results

	Nek2				**Nek3**			
	Scintillation count		**Percentage**		**Scintillation count**		**Percentage**	
177	-	+	-	+	-	+	-	+
	242604.5	47794.2	100	19.7	44531.0	44748.0	100	100.5
	266813.0	52359.0	100	19.6	32110.1	54141.5	100	168.6
	321872.9	47351.6	100	14.7	73606.4	61951.3	100	84.2
Avg.			100	18.0			100	117.8
Std. dev.			-	2.86			-	44.8
Std. err.			-	1.68			-	26.3

	Nek6				**Nek7**			
	Scintillation count		**Percentage**		**Scintillation count**		**Percentage**	
177	-	+	-	+	-	+	-	+
	86220.4	55.360.5	100	64.2	233102.5	219120.4	100	94.0
	67342.0	61657.3	100	91.6	391537.6	236611.8	100	60.4
	98924.9	60411.6	100	61.1	432639.5	445174.5	100	102.9

Avg.			100	72.3			100	85.8
Std. dev.			-	16.8			-	22.4
Std. err.			-	9.87			-	13.2

	Nek11				**Cdk1/Cyclin A2**			
	Scintillation count		**Percentage**		**Scintillation count**		**Percentage**	
177	**-**	**+**	**-**	**+**	**-**	**+**	**-**	**+**
	17021.4	9724.4	100	57.1	39534.9	37965.9	100	96.0
	20255.0	13585.0	100	67.1	43801.2	27502.2	100	62.8
	11399.0	10546.0	100	92.5	64297.8	51110.3	100	79.5
Avg.			100	72.2			100	79.4
Std. dev.			-	18.3			-	16.6
Std. err.			-	10.7			-	9.78

	Aurora A				**Plk1**			
	Scintillation count		**Percentage**		**Scintillation count**		**Percentage**	
177	**-**	**+**	**-**	**+**	**-**	**+**	**-**	**+**
	70337.2	14818.2	100	21.1	443152.0	351452.6	100	79.3
	52628.6	30293.6	100	57.6	441453.2	338621.7	100	76.7
	44562.2	11011.4	100	24.7	-	-	100	-
Avg.			100	34.4			100	78.0
Std. dev.			-	20.1			-	1.84
Std. err.			-	11.6			-	1.08

Table 26: Scintillation count data for NCL-00017509 (**177**) in ^{32}P *in vitro* kinase assays.

Chapter 8: Experimental

8.1. Chemicals and Solvents

All chemical reagents were purchased from the Aldrich Chemical Company, Apollo Scientific or Alfa Aesar Chemicals and were of the highest available purity. Chemicals were used as supplied with no further treatment. If chemicals used were stated as dry/anhydrous, they were stored in SureSeal™ septum-sealed bottles and removed under an inert nitrogen environment, with the reaction being carried out under the relevant inert atmosphere. Palladium catalysts were stored and measured out under an inert atmosphere.

8.2. Chromatography

Reaction monitoring and compounds identification was aided using Thin Layer Chromatography (TLC) and Retardation factor (R_f) values. TLC was conducted with Merck aluminium backed Si F_{254}, NH_2 F_{254s} and RP-18 F_{254s} plates. Fluorescent compounds were visualised under short wave (254 nm) UV irradiation. Compound purification was achieved using medium pressure 'Flash' column chromatography, with the use of Davisil silica 40-60μm as the stationary phase, or Biotage automated chromatography using pre-packed silica cartridges. A Biotage SP4 automated flash purification system was used with UV monitoring at 298 nm and compound collection at 254 nm. Biotage KP-NH cartridges were employed for the separation of secondary, tertiary, and heterocyclic amines; using a primary amine (propyl amine) bonded silica. When stated, compounds were purified *via* semi-preparative HPLC, using an ACE 5 Phenyl 150 x 21.2 mm column using an Agilent 1200 Modular Preparative HPLC system.

8.3. Analytical Techniques

All melting points were determined using a Stuart Scientific SMP3 or a Stuart Scientific SMP40 melting point apparatus and are uncorrected. ^{1}H and ^{13}C nuclear magnetic resonance (NMR) spectra were obtained as solutions in deuterated solvents DMSO-d_6, MeOD or $CDCl_3$ using a Bruker Avance III 500 spectrometer recording at 500 MHz. Chemical shifts (δ) are reported in parts per million (ppm) and the spin-multiplicity abbreviated as: s (singlet), d (doublet), t (triplet), q (quartet), quin (quintet), sept (septet), m (multiplet), or br (broad), with coupling constants (*J*) given in Hertz (Hz). Liquid Chromatography – Mass Spectrometry

(LC-MS) was carried out on a Micromass Platform LC running in both positive and negative electrospray mode with a PDA 240-400 nm detector using a Waters Symmetry Shield RP18 3 µm, 4.6 x 20 mm column with a flow rate of 3.0 mL/min. Alternatively, a Waters Acquity UPLC system was used, with a Waters SQD ESCi source using an Acquity UPLC BEH C18 1.7 µm, 2.1 x 50 mm column with a flow rate of 0.6 ml/min. The mobile phase used was 0.1% v/v Formic acid (aq.)/MeCN. Fourier Transform Infrared (FTIR) spectra were obtained using a Bio-Rad FTS 3000MX diamond ATR as a neat sample. Ultraviolet (UV) absorption data were collected using a Hitachi U-2800A spectrophotometer in ethanol. High-resolution mass spectra were performed by the ESPRC National Mass Spectrometry Service, University of Wales Swansea, Singleton Park, Swansea, SA2 8PP.

8.4. Microwave Assisted Synthesis

When stated, reactions were carried out under microwave irradiation, in sealed vessels, using the Biotage Initiator Sixty with robotic sample bed. Samples were irradiated at 2.45 GHz, able to reach temperatures of 60 - 250 ºC with a rate of heating at 2-5 °C/sec, and pressures of up to 20 bar.

8.5. Biological Evaluation

Inhibitors were tested for their Nek2 inhibitory activity by Kathy Boxall, Sam Burns, Yvette Newblatt and Maura Westlake under the supervision of Dr. Wynne Aherne in the Analytical Screening and Technology Laboratory of the CR UK Centre for Cancer Therapeutics, The Institute for Cancer Research, Sutton, Surrey, UK, SM2 5NG. Inhibitory potencies are reported as half maximal inhibitory concentrations (IC_{50}) or percentage inhibition where necessary. Assays were performed in the presence of 30 µM ATP, 1 µM 'peptide 11' substrate (5-FAM-KKLNRTLSVA-COOH) and 4 nM Nek2, using a microfluidic Caliper methodology as previously reported.[191]

Inhibitors were tested for their CDK2/cyclin A3 inhibitory activity by Lan-Zhen Wang at The Northern Institute for Cancer Research, Paul O'Gorman Building, Newcastle University, Newcastle upon Tyne, NE2 4HH. Assays were performed in the presence of 12.5 µM ATP, 14 µM histone H1 substrate and 1.9 µM recombinant CDK2/cyclin A3, using a scintillation count ^{32}P kinase assay according to literature procedure.[232]

8.6. General Procedures

General procedure A: Balz-Schiemann Reaction of 2-aminopurines

A solution of sodium nitrite (2.0 equiv.) in water (1 ml/mmol) was added to a solution of the purine substrate (1.0 equiv.) in HBF_4 (48 wt. % in H_2O, 3.5 ml/mmol), cooled to 0 °C, over 50 min. Upon completion of addition the reaction mixture was stirred at RT for 20 min, after which the solution was cooled to 0 °C and neutralised with a saturated aqueous solution of NaOH. The product was extracted with EtOAc (3 x 10 ml/mmol) and the combined extracts were dried ($MgSO_4$) and concentrated *in vacuo*. Further purification was carried out if necessary.

General Procedure B: TFA/TFE coupling of anilines with 2-fluoropurines using conventional heating

TFA (2.5-5.0 equiv.) was added to a solution of the purine substrate (1.0 equiv.) and the required aniline (2.0 equiv.) in TFE (10 ml/mmol). The reaction mixture was heated at reflux for 24 h unless otherwise stated, after which the solution was cooled and evaporated to dryness. The resulting residue was dissolved in EtOAc (10 ml/mmol) and washed with a saturated aqueous solution of $NaHCO_3$ (5 ml/mmol) and brine (5 ml/mmol). The combined aqueous layers were extracted with EtOAc (10 ml/mmol), and the combined organic extracts were dried ($MgSO_4$) and concentrated *in vacuo* to give the crude product for chromatographic purification.

General Procedure C: Nucleophilic substitution of 2,4-dichloro-5-nitropyrimidine with amines

The required amine (2.2-3.3 equiv.) was added to a solution of 2,4-dichloro-5-nitropyrimidine (1.0 equiv.) in THF (10 ml/mmol) at 0 °C. The reaction mixture was stirred at 0 °C for 30 min before being evaporated to dryness, and the crude product purified *via* chromatography.

General Procedure D: Aromatic nitro group reduction using tin(II) chloride in ethanol

Tin(II) chloride (4.0 equiv.) was added to a mixture of the aromatic nitro substrate (1.0 equiv.) in ethanol (10 ml/mmol). The reaction mixture was heated at reflux for 1.5 h, unless otherwise stated, after which the solvent was removed *in vacuo*. The resulting residue was dissolved in EtOAc (20 ml/mmol) and a saturated aqueous solution of $NaHCO_3$ was added until the aqueous phase was at pH 9-10. The resulting precipitate was removed by filtration through Celite® and the organic phase was collected, washed with brine (5 ml/mmol) and evaporated to dryness. The crude residue was subsequently purified by chromatography to give the desired compound.

General Procedure E: Synthesis of 8-methylpurine derivatives using 4,5-diaminopyrimidines and triethyl orthoacetate

The pyrimidine substrate (1.0 equiv.), triethyl orthoacetate (2.5 equiv.) and TFA (0.1 equiv.) were combined in TFE (5 ml/mmol) and heated under microwave irradiation at 140 °C for 1.5 h, unless otherwise stated, before being concentrated to dryness. The resulting residue was dissolved in EtOAc (10 ml/mmol) and washed with a saturated aqueous solution of $NaHCO_3$ (5 ml/mmol) and brine (5 ml/mmol). The combined aqueous layers were extracted with EtOAc (10 ml/mmol), and the combined organic extracts were dried ($MgSO_4$) and concentrated *in vacuo* to give the crude product for chromatographic purification.

General Procedure F: TFA/TFE coupling of anilines with 2-chloro-8-methylpurines using microwave heating

The purine substrate (1.0 equiv.), the required aniline (2.0 equiv.) and TFA (2.5-5.0 equiv.) were dissolved in TFE (10 ml/mmol) and heated under microwave irradiation at 160 °C for 1 h, unless otherwise stated. Following removal of the solvent *in vacuo*, the resulting residue was dissolved in EtOAc (10 ml/mmol) and washed with a saturated aqueous solution of $NaHCO_3$ (5 ml/mmol) and brine (5 ml/mmol). The combined aqueous layers were extracted with EtOAc (10 ml/mmol), and the combined organic extracts were dried ($MgSO_4$) and concentrated *in vacuo* to give the crude product for chromatographic purification.

General Procedure G: Reduction of aromatic nitro groups using palladium-catalysed transfer hydrogenation

Palladium on carbon (10% w/w) and ammonium formate (10.0 equiv.) were added to a solution of the nitro aromatic substrate (1.0 equiv.) in methanol (10 ml/mmol). The reaction mixture was stirred at RT for 18 h, before being filtered through Celite®. The solvent was removed *in vacuo* and the resulting residue was purified *via* chromatography to give the target compound.

General Procedure H: Alkylation of phenols with benzyl halides

The required benzyl halide (1.2-4.0 equiv.) was added to a mixture of the phenol substrate (1.0 equiv.) and K_2CO_3 (1.1 equiv.) in dry DMF (10 ml/mmol) in a sealed vial. The reaction mixture was heated at 60 °C for 18 h before being evaporated to dryness. The resulting residue was dissolved in EtOAc (10 ml/mmol) and washed with brine (10 ml/mmol) before being dried ($MgSO_4$) and concentrated *in vacuo*. The crude residue was subsequently purified *via* chromatography to give the desired product.

General Procedure I: Removal of TIPS-protecting groups using TBAF

TBAF (1.2 equiv.) was added to a solution of the TIPS-protected substrate (1.0 equiv.) in THF (10-20 ml/mmol). The reaction mixture was stirred at RT for 5 min before being concentrated *in vacuo* and the crude residue purified by chromatography to afford the target compound.

General Procedure J: CDI mediated amide coupling reactions

CDI (2.0 equiv.) and DIPEA (2.0 equiv.) were added to a solution of the carboxylic acid substrate (1.0 equiv.) in dry DMF (10 ml/mmol). The mixture was stirred at RT for 1.5 h, at which point the required amine (4.0 equiv.) was added. Following a further 18 h stirring at RT, the solvent was removed *in vacuo* and the resulting residue was purified by chromatography to give the desired product.

General Procedure K: Removal of PMB protecting groups using TFA

The PMB-protected substrate (1.0 equiv.) was dissolved in TFA (10-20 ml/mmol) and the resulting solution was heated at reflux for 24 h, unless stated otherwise. The reaction mixture

was evaporated to dryness and the resulting residue was dissolved in EtOAc (20 ml/mmol) and washed with a saturated aqueous solution of $NaHCO_3$ (2 x 10 ml/mmol) and brine (10 ml/mmol). The combined aqueous layers were extracted with EtOAc (20 ml/mmol) and the combined organic extracts were dried ($MgSO_4$), concentrated *in vacuo*, and the residue purified by chromatography to give the desired compound.

General Procedure L: Cleavage of N-Boc protecting groups using TFA

TFA (10.0 equiv.) was added to a solution of the Boc-protected substrate (1.0 equiv.) in DCM (10 ml/mmol). The resulting mixture was stirred at RT for 18 h, before being diluted with DCM (10 ml/mmol) and washed with a saturated aqueous solution of $NaHCO_3$ (10 ml/mmol). The biphasic mixture was passed through an Isolute® phase separator, and the organic phase concentrated to dryness. The resulting crude residue was purified by chromatography to give the target compound.

General Procedure M: Palladium-mediated Buchwald amination reactions

The aryl halide substrate (1.0 equiv.) and the required aniline (1.2 equiv.) were combined with *tris*(dibenzylideneacetone)dipalladium(0) ($Pd_2(dba)_3$, 10 mol. %), 2-dicyclohexyl phosphino-2′,4′,6′-triisopropylbiphenyl (XPhos, 10 mol. %) and K_2CO_3 (2.2 equiv.) in dry MeCN (10 ml/mmol) in a sealed vial. The solution was degassed with a stream of N_2, after which the reaction mixture was heated at 100 °C for 1 h, unless otherwise stated, before being cooled and filtered through Celite®. The filtrate was concentrated *in vacuo* and purified by chromatography to afford the desired product.

General Procedure N: Palladium-mediated Sonogashira couplings

The aryl halide substrate (1.0 equiv.), copper iodide (2 mol. %) and *bis*(triphenylphosphine) palladium(II) dichloride ($Pd(PPh_3)_2Cl_2$, 2 mol. %) were combined in dry THF or dry DMF (10 mmol/ml) in a sealed vial. Triethylamine (2.5 equiv.) and (triisopropylsilyl)acetylene (1.1 equiv.) were added and the mixture was degassed with a stream of N_2 for 15 min. The reaction mixture was stirred at RT for 18 h before being filtered through Celite®. The filtrate was concentrated *in vacuo* and purified by chromatography to give the desired product.

General Procedure O: Sulfonamide synthesis by treatment of trifluoroethyl sulfonate esters with amines

The trifluoroethyl sulfonate ester substrate (1.0 equiv.), the required amine (1.3 equiv.) and DBU (2.0 equiv.) were combined in dry THF (10 ml/mmol) in a sealed vial. The reaction mixture was heated under microwave irradiation at 160 °C for 15 min, before being evaporated to dryness. The resulting residue was dissolved in DCM (10 ml/mmol) and washed with a saturated aqueous solution of $NaHCO_3$ (10 ml/mmol), after which the biphasic mixture was passed through an Isolute® phase separator and the organic phase was concentrated *in vacuo*. The crude residue was purified *via* chromatography to give the target compound.

General Procedure P: Boc-protection of anilines bearing carboxylic acid moieties

Di-*tert*-butyl dicarbonate (1.1 equiv.) was added to a solution of the aniline substrate (1.0 equiv.) in a mixture of 1,4-dioxane (2.0 ml/mmol), 1 M NaOH solution (1.0 ml/mmol) and water (1.0 ml/mmol). The reaction mixture was stirred at RT for 18 h, after which the volume was reduced by half *in vacuo* and the solution taken to pH 3 with 2M $KHSO_4$ solution. The aqueous mixture was extracted with EtOAc (2 x 10 ml/mmol) and the combined organic extracts were dried ($MgSO_4$) and concentrated *in vacuo*. The crude residue was purified by chromatography to give the desired product.

General Procedure Q: Removal of TIPS-protecting groups using KF and 18-crown-6

KF (1.2 equiv.) and 18-crown-6 (0.1 equiv.) were added to a solution of the TIPS-protected substrate (1.0 equiv.) in THF (10 ml/mmol) and the reaction mixture was stirred at RT for 24 h. The solvent was removed *in vacuo* and the crude product was purified by chromatography.

General Procedure R: Esterification of carboxylic acids

Thionyl chloride (2.0 equiv.) was added to a solution of the carboxylic acid substrate (1.0 equiv.) in methanol (10 ml/mmol). The resulting solution was heated at reflux for 1 h, after which the solvent was removed *in vacuo*. The crude residue was purified by chromatography to give the target compound.

General Procedure S: Synthesis of carboxamides by treatment of methyl esters with amines

The methyl ester substrate (1.0 equiv.) was suspended in a concentrated aqueous solution of the required amine (10 ml/mmol) and the reaction mixture was stirred at RT for 24 h, unless otherwise stated. The solvent was removed *in vacuo* and the crude residue was purified by chromatography to give the target product.

General Procedure T: Reduction of aromatic nitro groups using iron powder in acetic acid

Iron powder (10.0 equiv.) was added to a solution of the aromatic nitro substrate (1.0 equiv.) in acetic acid (10 ml/mmol). The reaction mixture was heated at 50 °C for 15 min, before being filtered through Celite® and the filtrate concentrated *in vacuo*. The residue was dissolved in EtOAc (20 ml/mmol) and washed with a saturated aqueous solution of $NaHCO_3$ (2 x 20 ml/mmol) and brine (10 ml/mmol). The combined aqueous layers were extracted with EtOAc (20 ml/mmol) and the combined organic extracts were dried ($MgSO_4$) and evaporated to dryness. The resulting residue was purified by chromatography to afford the target compound.

General Procedure U: Removal of TIPS-protecting groups using TBAF followed by removal of TBAF contaminant

TBAF (1.2 equiv.) was added to a solution of the TIPS-protected substrate (1.0 equiv.) in THF (10-20 ml/mmol). The reaction mixture was stirred at RT for 5 min before being diluted with THF (100-200 ml/mmol) and the TBAF scavenger bead system (**231**, 10x w/w) added. The resulting suspension was agitated at RT for 48 h, before being filtered and the filtrate concentrated *in vacuo*. The resulting residue was purified by chromatography to afford the target compound.

General Procedure V: TFA/TFE coupling of anilines with 2-fluoropurines using microwave heating

The purine substrate (1.0 equiv.), the required aniline (2.0 equiv.) and TFA (2.5-5.0 equiv.) were dissolved in TFE (10 ml/mmol) and heated under microwave irradiation at 140 °C for 2 h, unless otherwise stated. Following removal of the solvent *in vacuo*, the resulting residue

was dissolved in EtOAc (10 ml/mmol) and washed with a saturated aqueous solution of $NaHCO_3$ (5 ml/mmol) and brine (5 ml/mmol). The combined aqueous layers were extracted with EtOAc (10 ml/mmol), and the combined organic extracts were dried ($MgSO_4$) and concentrated *in vacuo* to give the crude product for chromatographic purification.

General Procedure W: Direct synthesis of carboxamides from carboxylic acids *via* a methyl ester intermediate

Thionyl chloride (2.0 equiv.) was added to a solution of the carboxylic acid substrate (1.0 equiv.) in methanol (10 ml/mmol). The resulting solution was heated at reflux for 1 h, after which the solvent was removed *in vacuo*. A concentrated aqueous solution of the required amine (10 ml/mmol) was added to the residue and the reaction mixture was stirred at RT for 24 h, unless otherwise stated. The solvent was removed *in vacuo* and the crude residue was purified by chromatography to give the target product.

General Procedure X: Phosphorus trichloride mediated amide coupling reactions

Phosphorus trichloride (1.1 equiv.) was added to a solution of the carboxylic acid substrate (1.0 equiv.) and the required amine (2.5 equiv.) in dry MeCN (5 ml/mmol) in a sealed vial. The reaction mixture was heated under microwave irradiation at 150 C for 5 min, before being concentrated to dryness. The resulting residue was dissolved in DCM (10 ml/mmol) and washed with a saturated aqueous solution of $NaHCO_3$ (10 ml/mmol). The biphasic mixture was passed through an Isolute® phase separator and the organic phase was concentrated *in vacuo*. The crude residue was purified by chromatography to afford the target compound.

8.7. Index of Synthesised Compounds

8.8. Intermediates and Final Compounds

6-Chloro-2-fluoro-9*H*-purine (50)[233]

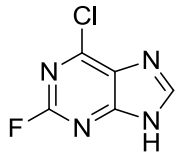

2-Amino-6-chloropurine (9.0 g, 53 mmol), sodium nitrite (7.3 g, 106 mmol) and HBF_4 (48 wt. % in H_2O, 180 mL) were reacted according to **general procedure A**, yielding the desired product as a pale yellow solid (5.57 g, 32.3 mmol, 61%). R_f 0.41 (9:1 DCM/MeOH); M.p. 169-173 °C (Lit.[233] 161-162 °C); λ_{max} (EtOH/nm) 271; IR (cm^{-1}) 3488, 2961, 2802, 2569, 2155, 1584; ^{1}H NMR (500 MHz, DMSO-d_6) 8.62 (1H, s, H-8), 14.01 (1H, s, br, H-9); ^{13}C NMR (125 MHz, DMSO-d_6) 147.5 (C-Ar), 156.2 (d, J_{CF} = 210.1 Hz, C^2-Ar), 162.3 (C-Ar); ^{19}F NMR (470 MHz, DMSO-d_6) -52.8 (C^2-F); LRMS (ES+) *m/z* 173.2 $[M^{35}Cl+H]^+$, 175.2 $[M^{37}Cl+H]^+$.

Note: Unable to visualise all quaternary carbon signals by ^{13}C NMR.

6-Chloro-2-fluoro-9-(tetrahydro-2*H*-pyran-2-yl)-9*H*-purine (51)[234]

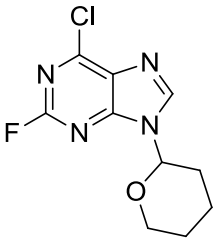

3,4-Dihydro-2*H*-pyran (2.12 mL, 23.2 mmol) was added dropwise over 10 min to a rapidly stirred mixture of purine **50** (4.00 g, 23.2 mmol) and (*Rac*)-camphor sulfonic acid (0.186 g, 0.80 mmol) in dry EtOAc (350 mL). The mixture was heated at reflux for 18 h before being cooled, neutralised (conc. NH_3), and washed with water (2 × 100 mL) and brine (80 mL). The organic phase was dried ($MgSO_4$) and concentrated, and the resulting residue purified by chromatography on silica (7:3 Petrol/EtOAc) to give the desired product as an off-white crystalline solid (4.38 g, 17.2 mmol, 74%). R_f 0.22 (7:3 Petrol/EtOAc); M.p. 92-94 °C; λ_{max} (EtOH/nm) 269; IR (cm^{-1}) 3132, 2955, 2876, 1574; ^{1}H NMR: (500 MHz, DMSO-d_6) 1.57-1.64 (2H, m, OCH_2CH_2), 1.70-1.80 (1H, m, CHCH*H'*), 1.94-2.02 (2H, m, $CHCH_2CH_2$), 2.23-

2.32 (1H, m, CHC*H*H'), 3.70-3.77 (1H, m, CHOCH*H'*), 4.00-4.06 (1H, m, CHOC*H*H'), 5.71 (1H, dd, *J* = 2.3 and 10.9 Hz, C*H*), 8.92 (1H, s, H-8); ^{13}C NMR (125 MHz, DMSO-d_6) 22.0 (CH*C*H$_2$), 24.3 (OCH$_2$*C*H$_2$), 29.6 (CHCH$_2$*C*H$_2$), 67.7 (NO*C*H$_2$), 81.7 (*C*H), 130.1 (d, J_{CF} = 4.8 Hz, C-Ar), 146.4 (d, J_{CF} = 2.8 Hz, C-Ar), 150.6 (d, J_{CF} = 18.5 Hz, C-Ar), 153.2 (d, J_{CF} = 17.6 Hz, C-Ar), 156.2 (d, J_{CF} = 213.7 Hz, C^2-Ar); LRMS (ES+) *m/z* 257.2 [M^{35}Cl+H]$^+$, 259.2 [M^{37}Cl+H]$^+$.

8-Bromo-6-chloro-2-fluoro-9-(tetrahydro-2*H*-pyran-2-yl)-9*H*-purine (52)

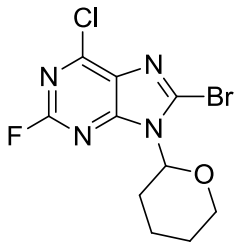

n-Butyllithium (2.5 M in THF, 234 µl, 0.58 mmol) was added dropwise to a solution of diisopropylamine (82 µl, 0.58 mmol) in dry THF (1.5 ml) at -78 °C under N_2. After addition, the mixture was allowed to warm to RT for 20 min before being cooled to -78 °C. The resulting LDA solution was added dropwise to a solution of the THP-protected purine **51** (0.100 g, 0.39 mmol) in dry THF (2.5 ml) at -78 °C under N_2. The mixture was stirred at -78 °C for 25 min, after which a solution of 1,2-dibromotetrachloroethane (0.254 g, 0.78 mmol) in dry THF (1 ml) cooled to -78 °C was added dropwise to the reaction mixture. The solution was allowed to warm to RT whilst stirred under N_2 over 3 h. The reaction solvent was removed *in vacuo* and the residue was purified *via* chromatography on silica (7:3 Petrol/EtOAc) to give the desired compound as an off-white solid (91 mg, 0.27 mmol, 69%). R_f 0.50 (7:3 Petrol/EtOAc); M.p. 110-112 °C; λ_{max} (EtOH/nm) 275; IR (cm^{-1}) 2963, 2931, 2837, 2161, 1576; ^{1}H NMR (500 MHz, DMSO-d_6) 1.57-1.64 (2H, m, OCH$_2$C*H$_2$*), 1.70-1.78 (1H, m, CHCH$_2$C*H*H'), 1.92-1.98 (1H, m, CHCH$_2$CH*H'*), 1.98-2.05 (1H, m, CHC*H*H'), 2.73-2.80 (1H, m, CHCH*H'*), 3.72 (1H, ddd, *J* = 3.7, 11.2 and 11.4 Hz, OC*H*H'), 4.02-4.10 (1H, br, OCH*H'*), 5.69 (1H, dd, *J* = 2.4 and 11.1 Hz, CH); ^{13}C NMR (125 MHz, DMSO-d_6) 22.3 (CH*C*H$_2$), 24.3 (OCH$_2$*C*H$_2$), 27.8 (CHCH$_2$*C*H$_2$), 68.2 (OCH$_2$), 85.0 (CH), 120.1 (C-Ar), 156.0 (d, J_{CF} = 212.8 Hz, C^2-Ar); LRMS (EI) *m/z* 333.9 [M^{35}Cl^{79}Br+H]$^+$, 335.9 [M^{37}Cl^{79}Br+H]$^+$ /[M^{35}Cl^{81}Br+H]$^+$, 337.9 [M^{37}Cl^{81}Br+H]$^+$.

Note: Unable to visualise all quaternary carbon signals by ^{13}C NMR.

6-Chloro-2-fluoro-9-(tetrahydro-2*H*-pyran-2-yl)-8-methyl-9*H*-purine (53)

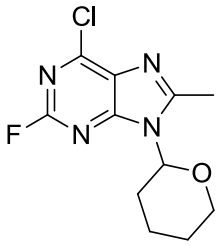

2.5 M *n*-butyllithium (133 µl, 0.33 mmol) was added to a solution of the 8-bromopurine **52** (0.102 g, 0.30 mmol) in dry THF (2 ml) at -78 °C under N_2. The solution was stirred at -78 °C for 20 min, after which iodomethane (37 µl, 0.61 mmol) was added dropwise. The mixture was allowed to warm to RT whilst stirred under N_2 over 3 h. The reaction solvent was removed *in vacuo* and the residue was purified *via* chromatography on silica (7:3 Petrol/EtOAc) to give the desired compound as an off-white waxy solid (76 mg, 0.28 mmol, 93%). R_f 0.24 (7:3 Petrol/EtOAc); M.p. 98-100 °C; λ_{max} (EtOH/nm) 273; IR (cm^{-1}) 2945, 2855, 2157, 2021, 1607; ^{1}H NMR (500 MHz, $CDCl_3$) 1.59-1.70 (3H, m, OCH_2CH_2 & $CHCH_2CHH$'), 1.80-1.87 (1H, m, $CHCH_2CHH'$), 2.01-2.08 (1H, m, $CHCHH$'), 2.32-2.39 (1H, m, $CHCHH'$), 2.72 (3H, s, C^8-CH_3), 3.66 (1H, ddd, J = 2.5, 11.8 and 11.9 Hz, $OCHH'$), 4.10-4.17 (1H, m, $OCHH$'-), 5.63 (1H, dd, J = 2.5 and 11.3 Hz, CH); ^{13}C NMR (125 MHz, $CDCl_3$) 16.4 (C^8-CH_3), 23.0 ($CHCH_2$), 24.8 (OCH_2CH_2), 30.1 ($CHCH_2CH_2$), 69.3 (OCH_2), 83.4 (*C*H), 129.2 (C-Ar), 150.4 (d, J_{CF} = 17.4 Hz, C-Ar), 154.4 (d, J_{CF} = 16.3 Hz, C-Ar), 156.0 (d, J_{CF} = 3.2 Hz, C-Ar), 156.6 (d, J_{CF} = 218.1 Hz, C^2-Ar); LRMS (ES+) *m*/*z* 187.0 $[M^{35}Cl\text{-}THP+H]^+$, 189.0 $[M^{37}Cl\text{-}THP+H]^+$.

2-Fluoro-9-(tetrahydro-2*H*-pyran-2-yl)-8-methyl-9*H*-purine (54)

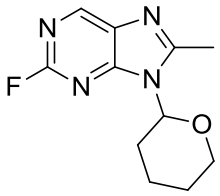

Palladium hydroxide (0.102 g, 100% w/w) and ammonium formate (70 mg, 1.11 mmol) were added to a solution of the 6-chloropurine **53** (0.101 g, 0.37 mmol) in methanol (10 ml). The mixture was heated at reflux for 2 h, after which the catalyst was removed by filtration through Celite®. The solvent was removed *in vacuo* and the residue was purified *via* chromatography on silica (7:3 Petrol/EtOAc) to give the desired compound as an off-white

waxy solid (74 mg, 0.32 mmol, 86%). R_f 0.37 (7:3 Petrol/EtOAc); M.p. 92-94 °C; λ_{max} (EtOH/nm) 270; IR (cm^{-1}) 2922, 2155, 2030, 1664; ^{1}H NMR (500 MHz, DMSO-d_6) 1.60-1.70 (3H, m, OCH_2CH_2 & $CHCH_2CHH'$), 1.82-1.91 (1H, m, $CHCH_2CHH'$), 2.00-2.07 (1H, m, $CHCHH'$), 2.38 (1H, m, $CHCHH'$), 2.71 (3H, s, C^8-CH_3), 3.67 (1H, ddd, J = 2.4, 11.7 and 11.8 Hz, $OCHH'$), 4.09-4.15 (1H, m, $OCHH'$), 5.67 (1H, dd, J = 2.5 and 11.3 Hz, CH), 8.69 (1H, s, H-6); ^{13}C NMR (125 MHz, DMSO-d_6) 16.4 (C^8-CH_3), 23.1 ($CHCH_2$), 24.9 (OCH_2CH_2), 30.1 ($CHCH_2CH_2$), 69.2 (OCH_2), 82.9 (CH), 131.8 (d, J_{CF} = 3.5 Hz, C-Ar), 148.5 (d, J_{CF} = 13.2 Hz, C-Ar), 155.8 (m, C-Ar); LRMS (ES+) m/z 153.1 $[M+H]^+$.

Note: Unable to visualise all quaternary carbon signals by ^{13}C NMR.

2-Fluoro-8-methyl-9*H*-purine (55)

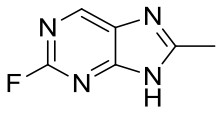

The THP-protected purine **54** (0.136 g, 0.58 mmol) was combined with TFA (1 ml) and H_2O (1 ml) in 2-propanol (6 ml) and heated under microwave irradiation at 130 °C for 15 min, after which the reaction mixture was taken to pH 7 (conc. NH_3) and concentrated to dryness. The residue was dissolved in EtOAc (15 ml) and washed with sat. $NaHCO_3$ solution (10 ml), and the organic phase was dried (Na_2SO_4) and the solvent removed *in vacuo*. The crude residue was purified on silica gel (9:1 DCM/MeOH) to give the desired compound as a white solid (79 mg, 0.52 mmol, 90%). R_f 0.36 (9:1 DCM/MeOH); M.p. 225-228 °C; λ_{max} (EtOH/nm) 394; IR (cm^{-1}) 2898, 2584, 1610, 1562; ^{1}H NMR (500 MHz, DMSO-d_6) 2.58 (3H, s, C^8-CH_3), 8.31 (1H, d, J = 0.9 Hz, H-6), 13.32 (1H, s, H-9); ^{13}C NMR (125 MHz, DMSO-d_6) 15.24 (C^8-CH_3), 144.2 (d, J_{CF} = 17.8 Hz, C-Ar), 157.8 (d, J_{CF} = 206.5 Hz, C-Ar); LRMS (ES+) m/z 153.1 $[M+H]^+$.

Note: Unable to visualise all quaternary carbon signals by ^{13}C NMR.

8-Methyl-*N*-(4-phenoxyphenyl)-9*H*-purin-2-amine (48)

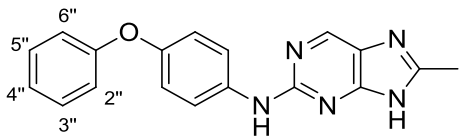

2-Fluoropurine intermediate **55** (0.070 g, 0.46 mmol) and 4-phenoxyaniline (0.170 g, 0.92 mmol) were reacted with TFA (177µl, 2.30 mmol) in TFE (6 ml) according to **general procedure B**. Chromatgraphy on silica (19:1 DCM/MeOH) afforded the target compound as a pale pink solid (0.101 g, 0.32 mmol, 75%). R_f 0.39 (19:1 DCM/MeOH); M.p. 228-231 °C; λ_{max} (EtOH/nm) 277; IR (cm^{-1}) 3454, 3253, 3194, 3044, 2924, 2161, 1617; ^{1}H NMR (500 MHz, DMSO-d_6) 2.46 (3H, s, C^8-CH_3), 6.95 (2H, dd, *J* = 1.1 and 7.7 Hz, H-2''/H-6''), 7.00 (2H, d, *J* = 9.0 Hz, H-3'/H-5'), 7.07 (1H, dddd, *J* = 1.1, 1.1, 7.4 and 7.4 Hz, H-4''), 7.36 (2H, ddd, *J* = 1.1,7.4 and 7.7 Hz, H-3''/H-5''), 7.83 (2H, d, *J* = 9.0 Hz, H-2'/H-6'), 8.63 (1H, s, H-6), 9.45 (1H, s, C^2-NH), 12.68 (1H, s, H-9); ^{13}C NMR (125 MHz, DMSO-d_6) 14.93 (C^8-CH_3), 117.1 (C-Ar), 119.7 (C-Ar), 119.8 (C-Ar), 122.4 (C-Ar), 128.3 (C-Ar), 129.8 (C-Ar), 137.5 (C-Ar), 146.4 (C-Ar), 149.3 (C-Ar), 151.4 (C-Ar), 154.3 (C-Ar), 155.9 (C-Ar), 158.1 (C-Ar); HRMS calcd. for $C_{18}H_{16}N_5O$ (ES+) *m*/*z* 318.1349 $[M+H]^+$, found 318.1352.

2-Chloro-5-nitropyrimidin-4-amine (58)[235]

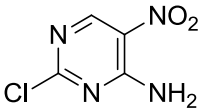

2,4-Dichloro-5-nitropyrimidine (1.00 g, 5.16 mmol) and ammonia (2M in EtOH, 6.00 ml, 12.0 mmol) were reacted in THF (50 ml) according to **general procedure C**. Purification on silica gel (9:1 Petrol/EtOAc) gave the desired product as a yellow solid (0.557 g, 3.19 mmol, 57%). R_f 0.20 (9:1 Petrol/EtOAc); M.p. 207-209 °C (Lit.[235] 215-217 °C); λ_{max} (EtOH/nm) 217, 258; IR (cm^{-1}) 3435, 3344, 3063, 1717, 1649, 1567, 1509; ^{1}H NMR (500 MHz, DMSO-d_6) 8.61 (1H, s, H-6), 9.02 (1H, s, N*H*H'), 9.20 (1H, s, NH*H'*); ^{13}C NMR (125 Hz, DMSO-d_6) 126.6 (C-Ar), 157.1 (C-Ar), 157.6 (C-Ar), 162.1 (C-Ar); LRMS (ES+) *m*/*z* 175.1 $[M^{35}Cl+H]^+$, 177.1 $[M^{37}Cl+H]^+$.

2-Chloropyrimidine-4,5-diamine (60)[236]

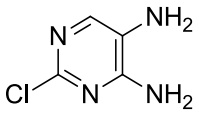

5-Nitropyrimidine **58** (0.203 g, 1.15 mmol) and tin(II) chloride (0.870 g, 4.58 mmol) were reacted in ethanol (12 ml) according to **general procedure D**. Purification *via* chromatography on silica (9:1 DCM/MeOH) afforded the desired compound as a white solid (0.138 g, 0.95 mmol, 83%). R_f 0.33 (9:1 DCM/MeOH); M.p. 218-221 °C (Lit.[236] 230-232 °C); λ_{max} (EtOH/nm) 268, 315; IR (cm^{-1}) 3162, 3031, 2024, 1603; ^{1}H NMR (500 MHz, DMSO-d_6) 4.85 (2H, s, C^5-NH_2), 6.85 (2H, br, C^4-NH_2), 7.41 (1H, s, H-6); ^{13}C NMR (125 Hz, DMSO-d_6) 126.7 (C-Ar), 136.7 (C-Ar), 146.7 (C-Ar), 155.2 (C-Ar); LRMS (ES+) *m*/*z* 145.1 $[M^{35}Cl+H]^+$, 147.1 $[M^{37}Cl+H]^+$.

2-Chloro-8-methyl-9*H*-purine (62)

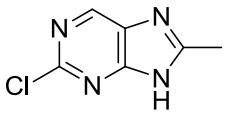

The diaminopyrimidine **60** (0.460 g, 3.18 mmol), triethyl orthoacetate (1.50 ml, 7.95 mmol) and TFA (25 µl, 0.32 mmol) were reacted in TFE (20 ml) according to **general procedure E**. Silica gel purification (19:1 DCM/MeOH) gave the target compound as a beige solid (0.461 g, 2.73 mmol, 86%). R_f 0.50 (19:1 DCM/MeOH); M.p. 239-241 °C; λ_{max} (EtOH/nm) 275; IR (cm^{-1}) 3414, 2889, 2804, 1537; ^{1}H NMR (500 MHz, DMSO-d_6) 2.59 (3H, s, C^8-CH_3), 8.87 (1H, s, H-6), 13.36 (1H, br, H-9); ^{13}C NMR (125 MHz, DMSO-d_6) 15.2 (C^8-CH_3), 137.6 (C-Ar), 144.3 (C-Ar), 151.9 (C-Ar), 158.4 (C-Ar); HRMS calcd. for $C_6H_6ClN_4$ (ES+) *m*/*z* 169.0276 $[M+H]^+$, found 169.0274.

Note: Unable to visualise all quaternary carbon signals by ^{13}C NMR.

2-Chloro-*N*-methyl-5-nitropyrimidin-4-amine (59)[237]

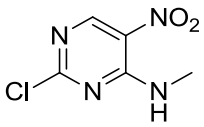

2,4-Dichloro-5-nitropyrimidine (0.502 g, 2.58 mmol) and methylamine (2M in THF, 3.9 ml, 7.75 mmol) were reacted in THF (25 ml) according to **general procedure C**. Purification on silica gel (9:1 Petrol/EtOAc) gave the desired product as a yellow solid (0.423 g, 2.24 mmol, 87%). R_f 0.22 (9:1 Petrol/EtOAc); M.p. 86-89 °C (Lit.[237] 85-86 °C); λ_{max} (EtOH/nm) 356, 256, 233; IR (cm^{-1}) 3377, 3280, 3054, 2166, 1608; ^{1}H NMR (500 MHz, DMSO-d_6) 2.89 (3H, d, J = 5.0 Hz, NHCH_3), 8.89 (1H, s, H-6), 9.02 (1H, br, NH); ^{13}C NMR (125 MHz, DMSO-d_6) 28.66 (NHCH$_3$), 119.0 (C-Ar), 151.1 (C-Ar), 155.2 (C-Ar); LRMS (ES+) m/z 189.1 $[M^{35}Cl+H]^+$, 191.1 $[M^{37}Cl+H]^+$.

2-Chloro-N^4-methylpyrimidine-4,5-diamine (61)[238]

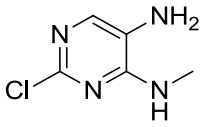

5-Nitropyrimidine **59** (0.502 g, 2.66 mmol) and tin(II) chloride (2.01 g, 10.6 mmol) were reacted in ethanol (20 ml) according to **general procedure D**. Purification *via* chromatography on silica (9:1 DCM/MeOH) afforded the desired compound as a white solid (0.330 g, 2.10 mmol, 78%). R_f 0.45 (9:1 DCM/MeOH); M.p. 118-121 °C (Lit.[238] 145.5-146.5 °C); λ_{max} (EtOH/nm) 264, 301; IR (cm^{-1}) 3162, 3031, 2024, 1603; ^{1}H NMR (500 MHz, DMSO-d_6) 2.86 (3H, d, J = 4.5 Hz, NHCH_3), 4.83 (2H, s, Ar-NH$_2$), 6.94 (1H, br, NHCH$_3$), 7.37 (1H, s, H-6); ^{13}C NMR (125 MHz, DMSO-d_6) 27.4 (NHCH$_3$), 127.2 (C-Ar), 135.3 (C-Ar), 147.2 (C-Ar), 154.4 (C-Ar); LRMS (ES+) m/z 159.1 $[M^{35}Cl+H]^+$, 161.1 $[M^{37}Cl+H]^+$.

2-Chloro-8,9-dimethyl-9*H*-purine (56)

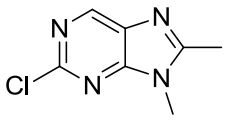

The diaminopyrimidine **61** (0.250 g, 1.57 mmol), triethyl orthoacetate (740 µl, 3.93 mmol) and TFA (12 µl, 0.16 mmol) were reacted in TFE (10 ml) according to **general procedure E**.

Chromatography on silica (19:1 DCM/MeOH) gave the desired compound as a white solid (0.265 g, 1.45 mmol, 94%). R_f 0.55 (19:1 DCM/MeOH); M.p. 189-192 °C; λ_{max} (EtOH/nm) 274; IR (cm^{-1}) 2924, 2159, 1989, 1600; ^{1}H NMR (500 MHz, DMSO-d_6) 2.62 (3H, s, C^8-CH_3), 3.72 (3H, s, N^9-CH_3), 8.90 (1H, s, H-6); ^{13}C NMR (125 MHz, DMSO-d_6) 14.0 (C^8-CH_3), 28.6 (N^9-CH_3), 132.5 (C-Ar), 147.3 (C-Ar), 151.7 (C-Ar), 154.6 (C-Ar), 157.4 (C-Ar); HRMS calcd. for $C_7H_8ClN_4$ (ES+) *m*/*z* 183.0432 $[M+H]^+$, found 183.0431.

_N_-(4-Methoxyphenyl)-8,9-dimethyl-9_H_-purin-2-amine (63)

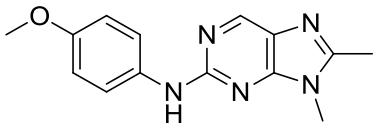

The 2-chloropurine intermediate **56** (30 mg, 0.16 mmol), 4-methoxyaniline (39 mg, 0.32 mmol) and TFA (63 µl, 0.82 mmol) were reacted in TFE (6 ml) according to **general procedure F**. Silica gel chromatography (9:1 DCM/MeOH) afforded the target compound as a beige solid (27 mg, 0.10 mmol, 61%). R_f 0.47 (9:1 DCM/MeOH); M.p. 183-185 °C; λ_{max} (EtOH/nm) 275; IR (cm^{-1}) 3261, 3051, 2925, 2839, 2040, 1602; ^{1}H NMR (500 MHz, DMSO-d_6) 2.35 (3H, s, C^8-CH_3), 3.49 (3H, s, N^9-CH_3), 3.57 (3H, s, OCH_3), 6.67 (2H, d, J = 9.1 Hz, H-3'/H-5'), 7.40 (2H, d, J = 9.1 Hz, H-2'/H-6'), 8.28 (1H, s, H-6); ^{13}C NMR (125 MHz, DMSO-d_6) 13.8 (C^8-CH_3), 28.0 (N^9-CH_3), 55.1 (OCH_3), 113.7 (C-Ar), 119.7 (C-Ar), 127.1 (C-Ar), 134.4 (C-Ar), 146.6 (C-Ar), 152.1 (C-Ar), 153.7 (C-Ar), 153.8 (C-Ar), 156.1 (C-Ar); HRMS calcd. for $C_{14}H_{16}N_5O$ (ES+) *m*/*z* 270.1349 $[M+H]^+$, found 270.1348.

8,9-Dimethyl-_N_-(4-phenoxyphenyl)-9_H_-purin-2-amine (74)

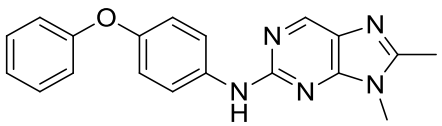

The 2-chloropurine intermediate **56** (70 mg, 0.38 mmol), 4-phenoxyaniline (0.142 g, 0.77 mmol) and TFA (146 µl, 1.90 mmol) were reacted in TFE (6 ml) according to **general procedure F**. Purification by chromatography on silica (19:1 DCM/MeOH) gave the desired compound as a pale pink solid (0.098 g, 0.30 mmol, 78%). R_f 0.48 (19:1 DCM/MeOH); M.p. 185-188 °C; λ_{max} (EtOH/nm) 277, 331; IR (cm^{-1}) 3262, 3193, 3117, 3038, 2026, 1617; ^{1}H NMR (500 MHz, DMSO-d_6) 2.29 (3H, s, C^8-CH_3), 3.43 (3H, s, N^9-CH_3), 6.73 (2H, ddd, J = 1.0 and 8.7 Hz, H-2''/H-6''), 6.77 (2H, d, J = 8.9 Hz, H-3'/H-5'), 6.82-6.85 (1H, m, H-4''),

7.13 (2H, ddd, *J* = 1.1, 8.6 and 8.7 Hz, H-3''/H-5''), 7.66 (2H, d, *J* = 8.9 Hz, H-2'/H-6'), 8.41 (1H, s, H-6), 9.34 (1H, s, C^2-NH); ^{13}C NMR (125 MHz, DMSO-d_6) 13.8 (C^8-CH_3), 28.0 (N^9-CH_3), 117.3 (C-Ar), 119.6 (C-Ar), 119.7 (C-Ar), 122.5 (C-Ar), 127.4 (C-Ar), 129.8 (C-Ar), 137.4 (C-Ar), 146.5 (C-Ar), 149.5 (C-Ar), 152.5 (C-Ar), 153.8 (C-Ar), 155.8 (C-Ar), 158.0 (C-Ar); HRMS calcd. for $C_{19}H_{18}N_5O$ (ES+) *m*/*z* 332.1506 $[M+H]^+$, found 332.1509.

8-Methyl-*N*-phenyl-9*H*-purin-2-amine (64)

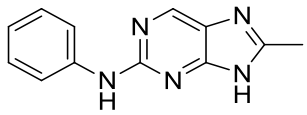

2-Chloropurine intermediate **62** (20 mg, 0.12 mmol), aniline (22 µl, 0.24 mmol) and TFA (45 µl, 0.59 mmol) were reacted in TFE (1 ml) according to **general procedure F**. Purification *via* chromatography on KP-NH silica (19:1 DCM/MeOH) afforded the desired compound as a pale pink solid (23 mg, 0.10 mmol, 83%). R_f 0.41 (19:1 DCM/MeOH, KP-NH); M.p. 238-240 °C; λ_{max} (EtOH/nm) 260, 330; IR (cm^{-1}) 3260, 3187, 3044, 2362, 1601; ^{1}H NMR (500 MHz, DMSO-d_6) 2.46 (3H, s, C^8-CH_3), 6.87-6.92 (1H, m, H-4'), 7.25 (2H, dd, *J* = 7.4 and 7.4 Hz, H-3'/H-5'), 7.79-7.83 (2H, m, H-2'/H-6'), 8.62 (1H, s, H-6), 9.38 (1H, s, C^2-NH), 12.67 (1H, br, H-9); ^{13}C NMR (125 MHz, DMSO-d_6) 15.0 (C^8-CH_3), 118.0 (C-Ar), 120.4 (C-Ar), 128.3 (C-Ar), 141.3 (C-Ar), 155.9 (C-Ar); HRMS calcd. for $C_{12}H_{12}N_5$ (ES+) *m*/*z* 226.1088 $[M+H]^+$, found 226.1087.

Note: Unable to visualise all carbon signals by NMR.

***N*-(4-Ethylphenyl)-8-methyl-9*H*-purin-2-amine (66)**

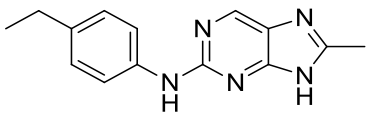

2-Chloropurine intermediate **62** (20 mg, 0.12 mmol), 4-ethylaniline (30 µl, 0.24 mmol) and TFA (45 µl, 0.59 mmol) were reacted in TFE (1 ml) according to **general procedure F**. Purification *via* chromatography on KP-NH silica (19:1 DCM/MeOH) afforded the desired compound as a pale pink solid (23 mg, 0.09 mmol, 76%). R_f 0.39 (19:1 DCM/MeOH, KP-NH); M.p. 286-289 °C; λ_{max} (EtOH/nm) 283, 331; IR (cm^{-1}) 3262, 3192, 2963, 2156, 2030, 1603; ^{1}H NMR (500 MHz, DMSO-d_6) 1.17 (3H, t, *J* = 7.6 Hz, -$CH_2C\mathit{H}_3$), 2.46 (3H, s, C^8-CH_3), 2.55 (2H, q, *J* = 7.6 Hz, -$C\mathit{H}_2CH_3$), 7.10 (2H, d, *J* = 8.6 Hz, H-3'/H-5'), 7.70 (2H, d, *J*

= 8.6 Hz, H-2'/H-6'), 8.60 (1H, s, H-6), 9.28 (1H, s, C^2-NH), 12.64 (1H, br, H-9); ^{13}C NMR (125 MHz, DMSO-d_6) 15.0 (C^8-CH_3), 15.9 (CH_2CH_3), 27.5 (CH_2CH_3), 118.3 (C-Ar), 127.6 (C-Ar), 135.8 (C-Ar), 139.0 (C-Ar), 156.1 (C-Ar); HRMS calcd. for $C_{14}H_{16}N_5$ (ES+) *m*/*z* 254.1402 $[M+H]^+$, found 254.1400.

Note: Unable to visualise all carbon signals by NMR.

***N*-(4-Isopropylphenyl)-8-methyl-9*H*-purin-2-amine (68)**

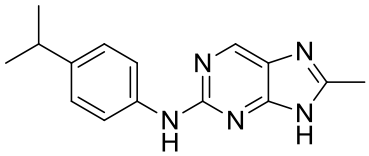

2-Chloropurine intermediate **62** (20 mg, 0.12 mmol), 4-isopropylaniline (34 µl, 0.24 mmol) and TFA (45 µl, 0.59 mmol) were reacted in TFE (1 ml) according to **general procedure F**. Purification *via* chromatography on KP-NH silica (19:1 DCM/MeOH) afforded the desired compound as a pale pink solid (17 mg, 0.06 mmol, 53%). R_f 0.33 (19:1 DCM/MeOH, KP-NH); M.p. 276-278 °C; λ_{max} (EtOH/nm) 273, 332; IR (cm^{-1}) 3455, 3225, 3190, 3107, 3049, 2957, 2160, 1976, 1610; ^{1}H NMR (500 MHz, DMSO-d_6) 1.20 (6H, d, *J* = 6.8 Hz, -$CH(CH_3)_2$), 2.46 (3H, s, C^8-CH_3), 2.83 (1H, sept, *J* = 6.8 Hz, -$CH(CH_3)_2$), 7.13 (2H, d, J = 8.2 Hz, H-3'/H-5'), 7.69 (2H, d, J = 8.2 Hz, H-2'/H-6'), 8.60 (1H, s, H-6), 9.27 (1H, s, C^2-NH), 12.63 (1H, br, H-9); ^{13}C NMR (125 MHz, DMSO-d_6) 15.0 (C^8-CH_3), 24.1 (-$CH(CH_3)_2$), 32.8 (-$CH(CH_3)_2$), 118.4 (C-Ar), 126.0 (C-Ar), 139.0 (C-Ar), 140.6 (C-Ar), 156.2 (C-Ar); HRMS calcd. for $C_{15}H_{18}N_5$ (ES+) *m*/*z* 268.1559 $[M+H]^+$, found 268.1557.

Note: Unable to visualise all carbon signals by NMR.

8,9-Dimethyl-*N*-phenyl-9*H*-purin-2-amine (65)

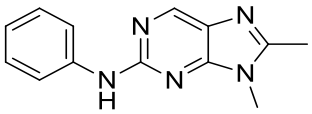

2-Chloropurine intermediate **56** (20 mg, 0.11 mmol), aniline (20 µl, 0.22 mmol) and TFA (42 µl, 0.55 mmol) were reacted in TFE (1 ml) according to **general procedure F**. Purification *via* chromatography on KP-NH silica (1:1 Petrol/EtOAc) afforded the desired compound as a pale pink solid (15 mg, 0.06 mmol, 57%). R_f 0.35 (1:1 Petrol/EtOAc, KP-NH); M.p. 238-240

°C; λ_{max} (EtOH/nm) 273, 328; IR (cm^{-1}) 3360, 3258, 3196, 3020, 1603; ^{1}H NMR (500 MHz, MeOD) 2.58 (3H, s, C^{8}-CH_3), 3.74 (3H, s, N^{9}-CH_3), 6.97 (1H, dddd, *J* = 1.0, 1.0, 7.4 and 7.4 Hz, H-4'), 7.29 (2H, ddd, *J* = 7.0, 7.4 and 7.4 Hz, H-3'/H-5'), 7.74-7.77 (2H, m, H-2'/H-6'), 8.45 (1H, s, H-6), 9.48 (1H, s, C^{2}-NH); ^{13}C NMR (125 MHz, DMSO-d_6) 13.8 (C^{8}-CH_3), 28.0 (N^{9}-CH_3), 118.1 (C-Ar), 120.6 (C-Ar), 127.4 (C-Ar), 128.4 (C-Ar), 141.2 (C-Ar), 146.5 (C-Ar), 152.6 (C-Ar), 153.8 (C-Ar), 155.8 (C-Ar); HRMS calcd. for $C_{13}H_{14}N_5$ (ES+) *m*/*z* 240.1246 $[M+H]^+$, found 240.1244.

_N_-(4-Ethylphenyl)-8,9-dimethyl-9_H_-purin-2-amine (67)

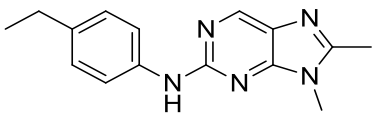

2-Chloropurine intermediate **56** (20 mg, 0.11 mmol), 4-ethylaniline (28 µl, 0.22 mmol) and TFA (42 µl, 0.55 mmol) were reacted in TFE (1 ml) according to **general procedure F**. Purification *via* chromatography on KP-NH silica (1:1 Petrol/EtOAc) afforded the desired compound as a pale pink solid (17 mg, 0.06 mmol, 57%). R_f 0.32 (1:1 Petrol/EtOAc, KP-NH); M.p. 197-199 °C; λ_{max} (EtOH/nm) 275, 333; IR (cm^{-1}) 3372, 2962, 2926, 2866, 2158, 1615; ^{1}H NMR (500 MHz, DMSO-d_6) 1.18 (3H, t, *J* = 7.6 Hz, -$CH_2C\mathit{H}_3$), 2.56 (2H, q, *J* = 7.6 Hz, -$C\mathit{H}_2CH_3$), 2.50 (3H, s, C^{8}-CH_3), 3.66 (3H, s, N^{9}-CH_3), 7.12 (2H, d, *J* = 8.7 Hz, H-3'/H-5'), 7.75 (2H, d, *J* = 8.7 Hz, H-2'/H-6'), 8.62 (1H, s, H-6), 9.41 (1H, s, C^{2}-NH); ^{13}C NMR (125 MHz, DMSO-d_6) 13.8 (C^{8}-CH_3), 15.9 ($CH_2\mathit{C}H_3$), 27.5 ($\mathit{C}H_2CH_3$), 28.0 (N^{9}-CH_3), 118.3 (C-Ar), 127.3 (C-Ar), 127.6 (C-Ar), 135.9 (C-Ar), 138.8 (C-Ar), 146.5 (C-Ar), 152.3 (C-Ar), 153.8 (C-Ar), 155.9 (C-Ar); HRMS calcd. for $C_{15}H_{18}N_5$ (ES+) *m*/*z* 268.1559 $[M+H]^+$, found 268.1557.

_N_-(4-Isopropylphenyl)-8,9-dimethyl-9_H_-purin-2-amine (69)

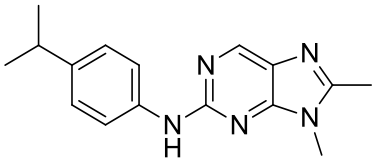

2-Chloropurine intermediate **56** (20 mg, 0.11 mmol), 4-isopropylaniline (31 µl, 0.22 mmol) and TFA (42 µl, 0.55 mmol) were reacted in TFE (1 ml) according to **general procedure F**. Purification *via* chromatography on KP-NH silica (1:1 Petrol/EtOAc) afforded the desired

compound as a pale pink solid (18 mg, 0.06 mmol, 58%). R_f 0.31 (1:1 Petrol/EtOAc, KP-NH); M.p. 188-190 °C; λ_{max} (EtOH/nm) 275, 333; IR (cm^{-1}) 3359, 2957, 2868, 2158, 2031, 1615; ^{1}H NMR (500 MHz, MeOD) 1.07 (6H, d, *J* = 7.0 Hz, -CH(C*H*$_3$)$_2$), 2.39 (3H, s, C^8-CH$_3$), 2.69 (1H, sept, *J* = 7.0 Hz, -C*H*(CH$_3$)$_2$), 3.55 (3H, s, N^9-CH$_3$), 7.00 (2H, d, *J* = 8.8 Hz, H-3'/H-5'), 7.47 (2H, d, *J* = 8.8 Hz, H-2'/H-6'), 8.34 (1H, s, H-6), 9.41 (1H, s, C^2-NH); ^{13}C NMR (125 MHz, DMSO-*d*$_6$) 13.8 (C^8-CH$_3$), 24.1 (-CH(*C*H$_3$)$_2$), 28.0 (N^9-CH$_3$), 32.8 (-*C*H(CH$_3$)$_2$), 118.3 (C-Ar), 126.1 (C-Ar), 127.2 (C-Ar), 138.9 (C-Ar), 140.7 (C-Ar), 146.5 (C-Ar), 152.3 (C-Ar), 153.8 (C-Ar), 155.9 (C-Ar); HRMS calcd. for $C_{16}H_{20}N_5$ (ES+) *m*/*z* 282.1715 $[M+H]^+$, found 282.1713.

1-Isopropoxy-4-nitrobenzene (77)[239]

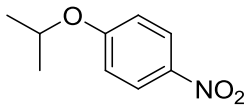

Sodium hydride (92 mg, 3.90 mmol) was added portionwise to dry isopropanol (3 ml). Once the resultant reaction had subsided, the solution was cooled to 0 °C and a solution of 4-fluoronitrobenzene (0.501 g, 3.54 mmol) in dry isopropanol (2 ml) was added drop-wise. The reaction mixture was stirred at RT for 18 h, after which point the solvent was removed *in vacuo*. The crude residue was purified *via* chromatography on silica (9:1 Petrol/EtOAc) to give the desired compound as a golden oil (0.550 g, 3.04 mmol, 86%). R_f 0.38 (1:1 Petrol/EtOAc); λ_{max} (EtOH/nm) 229, 318; IR (cm^{-1}) 2981, 2936, 1912, 1591; ^{1}H NMR (500 MHz, $CDCl_3$) 1.41 (6H, d, *J* = 6.1 Hz, OCH(C*H*$_3$)$_2$), 4.69 (1H, sept, *J* = 6.1 Hz, OC*H*(CH$_3$)$_2$), 6.94 (2H, d, *J* = 9.3 Hz, H-2/H-6), 8.21 (2H, d, *J* = 9.3 Hz, H-3/H-5); ^{13}C NMR (125 MHz, $CDCl_3$) 21.8 (OCH(*C*H$_3$)$_2$), 70.9 (OCH(CH$_3$)$_2$), 115.2 (C-Ar), 126.0 (C-Ar), 141.1 (C-Ar), 163.2 (C-Ar); LRMS (ES+) *m*/*z* 182.2 $[M+H]^+$.

4-Isopropoxyaniline (75)[240]

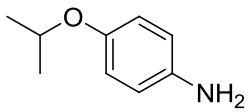

Nitro aromatic **77** (0.448 g, 2.47 mmol), palladium on carbon (50 mg, 10% w/w) and ammonium formate (1.56 g, 24.7 mmol) were reacted in methanol (25 ml) according to **general procedure G**. Chromatography on silica (7:3 Petrol/EtOAc) afforded the target

compound as an orange oil (0.307 g, 2.03 mmol, 82%). R_f 0.44 (7:3 Petrol/EtOAc); λ_{max} (EtOH/nm) 231, 273; IR (cm^{-1}) 3433, 3352, 3228, 2975, 2360, 1624, 1505; ^1H NMR (500 MHz, DMSO-d_6) 1.18 (6H, d, J = 6.0 Hz, OCH(CH_3)$_2$), 4.31 (1H, sept, J = 6.0 Hz, OCH(CH$_3$)$_2$), 4.60 (2H, s, Ar-NH$_2$), 6.49 (2H, d, J = 8.8 Hz, H-2/H-6), 6.62 (2H, d, J = 8.8 Hz, H-3/H-5); ^{13}C NMR (125 MHz, DMSO-d_6) 22.0 (OCH(*C*H$_3$)$_2$), 70.0 (OCH(CH$_3$)$_2$), 114.9 (C-Ar), 117.4 (C-Ar), 142.5 (C-Ar), 148.4 (C-Ar); LRMS (ES+) *m*/*z* 152.1 $[M+H]^+$.

***N*-(4-Isopropoxyphenyl)-8-methyl-9*H*-purin-2-amine (70)**

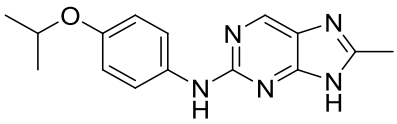

2-Chloropurine intermediate **62** (20 mg, 0.12 mmol), aniline **75** (36 mg, 0.24 mmol) and TFA (45 µl, 0.59 mmol) were reacted in TFE (1 ml) according to **general procedure F**. Purification *via* chromatography on KP-NH silica (19:1 DCM/MeOH) afforded the desired compound as a pale pink solid (23 mg, 0.08 mmol, 70%). R_f 0.36 (19:1 DCM/MeOH, KP-NH); M.p. 196-198 °C; λ_{max} (EtOH/nm) 274; IR (cm^{-1}) 3254, 3048, 2977, 1612; ^1H NMR (500 MHz, DMSO-d_6) 1.25 (6H, d, J = 6.0 Hz, OCH(CH_3)$_2$), 2.45 (3H, s, C^8-CH$_3$), 4.52 (1H, sept, J = 6.0 Hz, OCH(CH$_3$)$_2$), 6.85 (2H, d, J = 8.9 Hz, H-3'/H-5'), 7.66 (2H, d, J = 8.9 Hz, H-2'/H-6'), 8.58 (1H, s, H-6), 9.17 (1H, s, C^2-NH), 12.60 (1H, s, H-9); ^{13}C NMR (125 MHz, DMSO-d_6) 14.9 (C^8-CH$_3$), 21.9 (OCH(*C*H$_3$)$_2$), 69.4 (OCH(CH$_3$)$_2$), 115.9 (C-Ar), 119.9 (C-Ar); HRMS calcd. for $C_{15}H_{18}N_5O$ (ES+) *m*/*z* 284.1509 $[M+H]^+$, found 284.1506.

Note: Unable to visualise all carbon signals by NMR.

***N*-(4-Isopropoxyphenyl)-8,9-dimethyl-9*H*-purin-2-amine (71)**

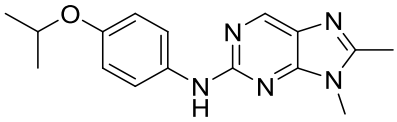

2-Chloropurine intermediate **56** (20 mg, 0.11 mmol), aniline **75** (33 mg, 0.22 mmol) and TFA (42 µl, 0.55 mmol) were reacted in TFE (1 ml) according to **general procedure F**. Purification *via* chromatography on KP-NH silica (1:1 Petrol/EtOAc) afforded the desired compound as a pale pink solid (28 mg, 0.09 mmol, 86%). R_f 0.27 (1:1 Petrol/EtOAc, KP-NH); M.p. 204-205 °C; λ_{max} (EtOH/nm) 276; IR (cm^{-1}) 3251, 3195, 3115, 3045, 2975, 2932,

2164, 1613; ^{1}H NMR (500 MHz, DMSO-d_6) 1.26 (6H, d, J = 6.0 Hz, OCH(CH_3)$_2$), 2.52 (3H, s, C^8-CH$_3$), 3.65 (3H, s, N^9-CH$_3$), 4.52 (1H, sept, J = 6.0 Hz, OCH(CH$_3$)$_2$), 6.86 (2H, d, J = 9.0 Hz, H-3'/H-5'), 7.72 (2H, d, J = 9.0 Hz, H-2'/H-6'), 8.59 (1H, s, H-6), 9.31 (1H, s, C^2-NH); ^{13}C NMR (125 MHz, DMSO-d_6) 13.8 (C^8-CH$_3$), 21.9 (OCH(CH_3)$_2$), 28.0 (N^9-CH$_3$), 69.4 (OCH(CH$_3$)$_2$), 115.9 (C-Ar), 119.7 (C-Ar), 127.3 (C-Ar),134.4 (C-Ar), 146.5 (C-Ar), 151.7 (C-Ar), 152.1 (C-Ar), 153.8 (C-Ar), 156.1 (C-Ar); HRMS calcd. for $C_{16}H_{20}N_5O$ (ES+) m/z 298.1665 $[M+H]^+$, found 298.1662.

2-Benzyl-4-((8,9-dimethyl-9*H*-purin-2-yl)amino)phenol (79)

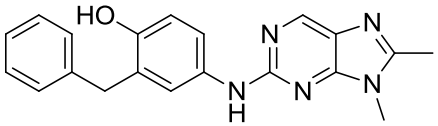

2-Chloropurine intermediate **56** (70 mg, 0.38 mmol), 4-benzyloxyaniline hydrochloride (0.180 g, 0.77 mmol) and TFA (150 µl, 1.92 mmol) were reacted in TFE (2 ml) according to **general procedure F**. Purification *via* chromatography on KP-NH silica (1:1 Petrol/EtOAc) afforded the described compound as a beige solid (16 mg, 0.05 mmol, 12%). R_f 0.21 (1:1 Petrol/EtOAc, KP-NH); M.p. 170-190 °C (decomposed); λ_{max} (EtOH/nm) 277, 336; IR (cm^{-1}) 3026, 2158, 2015, 1613, 1589; ^{1}H NMR (500 MHz, DMSO-d_6) 2.49 (3H, s, C^8-CH$_3$), 3.55 (3H, s, N^9-CH$_3$), 3.87 (2H, s, OCH$_2$Ar), 6.74 (1H, d, J = 8.7 Hz, H-6'), 7.14-7.19 (1H, m, H-4''), 7.25-7.29 (4H, m, H-2''/H-3''/H-5''/H-6''), 7.36 (1H, dd, J = 2.7 and 8.7 Hz, H-5'), 7.56 (1H, d, J = 2.7 Hz, H-3'), 8.53 (1H, s, H-6), 9.01 (1H, br, Ar-OH), 9.10 (1H, s, C^2-NH); HRMS calcd. for $C_{20}H_{20}N_5O$ (ES+) m/z 346.1668 $[M+H]^+$, found 346.1662.

Note: Insufficient material for ^{13}C NMR.

4-(8,9-Dimethyl-9*H*-purin-2-ylamino)phenol (80)

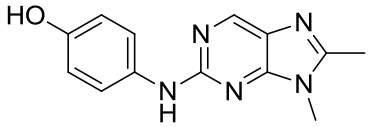

2-Chloropurine intermediate **56** (0.200 g, 1.10 mmol), 4-aminophenol (0.240 g, 2.20 mmol) and TFA (0.420 µl, 5.50 mmol) were reacted in TFE (6 ml) according to **general procedure F**. Purification *via* chromatography on KP-NH silica (19:1 DCM/MeOH) afforded the desired compound as a pale pink solid (0.174 g, 0.68 mmol, 62%). R_f 0.24 (19:1 DCM/MeOH, KP-

NH); M.p. 260-270 °C (decomposed); λ_{max} (EtOH/nm) 249, 338; IR (cm^{-1}) 1696, 2597, 2676, 3037, 3262; ^{1}H NMR (500 MHz, DMSO-d_6) 2.50 (3H, s, C^8-CH_3), 3.63 (3H, s, N^9-CH_3), 6.70 (2H, d, *J* = 8.8 Hz, H-2'/H-6'), 7.59 (2H, d, *J* = 8.8 Hz, H-3'/H-5'), 8.56 (1H, s, H-6), 8.96 (1H, br, Ar-OH), 9.17 (1H, s, C^2-NH); ^{13}C NMR (125 MHz, DMSO-d_6) 13.7 (C^8-CH_3), 27.9 (N^9-CH_3), 114.9 (C-Ar), 120.2 (C-Ar), 126.9 (C-Ar), 132.9 (C-Ar), 146.5 (C-Ar), 151.7 (C-Ar), 151.9 (C-Ar), 153.9 (C-Ar), 156.3 (C-Ar); HRMS calcd. for $C_{13}H_{14}N_5O$ (ES+) *m*/*z* 256.1193 $[M+H]^+$, found 256.1197.

_N_-(4-(Benzyloxy)phenyl)-8,9-dimethyl-9_H_-purin-2-amine (78)

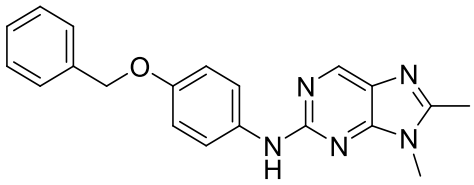

Phenol **80** (40 mg, 0.16 mmol), benzyl chloride (74µl, 0.64 mmol) and potassium carbonate (26 mg, 0.18 mmol) were reacted in dry DMF (1.5 ml) according to **general procedure H**. Purification *via* chromatography on KP-NH silica (1:1 Petrol/EtOAc) afforded the desired compound as a beige solid (24 mg, 0.07 mmol, 18%). R_f 0.21 (1:1 Petrol/EtOAc, KP-NH); M.p. 202-204 °C; λ_{max} (EtOH/nm) 277, 336; IR (cm^{-1}) 3255, 3155, 3116, 3051, 1624, 1548, 1510; ^{1}H NMR (500 MHz, DMSO-d_6) 2.50 (3H, s, C^8-CH_3), 3.64 (3H, s, N^9-CH_3), 5.07 (2H, s, $ArCH_2$), 6.96 (2H, d, *J* = 9.1 Hz, H-3'/H-5'), 7.31-7.36 (1H, m, H-4''), 7.40 (2H, dd, *J* = 7.3 and 7.6 Hz, H-3''/H-5''), 7.44-7.48 (2H, m, H-2''/H-6''), 7.74 (2H, d, *J* = 9.1 Hz, H-2'/H-6'), 8.60 (1H, s, H-6), 9.35 (1H, s, C^2-NH); ^{13}C NMR (125 MHz, DMSO-d_6) 13.8 (C^8-CH_3), 28.0 (N^9-CH_3), 69.4 ($ArCH_2$), 114.7 (C-Ar), 119.7 (C-Ar), 127.1 (C-Ar), 127.6 (C-Ar), 127.7 (C-Ar), 128.4 (C-Ar), 134.7 (C-Ar), 137.4 (C-Ar), 146.5 (C-Ar), 152.2 (C-Ar), 152.7 (C-Ar), 153.8 (C-Ar), 156.0 (C-Ar); HRMS calcd. for $C_{20}H_{20}N_5O$ (ES+) *m*/*z* 346.1668 $[M+H]^+$, found 346.1665.

***N*-(4-(4-Methoxybenzyloxy)phenyl)-8,9-dimethyl-9*H*-purin-2-amine (81)**

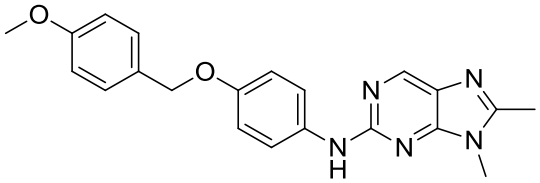

Phenol **80** (40 mg, 0.16 mmol), 4-methoxybenzyl chloride (26 μl, 0.18 mmol) and potassium carbonate (26 mg, 0.18 mmol) were reacted in dry DMF (1.5 ml) according to **general procedure H**. Purification *via* chromatography on silica (19:1 DCM/MeOH) afforded the desired compound as a pale pink solid (48 mg, 0.13 mmol, 80%) R_f 0.31 (19:1 DCM/MeOH); M.p. 178-180 °C; λ_{max} (EtOH/nm) 276; IR (cm^{-1}) 3257, 3199, 3117, 3059, 2836, 1609; ^{1}H NMR (500 MHz, DMSO-d_6) 2.52 (3H, s, C^8-CH_3), 3.64 (3H, s, N^9-CH_3), 3.76 (3H, s, OCH_3), 4.98 (2H, s, OCH_2Ar), 6.94 (2H, d, *J* = 9.2 Hz, H-3'/H-5'), 6.95 (2H, d, *J* = 8.5 Hz, H-3''/H-5''), 7.38 (2H, d, *J* = 8.5 Hz, H-2''/H-6''), 7.74 (2H, d, *J* = 9.2 Hz, H-2'/H-6'), 8.60 (1H, s, H-6), 9.34 (1H, s, C^2-NH); ^{13}C NMR (125 MHz, DMSO-d_6) 13.8 (C^8-CH_3), 28.0 (N^9-CH_3), 55.1 (OCH_3), 69.2 (OCH_2Ar), 113.7 (C-Ar), 114.8 (C-Ar), 119.6 (C-Ar), 127.1 (C-Ar), 129.3 (C-Ar), 129.4 (C-Ar), 134.6 (C-Ar), 146.6 (C-Ar), 152.1 (C-Ar), 152.8 (C-Ar), 152.8 (C-Ar), 156.0 (C-Ar), 158.9 (C-Ar); HRMS calcd. for $C_{21}H_{22}N_5O_2$ (ES+) *m*/*z* 376.1768 $[M+H]^+$, found 376.1768.

***N*-(4-(4-Chlorobenzyloxy)phenyl)-8,9-dimethyl-9*H*-purin-2-amine (82)**

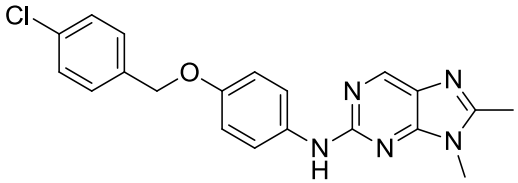

Phenol **80** (30 mg, 0.12 mmol), 4-chlorobenzyl chloride (57 mg, 0.35 mmol) and potassium carbonate (18 mg, 0.14 mmol) were reacted in dry DMF (1 ml) according to **general procedure H**. Purification *via* chromatography on silica (19:1 DCM/MeOH) afforded the desired compound as a pale pink solid (31 mg, 0.08 mmol, 68%). R_f 0.32 (19:1 DCM/MeOH); M.p. 206-207 °C; λ_{max} (EtOH/nm) 276; IR (cm^{-1}) 3263, 3201, 3125, 3065, 1618; ^{1}H NMR (500 MHz, DMSO-d_6) 2.52 (3H, s, C^8-CH_3), 3.64 (3H, s, N^9-CH_3), 5.08 (2H, s, OCH_2Ar), 6.96 (2H, d, *J* = 9.0 Hz, H-3'/H-5'), 7.46 (2H, d, *J* = 8.7 Hz, H-2''/H-6''), 4.49 (2H, d, *J* = 8.7 Hz, H-3''/H-5''), 7.75 (2H, d, *J* = 9.0 Hz, H-2'/H-6'), 8.60 (1H, s, H-6), 9.35

(1H, s, C^2-NH); ^{13}C NMR (125 MHz, DMSO-d_6) 13.8 (C^8-CH_3), 28.0 (N^9-CH_3), 68.6 (OCH_2Ar), 114.8 (C-Ar), 119.6 (C-Ar), 128.4 (C-Ar), 129.4 (C-Ar), 134.8 (C-Ar), 136.5 (C-Ar), 146.6 (C-Ar), 152.5 (C-Ar), 153.8 (C-Ar), 156.0 (C-Ar); HRMS calcd. for $C_{20}H_{19}ClN_5O$ (ES+) *m*/*z* 380.1272 $[M+H]^+$, found 380.1273.

Note: Unable to visualise all carbon signals by NMR.

N-(4-(4-tert-Butylbenzyloxy)phenyl)-8,9-dimethyl-9H-purin-2-amine (83)

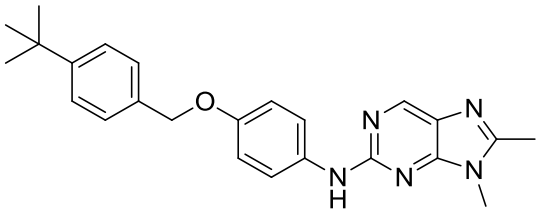

Phenol **80** (40 mg, 0.16 mmol), 4-*tert*-butylbenzyl chloride (35 µl, 0.18 mmol) and potassium carbonate (26 mg, 0.18 mmol) were reacted in dry DMF (1.5 ml) according to **general procedure H**. Purification *via* chromatography on silica (19:1 DCM/MeOH) afforded the desired compound as a pale pink solid (44 mg, 0.11 mmol, 69%) R_f 0.28 (19:1 DCM/MeOH); M.p. 228-229 °C; λ_{max} (EtOH/nm) 277; IR (cm^{-1}) 3272, 3202, 2958, 2853, 1608, 1558; ^{1}H NMR (500 MHz, DMSO-d_6) 1.29 (9H, s, -C(CH_3)$_3$), 2.52 (3H, s, C^8-CH_3), 3.64 (3H, s, N^9-CH_3), 5.03 (2H, s, OCH_2Ar), 6.95 (2H, d, *J* = 9.1 Hz, H-3'/H-5'), 7.38 (2H, d, *J* = 8.4 Hz, H-3''/H-5''), 7.42 (2H, d, *J* = 8.4 Hz, H-2''/H-6''), 7.45 (2H, d, *J* = 9.1 Hz, H-2'/H-6'), 8.59 (1H, s, H-6), 9.33 (1H, s, C^2-NH); ^{13}C NMR (125 MHz, DMSO-d_6) 13.8 (C^8-CH_3), 28.0 (N^9-CH_3), 31.1 (-C(*C*H_3)$_3$), 34.3 (-*C*(CH_3)$_3$), 69.1 (OCH_2Ar), 114.7 (C-Ar), 119.7 (C-Ar), 125.1 (C-Ar), 127.1 (C-Ar), 127.5 (C-Ar), 134.4 (C-Ar), 134.6 (C-Ar), 146.6 (C-Ar), 150.1 (C-Ar), 152.2 (C-Ar), 152.8 (C-Ar), 153.8 (C-Ar), 156.0 (C-Ar); HRMS calcd. for $C_{24}H_{28}N_5O$ (ES+) *m*/*z* 402.2285 $[M+H]^+$, found 402.2288.

1-(2-(4-Nitrophenoxy)ethyl)benzene (84)[241]

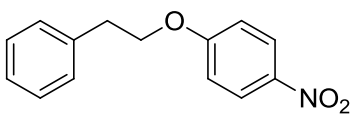

Sodium hydride (60% dispersion in mineral oil, 0.17 g, 4.3 mmol) was added portion-wise to a solution of 2-phenylethanol (0.51 ml, 4.3 mmol) in dry THF (4 ml) at 0 °C. The suspension was allowed to warm to room-temperature, after which point a solution of 1-fluoro-4-

nitrobenzene (0.500 g, 3.54 mmol) in dry THF (3 ml) was added drop-wise. The mixture was stirred at room-temperature for 18 h, after which point the solvent was removed *in vacuo*. The crude residue was purified *via* chromatography on silica (4:1 Petrol/EtOAc) to give the desired compound as a yellow oil (0.868 g, 3.57 mmol, 84%). R_f 0.64 (4:1 Petrol/EtOAc); λ_{max} (EtOH/nm) 232, 323; IR (cm^{-1}) 3116, 3025, 2935, 1591, 1507; ^{1}H NMR (500 MHz, DMSO-d_6) 3.09 (2H, t, J = 6.8 Hz, OCH_2CH_2), 4.36 (2H, t, J = 6.8 Hz, OCH_2CH_2), 7.16 (2H, d, J = 9.2 Hz, H-2/H-6), 7.22-7.26 (1H, m, H-4'), 7.30-7.37 (4H, m, H-2'/3'/5'/6'), 8.20 (2H, d, J = 9.2 Hz, H-3/H-5); ^{13}C NMR (125 MHz, DMSO-d_6) 34.6 (CH_2CH_2O), 69.1 (CH_2CH_2O), 115.0 (C-Ar), 125.9 (C-Ar), 126.4 (C-Ar), 128.3 (C-Ar), 129.0 (C-Ar), 137.8 (C-Ar), 140.8 (C-Ar), 163.7 (C-Ar); LRMS (ES+) m/z 244.3 $[M+H]^+$.

4-(Phenethyloxy)aniline (85)[242]

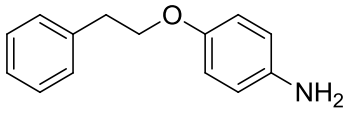

Nitro aromatic **84** (0.651 g, 2.67 mmol), palladium on carbon (65 mg, 10% w/w) and ammonium formate (1.70 g, 26.7 mmol) were reacted in methanol (25 ml) according to **general procedure G**. Silica gel chromatography (4:1 Petrol/EtOAc) afforded the target compound as an orange/red oil (0.307 g, 2.03 mmol, 82%). R_f 0.35 (4:1 Petrol/EtOAc); λ_{max} (EtOH/nm) 229, 273; IR (cm^{-1}) 3318, 3034, 2937, 2872, 1626, 1508; ^{1}H NMR (500 MHz, DMSO-d_6) 2.97 (2H, t, J = 6.9 Hz, OCH_2CH_2), 4.03 (2H, t, J = 6.9 Hz, OCH_2CH_2), 4.61 (2H, s, Ar-NH_2), 6.50 (2H, d, J = 8.9 Hz, H-2/H-6), 6.65 (2H, d, J = 8.9 Hz, H-3/H-5), 7.20-7.25 (1H, m, H-4'), 7.29-7.33 (4H, m, H-2'/3'/5'/6'); ^{13}C NMR (125 MHz, DMSO-d_6) 35.2 (CH_2CH_2O), 68.7 (CH_2CH_2O), 114.9 (C-Ar), 115.4 (C-Ar), 126.1 (C-Ar), 128.2 (C-Ar), 128.9 (C-Ar), 138.6 (C-Ar), 142.4 (C-Ar), 149.6 (C-Ar); LRMS (ES+) m/z 214.2 $[M+H]^+$.

8,9-Dimethyl-*N*-(4-(phenethyloxy)phenyl)-9*H*-purin-2-amine (86)

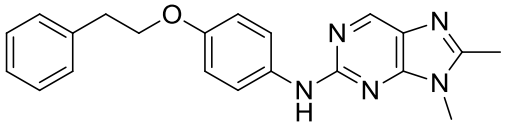

2-Chloropurine intermediate **56** (50 mg, 0.27 mmol), aniline **84** (0.117 g, 0.55 mmol) and TFA (53 µl, 0.69 mmol) were reacted in TFE (1.5 ml) according to **general procedure F**. Purification *via* chromatography on silica (19:1 DCM/MeOH) afforded the desired compound

as a pale pink solid (66 mg, 0.18 mmol, 68%). R_f 0.19 (19:1 DCM/MeOH); M.p. 180-182 °C; λ_{max} (EtOH/nm) 276; IR (cm^{-1}) 3266, 3203, 3023, 2891, 1970, 1607, 1550; ^{1}H NMR (500 MHz, DMSO-d_6) 2.52 (3H, s, C^8-CH_3), 3.03 (2H, t, J = 7.0 Hz, CH_2), 3.64 (3H, s, N^9-CH_3), 4.16 (2H, t, J = 7.0 Hz, CH_2), 6.89 (2H, d, J = 8.9 Hz, H-3'/H-5'), 7.2-7.4 (5H, m, H-2''/3''/4''/5''/6''), 7.73 (2H, d, J = 8.9 Hz, H-2'/H-6'), 8.59 (1H, s, H-6), 9.32 (1H, s, C^2-NH); ^{13}C NMR (125 MHz, DMSO-d_6) 13.8 (C^8-CH_3), 27.9 (N^9-CH_3), 35.1 (CH_2CH_2O), 68.3 (CH_2CH_2O), 114.4 (C-Ar), 119.7 (C-Ar), 126.2 (C-Ar), 128.3 (C-Ar), 128.9 (C-Ar), 134.5 (C-Ar), 138.5 (C-Ar), 146.5 (C-Ar), 147.3 (C-Ar), 152.2 (C-Ar), 152.8 (C-Ar), 153.8 (C-Ar), 156.0 (C-Ar); HRMS calcd. for $C_{21}H_{22}N_5O$ (ES+) m/z 360.1819 $[M+H]^+$, found 360.1821.

***N*-(4-Bromophenyl)-8,9-dimethyl-9*H*-purin-2-amine (90)**

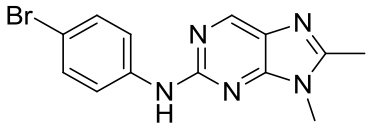

2-Chloropurine intermediate **56** (0.200 g, 1.10 mmol), 4-bromoaniline (0.380 g, 2.20 mmol) and TFA (420 µl, 5.50 mmol) were reacted in TFE (6 ml) according to **general procedure F**. Purification *via* chromatography on KP-NH silica (1:1 Petrol/EtOAc) afforded the desired compound as a pale pink solid (0.247 g, 0.78 mmol, 71%). R_f 0.39 (1:1 Petrol/EtOAc, KP-NH); M.p. 248-250 °C; λ_{max} (EtOH/nm) 274, 323; IR (cm^{-1}) 3362, 3110, 1619; ^{1}H NMR (500 MHz, DMSO-d_6) 2.53 (3H, s, C^8-CH_3), 3.68 (3H, s, N^9-CH_3), 7.45 (2H, d, J = 9.0 Hz, H-2'/H-6'), 7.86 (2H, d, J = 9.0 Hz, H-3'/H-5'), 8.67 (1H, s, H-6), 9.72 (1H, s, C^2-NH); ^{13}C NMR (125 MHz, DMSO-d_6) 13.8 (C^8-CH_3), 28.1 (N^9-CH_3), 118.8 (C-Ar), 119.9 (C-Ar), 131.1 (C-Ar), 146.5 (C-Ar), 155.4 (C-Ar); HRMS calcd. for $C_{13}H_{13}N_5Br$ (ES+) m/z 318.0349 $[M+H]^+$, found 318.0358.

Note: Unable to visualise all carbon signals by NMR.

8,9-Dimethyl-*N*-(4-((triisopropylsilyl)ethynyl)phenyl)-9*H*-purin-2-amine (91)

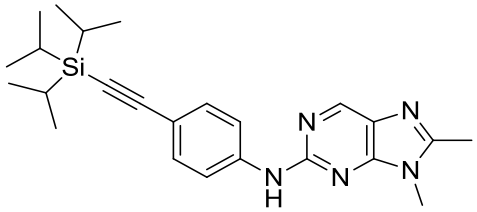

Acetonitrile (1 ml) and triisopropylsilylacetylene (65µl, 0.20 mmol) were added to a vial charged with arylbromide **90** (50 mg, 0.16 mmol), XPhos (4 mg, 0.008 mmol), $PdCl_2(CH_3CN)_2$ (2 mg, 0.008 mmol) and Cs_2CO_3 (0.135 g, 0.41 mmol). The resultant mixture was degassed for 15 min, before being heated at 80 °C for 2 h. The reaction mixture was passed through Celite® and evaporated to dryness, and the resultant residue was purified by reverse phase chromatography (9:1 MeOH/H_2O, 0.1% HCOOH) to give the target compound as a pale orange oil/gum (62 mg, 0.15 mmol, 93%). R_f 0.17 (9:1 MeOH/H_2O, 0.1% HCOOH); λ_{max} (EtOH/nm) 302; IR (cm^{-1}) 3257, 2940, 2864, 2145, 1601, 1513; ^{1}H NMR (500 MHz, DMSO-d_6) 1.02-1.18 (21H, m, $Si(CH(CH_3)_2)_3$), 2.54 (3H, s, C^8-CH_3), 3.69 (3H, s, N^9-CH_3), 7.39 (2H, d, *J* = 8.8 Hz, H-3'/H-5'), 7.90 (2H, d, *J* = 8.8 Hz, H-2'/H-6'), 8.69 (1H, s, H-6), 9.86 (1H, s, C^2-NH); ^{13}C NMR (125 MHz, DMSO-d_6) 10.8 ($Si(CH(CH_3)_2)_3$), 13.8 (C^8-CH_3), 18.5 ($Si(CH(CH_3)_2)_3$), 28.1 (N^9-CH_3), 117.7 (C-Ar), 132.3 (C-Ar), 146.5 (C-Ar); HRMS calcd. for $C_{24}H_{34}N_5Si$ (ES+) *m*/*z* 420.2578 $[M+H]^+$, found 420.2578.

Note: Unable to visualise all carbon environments by ^{13}C NMR.

***N*-(4-Ethynylphenyl)-8,9-dimethyl-9*H*-purin-2-amine (87)**

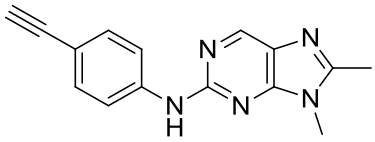

The TIPS-protected purine **91** (50 mg, 0.15 mmol) and TBAF (1M in THF, 0.13 ml, 0.13 mmol) were reacted in THF (5 ml) according to **general procedure I**. Silica gel chromatography (19:1 DCM/MeOH) afforded the desired compound as a white solid (12 mg, 0.05 mmol, 42%). R_f 0.27 (19:1 DCM/MeOH); M.p. 210-214 °C; λ_{max} (EtOH/nm) 294, 329; IR (cm^{-1}) 3314, 3273, 2104, 1607, 1517; ^{1}H NMR (500 MHz, DMSO-d_6) 2.54 (3H,s, C^8-CH_3), 3.68 (3H, s, N^9-CH_3), 4.01 (1H, s, C≡CH), 7.39 (2H, d, *J* = 8.7 Hz, H-3'/H-5'), 7.90 (2H, d, *J* = 8.7 Hz, H-2'/H-6'), 8.69 (1H, s, H-6), 9.81 (1H, s, C^2-NH); ^{13}C NMR (125 MHz,

DMSO-d_6) 13.8 (C^8-CH_3), 28.1 (N^9-CH_3), 79.0 (C≡*C*H), 84.2 (*C*≡CH), 113.1 (C-Ar), 117.6 (C-Ar), 127.8 (C-Ar), 132.2 (C-Ar), 141.8 (C-Ar), 146.5 (C-Ar), 153.0 (C-Ar), 153.7 (C-Ar), 155.2 (C-Ar); HRMS calcd. for $C_{15}H_{14}N_5$ (ES+) *m*/*z* 264.1244 $[M+H]^+$, found 264.1243.

3-Fluoro-4-methoxyaniline (94)[243]

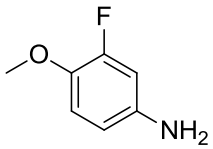

2-Fluoro-4-nitroanisole (0.250 g, 1.46 mmol), palladium on carbon (25 mg, 10% w/w) and ammonium formate (0.920 g, 14.6 mmol) were reacted in methanol (15 ml) according to **general procedure G**. Purification by silica gel chromatography (7:3 Petrol/EtOAc) gave the product as an off-white solid (0.183 g, 1.30 mmol, 89%). R_f 0.38 (7:3 Petrol/EtOAc); M.p. 80-83 °C (Lit.[243] 83-83.5 °C); λ_{max} (EtOH/nm) 235, 296; IR (cm^{-1}) 3412, 3307, 3212, 2971, 2844, 2040, 1633, 1588, 1511; ^{1}H NMR (500 MHz, DMSO-d_6) 3.68 (3H, s, OCH_3), 4.90 (2H, s, Ar-NH_2), 6.31 (1H, ddd, *J* = 1.3, 2.6 and 8.7 Hz, H-6), 6.41 (1H, dd, *J* = 2.6 and 13.9 Hz, H-2), 6.84 (1H, dd, *J* = 8.7 and 9.8 Hz, H-5); ^{13}C NMR (125 MHz, DMSO-d_6) 57.0 (OCH_3), 102.1 (d, J_{CF} = 20.5 Hz, C-Ar), 109.2 (d, J_{CF} = 2.8 Hz, C-Ar), 116.1 (d, J_{CF} = 2.7 Hz, C-Ar), 137.5 (d, J_{CF} = 11.0 Hz, C-Ar), 143.7 (d, J_{CF} = 10.0 Hz, C-Ar), 152.4 (d, J_{CF} = 240.4 Hz, C-Ar); LRMS (ES+) *m*/*z* 142.1 $[M+H]^+$.

***N*-(3-fluoro-4-methoxyphenyl)-8,9-dimethyl-9*H*-purin-2-amine (92)**

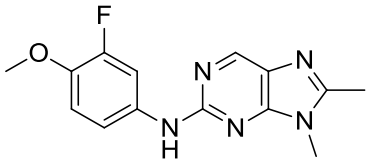

3-Fluoro-4-methoxyaniline **94** (62 mg, 0.44 mmol), 2-chloropurine intermediate **56** (40 mg, 0.22 mmol) and TFA (42 µl, 0.55 mmol) were reacted in TFE (2 ml) according to **general procedure F**. Chromatography on KP-NH silica (1:1 Petrol/EtOAc) gave the desired product was an off-white solid (39 mg, 0.14 mmol, 62%). R_f 0.27 (1:1 Petrol/EtOAc, KP-NH Si); M.p. 193-195 °C; λ_{max} (EtOH/nm) 274.5, 329.5; IR (cm^{-1}) 3356, 2934, 1978, 1621; ^{1}H NMR (500 MHz, DMSO-d_6) 2.52 (3H, s, C^8-CH_3), 3.66 (3H, s, N^9-CH_3), 3.81 (3H, s, OCH_3), 7.10 (1H, dd, *J* = 9.5 Hz, H-5'), 7.50-7.53 (1H, m, H-6'), 7.88 (1H, dd, *J* = 2.5 and 14.5 Hz, H-2'), , 8.64 (1H, s, H-6), 9.53 (1H, s, C^2-NH); ^{13}C NMR (125 MHz, DMSO-d_6) 13.8 (C^8-CH_3),

28.0 (N^9-CH_3), 56.4 (OCH_3), 113.8 (d, J_{CF} = 2.1 Hz, C-Ar), 114.4 (d, J_{CF} = 4.1 Hz, C-Ar), 135.1 (d, J_{CF} = 13.0 Hz, C-Ar), 146.5 (C-Ar); HRMS calcd. for $C_{14}H_{15}FN_5O$ (ES+) *m*/*z* 288.1257 $[M+H]^+$, found 288.1255.

Note: Unable to visualise all carbon environments by ^{13}C NMR.

_N_-(3,5-Difluoro-4-methoxyphenyl)-8,9-dimethyl-9_H_-purin-2-amine (93)

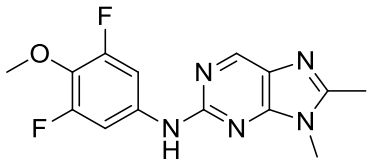

The 2-chloropurine intermediate **56** (80 mg, 0.44 mmol), 3,5-difluoro-4-methoxyaniline (0.140 g, 0.88 mmol) and TFA (85 µl, 1.10 mmol) were reacted in TFE (4 ml) according to **general procedure F**. Purification through chromatography on silica (19:1 DCM/MeOH) afforded the desired compound as a pale brown solid (26 mg, 0.09 mmol, 20%). R_f 0.23 (19:1 DCM/MeOH); M.p. 239-241 °C; λ_{max} (EtOH/nm) 273.5, 324.5; IR (cm^{-1}) 3256, 3197, 3069, 3003, 2834, 1611; ^1H NMR (500 MHz, DMSO-d_6) 2.54 (3H, s, C^8-CH_3), 3.68 (3H, s, N^9-CH_3), 3.85 (3H, s, OCH_3), 7.67 (2H, d, *J* = 11.7 Hz, H-2'/H-6'), 8.70 (1H, s, H-6), 9.84 (1H, s, C^2-NH); ^{13}C NMR (125 MHz, DMSO-d_6) 13.8 (C^8-CH_3), 28.1 (N^9-CH_3), 62.0 (OCH3), 101.5 (d, J_{CF} = 27.8 Hz, C-Ar), 127.9 (C-Ar), 128.9 (C-Ar), 137.2 (dd, J_{CF} = 13.4 and 13.7 Hz, C-Ar), 146.5 (C-Ar), 153.2 (C-Ar), 153.6 (C-Ar), 155.0 (C-Ar), 155.1 (dd, J_{CF} = 8.2 and 241.9 Hz, Ar-CF); HRMS calcd. for $C_{14}H_{14}F_2N_5O$ (ES+) *m*/*z* 306.1161 $[M+H]^+$, found 306.1163.

2-Chloro-_N_-ethyl-5-nitropyrimidin-4-amine (102)

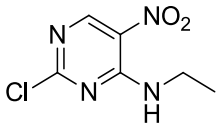

2,4-Dichloro-5-nitropyrimidine (0.550 g, 2.84 mmol) and ethylamine (2M in THF, 4.70 ml, 9.37 mmol) were reacted in THF (12 ml) according to **general procedure C**. Chromatography on silica (9:1 Petrol/EtOAc) afforded the target compound as a yellow solid (0.331 g, 1.63 mmol, 57%). R_f 0.41 (9:1 Petrol/EtOAc); M.p. 62-64 °C; λ_{max} (EtOH/nm) 261, 322; IR (cm^{-1}) 3362, 2977, 2933, 2871, 1613, 1565; ^1H NMR (500 MHz, DMSO-d_6) 1.18 (3H, t, *J* = 7.1 Hz, $NHCH_2C\mathit{H_3}$), 3.56 (2H, dt, *J* = 6.0 and 7.1 Hz, $NHC\mathit{H_2}CH_3$), 9.01 (1H, s,

H-6), 9.14-9.17 (1H, m, C^4-NH); ^{13}C NMR (125 MHz, DMSO-d_6) 13.9 (CH_3), 36.1 (CH_2), 127.2 (C-Ar), 154.7 (C-Ar), 157.3 (C-Ar), 162.4 (C-Ar); LRMS (ES+) *m*/*z* 203.2 $[M^{35}Cl+H]^+$, 205.2 $[M^{37}Cl+H]^+$.

2-Chloro-*N*-isopropyl-5-nitropyrimidin-4-amine (103)

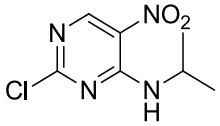

2,4-Dichloro-5-nitropyrimidine (0.520 g, 2.68 mmol) and isopropylamine (500 µl, 5.90 mmol) were reacted in THF (12 ml) according to **general procedure C**. Purification *via* chromatography on silica (9:1 Petrol/EtOAc) afforded the desired compound as a yellow solid (0.403 g, 1.85 mmol, 69%). R_f 0.48 (9:1 Petrol/EtOAc); M.p. 84-87 °C; λ_{max} (EtOH/nm) 261, 348; IR (cm^{-1}) 3354, 2985, 2931, 2881, 1565; ^{1}H NMR (500 MHz, DMSO-d_6) 1.27 (6H, d, *J* = 6.6 Hz, NHCH(CH_3)$_2$), 4.44 (1H, d sept, J = 6.6 and 7.8 Hz, NHC*H*(CH_3)$_2$), 8.60 (1H, d, *J* = 7.8 Hz, C^4-NH), 9.02 (1H, s, H-6); ^{13}C NMR (125 MHz, DMSO-d_6) 21.6 (-CH(CH_3)$_2$), 43.4 (-*C*H(CH_3)$_2$), 127.0 (C-Ar), 154.0 (C-Ar), 157.3 (C-Ar), 162.0 (C-Ar); LRMS (ES+) *m*/*z* 217.2 $[M^{35}Cl+H]^+$, 219.2 $[M^{37}Cl+H]^+$.

***N*-*tert*-Butyl-2-chloro-5-nitropyrimidin-4-amine (104)**

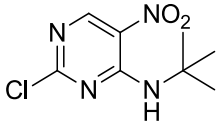

2,4-Dichloro-5-nitropyrimidine (0.519 g, 2.68 mmol) and *tert*-butylamine (620 µl, 5.90 mmol) were reacted in THF (12 ml) according to **general procedure C**. Purification *via* chromatography on silica (9:1 Petrol/EtOAc) afforded the desired compound as a yellow solid (0.392 g, 1.70 mmol, 63%). R_f 0.55 (9:1 Petrol/EtOAc); M.p. 71-74 °C; λ_{max} (EtOH/nm) 234, 259, 363; IR (cm^{-1}) 3336, 2981, 1573; ^{1}H NMR (500 MHz, DMSO-d_6) 1.51 (9H, s, NHC(CH_3)$_3$), 8.33 (1H, s, C^4-NH), 9.04 (1H, s, H-6); ^{13}C NMR (125 MHz, DMSO-d_6) 28.1 (-C(CH_3)$_3$), 53.7 (-*C*(CH_3)$_3$), 127.5 (C-Ar), 154.6 (C-Ar), 157.4 (C-Ar), 161.3 (C-Ar); LRMS (ES+) *m*/*z* 231.2 $[M^{35}Cl+H]^+$, 233.2 $[M^{37}Cl+H]^+$.

2-Chloro-*N*-isobutyl-5-nitropyrimidin-4-amine (105)

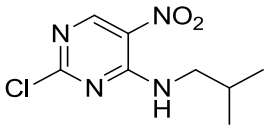

2,4-Dichloro-5-nitropyrimidine (0.543 g, 2.80 mmol) and isobutylamine (610 µl, 6.16 mmol) were reacted in THF (12 ml) according to **general procedure C**. Purification *via* chromatography on silica (9:1 Petrol/EtOAc) afforded the desired compound as a yellow solid (0.225 g, 0.98 mmol, 35%). R_f 0.50 (9:1 Petrol/EtOAc); M.p. 66-69 °C; λ_{max} (EtOH/nm) 260, 367; IR (cm^{-1}) 3386, 2970, 2936, 2873, 1572; ^{1}H NMR (500 MHz, DMSO-d_6) 0.91 (6H, d, J = 7.0 Hz, $CH_2CH(CH_3)_2$), 2.00 (1H, sept, J = 7.0 Hz, $CH_2CH(CH_3)_2$), 3.38 (2H, dd, J = 6.2 and 7.0 Hz, $CH_2CH(CH_3)_2$), 9.02 (1H, s, H-6), 9.08 (1H, t, J = 6.2 Hz, C^4-NH); ^{13}C NMR (125 MHz, DMSO-d_6) 19.9 ($CH_2CH(CH_3)_2$), 27.5 ($CH_2CH(CH_3)_2$), 48.0 ($CH_2CH(CH_3)_2$), 127.3 (C-Ar), 155.1 (C-Ar), 157.3 (C-Ar), 162.3 (C-Ar); LRMS (ES+) *m*/*z* 231.2 $[M^{35}Cl+H]^+$, 233.2 $[M^{37}Cl+H]^+$.

2-Chloro-5-nitro-*N*-phenylpyrimidin-4-amine (106)

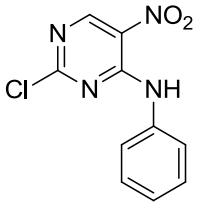

2,4-Dichloro-5-nitropyrimidine (0.508 g, 2.63 mmol) and aniline (530 µl, 5.79 mmol) were reacted in THF (12 ml) according to **general procedure C**. Purification *via* chromatography on silica (9:1 Petrol/EtOAc) afforded the desired compound as an orange solid (0.226 g, 0.90 mmol, 34%). R_f 0.42 (9:1 Petrol/EtOAc); M.p. 169-171 °C; λ_{max} (EtOH/nm) 234, 274, 364; IR (cm^{-1}) 3305, 3052, 1574; ^{1}H NMR (500 MHz, DMSO-d_6) 7.30 (1H, dddd, J = 1.2, 1.2, 7.4 and 7.4 Hz, H-4'), 7.46 (2H, ddd, J = 1.2, 7.4 and 7.4 Hz, H-3'/H-5'), 7.55 (2H, ddd, J = 1.2, 1.2 and 7.4 Hz, H-2'/H-6'), 9.17 (1H, s, H-6), 10.46 (1H, s, C^4-NH); ^{13}C NMR (125 MHz, DMSO-d_6) 123.6 (C-Ar), 124.8 (C-Ar), 126.3 (C-Ar), 128.6 (C-Ar), 128.7 (C-Ar), 136.2 (C-Ar), 153.8 (C-Ar), 157.6 (C-Ar); LRMS (ES+) *m*/*z* 251.2 $[M^{35}Cl+H]^+$, 253.2 $[M^{37}Cl+H]^+$.

***N*-Benzyl-2-chloro-5-nitropyrimidin-4-amine (107)**

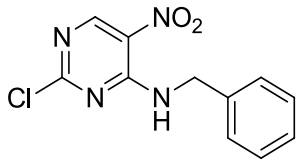

2,4-Dichloro-5-nitropyrimidine (0.501 g, 2.58 mmol) and benzylamine (620 µl, 5.67 mmol) were reacted in THF (12 ml) according to **general procedure C**. Purification *via* chromatography on silica (9:1 Petrol/EtOAc) afforded the desired compound as a yellow solid (0.249 g, 0.94 mmol, 36%). R_f 0.38 (9:1 Petrol/EtOAc); M.p. 101-104 °C; λ_{max} (EtOH/nm) 259, 357; IR (cm^{-1}) 3066, 3033, 1739, 1574, 1376; ^{1}H NMR (500 MHz, DMSO-d_6) 4.75 (2H, d, J = 6.2 Hz, NHCH_2), 7.27 (1H, dddd, J = 1.4, 1.4, 7.1 and 7.1 Hz, H-4'), 7.32-7.40 (4H, m, H-2'/H-3'/H-5'/H-6'), 9.05 (1H, s, H-6), 9.63 (1H, t, J = 6.2 Hz, NHCH_2); ^{13}C NMR (125 MHz, DMSO-d_6) 44.2 (NHCH$_2$), 127.1 (C-Ar), 127.4 (C-Ar), 127.5 (C-Ar), 128.3 (C-Ar), 137.7 (C-Ar), 155.0 (C-Ar), 157.3 (C-Ar), 162.2 (C-Ar); LRMS (ES+) *m*/*z* 265.2 $[M^{35}Cl+H]^+$, 267.2 $[M^{37}Cl+H]^+$.

2-Chloro-5-nitro-*N*-(2,2,2-trifluoroethyl)pyrimidin-4-amine (108)

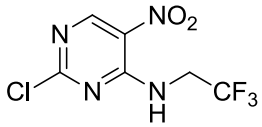

2,4-Dichloro-5-nitropyrimidine (0.602 g, 3.09 mmol) and 2,2,2-trifluoroethylamine (730 µl, 9.28 mmol) were reacted in THF (15 ml) according to **general procedure C**. Purification by silica gel chromatography (9:1 Petrol/EtOAc) gave the desired compound as a pale yellow solid (0.497 g, 1.93 mmol, 62%). R_f 0.54 (9:1 Petrol/EtOAc); M.p. 280-282 °C; λ_{max} (EtOH/nm) 225, 314; IR (cm^{-1}) 3333, 3178, 3035, 1687, 1622, 1568, 1515; ^{1}H NMR (500 MHz, $CDCl_3$) 4.40 (2H, dq, J = 6.4 and 8.6 Hz, CH_2), 8.57 (1H, br, NH), 9.13 (1H, s, H-6); ^{13}C NMR (125 MHz, $CDCl_3$) 42.0 (q, J_{CF} = 35.4 Hz, CH_2), 123.5 (q, J_{CF} = 279.6 Hz, CF_3), 127.2 (C-Ar), 156.1 (C-Ar), 157.5 (C-Ar), 164.5 (C-Ar); LRMS (ES+) *m*/*z* 257.1 $[M^{35}Cl+H]^+$, 259.1$[M^{37}Cl+H]^+$.

2-Chloro-5-nitro-*N*-(3,3,3-trifluoropropyl)pyrimidin-4-amine (109)

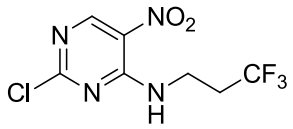

3,3,3-Trifluoropropylamine hydrochloride (0.118 g, 0.78 mmol) was added to a mixture of 2,4-dichloro-5-nitropyrimidine (0.100 g, 0.52 mmol) and cesium carbonate (0.423 g, 1.30 mmol) in THF (5 ml) at 0 °C. After stirring at 0 °C for 20 mins, the reaction mixture was filtered, and the filtrate was concentrated *in vacuo*. The resultant residue was purified by chromatography on silica (9:1 Petrol/EtOAc) to give the target compound as a yellow solid (91 mg, 0.34 mmol, 65%). R_f 0.44 (9:1 Petrol/EtOAc); M.p. 176-179 °C; λ_{max} (EtOH/nm) 228, 324; IR (cm^{-1}) 3056, 2651, 1751, 1649, 1538; ^{1}H NMR (500 MHz, $CDCl_3$) 2.58 (2H, tq, J = 6.5 and 10.5 Hz, CH_2CF$_3$), 3.98 (2H, t, J = 6.5 Hz, NHCH_2), 8.58 (1H, br, NH), 9.11 (1H, s, H-6); ^{13}C NMR (125 MHz, DMSO-d_6) 33.2 (q, J_{CF} = 28.5 Hz, CH$_2$CF$_3$), 35.0 (q, J_{CF} = 3.5 Hz, NHCH$_2$), 155.7 (C-Ar), 157.2 (C-Ar), 158.2 (C-Ar); LRMS (ES+) *m*/*z* 271.1 [M^{35}Cl+H]$^+$, 273.1 [M^{37}Cl+H]$^+$.

Note: Unable to visualise all carbon environments by ^{13}C NMR.

2-Chloro-N^4-ethylpyrimidine-4,5-diamine (110)[244]

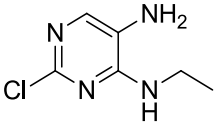

5-Nitropyrimidine **102** (0.298 g, 1.47 mmol) and tin(II) chloride (1.12 g, 5.88 mmol) were reacted in ethanol (6 ml) according to **general procedure D**. Purification *via* chromatography on silica (9:1 DCM/MeOH) afforded the desired compound as a beige solid (0.178 g, 1.03 mmol, 70%). R_f 0.38 (9:1 DCM/MeOH); M.p. 102-104 °C; λ_{max} (EtOH/nm) 260, 306; IR (cm^{-1}) 3385, 3359, 3326, 3249, 3036, 2972, 1584; ^{1}H NMR (500 MHz, DMSO-d_6) 1.17 (3H, t, J = 7.2 Hz, NHCH$_2$CH_3), 3.35 (2H, dt, J = 5.0 and 7.2 Hz, NHCH_2CH$_3$), 4.88 (2H, s, C^5-NH$_2$), 6.84 (1H, t, J = 5.0 Hz, C^4-NH), 7.37 (1H, s, H-6); ^{13}C NMR (125 MHz, DMSO-d_6) 14.2 (CH$_3$), 35.2 (CH$_2$), 127.0 (C-Ar), 135.5 (C-Ar), 147.1 (C-Ar), 153.5 (C-Ar); LRMS (ES+) *m*/*z* 173.1 [M^{35}Cl+H]$^+$, 175.1 [M^{37}Cl+H]$^+$.

2-Chloro-N^4-isopropylpyrimidine-4,5-diamine (111)

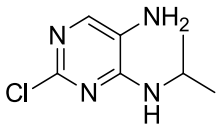

5-Nitropyrimidine **103** (0.324 g, 1.50 mmol) and tin(II) chloride (1.13 g, 5.98 mmol) were reacted in ethanol (6 ml) according to **general procedure D**. Purification *via* chromatography on silica (9:1 DCM/MeOH) afforded the desired compound as a beige solid (0.238 g, 1.28 mmol, 85%). R_f 0.45 (9:1 DCM/MeOH); M.p. 111-113 °C; λ_{max} (EtOH/nm) 263, 309; IR (cm^{-1}) 3345, 3248, 2970, 1584; ^{1}H NMR (500 MHz, DMSO-d_6) 1.19 (6H, d, *J* = 6.5 Hz, NHCH(CH_3)$_2$), 4.14 (1H, d sept, J = 6.5 and 7.2 Hz, NHC*H*(CH_3)$_2$), 4.92 (2H, s, C^5-NH_2), 6.59 (1H, d, *J* = 7.2 Hz, C^4-NH), 7.36 (1H, s, H-6); ^{13}C NMR (125 MHz, DMSO-d_6) 22.2 (-CH(*C*H_3)$_2$), 41.9 (-*C*H(CH_3)$_2$), 126.9 (C-Ar), 135.5 (C-Ar), 147.0 (C-Ar), 152.7 (C-Ar); HRMS calcd. for $C_7H_{12}N_4Cl$ (ES+) *m*/*z* 187.0745 $[M+H]^+$, found 187.0745.

***N^4*-*tert*-Butyl-2-chloropyrimidine-4,5-diamine (112)**

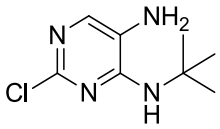

5-Nitropyrimidine **104** (0.337 g, 1.46 mmol) and tin(II) chloride (1.11 g, 5.85 mmol) were reacted in ethanol (6 ml) according to **general procedure D**. Purification *via* chromatography on silica (9:1 DCM/MeOH) afforded the desired compound as an off-white solid (0.250 g, 1.25 mmol, 86%). R_f 0.48 (9:1 DCM/MeOH); M.p. 123-125 °C; λ_{max} (EtOH/nm) 221, 298; IR (cm^{-1}) 3340, 3242, 3197, 2965, 2934, 1579; ^{1}H NMR (500 MHz, DMSO-d_6) 1.43 (9H, s, NHC(CH_3)$_3$), 5.00 (2H, s, C^5-NH_2), 6.08 (1H, s, C^4-NH), 7.37 (1H, s, H-6); ^{13}C NMR (125 MHz, DMSO-d_6) 28.4 (-C(*C*H_3)$_3$), 51.7 (-*C*(CH_3)$_3$), 127.4 (C-Ar), 135.9 (C-Ar), 146.2 (C-Ar), 153.0 (C-Ar); HRMS calcd. for $C_8H_{14}N_4Cl$ (ES+) *m*/*z* 201.0902 $[M+H]^+$, found 201.0902.

2-Chloro-N^4-isobutylpyrimidine-4,5-diamine (113)

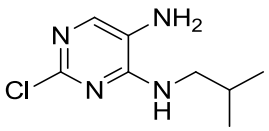

5-Nitropyrimidine **105** (0.190 g, 0.82 mmol) and tin(II) chloride (0.625 g, 3.29 mmol) were reacted in ethanol (4 ml) according to **general procedure D**. Purification *via* chromatography on silica (9:1 DCM/MeOH) afforded the desired compound as a orange/brown oil (0.111 g, 0.55 mmol, 67%). R_f 0.50 (9:1 DCM/MeOH); λ_{max} (EtOH/nm) 260, 311; IR (cm^{-1}) 3351, 3254, 2959, 2871, 2360, 1585; ^{1}H NMR (500 MHz, DMSO-d_6) 0.92 (6H, d, J = 6.7 Hz, $NHCH_2CH(CH_3)_2$), 1.89 (1H, sept, J = 6.7 Hz, $NHCH_2CH(CH_3)_2$), 3.16 (2H, dd, J = 5.5 and 6.7 Hz, $NHCH_2CH(CH_3)_2$), 4.93 (2H, s, C^5-NH_2), 6.80 (1H, t, J = 5.5 Hz, C^4-NH), 7.37 (1H, s, H-6); ^{13}C NMR (125 MHz, DMSO-d_6) 20.2 ($CH_2CH(CH_3)_2$), 27.4 ($CH_2CH(CH_3)_2$), 47.9 ($CH_2CH(CH_3)_2$), 126.9 (C-Ar), 135.5 (C-Ar), 146.9 (C-Ar), 153.7 (C-Ar); LRMS (ES+) *m*/*z* 201.2 $[M^{35}Cl+H]^+$, 203.2 $[M^{37}Cl+H]^+$.

2-Chloro-N^4-phenylpyrimidine-4,5-diamine (114)

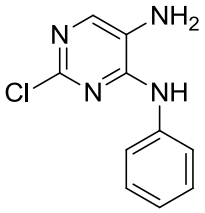

5-Nitropyrimidine **106** (0.220 g, 0.88 mmol) and tin(II) chloride (0.665 g, 3.51 mmol) were reacted in ethanol (4 ml) according to **general procedure D**. Purification *via* chromatography on silica (9:1 DCM/MeOH) afforded the desired compound as a brown oil (0.179 g, 0.81 mmol, 92%). R_f 0.28 (9:1 DCM/MeOH); λ_{max} (EtOH/nm) 270, 318; IR (cm^{-1}) 3347, 3284, 2360, 1570; ^{1}H NMR (500 MHz, DMSO-d_6) 5.32 (2H, s, C^5-NH_2), 7.07 (1H, dddd, J = 1.1, 1.1, 7.3 and 7.3 Hz, H-4'), 7.36 (2H, ddd, J = 1.1, 7.3 and 7.3 Hz, H-3'/H-5'), 7.66 (1H, s, H-6), 7.68 (2H, ddd, J = 1.1, 1.1 and 7.3 Hz, H-2'/H-6'), 8.64 (1H, s, C^4-NH); ^{13}C NMR (125 MHz, DMSO-d_6) 120.4 (C-Ar), 122.9 (C-Ar), 128.0 (C-Ar), 128.7 (C-Ar), 138.5 (C-Ar), 139.2 (C-Ar), 145.7 (C-Ar), 150.2 (C-Ar); HRMS calcd. for $C_{10}H_{10}N_4Cl$ (ES+) *m*/*z* 221.0589 $[M+H]^+$, found 221.0591.

N^4-Benzyl-2-chloropyrimidine-4,5-diamine (115)

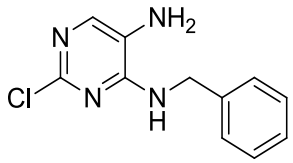

5-Nitropyrimidine **107** (0.219 g, 0.83 mmol) and tin(II) chloride (0.631 g, 3.31 mmol) were reacted in ethanol (4 ml) according to **general procedure D**. Purification *via* chromatography on silica (9:1 DCM/MeOH) afforded the desired compound as a brown/red solid (0.152 g, 0.65 mmol, 78%). R_f 0.37 (9:1 DCM/MeOH); M.p. 186-188 °C; λ_{max} (EtOH/nm) 260, 311; IR (cm^{-1}) 3423, 3356, 3300, 3250, 3026, 2869, 1580; ^{1}H NMR (500 MHz, DMSO-d_6) 4.58 (2H, d, J = 5.7 Hz, NHCH_2), 4.97 (2H, s, C^5-NH_2), 7.25-7.29 (1H, m, H-4'), 7.32-7.39 (5H, m, C^4-NH/H-2'/H-3'/H-5'/H-6'), 7.43 (1H, s, H-6); ^{13}C NMR (125 MHz, DMSO-d_6) 43.7 (NH*C*H_2), 126.9 (C-Ar), 127.1 (C-Ar), 127.5 (C-Ar), 128.3 (C-Ar), 136.0 (C-Ar), 139.0 (C-Ar), 146.8 (C-Ar), 153.4 (C-Ar); HRMS calcd. for $C_{11}H_{12}N_4Cl$ (ES+) m/z 235.0745 $[M+H]^+$, found 235.0750.

2-Chloro-N^4-(2,2,2-trifluoroethyl)pyrimidine-4,5-diamine (116)

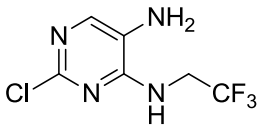

The nitropyrimidine **108** (0.461 g, 1.80 mmol) and tin(II) chloride (1.36 g, 7.20 mmol) were reacted in ethanol (18 ml) according to **general procedure D**. Purification on silica (9:1 DCM/MeOH) afforded the desired compound as a red waxy solid (0.342 g, 1.51 mmol, 84%). R_f 0.33 (9:1 DCM/MeOH); M.p. 137-139 °C; λ_{max} (EtOH/nm) 259, 303; IR (cm^{-1}) 3429, 3344, 3258, 3057, 1588; ^{1}H NMR (500 MHz, $CDCl_3$) 3.08 (2H, br, C^5-NH_2), 4.23 (2H, dq, J = 6.6 and 8.9 Hz, CH_2), 5.38 (1H, br, C^4-NH), 7.75 (1H, s, H-6); ^{13}C NMR (125 MHz, $CDCl_3$) 41.8 (q, J_{CF} = 35.3, CH_2), 123.9 (C-Ar) 124.3 (q, J_{CF} = 278.9 Hz, CF_3), 144.3 (C-Ar), 152.7 (C-Ar), 156.6 (C-Ar); HRMS calcd. for $C_6H_7ClF_3N_4$ (ES+) m/z 227.0306 $[M+H]^+$, found 227.0310.

2-Chloro-N^4-(3,3,3-trifluoropropyl)pyrimidine-4,5-diamine (117)

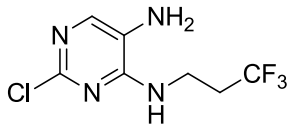

The nitropyrimidine **109** (0.506 g, 1.87 mmol) and tin(II) chloride (1.42 g, 7.48 mmol) were reacted in ethanol (19 ml) according to **general procedure D**. Silica chromatography (9:1 DCM/MeOH) gave the target compound as a red oil (0.394 g, 1.64 mmol, 88%). R_f 0.36 (9:1 DCM/MeOH); λ_{max} (EtOH/nm) 262, 302; IR (cm^{-1}) 3340, 3247, 3045, 1586; ^{1}H NMR (500 MHz, $CDCl_3$) 2.49 (2H, tq, J = 6.4 and 10.8 Hz, CH_2CF$_3$), 2.99 (2H, br, C^5-NH$_2$), 3.78 (2H, q, J = 6.4 Hz, NHCH_2), 5.33 (1H, br, C^4-NH), 7.66 (1H, s, H-6); ^{13}C NMR (125 MHz, $CDCl_3$) 33.3 (q, J_{CF} = 27.6 Hz, CH$_2$CF$_3$), 34.5 (q, J_{CF} = 3.4 Hz, NHCH$_2$), 123.8 (C-Ar), 126.6 (q, J_{CF} = 276.5 Hz, CF$_3$), 142.9 (C-Ar), 152.9 (C-Ar), 156.9 (C-Ar); HRMS calcd. for $C_7H_9ClF_3N_4$ (ES+) m/z 241.0462 $[M+H]^+$, found 241.0466.

2-Chloro-9-ethyl-8-methyl-9*H*-purine (118)

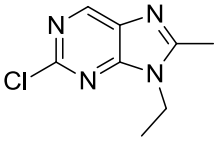

Diaminopyrimidine **110** (0.157 g, 0.91 mmol), triethyl orthoacetate (430 µl, 2.27 mmol) and TFA (7 µl, 0.09 mmol) were reacted in TFE (5 ml) according to **general procedure E**. Purification *via* chromatography on silica (19:1 DCM/MeOH) afforded the desired compound as a pale yellow solid (0.140 g, 0.71 mmol, 78%). R_f 0.36 (19:1 DCM/MeOH); M.p. 103-105 °C; λ_{max} (EtOH/nm) 224, 264; IR (cm^{-1}) 2975, 1600; ^{1}H NMR (500 MHz, DMSO-d_6) 1.31 (3H, t, J = 7.2 Hz, N^9-CH$_2$CH_3), 2.61 (3H, s, C^8-CH$_3$), 4.19 (2H, q, J = 7.2 Hz, N^9-CH_2CH$_3$), 8.82 (1H, s, H-6); ^{13}C NMR (125 MHz, DMSO-d_6) 13.8 (C^8-CH$_3$), 14.2 (CH$_2$$CH_3$), 37.5 ($CH_2CH_3$), 132.2 (C-Ar), 147.2 (C-Ar), 151.8 (C-Ar), 153.9 (C-Ar), 157.0 (C-Ar); HRMS calcd. for $C_8H_{10}N_4Cl$ (ES+) m/z 197.0589 $[M+H]^+$, found 197.0589.

2-Chloro-9-isopropyl-8-methyl-9*H*-purine (119)

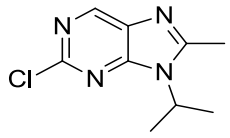

Diaminopyrimidine **111** (0.181 g, 0.97 mmol), triethyl orthoacetate (455 µl, 2.42 mmol) and TFA (7 µl, 0.10 mmol) were reacted in TFE (5 ml) according to **general procedure E**. Purification *via* chromatography on silica (19:1 DCM/MeOH) afforded the desired compound as a pale yellow solid (0.118 g, 0.56 mmol, 58%). R_f 0.46 (19:1 DCM/MeOH); M.p. 133-136 °C; λ_{max} (EtOH/nm) 260; IR (cm^{-1}) 2987, 1597; ^{1}H NMR (500 MHz, DMSO-d_6) 1.57 (6H, d, J = 6.8 Hz, N^9-CH(CH_3)$_2$), 2.62 (3H, s, C^8-CH_3), 4.74 (1H, sept, J = 6.8 Hz, N^9-CH(CH_3)$_2$), 8.82 (1H, s, H-6); ^{13}C NMR (125 MHz, DMSO-d_6) 14.7 (C^8-CH_3), 20.4 (N^9-CH(CH_3)$_2$), 48.4 (N^9-CH(CH_3)$_2$), 132.3 (C-Ar), 147.4 (C-Ar), 150.7 (C-Ar), 153.8 (C-Ar), 157.0 (C-Ar); HRMS calcd. for $C_9H_{12}N_4Cl$ (ES+) m/z 211.0745 $[M+H]^+$, found 211.0747.

2-Chloro-9-isobutyl-8-methyl-9*H*-purine (120)

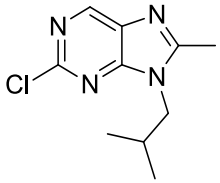

Diaminopyrimidine **113** (0.105 g, 0.52 mmol), triethyl orthoacetate (245 µl, 1.31 mmol) and TFA (4 µl, 0.05 mmol) were reacted in TFE (3 ml) according to **general procedure E**. Purification *via* chromatography on silica (19:1 DCM/MeOH) afforded the desired compound as a pale yellow solid (74 mg, 0.33 mmol, 63%). R_f 0.36 (19:1 DCM/MeOH); M.p. 101-104 °C; λ_{max} (EtOH/nm) 219, 275; IR (cm^{-1}) 2965, 1595; ^{1}H NMR (500 MHz, DMSO-d_6) 0.88 (6H, d, J = 6.8 Hz, -CH(CH_3)$_2$), 2.20 (1H, d sept, J = 6.8 and 7.8 Hz, -CH(CH_3)$_2$), 2.63 (3H, s, C^8-CH_3), 4.01 (2H, d, J = 7.8 Hz, N^9-CH_2), 8.90 (1H, s, H-6); ^{13}C NMR (125 MHz, DMSO-d_6) 14.3 (C^8-CH_3), 19.6 (CH_3), 28.0 (CH), 49.4 (CH_2), 132.3 (C-Ar), 147.6 (C-Ar), 151.8 (C-Ar), 154.6 (C-Ar), 157.0 (C-Ar); HRMS calcd. for $C_{10}H_{14}N_4Cl$ (ES+) m/z 225.0902 $[M+H]^+$, found 225.0905.

2-Chloro-8-methyl-9-phenyl-9*H*-purine (121)

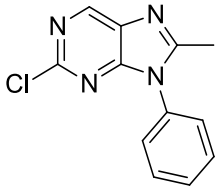

Diaminopyrimidine **114** (0.175 g, 0.79 mmol), triethyl orthoacetate (370 µl, 1.98 mmol) and TFA (6 µl, 0.08 mmol) were reacted in TFE (4 ml) according to **general procedure E** over 2.5 h. Purification *via* chromatography on silica (19:1 DCM/MeOH) afforded the desired compound as a orange solid (0.156 g, 0.64 mmol, 81%). R_f 0.44 (19:1 DCM/MeOH); M.p. 157-160 °C; λ_{max} (EtOH/nm) 227, 274; IR (cm^{-1}) 3060, 1588; ^{1}H NMR (500 MHz, DMSO-d_6) 2.49 (C^8-CH_3), 7.58-7.68 (5H, m, H-2'/3'/4'/5'/6'), 9.01 (1H, s, H-6); ^{13}C NMR (125 MHz, DMSO-d_6) 14.7 (C^8-CH_3), 127.5 (C-Ar), 129.6 (C-Ar), 129.8 (C-Ar), 132.5 (C-Ar), 132.9 (C-Ar), 148.0 (C-Ar), 152.4 (C-Ar), 154.9 (C-Ar), 156.4 (C-Ar); HRMS calcd. for $C_{12}H_{10}N_4Cl$ (ES+) *m/z* 245.0589 $[M+H]^+$, found 245.0594.

9-Benzyl-2-chloro-8-methyl-9*H*-purine (122)

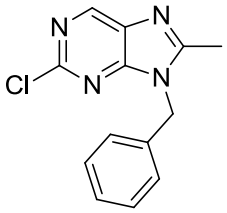

Diaminopyrimidine **115** (0.122 g, 0.52 mmol), triethyl orthoacetate (245 µl, 1.30 mmol) and TFA (4 µl, 0.05 mmol) were reacted in TFE (3 ml) according to **general procedure E**. Purification *via* chromatography on silica (19:1 DCM/MeOH) afforded the desired compound as a pale pink solid (97 mg, 0.38 mmol, 73%). R_f 0.42 (19:1 DCM/MeOH); M.p. 128-130 °C; λ_{max} (EtOH/nm) 223, 273; IR (cm^{-1}) 3031, 1598; ^{1}H NMR (500 MHz, DMSO-d_6) 2.54 (3H, s, C^8-CH_3), 5.46 (2H, s, N^9-CH_2), 7.17-7.21 (2H, m, H-2'/H-6'), 7.29-7.38 (3H, m, H-3'/H-4'/H-5'), 8.94 (1H, s, H-6); ^{13}C NMR (125 MHz, DMSO-d_6) 14.2 (C^8-CH_3), 45.2 (N^9-CH_2), 126.9 (C-Ar), 127.9 (C-Ar), 128.9 (C-Ar), 132.3 (C-Ar), 135.5 (C-Ar), 147.8 (C-Ar), 152.1 (C-Ar), 154.4 (C-Ar), 156.9 (C-Ar); HRMS calcd. for $C_{13}H_{12}N_4Cl$ (ES+) *m/z* 259.0745 $[M+H]^+$, found 259.0752.

2-Chloro-8-methyl-9-(2,2,2-trifluoroethyl)-9*H*-purine (123)

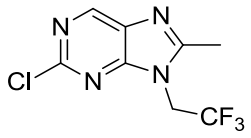

The diaminopyrimidine **116** (0.297 g, 1.31 mmol), triethyl orthoacetate (615 µl, 3.28 mmol) and TFA (10 µl, 0.13 mmol) were reacted in TFE (13 ml) according to **general procedure E**. Purification on silica (9:1 DCM/MeOH) gave the desired compound as a beige solid (0.250 g, 1.00 mmol, 76%). R_f 0.41 (9:1 DCM/MeOH); M.p. 140-143 °C; λ_{max} (EtOH/nm) 273; IR (cm^{-1}) 3000, 2955, 1599, 1577; ^{1}H NMR (500 MHz, DMSO-d_6) 2.68 (3H, s, C^8-CH_3), 5.29 (2H, q, J = 9.2 Hz, CH_2CF$_3$), 9.02 (1H, s, H-6); ^{13}C NMR (125 MHz, DMSO-d_6) 13.9 (CH_3), 42.9 (q, J_{CF} = 35.1 Hz, CH$_2$CF$_3$), 123.7 (q, J_{CF} = 279.5 Hz, CF$_3$), 132.3 (C-Ar), 140.5 (C-Ar), 152.4 (C-Ar), 154.6 (C-Ar), 156.9 (C-Ar); HRMS calcd. for $C_8H_7ClF_3N_4$ (ES+) m/z 251.0306 $[M+H]^+$, found 251.0310.

2-Chloro-8-methyl-9-(3,3,3-trifluoropropyl)-9*H*-purine (124)

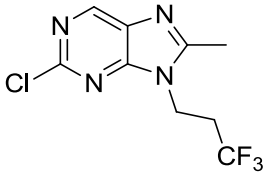

The diaminopyrimidine **117** (0.262 g, 1.09 mmol), triethyl orthoacetate (510 µl, 2.72 mmol) and TFA (8 µl, 0.11 mmol) were reacted in TFE (11 ml) according to **general procedure E**. Chromatography on silica (9:1 DCM/MeOH) gave the target compound as a beige solid (0.214 g, 0.81 mmol, 74%). R_f 0.43 (9:1 DCM/MeOH); M.p. 81-84 °C; λ_{max} (EtOH/nm) 274; IR (cm^{-1}) 3045, 1599, 1523; ^{1}H NMR (500 MHz, DMSO-d_6) 2.68 (3H, s, C^8-CH_3), 2.94 (2H, tq, J = 7.0 and 11.3 Hz, CH_2CF$_3$), 4.48 (2H, t, J = 7.0 Hz, N^9-CH_2), 8.94 (1H, s, H-6); ^{13}C NMR (125 MHz, DMSO-d_6) 14.0 (CH_3), 31.7 (q, J_{CF} = 27.9 Hz, CH$_2$CF$_3$), 35.8 (q, J_{CF} = 3.6 Hz, N-CH$_2$), 126.3 (q, J_{CF} = 277.8 Hz, CF$_3$), 132.5 (C-Ar), 147.7 (C-Ar), 151.9 (C-Ar), 154.3 (C-Ar), 156.7 (C-Ar); HRMS calcd. for $C_9H_9ClF_3N_4$ (ES+) m/z 265.0462 $[M+H]^+$, found 265.0469.

9-Ethyl-*N*-(4-methoxyphenyl)-8-methyl-9*H*-purin-2-amine (96)

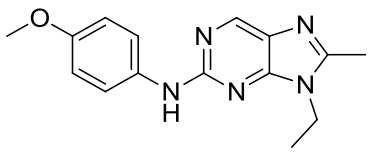

N^9-Ethylpurine **118** (30 mg, 0.15 mmol), 4-methoxyaniline (38 mg, 0.31 mmol) and TFA (60 µl, 0.77 mmol) were reacted in TFE (1 ml) according to **general procedure F**. Purification *via* chromatography on KP-NH silica (1:1 Petrol/EtOAc) afforded the desired compound as a pink solid (21 mg, 0.07 mmol, 49%). R_f 0.20 (1:1 Petrol/EtOAc, KP-NH); M.p. 160-163 °C; λ_{max} (EtOH/nm) 250, 335; IR (cm^{-1}) 3252, 3197, 3054, 3004, 1617; ^{1}H NMR (500 MHz, DMSO-d_6) 1.35 (3H, t, *J* = 7.3 Hz, -CH_2CH_3), 2.54 (3H, s, C^8-CH_3), 3.73 (3H, s, OCH_3), 4.15 (2H, q, *J* = 7.3 Hz, -CH_2CH_3), 6.88 (2H, d, *J* = 9.1 Hz, H-3'/H-5'), 7.73 (2H, d, *J* = 9.1 Hz, H-2'/H-6'), 8.60 (1H, s, H-6), 9.31 (1H, s, C^2-NH); ^{13}C NMR (125 MHz, DMSO-d_6) 13.7 (CH_2CH_3), 14.5 (C^8-CH_3), 36.7 (CH_2CH_3), 55.1 (OCH_3), 113.7 (C-Ar), 119.7 (C-Ar), 128.7 (C-Ar), 134.4 (C-Ar), 142.1 (C-Ar), 154.2 (C-Ar); HRMS calcd. for $C_{15}H_{18}N_5O$ (ES+) *m/z* 284.1506 $[M+H]^+$, found 284.1508.

Note: Unable to visualise all carbon signals by NMR.

9-Isobutyl-*N*-(4-methoxyphenyl)-8-methyl-9*H*-purin-2-amine (97)

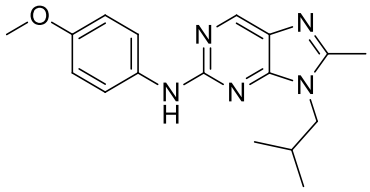

N^9-isobutylpurine **120** (30 mg, 0.13 mmol), 4-methoxyaniline (33 mg, 0.27 mmol) and TFA (50 µl, 0.67 mmol) were reacted in TFE (1 ml) according to **general procedure F**. Purification *via* chromatography on KP-NH silica (1:1 Petrol/EtOAc) afforded the desired compound as a pink solid (19 mg, 0.06 mmol, 47%). R_f 0.24 (1:1 Petrol/EtOAc, KP-NH); M.p. 152-154 °C; λ_{max} (EtOH/nm) 252, 332; IR (cm^{-1}) 3246, 3193, 3116, 2956, 2021, 1619; ^{1}H NMR (500 MHz, DMSO-d_6) 0.93 (6H, d, *J* = 6.8 Hz, -$CH(CH_3)_2$), 2.20-2.26 (1H, m, -$CH(CH_3)_2$), 2.52 (3H, s, C^8-CH_3), 3.73 (3H, s, OCH_3), 3.92 (2H, d, *J* = 7.5 Hz, N^9-CH_2), 6.88 (2H, d, *J* = 9.1 Hz, H-3'/H-5'), 7.73 (2H, d, *J* = 9.1 Hz, H-2'/H-6'), 8.61 (1H, s, H-6), 9.30 (1H, s, C^2-NH); ^{13}C NMR (125 MHz, DMSO-d_6) 14.2 (C^8-CH_3), 19.9 ($CH(CH_3)_2$), 28.4

($CH(CH_3)_2$), 49.2 (N^9-CH_2), 55.2 (OCH_3), 113.6 (C-Ar), 119.7 (C-Ar), 135.6 (C-Ar), 154.3 (C-Ar); HRMS calcd. for $C_{17}H_{22}N_5O$ (ES+) *m*/*z* 312.1822 $[M+H]^+$, found 312.1819.

Note: Unable to visualise all carbon signals by NMR.

_N_-(4-Methoxyphenyl)-8-methyl-9-phenyl-9*H*-purin-2-amine (98)

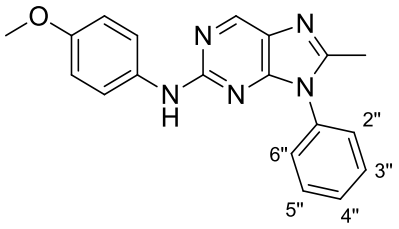

N^9-Phenylpurine **121** (30 mg, 0.14 mmol), 4-methoxyaniline (36 mg, 0.29 mmol) and TFA (55 µl, 0.71 mmol) were reacted in TFE (1 ml) according to **general procedure F**. KP-NH silica gel chromatography (1:1 Petrol/EtOAc) gave the target compound as a pale pink solid (14 mg, 0.05 mmol, 36%). R_f 0.26 (1:1 Petrol/EtOAc, KP-NH); M.p. 192-195 °C; λ_{max} (EtOH/nm) 276; IR (cm^{-1}) 3267, 3119, 2162, 1603; ^{1}H NMR (500 MHz, DMSO-d_6) 2.42 (3H, s, C^8-CH_3), 3.70 (3H, s, OCH_3), 6.79 (2H, d, *J* = 9.0 Hz, H-3'/H-5'), 7.57-7.67 (7H, m, H-2'/H-6' & H-2''/3''/4''/5''/6''), 8.72 (1H, s, H-6), 9.32 (1H, s, C2-NH); ^{13}C NMR (125 MHz, DMSO-d_6) 14.6 (C^8-CH_3), 55.1 (OCH_3), 113.6 (C-Ar), 119.9 (C-Ar), 127.4 (C-Ar), 128.9 (C-Ar), 129.5 (C-Ar), 134.2 (C-Ar), 139.5 (C-Ar), 139.8 (C-Ar), 147.1 (C-Ar), 153.7 (C-Ar); HRMS calcd. for $C_{19}H_{18}N_5O$ (ES+) *m*/*z* 332.1506 $[M+H]^+$, found 332.1508.

Note: Unable to visualise all carbon signals by NMR.

9-Benzyl-_N_-(4-methoxyphenyl)-8-methyl-9*H*-purin-2-amine (99)

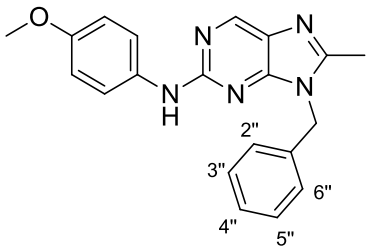

N^9-Benzylpurine **122** (30 mg, 0.12 mmol), 4-methoxyaniline (28 mg, 0.23 mmol) and TFA (45 µl, 0.58 mmol) were reacted in TFE (1 ml) according to **general procedure F**. Purification *via* chromatography on KP-NH silica (1:1 Petrol/EtOAc) afforded the desired

compound as a pink solid (16 mg, 0.05 mmol, 42%). R_f 0.24 (1:1 Petrol/EtOAc); M.p. 185-187 °C; λ_{max} (EtOH/nm) 275; IR (cm^{-1}) 3248, 3194, 2956, 2922, 2362, 1617; ^{1}H NMR (500 MHz, DMSO-d_6) 2.46 (3H, s, C^8-CH_3), 3.72 (3H, s, OCH_3), 5.37 (2H, s, N^9-CH_2), 6.86 (2H, d, *J* = 9.1 Hz, H-3'/H-5'), 7.25-7.28 (2H, m, H-2''/H-6''), 7.28-7.32 (1H, m, H-4''), 7.35-7.39 (2H, m, H-3''/H-5''), 7.69 (2H, d, *J* = 9.1 Hz, H-2'/H-6'), 8.65 (1H, s, H-6), 9.35 (1H, s, C^2-NH); ^{13}C NMR (125 MHz, DMSO-d_6) 55.2 (OCH_3), 113.7 (C-Ar), 119.8 (C-Ar), 127.0 (C-Ar), 128.8 (C-Ar), 135.2 (C-Ar), 140.5 (C-Ar), 141.5 (C-Ar), 148.0 (C-Ar), 156.6 (C-Ar); HRMS calcd. for $C_{20}H_{19}N_5O$ (ES+) *m*/*z* 346.1665 $[M+H]^+$, found 346.1662.

Note: Unable to visualise all carbon signals by NMR.

***N*-(4-methoxyphenyl)-8-methyl-9-(2,2,2-trifluoroethyl)-9*H*-purin-2-amine (100)**

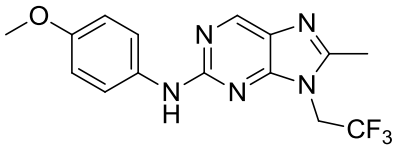

The 2-chloropurine intermediate **123** (98 mg, 0.39 mmol), 4-methoxyaniline (0.100 g, 0.80 mmol) and TFA (77 µl, 1.00 mmol) were reacted in TFE (4 ml) according to **general procedure F**. Purification on KP-NH silica (1:1 Petrol/EtOAc) afforded the desired compound as an off-white solid (89 mg, 0.27 mmol, 68%). R_f 0.21 (1:1 Petrol/EtOAc, KP-NH); M.p. 187-189 °C; λ_{max} (EtOH/nm) 275, 329; IR (cm^{-1}) 3253, 3199, 3125, 3070, 2965, 2836, 2361, 1621; ^{1}H NMR (500 MHz, DMSO-d_6) 2.56 (3H, s, C^8-CH_3), 3.74 (3H, s, OCH_3), 5.11 (2H, q, *J* = 9.0 Hz, CH_2CF_3), 6.88 (2H, d, *J* = 9.2 Hz, H-3'/H-5'), 7.73 (2H, d, *J* = 9.2 Hz, H-2'/H-6'), 8.68 (1H, s, H-6), 9.45 (1H, s, C^2-NH); ^{13}C NMR (125 MHz, DMSO-d_6) 13.6 (C^8-CH_3), 55.2 (OCH_3), 113.7 (C-Ar), 120.0 (C-Ar), 126.6 (C-Ar), 134.0 (C-Ar), 147.6 (C-Ar), 151.3 (C-Ar), 153.9 (C-Ar), 156.4 (C-Ar); HRMS calcd. for $C_{15}H_{15}F_3N_5O$ (ES+) *m*/*z* 338.1222 $[M+H]^+$, found 338.1223.

Note: Unable to visualise all carbon environments by ^{13}C NMR – masked by solvent peak.

***N*-(4-methoxyphenyl)-8-methyl-9-(3,3,3-trifluoropropyl)-9*H*-purin-2-amine (101)**

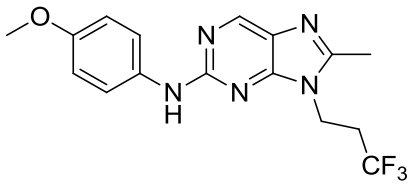

The 2-chloropurine intermediate **124** (0.100 mg, 0.38 mmol), 4-methoxyaniline (94 mg, 0.76 mmol) and TFA (73 µl, 0.94 mmol) were reacted in TFE (4 ml) according to **general procedure F**. Chromatography on silica (9:1 DCM/MeOH) gave the desired compound as an off-white solid (83 mg, 0.24 mmol, 62%). R_f 0.20 (1:1 Petrol/EtOAc, KP-NH); M.p. 148-150 °C; λ_{max} (EtOH/nm) 277, 330; IR (cm^{-1}) 3261, 3197, 1608; ^{1}H NMR (500 MHz, DMSO-d_6) 2.55 (3H, s, C^8-CH_3), 2.94 (2H, tq, J = 6.8 and 10.5 Hz, CH_2CF_3), 3.73 (3H, s, OCH_3), 4.38 (2H, t, J = 6.8 Hz, N^9-CH_2), 6.87 (2H, d, J = 9.0 Hz, H-3'/H-5'), 7.73 (2H, d, J = 9.0 Hz, H-2'/H-6'), 8.62 (1H, s, H-6), 9.36 (1H, s, C^2-NH); ^{13}C NMR (125 MHz, DMSO-d_6) 13.7 (C^8-CH_3), 31.7 (q, J_{CF} = 27.8 Hz, CH_2CF_3), 35.2 (q, J_{CF} = 4.0 Hz, N^9-CH_2), 55.1 (OCH_3), 113.6 (C-Ar), 119.9 (C-Ar), 126.9 (C-Ar), 134.3 (C-Ar), 147.0 (C-Ar), 151.3 (C-Ar), 153.8 (C-Ar), 156.1 (C-Ar); HRMS calcd. for $C_{16}H_{17}F_3N_5O$ (ES+) m/z 352.1380 $[M+H]^+$, found 352.1380.

Note: Unable to visualise all carbon environments by ^{13}C NMR.

Methyl 4-((8,9-dimethyl-9*H*-purin-2-yl)amino)benzoate (133)

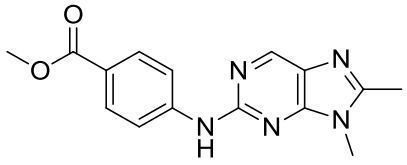

Methyl-4-aminobenzoate (0.497 g, 3.29 mmol), 2-chloropurine intermediate **56** (0.308 g, 1.64 mmol) and TFA (315 µl, 4.11 mmol) were reacted in TFE (16 ml) according to **general procedure B** over 72 h. Purification on KP-NH silica (1:1 Petrol/EtOAc) gave the desired product as a pale yellow solid (0.213 g, 0.71 mmol, 43%). R_f 0.16 (1:1 Petrol/EtOAc); M.p. 259-261 °C; λ_{max} (EtOH/nm) 225, 302, 330; IR (cm^{-1}) 3250, 3183, 2953, 1706, 1596, 1533; ^{1}H NMR (500 MHz, DMSO-d_6) 2.54 (3H, s, C^8-CH_3), 3.70 (3H, s, N^9-CH_3), 3.82 (3H, s, OCH_3), 7.90 (2H, d, J = 8.9 Hz, H-3'/H-5'), 8.01 (2H, d, J = 8.9 Hz, H-2'/H-6'), 8.72 (1H, H-6), 10.06 (1H, s, C^2-NH); ^{13}C NMR (125 MHz, DMSO-d_6) 13.8 (C^8-CH_3), 28.2 (N^9-CH_3), 51.6 (OCH_3), 117.0 (C-Ar), 120.9 (C-Ar), 128.1 (C-Ar), 130.2 (C-Ar), 145.8 (C-Ar), 146.4

(C-Ar), 153.4 (C-Ar), 153.6 (C-Ar), 154.9 (C-Ar), 166.1 (C=O); HRMS calcd. for $C_{15}H_{16}N_5O_2$ (ES+) *m*/*z* 298.1299 $[M+H]^+$, found 298.1307.

4-((8,9-Dimethyl-9*H*-purin-2-yl)amino)benzoic acid (132)

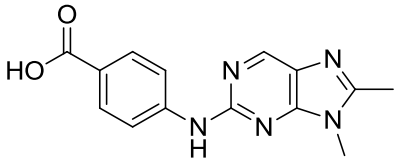

Lithium hydroxide (0.305 g, 12.8 mmol) was added to a suspension of the methyl ester **133** (0.190 g, 0.64 mmol) in THF/H_2O (1:1, 12 ml) at 65 °C. After stirring at this temperature for 2 h, the mixture was allowed to cool to RT and the pH adjusted to pH 7 with 2M HCl. The resultant white precipitate was collected by filtration, washed with cold water (5 ml) and dried in a vacuum oven. The desired product was obtained as an off-white solid (0.154 g, 0.54 mmol, 85%). R_f 0.24 (9:1 DCM/MeOH, 0.1% AcOH); M.p. 346-349 °C; λ_{max} (EtOH/nm) 293.5, 329.0; IR (cm^{-1}) 3297, 3037, 2157, 1976, 1684; ^{1}H NMR (500 MHz, DMSO-d_6) 2.58 (3H, s, C^8-CH_3), 3.72 (3H, s, N^9-CH_3), 7.88 (2H, d, *J* = 8.9 Hz, H-3', H-5'), 7.99 (2H, d, *J* = 8.9 Hz, H-2', H-6'), 8.76 (1H, s, H-6), 10.06 (1H, s, C^2-NH), 12.47 (1H, br, COOH); ^{13}C NMR (125 MHz, TFA) 10.9 (C^8-CH_3), 28.4 (N^9-CH_3), 115.3 (C-Ar), 120.4 (C-Ar), 124.9 (C-Ar), 130.6 (C-Ar), 138.0 (C-Ar), 139.6 (C-Ar), 150.8 (C-Ar), 153.7 (C-Ar), 161.6 (C-Ar), 170.8 (C=O); HRMS calcd. for $C_{14}H_{14}N_5O_2$ (ES+) *m*/*z* 284.1142 $[M+H]^+$, found 284.1144.

4-((8,9-Dimethyl-9*H*-purin-2-yl)amino)-*N*-(4-methoxybenzyl)benzamide (134)

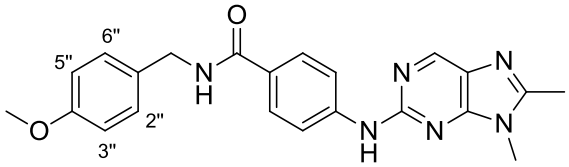

The carboxylic acid **132** (50 mg, 0.18 mmol), CDI (57 mg, 0.35 mmol), DIPEA (62 µl, 0.35 mmol) and 4-methoxybenzylamine (92 µl, 0.71 mmol) were reacted in dry DMF (2 ml) according to **general procedure J**. Purification on silica gel (9:1 DCM/MeOH) gave the desired compound as an off-white waxy solid (71 mg, 0.18 mmol, 100%). R_f 0.44 (9:1 DCM/MeOH); M.p. 246-248 °C; λ_{max} (EtOH/nm) 300, 329; IR (cm^{-1}) 3340, 2922, 2834, 1609, 1509; ^{1}H NMR (500 MHz, DMSO-d_6) 2.54 (3H, s, C^8-CH_3), 3.69 (3H, s, N^9-CH_3),

3.73 (3H, s, OCH_3), 4.41 (2H, d, *J* = 6.0 Hz, NHCH_2), 6.89 (2H, d, *J* = 8.7 Hz, H-3’’/H-5’’), 7.25 (2H, d, *J* = 8.7 Hz, H-2’’/H-6’’), 7.84 (2H, d, *J* = 8.9 Hz, H-2’/H-6’), 7.94 (2H, d, *J* = 8.9 Hz, H-3’/H-5’), 8.70 (1H, s, H-6), 8.77 (1H, t, *J* = 6.0 Hz, N*H*CH_2), 9.86 (1H, s, C^2-NH); ^{13}C NMR (125 MHz, DMSO-d_6) 13.8 (C^8-CH_3), 28.1 (N^9-CH_3), 41.9 ($NHCH_2$), 55.0 (OCH_3), 113.6 (C-Ar), 116.9 (C-Ar), 126.1 (C-Ar), 127.8 (C-Ar), 128.0 (C-Ar), 128.5 (C-Ar), 132.0 (C-Ar), 143.9 (C-Ar), 146.5 (C-Ar), 153.1 (C-Ar), 153.7 (C-Ar), 155.2 (C-Ar), 158.1 (C-Ar), 165.8 (C=O); HRMS calcd. for $C_{22}H_{23}N_6O_2$ (ES+) *m*/*z* 403.1877 $[M+H]^+$, found 403.1879.

4-((8,9-Dimethyl-9*H*-purin-2-yl)amino)benzamide (126)

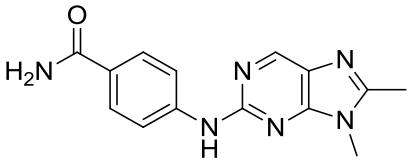

4-Methoxybenzamide **134** (55 mg, 0.14 mmol) and TFA (1.5 ml) were reacted according to **general procedure K**. Chromatography on silica (9:1 DCM/MeOH) gave the desired compound as an off-white solid (18 mg, 0.06 mmol, 45%). R_f 0.31 (9:1 DCM/MeOH); M.p. 314-317 °C; λ_{max} (EtOH/nm) 299.0, 329.0; IR (cm^{-1}) 3366, 3269, 3172, 2938, 2161, 1666, 1605; ^{1}H NMR (500 MHz, DMSO-d_6) 2.54 (3H, s, C^8-CH_3), 3.69 (3H, s, N^9-CH_3), 7.13 (1H, br, CON*H*H’), 7.77 (1H, br, CONH*H’*), 7.83 (2H, d, *J* = 8.9 Hz, H-2’/H-6’), 7.93 (2H, d, *J* = 8.9 Hz, H-3’/H-5’), 8.70 (1H, s, H-6), 9.85 (1H, s, C^2-NH); ^{13}C NMR (125 MHz, DMSO-d_6) 13.8 (C^8-CH_3), 28.1 (N^9-CH_3), 116.8 (C-Ar), 128.3 (C-Ar), 146.7 (C-Ar); HRMS calcd. for $C_{14}H_{15}N_6O$ (ES+) *m*/*z* 283.1302 $[M+H]^+$, found 283.1299.

Note: Unable to visualise all carbon environments by ^{13}C NMR – insufficient material.

4-((8,9-Dimethyl-9*H*-purin-2-yl)amino)-*N*-methylbenzamide (127)

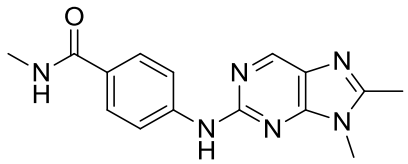

The carboxylic acid **132** (50 mg, 0.18 mmol), CDI (58 mg, 0.35 mmol), DIPEA (62 µl, 0.35 mmol) and methylamine (2M solution in THF, 0.35 ml) were reacted in dry DMF (2 ml) according to **general procedure J**. Purification by column chromatography on silica (9:1 DCM/MeOH) gave the target compound with imidazole contamination observed by ^{1}H

NMR. The crude product was suspended in water and stirred at RT for 30 mins, before being filtered, washed with cold water (1 ml) and dried in a vacuum oven. The pure target compound was acquired as an off-white solid (39 mg, 0.13 mmol, 72%). R_f 0.33 (9:1 DCM/MeOH); M.p. 313-315 °C; λ_{max} (EtOH/nm) 297.0; IR (cm^{-1}) 3585, 3277, 3108, 3012, 2914, 2796, 2609, 1605, 1507; ^{1}H NMR (500 MHz, DMSO-d_6) 2.54 (3H, s, C^8-CH_3), 2.78 (3H, d, J = 4.5 Hz, NHCH_3), 3.69 (3H, s, N^9-CH_3), 7.79 (2H, d, J = 8.8 Hz, H-2'/H-6'), 7.93 (2H, d, J = 8.8 Hz, H-3'/H-5'), 8.22 (1H, q, J = 4.5 Hz, N$H$$CH_3$), 8.70 (1H, s, H-6), 9.84 (1H, s, C^2-NH); ^{13}C NMR (125 MHz, DMSO-d_6) 13.8 (C^8-CH_3), 26.1 (NHCH_3), 28.1 (N^9-CH_3), 116.9 (C-Ar), 127.7 (C-Ar), 143.7 (C-Ar), 146.5 (C-Ar), 166.3 (C=O); HRMS calcd. for $C_{15}H_{17}N_6O$ (ES+) m/z 297.1458 $[M+H]^+$, found 297.1461.

Note: Unable to visualise all carbon environments by ^{13}C NMR.

4-((8,9-Dimethyl-9*H*-purin-2-yl)amino)-*N*-phenylbenzamide (128)

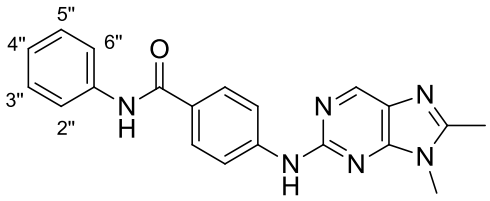

The carboxylic acid **132** (50 mg, 0.18 mmol), CDI (55 mg, 0.34 mmol), DIPEA (62 µl, 0.35 mmol) and aniline (65 µl, 0.71 mmol) were reacted in dry DMF (2 ml) according to **general procedure J**. Purification *via* silica gel chromatography (9:1 DCM/MeOH) gave the desired compound as an off-white solid (50 mg, 0.14 mmol, 77%). R_f 0.38 (9:1 DCM/MeOH); M.p. 282-285 °C; λ_{max} (EtOH/nm) 306, 333; IR (cm^{-1}) 3470, 3331, 3033, 1595, 1525; ^{1}H NMR (500 MHz, DMSO-d_6) 2.55 (3H, s, C^8-CH_3), 3.71 (3H, s, N^9-CH_3), 7.06-7.11 (1H, m, H-4''), 7.33-7.37 (2H, m, H-3''/H-5''), 7.77-7.81 (2H, m, H-2''/H-6''), 7.94 (2H, d, J = 8.8 Hz, H-2'/H-6'), 8.02 (2H, d, J = 8.8 Hz, H-3'/H-5'), 8.73 (1H, s, H-6), 9.96 (1H, s, NH), 10.04 (1H, s, NH); ^{13}C NMR (125 MHz, DMSO-d_6) 13.8 (C^8-CH_3), 28.1 (N^9-CH_3), 116.9 (C-Ar), 120.2 (C-Ar), 123.2 (C-Ar), 126.3 (C-Ar), 127.9 (C-Ar), 128.5 (C-Ar), 139.5 (C-Ar), 144.3 (C-Ar), 146.6 (C-Ar), 153.7 (C-Ar), 155.2 (C-Ar), 165.1 (C=O); HRMS calcd. for $C_{20}H_{19}N_6O$ (ES+) m/z 359.1615 $[M+H]^+$, found 359.1610.

Note: Unable to visualise all carbon environments by ^{13}C NMR.

8,9-Dimethyl-*N*-(4-nitrophenyl)-9*H*-purin-2-amine (136)

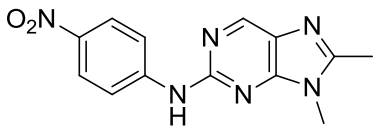

The 2-chloropurine intermediate **56** (0.500 mg, 2.74 mmol), 4-nitroaniline (0.755 g, 5.48 mmol) and TFA (1.05 ml, 13.7 mmol) were reacted in TFE (20 ml) according to **general procedure F** over 6 h. Purification through chromatography on silica (19:1 DCM/MeOH) afforded the desired compound as a pale brown solid (0.232 g, 0.82 mmol, 30%). R_f 0.40 (19:1 DCM/MeOH); M.p. 267-268 °C; λ_{max} (EtOH/nm) 237, 370; IR (cm^{-1}) 3245, 3197, 3120, 3063, 2413, 1586, 1551; ^{1}H NMR (500 MHz, DMSO-d_6) 2.57 (3H, s, C^8-CH_3), 3.73 (3H, s, N^9-CH_3), 8.12 (2H, d, J = 9.4 Hz, H-2'/H-6'), 8.21 (2H, d, J = 9.4 Hz, H-3'/H-5'), 8.78 (1H, s, H-6), 10.45 (1H, s, C^2-NH); ^{13}C NMR (125 MHz, DMSO-d_6) 13.8 (C^8-CH$_3$), 28.3 (N^9-CH$_3$), 116.9 (C-Ar), 125.1 (C-Ar), 128.6 (C-Ar), 139.7 (C-Ar), 146.4 (C-Ar), 147.7 (C-Ar), 153.6 (C-Ar), 154.0 (C-Ar), 154.4 (C-Ar); HRMS calcd. for $C_{13}H_{13}N_6O_2$ (ES+) *m*/*z* 285.1095 $[M+H]^+$, found 285.1092.

N^1-(8,9-Dimethyl-9*H*-purin-2-yl)benzene-1,4-diamine (135)

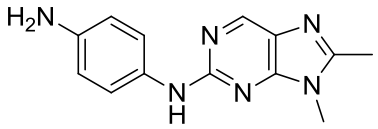

The nitro compound **136** (0.197 g, 0.69 mmol), palladium on carbon (20 mg, 10% w/w) and ammonium formate (0.435 g, 6.93 mmol) were reacted in methanol (7 ml) according to **general procedure G**. Silica gel chromatography (9:1 DCM/MeOH) gave the target compound as a pale brown solid (0.156 g, 0.61 mmol, 89%). R_f 0.36 (9:1 DCM/MeOH); M.p. 198-201 °C; λ_{max} (EtOH/nm) 281, 334; IR (cm^{-1}) 3590, 3439, 3333, 3247, 3192, 3052, 1639, 1512; ^{1}H NMR (500 MHz, DMSO-d_6) 2.49 (3H, s, C^8-CH_3), 3.61 (3H, s, N^9-CH_3), 5.11 (2H, br, Ar-NH_2), 6.53 (2H, d, J = 8.7 Hz, H-3'/H-5'), 7.43 (2H, d, J = 8.7 Hz, H-2'/H-6'), 8.53 (1H, s, H-6), 8.97 (1H, s, C^2-NH); ^{13}C NMR (125 MHz, DMSO-d_6) 13.7 (C^8-CH_3), 28.0 (N^9-CH_3), 114.0 (C-Ar), 120.5 (C-Ar), 126.7 (C-Ar), 130.5 (C-Ar), 143.1 (C-Ar), 146.5 (C-Ar), 151.6 (C-Ar), 153.9 (C-Ar), 156.5 (C-Ar); HRMS calcd. for $C_{13}H_{15}N_6$ (ES+) *m*/*z* 255.1353 $[M+H]^+$, found 255.1359.

1-(4-((8,9-Dimethyl-9*H*-purin-2-yl)amino)phenyl)urea (129)

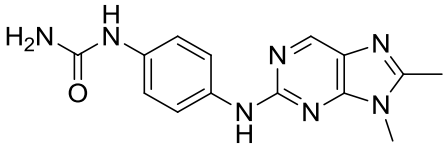

Sodium cyanate (12 mg, 0.19 mmol) in water (1 ml) was added to a solution of the aniline **135** (40 mg, 0.16 mmol) in acetic acid (1 ml) and water (2 ml). The mixture was stirred at RT for 30 min, before being taken to pH 7-8 through addition of sat. $NaHCO_3$ solution and extracted with EtOAc (4 x 15 ml). The combined organic extracts were dried ($MgSO_4$) and concentrated, and the crude residue purified on silica (9:1 DCM/MeOH) to afford the desired compound as a white solid (20 mg, 0.07 mmol, 44%). R_f 0.34 (9:1 DCM/MeOH); M.p. 316-319 °C; λ_{max} (EtOH/nm) 282.0; IR (cm^{-1}) 3362, 3285, 3178, 2361, 2164, 1662, 1604; ^1H NMR (500 MHz, DMSO-d_6) 3.65 (3H, s, N^9-CH_3), 5.73 (2H, s, NHCONH_2), 7.29 (2H, d, *J* = 9.0 Hz, H-3'/H-5'), 7.69 (2H, d, *J* = 9.0 Hz, H-2'/H-6'), 8.33 (1H, s, N*H*CONH$_2$), 8.59 (1H, s, H-6), 9.32 (1H, s, C^2-NH); ^{13}C NMR (125 MHz, DMSO-d_6) 13.8 (C^8-CH_3), 28.0 (N^9-CH_3), 118.4 (C-Ar), 118.8 (C-Ar), 126.2 (C-Ar), 127.1 (C-Ar), 135.1 (C-Ar), 146.6 (C-Ar), 156.0 (quat-C); HRMS calcd. for $C_{14}H_{16}N_7O$ (ES+) *m*/*z* 298.1411 $[M+H]^+$, found 298.1414.

Note: Unable to visualise all carbon environments by ^{13}C NMR.

***tert*-Butyl (4-aminophenyl) carbamate (138)[245]**

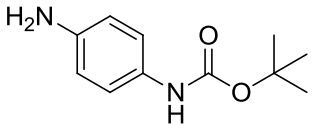

K_2CO_3 (0.470 g, 3.39 mmol) in water (2 ml) was added to a solution of 4-phenylenediamine (1.00 g, 9.25 mmol) in THF (10 ml) and DMF (3 ml). Boc_2O (0.672 g, 3.08 mmol) in THF (2 ml) was added dropwise and the resultant solution was stirred at RT for 4 h. The reaction mixture was poured onto ice (15 g) and extracted with chloroform (3 x 20 ml). The combined organic extracts were dried through a phase separator, evaporated to dryness, and the resultant residue was purified though chromatography on silica (1:1 Petrol/EtOAc). The target compound was obtained as a pale orange oil which crystallised on cooling (0.612 g, 2.94 mmol, 95%). R_f 0.39 (1:1 Petrol/EtOAc); M.p. 114-117 °C (Lit.[245] 105-106 °C); λ_{max} (EtOH/nm) 251, 300; IR (cm^{-1}) 3372, 3298, 3213, 2989, 1687, 1523; ^1H NMR (500 MHz,

DMSO-d_6) 1.45 (9H, s, OC(CH_3)$_3$), 4.73 (2H, s, Ar-NH_2), 6.47 (2H, d, *J* = 8.8 Hz, H-3/H-5), 7.07 (2H, d, *J* = 8.8 Hz, H-2/H-6), 8.78 (1H, s, NHCO); ^{13}C NMR (125 MHz, DMSO-d_6) 28.2 (-OC(*C*H_3)$_3$), 78.1 (-O*C*(CH$_3$)$_3$), 113.9 (C-Ar), 120.1 (C-Ar), 128.5 (C-Ar), 143.9 (C-Ar), 153.1 (C=O); LRMS (ES+) *m*/*z* 209.2 $[M+H]^+$.

tert-Butyl (4-(3-methylureido)phenyl) carbamate (139)

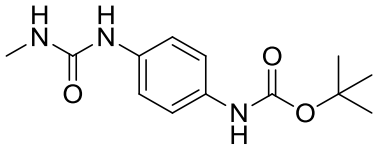

N-Succinimidyl *N*-methyl carbamate (0.605 g, 3.51 mmol) was added to a solution of the aniline **138** (0.488 g, 2.34 mmol) and DIPEA (0.61 ml, 3.51 mmol) in dry DMF (12 ml). The reaction mixture was heated at 70 °C for 18 h, before being cooled to RT and concentrated *in vacuo*. The crude residue was purified using silica gel chromatography (19:1 DCM/MeOH) to afford the target compound as pale yellow oil which solidified on cooling (0.410 g, 1.54 mmol, 66%). R_f 0.41 (19:1 DCM/MeOH); M.p. 155-158 °C; λ_{max} (EtOH/nm) 257; IR (cm^{-1}) 3380, 3263, 2976, 2929, 1696, 1662, 1537; ^{1}H NMR (500 MHz, DMSO-d_6) 1.45 (9H, s, OC(CH_3)$_3$), 2.62 (3H, d, *J* = 4.6 Hz, NHCH_3), 5.91 (1H, q, *J* = 4.6 Hz, N*H*CH$_3$), 7.22-7.31 (4H, m, H-2/H-3/H-5/H-6), 8.32 (1H, s, NH), 9.10 (1H, s, NH); ^{13}C NMR (125 MHz, DMSO-d_6) 25.2 (NH*C*H$_3$), 28.1 (-OC(*C*H$_3$)$_3$), 78.6 (-O*C*(CH$_3$)$_3$), 118.2 (C-Ar), 118.7 (C-Ar), 133.1 (C-Ar), 135.2 (C-Ar), 152.9 (C=O), 155.9 (C=O); LRMS (ES+) *m*/*z* 266.1 $[M+H]^+$, 166.1 $[M+H\text{-Boc}]^+$.

1-(4-Aminophenyl)-3-methylurea (140)[246]

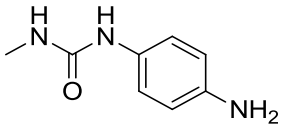

The Boc-protected aniline **139** (0.578 g, 2.18 mmol) and TFA (1.68 ml, 21.8 mmol) were reacted in DCM (20 ml) according to **general procedure L**. Silica gel chromatography (9:1 DCM/MeOH) gave the target compound as an off-white solid (0.328 g, 1.98 mmol, 91%). R_f 0.26 (9:1 DCM/MeOH); M.p. 150-153 °C (Lit.[246] 147-148 °C); λ_{max} (EtOH/nm) 252, 302; IR (cm^{-1}) 3331, 3302, 3038, 2944, 2902, 2808, 1876, 1596, 1577, 1506; ^{1}H NMR (500 MHz, DMSO-d_6) 2.60 (3H, d, *J* = 4.7 Hz, NHCH_3), 4.67 (2H, s, Ar-NH_2), 5.74 (1H, q, *J* = 4.7 Hz,

N*H*CH_3), 6.46 (2H, d, *J* = 8.7 Hz, H-3/H-5), 6.99 (2H, d, *J* = 8.7 Hz, H-2/H-6), 7.89 (1H, s, CONH); ^{13}C NMR (125 MHz, DMSO-d_6) 26.3 (NH*C*H_3), 114.1 (C-Ar), 120.5 (C-Ar), 129.6 (C-Ar), 143.4 (C-Ar), 156.4 (C=O); LRMS (ES-) *m*/*z* 166.1 $[M+H]^+$.

1-(4-((8,9-Dimethyl-9*H*-purin-2-yl)amino)phenyl)-3-methylurea (130)

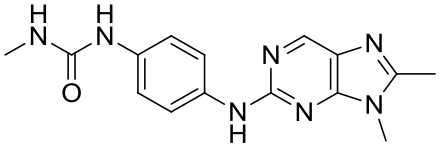

The 2-chloropurine **56** (50mg, 0.27 mmol), aniline **140** (55 mg, 0.33 mmol), $Pd_2(dba)_3$ (26 mg, 0.03 mmol), XPhos (15 mg, 0.03 mmol) and K_2CO_3 (84 mg, 0.60 mmol) were reacted in MeCN (3 ml) according to **general procedure M**. Purification on silica (9:1 DCM/MeOH) afforded the target compound as an off-white solid (41 mg, 0.13 mmol, 49%). R_f 0.20 (9:1 DCM/MeOH); M.p. 253-256 °C; λ_{max} (EtOH/nm) 283; IR (cm^{-1}) 3363, 3281, 1613, 1551, 1510; ^{1}H NMR (500 MHz, DMSO-d_6) 2.52 (3H, s, C8-CH3), 2.64 (3H, d, *J* = 4.6 Hz, NHC*H3*), 3.65 (3H, s, N9-CH3), 5.92 (1H, q, *J* = 4.6 Hz, N*H*CH3), 7.29 (2H, d, *J* = 8.9 Hz, H-3'/H-5'), 7.68 (2H, d, *J* = 8.9 Hz, H-2'/H-6'), 8.30 (1H, s, CONH), 8.59 (1H, s, H-6), 9.32 (1H, s, C2-NH); ^{13}C NMR (125 MHz, DMSO-d_6) 13.8 (C^8-CH_3), 26.2 (NHCH_3), 28.0 (N^9-CH_3), 118.4 (C-Ar), 118.8 (C-Ar), 127.1 (C-Ar), 134.1 (C-Ar), 135.0 (C-Ar), 146.5 (C-Ar), 152.1 (C-Ar), 153.8 (C-Ar), 156.0, 156.1; HRMS calcd. for $C_{15}H_{18}N_7O$ (ES+) *m*/*z* 312.1567 $[M+H]^+$, found 312.1566.

Note: Unable to distinguish carbon signals at 156.0 and 156.1 by ^{13}C NMR.

1-(4-((8,9-Dimethyl-9*H*-purin-2-yl)amino)phenyl)-3-phenylurea (131)

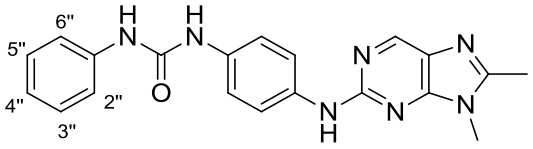

Phenyl isocyanate (21 µl, 0.19 mmol) in dry THF (0.5 ml) was added dropwise to a solution of the 2-anilinopurine **135** (40 mg, 0.16 mmol) in dry THF (2 ml). The mixture was stirred at RT for 18 h, before being concentrated *in vacuo* and the residue dissolved in EtOAc (5 ml). The organic was washed with sat. $NaHCO_3$ solution (5 ml) and brine (5 ml) before being dried ($MgSO_4$) and evaporated to dryness. The crude residue was purified by silica gel

chromatography (9:1 DCM/MeOH) to give the desired compound as an off-white solid (44 mg, 0.12 mmol, 73%). R_f 0.36 (9:1 DCM/MeOH); M.p. 310-313 °C; λ_{max} (EtOH/nm) 253.5, 286.5; IR (cm^{-1}) 3271, 3048, 2159, 1617; ^{1}H NMR (500 MHz, DMSO-d_6) 2.52 (3H, s, C^8-CH_3), 3.66 (3H, s, N^9-CH_3), 6.96 (1H, dddd, *J* = 1.2, 1.2, 7.4 and 7.4 Hz, H-4''), 7.28 (2H, dd, *J* = 7.4 and 7.5 Hz, H-3''/H-5''), 7.36 (2H, d, *J* = 8.9 Hz, H-3'/H-5'), 7.45 (2H, dd, *J* = 1.2 and 7.5 Hz, H-2''/H-6''), 7.76 (2H, d, *J* = 8.9 Hz, H-2'/H-6'), 8.50 (1H, br, N*H*CONH), 8.60-8.64 (2H, m, H-6 & NHCON*H*), 9.40 (1H, s, C^2-NH); ^{13}C NMR (125 MHz, DMSO-d_6) 13.8 (C^8-CH_3), 28.0 (N^9-CH_3), 118.0 (C-Ar), 118.8 (C-Ar), 118.9 (C-Ar), 128.7 (C-Ar), 131.8 (C-Ar), 133.0 (C-Ar), 152.6 (quat-C), 153.8 (quat-C), 155.9 (quat-C); HRMS calcd. for $C_{20}H_{20}N_7O$ (ES+) *m/z* 374.1724 $[M+H]^+$, found 374.1727.

Note: Unable to visualise all carbon environments by ^{13}C NMR.

***N*-(4-((8,9-Dimethyl-9*H*-purin-2-yl)amino)phenyl)acetamide (141)**

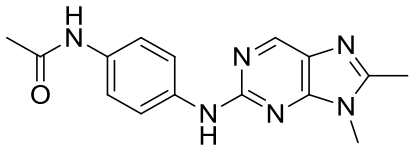

The 2-chloropurine **56** (50mg, 0.27 mmol), 4-aminoacetanilide (49 mg, 0.33 mmol), $Pd_2(dba)_3$ (27 mg, 0.03 mmol), XPhos (14 mg, 0.03 mmol) and K_2CO_3 (83 mg, 0.60 mmol) were reacted in MeCN (3 ml) according to **general procedure M**. Silica gel chromatography (9:1 DCM/MeOH) gave the desired compound as a beige solid (49 mg, 0.17 mmol, 62%). R_f 0.22 (9:1 DCM/MeOH); M.p. 291-293 °C; λ_{max} (EtOH/nm) 286.5, 333.0; IR (cm^{-1}) 3635, 3292, 3061, 1616, 1563, 1511; ^{1}H NMR (500 MHz, DMSO-d_6) 2.02 (3H, s, $COCH_3$), 2.49 (3H, s, C^8-CH_3), 3.66 (3H, s, N^9-CH_3), 7.48 (2H, d, *J* = 9.0 Hz, H-3'/H-5'), 7.76 (2H, d, *J* = 9.0 Hz, H-2'/H-6'), 8.61 (1H, s, H-6), 9.43 (1H, s, C^2-NH); ^{13}C NMR (125 MHz, DMSO-d_6) 13.8 (C^8-CH_3), 23.8 ($COCH_3$), 28.0 (N^9-CH_3), 118.4 (C-Ar), 119.5 (C-Ar), 127.2 (C-Ar), 132.7 (C-Ar), 136.6 (C-Ar), 146.5 (C-Ar), 152.3 (C-Ar), 153.8 (C-Ar), 155.8 (C-Ar), 167.6 (C=O); HRMS calcd. for $C_{15}H_{17}N_6O$ (ES+) *m/z* 297.1458 $[M+H]^+$, found 297.1464.

***N*-(4-Methoxyphenyl)-9-methyl-8-((phenylamino)methyl)-9*H*-purin-2-amine (144)**

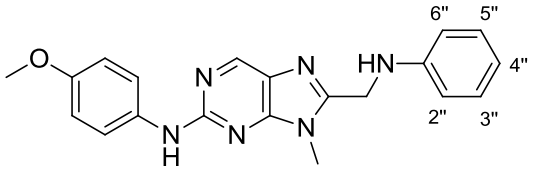

n-Butyllithium (0.37 ml, 0.94 mmol) was added dropwise to a solution of distilled DIPA (0.13 ml, 0.94 mmol) in dry THF (1.5 ml) at -90 °C under N_2. After 10 min, the LDA solution added dropwise to a solution of the purine **144** (100 mg, 0.39 mmol) in dry THF (3.5 ml) at -90 °C under N_2. The mixture was maintained at -90 °C for 15 min, before dry DMF (0.18 ml, 2.34 mmol) was added dropwise. The resultant suspension was allowed to warm to RT over 2 h and quenched with sat. NH_4Cl solution (2 ml). The mixture was extracted with EtOAc (2 x 8 ml) and the combined organic extracts were evaporated to dryness. The crude aldehyde residue was dissolved in DCM (4 ml) to which $MgSO_4$ was added, followed by aniline (35 µl, 0.39 mmol). The reaction mixture was stirred at RT for 2 h, before $NaBH_4$ (44 mg, 1.17 mmol) was added, and the mixture stirred at RT for a further 6 h. The drying reagent was removed through filtration and the filtrate concentrated *in vacuo*. Chromatography on silica (19:1 DCM/MeOH) of the crude residue gave the target compound as a yellow solid (52 mg, 0.14 mmol, 36%). R_f 0.38 (19:1 DCM/MeOH); M.p. 174-176 °C; λ_{max} (EtOH/nm) 245.0, 276.5, 340.5; IR (cm^{-1}) 3387, 3001, 2901, 2831, 1626, 1599, 1506; ^{1}H NMR (500 MHz, DMSO-d_6) 3.72-3.75 (6H, m, N^9-CH_3 & -OCH_3), 4.52 (2H, d, *J* = 5.7 Hz, NHC*H*$_2$), 6.25 (1H, t, *J* = 5.7 Hz, N*H*CH_2), 6.58 (1H, dddd, *J* = 0.9, 0.9, 7.3 and 7.3 Hz, H-4''), 6.76 (2H, dd, *J* = 0.9 and 8.5 Hz, H-2''/H-6''), 6.88 (2H, d, *J* = 9.1 Hz, H-3'/H-5'), 7.09 (2H, dd, *J* = 7.3 and 8.5 Hz, H-3''/H-5''), 7.74 (2H, d, *J* = 9.1 Hz, H-2'/H-6'), 8.70 (1H, s, H-6), 9.38 (1H, s, C^2-NH); ^{13}C NMR (125 MHz, DMSO-d_6) 28.2 (N^9-CH_3), 40.8 ($NHCH_2$), 55.1 (OCH_3), 112.4 (C-Ar), 113.7 (C-Ar), 116.4 (C-Ar), 119.9 (C-Ar), 126.7 (C-Ar), 128.9 (C-Ar), 134.3 (C-Ar), 147.7 (C-Ar), 148.2 (C-Ar), 152.4 (C-Ar), 153.8 (C-Ar), 153.9 (C-Ar), 156.4 (C-Ar); HRMS calcd. for $C_{20}H_{21}N_6O$ (ES+) *m*/*z* 361.1771 $[M+H]^+$, found 361.1776.

2-Fluoro-9-(tetrahydro-2*H*-pyran-2-yl)-6-(2-(triisopropylsilyl)ethynyl)-9*H*-purine (159)

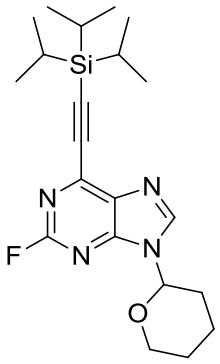

6-Chloropurine intermediate **51** (0.500 g, 1.95 mmol), (triisopropylsilyl)acetylene (0.49 ml, 2.20 mmol), copper iodide (7 mg, 0.02 mmol), $Pd(PPh_3)_2Cl_2$ (27 mg, 0.02 mmol) and triethylamine (0.68 ml, 4.88 mmol) were reacted in THF (20 ml) according to **general procedure N**. Purification by chromatography on silica (9:1 Petrol/EtOAc) gave the target compound as a golden oil (0.754 g, 1.87 mmol, 96%). R_f 0.30 (9:1 Petrol/EtOAc); λ_{max} (EtOH/nm) 303; IR (cm^{-1}) 3433, 2946, 2866, 2706, 2361, 1703; ^{1}H NMR (500 MHz, DMSO-d_6) 1.12-1.25 (21H, m, Si(C*H*(C*H*$_3$)$_2$)$_3$), 1.56-1.63 (2H, m, OCH$_2$C*H*$_2$), 1.71-1.80 (1H, m, CHCH*H'*), 1.94-2.03 (2H, m, CHCH$_2$C*H*$_2$), 2.20-2.30 (1H, m, CHC*H*H'), 3.70-3.78 (1H, m, OCH*H'*), 4.01-4.07 (1H, m, OC*H*H'), 5.70 (1H, dd, J = 2.2 and 10.8 Hz, CH), 8.89 (1H, s, H-8); ^{13}C NMR (125 MHz, DMSO-d_6) 10.5 (Si(*C*H(CH$_3$)$_2$)$_3$), 18.4 (Si(CH(*C*H$_3$)$_2$)$_3$), 22.0 (CH*C*H$_2$), 24.4 (OCH$_2$*C*H$_2$), 29.7 (CHCH$_2$*C*H$_2$), 67.7 (OCH$_2$), 81.4 (CH), 100.2 (C≡C), 102.8 (C≡C), 133.9 (d, J_{CF} = 4.6 Hz, C-Ar), 140.8 (d, J_{CF} = 17.9 Hz, C-Ar), 146.6 (d, J_{CF} = 2.8 Hz, C-Ar), 153.8 (d, J_{CF} = 17.8 Hz, C-Ar), 157.4 (d, J_{CF} = 210.6 Hz, C^2-Ar); HRMS calcd. for $C_{21}H_{32}FN_4OSi$ (ES+) m/z 403.2324 $[M+H]^+$, found 403.2324.

2-Fluoro-6-(2-(triisopropylsilyl)ethynyl)-9*H*-purine (160)

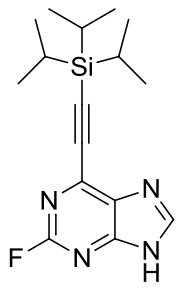

TFA (3 mL) was added to a solution of THP-protected purine **159** (0.644 g, 1.60 mmol) in IPA (15 mL). Water (3 mL) was added and the solution was heated to reflux for 2 h. The

mixture was cooled and neutralised (conc. NH_3) before being extracted with EtOAc (3 × 50 mL) and the combined organic extracts dried ($MgSO_4$) and concentrated. The resulting residue was purified by chromatography on silica (7:3 Petrol/EtOAc) to give the desired product as a pale yellow oil (0.461 g, 1.45 mmol, 91%). R_f 0.25 (7:3 Petrol/EtOAc); λ_{max} (EtOH/nm) 302; IR (cm^{-1}) 2945, 2866, 2361, 2000, 1584; ^{1}H NMR (500 MHz, DMSO-d_6) 1.12-1.21 (21H, m, Si(C*H*(C*H*$_3$)$_2$)$_3$), 8.68 (1H, s, H-8), 13.89 (1H, br, H-9); ^{13}C NMR (125 MHz, $CDCl_3$) 11.1 (Si(*C*H(CH$_3$)$_2$)$_3$), 18.5 (Si(CH(*C*H$_3$)$_2$)$_3$), 99.5 (C≡C), 106.1 (C≡C), 131.2 (m, C-Ar), 141.6 (m, C-Ar), 145.3 (m, C-Ar), 156.6 (m, C-Ar), 158.6 (d, J_{CF} = 217.4 Hz, C^2-Ar); HRMS calcd. for $C_{16}H_{24}FN_4Si$ (ES+) *m*/*z* 319.1749 $[M+H]^+$, found 319.1752.

6-(2-(Triisopropylsilyl)ethynyl)-*N*-phenyl-9*H*-purin-2-amine (164)

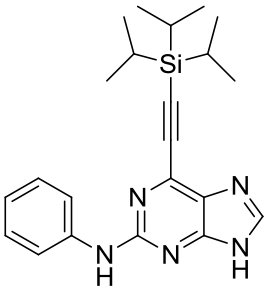

2-Fluoropurine intermediate **160** (0.455 g, 1.43 mmol), aniline (260 µL, 2.86 mmol), TFA (551 µL, 7.15 mmol) and TFE (7 mL) were reacted according to **general procedure B**. The dried ($MgSO_4$) and concentrated crude material was purified using chromatography on silica (19:1 DCM/MeOH) to give the desired product as a yellow oil/gum (0.390 g, 1.00 mmol, 70%). R_f 0.39 (19:1 DCM/MeOH); λ_{max} (EtOH/nm) 276; IR (cm^{-1}) 3389, 2361, 2021; ^{1}H NMR (500 MHz, $CDCl_3$) 1.09-1.22 (21H, m, Si(C*H*(C*H*$_3$)$_2$)$_3$), 7.00-7.04 (1H, m, H-4'), 7.22 (1H, s, C^2-NH), 7.29 (2H, dd, *J* = 7.7 and 8.1 Hz, H-3'/H-5'), 7.46 (1H, s, H-8), 7.52 (2H, dd, *J* = 1.7 and 7.7 Hz, H-2'/H-6'), 10.42 (1H, s, H-9); ^{13}C NMR (125 MHz, $CDCl_3$) 11.3 (Si(*C*H(CH$_3$)$_2$)$_3$), 18.7 (Si(CH(*C*H$_3$)$_2$)$_3$), 100.8 (C≡C), 101.8 (C≡C), 120.7 (C-Ar), 123.7 (C-Ar), 129.4 (C-Ar), 139.2 (C-Ar), 141.0 (C-Ar), 142.6 (C-Ar), 153.4 (C-Ar), 156.5 (C-Ar); HRMS calcd. for $C_{22}H_{30}N_5Si$ (ES+) *m*/*z* 392.2271 $[M+H]^+$, found 392.2263.

Note: Unable to visualise all carbon environments by ^{13}C NMR.

6-(2-(Triisopropylsilyl)ethynyl)-*N*-*p*-tolyl-9*H*-purin-2-amine (165)

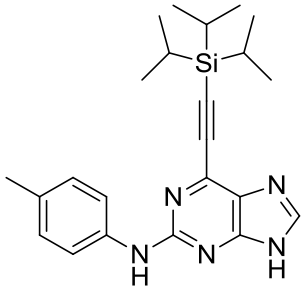

2-Fluoropurine intermediate **160** (0.357 g, 1.12 mmol) and 4-methylaniline (0.241 g, 2.25 mmol) were reacted with TFA (432 µl, 5.61 mmol) in TFE (6 ml) according to **general procedure B**. The resulting crude residue was purified by chromatography on reverse phase silica (19:1 MeOH/H_2O 0.1% HCOOH) to give the desired compound as a yellow oil (0.215 g, 0.53 mmol, 47%). R_f 0.27 (19:1 MeOH/H_2O, 0.1% HCOOH, C18); λ_{max} (EtOH/nm) 276; IR (cm^{-1}) 2942, 2865, 2361, 2336, 1605; ^{1}H NMR (500 MHz, DMSO-d_6) 1.13-1.22 (21H, m, Si(C*H*(C*H*$_3$)$_2$)$_3$), 2.31 (3H, s, -CH_3), 7.14 (2H, d, *J* = 8.4 Hz, H-3'/H-5'), 7.74 (2H, d, *J* = 8.4 Hz, H-2'/H-6'), 8.28 (1H, s, H-8), 9.65 (1H, s, C^2-NH), 13.11 (1H, br, H-9); ^{13}C NMR (125 MHz, $CDCl_3$) 11.3 (Si(*C*H(CH$_3$)$_2$)$_3$), 18.7 (Si(CH(*C*H$_3$)$_2$)$_3$), 20.9 (CH_3), 120.8 (C-Ar), 129.8 (C-Ar), 136.4 (C-Ar); HRMS calcd. for $C_{23}H_{32}N_5Si$ (ES+) *m*/*z* 406.2421 $[M+H]^+$, found 406.2423.

Note: Unable to visualise all carbon environments by ^{13}C NMR.

***N*-(4-Ethylphenyl)-6-(2-(triisopropylsilyl)ethynyl)-9*H*-purin-2-amine (166)**

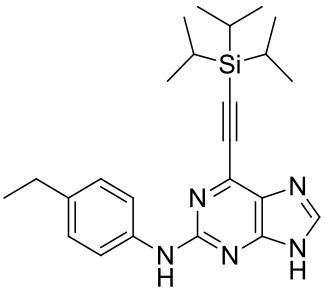

2-Fluoropurine intermediate **160** (0.394 g, 1.24 mmol) and 4-ethylaniline (310 µl, 2.48 mmol) were reacted with TFA (477 µl, 6.19 mmol) in TFE (6 ml) according to **general procedure B**. The resulting residue was purified by chromatography on reverse phase silica (19:1 MeOH/H_2O 0.1% HCOOH) to give the desired compound as a yellow oil/gum (0.281 g, 0.67 mmol, 54%). R_f 0.27 (19:1 MeOH/H_2O, 0.1% HCOOH, C18); λ_{max} (EtOH/nm) 277;

IR (cm^{-1}) 2941, 2865, 2361, 2338, 2160, 1605; ^{1}H NMR (500 MHz, DMSO-d_6) 1.13-1.21 (21H, m, Si(C*H*(CH_3)$_2$)$_3$), 1.23 (3H, t, *J* = 7.6 Hz, -CH_2CH_3), 2.61 (2H, q, *J* = 7.6 Hz, -CH_2CH_3) 7.17 (2H, d, *J* = 8.4 Hz, H-3'/H-5'), 7.75 (2H, d, *J* = 8.4 Hz, H-2'/H-6'), 8.27 (1H, s, H-8), 9.66 (1H, s, C^2-NH), 13.11 (1H, br, H-9); ^{13}C NMR (125 MHz, $CDCl_3$) 11.3 (Si(*C*H(CH_3)$_2$)$_3$), 15.7 (CH_3), 18.7 (Si(CH(*C*H_3)$_2$)$_3$), 28.3 (CH_2), 100.6 (C≡C), 121.0 (C-Ar), 128.7 (C-Ar), 136.7 (C-Ar), 139.9 (C-Ar), 140.8 (C-Ar), 156.7 (C-Ar); HRMS calcd. for $C_{24}H_{34}N_5Si$ (ES+) *m*/*z* 420.2578 $[M+H]^+$, found 420.2579.

Note: Unable to visualise all carbon environments by ^{13}C NMR.

***N*-(4-Isopropylphenyl)-6-(2-(triisopropylsilyl)ethynyl)-9*H*-purin-2-amine (167)**

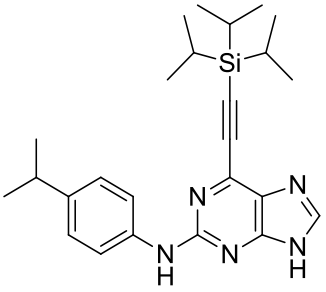

2-Fluoropurine intermediate **160** (0.395 g, 1.24 mmol) and 4-isopropylaniline (353 µl, 2.48 mmol) were reacted with TFA (478 µl, 6.21 mmol) in TFE (6 ml) according to **general procedure B**. The resulting residue was purified by chromatography on reverse phase silica (19:1 MeOH/H_2O, 0.1% HCOOH) to give the desired compound as a yellow oil/gum (0.314 g, 0.72 mmol, 58%). R_f 0.23 (19:1 MeOH/H_2O, 0.1% HCOOH, C18); λ_{max} (EtOH/nm) 277; IR (cm^{-1}) 2956, 2866, 2360, 2157, 1607; ^{1}H NMR (500 MHz, DMSO-d_6) 1.12-1.21 (21H, m, Si(C*H*(CH_3)$_2$)$_3$), 1.25 (6H, d, *J* = 7.0 Hz, -CH(CH_3)$_2$), 2.89 (1H, sept, *J* = 7.0 Hz, -C*H*(CH_3)$_2$), 7.19 (2H, d, *J* = 8.6 Hz, H-3'/H-5'), 7.74 (2H, d, *J* = 8.6 Hz, H-2'/H-6'), 8.26 (1H, s, H-8), 9.65 (1H, s, C^2-NH), 13.10 (1H, br, H-9); ^{13}C NMR (125 MHz, $CDCl_3$) 11.3 (Si(*C*H(CH_3)$_2$)$_3$), 18.7 (Si(CH(*C*H_3)$_2$)$_3$), 24.1 (CH_3), 33.6 (CH), 100.7 (C≡C), 120.5 (C-Ar), 127.1 (C-Ar), 136.7 (C-Ar), 155.7 (C-Ar); HRMS calcd. for $C_{25}H_{36}N_5Si$ (ES+) *m*/*z* 434.2734 $[M+H]^+$, found 434.2735.

Note: Unable to visualise all carbon environments by ^{13}C NMR.

(4-Nitrophenoxy)triisopropylsilane (162)[247]

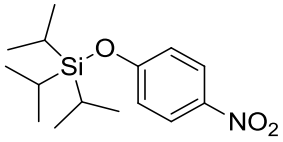

Imidazole (0.735 g, 10.8 mmol) was added to a solution of 4-nitrophenol (0.502 g, 3.60 mmol) in dry DCM (10 ml). Triisopropylsilyl chloride (1.5 ml, 7.20 mmol) was added, and the reaction mixture was stirred at RT for 2 h. The mixture was washed with sat. brine solution (2 x 10 ml) and the combined aqueous washings were extracted with DCM (3 x 10 ml). The combined organic extracts were dried (Na_2SO_4) and concentrated, and the resulting residue was purified using chromatography on silica (Petrol). The desired compound was obtained as a colourless oil (0.998 g, 3.38 mmol, 94%). R_f 0.40 (Petrol); λ_{max} (EtOH/nm) 245, 295; IR (cm^{-1}) 2980, 2930, 2156; ^{1}H NMR (500 MHz, DMSO-d_6) 1.13 (18H, d, J = 7.6 Hz, Si(CH(CH_3)$_2$)$_3$), 1.38 (3H, sept, J = 7.6 Hz, Si(CH(CH$_3$)$_2$)$_3$), 7.14 (2H, d, J = 9.2 Hz, H-2/H-6), 8.24 (2H, d, J = 9.2 Hz, H-3/H-5); LRMS (ES+) m/z 296.2 $[M+H]^+$.

4-Triisopropylsilyloxyaniline (163)[248]

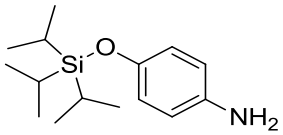

Zinc (0.454 g, 6.94 mmol) was added to a solution of the nitro compound **162** (0.205 g, 0.69 mmol) in acetic acid (10 ml) and the mixture was stirred at RT for 2.5 h. The solvent was removed *in vacuo* and the residue was dissolved in water. The solution was adjusted to pH 8 (conc. NH_3) and extracted with EtOAc (2 x 20 ml). The combined organic extracts were dried (Na_2SO_4) and concentrated, and the residue was purified by chromatography on silica (9:1 Petrol/EtOAc). The desired compound was obtained as an orange oil (0.132 g, 0.50 mmol, 72%). R_f 0.76 (7:3 Petrol/EtOAc); λ_{max} (EtOH/nm) 236, 301; IR (cm^{-1}) 2944, 2866, 1613; ^{1}H NMR (500 MHz, DMSO-d_6) 0.94 (18H, d, J = 7.3 Hz, Si(CH(CH_3)$_2$)$_3$), 1.07 (3H, sept, J = 7.3 Hz, Si(CH(CH$_3$)$_2$)$_3$), 4.64 (2H, s, Ar-NH_2), 6.36 (2H, d, J = 8.9 Hz, H-2/H-6), 6.47 (2H, d, J = 8.9 Hz, H-3/H-5); ^{13}C NMR (125 MHz, $CDCl_3$) 12.6 (Si(CH(CH$_3$)$_2$)$_3$), 17.9 (Si(CH(CH$_3$)$_2$)$_3$), 116.5 (C-Ar), 120.4 (C-Ar), 139.6 (C-Ar), 148.9 (C-Ar); LRMS (ES+) m/z 266.2 $[M+H]^+$.

6-((Triisopropylsilyl)ethynyl)-*N*-(4-((triisopropylsilyl)oxy)phenyl)-9*H*-purin-2-amine (168)

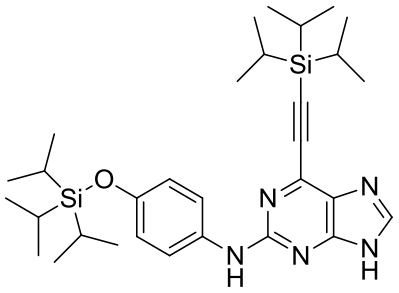

2-Fluoropurine intermediate **160** (0.379 g, 1.19 mmol) and aniline **163** (0.610 g, 2.38 mmol) were reacted with TFA (460 µl, 5.96 mmol) in TFE (8 ml) according to **general procedure B**. Purification on silica (7:3 Petrol/EtOAc)) gave the target compound as an orange oil (0.181 g, 0.32 mmol, 27%). R_f 0.44 (7:3 Petrol/EtOAc); λ_{max} (EtOH/nm) 277; IR (cm^{-1}) 2944, 2866, 2367, 2343, 2187, 1607; ^{1}H NMR (500 MHz, DMSO-d_6) 1.08 (18H, d, J = 7.3 Hz, OSi(CH(CH_3)$_2$)$_3$), 1.12-1.24 (24H, m, OSi(CH(CH$_3$)$_2$)$_3$ & Si(CH(CH_3)$_2$)$_3$), 6.80 (2H, d, J = 9.3 Hz, H-3'/H-5'), 7.64 (2H, d, J = 9.3 Hz, H-2'/H-6'), 8.20 (1H, s, H-8), 9.54 (1H, s, C^2-NH), 13.01 (1H, br, H-9); ^{13}C NMR (125 MHz, $CDCl_3$) 11.2 (Si(CH(CH$_3$)$_2$)$_3$), 12.7 (Si(CH(CH$_3$)$_2$)$_3$), 17.9 (Si(CH(CH$_3$)$_2$)$_3$), 18.7 (Si(CH(CH$_3$)$_2$)$_3$), 101.3 (C≡C), 115.1 (C-Ar), 117.5 (C-Ar), 120.2 (C-Ar), 122.1 (C-Ar), 156.7 (C-Ar); HRMS calcd. for $C_{31}H_{50}N_5OSi_2$ (ES+) m/z 564.3548 $[M+H]^+$, found 564.3543.

Note: Unable to visualise all carbon environments by ^{13}C NMR.

6-(2-(Triisopropylsilyl)ethynyl)-*N*-(3-methoxyphenyl)-9*H*-purin-2-amine (169)

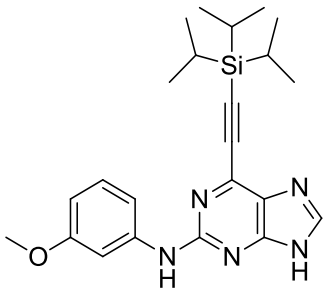

2-Fluoropurine intermediate **160** (0.421 g, 1.32 mmol) and 3-methoxyaniline (298 µl, 2.65 mmol) were reacted with TFA (510 µl, 6.62 mmol) in TFE (6 ml) according to **general procedure B**. Chromatography on reverse phase silica (19:1 MeOH/H_2O 0.1% HCOOH) afforded the target compound as a yellow oil/gum (0.297 g, 0.70 mmol, 53%). R_f 0.33 (19:1

MeOH/H_2O, 0.1% HCOOH, C18); λ_{max} (EtOH/nm) 274; IR (cm^{-1}) 3147, 2943, 2865, 2360, 1600; ^1H NMR (500 MHz, DMSO-d_6) 1.14-1.23 (21H, m, Si(CH(CH_3)$_2$)$_3$), 3.76 (3H, s, OCH_3), 6.52 (1H, ddd, *J* = 2.3, 2.5 and 8.5 Hz, H-4'), 7.17 (1H, dd, *J* = 8.1 and 8.2 Hz, H-5'), 7.29-7.33 (1H, m, H-6'), 7.64-7.67 (1H, m, H-2'), 8.26 (1H, s, H-8), 9.71 (1H, s, C^2-NH), 13.12 (1H, br, H-9); ^{13}C NMR (125 MHz, $CDCl_3$) 11.3 (Si(*C*H(CH_3)$_2$)$_3$), 18.7 (Si(CH(*C*H_3)$_2$)$_3$), 55.3 (OCH_3), 101.6 (C≡C), 108.0 (C-Ar), 117.9 (C-Ar), 129.8 (C-Ar), 138.7 (C-Ar), 160.3 (C-Ar); HRMS calcd. for $C_{23}H_{32}N_5OSi$ (ES+) *m*/*z* 422.2371 $[M+H]^+$, found 422.2372.

Note: Unable to visualise all carbon environments by ^{13}C NMR.

***N*-(2-Methoxyphenyl)-6-((triisopropylsilyl)ethynyl)-9*H*-purin-2-amine (170)**

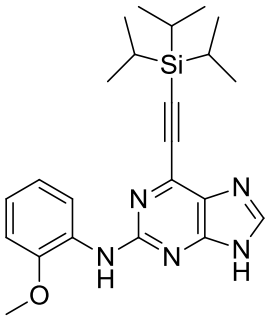

2-Fluoropurine **160** (0.169 g, 0.53 mmol), 2-methoxyaniline (120 µl, 1.06 mmol) and TFA (102 µl, 1.33 mmol) were reacted in TFE (5 ml) according to **general procedure V**. Purification by KP-NH silica chromatography (19:1 DCM/MeOH) afforded the target compound as a yellow oil/gum (98 mg, 0.23 mmol, 43%). R_f 0.39 (19:1 DCM/MeOH, KP-NH); λ_{max} (EtOH/nm) 271; IR (cm^{-1}) 3421, 3071, 2942, 2864, 1600, 1572, 1531; ^1H NMR (500 MHz, DMSO-d_6) 1.13-1.22 (21H, m, Si(C*H*(CH_3)$_2$)$_3$), 3.86 (3H, s, OCH_3), 6.95 (1H, ddd, *J* = 1.5, 7.5 and 7.7 Hz, H-5'), 7.01 (1H, dd, *J* = 1.5 and 8.0 Hz, H-3'), 7.04 (1H, ddd, *J* = 1.6, 7.5 and 8.0 Hz, H-4'), 8.11 (1H, s, C^2-NH), 8.20-8.23 (1H, m, H-6'), 8.26 (1H, s, H-8), 13.10 (1H, br, H-9); ^{13}C NMR (125 MHz, DMSO-d_6) 10.6 (Si(*C*H(CH_3)$_2$)$_3$), 18.4 (Si(CH(*C*H_3)$_2$)$_3$), 55.7 (OCH_3), 98.1 (C≡C), 101.8 (C≡C), 110.9 (C-Ar), 119.8 (C-Ar), 120.3 (C-Ar), 122.4 (C-Ar), 129.0 (C-Ar), 143.0 (C-Ar), 149.1 (C-Ar), 156.2 (C-Ar); HRMS calcd. for $C_{23}H_{32}N_5OSi$ (ES+) *m*/*z* 422.2371 $[M+H]^+$, found 422.2375.

Note: Unable to visualise all carbon environments by ^{13}C NMR.

6-(2-(Triisopropylsilyl)ethynyl)-*N*-(4-chlorophenyl)- 9*H*-purin-2-amine (171)

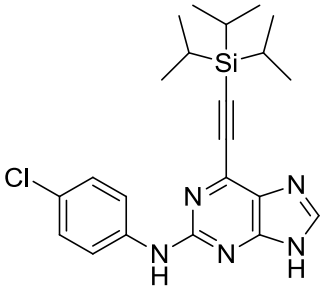

2-Fluoropurine intermediate **160** (0.200 g, 0.62 mmol), 4-chloroaniline (0.161 g, 1.26 mmol), TFA (242 µL, 3.14 mmol) and TFE (6 mL) were reacted according to **general procedure B**. The dried ($MgSO_4$) and concentrated crude material was purified using chromatography on silica (7:3 Petrol/EtOAc) to give the desired product as a yellow oil (0.165 g, 0.38 mmol, 61%). R_f 0.25 (7:3 Petrol/EtOAc); λ_{max} (EtOH/nm) 289; IR (cm^{-1}) 3118, 2945, 2866, 2361, 1541; ^{1}H NMR (500 MHz, DMSO-d_6) 1.13-1.22 (21H, m, Si(C*H*(C*H*$_3$)$_2$)$_3$), 7.33 (2H, d, *J* = 8.9 Hz, H-2'/H-6'), 7.85 (2H, d, *J* = 8.9 Hz, H-3'/H-5'), 8.27 (1H, s, H-8), 9.91 (1H, s, C^2-NH), 13.17 (1H, br, H-9); LRMS (ES+) *m/z* 426.2 $[M^{35}Cl+H]^+$, 428.2 $[M^{37}Cl+H]^+$.

***N*-(3-Chlorophenyl)-6-(2-(triisopropylsilyl)ethynyl)-9*H*-purin-2-amine (172)**

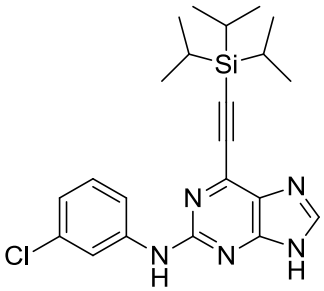

2-Fluoropurine intermediate **160** (0.354 g, 1.11 mmol) and 3-chloroaniline (234 µl, 2.23 mmol) were reacted with TFA (429 µl, 5.57 mmol) in TFE (6 ml) according to **general procedure B**. Purification of the crude residue by chromatography on reverse phase silica (19:1 MeOH/H_2O 0.1% HCOOH) gave the desired compound as a yellow oil/gum (0.281 g, 0.66 mmol, 59%). R_f 0.27 (19:1 MeOH/H_2O, 0.1% HCOOH, C18); λ_{max} (EtOH/nm) 276; IR (cm^{-1}) 3278, 2944, 2866, 2363, 1596; ^{1}H NMR (500 MHz, DMSO-d_6) 1.13-1.22 (21H, m, Si(C*H*(C*H*$_3$)$_2$)$_3$), 6.96 (1H, ddd, *J* = 2.0, 2.2 and 8.0 Hz, H-4'), 7.29 (1H, dd, *J* = 8.0 and 8.1 Hz, H-5'), 7.64 (1H, ddd, *J* = 2.0, 2.1 and 8.1 Hz, H-6'), 8.11-8.14 (1H, m, H-2'), 8.30 (1H, s, H-8), 9.96 (1H, s, C^2-NH), 13.21 (1H, br, H-9); ^{13}C NMR (125 MHz, $CDCl_3$) 11.2

(Si(*C*H(CH$_3$)$_2$)$_3$), 18.7 (Si(CH(*C*H$_3$)$_2$)$_3$), 117.1 (C-Ar), 118.9 (C-Ar), 122.6 (C-Ar), 129.9 (C-Ar), 134.7 (C-Ar), 135.7 (C-Ar), 140.2 (C-Ar); HRMS calcd. for $C_{22}H_{29}ClN_5Si$ (ES+) *m*/*z* 426.1875 $[M+H]^+$, found 426.1877.

Note: Unable to visualise all carbon environments by ^{13}C NMR.

6-Ethynyl-*N*-phenyl-9*H*-purin-2-amine (148)

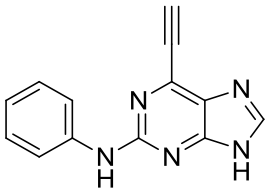

The TIPS-protected purine **164** (0.330 g, 0.84 mmol) and TBAF (1M in THF, 930 µL, 0.93 mmol) were reacted in THF (10 ml) according to **general procedure I**, with purification by chromatography on silica (EtOAc) to give the desired product as a yellow solid (0.201 g, 0.85 mmol, 100%). R_f 0.27 (EtOAc); M.p. 140-160 °C (decomposed); λ_{max} (EtOH/nm) 243; IR (cm^{-1}) 3414, 3111, 3072, 2920, 2110, 1704; ^1H NMR (500 MHz, DMSO-d_6) 4.86 (1H, s, C≡CH), 6.91-6.96 (1H, m, H-4'), 7.29 (2H, dd, *J* = 7.6 and 8.0 Hz, H-3'/H-5'), 7.80 (2H, dd, *J* = 2.0 and 8.0 Hz, H^3), 8.30 (1H, s, H-8), 9.70 (1H, s, C^2-NH), 13.17 (1H, br, H-9); ^{13}C NMR (125 MHz, DMSO-d_6) 87.0 (C≡*C*H), 118.3 (C-Ar), 120.0 (C-Ar), 128.4 (C-Ar), 140.8 (C-Ar), 156.2 (C-Ar); HRMS calcd. for $C_{13}H_{10}N_5$ (ES+) *m*/*z* 236.0934 $[M+H]^+$, found 236.0931.

Note: Unable to visualise all carbon environments by ^{13}C NMR.

6-Ethynyl-*N*-*p*-tolyl-9*H*-purin-2-amine (149)

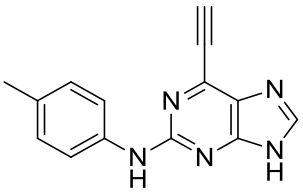

The TIPS-protected purine **165** (0.208 g, 0.51 mmol) was reacted with TBAF (1M in THF, 770 µl, 0.77 mmol) in THF (5 ml) according to **general procedure I**. Chromatography on silica (1:4 Petrol/EtOAc) afforded the desired compound as a yellow solid (0.102 g, 0.41 mmol, 80%). R_f 0.33 (EtOAc); M.p. 110-120 °C (decomposed); λ_{max} (EtOH/nm) 271; IR (cm$^-$

[1]) 3409, 3268, 2852, 2721, 2110; ^{1}H NMR (500 MHz, DMSO-d_6) 2.26 (3H, s, -CH_3), 4.82 (1H, s, C≡CH), 7.10 (2H, d, *J* = 8.4 Hz, H-2'/H-6'), 7.67 (2H, d, *J* = 8.4 Hz, H-3'/H-5'), 8.24 (1H, s, H-8), 9.57 (1H, s, C^2-NH), 13.09 (1H, br, H-9); HRMS calcd. for $C_{14}H_{12}N_5$ (ES+) *m*/*z* 250.1087 $[M+H]^+$, found 250.1084.

_N_-(4-Ethylphenyl)-6-ethynyl-9_H_-purin-2-amine (150)

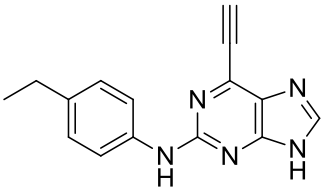

The TIPS-protected purine **166** (0.258 g, 0.61 mmol) was reacted with TBAF (1M in THF, 920 µl, 0.92 mmol) in THF (6 ml) according to **general procedure I**. Purification *via* chromatography on silica (1:4 Petrol/EtOAc) gave the desired compound as a yellow solid (0.119 g, 0.45 mmol, 74%). R_f 0.36 (EtOAc); M.p. 120-140 °C (decomposed); λ_{max} (EtOH/nm) 274; IR (cm^{-1}) 3408, 3109, 2961, 2923, 2110, 1748; ^{1}H NMR (500 MHz, DMSO-d_6) 1.17 (3H, t, *J* = 7.7 Hz, -$CH_2C\mathit{H}_3$), 2.56 (2H, q, *J* = 7.7 Hz, -$C\mathit{H}_2CH_3$), 4.83 (1H, s, C≡CH), 7.13 (2H, d, *J* = 8.5 Hz, H-3'/H-5'), 7.68 (2H, d, *J* = 8.5 Hz, H-2'/H-6'), 8.26 (1H, s, H-8), 9.57 (1H, s, C^2-NH), 13.11 (1H, br, H-9); HRMS calcd. for $C_{15}H_{14}N_5$ (ES+) *m*/*z* 264.1246 $[M+H]^+$, found 264.1244.

_N_-(4-Isopropylphenyl)-6-ethynyl-9_H_-purin-2-amine (151)

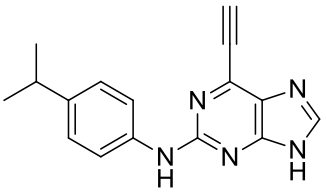

The TIPS-protected purine **167** (0.259 g, 0.60 mmol) was reacted with TBAF (1M in THF, 900 µl, 0.90 mmol) in THF (6 ml) according to **general procedure I**. Purification by silica gel chromatography (1:4 Petrol/EtOAc) afforded the target compound as a yellow solid (0.104 g, 0.37 mmol, 62%). R_f 0.40 (EtOAc); M.p. 120-140 °C (decomposed); λ_{max} (EtOH/nm) 277; IR (cm^{-1}) 3408, 3275, 2957, 2814, 2366, 2111; ^{1}H NMR (500 MHz, DMSO-d_6) 0.97 (6H, d, *J* = 7.1 Hz, -$CH(C\mathit{H}_3)_2$), 2.61 (1H, sept, *J* = 7.1 Hz, -$C\mathit{H}(CH_3)_2$), 4.59 (1H, s, C≡CH), 6.92 (2H, d, *J* = 8.5 Hz, H-3'/H-5'), 7.44 (2H, d, *J* = 8.5 Hz, H-2'/H-6'), 8.02 (1H, s,

H-8), 9.32 (1H, s, C^2-NH), 12.88 (1H, br, H-9); HRMS calcd. for $C_{16}H_{16}N_5$ (ES+) *m*/*z* 278.1404 $[M+H]^+$, found 278.1400.

4-(6-Ethynyl-9*H*-purin-2-ylamino)phenol (152)

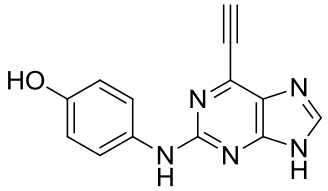

The TIPS-protected purine **168** (0.167 g, 0.30 mmol) was reacted with TBAF (1M in THF, 0.66 ml, 0.66 mmol) in THF (3 ml) according to **general procedure I**. Silica gel chromatography (9:1 DCM/MeOH) afforded the desired compound as a beige solid (36 mg, 0.14 mmol, 48%). R_f 0.36 (9:1 DCM/MeOH); M.p. 275-290 °C (decomposed); λ_{max} (EtOH/nm) 274; IR (cm^{-1}) 3391, 3257, 3059, 2921, 2849, 2567, 2114, 1623; ^{1}H NMR (500 MHz, DMSO-d_6) 4.60 (1H, s, C≡CH), 6.51 (2H, d, *J* = 8.9 Hz, H-2'/H-6'), 7.32 (2H, d, *J* = 8.9 Hz, H-3'/H-5'), 8.00 (1H, s, H-8), 8.83 (1H, s, C^2-NH), 9.12 (1H, s, OH), 12.80 (1H, s, H-9); HRMS calcd. for $C_{13}H_{10}N_5O$ (ES+) *m*/*z* 252.0886 $[M+H]^+$, found 252.0880.

Note: Insufficient material for 13C NMR.

6-Ethynyl-*N*-(3-methoxyphenyl)-9*H*-purin-2-amine (154)

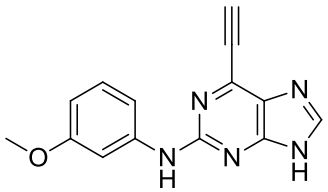

The TIPS-protected purine **169** (0.271 g, 0.64 mmol) was reacted with TBAF (1M in THF, 960 µl, 0.96 mmol) in THF (6 ml) according to **general procedure I**. Silica gel chromatography (1:4 Petrol/EtOAc) gave the target compound as a yellow solid (0.119 g, 0.45 mmol, 70%). R_f 0.30 (EtOAc); M.p. 130-150 °C (decomposed); λ_{max} (EtOH/nm) 272; IR (cm^{-1}) 3410, 3264, 3108, 2958, 2868, 2112, 1703; ^{1}H NMR (500 MHz, DMSO-d_6) 3.76 (3H, s, OCH_3), 4.86 (1H, s, C≡CH), 6.53 (1H, ddd, *J* = 2.1 and 8.1 Hz, H-4'), 7.18 (1H, dd, *J* = 8.2 Hz, H-5'), 7.30-7.34 (1H, m, H-6'), 7.59-7.62 (1H, m, H-2'), 8.30 (1H, s, H-8), 9.68 (1H, s, C^2-NH), 13.20 (1H, s, H-9); HRMS calcd. for $C_{14}H_{12}N_5O$ (ES+) *m*/*z* 266.1036 $[M+H]^+$, found 266.1038.

***N*-(4-Chlorophenyl)-6-ethynyl-9*H*-purin-2-amine (156)**

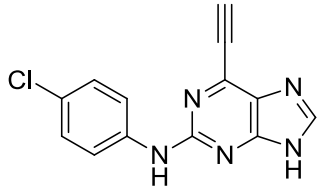

The TIPS-protected purine **171** (0.125 g, 0.29 mmol) and TBAF (1M in THF, 440 µL, 0.44 mmol) were reacted in THF (5 ml) according to **general procedure I**, with purification by chromatography on silica (EtOAc) to give the desired product as a yellow solid (77 mg, 0.28 mmol, 81%). R_f 0.34 (EtOAc); M.p. 180-200 °C (decomposed); λ_{max} (EtOH/nm) 241; IR (cm^{-1}) 3414, 3278, 2921, 2848, 2108, 1576, 1522; ^{1}H NMR (500 MHz, DMSO-d_6) 4.87 (1H, s, C≡CH), 7.34 (2H, d, *J* = 8.9 Hz, H-2'/H-6'), 7.84 (2H, d, *J* = 8.9 Hz, H-3'/H-5'), 8.32 (1H, s, H-8), 9.85 (1H, s, C^2-NH), 13.21 (1H, br, H-9); HRMS calcd. for $C_{13}H_9N_5Cl$ (ES+) *m*/*z* 270.0541 $[M+H]^+$, found 270.0540.

***N*-(3-Chlorophenyl)-6-ethynyl-9*H*-purin-2-amine (157)**

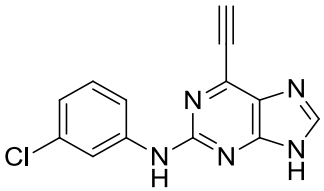

The TIPS-protected purine **172** (0.255 g, 0.60 mmol) was reacted with TBAF (1M in THF, 900 µl, 0.90 mmol) in THF (6 ml) according to **general procedure I**. Purification by chromatography on silica (1:4 Petrol/EtOAc) afforded the desired compound as a yellow solid (0.126 g, 0.47 mmol, 78%). R_f 0.35 (EtOAc); M.p. 130-150 °C (decomposed); λ_{max} (EtOH/nm) 273; IR (cm^{-1}) 3407, 3282, 3078, 2926, 2812, 2110, 1706; ^{1}H NMR (500 MHz, DMSO-d_6) 4.93 (1H, s, C≡CH), 7.00 (1H, ddd, *J* = 2.0, 2.1 and 8.0 Hz, H-6'), 7.34 (1H, dd, *J* = 8.0 Hz, H-5'), 7.71 (1H, ddd, *J* = 2.0, 2.1 and 8.1 Hz, H-4'), 8.09 (1H, br, H-2'), 8.37 (1H, s, H-8), 9.97 (1H, s, C^2-NH), 13.31 (1H, s, H-9); HRMS calcd. for $C_{13}H_9ClN_5$ (ES+) *m*/*z* 270.0541 $[M+H]^+$, found 270.0546.

3-(4-Nitrophenoxy)-*N*,*N*-dimethylpropan-1-amine (183)[249]

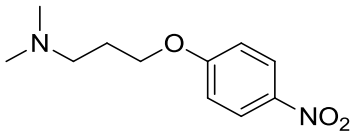

K_2CO_3 (2.78 g, 20.1 mmol) was added to a solution of 4-nitrophenol (1.00 g, 7.20 mmol) in DMF (20 mL) and the mixture was stirred at RT for 15 min. 3-Dimethylaminopropylchloride hydrochloride (2.02 g, 12.9 mmol) was added portionwise and the mixture was heated at 80 °C for 2 h. The solvent was removed *in vacuo* and the residue was dissolved in water (70 mL) and extracted with DCM (4 × 40 mL). The combined organic extracts were washed with 1M NaOH (100 mL), dried ($MgSO_4$) and concentrated to give the desired product as a yellow oil (1.18 g, 5.25 mmol, 73%). R_f 0.34 (19:1 DCM/MeOH); λ_{max} (EtOH/nm) 331; IR (cm^{-1}) 3412, 2948, 2819, 2770, 1592; ^{1}H NMR (500 MHz, DMSO-d_6) 1.89 (2H, tt, *J* = 6.8 and 6.9 Hz, OCH_2CH_2), 2.15 (6H, s, $N(CH_3)_2$), 2.36 (2H, t, *J* = 6.9 Hz, $CH_2N(CH_3)_2$), 4.15 (2H, t, *J* = 6.8 Hz, OCH_2CH_2), 7.15 (2H, d, *J* = 9.2 Hz, H-2/H-6), 8.21 (2H, d, *J* = 9.2 Hz, H-3/H-5); LRMS (ES+) *m/z* 225.2 $[M+H]^+$.

4-(3-(Dimethylamino)propoxy)benzenamine (184)[249]

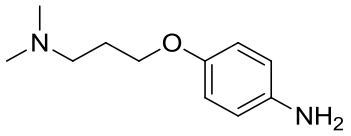

Palladium on carbon (0.10 g, 10% w/w) was added to a solution of the nitro compound **183** (1.00 g, 4.50 mmol) in EtOH (20 mL) and the mixture was hydrogenated at RT for 18 h. The catalyst was removed by filtration through Celite® and the solvent removed *in vacuo* to give the desired product as a pale red oil (0.789 g, 4.06 mmol, 91%). R_f 0.40 (9:1 DCM/MeOH); λ_{max} (EtOH/nm) 235; IR (cm^{-1}) 3323, 2359, 2180, 2004, 1630, 1511; ^{1}H NMR (500 MHz, DMSO-d_6) 1.77 (2H, tt, *J* = 6.7 and 6.9 Hz, OCH_2CH_2), 2.13 (6H, s, $N(CH_3)_2$), 2.32 (2H, t, *J* = 6.9 Hz, $CH_2N(CH_3)_2$), 3.84 (2H, t, *J* = 6.7 Hz, OCH_2CH_2), 4.58 (2H, s, Ar-NH_2), 6.50 (2H, d, *J* = 8.6 Hz, H-3/H-5), 6.63 (2H, d, *J* = 8.6 Hz, H-2/H-6); LRMS (ES+) *m/z* 195.1 $[M+H]^+$.

***N*-(4-(3-(Dimethylamino)propoxy)phenyl)-6-((triisopropylsilyl)ethynyl)-9*H*-purin-2-amine (185)**

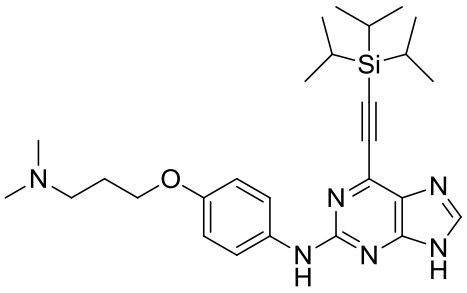

2-Fluoropurine intermediate **160** (0.179 g, 0.56 mmol), aniline **184** (0.225 g, 1.15 mmol), TFA (216 µL, 2.81 mmol) and TFE (6 mL) were reacted according to **general procedure B**. The crude material was purified using chromatography on C18 silica (1:19 H_2O/MeOH, 0.1% HCOOH) to give the desired compound as a yellow oil/gum (0.116 g, 0.24 mmol, 41%). R_f 0.40 (19:1 MeOH/H_2O, 0.1% HCOOH, C18); λ_{max} (EtOH/nm) 279; IR (cm^{-1}) 3401, 2945, 2866, 1704, 1573; ^{1}H NMR (500 MHz, DMSO-d_6) 1.13-1.26 (23H, m, Si(C*H*(CH_3)$_2$)$_3$ & -OCH_2CH_2), 2.95 (6H, s, N(CH_3)$_2$), 3.37 (2H, t, *J* = 6.5 Hz, $CH_2N(CH_3)_2$), 4.11 (2H, t, *J* = 5.7 Hz, OCH_2CH_2), 6.92, (2H, d, *J* = 9.0 Hz, H-3'/H-5'), 7.67 (2H, d, *J* = 9.0 Hz, H-2'/H-6'), 8.27 (1H, s, H-8), 9.52 (1H, s, C^2-NH); ^{13}C NMR (125 MHz, DMSO-d_6) 10.6 (Si(*C*H(CH_3)$_2$)$_3$), 18.4 (Si(CH(*C*H_3)$_2$)$_3$), 25.8 (CH_2), 43.9 (N(CH_3)$_2$), 55.1 (CH_2), 65.6 (CH_2), 97.5 (C≡C), 101.8 (C≡C), 114.4 (C-Ar), 120.0 (C-Ar), 134.2 (C-Ar), 139.5 (C-Ar), 142.7 (C-Ar), 153.1 (C-Ar), 156.5 (C-Ar), 164.2 (C-Ar); HRMS calcd. for $C_{27}H_{41}N_6OSi$ (ES+) *m*/*z* 493.3106 $[M+H]^+$, found 493.3100.

Note: Unable to visualise all carbon environments by ^{13}C NMR.

2-(3-(6-(2-(Triisopropylsilyl)ethynyl)-9*H*-purin-2-ylamino) phenyl)acetic acid (186)

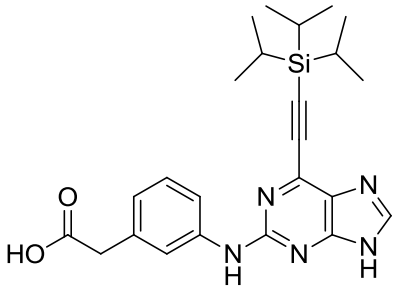

2-Fluoropurine intermediate **160** (1.06 g, 3.32 mmol) and 3-aminophenyl acetic acid (1.00 g, 6.64 mmol) were reacted with TFA (1.28 ml, 16.6 mmol) in TFE (25 ml) according to

general procedure B. Upon completion of the reaction, the reaction solvent was removed *in vacuo* and the resultant residue was dissolved in THF (20 ml) and 1M NaOH solution (15 ml). The mixture was stirred at RT for 18 h before the THF was removed *in vacuo*. The aqueous solution was then taken to pH 3 with 4M HCl solution and extracted with EtOAc (3 x 75 ml). The combined organic extracts were dried (Na_2SO_4) and concentrated, and the resulting orange residue was purified *via* chromatography on silica (9:1 DCM/MeOH) followed by chromatography on reverse phase silica (9:1 MeOH/H_2O 0.1% HCOOH). The desired product was obtained as an orange oil/gum (0.952 g, 2.12 mmol, 64%). R_f 0.32 (9:1 DCM/MeOH); λ_{max} (EtOH/nm) 275; IR (cm^{-1}) 2972, 2360, 2340, 1977, 1702; ^{1}H NMR (500 MHz, DMSO-d_6) 1.13-1.22 (21H, m, Si(C*H*(CH_3)$_2$)$_3$), 3.51 (2H, s, -CH_2CO$_2$H), 6.82-6.85 (1H, m, H-6'), 7.22 (1H, dd, *J* = 7.7 and 7.8 Hz, H-5'), 7.65-7.68 (1H, m, H-2'), 7.72-7.76 (1H, m, H-4'), 8.25 (1H, s, H-8), 9.71 (1H, s, C^2-NH), 12.33 (1H, br, -CO$_2$H), 13.10 (1H, br, H-9); ^{13}C NMR (125 MHz, DMSO-d_6) 10.6 (Si(*C*H(CH$_3$)$_2$)$_3$), 18.4 (Si(CH(*C*H$_3$)$_2$)$_3$), 41.2 (CO*C*H$_2$), 116.7 (C-Ar), 119.2 (C-Ar), 122.0 (C-Ar), 128.2 (C-Ar), 135.2 (C-Ar), 140.9 (C-Ar), 156.2 (C-Ar), 172.6 (C=O); HRMS calcd. for $C_{24}H_{32}N_5O_2Si$ (ES+) *m*/*z* 450.2320 $[M+H]^+$, found 450.2320.

Note: Unable to visualise quaternary carbon signals by ^{13}C NMR.

N-(4-Methoxybenzyl)-2-(3-(6-(2-(triisopropylsilyl)ethynyl)-9*H*-purin-2-ylamino)phenyl)acetamide (187)

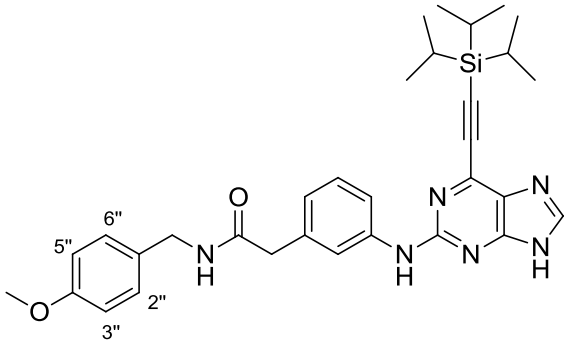

Carboxylic acid **186** (0.193 g, 0.43 mmol), CDI (0.140 g, 0.86 mmol), DIPEA (150 µl, 0.86 mmol) and 4-methoxybenzylamine (223 µl, 1.72 mmol) were reacted in dry DMF (5 ml) according to **general procedure J**. Chromatography on KP-NH silica (19:1 DCM/MeOH) gave the desired compound as a yellow oil/gum (0.238 g, 0.42 mmol, 99%). R_f 0.48 (19:1 DCM/MeOH, KP-NH); λ_{max} (EtOH/nm) 277; IR (cm^{-1}) 2360, 2153, 2120, 1980; ^{1}H NMR

(500 MHz, DMSO-d_6) 1.12-1.25 (21H, m, Si(C*H*(C*H*$_3$)$_2$)$_3$), 3.42 (2H, s, COC*H*$_2$), 3.71 (3H, s, OCH$_3$), 4.20 (2H, d, *J* = 5.8 Hz, NHC*H*$_2$), 6.85 (2H, d, *J* = 8.8 Hz, H-3''/H-5''), 6.86-6.91 (1H, m, H-6'), 7.17 (2H, d, *J* = 8.8 Hz, H-2''/H-6''), 7.20 (1H, dd, *J* = 7.9 and 8.0 Hz, H-5'), 7.59-7.62 (1H, m, H-2'), 7.74-7.78 (1H, m, H-4'), 8.24 (1H, s, H-8), 8.44 (1H, t, *J* = 5.8 Hz, N*H*CH$_2$), 9.65 (1H, s, C^2-NH), 12.06 (1H, br, H-9); ^{13}C NMR (125 MHz, DMSO-d_6) 10.6 (Si(*C*H(CH$_3$)$_2$)$_3$), 18.5 (Si(CH(*C*H$_3$)$_2$)$_3$), 41.7 (CH2), 42.6 (CH2), 55.0 (OCH3), 97.9 (C≡C), 113.6 (C-Ar), 121.8 (C-Ar), 128.6 (C-Ar), 131.7 (C-Ar), 136.7 (C-Ar), 141.0 (C-Ar), 156.4 (C-Ar), 158.1 (C-Ar), 169.9 (C=O); HRMS calcd. for $C_{32}H_{41}N_6O_2Si$ (ES+) *m*/*z* 569.3055 $[M+H]^+$, found 569.3057.

Note: Unable to visualise all quaternary carbon signals by ^{13}C NMR.

2-(3-(6-(2-(Triisopropylsilyl)ethynyl)-9*H*-purin-2-ylamino)phenyl) acetamide (189)

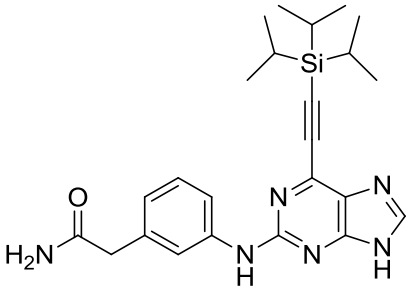

The PMB-amide **187** (0.232 g, 0.41 mmol) was reacted in TFA (6 ml) according to **general procedure K** over 72 h. Purification *via* chromatography on KP-NH silica (19:1 DCM/MeOH) gave the desired compound as a yellow oil/gum (0.170 g, 0.37 mmol, 90%). R_f 0.24 (19:1 DCM/MeOH, KP-NH); λ_{max} (EtOH/nm) 276; IR (cm^{-1}) 3282, 2965, 2943, 2362, 1669; ^{1}H NMR (500 MHz, DMSO-d_6) 1.13-1.21 (21H, m, Si(C*H*(C*H*$_3$)$_2$)$_3$), 3.34 (2H, s, COC*H*$_2$), 6.83-6.86 (1H, m, H-6'), 6.88 (1H, s, -CON*H*H'), 7.19 (1H, dd, *J* = 8.5 and 8.7 Hz, H-5'), 7.42 (1H, s, -CONH*H'*), 7.57-7.60 (1H, m, H-2'), 7.72-7.76 (1H, m, H-4'), 8.23 (1H, s, H-8), 9.65 (1H, s, C^2-NH), 13.08 (1H, s, H-9); ^{13}C NMR (125 MHz, $CDCl_3$) 11.2 (Si(*C*H(CH$_3$)$_2$)$_3$), 18.7 (Si(CH(*C*H$_3$)$_2$)$_3$), 46.9 (CO*C*H$_2$), 98.3 (C≡C), 119.0 (C-Ar), 120.6 (C-Ar), 123.6 (C-Ar), 124.8 (C-Ar), 135.5 (C-Ar), 153.4 (C-Ar); HRMS calcd. for $C_{24}H_{33}N_6OSi$ (ES+) *m*/*z* 449.2480 $[M+H]^+$, found 449.2480.

Note: Unable to visualise all quaternary carbon signals by ^{13}C NMR.

2-(3-(6-(2-(Triisopropylsilyl)ethynyl)-9*H*-purin-2-ylamino)phenyl)-*N*-(2-(dimethylamino)ethyl)acetamide (188)

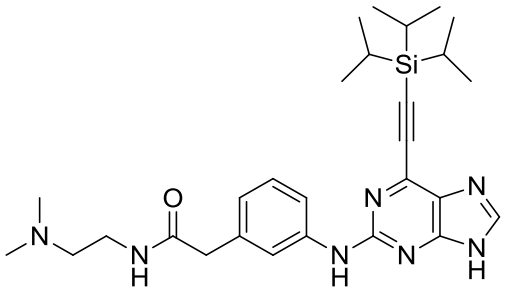

Carboxylic acid **186** (0.188 g, 0.42 mmol), CDI (0.136 g, 0.84 mmol), DIPEA (145 µl, 0.84 mmol) and *N*,*N*-dimethylethylenediamine (183 µl, 1.67 mmol) were reacted in dry DMF (5 ml) according to **general procedure J**. Chromatography on KP-NH silica (19:1 DCM/MeOH) afforded the desired compound as a yellow oil/gum (0.222 g, 0.42 mmol, 100%). R_f 0.42 (19:1 DCM/MeOH, KP-NH); λ_{max} (EtOH/nm) 276; IR (cm^{-1}) 2966, 2942, 2344, 2158, 1653; ^{1}H NMR (500 MHz, DMSO-d_6) 1.13-1.22 (21H, m, Si(C*H*(C*H*$_3$)$_2$)$_3$), 2.13 (6H, s, N(CH$_3$)$_2$), 2.28 (2H, t, *J* = 6.7 Hz, CH$_2$C*H*$_2$N(CH$_3$)$_2$), 3.15 (2H, dt, *J* = 5.8 and 6.7 Hz, C*H*$_2$CH$_2$N(CH$_3$)$_2$), 3.37 (2H, s, COC*H*$_2$) 6.82-6.86 (1H, m, H-6'), 7.19 (1H, dd, *J* = 7.7 and 7.8 Hz, H-5'), 7.55-7.58 (1H, m, H-2'), 7.73-7.77 (1H, m, H-4'), 7.93 (1H, t, *J* = 5.8 Hz, CON*H*), 8.24 (1H, s, H-8), 9.66 (1H, s, C^2-NH), 13.06 (1H, s, H-9); ^{13}C NMR (125 MHz, DMSO-d_6) 10.6 (Si(*C*H(CH$_3$)$_2$)$_3$), 18.4 (Si(CH(*C*H$_3$)$_2$)$_3$), 36.8 (CH$_2$), 40.1 (CH$_2$), 45.2 (N(CH$_3$)$_2$), 58.2 (CH$_2$), 113.6 (C-Ar), 122.6 (C-Ar), 128.1 (C-Ar), 135.2 (C-Ar), 136.6 (C-Ar), 143.7 (C-Ar), 156.3 (C-Ar), 169.9 (C=O); HRMS calcd. for $C_{28}H_{42}N_7OSi$ (ES+) *m*/*z* 520.3215 $[M+H]^+$, found 520.3211.

Note: Unable to visualise quaternary carbon signals by ^{13}C NMR.

2,2,2-Trifluoroethyl (3-nitrophenyl)methanesulfonate (190)[250]

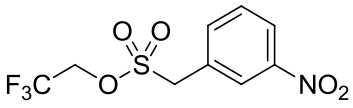

3-Nitro-α-toluenesulfonyl chloride (1.00 g, 4.24 mmol) was added to a solution of DMAP (0.052 g, 0.42 mmol) and triethylamine (1.77 ml, 12.7 mmol) in TFE (10 ml). The mixture was stirred at RT for 3 hour, after which the solvent was removed *in vacuo*. The residue was dissolved in DCM (60 ml) and washed with 0.05 M HCl (60 ml) and water (60 ml), and the

organic phase was passed through a phase separator and concentrated. The resulting oil was sonicated with water (5 ml), resulting in the formation of the product as a white precipitate which was collected *via* filtration and dried (1.25 g, 4.19 mmol, 99%). R_f 0.73 (7:3 Petrol/EtOAc); M.p. 89-91 °C (Lit.[250] 84-85 °C); λ_{max} (EtOH/nm) 257; IR (cm^{-1}) 2998, 2950, 2160, 1977, 1531; ^{1}H NMR (500 MHz, DMSO-d_6) 5.00 (2H, q, J = 8.4 Hz, F_3CCH_2), 5.19 (2H, s, Ar-CH_2), 7.76 (1H, dd, J = 8.0 and 8.2 Hz, H-5), 7.90-7.95 (1H, m, H-6), 8.30 (1H, ddd, J = 2.3, 2.4 and 8.2 Hz, H-4), 8.37-8.39 (1H, m, H-2); ^{13}C NMR (125 MHz, DMSO-d_6) 53.9 (Ar-CH_2), 65.0 (q, J_{CF} = 36.6 Hz, CH_2CF_3), 122.5 (q, J_{CF} = 276.9 Hz, CF_3), 123.8 (C-Ar), 125.5 (C-Ar), 130.2 (C-Ar), 130.3 (C-Ar), 137.4 (C-Ar), 147.8 (C-Ar); ^{19}F NMR (470 MHz, DMSO-d_6) -72.9 (CF_3); LRMS (ES-) m/z 298.1 $[M-H]^-$.

2,2,2-Trifluoroethyl (3-aminophenyl)methanesulfonate (192)[250]

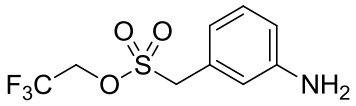

Palladium on carbon (0.30 g, 10% w/w) was added to a solution of the nitro compound **190** (1.00 g, 3.34 mmol) in TFE (10 ml) and EtOAc (3 ml). The mixture was hydrogenated at RT for 18 h before being passed through Celite® and concentrated. The crude oil was purified *via* chromatography on silica (7:3 Petrol/EtOAc) to give an oil, which was triturated with petrol (10 ml) to give the desired compound as a white solid (0.789 g, 2.93 mmol, 88%). R_f 0.36 (7:3 Petrol/EtOAc); M.p. 74-76 °C (Lit.[250] 77-78 °C); λ_{max} (EtOH/nm) 243; IR (cm^{-1}) 3502, 3397, 2945, 2359, 1619; ^{1}H NMR (500 MHz, DMSO-d_6) 4.76 (2H, s, Ar-NH_2), 4.95 (2H, q, J = 8.7 Hz, F_3CCH_2O), 5.28 (2H, s, Ar-CH_2), 6.59-6.64 (2H, m, H-4/H-6), 6.65-6.68 (1H, m, H-2), 7.09 (1H, dd, J = 7.7 and 7.9 Hz, H-5); ^{13}C NMR (125 MHz, DMSO-d_6) 55.6 (Ar-CH_2), 64.8 (q, J_{CF} = 35.0 Hz, CH_2CF_3), 114.3 (C-Ar), 115.9 (C-Ar), 118.1 (C-Ar), 122.6 (q, J_{CF} = 276.9 Hz, CF_3), 128.0 (C-Ar), 129.1 (C-Ar), 148.9 (C-Ar); ^{19}F NMR (470 MHz, DMSO-d_6) -72.87 (CF_3); LRMS (ES+) m/z 270.0 $[M+H]^+$.

2,2,2-Trifluoroethyl (3-((6-((triisopropylsilyl)ethynyl)-9*H*-purin-2-yl)amino)phenyl) methanesulfonate (193)

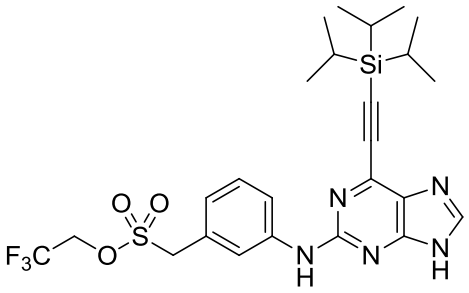

2-Fluoropurine intermediate **160** (0.416 g, 1.31 mmol) and aniline **192** (0.704 g, 2.62 mmol) were reacted with TFA (504 µl, 6.54 mmol) in TFE (10 ml) according to **general procedure B**. The resulting orange oil was purified *via* chromatography on reverse phase silica (19:1 MeOH/H_2O 0.1% HCOOH) followed by chromatography on silica (7:3 Petrol/EtOAc) to give the desired compound as a yellow/orange oil/gum (0.506 g, 0.89 mmol, 68%). R_f 0.34 (9:1 MeOH/H_2O, 0.1% HCOOH, C18); λ_{max} (EtOH/nm) 368, 277; IR (cm^{-1}) 2950, 2365, 2161, 2011, 1967, 1601; ^{1}H NMR (500 MHz, DMSO-d_6) 1.13-2.23 (21H, m, Si(C*H*(CH_3)$_2$)$_3$), 4.85 (2H, s, Ar-CH_2), 4.95 (2H, q, *J* = 8.7 Hz, F_3CCH_2O), 7.00-7.04 (1H, m, H-6'), 7.34 (1H, dd, *J* = 7.9 and 8.1 Hz, H-5'), 7.74-7.77 (1H, m, H-2'), 7.96-8.00 (1H, m, H-4'), 8.28 (1H, s, H-8), 9.84 (1H, s, C^2-NH), 13.12 (1H, br, H-9); ^{13}C NMR (125 MHz, $CDCl_3$) 11.2 (Si(*C*H(CH_3)$_2$)$_3$), 18.7 (Si(CH(*C*H_3)$_2$)$_3$), 57.8 (Ar-CH_2), 65.2 (q, J_{CF} = 38.0 Hz, *C*H_2CF_3), 102.0 (C≡C), 120.0 (C-Ar), 121.0 (C-Ar), 121.9 (q, J_{CF} = 277.8 Hz, CF_3), 124.5 (C-Ar), 127.4 (C-Ar), 129.7 (C-Ar), 140.5 (C-Ar), 156.1 (C-Ar); HRMS calcd. for $C_{25}H_{33}F_3N_5O_3SSi$ (ES+) *m*/*z* 568.2020 $[M+H]^+$, found 568.2015.

Note: Unable to visualise all quaternary carbon signals by ^{13}C NMR.

***N*-(4-Methoxybenzyl)-1-(3-((6-((triisopropylsilyl)ethynyl)-9*H*-purin-2-yl)amino)phenyl)methanesulfonamide (194)**

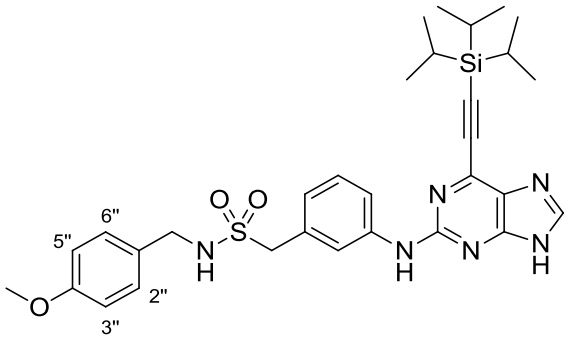

Trifluoroethylsulfonate ester **193** (0.215 g, 0.38 mmol), 4-methoxybenzylamine (64 µl, 0.49 mmol) and DBU (115 µl, 0.76 mmol) were reacted in dry THF (3 ml) according to **general procedure O**. Chromatography on silica (19:1 DCM/MeOH) gave the desired compound as a yellow oil (0.224 g, 0.37 mmol, 97%). R_f 0.44 (19:1 DCM/MeOH); λ_{max} (EtOH/nm) 276; IR (cm^{-1}) 2361, 2341, 2162, 1992, 1969, 1609; ^{1}H NMR (500 MHz, DMSO-d_6) 1.13-1.22 (21H, m, Si(C*H*(CH_3)$_2$)$_3$), 3.72 (3H, s, OCH_3), 4.05 (2H, d, *J* = 6.0 Hz, NHCH_2), 4.23 (2H, s, Ar-CH_2), 6.87 (2H, d, *J* = 8.7 Hz, H-3''/H-5''), 6.91-6.95 (1H, m, H-6'), 7.23 (2H, d, *J* = 8.7 Hz, H-2''/H-6''), 7.28 (1H, dd, *J* = 8.0 and 8.2 Hz, H-5'), 7.55 (1H, t, *J* = 6.0 Hz, N*H*CH_2), 7.72-7.75 (1H, m, H-2'), 7.87-7.91 (1H, m, H-4'), 8.26 (1H, s, H-8), 9.76 (1H, s, C^2-NH), 13.06 (1H, s, H-9); ^{13}C NMR (125 MHz, DMSO-d_6) 10.6 (Si(*C*H(CH_3)$_2$)$_3$), 18.4 (Si(CH(*C*H_3)$_2$)$_3$), 45.7 (NH*C*H_2), 55.0 (OCH3), 58.1 (Ar-CH_2), 97.9 (C≡C), 113.6 (C-Ar), 118.0 (C-Ar), 120.7 (C-Ar), 123.4 (C-Ar), 128.3 (C-Ar), 129.0 (C-Ar), 130.0 (C-Ar), 130.4 (C-Ar), 140.9 (C-Ar), 156.2 (C-Ar), 158.4 (C-Ar); HRMS calcd. for $C_{31}H_{41}N_6O_3SSi$ (ES+) *m*/*z* 605.2725 $[M+H]^+$, found 605.2723.

Note: Unable to visualise all carbon signals by ^{13}C NMR.

(3-((6-((Triisopropylsilyl)ethynyl)-9*H*-purin-2-yl)amino)phenyl) methanesulfonamide (195)

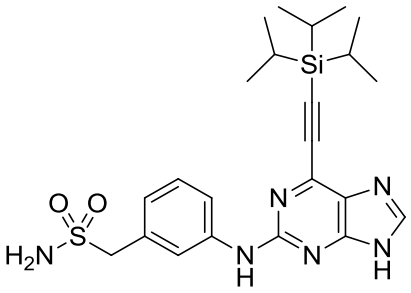

PMB-sulfonamide **194** (0.221 g, 0.37 mmol) was reacted in TFA (6 ml) according to **general procedure K** over 3 h. The crude product was purified *via* chromatography on KP-NH silica (19:1 DCM/MeOH) to give the desired compound as a yellow oil/gum (0.108 g, 0.22 mmol, 60%). R_f 0.21 (19:1 DCM/MeOH, KP-NH); λ_{max} (EtOH/nm) 276; IR (cm^{-1}) 3367, 2943, 2865, 2160, 2021, 1606; ^{1}H NMR (500 MHz, DMSO-d_6) 1.13-1.23 (21H, m, Si(C*H*(C*H*$_3$)$_2$)$_3$), 4.21 (2H, s, Ar-C*H*$_2$), 6.84 (2H, s, SO_2NH_2), 6.95-6.98 (1H, br, H-6'), 7.13 (1H, dd, *J* = 7.9 and 8.0 Hz, H-5'), 7.68-7.71 (1H, m, H-2'), 7.90 (1H, ddd, *J* = 1.0, 1.9 and 8.0 Hz, H-4'), 8.25 (1H, s, H-8), 9.75 (1H, s, C^2-NH), 13.07 (1H, s, H-9); ^{13}C NMR (125 MHz, DMSO-d_6) 10.6 (Si(*C*H(CH$_3$)$_2$)$_3$), 18.4 (Si(CH(*C*H$_3$)$_2$)$_3$), 60.6 (Ar-*C*H$_2$), 97.9 (C≡C), 117.9 (C-Ar), 120.8 (C-Ar), 123.4 (C-Ar), 128.3 (C-Ar), 130.8 (C-Ar), 139.8 (C-Ar), 140.8 (C-Ar), 156.2 (C-Ar); HRMS calcd. for $C_{23}H_{33}N_6O_2SSi$ (ES+) *m*/*z* 485.2149 $[M+H]^+$, found 485.2147.

Note: Unable to visualise all carbon signals by ^{13}C NMR.

***N*-(3-(Dimethylamino)propyl)-1-(3-((6-((triisopropylsilyl)ethynyl)-9*H*-purin-2-yl)amino)phenyl)methanesulfonamide (196)**

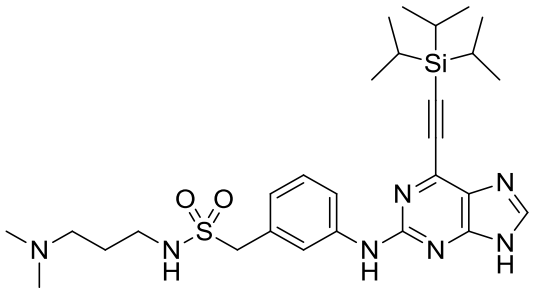

Trifluoroethylsulfonate ester **193** (0.227 g, 0.40 mmol), *N*,*N*-dimethylpropane-1,3-diamine (65 μl, 0.52 mmol) and DBU (120 μl, 0.80 mmol) were reacted in dry THF (3 ml) according to **general procedure O**. Purification by chromatography on KP-NH silica (9:1

DCM/MeOH) afforded the target compound as a yellow oil/gum (0.130 g, 0.23 mmol, 58%). R_f 0.38 (9:1 DCM/MeOH, KP-NH); λ_{max} (EtOH/nm) 372, 276; IR (cm^{-1}) 2941, 2864, 2364, 2166, 2015, 1602; ^{1}H NMR (500 MHz, DMSO-d_6) 1.13-1.21 (21H, m, S(C*H*(CH_3)$_2$)$_3$), 1.58 (2H, tt, *J* = 6.9, 7.0 Hz, NHCH$_2$C*H*$_2$), 2.11 (6H, s, N(CH_3)$_2$), 2.25 (2H, t, *J* = 6.9 Hz, -C*H*$_2$N(CH_3)$_2$), 2.97 (2H, dt, *J* = 4.7 and 7.0 Hz, NHC*H*$_2$CH$_2$), 4.25 (2H, s, Ar-CH$_2$), 6.92-6.96 (1H, m, H-6'), 7.11 (1H, q, *J* = 4.7 Hz, N*H*CH$_2$), 7.28 (1H, dd, *J* = 7.9 and 8.1 Hz, H-5'), 7.77-7.80 (1H, m, H-2'), 7.82-7.86 (1H, m, H-4'), 8.28 (1H, s, H-8), 9.80 (1H, s, C^2-NH); ^{13}C NMR (125 MHz, DMSO-d_6) 10.6 (Si(*C*H(CH_3)$_2$)$_3$), 18.4 (Si(CH(*C*H$_3$)$_2$)$_3$), 27.4 (CH$_2$), 41.1 (CH$_2$), 44.8 (N(CH_3)$_2$), 56.3 (CH$_2$), 57.4 (CH$_2$), 97.9 (C≡C), 117.9 (C-Ar), 120.4 (C-Ar), 123.4 (C-Ar), 128.3 (C-Ar), 130.5 (C-Ar), 140.9 (C-Ar), 156.1 (C-Ar); HRMS calcd. for $C_{28}H_{44}N_7O_2SSi$ (ES+) *m*/*z* 570.3041 $[M+H]^+$, found 570.3043.

Note: Unable to visualise all quaternary carbon signals by ^{13}C NMR.

***tert*-Butyl-4-((3-((6-((triisopropylsilyl)ethynyl)-9*H*-purin-2-yl)amino)benzyl)sulfonyl) piperazine-1-carboxylate (198)**

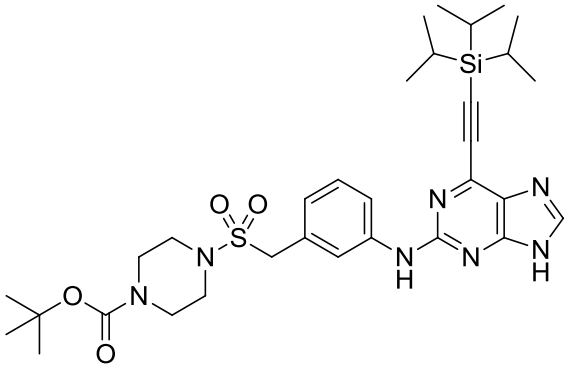

Trifluoroethylsulfonate ester **193** (0.233 g, 0.41 mmol), *tert*-butyl piperazine-1-carboxylate (0.100 g, 0.53 mmol) and DBU (123 µl, 0.82 mmol) were reacted in dry THF (3 ml) according to **general procedure O**. Chromatography on KP-NH silica (9:1 DCM/MeOH) gave the desired compound as a yellow oil (0.186 g, 0.28 mmol, 68%). R_f 0.44 (9:1 DCM/MeOH, KP-NH); λ_{max} (EtOH/nm) 370, 277; IR (cm^{-1}) 2941, 2866, 2362, 2159, 2031, 1691, 1604; ^{1}H NMR (500 MHz, DMSO-d_6) 1.13-1.22 (21H, m, Si(C*H*(CH_3)$_2$)$_3$), 1.33 (9H, s, C(CH_3)$_3$), 3.06-3.12 (4H, m, SO$_2$N(C*H*$_2$CH$_2$)$_2$), 3.30-3.35 (4H, br, SO$_2$N(CH$_2$C*H*$_2$)$_2$), 4.36 (2H, s, Ar-CH$_2$), 6.81-6.85 (1H, m, H-6'), 7.30 (1H, dd, *J* = 7.9 and 8.0 Hz, H-5'), 7.80-7.82 (1H, m, H-2'), 7.88-7.92 (1H, m, H-4'), 8.27 (1H, s, H-8), 9.84 (1H, s, C^2-NH), 13.10 (1H, s, H-9); ^{13}C NMR (125 MHz, DMSO-d_6) 10.6 (Si(*C*H(CH_3)$_2$)$_3$), 18.4 (Si(CH(*C*H$_3$)$_2$)$_3$), 27.87

(CH_2), 30.68 (CH_2), 45.26 Ar-*C*H_2), 79.18 (C≡C), 122.6 (C-Ar), 127.1 (C-Ar), 153.52 (quat-C); HRMS calcd. for $C_{32}H_{48}N_7O_4SSi$ (ES+) *m*/*z* 654.3252 $[M+H]^+$, found 654.3262.

Note: Unable to visualise all quaternary carbon signals by ^{13}C NMR.

***N*-(3-((Piperazin-1-ylsulfonyl)methyl)phenyl)-6-((triisopropylsilyl)ethynyl)-9*H*-purin-2-amine (197)**

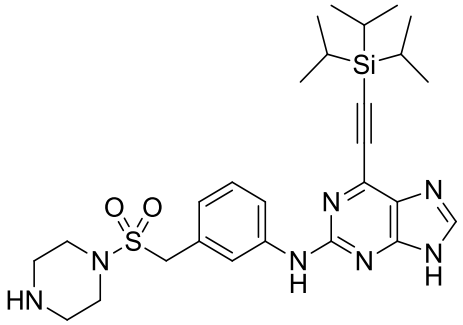

The Boc-protected amine **198** (0.179 g, 0.27 mmol) and TFA (210 μl, 2.70 mmol) were reacted in DCM (5 ml) according to **general procedure L**. Purification *via* chromatography on silica (19:1 DCM/MeOH) afforded the desired compound as a yellow oil/gum (0.140 g, 0.25 mmol, 93%). R_f 0.36 (19:1 DCM/MeOH); λ_{max} (EtOH/nm) 276; IR (cm^{-1}) 3325, 3252, 2940, 2864, 2456, 1733; ^1H NMR (500 MHz, DMSO-d_6) 1.12-1.25 (21H, m, Si(C*H*(CH_3)$_2$)$_3$), 2.72-2.78 (4H, m, SO_2N(C$H_2$$CH_2$)$_2$), 3.20-3.25 (4H, br, SO_2N(CH_2CH_2)$_2$), 4.36 (2H, s, Ar-CH_2), 6.98 (1H, dd, *J* = 1.4, 1.5 and 7.6 Hz, H-6'), 7.27 (1H, dd, *J* = 7.6 and 7.8 Hz, H-5'), 7.52-7.56 (1H, m, H-4'), 7.86-7.89 (1H, m, H-2'), 8.20 (1H, s, H-8), 9.72 (1H, s, C^2-NH); ^{13}C NMR (125 MHz, DMSO-d_6) 10.6 (Si(*C*H(CH_3)$_2$)$_3$), 18.5 (Si(CH(*C*H_3)$_2$)$_3$), 27.2 (CH_2), 33.8 (CH_2), 43.6 (Ar-CH_2), 94.3 (C≡C), 118.3 (C-Ar), 130.4 (C-Ar), 156.1 (C-Ar); HRMS calcd. for $C_{27}H_{40}N_7O_2SSi$ (ES+) *m*/*z* 554.2728 $[M+H]^+$, found 554.2724.

Note: Unable to visualise all carbon signals by ^{13}C NMR.

2-(3-(6-Ethynyl-9*H*-purin-2-ylamino)phenyl)acetamide (177)

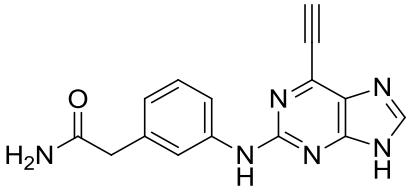

The TIPS-protected purine **189** (0.165 g, 0.37 mmol) was reacted with TBAF (1M in THF, 0.55 ml, 0.55 mmol) in THF (4 ml) according to **general procedure I**. The residue was purified *via* semi-preparative HPLC (17:3 H_2O/MeCN), to give the desired compound as a yellow solid (0.084 g, 0.28 mmol, 76 %). R_f 0.32 (17:3 DCM/MeOH, KP-NH); M.p. 250-270 °C (decomposed); λ_{max} (EtOH/nm) 274; IR (cm^{-1}) 3359, 3170, 2921, 2107, 1658; ^{1}H NMR (500 MHz, DMSO-d_6) 4.76 (1H, s, C≡CH), 6.77-6.81 (1H, m, H-6'), 6.83 (1H, s, CON*H*H'), 7.15 (1H, dd, *J* = 8.0 and 8.1 Hz, H-5'), 7.38 (1H, s, CONH*H'*), 7.47-7.50 (1H, m, H-2'), 7.68-7.73 (1H, m, H-4'), 8.19 (1H, s, H-8), 9.52 (1H, s, C^2-NH), 13.06 (1H, s, H-9); ^{13}C NMR (125 MHz, DMSO-d_6) 48.6 (CO*C*H_2), 79.1 (*C*≡CH), 86.7 (C≡*C*H), 116.4 (C-Ar), 119.2 (C-Ar), 121.8 (C-Ar), 128.2 (C-Ar), 136.6 (C-Ar), 140.8 (C-Ar), 144.5 (C-Ar), 156.1 (C-Ar), 172.2 (C=O); HRMS calcd. for $C_{15}H_{13}N_6O$ (ES+) *m/z* 293.1149 $[M+H]^+$, found 293.1145.

(3-((6-Ethynyl-9*H*-purin-2-yl)amino)phenyl)methanesulfonamide (178)

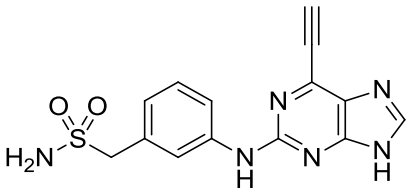

The TIPS-protected purine **195** (60 mg, 0.12 mmol), TBAF (1M in THF, 0.15 ml, 0.15 mmol) and the TBAF scavenger bead system **231** (0.60 g, 10 x w/w) were reacted in THF (5 ml) according to **general procedure U**. Silica gel chromatography (9:1 DCM/MeOH) gave the target compound as a pale yellow solid (23 mg, 0.07 mmol, 58%). R_f 0.29 (9:1 DCM/MeOH); M.p. 190-210 °C (decomposed); λ_{max} (EtOH/nm) 273.5, 359.0; IR (cm^{-1}) 3361, 3248, 2976, 2809, 2707, 2114, 1701, 1610, 1583, 1491; ^{1}H NMR (500 MHz, DMSO-d_6) 4.22 (2H, s, SO_2CH_2), 4.85 (1H, s, C≡CH), 6.86 (2H, s, SO_2NH_2), 6.94-6.98 (1H, m, H-6'), 7.30 (1H, dd, *J* = 7.7 and 8.0 Hz, H-5'), 7.64-7.68 (1H, m, H-2'), 7.88-7.92 (1H, m, H-4'), 8.29 (1H, s, H-8), 9.72 (1H, s, C^2-NH), 13.13 (1H, br, H-9); ^{13}C NMR (125 MHz,

DMSO-d_6) 60.6 (SO_2CH_2), 78.9 (*C*≡CH), 87.1 (C≡*C*H), 118.0 (C-Ar), 120.8 (C-Ar), 123.5 (C-Ar), 128.3 (C-Ar), 130.8 (C-Ar), 140.8 (C-Ar), 156.2 (C-Ar); HRMS calcd. for $C_{14}H_{13}N_6O_2S$ (ES+) *m*/*z* 329.0815 $[M+H]^+$, found 329.0821.

Note: Unable to visualise all carbon environments by ^{13}C NMR.

2-(3-(6-(2-(Triisopropylsilyl)ethynyl)-9*H*-purin-2-ylamino)phenyl)-*N*,*N*-dimethylacetamide (214)

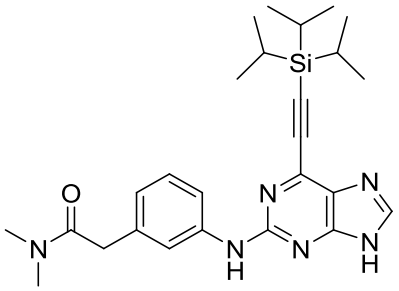

Carboxylic acid **186** (54 mg, 0.12 mmol), CDI (40 mg, 0.24 mmol), DIPEA (125 µl, 0.72 mmol) and dimethylamine hydrochloride (40 mg, 0.48 mmol) were reacted in dry DMF (1 ml) according to **general procedure J**. Chromatography on KP-NH silica (19:1 DCM/MeOH) gave the desired compound as a yellow oil (51 mg, 0.11 mmol, 92%). R_f 0.38 (19:1 DCM/MeOH, KP-NH); λ_{max} (EtOH/nm) 275, 368; IR (cm^{-1}) 3117, 2965, 2943, 2363, 2160, 1711, 1598; ^1H NMR (500 MHz, $CDCl_3$) 1.14-1.18 (21H, m, Si(C*H*(CH_3)$_2$)$_3$), 2.96 (3H, s, N-CH_3), 3.01 (3H, s, N-CH_3), 3.68 (2H, s, CH_2), 6.82-6.85 (1H, m, H-6'), 7.16 (1H, dd, *J* = 7.9 and 8.0 Hz, H-5'), 7.34-7.38 (1H, m, H-4'), 7.61 (1H, s, H-8), 7.65 (1H, br, H-2'), 7.86 (1H, s, C^2-NH); ^{13}C NMR (125 MHz, $CDCl_3$) 11.3 (Si(*C*H(CH_3)$_2$)$_3$), 18.7 (Si(CH(*C*H_3)$_2$)$_3$), 35.8 (N-CH_3), 37.8 (N-CH_3), 40.9 (CO*C*H_2), 100.9 (C≡C), 101.1 (C≡C), 117.9 (C-Ar), 119.7 (C-Ar), 122.8 (C-Ar), 129.2 (C-Ar), 135.6 (C-Ar), 137.0 (C-Ar), 140.3 (C-Ar), 142.4 (C-Ar), 156.2 (C-Ar), 171.6 (C=O); HRMS calcd. for $C_{26}H_{37}N_6OSi$ (ES+) *m*/*z* 477.2793 $[M+H]^+$, found 477.2797.

2-(4-(6-(2-(Triisopropylsilyl)ethynyl)-9*H*-purin-2-ylamino)phenyl)acetic acid (215)

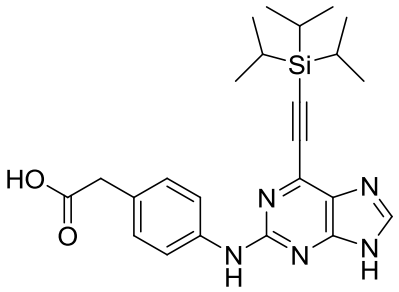

2-Fluoropurine intermediate **160** (0.485 g, 1.53 mmol), (4-aminophenyl)acetic acid (0.460 g, 3.05 mmol) and TFA (588 µl, 7.63 mmol) were reacted in TFE (15 ml) according to **general procedure B**. Upon completion of the reaction, the residue was dissolved in THF (15 ml) and 1M NaOH solution (10 ml). The mixture was stirred at RT for 18 h before the THF was removed *in vacuo*. The aqueous solution was then taken to pH 3 with 4M HCl solution and extracted with EtOAc (3 x 30 ml). The combined organic extracts were dried (Na_2SO_4) and concentrated, and the resulting orange residue was purified *via* chromatography on reverse phase silica (9:1 MeOH/H_2O 0.1% HCOOH). The desired product was obtained as an orange oil (0.365 g, 0.81 mmol, 53%). R_f 0.44 (9:1 MeOH/H_2O, 0.1% HCOOH, C18); λ_{max} (EtOH/nm) 263, 368; IR (cm^{-1}) 2942, 2866, 2540, 2161, 2037, 1636; ^{1}H NMR (500 MHz, DMSO-d_6) 1.16 (21H, m, Si(CH(CH_3)$_2$)$_3$), 3.34 (2H, s, CH_2), 7.16 (2H, d, *J* = 8.6 Hz, H-2'/H-6'), 7.73 (2H, d, *J* = 8.6 Hz, H-3'/H-5'), 8.24 (1H, s, H-8), 9.66 (1H, s, C^2-NH), 13.10 (1H, br, H-9); ^{13}C NMR (125 MHz, MeOD) 12.5 (Si(*C*H(CH_3)$_2$)$_3$), 19.1 (Si(CH(*C*H_3)$_2$)$_3$), 41.4 (CO*C*H_2), 100.4 (C≡C), 102.5 (C≡C), 120.0 (C-Ar), 109.2 (C-Ar), 130.5 (C-Ar), 140.8 (C-Ar), 143.9 (C-Ar), 158.4 (C-Ar), 176.1 (C=O); HRMS calcd. for $C_{24}H_{30}N_5O_2Si$ (ES-) *m*/*z* 448.2174 $[M-H]^-$ found 448.2163.

Note: Unable to visualise all carbon signals by NMR.

***N*-(4-Methoxybenzyl)-2-(4-(6-(2-(triisopropylsilyl)ethynyl)-9*H*-purin-2-ylamino)phenyl) acetamide (216)**

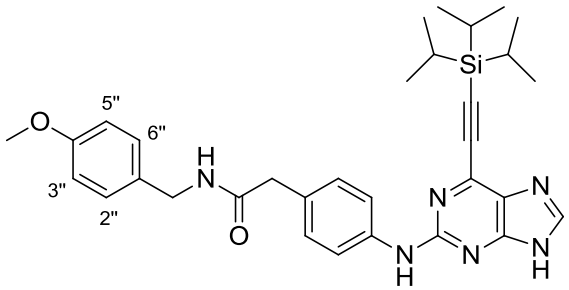

The carboxylic acid **215** (0.160 g, 0.36 mmol), CDI (0.115 g, 0.71 mmol), DIPEA (125 µl, 0.71 mmol) and 4-methoxybenzylamine (185 µl, 1.43 mmol) were reacted in dry DMF (2 ml) according to **general procedure J**. Purification on KP-NH silica (19:1 DCM/MeOH) gave the desired compound as a yellow oil (0.159 g, 0.28 mmol, 78%). R_f 0.48 (19:1 DCM/MeOH, KP-NH); λ_{max} (EtOH/nm) 278, 370; IR (cm^{-1}) 3102, 2965, 2943, 2364, 2154, 1646; ^{1}H NMR (500 MHz, $CDCl_3$) 1.14-1.23 (21H, m, Si(C*H*(CH_3)$_2$)$_3$), 3.62 (2H, s, CH_2CO), 3.80 (3H, s, OCH_3), 4.41 (2H, d, *J* = 5.8 Hz, C*H*$_2$NH), 6.13 (1H, br, CH_2N*H*), 6.86 (2H, d, *J* = 8.8 Hz, H-2'/H-6'), 7.18 (2H, d, *J* = 8.8 Hz, H-3'/H-5'), 7.21 (2H, d, *J* = 8.5 Hz, H-3''/H-5''), 7.56 (2H, d, *J* = 8.5 Hz, H-2''/H-6''), 8.08 (1H, s, C^2-NH), 8.23 (1H, s, H-8); ^{13}C NMR (125 MHz, $CDCl_3$) 11.3 (Si(*C*H(CH_3)$_2$)$_3$), 18.7 (Si(CH(*C*H_3)$_2$)$_3$), 43.0 (CH_2), 43.3 (CH_2), 55.3 (OCH_3), 114.1 (C-Ar), 120.8 (C-Ar), 121.6 (C-Ar), 129.0 (C-Ar), 129.9 (C-Ar), 134.8 (C-Ar), 141.9 (C-Ar), 174.6 (C=O); HRMS calcd. for $C_{32}H_{41}N_6O_2Si$ (ES+) *m*/*z* 569.3055 $[M+H]^+$, found 569.3051.

Note: Unable to visualise all carbon signals by NMR.

2-(4-(6-(2-(Triisopropylsilyl)ethynyl)-9*H*-purin-2-ylamino)phenyl) acetamide (217)

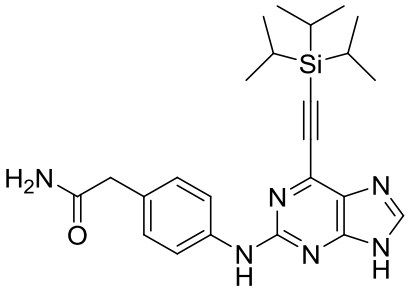

PMB-carboxamide **216** (87 mg, 0.15 mmol) and TFA (2 ml) were reacted according to **general procedure K**. Chromatography on KP-NH silica (9:1 DCM/MeOH) gave the target

compound as a yellow oil (60 mg, 0.13 mmol, 87%). R_f 0.37 (9:1 DCM/MeOH, KP-NH); λ_{max} (EtOH/nm) 278, 370; IR (cm^{-1}) 3472, 2943, 2865, 2040, 1659; ^{1}H NMR (500 MHz, DMSO-d_6) 1.13-1.23 (21H, m, Si(C*H*(CH_3)$_2$)$_3$), 3.31 (2H, s, $COCH_2$), 6.83 (1H, s, -CON*H*H'), 7.16 (2H, d, *J* = 8.6 Hz, H-2'/H-6'), 7.38 (1H, s, CONH*H'*), 7.71 (2H, d, *J* = 8.6 Hz, H-3'/H-5'), 8.22 (1H, s, H-8), 9.64 (1H, s, C^2-NH), 13.06 (1H, br, H-9); ^{13}C NMR (125 MHz, DMSO-d_6) 10.4 (Si(*C*H(CH_3)$_2$)$_3$), 18.4 (Si(CH(*C*H_3)$_2$)$_3$), 118.4 (C-Ar), 129.0 (C-Ar), 142.6 (C-Ar), 172.6 (C=O); HRMS calcd. for $C_{24}H_{33}N_6OSi$ (ES+) *m*/*z* 449.2480 $[M+H]^+$, found 449.2480.

Note: Unable to visualise all carbon signals by NMR.

3-(3-(*tert*-Butoxycarbonylamino)phenyl)propanoic acid (220)

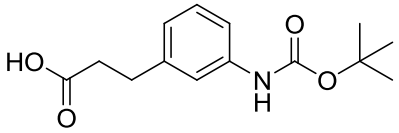

(3-Aminophenyl)propionic acid (1.00 g, 6.06 mmol) and di-*tert*-butyl dicarbonate (1.45 g, 6.66 mmol) were reacted in 1,4-dioxane (12 ml), 1 M NaOH (6 ml) and water (6 ml) according to **general procedure P**. The desired compound was obtained as an off-white waxy solid (1.42 g, 5.35mmol, 88%). R_f 0.18 (1:1 Petrol/EtOAc); M.p. 120-123 °C; λ_{max} (EtOH/nm) 249, 276; IR (cm^{-1}) 3307, 2927, 1690; ^{1}H NMR (500 MHz, DMSO-d_6) 1.48 (9H, s, C(CH_3)$_3$), 2.50 (2H, t, *J* = 7.7 Hz, ArCH_2), 2.76 (2H, t, *J* = 7.7 Hz, $COCH_2$), 6.81-6.85 (1H, m, H-6), 7.11-7.16 (1H, m, H-5), 7.22-7.26 (1H, m, H-4), 7.34-7.37 (1H, m, H-2), 9.27 (1H, s, Ar-NH), 12.13 (1H, s, COOH); ^{13}C NMR (125 MHz, DMSO-d_6) 28.1 (-C(*C*H_3)$_3$), 30.5 (CH_2), 35.2 (CH2), 78.9 (-*C*(CH_3)$_3$), 116.0 (C-Ar), 117.9 (C-Ar), 121.9 (C-Ar), 128.5 (C-Ar), 139.5 (C-Ar), 141.3 (C-Ar), 152.7 (carbamate C=O), 173.6 (acid C=O); HRMS calcd. for $C_{14}H_{18}NO_4$ (ES-) *m*/*z* 264.1241 $[M-H]^-$ found 264.1233.

***tert*-Butyl-3-(2-(4-methoxybenzylcarbamoyl)ethyl)phenyl carbamate (222)**

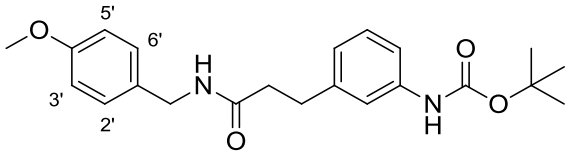

Carboxylic acid **220** (0.762 g, 2.87 mmol), CDI (0.932 g, 5.74 mmol), DIPEA (1.00 ml, 5.74 mmol) and 4-methoxybenzylamine (1.50 ml, 11.5 mmol) were reacted in dry DMF (15 ml) according to **general procedure J**. Chromatography on silica (1:1 Petrol/EtOAc) gave the desired compound as a colourless oil (1.08 g, 2.80 mmol, 98%). R_f 0.48 (1:1 Petrol/EtOAc); λ_{max} (EtOH/nm) 232, 274; IR (cm^{-1}) 3363, 3271, 2971, 2933, 1698, 1643; ^{1}H NMR (500 MHz, DMSO-d_6) 1.47 (9H, s, -C(CH_3)$_3$), 2.40 (2H, t, *J* = 7.6 Hz, C$H_2$$CH_2$), 2.78 (2H, t, *J* = 7.6 Hz, CH_2CH_2), 3.72 (3H, s, OCH_3), 4.18 (2H, d, *J* = 5.9 Hz, CH_2NH), 6.79-6.83 (1H, m, H-4'), 6.84 (2H, d, *J* = 8.4 Hz, H-3'/H-5'), 7.07 (2H, d, *J* = 8.4 Hz, H-2'/H-6'), 7.14 (1H, dd, *J* = 8.1 and 8.2 Hz, H-5'), 7.21-7.24 (1H, m, H-6'), 7.35-7.38 (1H, m, H-2'), 8.25 (1H, t, *J* = 5.9 Hz, CH_2N*H*), 9.27 (1H, s, Ar-NH); ^{13}C NMR (125 MHz, DMSO-d_6) 28.1 (-C(*C*H_3)$_3$), 31.4 (CH_2), 37.1 (CH_2), 41.4 (CH_2), 55.0 (OCH_3), 79.2 (-*C*(CH_3)$_3$), 113.6 (C-Ar), 115.9 (C-Ar), 118.1 (C-Ar), 122.0 (C-Ar), 128.4 (C-Ar), 131.4 (C-Ar), 139.5 (C-Ar), 141.7 (C-Ar), 152.7 (carbamate C=O), 158.1 (C-Ar), 160.8 (C-Ar), 171.0 (amide C=O); HRMS calcd. for $C_{22}H_{29}N_2O_4$ (ES+) *m*/*z* 385.2122 $[M+H]^+$, found 385.2126.

***N*-(4-Methoxybenzyl)-3-(3-aminophenyl)propanamide (224)**

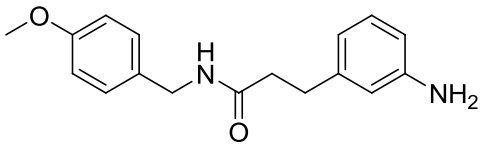

Boc-protected aniline **222** (1.00 g, 2.60 mmol) was reacted with TFA (2.00 ml, 26.0 mmol) in DCM (25 ml) according to **general procedure L**. Silica gel chromatography (1:1 Petrol/EtOAc) afforded the desired compound as a white solid (0.643 g, 2.26 mmol, 87%). R_f 0.46 (1:1 Petrol/EtOAc); M.p. 88-91 °C; λ_{max} (EtOH/nm) 231, 274; IR (cm^{-1}) 3424, 3337, 3241, 3063, 2945, 2904, 1629; ^{1}H NMR (500 MHz, DMSO-d_6) 2.36 (2H, t, *J* = 7.8 Hz, C$H_2$$CH_2$), 2.67 (2H, t, *J* = 7.8 Hz, CH_2CH_2), 3.73 (3H, s, OCH_3), 4.18 (2H, d, *J* = 5.9 Hz, CH_2NH), 4.95 (2H, s, Ar-NH_2), 6.33-6.40 (3H, m, H-2/H-4/H-6), 6.86 (2H, d, *J* = 7.9 Hz, H-3'/H-5'), 6.90 (1H, dd, *J* = 7.4 and 7.5 Hz, H-5), 7.11 (2H, d, *J* = 7.9 Hz, H-2'/H-6'), 8.25

(1H, t, *J* = 5.9 Hz, CH_2NH); ^{13}C NMR (125 MHz, DMSO-d_6) 31.4 (CH_2), 37.1 (CH_2), 41.4 (CH_2), 55.0 (OCH_3), 111.6 (C-Ar), 113.6 (C-Ar), 113.9 (C-Ar), 115.7 (C-Ar), 128.4 (C-Ar), 128.7 (C-Ar), 131.5 (C-Ar), 141.8 (C-Ar), 148.5 (C-Ar), 158.1 (C-Ar), 171.3 (C=O); HRMS calcd. for $C_{17}H_{21}N_2O_2$ (ES+) *m/z* 285.1598 $[M+H]^+$, found 285.1603.

_N_-(4-Methoxybenzyl)-3-(3-(6-(2-(triisopropylsilyl)ethynyl)-9_H_-purin-2-ylamino)phenyl)propanamide (226)

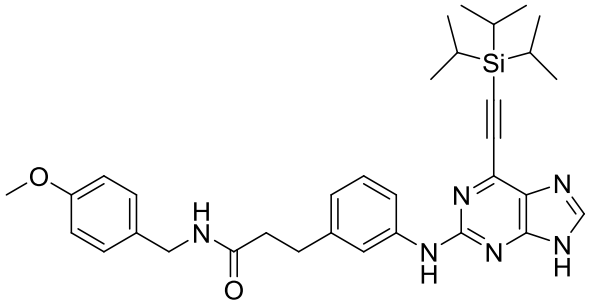

2-Fluoropurine intermediate **160** (0.273 g, 0.86 mmol), aniline **224** (0.490 g, 1.72 mmol) and TFA (330 µl, 4.29 mmol) were reacted in TFE (5 ml) according to **general procedure B**. Chromatography on KP-NH silica (19:1 DCM/MeOH) gave the target compound as a yellow oil (0.205 g, 0.35 mmol, 41%). R_f 0.35 (19:1 DCM/MeOH, KP-NH); λ_{max} (EtOH/nm) 277, 363; IR (cm^{-1}) 3278, 3082, 2944, 2865, 2359, 1644; ^1H NMR (500 MHz, $CDCl_3$) 1.17-1.31 (21H, m, $Si(CH(CH_3)_2)_3$), 2.57 (2H, t, *J* = 7.3 Hz, CH_2CH_2), 2.99 (2H, t, *J* = 7.3 Hz, CH_2CH_2), 3.73 (3H, s, OCH_3), 4.31 (2H, d, *J* = 5.5 Hz, CH_2NH), 6.12 (1H, br, CH_2NH), 6.72 (2H, d, *J* = 8.8 Hz, H-3''/H-5''), 6.82-6.86 (1H, m, H-6'), 7.01 (2H, d, *J* = 8.8 Hz, H-2''/H-6''), 7.17-7.23 (2H, m, H-4'/H-5'), 7.37 (1H, s, C^2-NH), 7.79 (1H, s, H-8), 7.83 (1H, br, H-2'), 11.94 (1H, br, H-9); ^{13}C NMR (125 MHz, $CDCl_3$) 11.3 ($Si(CH(CH_3)_2)_3$), 18.7 ($Si(CH(CH_3)_2)_3$), 31.8 (CH_2), 38.1 (CH_2), 43.2 (CH_2), 55.2 (OCH_3), 101.2 (C≡C), 113.9 (C-Ar), 117.3 (C-Ar), 119.0 (C-Ar), 122.5 (C-Ar), 129.0 (C-Ar), 129.1 (C-Ar), 129.9 (C-Ar), 139.9 (C-Ar), 141.4 (C-Ar), 156.3 (C-Ar), 158.9 (C-Ar), 172.5 (C=O); HRMS calcd. for $C_{33}H_{43}N_6O_2Si$ (ES+) *m/z* 583.3211 $[M+H]^+$, found 583.3212.

Note: Unable to visualise all carbon signals by NMR.

3-(3-(6-(2-(Triisopropylsilyl)ethynyl)-9*H*-purin-2-ylamino)phenyl) propanamide (228)

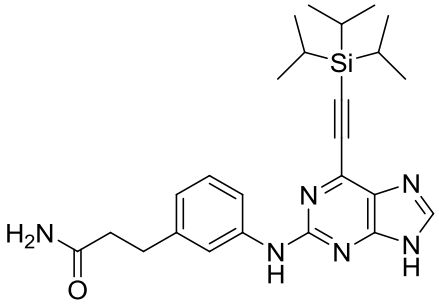

PMB-carboxamide **226** (0.178 g, 0.31 mmol) and TFA (3 ml) were reacted according to **general procedure K**. Chromatography on KP-NH silica (19:1 DCM/MeOH) gave the desired compound as a yellow oil (81 mg, 0.18 mmol, 58%). R_f 0.38 (19:1 DCM/MeOH, KP-NH); λ_{max} (EtOH/nm) 260, 368; IR (cm^{-1}) 3185, 2942, 2864, 2159, 2030, 1660; ^{1}H NMR (500 MHz, DMSO-d_6) 1.10-1.23 (21H, m, Si(C*H*(C*H*$_3$)$_2$)$_3$), 2.37 (2H, t, *J* = 7.6 Hz, C*H*$_2$CH$_2$), 2.78 (2H, t, *J* = 7.6 Hz, CH$_2$C*H*$_2$), 6.77-6.80 (2H, m, CON*H*H'/H-6'), 7.17 (1H, dd, *J* = 7.8 and 7.9 Hz, H-5'), 7.31 (1H, s, CONH*H'*), 7.61-7.64 (1H, m, H-4'), 7.66-7.69 (1H, m, H-2'), 8.25 (1H, s, H-8), 9.63 (1H, s, C^2-NH), 13.08 (1H, br, H-9); ^{13}C NMR (125 MHz, DMSO-d_6) 10.6 (Si(*C*H(CH$_3$)$_2$)$_3$), 18.4 (Si(CH(*C*H$_3$)$_2$)$_3$), 31.3 (CH$_2$), 36.8 (CH$_2$), 116.1 (C-Ar), 118.1 (C-Ar), 120.8 (C-Ar), 128.3 (C-Ar), 140.9 (C-Ar), 141.6 (C-Ar), 156.2 (C-Ar), 173.4 (C=O); HRMS calcd. for $C_{25}H_{35}N_6OSi$ (ES+) *m*/*z* 463.2636 $[M+H]^+$, found 463.2634.

Note: Unable to visualise all carbon signals by NMR.

3-((*tert*-Butoxycarbonyl)amino)benzoic acid (221)[251]

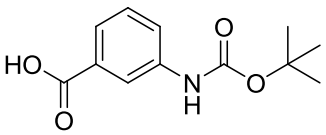

3-Aminobenzoic acid (1.00 g, 7.29 mmol) and di-*tert*-butyl dicarbonate (1.75 g, 8.02 mmol) were reacted in 1,4-dioxane (15 ml), 0.5M NaOH (15 ml) according to **general procedure P**. The desired compound was obtained as a white waxy solid (1.61 g, 6.77 mmol, 93%). R_f 0.15 (1:1 Petrol/EtOAc); M.p. 183-185 °C (Lit.[251] 189-190 °C); λ_{max} (EtOH/nm) 247, 301; IR (cm^{-1}) 3352, 3002, 2971, 1690; ^{1}H NMR (500 MHz, DMSO-d_6) 1.49 (9H, s, -C(CH$_3$)$_3$), 7.37 (1H, dd, *J* = 7.9 and 8.0 Hz, H-5), 7.54 (1H, ddd, *J* = 1.2, 1.3 and 7.9 Hz, H-6), 7.61-7.65 (1H, m, H-4), 8.13-8.16 (1H, m, H-2), 9.55 (1H, br, Ar-NH), 12.88 (1H, br, COOH); ^{13}C NMR (125

MHz, DMSO-d_6) 28.1 (C(CH$_3$)$_3$), 79.3 (C(CH$_3$)$_3$), 122.2 (C-Ar), 122.9 (C-Ar), 128.8 (C-Ar), 131.3 (C-Ar), 139.8 (C-Ar), 152.7 (carbamate C=O), 167.3 (acid C=O); LRMS (ES-) *m*/*z* 236.2 [M-H]$^-$.

tert-Butyl 3-(4-methoxybenzylcarbamoyl)phenyl carbamate (223)

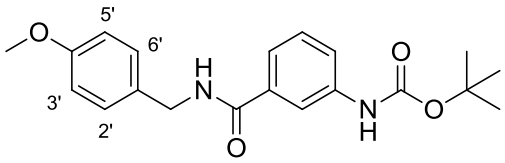

Carboxylic acid **221** (0.601 g, 2.53 mmol), CDI (0.823 g, 5.07 mmol), DIPEA (885 µl, 5.07 mmol) and 4-methoxybenzylamine (1.31 ml, 10.1 mmol) were reacted in dry DMF (13 ml) according to **general procedure J**. Purification *via* chromatography on silica (7:3 Petrol/EtOAc) gave the desired compound as a white solid (0.841 g, 2.36 mmol, 93%). R_f 0.27 (7:3 Petrol/EtOAc); M.p. 166-170 °C; λ_{max} (EtOH/nm) 234; IR (cm^{-1}) 3349, 3274, 3062, 2931, 2836, 1697, 1644; ^{1}H NMR (500 MHz, DMSO-d_6) 1.49 (9H, s, -C(CH$_3$)$_3$), 3.74 (3H, s, OCH$_3$), 4.38 (2H, d, J = 6.0 Hz, CH_2NH), 6.89 (2H, d, J = 8.4 Hz, H-3'/H-5'), 7.24 (2H, d, J = 8.4 Hz, H-2'/H-6'), 7.33 (1H, dd, J = 7.9 and 8.1 Hz, H-5), 7.43-7.47 (1H, m, H-4), 7.52-7.56 (1H, m, H-6), 7.98-8.00 (1H, m, H-2), 8.89 (1H, t, J = 6.0 Hz, CH$_2$NH), 9.48 (1H, s, Ar-NH); ^{13}C NMR (125 MHz, DMSO-d_6) 28.1 (C(CH$_3$)$_3$), 42.4 (NHCH$_2$), 55.0 (OCH$_3$), 79.2 (C(CH$_3$)$_3$), 113.8 (C-Ar), 117.4 (C-Ar), 120.8 (C-Ar), 128.3 (C-Ar), 128.5 (C-Ar), 128.6 (C-Ar), 132.8 (C-Ar), 135.3 (C-Ar), 139.6 (C-Ar), 152.8 (carbamate C=O), 160.9 (C-Ar), 166.3 (amide C=O); HRMS calcd. for $C_{20}H_{25}N_2O_4$ (ES+) *m*/*z* 357.1809 [M+H]$^+$, found 357.1812.

***N*-(4-Methoxybenzyl)-3-aminobenzamide (225)**

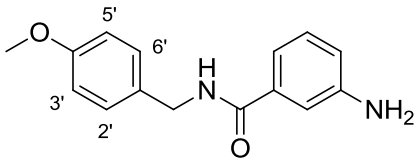

Boc-protected aniline **223** (0.831 g, 2.33 mmol) was reacted with TFA (1.80 ml, 23.3 mmol) in DCM (25 ml) according to **general procedure L**. Purification *via* chromatography on silica (1:1 Petrol/EtOAc) gave the target compound as a white waxy solid (0.472 g,1.84 mmol, 79%). R_f 0.30 (1:1 Petrol/EtOAc); M.p. 90-93 °C; λ_{max} (EtOH/nm) 242, 306; IR (cm^{-1}) 3349, 3274, 2972, 2930, 1697, 1643; ^{1}H NMR (500 MHz, DMSO-d_6) 3.73 (3H, s, OCH$_3$),

4.36 (2H, d, J = 6.1 Hz, CH_2NH), 5.22 (2H, s, Ar-NH_2), 6.89 (1H, ddd, J = 2.3, 2.4 and 7.9 Hz, H-4), 6.88 (2H, d, J = 8.8 Hz, H-3'/H-5'), 6.97-7.00 (1H, m, H-6), 7.04-7.09 (2H, m, H-2/H-5), 7.23 (2H, d, J = 8.8 Hz, H-2'/H-6'), 8.73 (1H, t, J = 6.1 Hz, CH_2NH); ^{13}C NMR (125 MHz, DMSO-d_6) 41.9 (CH_2), 55.0 (OCH_3), 112.8 (C-Ar), 113.6 (C-Ar), 113.7 (C-Ar), 114.2 (C-Ar), 116.3 (C-Ar), 128.5 (C-Ar), 128.6 (C-Ar), 131.9 (C-Ar), 135.4 (C-Ar), 148.6 (C-Ar), 166.8 (C=O); HRMS calcd. for $C_{15}H_{17}N_2O_2$ (ES+) m/z 257.1285 $[M+H]^+$, found 257.1289.

N-(4-Methoxybenzyl)-3-(6-(2-(triisopropylsilyl)ethynyl)-9H-purin-2-ylamino)benzamide (227)

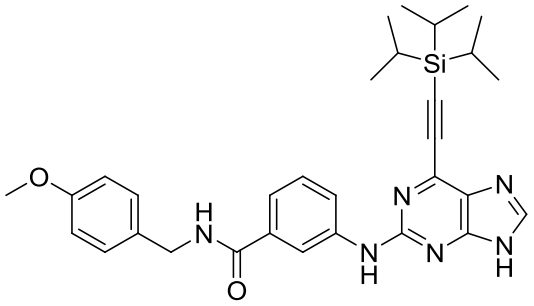

2-Fluoropurine intermediate **160** (0.265 g, 0.83 mmol), aniline **225** (0.428 g, 1.67 mmol) and TFA (320 μl, 4.17 mmol) were reacted in TFE (5 ml) according to **general procedure B**. Purification *via* chromatography on KP-NH silica (19:1 DCM/MeOH) followed by normal phase silica (1:1 Petrol/EtOAc) gave the desired compound as a yellow oil (88 mg, 0.16 mmol, 9%). R_f 0.42 (1:1 Petrol/EtOAc); λ_{max} (EtOH/nm) 279, 364; IR (cm^{-1}) 2864, 2159, 1739, 1641; ^{1}H NMR (500 MHz, DMSO-d_6) 1.13-1.18 (21H, m, Si(CH(CH_3)$_2$)$_3$), 3.74 (3H, s, OCH_3), 4.40 (2H, d, J = 5.9 Hz, CH_2NH), 6.90 (2H, d, J = 8.9 Hz, H-3''/H-5''), 7.27 (2H, d, J = 8.9 Hz, H-2''/H-6''), 7.35 (1H, m, H-5'), 7.41 (1H, m, H-6'), 7.95 (1H, m, H-4'), 8.22-8.25 (2H, m, H-8/H-2'), 8.89 (1H, t, J = 5.9 Hz, CH_2NH), 9.83 (1H, s, C^2-NH), 13.16 (1H, br, H-9); ^{13}C NMR (125 MHz, DMSO-d_6) 10.6 (Si(CH(CH_3)$_2$)$_3$), 18.4 (Si(CH(CH_3)$_2$)$_3$), 42.1 (CH_2), 55.0 (OCH_3), 113.6 (C-Ar), 117.9 (C-Ar), 121.0 (C-Ar), 128.2 (C-Ar), 128.6 (C-Ar), 131.8 (C-Ar), 135.3 (C-Ar), 156.1 (C-Ar), 158.1 (C-Ar), 166.5 (C=O); HRMS calcd. for $C_{31}H_{39}N_6O_2Si$ (ES+) m/z 555.2898 $[M+H]^+$, found 555.2893.

Note: Unable to visualise all carbon signals by NMR.

3-(6-(2-(Triisopropylsilyl)ethynyl)-9*H*-purin-2-ylamino)benzamide (229)

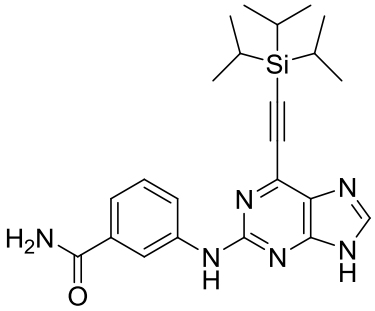

PMB-carboxamide **227** (82 mg, 0.15 mmol) and TFA (2 ml) were reacted according to **general procedure K** over 24 h. Chromatography on KP-NH silica (9:1 DCM/MeOH) afforded the target compound as a yellow oil (55 mg, 0.13 mmol, 87%). R_f 0.41 (9:1 DCM/MeOH, KP-NH); λ_{max} (EtOH/nm) 263, 365; IR (cm^{-1}) 3295, 2964, 2943, 1660; ^1H NMR (500 MHz, DMSO-d_6) 1.14-1.19 (21H, m, Si(C*H*(CH_3)$_2$)$_3$), 7.30-7.36 (2H, m, CON*H*H'/H-5'), 7.40-7.42 (1H, m, H-6'), 7.85 (1H, s, CONH*H'*), 7.90-7.93 (1H, m, H-4'), 8.23 (1H, br, H-2'), 8.31 (1H, s, H-8), 9.83 (1H, s, C^2-NH); ^{13}C NMR (125 MHz, DMSO-d_6) 10.6 (Si(*C*H(CH_3)$_2$)$_3$), 18.4 (Si(CH(*C*H_3)$_2$)$_3$), 98.1 (C≡C), 101.6 (C≡C), 118.0 (C-Ar), 119.9 (C-Ar), 121.1 (C-Ar), 128.1 (C-Ar), 135.1 (C-Ar), 139.1 (C-Ar), 140.8 (C-Ar), 143.2 (C-Ar), 156.2 (C-Ar), 168.4 (C=O); HRMS calcd. for $C_{23}H_{31}N_6OSi$ (ES+) *m*/*z* 435.2323 $[M+H]^+$, found 435.2325.

Note: Unable to visualise all carbon signals by NMR.

2-(3-(6-Ethynyl-9*H*-purin-2-ylamino)phenyl)-*N*,*N*-dimethylacetamide (201)

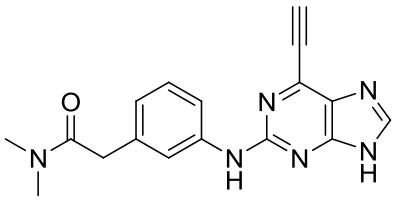

TIPS-protected purine **214** (48 mg, 0.10 mmol) and TBAF (1M in THF, 110 µl, 0.11 mmol) were reacted in THF (2 ml) according to **general procedure I**. Purification on silica gel (9:1 DCM/MeOH) afforded the desired compound as a yellow solid (28 mg, 0.087 mmol, 87%). R_f 0.45 (9:1 DCM/MeOH); M.p. 120-130 °C (decomposed); λ_{max} (EtOH/nm) 274; IR (cm^{-1}) 3084, 2818, 2161, 2110, 2029, 1596; ^1H NMR (500 MHz, DMSO-d_6) 2.65 (3H, s, N-CH_3), 2.83 (3H, s, -N-CH_3), 3.45 (2H, s, CH_2CO), 4.65 (1H, s, C≡CH), 6.57-6.60 (1H, m, H-6'),

7.02 (1H, dd, *J* = 7.8 and 8.0 Hz, H-5'), 7.31-7.34 (1H, m, H-2'), 7.54 (1H, ddd, *J* = 1.0, 1.2 and 7.8 Hz, H-4'), 8.08 (1H, s, H-8), 9.44 (1H, s, C^2-NH), 12.93 (1H, br, H-9); ^{13}C NMR (125 MHz, DMSO-d_6) 34.98 (N-CH_3), 37.29 (N-CH_3), 40.2 (CO*C*H_2) 87.0 (C≡*C*H), 116.5 (C-Ar), 119.1 (C-Ar), 121.8 (C-Ar), 128.3 (C-Ar), 136.1 (C-Ar), 140.8 (C-Ar), 156.2 (C-Ar), 170.2 (C=O); HRMS calcd. for $C_{17}H_{17}N_6O$ (ES+) *m/z* 321.1462 $[M+H]^+$, found 321.1458.

Note: Unable to visualise all carbon signals by NMR.

Solid supported TBAF scavenger (231)[209]

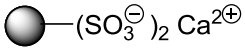

Amberlite 15 Ion exchange resin (SO_3H, 100 ml) was loaded into a column and washed with water (400 ml). The column was eluted with sat. calcium hydroxide solution whilst the pH of the eluent was monitored. Once the initially pH neutral eluent became strongly basic, the column was eluted with water until the pH of the eluent returned to neutral. The resin was washed with DCM (300 ml), THF (300 ml) and Et_2O (300 ml), before being removed from the column and dried in a vacuum oven at 40 °C.

2-(4-(6-Ethynyl-9*H*-purin-2-ylamino)phenyl)acetamide (202)

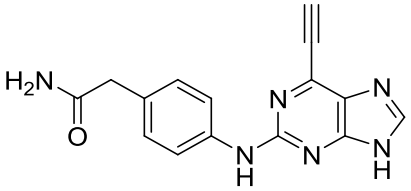

TIPS-protected purine **217** (53 mg, 0.12 mmol) and TBAF (1M in THF, 130 µl, 0.13 mmol) were reacted in THF (2 ml) according to **general procedure I**. Upon completion of the reaction, the solution was diluted with THF (10 ml) and treated with the solid supported TBAF scavenger **231** (0.20 g, 4 x w/w) at RT for 18 h. The resin was removed *via* filtration and the solvent removed *in vacuo*. The crude residue was purified *via* chromatography on silica (9:1 DCM/MeOH) to give the desired compound as a yellow solid (16 mg, 0.055 mmol, 46%). R_f 0.24 (9:1 DCM/MeOH); M.p. 140-150 °C (decomposed); λ_{max} (EtOH/nm) 275; IR (cm^{-1}) 3375, 3287, 3193, 3127, 2157, 2119, 2030, 1653, 1604; ^{1}H NMR (500 MHz, DMSO-d_6) 3.31 (2H, s, $COCH_2$), 4.84 (1H, s, -C≡CH), 6.85 (1H, s, -CON*H*H'), 7.17 (2H, d, *J* = 8.6 Hz, H-2'/H-6'), 7.40 (1H, s, -CONH*H'*), 7.69 (2H, d, *J* = 8.6 Hz, H-3'/H-5'), 8.27 (1H, s, H-

8), 9.62 (1H, s, C^2-NH), 13.12 (1H, br, H-9); ^{13}C NMR (125 MHz, DMSO-d_6) 41.7 (CO*C*H$_2$), 86.9 (C≡*C*H), 118.5 (C-Ar), 129.0 (C-Ar), 139.1 (C-Ar), 156.3 (C-Ar), 172.5 (C=O); HRMS calcd. for $C_{15}H_{13}N_6O$ (ES+) *m*/*z* 293.1148 $[M+H]^+$, found 293.1145.

Note: Unable to visualise all carbon signals by NMR.

3-(3-(6-Ethynyl-9*H*-purin-2-ylamino)phenyl)propanamide (212)

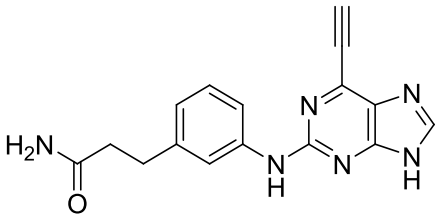

TIPS-protected purine **228** (45 mg, 0.097 mmol) and TBAF (1M in THF, 106 µl, 0.106 mmol) were reacted in THF (2 ml) according to **general procedure I**. Upon completion of the reaction, the solution was diluted with THF (10 ml) and treated with solid supported TBAF scavenger **231** (0.20 g, 4 x w/w) at RT for 18 h. The resin was removed *via* filtration and the solvent removed *in vacuo*. The crude residue was purified *via* chromatography on silica (17:3 DCM/MeOH) to give the desired compound as a yellow solid (16 mg, 0.055 mmol, 46%). R_f 0.45 (17:3 Petrol/EtOAc); M.p. 135-145 °C (decomposed); λ_{max} (EtOH/nm) 273; IR (cm^{-1}) 3380, 3249, 3093, 2828, 2779, 2160, 2116, 2030, 1653; ^{1}H NMR (500 MHz, DMSO-d_6) 2.37 (2H, t, *J* = 7.6 Hz, -COC*H*$_2$CH$_2$), 2.78 (2H, t, *J* = 7.6 Hz, -COCH$_2$C*H*$_2$), 4.84 (1H, s, -C≡CH), 6.77-6.81 (2H, m, -CON*H*H' & H-6'), 7.19 (1H, dd, *J* = 7.9 and 8.0 Hz, H-5'), 7.32 (1H, s, -CONH*H'*), 7.57-7.60 (1H, br, H-2'), 7.66-7.69 (1H, m, H-4'), 8.27 (1H, s, H-8), 9.60 (1H, s, C^2-NH), 13.13 (1H, br, H-9); ^{13}C NMR (125 MHz, DMSO-d_6) 31.3 (CH$_2$), 36.7 (CH$_2$), 86.9 (C≡*C*H), 116.1 (C-Ar), 118.2 (C-Ar), 120.9 (C-Ar), 128.3 (C-Ar), 140.8 (C-Ar), 141.6 (C-Ar), 156.2 (C-Ar), 173.4 (C=O); HRMS calcd. for $C_{16}H_{15}N_6O$ (ES+) *m*/*z* 307.1305 $[M+H]^+$, found 307.1302.

Note: Unable to visualise all carbon signals by NMR.

3-(6-Ethynyl-9*H*-purin-2-ylamino)benzamide (205)

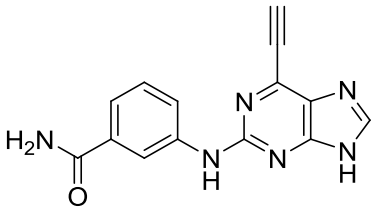

TIPS-protected purine **229** (33 mg, 0.076 mmol), KF (22 mg, 0.38 mmol) and 18-crown-6 (3 mg, 0.008 mmol) were reacted in THF (1 ml) according to **general procedure Q**. Purification *via* chromatography on silica (17:3 DCM/MeOH) afforded the desired compound as a yellow solid (20 mg, 0.071 mmol, 94%). R_f 0.38 (17:3 Petrol/EtOAc); M.p. 170-180 °C (decomposed); λ_{max} (EtOH/nm) 274; IR (cm^{-1}) 3254, 3085, 2830, 2775, 2551, 2162, 2117, 1659; ^{1}H NMR (500 MHz, DMSO-d_6) 4.89 (1H, s, -C≡CH), 7.35 (1H, s, -CON*H*H'), 7.39 (1H, dd, *J* = 7.8 and 7.9 Hz, H-5'), 7.43-7.46 (1H, m, H-6'), 7.90 (1H, s, -CONH*H'*), 7.97-7.80 (1H, m, H-4'), 8.20-8.23 (1H, m, H-2'), 8.32 (1H, s, H-8), 9.80 (1H, s, C^2-NH), 13.21 (1H, br, H-9); HRMS calcd. for $C_{14}H_{11}N_6O$ (ES+) *m*/*z* 279.0993 $[M+H]^+$, found 279.0989.

Note: Insufficient material for ^{13}C NMR.

Methyl 2-(3-aminophenyl)acetate (234)[252]

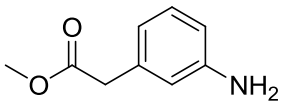

(3-Aminophenyl)acetic acid (1.00 g, 6.62 mmol) and thionyl chloride (970 µl, 13.2 mmol) were reacted in dry MeOH (35 ml) according to **general procedure R**. Chromatography on silica (7:3 Petrol/EtOAc) gave the target compound as a pale yellow oil (0.927 g, 5.61 mmol, 85%). R_f 0.32 (7:3 Petrol/EtOAc); λ_{max} (EtOH/nm) 221, 285; IR (cm^{-1}) 3369, 2952, 1724; ^{1}H NMR (500 MHz, DMSO-d_6) 3.50 (2H, s, CH_2), 3.61 (3H, s, OCH_3), 5.70 (2H, br, Ar-NH_2), 6.45-6.48 (1H, m, H-4), 6.51-6.54 (2H, m, H-2/H-6), 6.97-7.01 (1H, m, H-5); ^{13}C NMR (125 MHz, DMSO-d_6) 40.5 (CH_2), 51.6 (OCH_3), 113.3 (C-Ar), 115.3 (C-Ar), 117.7 (C-Ar), 128.9 (C-Ar), 134.8 (C-Ar), 147.2 (C-Ar), 171.7 (C=O); LRMS (ES+) *m*/*z* 166.2 $[M+H]^+$.

2-(3-Aminophenyl)-*N*-methylacetamide (236)[253]

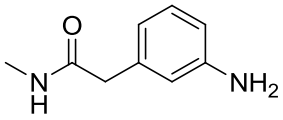

Methyl ester **234** (0.250 g, 1.51 mmol) and methylamine (40% aqueous solution, 8 ml) were reacted according to **general procedure S**. Chromatography on silica (9:1 DCM/MeOH) afforded the desired compound was obtained as a pale yellow oil (0.233 g, 1.42 mmol, 94%). R_f 0.38 (9:1 DCM/MeOH); λ_{max} (EtOH/nm) 220; IR (cm^{-1}) 3331, 3091, 2943, 1629; ^{1}H NMR (500 MHz, DMSO-d_6) 2.56 (3H, d, J = 4.8 Hz, NHCH_3), 3.20 (2H, s, CH_2), 4.98 (2H, s, Ar-NH_2), 6.37-6.41 (2H, m, H-4/H-6), 6.42-6.45 (1H, br, H-2), 6.91 (1H, dd, J = 7.7 and 7.9 Hz, H-5), 7.82 (1H, br, NHCH$_3$); ^{13}C NMR (125 MHz, DMSO-d_6) 25.6 (NHCH$_3$), 42.7 (CH_2), 112.0 (C-Ar), 114.4 (C-Ar), 116.5 (C-Ar), 128.6 (C-Ar), 136.8 (C-Ar), 148.5 (C-Ar), 170.7 (C=O); LRMS (ES+) m/z 165.2 $[M+H]^+$.

2-(3-(6-(2-(Triisopropylsilyl)ethynyl)-9*H*-purin-2-ylamino)phenyl)-*N*-methylacetamide (239)

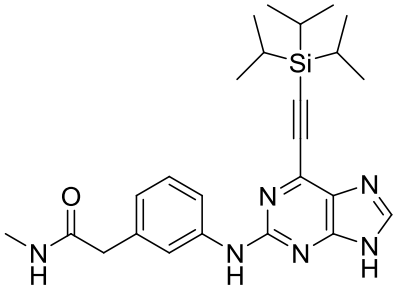

2-Fluoropurine intermediate **160** (0.127 g, 0.40 mmol), aniline **236** (0.130 g, 0.80 mmol) and TFA (155 μl, 2.00 mmol) were reacted in TFE (2 ml) according to **general procedure B**. Purification *via* chromatography on KP-NH silica (19:1 DCM/MeOH) afforded the desired compound as a yellow oil (70 mg, 0.15 mmol, 38%). R_f 0.41 (19:1 DCM/MeOH, KP-NH); λ_{max} (EtOH/nm) 264, 368; IR (cm^{-1}) 2942, 2864, 2159, 1641; ^{1}H NMR (500 MHz, DMSO-d_6) 1.13-1.17 (21H, m, Si(CH(CH_3)$_2$)$_3$), 2.59 (3H, d, J = 4.6 Hz, NHCH_3), 3.36 (2H, s, CH_2), 6.83-6.85 (1H, m, H-6'), 7.20 (1H, dd, J = 7.9 and 7.9 Hz, H-5'), 7.57 (1H, br, H-2'), 7.74-7.77 (1H, m, H-4'), 7.90 (1H, br, NHCH$_3$), 8.25 (1H, s, H-8), 9.66 (1H, s, C^2-NH), 13.08 (1H, s, H-9); ^{13}C NMR (125 MHz, DMSO-d_6) 10.6 (Si(CH(CH$_3$)$_2$)$_3$), 18.4 (Si(CH(CH$_3$)$_2$)$_3$), 25.6 (NHCH$_3$), 42.6 (CH_2), 116.6 (C-Ar), 119.3 (C-Ar), 121.7 (C-Ar), 128.2 (C-Ar), 136.5

(C-Ar), 140.8 (C-Ar), 156.3 (C-Ar), 170.4 (C=O); HRMS calcd. for $C_{25}H_{35}N_6OSi$ (ES+) *m*/*z* 463.2636 $[M+H]^+$, found 463.2640.

Note: Unable to visualise all carbon signals by NMR.

2-(3-(6-Ethynyl-9*H*-purin-2-ylamino)phenyl)-*N*-methylacetamide (200)

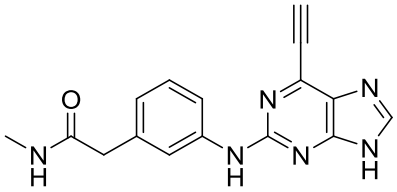

TIPS-protected purine **239** (50 mg, 0.11 mmol), KF (31 mg, 0.54 mmol) and 18-crown-6 (3 mg, 0.011 mmol) were reacted in THF (1 ml) according to **general procedure Q**. Purification *via* chromatography on silica (9:1 DCM/MeOH) afforded the desired compound as a yellow solid (24 mg, 0.078 mmol, 73%). R_f 0.41 (9:1 DCM/MeOH); M.p. 170-180 °C (decomposed); λ_{max} (EtOH/nm) 274; IR (cm^{-1}) 3270, 3088, 2158, 2025, 1596; ^{1}H NMR (500 MHz, DMSO-d_6) 2.59 (3H, d, *J* = 4.7 Hz, NHCH_3), 3.36 (2H, s, CH_2CO), 4.84 (1H, s, -C≡CH), 6.81-6.84 (1H, m, H-6'), 7.21 (1H, dd, *J* = 7.8 and 7.9 Hz, H-5'), 7.52-7.55 (1H, m, H-2'), 7.74-7.77 (1H, m, H-4'), 7.92 (1H, br, CONH), 8.27 (1H, s, H-8), 9.62 (1H, s, C^2-NH), 13.12 (1H, br, H-9); ^{13}C NMR (125 MHz, DMSO-d_6) 23.6 (NH*C*H_3), 42.6 ($COCH_2$), 87.0 (C≡*C*H), 116.6 (C-Ar), 119.2 (C-Ar), 121.8 (C-Ar), 128.2 (C-Ar), 136.6 (C-Ar), 140.7 (C-Ar), 156.3 (C-Ar), 170.4 (C=O); HRMS calcd. for $C_{16}H_{15}N_6O$ (ES+) *m*/*z* 307.1305 $[M+H]^+$, found 307.1302.

Note: Unable to visualise all carbon signals by NMR.

Methyl 4-aminobenzoate (235)[254]

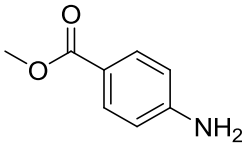

4-Aminobenzoic acid (0.500 g, 3.65 mmol) and thionyl chloride (0.53 ml, 7.29 mmol) were reacted in dry methanol (20 ml) according to **general procedure R**. Chromatography on silica (7:3 Petrol/EtOAc) afforded the desired compound as a white solid (0.520 g, 3.44 mmol, 94%). R_f 0.42 (7:3 Petrol/EtOAc); M.p. 111-114 °C (Lit.[254] 109-110 °C); λ_{max}

(EtOH/nm) 255, 309; IR (cm^{-1}) 3407, 3336, 3298, 2944, 1681; ^{1}H NMR (500 MHz, DMSO-d_6) 3.74 (3H, s, OCH_3), 5.97 (2H, s, Ar-NH_2), 6.57 (2H, d, *J* = 8.8 Hz, H-3/H-5), 7.64 (2H, d, *J* = 8.8 Hz, H-2/H-6); ^{13}C NMR (125 MHz, DMSO-d_6) 51.1 (OCH_3), 112.8 (C-Ar), 115.7 (C-Ar), 131.0 (C-Ar), 153.5 (C-Ar), 166.3 (C=O); LRMS (ES+) *m*/*z* 152.2 $[M+H]^+$.

4-Aminobenzamide (237)[255]

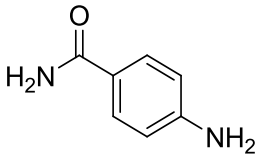

Methyl ester **235** (0.408 g, 2.70 mmol) was dissolved in concentrated ammonium hydroxide (10 ml) and the resulting solution was heated at 60 °C for 18 h. The solvent was removed *in vacuo* and the crude product was purified *via* chromatography on KP-NH silica (19:1 DCM/MeOH) to give the desired compound as a white solid (0.214 g, 1.57 mmol, 58%). R_f 0.31 (19:1 DCM/MeOH); M.p. 178-181 °C (Lit.[255] 175-179 °C); λ_{max} (EtOH/nm) 230, 262; IR (cm^{-1}) 3463, 3317, 3205, 1591; ^{1}H NMR (500 MHz, DMSO-d_6) 5.59 (2H, s, Ar-NH_2), 6.52 (2H, d, *J* = 8.6 Hz, H-3/H-5), 6.82 (1H, br, CONH*H'*), 7.50 (1H, br, CON*H*H'), 7.58 (2H, d, *J* = 8.6 Hz, H-2/H-6); ^{13}C NMR (125 MHz, DMSO-d_6) 112.4 (C-Ar), 120.9 (C-Ar), 129.1 (C-Ar), 151.6 (C-Ar), 168.0 (C=O); LRMS (ES+) *m*/*z* 137.1 $[M+H]^+$.

4-(6-(2-(Triisopropylsilyl)ethynyl)-9*H*-purin-2-ylamino)benzamide (240)

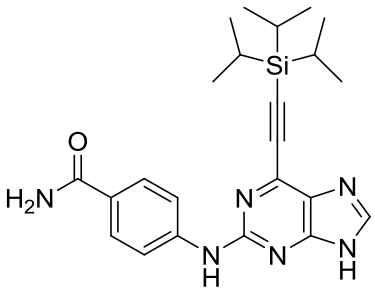

2-Fluoropurine intermediate **160** (0.216 g, 0.68 mmol), aniline **237** (0.185 g, 1.36 mmol) and TFA (262 μl, 3.40 mmol) were reacted in TFE (4 ml) according to **general procedure B**. Purification *via* chromatography on KP-NH silica (9:1 DCM/MeOH) afforded the desired compound as a yellow oil (0.114 g, 0.26 mmol, 38%). R_f 0.29 (9:1 DCM/MeOH); λ_{max} (EtOH/nm) 224, 301, 363; IR (cm^{-1}) 3113, 2942, 2864, 2160, 1653; ^{1}H NMR (500 MHz, DMSO-d_6) 1.14-1.18 (21H, m, $Si(CH(CH_3)_2)_3$), 7.16 (1H, br, CONHH'), 7.79-7.82 (3H, m,

CONHH'/H-3'/H-5'), 7.89 (2H, d, *J* = 8.9 Hz, H-2'/H-6'), 8.31 (1H, s, H-8), 10.01 (1H, s, C^2-NH), 13.17 (1H, br, H-9); ^{13}C NMR (125 MHz, DMSO-d_6) 10.6 (Si(*C*H(CH_3)$_2$)$_3$), 18.4 (Si(CH(*C*H_3)$_2$)$_3$), 98.2 (C≡C), 116.8 (C-Ar), 126.2 (C-Ar), 128.2 (C-Ar), 143.7 (C-Ar), 155.7 (C-Ar), 167.5 (C=O); HRMS calcd. for $C_{23}H_{31}N_6OSi$ (ES+) *m*/*z* 435.2323 $[M+H]^+$, found 435.2323.

Note: Unable to visualise all carbon signals by NMR.

4-(6-Ethynyl-9*H*-purin-2-ylamino)benzamide (208)

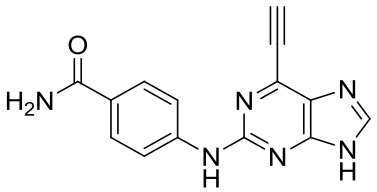

TIPS-protected purine **240** (86 mg, 0.20 mmol), KF (57 mg, 0.99 mmol) and 18-crown-6 (5 mg, 0.020 mmol) were reacted in THF (2 ml) according to **general procedure Q**. Purification *via* chromatography on silica (9:1 DCM/MeOH) afforded the desired compound as a yellow solid (41 mg, 0.15 mmol, 74%). R_f 0.25 (9:1 DCM/MeOH); M.p. 180-190 °C (decomposed); λ_{max} (EtOH/nm) 220, 302; IR (cm^{-1}) 3267, 2164, 2024, 1653, 1602; ^{1}H NMR (500 MHz, DMSO-d_6) 4.89 (1H, s, -C≡CH), 7.17 (1H, s, -CON*H*H'), 7.70 (1H, s, -CONH*H'*), 7.83 (2H, d, *J* = 8.7 Hz, H-2'/H-6'), 7.87 (2H, d, *J* = 8.7 Hz, H-3'/H-5'), 8.35 (1H, s, H-8), 10.00 (1H, s, C^2-NH), 13.23 (1H, br, H-9); ^{13}C NMR (125 MHz, DMSO-d_6) 87.3 (C≡*C*H), 116.9 (C-Ar), 126.3 (C-Ar), 128.2 (C-Ar), 143.6 (C-Ar), 155.7 (C-Ar), 167.6 (C=O); HRMS calcd. for $C_{14}H_{11}N_6O$ (ES+) *m*/*z* 279.0994 $[M+H]^+$, found 279.0989.

Note: Unable to visualise all carbon signals by NMR.

4-Amino-*N*-methylbenzamide (238)[255]

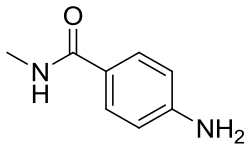

Methyl ester **235** (0.413 g, 2.70 mmol) and methylamine (40% aqueous solution, 10 ml) were reacted according to **general procedure S**. Chromatography on silica (19:1 DCM/MeOH) gave the desired compound as a pale yellow solid (0.396 g, 2.64 mmol, 98%). R_f 0.36 (19:1

DCM/MeOH); M.p. 173-176 °C (Lit.[255] 178-180 °C); λ_{max} (EtOH/nm) 236, 270; IR (cm^{-1}) 3399, 3336, 3228, 2934, 1627; ^{1}H NMR (500 MHz, DMSO-d_6) 2.72 (3H, d, *J* = 4.6 Hz, NHCH_3), 5.57 (2H, s, Ar-NH_2), 6.53 (2H, d, *J* = 8.6 Hz, H-3/H-5), 7.55 (2H, d, *J* = 8.6 Hz, H-2/H-6), 7.94 (1H, br, N*H*CH_3); ^{13}C NMR (125 MHz, DMSO-d_6) 26.0 ($NHCH_3$), 112.5 (C-Ar), 121.3 (C-Ar), 128.5 (C-Ar), 151.4 (C-Ar), 166.7 (C=O); LRMS (ES+) *m*/*z* 151.2 $[M+H]^+$.

4-(6-(2-(Triisopropylsilyl)ethynyl)-9*H*-purin-2-ylamino)-*N*-methyl benzamide (241)

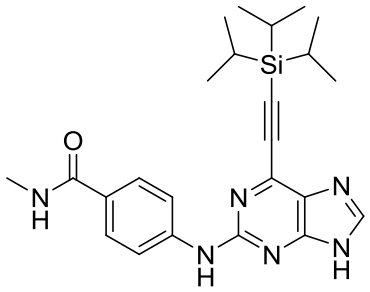

2-Fluoropurine intermediate **160** (0.270 g, 0.85 mmol), aniline **238** (0.255 g, 1.70 mmol) and TFA (330 μl, 4.25 mmol) were reacted in TFE (4 ml) according to **general procedure B**. Purification *via* chromatography on KP-NH silica (9:1 DCM/MeOH) afforded the desired compound as a yellow oil (0.117 g, 0.26 mmol, 31%). R_f 0.51 (9:1 DCM/MeOH, KP-NH); λ_{max} (EtOH/nm) 230, 283, 362; IR (cm^{-1}) 3278, 3082, 2942, 2864, 2154, 2027, 1602; ^{1}H NMR (500 MHz, DMSO-d_6) 1.14-1.19 (21H, m, $Si(CH(CH_3)_2)_3$), 2.78 (3H, d, *J* = 4.6 Hz, NHCH_3), 7.77 (2H, d, *J* = 8.8 Hz, H-3'/H-5'), 7.89 (2H, d, *J* = 8.8 Hz, H-2'/H-6'), 8.23 (1H, q, *J* = 4.6 Hz, N*H*CH_3), 8.31 (1H, s, H-8), 10.00 (1H, s, C^2-NH), 13.19 (1H, br, H-9); ^{13}C NMR (125 MHz, DMSO-d_6) 10.6 ($Si(CH(CH_3)_2)_3$), 18.4 ($Si(CH(CH_3)_2)_3$), 26.1 ($NHCH_3$), 116.9 (C-Ar), 126.5 (C-Ar), 127.7 (C-Ar), 143.5 (C-Ar), 155.7 (C-Ar), 166.3 (C=O); HRMS calcd. for $C_{24}H_{33}N_6OSi$ (ES+) *m*/*z* 449.2480 $[M+H]^+$, found 449.2480.

Note: Unable to visualise all carbon signals by NMR.

4-(6-Ethynyl-9*H*-purin-2-ylamino)-*N*-methylbenzamide (209)

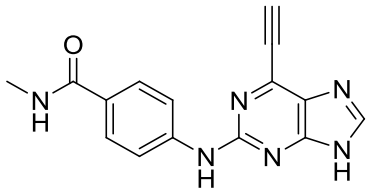

TIPS-protected purine **241** (0.105 g, 0.23 mmol), KF (67 mg, 1.15 mmol) and 18-crown-6 (6 mg, 0.023 mmol) were reacted in THF (2.5 ml) according to **general procedure Q**. Purification *via* chromatography on silica (9:1 DCM/MeOH) afforded the desired compound as a yellow solid (46 mg, 0.16 mmol, 69%). R_f 0.24 (9:1 DCM/MeOH); M.p. 180-190 °C (decomposed); λ_{max} (EtOH/nm) 221, 301; IR (cm^{-1}) 3275, 3109, 2163, 2111, 2022, 1605; ^{1}H NMR (500 MHz, DMSO-d_6) 2.78 (3H, d, J = 4.5 Hz, NHCH_3), 4.89 (1H, s, -C≡CH), 7.78 (2H, d, J = 8.8 Hz, H-2'/H-6'), 7.87 (2H, d, J = 8.8 Hz, H-3'/H-5'), 8.24 (1H, q, J = 4.5 Hz, CONH), 8.34 (1H, s, H-8), 9.99 (1H, s, C^2-NH), 13.25 (1H, br, H-9); ^{13}C NMR (125 MHz, DMSO-d_6) 26.1 ($NHCH_3$), 87.3 (C≡*C*H), 117.0 (C-Ar), 126.6 (C-Ar), 127.7 (C-Ar), 143.4 (C-Ar), 155.7 (C-Ar), 166.3 (C=O); HRMS calcd. for $C_{15}H_{13}N_6O$ (ES+) *m*/*z* 293.1148 $[M+H]^+$, found 293.1145.

Note: Unable to visualise all carbon signals by NMR.

4-Amino-*N*,*N*-dimethylbenzamide (243)[256]

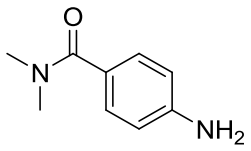

4-Aminobenzoic acid (0.500 g, 3.65 mmol) was dissolved thionyl chloride (5 ml) and 1 drop of DMF was added. The solution was refluxed for 1 hour, after which point the solution was concentrated to dryness. Remaining thionyl chloride was removed through addition of toluene (5 ml) and removal of the azeotrope *in vacuo*. The resultant orange residue was suspended in dry THF (4 ml) and triethylamine (530 µl, 3.65 mmol), and dimethylamine (2M in THF, 5.50 ml, 10.9 mmol) was added under nitrogen. The reaction mixture was stirred at RT for 18 h, after which the solvent was removed *in vacuo* and the resultant residue was purified by chromatography on silica (19:1 DCM/MeOH). The desired compound was obtained as an off-white solid (0.348 g, 2.12 mmol, 58%). R_f 0.40 (19:1 DCM/MeOH); M.p.

150-153 °C (Lit.[256] 153 °C); λ_{max} (EtOH/nm) 220, 272; IR (cm^{-1}) 3428, 3335, 3236, 2925, 1642; ^{1}H NMR (500 MHz, DMSO-d_6) 2.94 (6H, s, $N(CH_3)_2$), 5.47 (2H, s, Ar-NH_2), 6.54 (2H, d, *J* = 8.6 Hz, H-3/H-5), 7.14 (2H, d, *J* = 8.6 Hz, H-2/H-6); ^{13}C NMR (125 MHz, DMSO-d_6) 40.0 ($N(CH_3)_2$), 112.5 (C-Ar), 122.5 (C-Ar), 129.1 (C-Ar), 150.2 (C-Ar), 170.7 (C=O); LRMS (ES+) *m*/*z* 165.2 $[M+H]^+$.

4-(6-(2-(Triisopropylsilyl)ethynyl)-9*H*-purin-2-ylamino)-*N*,*N*-dimethyl benzamide (244)

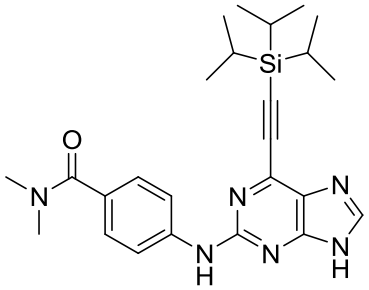

2-Fluoropurine intermediate **160** (0.205 g, 0.64 mmol), aniline **243** (0.210 g, 1.28 mmol) and TFA (248 µl, 3.22 mmol) were reacted in TFE (4 ml) according to **general procedure B**. Purification *via* chromatography on KP-NH silica (19:1 DCM/MeOH) afforded the desired compound as a yellow oil (79 mg, 0.17 mmol, 27%). R_f 0.48 (19:1 DCM/MeOH, KP-NH); λ_{max} (EtOH/nm) 283, 364; IR (cm^{-1}) 2942, 2862, 2160, 2028, 1601; ^{1}H NMR (500 MHz, DMSO-d_6) 1.14-1.18 (21H, m, Si(C*H*(CH_3)$_2$)$_3$), 2.98 (6H, s, $N(CH_3)_2$), 7.36 (2H, d, *J* = 8.5 Hz, H-3'/H-5'), 7.88 (2H, d, *J* = 8.5 Hz, H-2'/H-6'), 8.29 (1H, s, H-8), 9.96 (1H, s, C^2-NH), 13.19 (1H, br, H-9); ^{13}C NMR (125 MHz, $CDCl_3$) 11.3 (Si(*C*H(CH_3)$_2$)$_3$), 18.7 (Si(CH(*C*H_3)$_2$)$_3$), 40.0 ($N(CH_3)_2$), 100.6 (C≡C), 103.9 (C≡C), 118.5 (C-Ar), 128.3 (C-Ar), 128.7 (C-Ar), 141.5 (C-Ar), 155.8 (C-Ar), 172.4 (C=O); HRMS calcd. for $C_{25}H_{35}N_6OSi$ (ES+) *m*/*z* 463.2636 $[M+H]^+$, found 463.2641.

Note: Unable to visualise all carbon signals by NMR.

4-(6-Ethynyl-9*H*-purin-2-ylamino)-*N*,*N*-dimethylbenzamide (210)

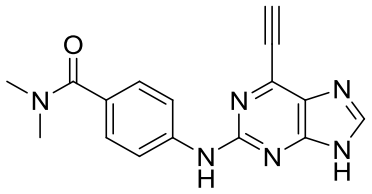

TIPS-protected purine **244** (63 mg, 0.14 mmol), KF (41 mg, 0.70 mmol) and 18-crown-6 (4 mg, 0.014 mmol) were reacted in THF (1.5 ml) according to **general procedure Q**. Purification *via* chromatography on silica (9:1 DCM/MeOH) afforded the desired compound as a yellow solid (27 mg, 0.088 mmol, 63%). R_f 0.29 (9:1 DCM/MeOH); M.p. 190-210 °C (decomposed); λ_{max} (EtOH/nm) 292; IR (cm^{-1}) 3101, 2111, 1599; ^{1}H NMR (500 MHz, DMSO-d_6) 2.98 (6H, s, $N(CH_3)_2$), 4.89 (1H, s, -C≡CH), 7.38 (2H, d, *J* = 8.4 Hz, H-2'/H-6'), 7.86 (2H, d, *J* = 8.4 Hz, H-3'/H-5'), 8.33 (1H, s, H-8), 9.95 (1H, s, C^2-NH), 13.23 (1H, s, H-9); ^{13}C NMR (125 MHz, DMSO-*d6*) 87.2 (C≡*C*H), 117.1 (C-Ar), 128.0 (C-Ar), 128.3 (C-Ar), 142.0 (C-Ar), 155.8 (C-Ar), 170.2 (C=O); HRMS calcd. for $C_{16}H_{15}N_6O$ (ES+) *m*/*z* 307.1302 $[M+H]^+$, found 307.1302.

Note: Unable to visualise all carbon signals by NMR – N-CH_3 masked by solvent.

***N*^{1},*N*^{3}-Dimethyl-2-(4-nitrophenyl)malonamide (248)**

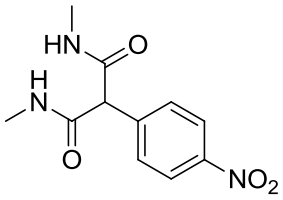

4-Nitrophenylacetic acid (0.598 g, 3.31 mmol), CDI (1.07 g, 6.62 mmol), DIPEA (1.15 ml, 6.62 mmol) and methylamine (2M in THF, 6.60 ml, 13.2 mmol) were reacted in dry DMF (30 ml) according to **general procedure J**. Purification *via* silica gel chromatography (7:3 Petrol/EtOAc) gave the desired compound as an off-white solid (0.608 g, 2.42 mmol, 73%). R_f 0.33 (7:3 Petrol/EtOAc); M.p. 221-224 °C; λ_{max} (EtOH/nm) 273; IR (cm^{-1}) 3405, 3311, 3111, 2932, 1655, 1512; ^{1}H NMR (500 MHz, DMSO-d_6) 2.62 (6H, d, *J* = 4.6 Hz, 2 x NHCH_3), 4.57 (1H, s, COC*H*CO), 7.65 (2H, d, *J* = 8.8 Hz, H-2/H-6), 8.11 (2H, q, *J* = 4.6 Hz, 2 x NH), 8.21 (2H, d, *J* = 8.8 Hz, H-3/H-5); ^{13}C NMR (125 MHz, DMSO-d_6) 25.9 ($N(CH_3)_2$),

57.9 (CO*C*HCO), 123.2 (C-Ar), 129.9 (C-Ar), 143.5 (C-Ar), 146.7 (C-Ar), 167.6 (2 x C=O); HRMS calcd. for $C_{11}H_{14}N_3O_4$ (ES+) *m*/*z* 252.0979 $[M+H]^+$, found 252.0983.

2-(4-Aminophenyl)-*N*^{1},*N*^{3}-dimethylmalonamide (254)

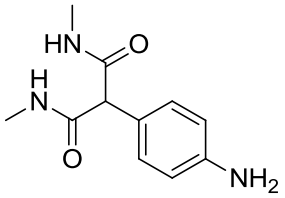

The nitro compound **248** (0.593 g, 3.05 mmol) and iron powder (1.70 g, 30.5 mmol) were reacted in acetic acid (30 ml) according to **general procedure T**. Purification on silica (9:1 DCM/MeOH) gave the desired compound as a beige waxy solid (0.380 g, 2.32 mmol, 76%). R_f 0.35 (9:1 DCM/MeOH); M.p. 148-150 °C; λ_{max} (EtOH/nm) 248, 292; IR (cm^{-1}) 3414, 3273, 3100, 2937, 1663, 1650, 1515; ^{1}H NMR (500 MHz, DMSO-d_6) 2.59 (6H, d, *J* = 4.6 Hz, 2 x NHC*H*$_3$), 4.11 (1H, s, COC*H*CO), 5.00 (2H, s, Ar-NH$_2$), 6.49 (2H, d, *J* = 8.5 Hz, H-3/H-5), 7.00 (2H, d, *J* = 8.5 Hz, H-2/H-6), 7.94 (2H, q, *J* = 4.6 Hz, 2 x N*H*CH$_3$); ^{13}C NMR (125 MHz, DMSO-d_6) 25.7 (2 x NHCH$_3$), 57.6 (CO*C*HCO), 113.6 (C-Ar), 123.4 (C-Ar), 128.6 (C-Ar), 147.8 (C-Ar), 169.7 (C=O); HRMS calcd. for $C_{11}H_{16}N_3O_2$ (ES+) *m*/*z* 222.1237 $[M+H]^+$, found 222.1239.

***N*^{1},*N*^{3}-Dimethyl-2-(4-((6-((triisopropylsilyl)ethynyl)-9*H*-purin-2-yl)amino) phenyl)malonamide (256)**

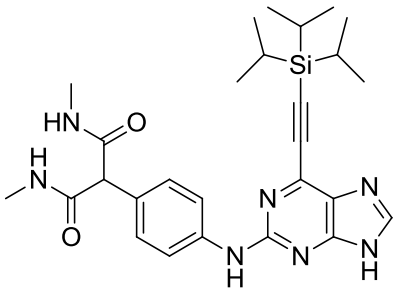

2-Fluoropurine **160** (0.198 g, 0.63 mmol), aniline **254** (0.277 g, 1.26 mmol) and TFA (120 µl, 1.57 mmol) were reacted in TFE (6 ml) according to **general procedure V**. Purification through chromatography on KP-NH silica (19:1 DCM/MeOH) gave the desired compound as a yellow oil/gum (0.167 g, 0.32 mmol, 51%). R_f 0.35 (19:1 DCM/MeOH, KP-NH); λ_{max} (EtOH/nm) 280, 354; IR (cm^{-1}) 3287, 3085, 2943, 2864, 1663, 1603, 1573, 1521; ^{1}H NMR (500 MHz, DMSO-d_6)) 1.13-1.23 (21H, m, Si(C*H*(C*H*$_3$)$_2$)$_3$), 2.62 (6H, d, *J* = 4.7 Hz, (2 x

NHC*H*$_3$), 4.28 (1H, s, COC*H*CO), 7.26 (2H, d, *J* = 8.7 Hz, H-2'/H-6'), 7.71 (2H, d, *J* = 8.7 Hz, H-3'/H-5'), 8.02 (2H, q, *J* = 4.7 Hz, 2 x N*H*CH$_3$), 8.23 (1H, s, H-8), 9.68 (1H, s, C^2-NH), 13.05 (1H, br, H-9); ^{13}C NMR (125 MHz, DMSO-d_6) 10.6 (Si(*C*H(CH$_3$)$_2$)$_3$), 18.4 (Si(CH(*C*H$_3$)$_2$)$_3$), 25.8 (CH3), 26.9 (CH3), 57.8 (CO*C*HCO), 118.4, 128.3 (C-Ar), 129.0 (C-Ar), 139.9 (C-Ar), 142.7 (C-Ar), 153.9 (C-Ar), 156.2 (C-Ar), 169.2 (C=O); HRMS calcd. for $C_{27}H_{38}N_7O_2Si$ (ES+) *m*/*z* 520.2851 $[M+H]^+$, found 520.2847.

Note: Unable to visualise all carbon environments by ^{13}C NMR.

2-(4-((6-Ethynyl-9*H*-purin-2-yl)amino)phenyl)-*N*^{1},*N*^{3}-dimethylmalonamide (257)

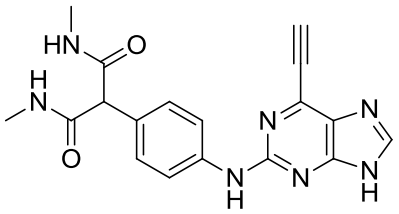

The TIPS-protected purine **256** (0.120 mg, 0.23 mmol), TBAF (1M in THF, 0.28 ml, 0.28 mmol) and the TBAF scavenger bead system **231** (1.20 g, 10 x w/w) were reacted in THF (5 ml) according to **general procedure U**. Chromatography on KP-NH silica (9:1 DCM/MeOH) afforded the target compound as a yellow solid (29 mg, 0.08 mmol, 35%). R_f 0.26 (9:1 DCM/MeOH, KP-NH); M.p. 160-180 °C (decomposed); λ_{max} (EtOH/nm) 277.0, 368.5; IR (cm^{-1}) 3274, 2550, 2160, 2111, 2030, 1660; ^{1}H NMR (500 MHz, DMSO-d_6) 2.61 (6H, d, *J* = 4.6 Hz, 2 x NHC*H*$_3$), 4.28 (1H, s, COC*H*CO), 4.84 (1H, s, C≡CH), 7.27 (2H, d, *J* = 8.7 Hz, H-2'/H-6'), 7.69 (2H, d, *J* = 8.7 Hz, H-3'/H-5'), 8.04 (2H, q, *J* = 4.6 Hz, 2 x N*H*CH$_3$), 8.28 (1H, s, H-8), 9.65 (1H, s, C^2-NH), 13.10 (1H, br, H-9); ^{13}C NMR (125 MHz, DMSO-d_6) 40.0 (NH*C*H$_3$), 58.7 (CO*C*HCO), 118.9 (C-Ar), 129.1 (C-Ar); HRMS calcd. for $C_{18}H_{18}N_7O_2$ (ES+) *m*/*z* 364.1516 $[M+H]^+$, found 364.1520.

Note: Unable to visualise all carbon environments by ^{13}C NMR – insufficient material.

***N*,*N*-Dimethyl-2-(4-nitrophenyl)acetamide (247)[257]**

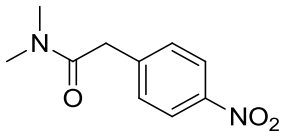

4-Nitrophenylacetic acid (0.600 g, 3.31 mmol), CDI (1.07 g, 6.62 mmol), DIPEA (1.15 ml, 6.62 mmol) and dimethylamine (2M in THF, 6.60 ml, 13.2 mmol) were reacted in dry DMF (30 ml) according to **general procedure J**. Silica gel chromatography (7:3 Petrol/EtOAc) afforeded the target compound as an off-white solid (0.204 g, 0.98 mmol, 30%). R_f 0.38 (7:3 Petrol/EtOAc); M.p. 80-83 °C (Lit.[257] 87 °C); λ_{max} (EtOH/nm) 270; IR (cm^{-1}) 2937, 2449, 1637, 1512; ^{1}H NMR (500 MHz, $CDCl_3$) 3.01 (3H, s, N-CH_3), 3.08 (3H, s, N-CH_3), 3.83 (2H, s, COCH_2), 7.45 (2H, d, *J* = 8.5 Hz, H-2/H-6), 8.21 (2H, d, *J* = 8.5 Hz, H-3/H-5); ^{13}C NMR (125 MHz, $CDCl_3$) 35.8 (N-CH_3), 37.6 (N-CH_3), 40.3 (CO*C*H_2), 123.8 (C-Ar), 130.1 (C-Ar), 142.7 (C-Ar), 154.1 (C-Ar), 169.4 (C=O); LRMS (ES+) *m*/*z* 209.1 $[M+H]^+$.

2-(4-Aminophenyl)-*N*,*N*-dimethylacetamide (253)[258]

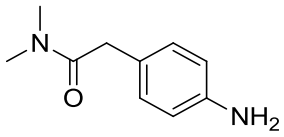

The nitro compound **247** (0.133 g, 0.64 mmol) and iron powder (0.355 g, 6.39 mmol) were reacted in acetic acid (6 ml) according to **general procedure T**. Chromatography on silica (9:1 DCM/MeOH) gave the desired compound as a pale red oil (0.105 g, 0.58 mmol, 92%). R_f 0.40 (9:1 DCM/MeOH); λ_{max} (EtOH/nm) 242, 291; IR (cm^{-1}) 3414, 3342, 3230, 2933, 1611, 1515; ^{1}H NMR (500 MHz, DMSO-d_6) 2.81 (3H, s, N-CH_3), 2.96 (3H, s, N-CH_3), 3.46 (2H, s, $COCH_2$), 4.89 (2H, s, Ar-NH_2), 6.50 (2H, d, *J* = 8.4 Hz, H-3/H-5), 6.86 (2H, d, *J* = 8.4 Hz, H-2/H-6); ^{13}C NMR (125 MHz, DMSO-d_6) 34.9 (N-CH_3), 37.1 (N-CH_3), 39.1 (CO*C*H_2), 113.9 (C-Ar), 122.5 (C-Ar), 129.2 (C-Ar), 146.9 (C-Ar), 170.9 (C=O); LRMS (ES+) *m*/*z* 179.1 $[M+H]^+$.

***N*,*N*-Dimethyl-2-(4-((6-((triisopropylsilyl)ethynyl)-9*H*-purin-2-yl)amino) phenyl)acetamide (255)**

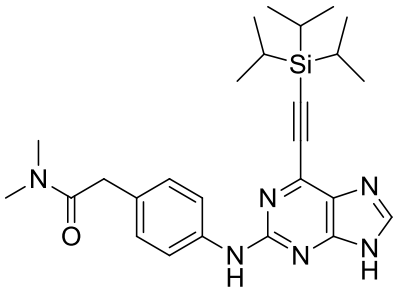

2-Fluoropurine **160** (73 mg, 0.23 mmol), aniline **253** (96 mg, 0.46 mmol) and TFA (45 µl, 0.58 mmol) were reacted in TFE (3 ml) according to **general procedure V**. Purification by KP-NH silica chromatography (19:1 DCM/MeOH) gave the desired compound as a yellow oil/gum (69 mg, 0.14 mmol, 61%). R_f 0.32 (19:1 DCM/MeOH, KP-NH); λ_{max} (EtOH/nm) 278, 379; IR (cm^{-1}) 3275, 3104, 2941, 2864, 1603, 1570; ^{1}H NMR (500 MHz, DMSO-d_6) 1.13-1.23 (21H, m, Si(C*H*(C*H*$_3$)$_2$)$_3$), 2.83 (3H, s, N-CH_3), 3.00 (3H, s, N-CH_3), 3.62 (2H, s, COCH_2), 7.12 (2H, d, *J* = 8.6 Hz, H-2'/H-6'), 7.71 (2H, d, *J* = 8.6 Hz, H-3'/H-5'), 8.22 (1H, s, H-8), 9.60 (1H, s, C^2-NH), 13.04 (1H, br, H-9); ^{13}C NMR (125 MHz, $CDCl_3$) 11.3 (Si(*C*H(CH$_3$)$_2$)$_3$), 18.8 (Si(CH(*C*H$_3$)$_2$)$_3$), 35.9 (N-CH$_3$), 37.7 (N-CH$_3$), 40.1 (CO*C*H$_2$), 114.9 (C-Ar), 115.5 (C-Ar), 120.9 (C-Ar), 121.6 (C-Ar), 129.6 (C-Ar), 140.1 (C-Ar), 171.6 (C=O); HRMS calcd. for $C_{26}H_{37}N_6OSi$ (ES+) *m*/*z* 477.2793 $[M+H]^+$, found 477.2779.

Note: Unable to visualise all carbon environments by ^{13}C NMR.

2-(4-((6-Ethynyl-9*H*-purin-2-yl)amino)phenyl)-*N*,*N*-dimethylacetamide (204)

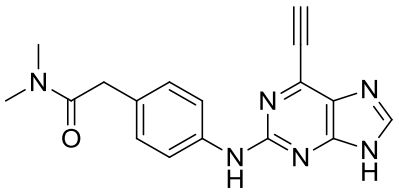

The TIPS-protected purine **255** (56 mg, 0.12 mmol), TBAF (1M in THF, 0.14 ml, 0.14 mmol) and the TBAF scavenger bead system **231** (0.60 g, 10 x w/w) were reacted in THF (5 ml) according to **general procedure U**. Chromatography on KP-NH silica (9:1 DCM/MeOH) afforded the desired compound as a yellow solid (27 mg, 0.08 mmol, 69%). R_f 0.33 (9:1 DCM/MeOH, KP-NH); M.p. 120-130 °C (decomposed); λ_{max} (EtOH/nm) 276.0, 378.0; IR (cm^{-1}) 2932, 2538, 2110, 1607, 1575, 1530; ^{1}H NMR (500 MHz, DMSO-d_6) 2.84 (3H, s, N-

CH_3), 3.01 (3H, s, N-CH_3), 3.62 (2H, s, $COCH_2$), 4.83 (1H, s, C≡CH), 7.13 (2H, d, *J* = 8.6 Hz, H-2'/H-6'), 7.69 (2H, d, *J* = 8.6 Hz, H-3'/H-5'), 8.26 (1H, s, H-8), 9.60 (1H, s, C^2-NH), 13.10 (1H, br, H-9); ^{13}C NMR (125 MHz, DMSO-d_6) 35.0 (N-CH_3), 37.2 (N-CH_3), 39.6 ($COCH_2$), 91.0 (C≡*C*H), 118.5 (C-Ar), 129.0 (C-Ar), 149.9 (C-Ar), 156.3 (C-Ar), 158.0 (C-Ar), 170.5 (C=O); HRMS calcd. for $C_{17}H_{17}N_6O$ (ES+) *m*/*z* 321.1458 $[M+H]^+$, found 321.1462.

Note: Unable to visualise all carbon environments by ^{13}C NMR.

2-(4-Aminophenyl)-*N*-methylacetamide (258)[255]

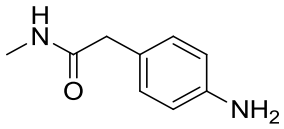

4-Aminophenylacetic acid (0.601 g, 3.97 mmol), thionyl chloride (0.58 ml, 7.94 mmol), methanol (20 ml) and methylamine (40% aqueous solution, 20 ml) were reacted together according to **general procedure W**. Silica gel chromatography (19:1 DCM/MeOH) afforded the desired product as a pale orange oil (0.573 g, 3.49 mmol, 88%). R_f 0.39 (19:1 DCM/MeOH); λ_{max} (EtOH/nm) 242, 291; IR (cm^{-1}) 3444, 3347, 3308, 3098, 1618, 1556, 1515; ^{1}H NMR (500 MHz, DMSO-d_6) 2.55 (3H, d, *J* = 4.6 Hz, NHC*H*$_3$), 3.18 (2H, s, $COCH_2$), 4.89 (2H, s, Ar-NH_2), 6.49 (2H, d, *J* = 8.4 Hz, H-3/H-5), 6.89 (2H, d, *J* = 8.4 Hz, H-2/H-6), 7.74 (1H, br, N*H*CH_3); ^{13}C NMR (125 MHz, DMSO-d_6) 25.6 ($NHCH_3$), 41.7 ($COCH_2$), 113.8 (C-Ar), 123.3 (C-Ar), 129.4 (C-Ar), 147.0 (C-Ar), 171.3 (C=O); LRMS (ES+) *m*/*z* 165.1 $[M+H]^+$.

***N*-Methyl-2-(4-((6-((triisopropylsilyl)ethynyl)-9*H*-purin-2-yl)amino)phenyl) acetamide (260)**

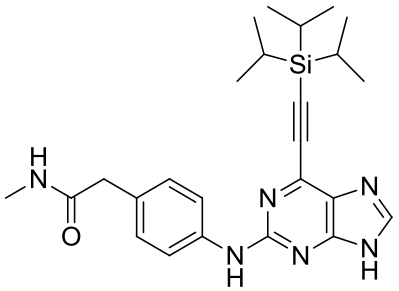

2-Fluoropurine **160** (0.200 g, 0.63 mmol), aniline **258** (0.206 g, 1.26 mmol) and TFA (120 µl, 1.57 mmol) were reacted in TFE (6 ml) according to **general procedure V**. Purification by KP-NH silica chromatography (19:1 DCM/MeOH) afforded the target compound as a yellow oil/gum (0.137 g, 0.30 mmol, 47%). R_f 0.37 (19:1 DCM/MeOH, KP-NH); λ_{max} (EtOH/nm) 279, 379; IR (cm^{-1}) 3275, 2942, 2864, 1604, 1573, 1523; ^{1}H NMR (500 MHz, DMSO-d_6) 1.13-1.23 (21H, m, Si(C*H*(C*H*$_3$)$_2$)$_3$), 2.58 (3H, d, *J* = 4.7 Hz, NHC*H*$_3$), 3.33 (2H, s, COCH$_2$), 7.15 (2H, d, *J* = 8.6 Hz, H-2'/H-6'), 7.70 (2H, d, *J* = 8.6 Hz, H-3'/H-5'), 7.84 (1H, q, *J* = 4.7 Hz, N*H*CH$_3$), 8.23 (1H, s, H-8), 9.61 (1H, s, C^2-NH), 13.04 (1H, br, H-9); ^{13}C NMR (125 MHz, DMSO-d_6) 10.6 (Si(*C*H(CH$_3$)$_2$)$_3$), 18.4 (Si(CH(*C*H$_3$)$_2$)$_3$), 25.6 (CH3), 41.8 (CO*C*H2), 118.4, 119.9, 128.9 (C-Ar), 133.1 (C-Ar), 142.7 (C-Ar), 156.3 (C-Ar), 170.8 (C=O); HRMS calcd. for $C_{25}H_{35}N_6OSi$ (ES+) *m/z* 463.2636 $[M+H]^+$, found 463.2631.

Note: Unable to visualise all carbon environments by ^{13}C NMR.

2-(4-((6-Ethynyl-9*H*-purin-2-yl)amino)phenyl)-*N*-methylacetamide (203)

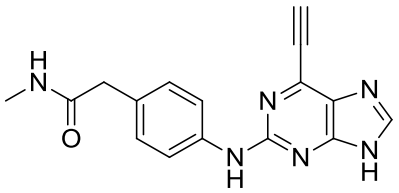

The TIPS-protected purine **260** (0.130 g, 0.28 mmol), TBAF (1M in THF, 0.34 ml, 0.34 mmol) and the TBAF scavenger bead system **231** (1.30 g, 10 x w/w) were reacted in THF (5 ml) according to **general procedure U**. Chromatography on KP-NH silica (9:1 DCM/MeOH) gave the target compound as a yellow solid (50 mg, 0.16 mmol, 58%). R_f 0.26 (9:1 DCM/MeOH, KP-NH); M.p. 140-160 °C (decomposed); λ_{max} (EtOH/nm) 276.0, 371.0; IR (cm^{-1}) 3414, 3092, 2531, 2112, 1611, 1577, 1530; ^{1}H NMR (500 MHz, DMSO-d_6) 2.58 (3H,

d, *J* = 4.6 Hz, NHC*H*$_3$), 3.33 (2H, s, COCH_2), 4.82 (1H, s, C≡CH), 7.16 (2H, d, *J* = 8.5 Hz, H-2'/H-6'), 7.68 (2H, d, *J* = 8.5 Hz, H-3'/H-5'), 7.86 (1H, q, *J* = 4.6 Hz, N*H*CH_3), 8.25 (1H, s, H-8), 9.60 (1H, s, C^2-NH), 13.09 (1H, br, H-9); ^{13}C NMR (125 MHz, DMSO-d_6) 25.6 (NH*C*H_3), 41.8 (*C*OCH_2), 86.9 (C≡*C*H), 118.5 (C-Ar), 129.0 (C-Ar), 139.1 (C-Ar), 142.7 (C-Ar), 156.3 (C-Ar), 170.8 (C=O); HRMS calcd. for $C_{16}H_{15}N_6O$ (ES+) *m*/*z* 307.1302 $[M+H]^+$, found 307.1306.

Note: Unable to visualise all carbon environments by ^{13}C NMR.

_N_-Methyl-3-nitrobenzamide (261)[259]

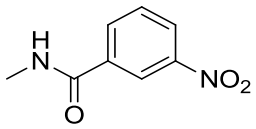

3-Nitrobenzoic acid (0.502 g, 2.99 mmol), phosphorus trichloride (288 µl, 3.29 mmol) and methylamine (2M in THF, 3.74 ml, 7.48 mmol) were reacted in dry MeCN (15 ml) according to **general procedure W**. Purification on silica (7:3 Petrol/EtOAc) gave the desired compound as a beige solid on cooling (0.535 g, 2.97 mmol, 99%). R_f 0.33 (7:3 Petrol/EtOAc); M.p. 175-177 °C (Lit.[259] 175 °C); λ_{max} (EtOH/nm) 241; IR (cm^{-1}) 3352, 3285, 3093, 1637, 1619, 1559, 1524; ^{1}H NMR (500 MHz, DMSO-d_6) 2.83 (3H, d, *J* = 4.6 Hz, NHC*H*$_3$), 7.79 (1H, dd, *J* = 7.9 and 8.0 Hz, H-5), 8.28 (1H, ddd, *J* = 1.0, 1.6 and 7.9 Hz, H-6), 8.38 (1H, ddd, *J* = 1.0, 2.4 and 8.0 Hz, H-4), 8.65-8.68 (1H, m, H-2), 8.84 (1H, br, N*H*CH_3); ^{13}C NMR (125 MHz, DMSO-d_6) 26.4 (NH*C*H_3), 121.8 (C-Ar), 125.7 (C-Ar), 130.1 (C-Ar), 133.4 (C-Ar), 135.8 (C-Ar), 147.8 (C-Ar), 164.4 (C=O); LRMS (ES+) *m*/*z* 181.1 $[M+H]^+$.

3-Amino-_N_-methylbenzamide (264)[260]

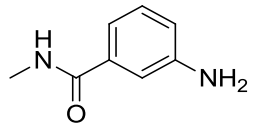

The nitro compound **261** (0.420 g, 2.33 mmol) and iron powder (1.30 g, 23.3 mmol) were reacted in acetic acid (20 ml) according to **general procedure T**. Purification of the crude using chromatography on silica (19:1 DCM/MeOH) gave the desired compound as a beige solid on cooling (0.276 g, 1.84 mmol, 79%). R_f 0.38 (19:1 DCM/MeOH); M.p. 98-100 °C;

λ_{max} (EtOH/nm) 217, 313; IR (cm^{-1}) 3465, 3412, 3294, 3221, 1634, 1580, 1547; ^{1}H NMR (500 MHz, DMSO-d_6) 2.74 (3H, d, J = 4.6 Hz, NHCH_3), 5.19 (2H, s, Ar-NH_2), 6.67 (1H, ddd, J = 1.0, 2.4 and 7.9 Hz, H-4), 6.92 (1H, ddd, J = 1.0, 1.6 and 7.7 Hz, H-6), 7.02 (1H, dd, J = 1.6 and 2.4 Hz, H-2), 7.06 (1H, dd, J = 7.7 and 7.9 Hz, H-5), 8.15 (1H, q, J = 4.6 Hz, N$H$$CH_3$); ^{13}C NMR (125 MHz, DMSO-d_6) 26.2 (CH_3), 112.7 (C-Ar), 114.0 (C-Ar), 116.2 (C-Ar), 128.6 (C-Ar), 135.5 (C-Ar), 148.6 (C-Ar), 167.4 (C=O); LRMS (ES+) m/z 151.1 $[M+H]^+$.

_N_-Methyl-3-((6-((triisopropylsilyl)ethynyl)-9_H_-purin-2-yl)amino) benzamide (266)

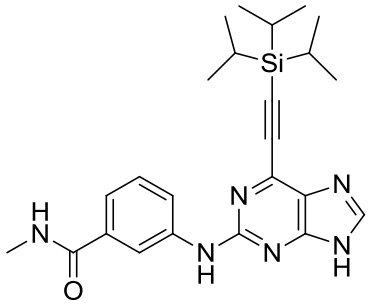

2-Fluoropurine **160** (0.202 g, 0.63 mmol), aniline **264** (0.190 g, 1.26 mmol) and TFA (120 µl, 1.57 mmol) were reacted in TFE (6 ml) according to **general procedure V** over 3 h. Chromatography on KP-NH silica (19:1 DCM/MeOH) gave the target compound as a yellow oil/gum (0.101 g, 0.23 mmol, 37%). R_f 0.30 (19:1 DCM/MeOH, KP-NH); λ_{max} (EtOH/nm) 276; IR (cm^{-1}) 3069, 2942, 2865, 2161, 1580; ^{1}H NMR (500 MHz, DMSO-d_6) 1.10-1.25 (21H, m, Si(CH(CH_3)$_2$)$_3$), 2.78 (3H, d, J = 4.5 Hz, NHCH_3), 7.32-7.36 (2H, m, H-5'/H-6'), 7.89-7.93 (1H, m, H-4'), 8.19-8.21 (1H, m, H-2'), 8.24 (1H, s, H-8), 8.30 (1H, q, J = 4.5 Hz, N$H$$CH_3$), 9.81 (1H, s, C^2-NH), 13.14 (1H, br, H-9); ^{13}C NMR (125 MHz, $CDCl_3$) 11.3 (Si(CH(CH_3)$_2$)$_3$), 18.7 (Si(CH($C$$H_3$)$_2$)$_3$), 27.0 (NH$CH_3$), 117.7 (C-Ar), 120.3 (C-Ar), 121.9 (C-Ar), 129.1 (C-Ar), 132.8 (C-Ar), 135.3 (C-Ar), 142.0 (C-Ar); HRMS calcd. for $C_{24}H_{33}N_6OSi$ (ES+) m/z 449.2480 $[M+H]^+$, found 449.2480.

Note: Unable to visualise all carbon environments by ^{13}C NMR.

3-((6-Ethynyl-9*H*-purin-2-yl)amino)-*N*-methylbenzamide (206)

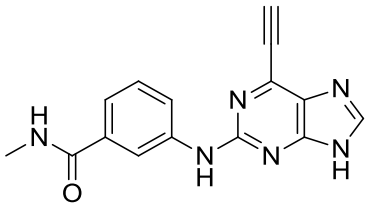

The TIPS-protected purine **266** (72 mg, 0.16 mmol), TBAF (1M in THF, 0.19 ml, 0.19 mmol) and the TBAF scavenger bead system **231** (0.70 g, 10 x w/w) were reacted in THF (5 ml) according to **general procedure U**. Chromatography on KP-NH silica (9:1 DCM/MeOH) gave the target compound as a yellow solid (29 mg, 0.10 mmol, 63%). R_f 0.24 (9:1 DCM/MeOH, KP-NH); M.p. 200-220 °C (decomposed); λ_{max} (EtOH/nm) 274.0, 363.5; IR (cm^{-1}) 3302, 3252, 3113, 1607; ^{1}H NMR (500 MHz, DMSO-d_6) 2.79 (3H, d, *J* = 4.5 Hz, NHC*H*$_3$), 4.86 (1H, s, C≡CH), 7.33-7.39 (2H, m, H-5'/H-6'), 7.92-7.97 (1H, m, H-4'), 8.16-8.18 (1H, m, H-2'), 8.29 (1H, s, H-8), 8.36 (1H, q, *J* = 4.5 Hz, N*H*CH$_3$), 9.78 (1H, s, C^2-NH), 13.20 (1H, br, H-9); ^{13}C NMR (125 MHz, DMSO-d_6) 26.3 (NH*C*H$_3$), 87.1 (C≡*C*H), 117.7 (C-Ar), 120.8 (C-Ar), 128.2 (C-Ar), 132.2 (C-Ar), 135.4 (C-Ar), 140.9 (C-Ar), 156.1 (C-Ar), 167.1 (C=O); HRMS calcd. for $C_{15}H_{13}N_6O$ (ES+) *m*/*z* 293.1145 $[M+H]^+$, found 293.1149.

Note: Unable to visualise all carbon environments by ^{13}C NMR.

***N*,*N*-Dimethyl-3-nitrobenzamide (262)[261]**

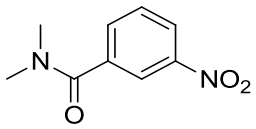

3-Nitrobenzoic acid (0.499 g, 2.99 mmol), phosphorus trichloride (288 µl, 3.29 mmol) and dimethylamine (2M in THF, 3.74 ml, 7.48 mmol) were reacted in dry MeCN (15 ml) according to **general procedure X**. Chromatography on silica (7:3 Petrol/EtOAc) gave the target compound as a beige solid (0.560 g, 2.88 mmol, 96%). R_f 0.36 (7:3 Petrol/EtOAc); M.p. 81-84 °C (Lit.[261] 83-84 °C); λ_{max} (EtOH/nm) 243; IR (cm^{-1}) 3083, 2941, 1626, 1527; ^{1}H NMR (500 MHz, $CDCl_3$) 3.03 (3H, s, N-CH_3), 3.18 (3H, s, N-CH_3), 7.64 (1H, dd, *J* = 7.7 and 8.0 Hz, H-5), 7.80 (1H, ddd, *J* = 1.2, 1.4 and 7.7 Hz, H-6), 8.29-8.33 (2H, m, H-2/H-4); ^{13}C NMR (125 MHz, $CDCl_3$) 35.5 (N-CH_3), 39.5 (N-CH_3), 122.3 (C-Ar), 124.4 (C-Ar), 129.7 (C-

Ar), 133.2 (C-Ar), 137.9 (C-Ar), 148.2 (C-Ar), 166.4 (C=O); LRMS (ES-) *m*/*z* 195.1 $[M+H]^+$.

3-Amino-*N*,*N*-dimethylbenzamide (265)[261]

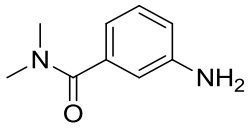

The nitro compound **262** (0.200 g, 1.03 mmol) and iron powder (0.57 g, 10.3 mmol) were reacted in acetic acid (10 ml) according to **general procedure T**. Purification on silica gel (19:1 DCM/MeOH) gave the target compound as a golden oil (0.142 g, 0.86 mmol, 84%). R_f 0.41 (19:1 DCM/MeOH); λ_{max} (EtOH/nm) 243, 302; IR (cm^{-1}) 3413, 3342, 3232, 2930, 1598, 1579; ^{1}H NMR (500 MHz, DMSO-d_6) 2.90 (3H, s, N-CH_3), 2.94 (3H, s, N-CH_3), 5.21 (2H, s, Ar-NH_2), 6.46 (1H, ddd, *J* = 1.1, 1.4 and 7.4 Hz, H-4), 6.54 (1H, dd, *J* = 1.4 and 2.3 Hz, H-2), 6.59 (1H, ddd, *J* = 1.1, 2.3 and 8.0 Hz, H-6), 7.05 (1H, dd, *J* = 7.4 and 8.0 Hz, H-5); ^{13}C NMR (125 MHz, DMSO-d_6) 112.0 (C-Ar), 113.9 (C-Ar), 114.5 (C-Ar), 128.6 (C-Ar), 137.2 (C-Ar), 148.6 (C-Ar), 170.8 (C=O); LRMS (ES+) *m*/*z* 165.1 $[M+H]^+$.

Note: Unable to visualise all carbon environments by ^{13}C NMR – masked by solvent peak.

***N*,*N*-Dimethyl-3-((6-((triisopropylsilyl)ethynyl)-9*H*-purin-2-yl)amino) benzamide (267)**

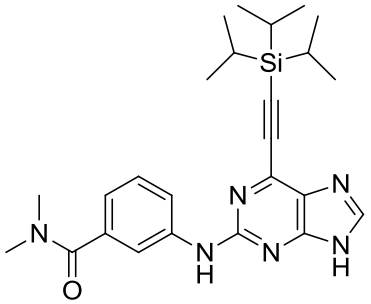

2-Fluoropurine **160** (0.121 g, 0.38 mmol), aniline **265** (0.125 g, 0.76 mmol) and TFA (73 µl, 0.95 mmol) were reacted in TFE (4 ml) according to **general procedure V** over 3 h. Purification by KP-NH silica chromatography (19:1 DCM/MeOH) gave the target compound as a yellow oil/gum (81 mg, 0.18 mmol, 47%). R_f 0.34 (19:1 DCM/MeOH, KP-NH); λ_{max} (EtOH/nm) 228, 317; IR (cm^{-1}) 3079, 2942, 2864, 2057, 1576, 1538; ^{1}H NMR (500 MHz, DMSO-d_6) 1.13-1.23 (21H, m, Si(C*H*(CH_3)$_2$)$_3$), 2.96 (3H, s, N-CH_3), 3.00 (3H, s, N-CH_3), 6.93 (1H, ddd, *J* = 1.1, 1.2 and 7.7 Hz, H-6'), 7.33 (1H, dd, *J* = 7.7 and 7.9 Hz, H-5'), 7.76-

7.80 (1H, m, H-4'), 7.95 (1H, m, H-2'), 8.27 (1H, s, H-8), 9.82 (1H, s, C^2-NH), 13.13 (1H, br, H-9); ^{13}C NMR (125 MHz, DMSO-d_6) 10.6 (Si(*C*H(CH$_3$)$_2$)$_3$), 18.4 (Si(CH(*C*H$_3$)$_2$)$_3$), 39.6 (N-CH$_3$), 116.3 (C-Ar), 119.0 (C-Ar), 128.4 (C-Ar), 136.9 (C-Ar), 141.0 (C-Ar), 147.7 (C-Ar); HRMS calcd. for $C_{25}H_{35}N_6OSi$ (ES+) *m*/*z* 463.2636 $[M+H]^+$, found 463.2632.

Note: Unable to visualise all carbon environments by ^{13}C NMR – masked by solvent.

3-((6-Ethynyl-9*H*-purin-2-yl)amino)-*N*,*N*-dimethylbenzamide (207)

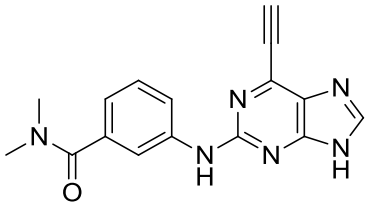

The TIPS-protected purine **267** (52 mg, 0.11 mmol), TBAF (1M in THF, 0.13 ml, 0.13 mmol) and the TBAF scavenger bead system **231** (0.50 g, 10 x w/w) were reacted in THF (5 ml) according to **general procedure U**. Chromatography on KP-NH silica (9:1 DCM/MeOH) gave the target compound as a yellow solid (23 mg, 0.08 mmol, 69%). R_f 0.33 (9:1 DCM/MeOH, KP-NH); M.p. 175-190 °C (decomposed); λ_{max} (EtOH/nm) 274.5, 362.5; IR (cm^{-1}) 3281, 2558, 2160, 2031, 1976, 1575; ^{1}H NMR (500 MHz, DMSO-d_6) 2.96 (3H, s, N-CH$_3$), 3.00 (3H, s, N-CH$_3$), 4.86 (1H, s, C≡CH), 6.94 (1H, ddd, *J* = 1.3, 2.0 and 7.6 Hz, H-6'), 7.34 (1H, dd, *J* = 7.6 and 7.7 Hz, H-5'), 7.80-7.83 (1H, m, H-4'), 7.88 (1H, dd, *J* = 1.3 and 1.4 Hz, H-2'), 8.30 (1H, s, H-8), 9.82 (1H, s, C^2-NH), 13.17 (1H, br, H-9); ^{13}C NMR (125 MHz, DMSO-d_6) 35.0 (N-CH$_3$), 39.4 (N-CH$_3$), 116.4 (C-Ar), 118.9 (C-Ar), 119.3 (C-Ar), 128.4 (C-Ar), 136.7 (C-Ar), 156.0 (C-Ar), 170.2 (C=O); HRMS calcd. for $C_{16}H_{15}N_6O$ (ES+) *m*/*z* 307.1302 $[M+H]^+$, found 307.1306.

Note: Unable to visualise all carbon environments by ^{13}C NMR.

***N*-(3-Nitrophenyl)acetamide (269)[262]**

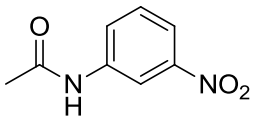

3-Nitroaniline (0.503 g, 3.62 mmol) was added to acetic anhydride at RT. The yellow solution was stirred at RT for 30 mins, over which time a white precipitate formed. Water (20

ml) was added, and the mixture was extracted with DCM (2 x 40 ml). The combined organic extracts were washed with 1M HCl (20 ml), sat. $NaHCO_3$ solution (20 ml) and brine (20 ml). The organic phase was dried ($MgSO_4$) and concentrated *in vacuo*, and the resultant crude was triturated with Et_2O (20 ml). The desired product was obtained as a white solid, collected by filtration (0.334 g, 1.85 mmol, 51%). R_f 0.27 (7:3 Petrol/EtOAc); M.p. 153-156 °C (Lit.[262] 152-153 °C); λ_{max} (EtOH/nm) 241, 329; IR (cm^{-1}) 3261, 3193, 3129, 3097, 1672, 1599, 1547, 1526; ^{1}H NMR (500 MHz, DMSO-d_6) 2.10 (3H, s, CH_3), 7.60 (1H, dd, J = 8.2 and 8.3 Hz, H-5), 7.88-7.91 (2H, m, H-4/H-6), 8.62 (1H, dd, J = 2.1 and 2.2 Hz, H-2); ^{13}C NMR (125 MHz, DMSO-d_6) 24.0 (CH_3), 113.0 (C-Ar), 117.5 (C-Ar), 124.9 (C-Ar), 130.1 (C-Ar), 140.4 (C-Ar), 147.9 (C-Ar), 169.0 (C=O); LRMS (ES+) m/z 181.1 $[M+H]^+$.

_N_-(3-Aminophenyl)acetamide (270)[263]

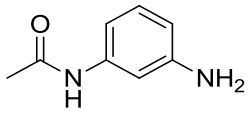

The nitro compound **269** (0.272 g, 1.51 mmol) and iron powder (0.845 g, 15.1 mmol) were reacted in acetic acid (15 ml) according to **general procedure T**. Purification on silica (9:1 DCM/MeOH) afforded the desired compound as a pale red oil (0.206 g, 1.37 mmol, 91%). R_f 0.46 (9:1 DCM/MeOH); λ_{max} (EtOH/nm) 223, 297; IR (cm^{-1}) 3245, 3074, 2621, 1658, 1608, 1545; ^{1}H NMR (500 MHz, DMSO-d_6) 1.99 (3H, s, CH_3), 5.01 (2H, s, Ar-NH_2), 6.21-6.25 (1H, m, H-4), 6.63-6.67 (1H, m, H-6), 6.89 (1H, dd, J = 7.9 and 8.0 Hz, H-5), 6.92 (1H, dd, J = 1.8 and 1.9 Hz, H-2), 9.58 (1H, s, NH); ^{13}C NMR (125 MHz, DMSO-d_6) 24.0 (CH_3), 104.7 (C-Ar), 106.9 (C-Ar), 109.1 (C-Ar), 128.8 (C-Ar), 139.9 (C-Ar), 148.9 (C-Ar), 167.8 (C=O); LRMS (ES+) m/z 151.1 $[M+H]^+$.

***N*-(3-((6-((Triisopropylsilyl)ethynyl)-9*H*-purin-2-yl)amino)phenyl) acetamide (271)**

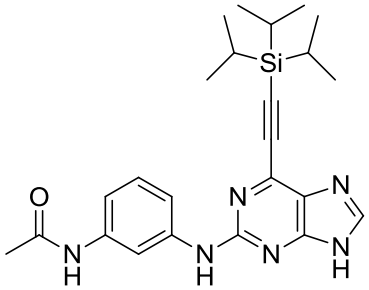

2-Fluoropurine **160** (0.230 g, 0.72 mmol), aniline **270** (0.216 g, 1.44 mmol) and TFA (140 µl, 1.80 mmol) were reacted in TFE (7 ml) according to **general procedure V**. Purification by KP-NH silica chromatography (19:1 DCM/MeOH) afforded the target compound as a yellow oil/gum (0.200 g, 0.45 mmol, 62%). R_f 0.29 (19:1 DCM/MeOH, KP-NH); λ_{max} (EtOH/nm) 276, 375; IR (cm^{-1}) 3109, 2942, 2862, 1667, 1603, 1577, 1534; ^{1}H NMR (500 MHz, DMSO-d_6) 1.13-1.19 (21H, m, Si(C*H*(CH_3)$_2$)$_3$), 2.04 (3H, s, CH_3), 7.17 (1H, dd, *J* = 7.9 and 8.0 Hz, H-5'), 7.21-7.25 (1H, m, H-6'), 7.53-7.57 (1H, m, H-4'), 7.76-7.80 (1H, m, H-2'), 8.23 (1H, s, H-8), 9.65 (1H, s, CONH), 9.85 (1H, s, C^2-NH), 13.05 (1H, br, H-9); ^{13}C NMR (125 MHz, DMSO-d_6) 10.6 (Si(*C*H(CH$_3$)$_2$)$_3$), 18.4 (Si(CH(*C*H$_3$)$_2$)$_3$), 23.9 (CH3), 110.1, 112.8, 113.9, 128.4 (C-Ar), 139.3 (C-Ar), 141.0 (C-Ar), 168.0 (C=O); HRMS calcd. for $C_{24}H_{33}N_6OSi$ (ES+) *m*/*z* 449.2480 $[M+H]^+$, found 449.2479.

Note: Unable to visualise all carbon environments by ^{13}C NMR.

***N*-(3-((6-Ethynyl-9*H*-purin-2-yl)amino)phenyl)acetamide (211)**

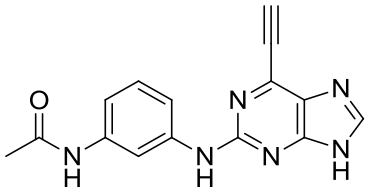

The TIPS-protected purine **271** (0.151 mg, 0.33 mmol), TBAF (1M in THF, 0.40 ml, 0.40 mmol) and the TBAF scavenger bead system **231** (1.50 g, 10 x w/w) were reacted in THF (5 ml) according to **general procedure U**. Chromatography on KP-NH silica (9:1 DCM/MeOH) gave the desired compound as a yellow solid (48 mg, 0.16 mmol, 48%). R_f 0.29 (9:1 DCM/MeOH, KP-NH); M.p. 160-180 °C (decomposed); λ_{max} (EtOH/nm) 251.5, 275.5, 362.0; IR (cm^{-1}) 3266, 2546, 2112, 1668, 1605, 1581, 1536; ^{1}H NMR (500 MHz, DMSO-d_6) 2.04 (3H, s, $COCH_3$), 4.84 (1H, s, C≡CH), 7.19 (1H, dd, *J* = 7.8 and 7.9 Hz, H-5'), 7.24 (1H,

m, H-6'), 7.55 (1H, m, H-4'), 7.77 (1H, m, H-2'), 8.27 (1H, s, H-8), 9.63 (1H, s, C^2-NH), 9.88 (1H, s, CONH), 13.12 (1H, br, H-9); ^{13}C NMR (125 MHz, DMSO-d_6) 23.9 (CO*C*H$_3$), 87.0 (C≡*C*H), 110.0 (C-Ar), 112.7 (C-Ar), 113.9 (C-Ar), 128.4 (C-Ar), 139.3 (C-Ar), 141.0 (C-Ar), 156.3 (C-Ar), 168.1 (C=O); HRMS calcd. for $C_{15}H_{13}N_6O$ (ES+) *m*/*z* 293.1145 $[M+H]^+$, found 293.1149.

Note: Unable to visualise all carbon environments by ^{13}C NMR.

2-(2-Nitrophenyl)acetamide (274)[264]

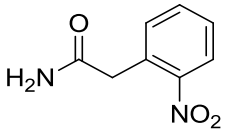

2-Nitrophenylacetic acid (1.00 g, 5.52 mmol), thionyl chloride (0.81 mmol, 11.0 mmol), methanol (50 ml) and ammonium hydroxide solution (50 ml) were reacted together according to **general procedure W**. Chromatography on silica (19:1 DCM/MeOH) gave the target compound as an off-white solid (0.837 g, 4.65 mmol, 84%). R_f 0.27 (19:1 DCM/MeOH); M.p. 156-159 °C (Lit.[264] 160-161 °C); λ_{max} (EtOH/nm) 257; IR (cm^{-1}) 3393, 3188, 2919, 2852, 1646, 1610, 1577, 1514; ^{1}H NMR (500 MHz, DMSO-d_6) 3.86 (2H, s, COC*H*$_2$), 6.99 (1H, s, CON*H*H'), 6.47-6.54 (3H, m, CONH*H'* and H-4/H-6), 7.66 (1H, ddd, *J* = 1.3, 7.4 and 7.6 Hz, H-5), 8.00 (1H, dd, *J* = 1.3 and 8.0 Hz, H-3); ^{13}C NMR (125 MHz, DMSO-d_6) 39.3 ($COCH_2$), 124.4 (C-Ar), 128.0 (C-Ar), 131.0 (C-Ar), 133.2 (C-Ar), 133.4 (C-Ar), 149.2 (C-Ar), 170.4 (C=O); LRMS (ES+) *m*/*z* 181.2 $[M+H]^+$.

2-(2-Aminophenyl)acetamide (276)[265]

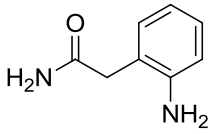

The nitro compound **274** (0.352 g, 1.94 mmol), ammonium formate (1.23 g, 19.4 mmol) and palladium on carbon (35 g, 10% w/w) were reacted in methanol (20 ml) according to **general procedure G**. Chromatography on silica (9:1 DCM/MeOH) gave the target compound as a pale pink solid (0.226 g, 1.51 mmol, 78%). R_f 0.35 (9:1 DCM/MeOH); M.p. 93-96 °C (Lit.[265] 114-115 °C); λ_{max} (EtOH/nm) 236, 288; IR (cm^{-1}) 3395, 3188, 1689, 1654, 1615; ^{1}H NMR (500 MHz, DMSO-d_6) 2.45 (2H, s, $COCH_2$), 5.10 (2H, br, Ar-NH_2), 6.52 (1H, ddd, *J* = 1.2,

7.4 and 7.7 Hz, H-5), 6.65 (1H, dd, *J* = 1.1 and 7.7 Hz, H-3), 6.92-6.96 (2H, m, H-4 and CON*H*H'), 7.00 (1H, dd, *J* = 1.2 and 7.4, H-6), 7.50 (1H, s, CONH*H'*); ^{13}C NMR (125 MHz, DMSO-d_6) 39.2 (CO*C*H$_2$), 115.0 (C-Ar), 116.4 (C-Ar), 120.5 (C-Ar), 127.2 (C-Ar), 130.3 (C-Ar), 147.0 (C-Ar), 173.0 (C=O); LRMS (ES+) *m*/*z* 151.1 [M+H]$^+$.

6-Chloro-9-(4-methoxybenzyl)-9*H*-purin-2-amine (279)

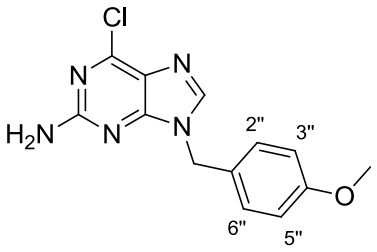

4-Methoxybenzylchloride (0.88 ml, 6.49 mmol) was added to a solution of 2-amino-6-chloropurine (1.00 g, 5.90 mmol) and K_2CO_3 (0.90 g, 6.49 mmol) in dry DMF (30 ml). The reaction mixture was heated at 60 °C for 18 h before being cooled to RT and evaporated to dryness *in vacuo*. The resultant residue was purified by silica gel chromatography (19:1 DCM/MeOH) to give the target compound as a pale yellow solid (1.47 g, 5.07 mmol, 86%). R_f 0.29 (19:1 DCM/MeOH); M.p. 170-173 °C; λ_{max} (EtOH/nm) 224, 310; IR (cm^{-1}) 3440, 3310, 3201, 3076, 2957, 2831, 1610, 1561, 1512; ^{1}H NMR (500 MHz, DMSO-d_6) 3.70 (3H, s, OCH$_3$), 5.19 (1.4 H, s, N^9-CH$_2$), 5.46 (0.6 H, s, N^7-CH$_2$), 6.64 (0.6 H, s, C^2-NH$_2$ [N^7-PMB]), 6.89 (2H, d, *J* = 8.8 Hz, H-3'/H-5'), 6.93 (1.4 H, s, C^2-NH$_2$ [N^9-PMB]), 7.12 (0.6 H, d, *J* = 8.8 Hz, N^7-[H-2'/H-6']), 7.23 (1.4 H, d, *J* = 8.8 Hz, N^9-[H-2'/H-6']), 8.19 (0.7 H, s, H-8 [N^9-PMB]), 8.52 (0.3 H, s, H-8 [N^7-PMB]); ^{13}C NMR (125 MHz, DMSO-d_6) 45.6 (N^9-CH$_2$), 48.7 (N^7-CH$_2$), 55.0 (N^7-OCH$_3$), 55.1 (N^9-OCH$_3$), 114.1 (C-Ar), 123.2 (C-Ar), 127.9 (C-Ar), 128.1 (C-Ar), 128.5 (C-Ar), 128.8 (C-Ar), 143.1 (C-Ar), 149.4 (C-Ar), 149.8 (C-Ar), 153.9 (C-Ar), 158.8 (C-Ar), 158.9 (C-Ar), 159.9 (C-Ar), 160.0 (C-Ar), 164.4 (C-Ar); HRMS calcd. for $C_{13}H_{13}ClN_5O$ (ES+) *m*/*z* 290.0803 [M+H]$^+$, found 290.0808.

Note: Greater number of ^{13}C NMR signals than environments due to regioisomers.

9-(4-Methoxybenzyl)-6-((triisopropylsilyl)ethynyl)-9*H*-purin-2-amine (280)

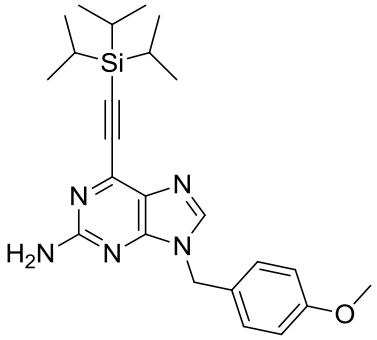

6-Chloropurine intermediate **279** (0.502 g, 1.73 mmol), (triisoproplsilyl)acetylene (0.46 ml, 2.07 mmol), copper iodide (6 mg, 0.03 mmol), $Pd(PPh_3)_2Cl_2$ (21 mg, 0.03 mmol) and triethylamine (0.60 ml, 4.31 mmol) were reacted in DMF (17 ml) according to **general procedure N**. Purification by chromatography on silica (1:1 Petrol/EtOAc) gave the target compound as a pale yellow solid (0.518 g, 1.19 mmol, 69%). R_f 0.59 (1:1 Petrol/EtOAc); M.p. 121-124 °C;λ_{max} (EtOH/nm) 230, 344; IR (cm^{-1}) 3487, 3296, 3183, 2944, 2866, 1594, 1567, 1511; ^{1}H NMR (500 MHz, DMSO-d_6) 1.09-1.17 (21H, m, Si(C*H*(C*H*$_3$)$_2$)$_3$), 3.72 (3H, s, OCH_3), 5.21 (2H, s, N^9-CH_2), 6.68 (2H, s, C^2-NH_2), 6.90 (2H, d, *J* = 8.7 Hz, H-3'/H-5'), 7.23 (2H, d, *J* = 8.7 Hz, H-2'/H-6'), 8.19 (1H, s, H-8); ^{13}C NMR (125 MHz, DMSO-d_6) 10.6 (Si(*C*H(CH$_3$)$_2$)$_3$), 18.4 (Si(CH(*C*H$_3$)$_2$)$_3$), 45.2 (N^9-CH_2), 55.1 (OCH_3), 97.1 (*C*≡C-Si), 101.9 (C≡*C*-Si), 114.0 (C-Ar), 127.9 (C-Ar), 128.6 (C-Ar), 128.8 (C-Ar), 140.3 (C-Ar), 143.4 (C-Ar), 153.7 (C-Ar), 158.8 (C-Ar), 160.4 (C-Ar); HRMS calcd. for $C_{24}H_{34}N_5OSi$ (ES+) *m*/*z* 436.2527 $[M+H]^+$, found 436.2527.

2-Iodo-9-(4-methoxybenzyl)-6-((triisopropylsilyl)ethynyl)-9*H*-purine (278)

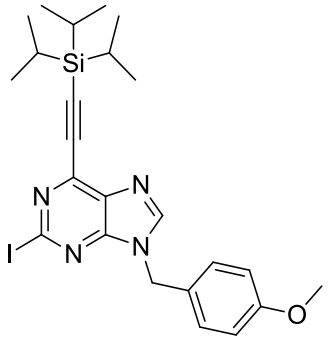

Isoamyl nitrite (140 µl, 0.69 mmol) was added to a solution of the 2-aminopurine **280** (100 mg, 0.23 mmol), diiodomethane (93 µl, 1.15 mmol) and copper iodide (48 mg, 0.25 mmol) in dry THF (2 ml). The reaction mixture was heated at reflux for 1 h, before being cooled and

evaporated to dryness. The residue was purified using silica gel chromatography (4:1 Petrol/EtOAc) to afford the target compound as pale yellow oil (0.110 g, 0.20 mmol, 87%). R_f 0.32 (4:1 Petrol/EtOAc); λ_{max} (EtOH/nm) 229, 312; IR (cm^{-1}) 2948, 2866, 1610, 1558, 1512; ^{1}H NMR (500 MHz, $CDCl_3$) 1.13-1.23 (21H, m, Si(C*H*(CH_3)$_2$)$_3$), 3.80 (3H, s, OCH_3), 5.30 (2H, s, N^9-CH_2), 6.88 (2H, d, *J* = 8.6 Hz, H-3'/H-5'), 7.23 (2H, d, *J* = 8.6 Hz, H-2'/H-6'), 7.90 (1H, s, H-8); ^{13}C NMR (125 MHz, $CDCl_3$) 11.2 (Si(*C*H(CH_3)$_2$)$_3$), 18.7 (Si(CH(*C*H_3)$_2$)$_3$), 47.1 (N^9-CH_2), 55.4 (OCH_3), 99.8 (C≡C-Si), 105.3 (C≡C-Si), 114.6 (C-Ar), 118.8 (C-Ar), 126.4 (C-Ar), 129.7 (C-Ar), 135.1 (C-Ar), 142.4 (C-Ar), 145.0 (C-Ar), 152.6 (C-Ar), 160.0 (C-Ar); HRMS calcd. for $C_{24}H_{32}IN_4OSi$ (ES+) *m*/*z* 547.1385 $[M+H]^+$, found 547.1377.

2-(2-((9-(4-Methoxybenzyl)-6-((triisopropylsilyl)ethynyl)-9*H*-purin-2-yl) amino)phenyl)acetamide (281)

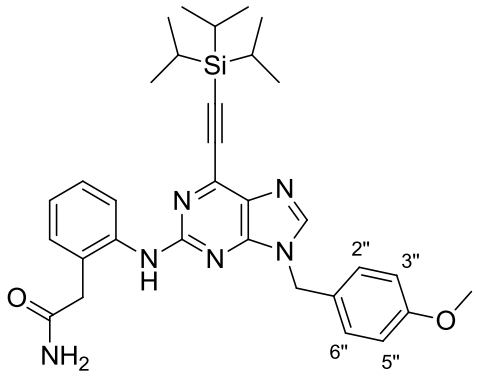

2-Iodopurine intermediate **278** (0.268 g, 0.49 mmol), aniline **276** (88 mg, 0.59 mmol), $Pd_2(dba)_3$ (45 mg, 0.05 mmol), XPhos (23 mg, 0.05 mmol) and K_2CO_3 (0.150 g, 1.09 mmol) were reacted in MeCN (5 ml) according to **general procedure M**. Purification by silica gel chromatography (3:2 Petrol/EtOAc) gave the desired compound as a pale yellow oil (0.102 g, 0.18 mmol, 37%). R_f 0.20 (3:2 Petrol/EtOAc); λ_{max} (EtOH/nm) 276; IR (cm^{-1}) 3422, 3283, 3150, 2942, 2864, 1667, 1593, 1575, 1512; ^{1}H NMR (500 MHz, DMSO-d_6) 1.12-1.21 (21H, m, Si(C*H*(CH_3)$_2$)$_3$), 3.50 (2H, s, N^9-CH_2), 3.73 (3H, s, OCH_3), 5.22 (2H, s, COCH_2), 6.92 (2H, d, *J* = 8.7 Hz, H-3''/H-5''), 7.05 (1H, ddd, *J* = 1.0, 7.3 and 7.4 Hz, H-4'), 7.18 (1H, s, CON*H*H'), 7.24-7.29 (2H, m, H-5'/H-6'), 7.30 (2H, d, *J* = 8.7 Hz, H-2''/H-6''), 7.78 (1H, s, CONH*H'*), 7.84-7.87 (1H, m, H-3'), 8.38 (1H, s, H-8), 9.75 (1H, s, C^2-NH); ^{13}C NMR (125 MHz, DMSO-d_6) 10.6 (Si(*C*H(CH_3)$_2$)$_3$), 18.4 (Si(CH(*C*H_3)$_2$)$_3$), 45.9 (CO*C*H_2), 55.1 (OCH_3), 98.5 (C≡*C*-Si), 101.6 (*C*≡C-Si), 114.0 (C-Ar), 122.2 (C-Ar), 122.9 (C-Ar), 126.8 (C-Ar),

127.7 (C-Ar), 128.4 (C-Ar), 129.2 (C-Ar), 129.4 (C-Ar), 130.2 (C-Ar), 138.8 (C-Ar), 140.4 (C-Ar), 144.4 (C-Ar), 152.8 (C-Ar), 156.3 (C-Ar), 158.9 (C-Ar), 173.8 (C=O); HRMS calcd. for $C_{32}H_{41}N_6O_2Si$ (ES+) *m/z* 569.3055 $[M+H]^+$, found 569.3051.

1-(3-Nitrophenyl)propan-2-one (284)[266]

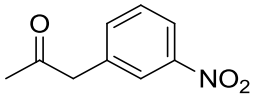

Acetic anhydride (10.4 ml, 110 mmol) was added to a solution of 3-nitrophenylacetic acid (2.00 g, 11.0 mmol) in dry pyridine (4.50 ml, 55.2 mmol). The reaction mixture was heated at reflux under N_2 for 4 h, before being concentrated *in vacuo*. The brown residue was suspended in a mixture of conc. HCl (1 ml) and EtOH (8 ml), and the suspension was heated at reflux for 1 h. The resultant solution was poured onto ice water (50 ml) and the mixture was extracted with EtOAc (3 x 30 ml). The combined organic extracts were dried ($MgSO_4$), concentrated *in vacuo*, and the crude product purified by silica gel chromatography (4:1 Petrol/EtOAc). The target compound was obtained as a pale yellow oil which crystallised on standing (1.33 g, 7.43 mmol, 68%). R_f 0.26 (4:1 Petrol/EtOAc); M.p. 62-65 °C (Lit.[266] 62 °C); λ_{max} (EtOH/nm) 263; IR (cm^{-1}) 3076, 1719, 1518; ^{1}H NMR (500 MHz, $CDCl_3$) 2.28 (3H, s, CH_3), 3.88 (2H, s, CH_2), 7.53-7.56 (2H, m, H-4/H-5), 8.07-8.10 (1H, m, H-2), 8.14-8.18 (1H, m, H-6); ^{13}C NMR (125 MHz, $CDCl_3$) 29.9 (CH_3), 49.7 (CH_2), 122.2 (C-Ar), 124.5 (C-Ar), 129.5 (C-Ar), 135.8 (C-Ar), 135.9 (C-Ar), 149.4 (C-Ar), 188.9 (C=O); LRMS (ES-) *m/z* 178.1 $[M-H]^-$.

2-Methyl-2-(3-nitrobenzyl)-1,3-dithiane (285)

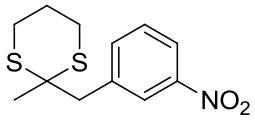

1,3-Propanedithiol (0.77 ml, 7.70 mmol) and boron trifluoride diethyl etherate (1.58 ml, 12.8 mmol) were added to a solution of ketone **284** (1.15 g, 6.42 mmol) in dry DCM (30 ml) at 0 °C. The solution was stirred under N_2 at RT for 18 h, before being washed with sat. $NaHCO_3$ solution (20 ml). The organic phase was dried through a phase separator, concentrated *in vacuo*, and the crude residue purified *via* silica gel chromatography (4:1 Petrol/EtOAc). The desired compound was obtained as an off-white crystalline solid on cooling (1.50 g, 5.56

mmol, 87%). R_f 0.44 (4:1 Petrol/EtOAc); M.p. 75-78 °C; λ_{max} (EtOH/nm) 261; IR (cm^{-1}) 2933, 2907, 1525; ^{1}H NMR (500 MHz, $CDCl_3$) 1.56 (3H, s, CH_3), 1.97-2.11 (2H, m, $C(SCH_2)_2CH_2$), 2.88-3.05 (4H, m, $C(SCH_2)_2CH_2$), 3.37 (2H, s, Ar-CH_2), 7.50 (1H, dd, *J* = 7.6 and 7.7 Hz, H-5), 7.61-7.65 (1H, m, H-6), 8.15-8.18 (2H, m, H-2/H-4); ^{13}C NMR (125 MHz, $CDCl_3$) 24.9 ($C(SCH_2)_2CH_2$), 26.7 ($C(SCH_2)_2CH_2$), 27.6 (CH_3), 46.8 (Ar-CH_2), 48.6 ($C(SCH_2)_2CH_2$), 122.1 (C-Ar), 125.7 (C-Ar), 128.6 (C-Ar), 137.1 (C-Ar), 138.1 (C-Ar), 147.9 (C-Ar); LRMS (ES+) *m*/*z* 270.2 $[M+H]^+$.

3-((2-Methyl-1,3-dithian-2-yl)methyl)aniline (286)

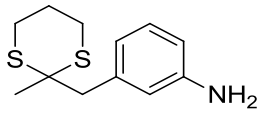

Nitro compound **285** (1.00 g, 3.71 mmol) and tin(II) chloride (2.81 g, 14.8 mmol) were reacted in ethanol (40 ml) according to **general procedure D**. Following silica gel chromatography (7:3 Petrol/EtOAc) the desired compound was obtained as an off-white solid on cooling (0.760 g, 3.17 mmol, 85%). R_f 0.41 (7:3 Petrol/EtOAc); M.p. 73-75 °C; λ_{max} (EtOH/nm) 235, 291; IR (cm^{-1}) 3444, 3349, 2941, 2913, 1612, 1585; ^{1}H NMR (500 MHz, DMSO-d_6) 1.48 (3H, s, CH_3), 1.80-1.92 (2H, m, $C(SCH_2)_2CH_2$), 2.82-2.99 (4H, m, $C(SCH_2)_2CH_2$), 3.02 (2H, s, Ar-CH_2), 4.94 (2H, s, Ar-NH_2), 6.41 (1H, ddd, *J* = 1.2, 1.6 and 7.6 Hz, H-6), 6.44 (1H, ddd, *J* = 1.2, 2.2 and 7.7 Hz, H-4), 6.46-6.48 (1H, m, H-2), 6.91 (1H, dd, *J* = 7.6 and 7.7 Hz, H-5); ^{13}C NMR (125 MHz, DMSO-d_6) 24.9 ($C(SCH_2)_2CH_2$), 25.8 ($C(SCH_2)_2CH_2$), 27.4 (CH_3), 47.2 (Ar-CH_2), 49.1 ($C(SCH_2)_2CH_2$), 112.3 (C-Ar), 116.6 (C-Ar), 118.7 (C-Ar), 128.0 (C-Ar), 136.5 (C-Ar), 147.9 (C-Ar); HRMS calcd. for $C_{12}H_{18}NS_2$ (ES+) *m*/*z* 240.0875 $[M+H]^+$, found 240.0878.

***N*-(3-((2-methyl-1,3-dithian-2-yl)methyl)phenyl)-6-((triisopropylsilyl)ethynyl)-9*H*-purin-2-amine (287)**

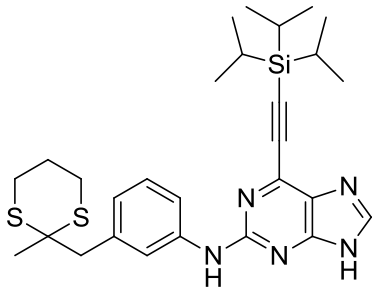

2-Fluoropurine **160** (0.195 g, 0.61 mmol), aniline **286** (0.220 g, 0.92 mmol) and TFA (117 µl, 1.53 mmol) were reacted in TFE (6 ml) according to **general procedure V**. Purification through chromatography on KP-NH silica (19:1 DCM/MeOH) gave the target compound as a yellow oil/gum (0.182 g, 0.34 mmol, 56%). R_f 0.41 (19:1 DCM/MeOH, KP-NH); λ_{max} (EtOH/nm) 276, 379; IR (cm^{-1}) 3072, 2942, 2863, 1595, 1575, 1533; ^{1}H NMR (500 MHz, $CDCl_3$) 1.17-1.26 (21H, m, Si(C*H*(CH_3)$_2$)$_3$), 1.58 (3H, s, CH_3), 1.97-2.03 (2H, m, C(SCH_2)$_2$C*H*$_2$), 2.87-2.93 (4H, m, C(SC*H*$_2$)$_2$$CH_2$), 3.19 (2H, s, Ar-$CH_2$), 7.00-7.04 (1H, m, H-6'), 7.28 (1H, dd, *J* = 7.7 and 7.8 Hz, H-5'), 7.38 (1H, s, H-8), 7.39 (1H, s, C^2-NH), 7.44-7.47 (1H, m, H-2'), 7.49-7.54 (1H, m, H-4'), 11.80 (1H, s, H-9); ^{13}C NMR (125 MHz, $CDCl_3$) 11.3 (Si(*C*H(CH_3)$_2$)$_3$), 18.7 (Si(CH(*C*H_3)$_2$)$_3$), 25.1 (C(SCH_2)$_2$*C*H_2), 26.7(C(S*C*H_2)$_2$$CH_2$), 27.6 ($CH_3$), 47.5 (Ar-$CH_2$), 49.2(*C*($SCH_2$)$_2$$CH_2$), 100.9 (C≡C), 101.6 (C≡C), 119.1 (C-Ar), 123.2 (C-Ar), 126.4 (C-Ar), 128.6 (C-Ar), 129.3 (C-Ar), 137.3 (C-Ar), 138.7 (C-Ar), 141.0 (C-Ar), 142.4 (C-Ar), 153.5 (C-Ar), 156.5 (C-Ar); HRMS calcd. for $C_{28}H_{40}N_5S_2Si$ (ES+) *m*/*z* 538.2489 $[M+H]^+$, found 538.2484.

1-(3-((6-((Triisopropylsilyl)ethynyl)-9*H*-purin-2-yl)amino)phenyl)propan-2-one (288)

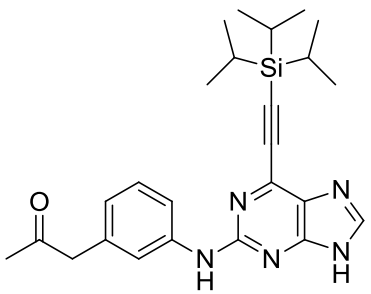

[Bis(trifluoroacetoxy)iodo]benzene (0.158 g, 0.37 mmol) was added to a solution of the dithiane protected purine **287** (0.132 g, 0.25 mmol) in MeOH/H_2O (9:1, 25 ml). After stirring

at RT for 10 min, the solution was diluted with sat. $NaHCO_3$ solution (30 ml) and the resultant suspension was extracted with DCM (2 x 20 ml). The combined organic extracts were dried through a phase separator, evaporated to dryness, and the resultant residue was purified by silica gel chromatography (19:1 DCM/MeOH). The desired compound was obtained as a yellow oil/gum (98 mg, 0.22 mmol, 88%). R_f 0.33 (19:1 DCM/MeOH); λ_{max} (EtOH/nm) 277; IR (cm^{-1}) 3402, 2943, 2865, 2363, 2160, 1705, 1597, 1577, 1542; ^{1}H NMR (500 MHz, $CDCl_3$) 1.14-1.25 (21H, m, Si(C*H*(CH_3)$_2$)$_3$), 2.16 (3H, s, CH_3), 3.67 (2H, s, CH_2), 6.85-6.89 (1H, m, H-6'), 7.27 (1H, dd, *J* = 7.7 and 7.9 Hz, H-5'), 7.40-7.45 (2H, m, H-4' & C^2-NH), 7.52-7.56 (1H, m, H-2'), 7.70 (1H, s, H-8), 11.44 (1H, br, H-9); ^{13}C NMR (125 MHz, $CDCl_3$) 11.3 (Si(*C*H(CH_3)$_2$)$_3$), 18.7 (Si(CH(*C*H_3)$_2$)$_3$), 29.4 (CH3), 51.0 (CH2), 100.8 (C≡C), 101.5 (C≡C), 118.5 (C-Ar), 120.5 (C-Ar), 123.9 (C-Ar), 129.4 (C-Ar), 135.1 (C-Ar), 139.9 (C-Ar), 156.4 (C-Ar), 206.8 (C=O); HRMS calcd. for $C_{25}H_{34}N_5OSi$ (ES+) *m*/*z* 448.2527 $[M+H]^+$, found 448.2527.

Note: Unable to visualise all carbon environments by ^{13}C NMR.

1-(3-((6-Ethynyl-9*H*-purin-2-yl)amino)phenyl)propan-2-one (199)

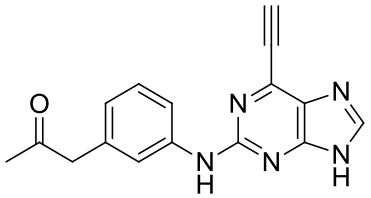

The TIPS-protected purine **288** (90 mg, 0.20 mmol), TBAF (1M in THF, 0.24 ml, 0.24 mmol) and the TBAF scavenger bead system **231** (0.90 g, 10 x w/w) were reacted in THF (5 ml) according to **general procedure U**. Silica gel chromatography (9:1 DCM/MeOH) gave the desired compound as a yellow solid (43 mg, 0.14 mmol, 70%). R_f 0.43 (9:1 DCM/MeOH); M.p. 90-110 °C (decomposed); λ_{max} (EtOH/nm) 273; IR (cm^{-1}) 3260, 3082, 2964, 2827, 2113, 1705, 1604, 1578, 1537; ^{1}H NMR (500 MHz, DMSO-d_6) 2.15 (3H, s, $COCH_3$), 3.71 (2H, s, $COCH_2$), 4.84 (1H, s, C≡CH), 6.77-6.80 (1H, m, H-6'), 7.24 (1H, dd, *J* = 7.8 and 7.9 Hz, H-5'), 7.52 (1H, dd, *J* = 1.4 and 1.6 Hz, H-2'), 7.75-7.78 (1H, m, H-4'), 8.28 (1H, s, H-8), 9.64 (1H, s, C^2-NH), 13.14 (1H, br, H-9); ^{13}C NMR (125 MHz, DMSO-d_6) 29.3 (CO*C*H_3), 50.2 (CO*C*H_2), 79.0 (C≡C), 87.0 (C≡C), 116.8 (C-Ar), 119.5 (C-Ar), 122.3 (C-Ar), 128.5 (C-Ar), 135.0 (C-Ar), 140.9 (C-Ar), 156.2 (C-Ar), 206.1 (C=O); HRMS calcd. for $C_{16}H_{14}N_5O$ (ES+) *m*/*z* 292.1193 $[M+H]^+$, found 292.1197.

***N*,*N*-Dimethyl-1-(3-((6-((triisopropylsilyl)ethynyl)-9*H*-purin-2-yl)amino)phenyl) methanesulfonamide (291)**

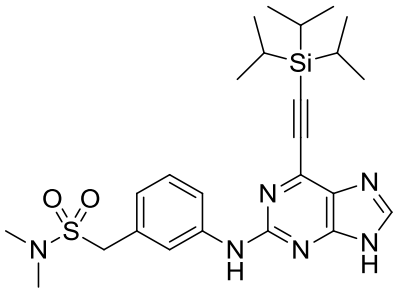

Trifluoroethylsulfonate ester **193** (0.164 g, 0.29 mmol), dimethylamine (2M in THF, 0.29 ml, 0.58 mmol) and DBU (86 µl, 0.58 mmol) were reacted in dry THF (3 ml) according to **general procedure O**. Chromatography on KP-NH silica (19:1 DCM/MeOH) afforded the target compound as a yellow oil/gum (0.148 g, 0.29 mmol, 100%). R_f 0.50 (19:1 DCM/MeOH, KP-NH); λ_{max} (EtOH/nm) 276, 366; IR (cm^{-1}) 3084, 2942, 2864, 2160, 1599, 1577, 1539; ^{1}H NMR (500 MHz, DMSO-d_6) 1.13-1.23 (21H, m, Si(C*H*(CH_3)$_2$)$_3$), 2.74 (6H, s, N-(CH_3)$_2$), 4.34 (2H, s, SO_2CH_2), 6.97-7.01 (1H, m, H-6'), 7.29 (1H, dd, *J* = 7.9 and 8.0 Hz, H-5'), 7.80 (1H, dd, *J* = 1.6 and 1.7 Hz, H-2'), 7.87 (1H, ddd, *J* = 1.0, 1.7 and 8.0 Hz, H-4'), 8.27 (1H, s, H-8), 9.78 (1H, s, C^2-NH), 12.25 (1H, br, H-9); ^{13}C NMR (125 MHz, DMSO-d_6) 10.6 (Si(*C*H(CH_3)$_2$)$_3$), 18.4 (Si(CH(*C*H_3)$_2$)$_3$), 37.4 (N-(*C*H_3)$_2$), 54.0 (SO_2CH_2), 98.0 (C≡*C*-Si), 101.7 (*C*≡C-Si), 118.0 (C-Ar), 120.5 (C-Ar), 123.5 (C-Ar), 128.4 (C-Ar), 129.7 (C-Ar), 141.0 (C-Ar), 156.1 (C-Ar); HRMS calcd. for $C_{25}H_{37}N_6O_2SSi$ (ES+) *m*/*z* 513.2462 $[M+H]^+$, found 513.2451.

Note: Unable to visualise all carbon environments by ^{13}C NMR.

1-(3-((6-Ethynyl-9*H*-purin-2-yl)amino)phenyl)-*N*,*N*-dimethylmethane sulfonamide (289)

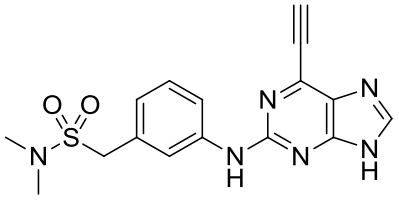

The TIPS-protected purine **291** (0.139 g, 0.27 mmol), TBAF (1M in THF, 0.33 ml, 0.33 mmol) and the TBAF scavenger bead system **231** (1.40 g, 10 x w/w) were reacted in THF (5 ml) according to **general procedure U**. Silica gel chromatography (9:1 DCM/MeOH) afforded the target compound as a yellow solid (56 mg, 0.16 mmol, 58%). R_f 0.42 (9:1

DCM/MeOH); M.p. 90-110 °C (decomposed); λ_{max} (EtOH/nm) 275, 367; IR (cm^{-1}) 3253, 3126, 2966, 2926, 2852, 2113, 1599, 1580, 1540; ^{1}H NMR (500 MHz, DMSO-d_6) 2.76 (6H, s, $N(CH_3)_2$), 4.36 (Ar-CH_2), 4.85 (1H, s, C≡CH), 6.98-7.01 (1H, m, H-6'), 7.31 (1H, dd, *J* = 7.8 and 8.0 Hz, H-5'), 7.73-7.76 (1H, m, H-2'), 7.84-7.89 (1H, m, H-4'), 8.29 (1H, s, H-8), 9.75 (1H, s, C^2-NH), 13.1 (1H, br, H-9); ^{13}C NMR (125 MHz, DMSO-d_6) 37.4 ($N(CH_3)_2$), 54.0 (Ar-CH_2), 90.7 (C≡C), 118.1 (C-Ar), 120.7 (C-Ar), 123.7 (C-Ar), 125.6 (C-Ar), 128.5 (C-Ar), 129.7 (C-Ar), 140.9 (C-Ar), 150.5 (C-Ar), 156.2 (C-Ar); HRMS calcd. for $C_{16}H_{17}N_6O_2S$ (ES+) *m*/*z* 357.1128 $[M+H]^+$, found 357.1134.

Note: Unable to visualise all carbon environments by ^{13}C NMR.

1-((Methylsulfonyl)methyl)-3-nitrobenzene (293)[267]

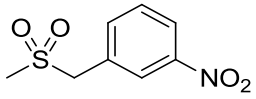

Sodium methanesulfinate (0.306 g, 3.01 mmol) in ethanol (2 ml) was added to a solution of 3-nitrobenzyl bromide (0.502 g, 2.31 mmol) in ethanol (6 ml). The mixture was heated at 80 °C for 2 h, before being cooled and concentrated *in vacuo*. The resultant residue was partitioned between DCM (15 ml) and water (10 ml), and the organic phase was dried through a phase separator. The solvent was removed and the crude residue purified on silica gel (1:1 Petrol/EtOAc) to give the target compound as a white solid (0.467 g, 2.17 mmol, 94%). R_f 0.39 (1:1 Petrol/EtOAc); M.p. 119-121 °C (Lit.[267] 105-106 °C); λ_{max} (EtOH/nm) 260; IR (cm^{-1}) 3018, 2989, 2935, 1521; ^{1}H NMR (500 MHz, $CDCl_3$) 2.91 (3H, s, CH_3), 4.40 (2H, s, CH_2), 7.66 (1H, dd, *J* = 7.6 and 7.7 Hz, H-5), 7.83 (1H, ddd, *J* = 1.3, 1.5 and 7.7 Hz, H-6), 8.29-8.33 (2H, m, H-2/H-4); ^{13}C NMR (125 MHz, $CDCl_3$) 39.9 (CH_3), 60.2 (CH_2), 124.2 (C-Ar), 125.5 (C-Ar), 130.0 (C-Ar), 130.2 (C-Ar), 136.8 (C-Ar), 153.7 (C-Ar); LRMS (ES-) *m*/*z* 214.1 $[M-H]^-$.

3-((Methylsulfonyl)methyl)aniline (294)[268]

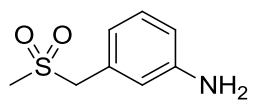

The nitro compound **293** (0.695 g, 3.23 mmol) and iron powder (1.80 g, 32.3 mmol) were reacted in acetic acid (30 ml) according to **general procedure T**. Silica gel chromatography

(9:1 DCM/MeOH) afforded the target compound as an off-white solid (0.532 g, 2.87 mmol, 89%). R_f 0.42 (9:1 DCM/MeOH); M.p. 123-126 °C (Lit.[268] 126 °C); λ_{max} (EtOH/nm) 243, 298; IR (cm^{-1}) 3463, 3373, 3221, 3011, 2970, 2930, 1625, 1603; ^{1}H NMR (500 MHz, DMSO-d_6) 2.87 (3H, s, CH_3), 4.27 (2H, s, CH_2), 5.16 (2H, s, Ar-NH_2), 6.52-6.55 (1H, m, H-6), 6.56 (1H, ddd, *J* = 1.0, 2.2 and 8.0 Hz, H-4), 6.58-6.60 (1H, m, H-2), 7.02 (1H, dd, *J* = 7.8 and 8.0 Hz, H-5); ^{13}C NMR (125 MHz, DMSO-d_6) 59.8 (CH_2), 113.9 (C-Ar), 116.1 (C-Ar), 118.2 (C-Ar), 128.9 (C-Ar), 129.4 (C-Ar), 148.7 (C-Ar); LRMS (ES+) *m*/*z* 186.1 $[M+H]^+$.

Note: Unable to visualise all carbon environments by ^{13}C NMR – masked by solvent peak.

_N_-(3-((Methylsulfonyl)methyl)phenyl)-6-((triisopropylsilyl)ethynyl)-9_H_-purin-2-amine (295)

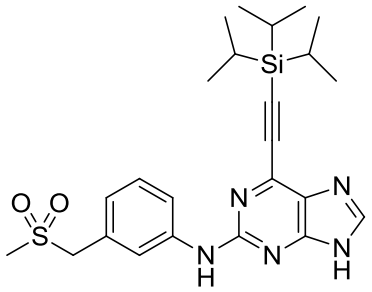

2-Fluoropurine intermediate **160** (0.213 g, 0.67 mmol), aniline **294** (0.248 g, 1.34 mmol) and TFA (130 µl, 1.67 mmol) were reacted in TFE (7 ml) according to **general procedure V**. KP-NH silica chromatography (19:1 DCM/MeOH) gave the target compound as a yellow oil/gum (0.134 g, 0.28 mmol, 42%). R_f 0.36 (19:1 DCM/MeOH, KP-NH); λ_{max} (EtOH/nm) 277, 369; IR (cm^{-1}) 3338, 2942, 2864, 1599, 1577, 1539; ^{1}H NMR (500 MHz, DMSO-d_6) 1.11-1.20 (21H, m, Si(C*H*(CH_3)$_2$)$_3$), 2.94 (3H, s, CH_3), 4.40 (2H, s, Ar-CH_2), 6.96-7.01 (1H, m, H-4'), 7.27-7.31 (1H, dd, *J* = 7.9 and 8.1 Hz, H-5'), 7.77-7.80 (1H, m, H-2'), 7.85-7.90 (1H, m, H-6'), 8.26 (1H, s, H-8), 9.79 (1H, s, C^2-NH), 13.11 (1H, br, H-9); ^{13}C NMR (125 MHz, DMSO-d_6) 10.6 (Si(*C*H(CH_3)$_2$)$_3$), 18.4 (Si(CH(*C*H_3)$_2$)$_3$), 39.7 (CH3), 59.9 (CH2), 98.0 (C≡C), 101.7 (C≡C) 118.4 (C-Ar), 120.8, 123.6 (C-Ar), 128.5 (C-Ar), 129.2 (C-Ar), 141.0 (C-Ar), 143.1 (C-Ar), 145.9 (C-Ar), 156.1 (C-Ar); HRMS calcd. for $C_{24}H_{34}N_5O_2SSi$ (ES+) *m*/*z* 484.2197 $[M+H]^+$, found 484.2197.

Note: Unable to visualise all carbon environments by ^{13}C NMR.

6-Ethynyl-*N*-(3-((methylsulfonyl)methyl)phenyl)-9*H*-purin-2-amine (290)

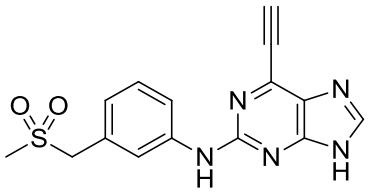

The TIPS-protected purine **295** (0.111 g, 0.23 mmol), TBAF (1M in THF, 0.28 ml, 0.28 mmol) and the TBAF scavenger bead system **231** (1.10 g, 10 x w/w) were reacted in THF (5 ml) according to **general procedure U**. Silica gel chromatography (9:1 DCM/MeOH) afforded the desired compound as a pale yellow solid (52 mg, 0.15 mmol, 66%). R_f 0.36 (9:1 DCM/MeOH); M.p. 180-200 °C (decomposed); λ_{max} (EtOH/nm) 275.0, 346.5; IR (cm^{-1}) 3330, 3257, 2982, 2919, 2116, 1607, 1548, 1492; ^{1}H NMR (500 MHz, DMSO-d_6) 2.97 (3H, s, -SO_2CH_3), 4.43 (2H, s, -SO_2CH_2), 4.83 (1H, s, C≡CH), 6.98-7.02 (1H, m, H-4'), 7.32 (1H, dd, *J* = 7.9 and 8.0 Hz, H-5'), 7.69-7.73 (1H, m, H-2'), 7.85-7.89 (1H, m, H-6'), 8.27 (1H, s, H-8), 9.77 (1H, s, C^2-NH), 13.11 (1H, br, H-9); ^{13}C NMR (125 MHz, DMSO-d_6) 59.8 (SO_2CH_2), 79.0 (*C*≡CH), 87.0 (C≡*C*H), 118.5 (C-Ar), 121.0 (C-Ar), 123.8 (C-Ar), 128.6 (C-Ar), 128.9 (C-Ar), 129.3 (C-Ar), 139.5 (C-Ar), 140.9 (C-Ar), 143.0 (C-Ar), 153.9 (C-Ar), 156.1 (C-Ar); HRMS calcd. for $C_{15}H_{14}N_5O_2S$ (ES+) *m*/*z* 328.0863 $[M+H]^+$, found 328.0868.

9-(4-Methoxybenzyl)-2-amino-9*H*-purine-6-carbonitrile (299)

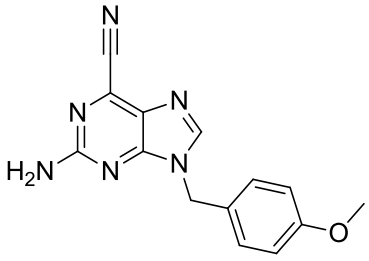

PMB-protected purine **277** (1.47 g, 5.07 mmol) was suspended in MeCN (100 ml), to which tetraethylammonium cyanide (1.59 g, 10.2 mmol) and DABCO (1.14 g, 10.2 mmol) were added, and the mixture was stirred at RT for 18 h. Conc. NH_3 solution (10 ml) was added and stirring was continued for a further 30 min. The solvent was removed *in vacuo* and the residue was suspended in sat. brine solution (100 ml) and extracted with THF (3 x 100 ml). The combined organic extracts were concentrated and purified *via* chromatography on silica (19:1 DCM/MeOH) to give the desired compound as a yellow solid (0.956 g, 3.40 mmol, 67%). R_f 0.66 (19:1 DCM/MeOH); M.p. 171-175 °C; λ_{max} (EtOH/nm) 357, 227; IR (cm^{-1})

3470, 3293, 3180, 3100, 2957, 2158, 2032, 1611; ^{1}H NMR (500 MHz, DMSO-d_6) 3.73 (3H, s, OCH_3), 5.24 (2H, s, N^9-CH_2), 6.91 (2H, d, J = 8.8 Hz, H-3'/H-5'), 7.12 (2H, s, C^2-NH_2), 7.27 (2H, d, J = 8.7 Hz, H-2'/H-6'), 8.44 (1H, s, H-8); ^{13}C NMR (125 MHz, DMSO-d_6) 45.5 (N^9-CH_2), 55.1 (OCH_3), 113.5 (quat-C), 114.1 (quat-C), 114.5 (quat-C), 128.2 (C-Ar), 129.0 (C-Ar), 129.7 (C-Ar), 146.3 (C-Ar), 154.9 (C-Ar), 158.9 (C-Ar), 160.5 (C-Ar); HRMS calcd. for $C_{14}H_{13}N_6O$ (ES+) m/z 281.1145 $[M+H]^+$, found 281.1152.

Note: Unable to distinguish between aromatic and nitrile ^{13}C NMR signals.

2-Amino-9*H*-purine-6-carbonitrile trifluoroacetate (300)

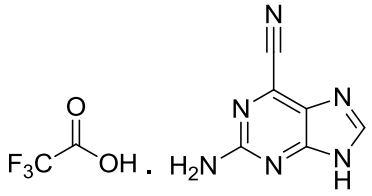

The PMB-protected purine **299** (0.803 g, 2.86 mmol) was reacted in TFA (15 ml) according to **general procedure K** for 5 h. Purification by chromatography on silica (9:1 DCM/MeOH) gave the target compound as a yellow solid (0.657 g, 2.40 mmol, 84%). R_f 0.31 (19:1 DCM/MeOH); M.p. 260-280 °C (decomposed); λ_{max} (EtOH/nm) 224, 352; IR (cm^{-1}) 3441, 3327, 3226, 2708, 2159, 1677, 1642; ^{1}H NMR (500 MHz, DMSO-d_6) 6.91 (2H, s, C^2-NH_2), 8.32 (1H, s, H-8), 12.22 (2H, br, $N^{9(+)}$-H_2); ^{13}C NMR (125 MHz, DMSO-d_6) 114.8 (C≡N), 116.0 (q, J_{CF} = 272.8 Hz, CF_3), 128.0 (C-Ar), 128.8 (C-Ar), 145.3 (C-Ar), 156.7 (C-Ar), 157.7 (C-Ar), 160.5 (C=O); ^{19}F NMR (470 MHz, DMSO-d_6) -73.5 (CF_3); HRMS calcd. for $C_6H_5N_6$ (ES+) m/z 161.0570 $[M+H]^+$, found 161.0568.

2-Fluoro-9*H*-purine-6-carbonitrile (301)

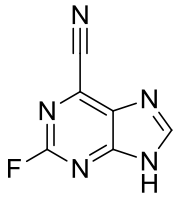

2-Aminopurine **300** (0.650 g, 2.37 mmol), sodium nitrite (0.329 g, 4.76 mmol) and HBF_4 (48 wt. % in H_2O, 20 ml) were reacted according to **general procedure A**. Purification *via* chromatography on silica (9:1 DCM/MeOH) afforded the desired compound as a beige solid (0.111 g, 0.67 mmol, 28%). R_f 0.44 (9:1 DCM/MeOH); M.p. 176-179 °C; λ_{max} (EtOH/nm)

195; IR (cm^{-1}) 3100, 2700, 2158, 2021, 1626; ^{1}H NMR (500 MHz, DMSO-d_6) 8.87 (1H, s, H-8), 14.36 (1H, s, H-9); ^{13}C NMR (125 MHz, DMSO-d_6) 113.7 (C≡N), 150.9 (d, J_{CF} = 5.7 Hz, C-Ar), 157.1 (d, J_{CF} = 211.3 Hz, C^2-Ar); ^{19}F NMR (470 MHz, DMSO-d_6) -52.01 (C^2-F); LRMS (ES+) *m*/*z* 164.1 $[M+H]^+$.

Note: Unable to visualise all quaternary carbon signals by ^{13}C NMR – poorly soluble.

2-(3-Aminophenyl)acetamide (297)

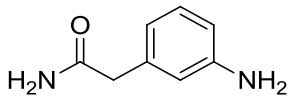

The methyl ester **234** (0.230 g, 1.39 mmol) and ammonium hydroxide solution (15 ml) were reacted together according to **general procedure S**. Chromatography on silica (7:3 Petrol/EtOAc) gave the target compound as an off-white solid (0.160 g, 1.07 mmol, 77%). R_f 0.32 (7:3 Petrol/EtOAc); M.p. 156-158 °C; λ_{max} (EtOH/nm) 238; IR (cm^{-1}) 3410, 3300, 3175, 1666, 1607; ^{1}H NMR (500 MHz, DMSO-d6) 3.19 (2H, s, $COCH_2$), 5.00 (2H, s, Ar-NH_2), 6.40-6.43 (2H, m, H-4/H-6), 6.46-6.48 (1H, br, H-2), 6.81 (1H, s, CON*H*H'), 6.92 (1H, dd, *J* = 7.7 and 7.8 Hz, H-5), 7.34 (1H, s, CONH*H'*); ^{13}C NMR (125 MHz, DMSO-d_6) 42.6 ($CO\mathit{C}H_2$), 112.0 (C-Ar), 114.6 (C-Ar), 116.6 (C-Ar), 128.6 (C-Ar), 136.9 (C-Ar), 148.4 (C-Ar), 172.4 (C=O); LRMS (ES+) *m*/*z* 151.2 $[M+H]^+$.

2-(3-(6-Cyano-9*H*-purin-2-ylamino)phenyl)acetamide (296)

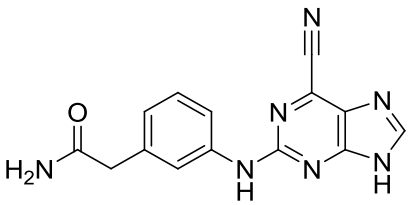

2-Fluoropurine intermediate **301** (10 mg, 0.06 mmol) and aniline **297** (18 mg, 0.12 mmol) were combined in DMSO (1 ml) and heated in a sealed vial at 100 °C for 72 h. The solvent was removed *in vacuo* and the residue was purified *via* chromatography on silica (9:1 DCM/MeOH) to give the desired product as a yellow solid (9 mg, 0.03 mmol, 50%). R_f 0.32 (9:1 DCM/MeOH); M.p. 170-180 °C (decomposed); λ_{max} (EtOH/nm) 273; IR (cm^{-1}) 3427, 3268, 3118, 2828, 2160, 2030, 1686; ^{1}H NMR (500 MHz, DMSO-d6) 3.36 (2H, s, $COCH_2$), 6.91 (2H, m, CON*H*H'/H-6'), 7.22-7.26 (1H, m, H-5'), 7.46 (1H, s, CONH*H'*), 7.50-7.54

(1H, m, H-2'), 7.69-7.73 (1H, m, H-4'), 8.50 (1H, s, H-8), 9.94 (1H, s, C^2-NH), 13.52 (1H, br, H-9); HRMS calcd. for $C_{14}H_{12}N_7O$ (ES+) *m/z* 294.1101 $[M+H]^+$, found 294.1098.

Note: Insufficient material for ^{13}C NMR.

Methyl 2-(3-nitrophenyl)acetate (303)[269]

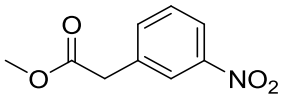

3-Nitrophenylacetic acid (0.500 g, 2.76 mmol) and thionyl chloride (400 µl, 5.52 mmol) were reacted in dry methanol (25 ml) according to **general procedure R**. The crude product was purified using silica gel chromatography (17:3 Petrol/EtOAc) to give the desired compound as a colourless oil (0.501 g, 2.56 mmol, 93%). R_f 0.36 (17:3 Petrol/EtOAc); λ_{max} (EtOH/nm) 272, 320; IR (cm^{-1}) 2985, 2359, 1728, 1530; ^1H NMR (500 MHz, DMSO-d_6) 3.65 (3H, s, OCH_3), 3.93 (2H, s, CH_2), 7.64 (1H, dd, *J* = 7.9 and 8.1 Hz, H-5), 7.75-7.78 (1H, m, H-6), 8.15 (1H, ddd, *J* = 0.9, 2.3 and 7.9 Hz, H-4), 8.18-8.21 (1H, m, H-2); ^{13}C NMR (125 MHz, DMSO-d_6) 51.9 (OCH_3), 121.9 (C-Ar), 124.3 (C-Ar), 129.7 (C-Ar), 136.5 (C-Ar), 136.7 (C-Ar), 147.7 (C-Ar), 171.1 (C=O); LRMS (ES+) *m/z* 196.3 $[M+H]^+$.

Note: Unable to visualise all carbon signals by NMR – masked by solvent.

Methyl 2-methyl-2-(3-nitrophenyl)propanoate (304)

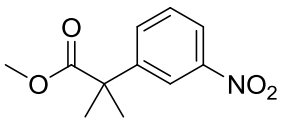

Sodium hydride (60% dispersion in mineral oil, 90 mg, 2.25 mmol) was added portion-wise to a solution of the ester **303** (0.200 g, 1.02 mmol) and methyl iodide (160 µl, 2.56 mmol) in dry THF (2 ml) at 0 °C. The reaction mixture was stirred at 0 °C for 20 min, before being warmed to RT and stirred for a further 18 h. The reaction was quenched with acetic acid (1 ml) and the solvent was removed *in vacuo*. The crude residue was purified on silica (17:3 Petrol/EtOAc) to give the desired compound as a pale orange oil (0.124 g, 0.56 mmol, 55%). R_f 0.45 (17:3 Petrol/EtOAc); λ_{max} (EtOH/nm) 270, 308; IR (cm^{-1}) 2983, 2954, 2361, 2341, 1730, 1527; ^1H NMR (500 MHz, DMSO-d_6) 1.59 (6H, s, $C(CH_3)_2$), 3.63 (3H, s, OCH_3), 7.67 (1H, dd, *J* = 7.9 and 8.1 Hz, H-5), 7.82 (1H, ddd, *J* = 1.0, 1.9 and 7.9 Hz, H-6), 8.12 (1H, dd,

J = 1.9 and 2.3 Hz, H-2), 8.15 (1H, ddd, *J* = 1.0, 2.3 and 8.1 Hz, H-4); ^{13}C NMR (125 MHz, DMSO-d_6) 26.1 (C(*C*H$_3$)$_2$), 46.3 (*C*(CH$_3$)$_2$), 52.4 (OCH$_3$), 120.2 (C-Ar), 121.9 (C-Ar), 130.0 (C-Ar), 132.9 (C-Ar), 146.5 (C-Ar), 147.8 (C-Ar), 175.6 (C=O); LRMS (ES+) *m*/*z* 224.2 [M+H]$^+$.

2-Methyl-2-(3-nitrophenyl)propanamide (305)

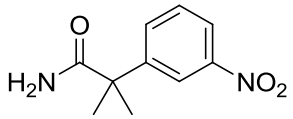

Methyl ester **304** (0.110 g, 0.49 mmol) was dissolved in concentrated ammonium hydroxide (5 ml) and the resultant solution was heated in a sealed vessel at 60 °C for 18 h. The solvent was removed *in vacuo* and the residue was dissolved in dry DCM (5 ml) and treated with thionyl chloride (72 µl, 0.98 mmol) and 1 drop of DMF. The solution was stirred at RT under nitrogen for 15 min, after which point the solvent was removed *in vacuo*. The residue was dissolved in dry THF (5 ml) and the solution was added drop-wise to concentrated ammonium hydroxide (3 ml). The mixture was stirred at RT for 18 h, before the solvent was removed *in vacuo*. The crude residue was purified *via* chromatography on KP-NH silica (7:3 Petrol/EtOAc) to give the desired compound as a white solid (72 mg, 0.35 mmol, 71%). R_f 0.29 (7:3 Petrol/EtOAc, KP-NH); M.p. 116-118 °C; λ_{max} (EtOH/nm) 220, 270; IR (cm^{-1}) 3391, 3208, 2965, 1650, 1535; ^{1}H NMR (500 MHz, DMSO-d_6) 1.51 (6H, s, C(CH$_3$)$_2$), 7.06 (1H, s, CON*H*H'), 7.11 (1H, s, CONH*H'*), 7.65 (1H, dd, *J* = 8.0 and 8.0 Hz, H-5), 7.81 (1H, ddd, *J* = 1.0, 1.8 and 8.0 Hz, H-6), 8.12 (1H, ddd, *J* = 1.0, 2.3 and 8.0 Hz, H-4), 8.15 (1H, dd, *J* = 1.8 and 2.3 Hz, H-2); ^{13}C NMR (125 MHz, DMSO-d_6) 26.4 (C(*C*H$_3$)$_2$), 48.1(*C*(*C*H$_3$)$_2$), 120.5 (C-Ar), 121.3 (C-Ar), 129.7 (C-Ar), 133.0 (C-Ar), 176.9 (C=O); HRMS calcd. for $C_{10}H_{13}N_2O_3$ (ES+) *m*/*z* 209.0921 [M+H]$^+$, found 209.0924.

2-(3-Aminophenyl)-2-methylpropanamide (307)

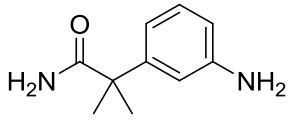

Nitro aromatic **305** (0.392 g, 1.88 mmol), pallladium on carbon (40 mg, 10% w/w) and ammonium formate (1.19 g, 18.8 mmol) were reacted in methanol (20 ml) according to **general procedure G** over 18 h. Chromatography on silica (19:1 DCM/MeOH) gave the

desired compound as an off-white solid (0.311 g, 1.75 mmol, 93%). R_f 0.21 (19:1 DCM/MeOH); M.p. 117-120 °C; λ_{max} (EtOH/nm) 243; IR (cm^{-1}) 3410, 3337, 3172, 2982, 1665; ^{1}H NMR (500 MHz, DMSO-d_6) 1.36 (6H, s, C(CH_3)$_2$), 5.10 (2H, br, Ar-NH_2), 6.40 (1H, ddd, *J* = 0.8, 2.1 and 7.9 Hz, H-6), 6.47-6.50 (1H, m, H-4), 6.54-6.56 (1H, m, H-2), 6.72 (1H, s, CON*H*H'), 6.78 (1H, s, CONH*H'*), 6.94 (1H, dd, *J* = 7.9 and 8.0 Hz, H-5); ^{13}C NMR (125 MHz, DMSO-d_6) 26.8 (C(*C*H_3)$_2$), 45.7 (*C*(CH_3)$_2$), 111.5 (C-Ar), 111.8 (C-Ar), 113.2 (C-Ar), 128.5 (C-Ar), 146.9 (C-Ar), 148.3 (C-Ar), 178.1 (C=O); HRMS calcd. for $C_{10}H_{15}N_2O$ (ES+) *m*/*z* 179.1179 $[M+H]^+$, found 179.1180.

2-(3-(6-(2-(Triisopropylsilyl)ethynyl)-9*H*-purin-2-ylamino)phenyl)-2-methylpropanamide (308)

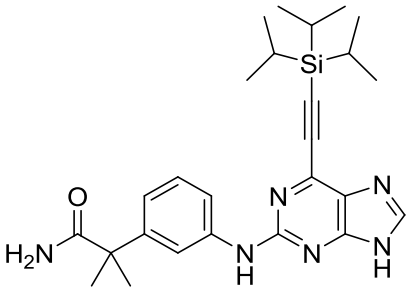

2-Fluoropurine intermediate **160** (0.197 g, 0.62 mmol), aniline **307** (0.220 g, 1.24 mmol) and TFA (240 μl, 3.10 mmol) were reacted in TFE (4 ml) according to **general procedure B**. Purification *via* chromatography on silica (19:1 DCM/MeOH) afforded the desired compound as a yellow oil (0.127 g, 0.27 mmol, 43%). R_f 0.28 (19:1 DCM/MeOH); λ_{max} (EtOH/nm) 270, 368; IR (cm^{-1}) 3094, 2964, 2943, 2162, 1970, 1659; ^{1}H NMR (500 MHz, DMSO-d_6) 1.13-1.19 (21H, m, Si(C*H*(CH_3)$_2$)$_3$), 1.45 (6H, s, C(CH_3)$_2$), 6.80 (1H, s, CON*H*H'), 6.89 (1H, s, CONH*H'*), 7.04-7.07 (1H, m, H-6'), 7.21 (1H, dd, *J* = 7.9 and 8.1 Hz, H-5'), 7.65-7.69 (1H, m, H-4'), 7.86-7.88 (1H, m, H-2'), 8.25 (1H, s, H-8), 9.65 (1H, s, C^2-NH), 13.07 (1H, br, H-9); ^{13}C NMR (125 MHz, DMSO-d_6) 10.6 (Si(*C*H(CH_3)$_2$)$_3$), 18.4 (Si(CH(*C*H_3)$_2$)$_3$), 26.8 (C(*C*H_3)$_2$), 46.0 (*C*(CH_3)$_2$), 97.7 (C≡C), 116.1 (C-Ar), 116.2 (C-Ar), 116.6 (C-Ar), 117.1 (C-Ar), 128.0 (C-Ar), 128.5 (C-Ar), 138.1 (C-Ar), 140.7 (C-Ar), 146.6 (C-Ar), 147.1 (C-Ar), 156.2 (C-Ar), 159.4 (C-Ar), 177.6 (C=O); HRMS calcd. for $C_{26}H_{37}N_6OSi$ (ES+) *m*/*z* 477.2793 $[M+H]^+$, found 477.2796.

2-(3-(6-Ethynyl-9*H*-purin-2-ylamino)phenyl)-2-methylpropanamide (302)

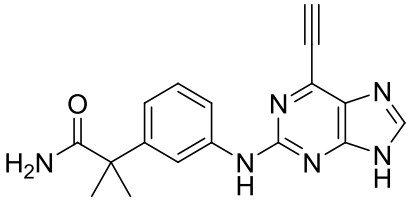

TIPS-protected purine **308** (0.108 g, 0.23 mmol), KF (65 mg, 1.13 mmol) and 18-crown-6 (6 mg, 0.023 mmol) were reacted in THF (2.5 ml) according to **general procedure Q**. Purification *via* chromatography on KP-NH silica (9:1 DCM/MeOH) afforded the desired compound as a yellow solid (37 mg, 0.12 mmol, 51%). R_f 0.29 (9:1 DCM/MeOH, KP-NH); M.p. 140-160 °C (decomposed); λ_{max} (EtOH/nm) 274; IR (cm^{-1}) 3270, 2975, 2853, 2155, 1979, 1659, 1599; ^{1}H NMR (500 MHz, DMSO-d_6) 1.45 (6H, s, -C(CH_3)$_2$), 4.82 (1H, s, -C≡CH), 6.80 (1H, s, -CON*H*H'), 6.84 (1H, s, -CONH*H'*), 6.90-6.92 (1H, m, H-6'), 7.22 (1H, dd, *J* = 8.1 and 8.2 Hz, H-5'), 7.74-7.76 (2H, m, H-2'/H-4'), 8.27 (1H, s, H-8), 9.60 (1H, s, C^2-NH), 13.11 (1H, br, H-9); ^{13}C NMR (125 MHz, MeOD) 23.8 (C(*C*H_3)$_2$), 49.4 (*C*(CH_3)$_2$), 102.4 (C≡C), 122.8 (C-Ar), 124.6 (C-Ar), 125.9 (C-Ar), 128.9 (C-Ar), 130.1 (C-Ar); HRMS calcd. for $C_{17}H_{17}N_6O$ (ES+) *m*/*z* 321.1463 $[M+H]^+$, found 321.1458.

Note: Unable to visualise all carbon signals by NMR.

5-(6-(2-(Triisopropylsilyl)ethynyl)-9*H*-purin-2-ylamino)indolin-2-one (319)

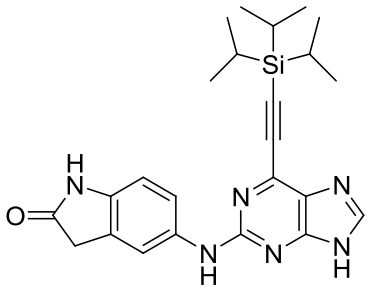

2-Fluoropurine intermediate **160** (0.319 g, 1.00 mmol), 5-amino-1,3-dihydro-2H-indol-2-one (0.298 g, 2.01 mmol) and TFA (390 µl, 5.02 mmol) were reacted in TFE (5 ml) according to **general procedure B**. Purification *via* chromatography on KP-NH silica (17:3 DCM/MeOH) afforded the desired compound as a orange oil (0.143 g, 0.32 mmol, 32%). R_f 0.45 (17:3 DCM/MeOH, KP-NH); λ_{max} (EtOH/nm) 255, 300, 374; IR (cm^{-1}) 2941, 2864, 2154, 1685; ^{1}H NMR (500 MHz, DMSO-d_6) 1.14-1.19 (21H, m, Si(CH(CH_3)$_2$)$_3$), 3.47 (2H, s, $COCH_2$), 6.74

(1H, d, *J* = 8.4 Hz, H-3'), 7.51-7.54 (1H, m, H-4'), 7.72-7.75 (1H, br, H-6'), 8.19 (1H, s, H-8), 9.54 (1H, s, indole NH), 10.23 (1H, s, C^2-NH), 13.03 (1H, br, H-9); ^{13}C NMR (125 MHz, DMSO-d_6) 10.6 (Si(*C*H(CH_3)$_2$)$_3$), 18.5 (Si(CH(*C*H_3)$_2$)$_3$), 36.1 (CO*C*H_2), 97.6 (C≡C), 101.9 (C≡C), 108.8 (C-Ar), 115.9 (C-Ar), 117.8 (C-Ar), 125.9 (C-Ar), 128.3 (C-Ar), 135.1 (C-Ar), 137.7 (C-Ar), 139.9 (C-Ar), 142.3 (C-Ar), 153.9 (C-Ar), 156.5 (C-Ar), 176.2 (C=O); HRMS calcd. for $C_{24}H_{31}N_6OSi$ (ES+) *m*/*z* 447.2323 $[M+H]^+$, found 447.2322.

5-((6-Ethynyl-9*H*-purin-2-yl)amino)indolin-2-one (309)

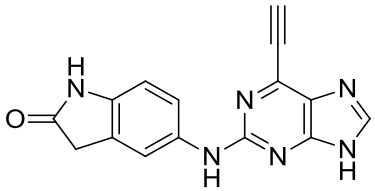

The TIPS-protected purine **319** (66 mg, 0.15 mmol), TBAF (1M in THF, 0.18 ml, 0.18 mmol) and the TBAF scavenger bead system **231** (0.60 g, 10 x w/w) were reacted in THF (5 ml) according to **general procedure U**. Chromatography on silica (9:1 DCM/MeOH) gave the desired compound as an orange solid (29 mg, 0.10 mmol, 67%). R_f 0.38 (9:1 DCM/MeOH); M.p. 130-160 °C (decomposed); λ_{max} (EtOH/nm) 285.0, 375.5; IR (cm^{-1}) 2835, 2161, 2112, 2028, 1977, 1668; ^{1}H NMR (500 MHz, DMSO-d_6) 3.48 (2H, s, CH_2), 4.83 (1H, s, C≡CH), 6.74 (1H, d, *J* = 8.4 Hz, H-7'), 7.53 (1H, dd, *J* = 1.4 and 8.4 Hz, H-6'), 7.69-7.71 (1H, m, H-4'), 8.24 (1H, s, H-8), 9.51 (1H, s, lactam-NH), 10.26 (1H, s, C^2-NH), 13.08 (1H, br, H-9); ^{13}C NMR (125 MHz, DMSO-d_6) 36.1 (CH_2), 86.7 (C≡*C*H), 108.8 (*C*≡CH), 115.9 (C-Ar), 117.9 (C-Ar), 125.9 (C-Ar), 135.0 (C-Ar), 156.5 (C-Ar), 176.2 (C=O); HRMS calcd. for $C_{15}H_{11}N_6O$ (ES+) *m*/*z* 291.0990 $[M+H]^+$, found 291.0989.

Note: Unable to visualise all carbon environments by ^{13}C NMR.

Di-*tert*-butyl 2-(3-fluoro-2-nitrophenyl)malonate (321)[270]

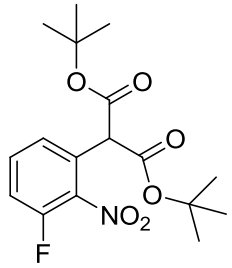

2,6-Difluoronitrobenzene (0.501 g, 3.14 mmol), di-*tert*-butyl malonate (775 µl, 3.46 mmol) and potassium carbonate (0.780 g, 5.65 mmol) were combined in dry DMF (9 ml) and heated at 60 °C for 18 h, after which the reaction mixture was neutralised with 1M HCl, and extracted with Et_2O (3 x 20 ml). The combined organic extracts were dried (Na_2SO_4), concentrated *in vacuo*, and purified *via* chromatography on silica (9:1 Petrol/EtOAc) to give the desired compound as a yellow oil (0.681 g, 1.92 mmol, 61%). R_f 0.56 (9:1 Petrol/EtOAc); λ_{max} (EtOH/nm) 230; IR (cm^{-1}) 2981, 2937, 1727; ^{1}H NMR (500 MHz, $CDCl_3$) 1.50 (18H, s, $(OC(CH_3)_3)_2$), 4.66 (1H, s, CH), 7.22-7.26 (1H, m, H-4), 7.42-7.45 (1H, m, H-6), 7.50-7.55 (1H, m, H-5); ^{13}C NMR (125 MHz, $CDCl_3$) 27.8 (-OC(*C*$H_3)_3$), 54.8 (CO*C*HCO), 83.3 (O*C*$(CH_3)_3$), 116.9 (C-Ar), 125.9 (C-Ar), 129.1 (C-Ar), 132.1 (C-Ar), 153.0 (C-Ar), 155.1 (C-Ar), 165.7 (C=O); LRMS (ES-) *m*/*z* 354.2 $[M-H]^-$.

Di-*tert*-butyl 2-(3-(4-methoxybenzylamino)-2-nitrophenyl)malonate (322)

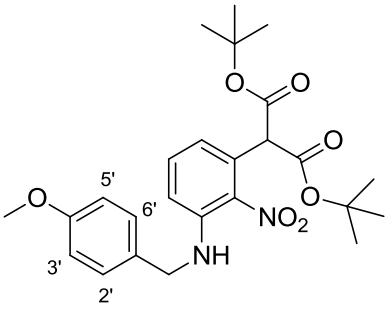

Malonate **321** (0.527 g, 1.48 mmol) was combined with 4-methoxybenzylamine (575 µl, 4.44 mmol) in THF (15 ml). The reaction mixture was heated at 80 °C for 18 h, after which the solvent was removed *in vacuo*. The crude residue was purified *via* chromatography on silica (9:1 Petrol/EtOAc) to give the desired product as a dark orange oil (0.460 g, 1.04 mmol, 70%). R_f 0.25 (9:1 Petrol/EtOAc); λ_{max} (EtOH/nm) 241; IR (cm^{-1}) 3409, 2980, 2360, 1727; ^{1}H NMR (500 MHz, DMSO-d_6) 1.49 (18H, s, $(OC(CH_3)_3)_2$), 3.81 (3H, s, OCH_3), 4.38 (2H, d,

J = 4.7 Hz, C*H*$_2$NH), 4.83 (1H, s, CH), 6.73 (1H, dd, *J* = 1.0 and 7.5 Hz, H-4), 6.80 (1H, dd, *J* = 1.0 and 8.7 Hz, H-6), 6.89 (2H, d, *J* = 8.8 Hz, H-3'/H-5'), 7.25 (2H, d, *J* = 8.8 Hz, H-2'/H-6'), 7.31 (1H, dd, *J* = 7.5 and 8.7 Hz, H-5); ^{13}C NMR (125 MHz, $CDCl_3$) 27.9 (-OC(*C*H$_3$)$_3$), 47.2 (NH*C*H$_2$), 55.3 (OCH$_3$), 57.5 (CO*C*HCO), 82.4 (-O*C*(CH$_3$)$_3$), 113.8 (C-Ar), 114.3 (C-Ar), 118.1 (C-Ar), 128.5 (C-Ar), 129.3 (C-Ar), 133.7 (C-Ar), 167.2 (C=O); HRMS calcd. for $C_{25}H_{33}N_2O_7$ (ES+) *m/z* 473.2282 $[M+H]^+$, found 473.2281.

7-Aminoindolin-2-one (324)[271]

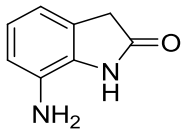

Ammonium formate (1.07 g, 17.0 mmol) and palladium on carbon (0.080 g, 10% w/w) were added to a solution of malonate **322** (0.802 g, 1.70 mmol) in acetic acid (17 ml). The mixture was heated under microwave irradiation at 100 °C for 80 min, after which point the microwave vial was vented, and the catalyst was removed *via* filtration through Celite®. The solvent was removed *in vacuo* and the resulting residue was dissolved in EtOAc (30 ml) and washed with sat. $NaHCO_3$ solution (3 x 30 ml). The organic extract was dried (Na_2SO_4) and concentrated, and the crude residue was purified *via* chromatography on silica (9:1 DCM/MeOH) to give the *N*-acetylated product as an off-white solid (0.146 g, 0.77 mmol, crude yield 45%). The solid was suspended in methanol (8 ml) and treated with acetyl chloride (330 µl, 4.62 mmol) at RT. The suspension slowly entered solution and after 1 hour the solvent was removed *in vacuo*. The residue was partitioned between EtOAc (10 ml) and sat. $NaHCO_3$ solution (10 ml) and the organic extract was dried (Na_2SO_4) and concentrated to dryness. Purification of the crude residue *via* chromatography on silica (1:4 Petrol/EtOAc) gave the desired compound as a beige solid (91 mg, 0.61 mmol, 36%). R_f 0.44 (1:4 Petrol/EtOAc); M.p. 249-251 °C (Lit.[271] 247-249 °C); λ_{max} (EtOH/nm) 255; IR (cm^{-1}) 3425, 3363, 3247, 1694; ^{1}H NMR (500 MHz, DMSO-d_6) 3.41 (2H, s, CH_2), 4.81 (2H, s, Ar-NH_2), 6.47-6.49 (1H, m, H-4), 6.50 (1H, dd, *J* = 1.0 and 8.0 Hz, H-6), 6.69 (1H, ddd, *J* = 8.0 and 8.1 Hz, H-5); ^{13}C NMR (125 MHz, DMSO-d_6) 36.3 (CO*C*H$_2$), 112.6 (C-Ar), 113.6 (C-Ar), 122.0 (C-Ar), 125.7 (C-Ar), 128.9 (C-Ar), 131.5 (C-Ar), 176.0 (C=O); LRMS (ES+) *m/z* 149.1 $[M+H]^+$.

7-(6-(2-(Triisopropylsilyl)ethynyl)-9H-purin-2-ylamino)indolin-2-one (325)

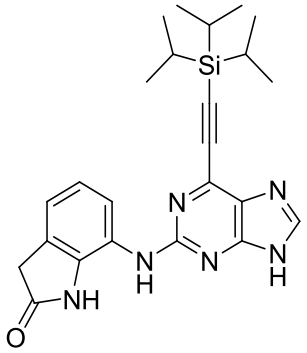

2-Fluoropurine intermediate **160** (0.120 g, 0.37 mmol), aminoindolinone **324** (0.110 g, 0.75 mmol) and TFA (142 µl, 1.85 mmol) were reacted in TFE (4 ml) according to **general procedure B**. Purification *via* chromatography on KP-NH silica (19:1 DCM/MeOH) afforded the desired compound as a orange oil (54 mg, 0.12 mmol, 32%). R_f 0.36 (19:1 DCM/MeOH); λ_{max} (EtOH/nm) 255, 359; IR (cm^{-1}) 3351, 3251, 3070, 2943, 2866, 2159, 1704; ^{1}H NMR (500 MHz, DMSO-d_6) 1.14-1.19 (21H, m, Si(C*H*(C*H*$_3$)$_2$)$_3$), 3.52 (2H, s, CH_2), 6.90-7.00 (2H, m, H-4'/H-5'), 7.58-7.62 (1H, m, H-6'), 8.20 (1H, s, H-8), 9.00 (1H, s, indole NH), 10.08 (1H, s, C^2-NH), 13.05 (1H, br, H-9); ^{13}C NMR (125 MHz, DMSO-d_6) 10.6 (Si(*C*H(CH$_3$)$_2$)$_3$), 18.4 (Si(CH(*C*H$_3$)$_2$)$_3$), 36.0 (CO*C*H$_2$), 119.2 (C-Ar), 121.1 (C-Ar), 126.3 (C-Ar), 156.6 (C-Ar), 175.9 (C=O); HRMS calcd. for $C_{24}H_{31}N_6OSi$ (ES+) *m/z* 447.2323 $[M+H]^+$, found 447.2323.

Note: Unable to visualise all carbon signals by NMR.

7-((6-Ethynyl-9*H*-purin-2-yl)amino)indolin-2-one (310)

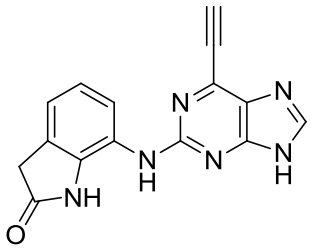

The TIPS-protected purine **325** (99 mg, 0.22 mmol), TBAF (1M in THF, 0.27 ml, 0.27 mmol) and the TBAF scavenger bead system **231** (1.00 g, 10 x w/w) were reacted in THF (5 ml) according to **general procedure U**. Purification on silica (9:1 DCM/MeOH) afforded the target compound as a pale orange solid (43 mg, 0.14 mmol, 67%). R_f 0.27 (9:1

DCM/MeOH); M.p. 195-225 °C (decomposed); λ_{max} (EtOH/nm) 244.0, 361.0; IR (cm^{-1}) 3248, 2363, 2169, 2013, 1978, 1662; ^{1}H NMR (500 MHz, DMSO-d_6) 3.52 (2H, s, CH_2), 4.81 (1H, s, C≡CH), 6.93 (1H, dd, *J* = 7.4 and 7.7 Hz, H-5'), 6.95-6.98 (1H, m, H-4'), 7.61-7.67 (1H, m, H-6'), 8.23 (1H, s, H-8), 8.96 (1H, s, lactam-NH), 10.11 (1H, s, C^2-NH), 13.08 (1H, br, H-9); ^{13}C NMR (125 MHz, DMSO-d_6) 36.4 (CH_2), 119.6 (C-Ar), 121.4 (C-Ar); HRMS calcd. for $C_{15}H_{11}N_6O$ (ES+) *m*/*z* 291.0990 $[M+H]^+$, found 291.0989.

Note: Unable to visualise all carbon environments by ^{13}C NMR – insufficient material.

Methyl methyl(phenethyl) carbamate (326)[272]

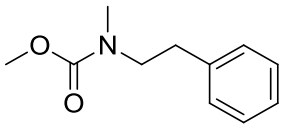

A solution of methyl chloroformate (1.59 ml, 20.6 mmol) in Et_2O (5 ml) was added dropwise over 30 min to the biphasic mixture of *N*-methyl-phenethylamine (2.00 ml, 13.8 mmol) and K_2CO_3 (5.71 g, 41.3 mmol) in Et_2O (20 ml) and water (20 ml). The mixture was stirred at RT for 1 hour, before the organic phase was removed and washed with 1M HCl (20 ml), dried ($MgSO_4$) and evaporated to dryness. The resultant crude residue was purified using silica gel chromatography (4:1 Petrol/EtOAc) to give the target compound as a colourless liquid (2.44 g, 11.9 mmol, 86%). R_f 0.44 (4:1 Petrol/EtOAc); λ_{max} (EtOH/nm) 259; IR (cm^{-1}) 3027, 2950, 1697; ^{1}H NMR (500 MHz, DMSO-d_6, 348 K) 2.79 (2H, t, *J* = 7.6 Hz, NCH_2CH_2), 2.80 (3H, s, N-CH3), 3.45 (2H, t, *J* = 7.6 Hz, NCH_2CH_2), 3.56 (3H, s, OCH_3), 7.19-7.23 (3H, m, H-2/H-4/H-6), 7.28-7.32 (2H, m, H-3/H-5); ^{13}C NMR (125 MHz, $CDCl_3$, 298 K) 34.1 (N-CH_3), 34.6 (N-CH_3), 50.6 (CH_2), 51.1 (CH_2), 52.5 (OCH_3), 126.3 (C-Ar), 128.5 (C-Ar), 128.8 (C-Ar), 139.0 (C-Ar), 153.7 (C=O); LRMS (ES+) *m*/*z* 194.2 $[M+H]^+$.

2-Methyl-3,4-dihydroisoquinolin-1(2*H*)-one (328)[273]

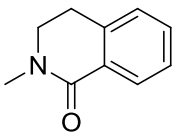

The methyl carbamate **326** (1.77 g, 9.16 mmol) was heated in Eaton's reagent (10 ml) under microwave irradiation conditions at 120 °C for 15 min. The resultant brown oil was dissolved in EtOAc (100 ml) and slowly added to a stirred sat. $NaHCO_3$ solution (100 ml). The mixture

was shaken, and the organic phase washed with brine (50 ml), dried ($MgSO_4$) and concentrated *in vacuo*. Chromatography on silica (4:1 Petrol/EtOAc) gave the desired compound as a colourless oil (1.30 g, 8.09 mmol, 88%). R_f 0.26 (4:1 Petrol/EtOAc); λ_{max} (EtOH/nm) 229; IR (cm^{-1}) 2941, 2871, 1641, 1604, 1578; ^1H NMR (500 MHz, $CDCl_3$) 3.02 (2H, t, *J* = 6.7 Hz, NCH_2CH_2), 3.17 (3H, s, $N\text{-}CH_3$), 3.58 (2H, t, *J* = 6.7 Hz, NCH_2CH_2), 7.17-7.20 (1H, m, H-5), 7.34 (1H, ddd, *J* = 1.1, 7.5 and 7.6 Hz, H-7), 7.42 (1H, ddd, *J* = 1.4, 7.4 and 7.5 Hz, H-6), 8.10 (1H, dd, *J* = 1.4 and 7.6 Hz, H-8); ^{13}C NMR (125 MHz, $CDCl_3$) 27.9 (NCH_2CH_2), 35.2 ($N\text{-}CH_3$), 48.1 (NCH_2CH_2), 126.9 (C-Ar), 127.0 (C-Ar), 128.1 (C-Ar), 129.4 (C-Ar), 131.5 (C-Ar), 138.0 (C-Ar), 164.8 (C=O); LRMS (ES+) *m*/*z* 162.1 $[M+H]^+$.

2-Methyl-7-nitro-3,4-dihydroisoquinolin-1(2*H*)-one (330)

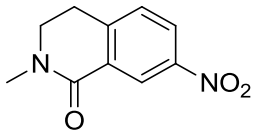

Fuming HNO_3 (42 µl, 1.01 mmol) was added to conc. H_2SO_4 (2 ml) at 0 °C. A solution of the isoquinolinone **328** (0.135 g, 0.84 mmol) in conc. H_2SO_4 (0.5 ml) was added dropwise, and the solution was stirred at 0 °C for 30 min. The mixture was poured onto ice water (15 ml) and the resulting precipitate collected by filtration and washed with cold water (5 ml). The filtrand was dried in a vacuum oven to give the target compound as a white solid (100 mg, 0.48 mmol, 57%). R_f 0.29 (19:1 DCM/MeOH); M.p. 137-140 °C; λ_{max} (EtOH/nm) 220, 255; IR (cm^{-1}) 2925, 2868, 1647, 1610, 1518; ^1H NMR (500 MHz, DMSO-d_6) 3.07 (3H, s, $N\text{-}CH_3$), 3.14 (2H, t, *J* = 6.7 Hz, NCH_2CH_2), 3.62 (2H, t, *J* = 6.7 Hz, NCH_2CH_2), 7.61 (1H, d, *J* = 8.3 Hz, H-5), 8.31 (1H, dd, *J* = 2.5 and 8.3 Hz, H-6), 8.56 (1H, d, *J* = 2.5 Hz, H-8); ^{13}C NMR (125 MHz, DMSO-d_6) 27.1 (NCH_2CH_2), 34.6 ($N\text{-}CH_3$), 46.7 (NCH_2CH_2), 121.7 (C-Ar), 125.8 (C-Ar), 129.2 (C-Ar), 130.2 (C-Ar), 146.2 (C-Ar), 146.6 (C-Ar), 161.6 (C=O); HRMS calcd. for $C_{10}H_{11}N_2O_3$ (ES+) *m*/*z* 207.0764 $[M+H]^+$, found 207.0765.

7-amino-2-methyl-3,4-dihydroisoquinolin-1(2H)-one (331)

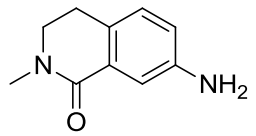

The nitro compound **330** (0.947 g, 4.59 mmol) and iron powder (2.56 g, 45.9 mmol) were reacted in acetic acid (45 ml) according to **general procedure T**. Purification on silica (19:1

DCM/MeOH) afforded the desired compound as a pale yellow solid (0.678 g, 3.85 mmol, 84%). R_f 0.24 (19:1 DCM/MeOH); M.p. 131-133 °C; λ_{max} (EtOH/nm) 224, 330; IR (cm^{-1}) 3439, 3359, 3330, 3234, 2931, 1635, 1599, 1576, 1498; ^{1}H NMR (500 MHz, DMSO-d_6) 2.77 (2H, t, J = 6.7 Hz, NCH_2CH_2), 2.99 (N-CH_3), 3.45 (2H, t, J = 6.7 Hz, NCH_2CH_2), 5.12 (2H, s, Ar-NH_2), 6.66 (1H, dd, J = 2.5 and 8.0 Hz, H-6), 6.91 (1H, d, J = 8.0 Hz, H-5), 7.15 (1H, d, J = 2.5 Hz, H-8); ^{13}C NMR (125 MHz, DMSO-d_6) 26.3 (NCH_2CH_2), 34.6 (N-CH_3), 47.9 (NCH_2CH_2), 112.3 (C-Ar), 117.1 (C-Ar), 125.4 (C-Ar), 127.6 (C-Ar), 129.4 (C-Ar), 147.4 (C-Ar), 164.1 (C=O); HRMS calcd. for $C_{10}H_{13}N_2O$ (ES+) m/z 177.1022 $[M+H]^+$, found 177.1021.

2-Methyl-7-((6-((triisopropylsilyl)ethynyl)-9*H*-purin-2-yl)amino)-3,4-dihydroisoquinolin-1(2*H*)-one (317)

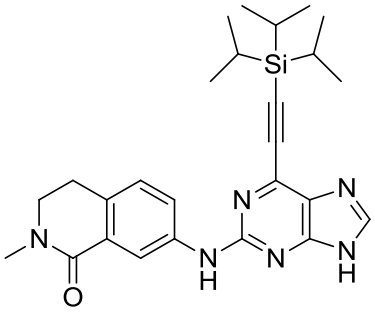

2-Fluoropurine **160** (0.225 g, 0.71 mmol), aniline **331** (0.250 g, 1.41 mmol) and TFA (136 µl, 1.77 mmol) were reacted in TFE (7 ml) according to **general procedure V**. Chromatography on KP-NH silica (19:1 DCM/MeOH) gave the desired product as a yellow oil/gum (0.142 g, 0.30 mmol, 42%). R_f 0.37 (19:1 DCM/MeOH, KP-NH); λ_{max} (EtOH/nm) 279; IR (cm^{-1}) 3390, 3136, 2941, 2864, 2167, 1609, 1577, 1538; ^{1}H NMR (500 MHz, DMSO-d_6) 1.12-1.23 (21H, m, $Si(CH(CH_3)_2)_3$), 2.91 (2H, t, J = 6.6 Hz, NCH_2CH_2), 3.04 (3H, s, N-CH_3), 3.53 (2H, t, J = 6.6 Hz, NCH_2CH_2), 7.19 (1H, d, J = 8.3 Hz, H-5'), 7.90 (1H, dd, J = 2.3 and 8.3 Hz, H-6'), 8.25 (1H, s, H-8), 8.27 (1H, d, J = 2.3 Hz, H-8'), 9.77 (1H, s, C^2-NH), 13.14 (1H, br, H-9); ^{13}C NMR (125 MHz, DMSO-d_6) 10.6 ($Si(CH(CH_3)_2)_3$), 18.4 ($Si(CH(CH_3)_2)_3$), 26.6 (NCH_2CH_2), 34.6 (N-CH_3), 47.6 (NCH_2CH_2), 97.9 (C≡C), 101.7 (C≡C), 117.3 (C-Ar), 121.6 (C-Ar), 127.2 (C-Ar), 129.2 (C-Ar), 131.0 (C-Ar), 139.5 (C-Ar), 156.2 (C-Ar), 163.7 (C=O); HRMS calcd. for $C_{26}H_{35}N_6OSi$ (ES+) m/z 475.2636 $[M+H]^+$, found 475.2635.

Note: Unable to visualise all carbon environments by ^{13}C NMR.

7-((6-Ethynyl-9*H*-purin-2-yl)amino)-2-methyl-3,4-dihydroisoquinolin-1(2*H*)-one (312)

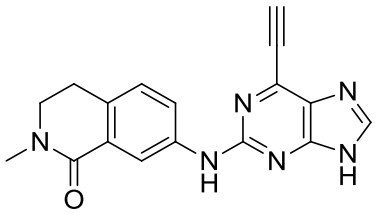

The TIPS-protected purine **317** (98 mg, 0.21 mmol), TBAF (1M in THF, 0.25 ml, 0.25 mmol) and the TBAF scavenger bead system **231** (1.00 g, 10 x w/w) were reacted in THF (5 ml) according to **general procedure U**. Chromatography on silica (9:1 DCM/MeOH) gave the target compound as a yellow solid (36 mg, 0.11 mmol, 54%). R_f 0.34 (9:1 DCM/MeOH); M.p. 280-300 °C (decomposed); λ_{max} (EtOH/nm) 276; IR (cm^{-1}) 3117, 2945, 2108, 1641, 1608, 1575, 1540; ^{1}H NMR (500 MHz, DMSO-d_6) 2.92 (2H, t, J = 6.6 Hz, NCH_2CH_2), 3.04 (3H, s, N-CH_3), 3.54 (2H, t, J = 6.6 Hz, NCH_2CH_2), 4.85 (1H, s, C≡CH), 7.20 (1H, d, J = 8.3 Hz, H-5'), 7.89 (1H, dd, J = 2.3 and 8.3 Hz, H-6'), 8.26 (1H, d, J = 2.3 Hz, H-8'), 8.28 (1H, s, H-8), 9.73 (1H, s, C^2-NH), 13.2 (1H, br, H-9); ^{13}C NMR (125 MHz, DMSO-d_6) 26.6 (NCH_2CH_2), 34.6 (N-CH_3), 47.6 (NCH_2CH_2), 87.0 (C≡C), 117.4 (C-Ar), 121.7 (C-Ar), 127.2 (C-Ar), 129.2 (C-Ar), 131.1 (C-Ar), 139.5 (C-Ar), 156.2 (C-Ar), 163.7 (C=O); HRMS calcd. for $C_{17}H_{15}N_6O$ (ES+) m/z 319.1302 $[M+H]^+$, found 319.1307.

Note: Unable to visualise all carbon environments by ^{13}C NMR.

***N*-Methyl-2-(4-nitrophenyl)acetamide (332)[274]**

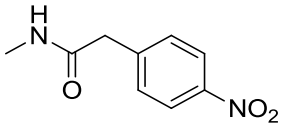

4-Nitrophenylacetic acid (1.00 g, 5.52 mmol), thionyl chloride (0.81 mmol, 11.0 mmol), methanol (50 ml) and methylamine (40% aqueous solution, 50 ml) were reacted together according to **general procedure W** over 72 h. Chromatography on silica (19:1 DCM/MeOH) gave the target compound as an off-white solid (0.916 g, 5.08 mmol, 92%). R_f 0.31 (19:1 DCM/MeOH); M.p. 157-160 °C (Lit.[274] 159 °C); λ_{max} (EtOH/nm) 271; IR (cm^{-1}) 3260, 3084, 2943, 2844, 1638, 1565, 1505; ^{1}H NMR (500 MHz, DMSO-d_6) 2.60 (3H, d, J = 4.7 Hz, $NHCH_3$), 3.58 (2H, s, $COCH_2$), 7.53 (2H, d, J = 9.0 Hz, H-2/H-6), 8.09 (1H, br, $NHCH_3$), 8.18 (2H, d, J = 9.0 Hz, H-3/H-5); ^{13}C NMR (125 MHz, DMSO-d_6) 25.6 ($NHCH_3$), 41.9

(Ar*C*H_2), 123.3 (C-Ar), 130.3 (C-Ar), 144.5 (C-Ar), 146.2 (C-Ar), 169.3 (C=O); LRMS (ES+) *m*/*z* 195.2 $[M+H]^+$.

2-Methyl-7-nitro-1,2-dihydroisoquinolin-3(4*H*)-one (333)[217]

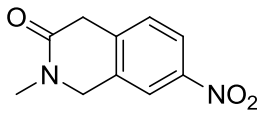

Paraformaldehyde (19 mg, 0.62 mmol) was added to a suspension of the *N*-methyl carboxamide **332** (102 mg, 0.51 mmol) in Eaton's reagent (1 ml). The mixture was heated in a sealed vial at 80 °C for 6 h, after which point the brown solution was cooled to RT, diluted with ice water (5 ml) and neutralised with 50% NaOH solution. The resultant suspension was extracted with EtOAc (3 x 10 ml) and the combined organic extracts were dried ($MgSO_4$) and concentrated *in vacuo*. The crude residue was purified by chromatography on silica gel (19:1 DCM/MeOH) to give the target compound as a pale orange solid (78 mg, 0.38 mmol, 75%). R_f 0.30 (19:1 DCM/MeOH); M.p. 151-154 °C; λ_{max} (EtOH/nm) 273; IR (cm^{-1}) 3041, 2875, 1637, 1597, 1500; ^{1}H NMR (500 MHz, DMSO-d_6) 2.98 (3H, s, N-CH_3), 3.70 (2H, s, N-CH_2), 4.64 (2H, s, COCH_2), 7.50 (1H, d, *J* = 8.4 Hz, H-5), 8.13 (1H, dd, *J* = 2.3 and 8.4 Hz, H-6), 8.20 (1H, d, *J* = 2.3 Hz, H-8); ^{13}C NMR (125 MHz, DMSO-d_6) 33.6 (N-CH_3), 37.0 (N-CH_2), 51.1 (CO*C*H_2), 120.4 (C-Ar), 122.1 (C-Ar), 128.3 (C-Ar), 134.0 (C-Ar), 141.0 (C-Ar), 146.0 (C-Ar), 166.9 (C=O); LRMS (ES+) *m*/*z* 207.1 $[M+H]^+$.

7-Amino-2-methyl-1,2-dihydroisoquinolin-3(4*H*)-one (334)

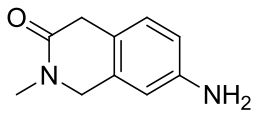

The nitro compound **333** (0.348 g, 1.69 mmol) and iron powder (0.943 g, 16.9 mmol) were reacted in acetic acid (17 ml) according to **general procedure T**. Purification *via* silica gel chromatography (19:1 DCM/MeOH) gave the desired compound as a pale orange solid (0.196 g, 1.11 mmol, 66%). R_f 0.25 (19:1 DCM/MeOH); M.p. 167-170 °C; λ_{max} (EtOH/nm) 241, 296; IR (cm^{-1}) 3426, 3343, 3241, 3023, 2871, 1612, 1502; ^{1}H NMR (500 MHz, DMSO-d_6) 2.94 (3H, s, N-CH_3), 3.31 (2H, s, COCH_2), 4.34 (2H, s, N-CH_2), 4.99 (2H, s, Ar-NH_2), 6.42 (1H, d, *J* = 2.2 Hz, H-8), 6.46 (1H, dd, *J* = 2.2 and 8.0 Hz, H-6), 6.82 (1H, d, *J* = 8.0 Hz, H-5); ^{13}C NMR (125 MHz, DMSO-d_6) 33.5 (N-CH_3), 35.8 (CO*C*H_2), 52.0 (N-CH_2), 110.1

(C-Ar), 113.2 (C-Ar), 119.1 (C-Ar), 127.3 (C-Ar), 132.1 (C-Ar), 147.0 (C-Ar), 168.6 (C=O); HRMS calcd. for $C_{10}H_{13}N_2O$ (ES+) *m*/*z* 177.1022 $[M+H]^+$, found 177.1019.

2-Methyl-7-((6-((triisopropylsilyl)ethynyl)-9*H*-purin-2-yl)amino)-1,2-dihydroisoquinolin-3(4*H*)-one (335)

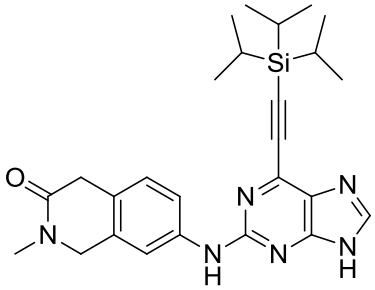

2-Fluoropurine **160** (0.145 g, 0.45 mmol), aniline **334** (0.160 g, 0.91 mmol) and TFA (87 µl, 1.14 mmol) were reacted in TFE (5 ml) according to **general procedure V**. Purification through chromatography on KP-NH silica (19:1 DCM/MeOH) gave the desired compound as a yellow oil/gum (0.138 g, 0.29 mmol, 64%). R_f 0.39 (19:1 DCM/MeOH, KP-NH); λ_{max} (EtOH/nm) 277; IR (cm^{-1}) 2943, 2864, 1605, 1577, 1537; ^{1}H NMR (500 MHz, DMSO-d_6) 1.13-1.22 (21H, m, Si(C*H*(C*H*$_3$)$_2$)$_3$), 2.98 (3H, s, N-CH_3), 3.46 (2H, s, $COCH_2$), 4.48 (2H, s, N-CH_2), 7.10 (1H, d, *J* = 8.4 Hz, H-5'), 7.66 (1H, dd, *J* = 2.1 and 8.4 Hz, H-6'), 7.73-7.77 (1H, m, H-8'), 8.25 (1H, s, H-8), 9.71 (1H, s, C^2-NH), 13.08 (1H, br, H-9); ^{13}C NMR (125 MHz, DMSO-d_6) 10.6 (Si(*C*H(CH$_3$)$_2$)$_3$), 18.4 (Si(CH(*C*H$_3$)$_2$)$_3$), 33.6 (N-*C*H$_3$), 36.1 (CO*C*H$_2$), 52.2 (N-CH_2), 97.8 (C≡*C*-Si), 101.8 (*C*≡C-Si), 114.7 (C-Ar), 117.5 (C-Ar), 124.8 (C-Ar), 127.0 (C-Ar), 131.8 (C-Ar), 139.2 (C-Ar), 142.7 (C-Ar), 156.2 (C-Ar), 168.2 (C=O); HRMS calcd. for $C_{26}H_{35}N_6OSi$ (ES+) *m*/*z* 475.2636 $[M+H]^+$, found 475.2631.

Note: Unable to visualise all carbon environments by ^{13}C NMR.

7-((6-Ethynyl-9*H*-purin-2-yl)amino)-2-methyl-1,2-dihydroisoquinolin-3(4*H*)-one (314)

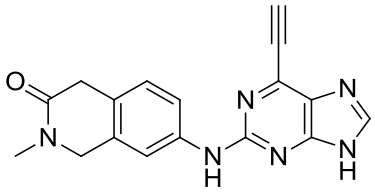

The TIPS-protected purine **335** (0.112 g, 0.24 mmol), TBAF (1M in THF, 0.28 ml, 0.28 mmol) and the TBAF scavenger bead system **231** (1.10 g, 10 x w/w) were reacted in THF (5

ml) according to **general procedure U**. Silica gel chromatography (9:1 DCM/MeOH) afforded the target compound as a yellow solid (41 mg, 0.13 mmol, 54%). R_f 0.41 (9:1 DCM/MeOH); M.p. 200-220 °C (decomposed); λ_{max} (EtOH/nm) 274.5, 346.5; IR (cm^{-1}) 3292, 3086, 2963, 2774, 2104, 1610, 1551, 1494; ^{1}H NMR (500 MHz, DMSO-d_6) 2.98 (3H, s, N-CH_3), 3.46 (2H, s, Ar-CH_2), 4.49 (2H, s, Ar-CH_2), 4.84 (1H, s, C≡CH), 7.11 (1H, d, *J* = 8.5 Hz, H-5'), 7.65-7.71 (2H, m, H-6'/H-8'), 8.28 (1H, s, H-8), 9.69 (1H, s, C^2-NH), 13.13 (1H, br, H-9); ^{13}C NMR (125 MHz, DMSO-d_6) 33.6 (N-CH_3), 36.1 (Ar-CH_2), 52.1 (Ar-CH_2), 78.9 (*C*≡CH), 87.0 (C≡*C*H), 114.8 (C-Ar), 117.6 (C-Ar), 124.9 (C-Ar), 127.0 (C-Ar), 131.8 (C-Ar), 139.1 (C-Ar), 156.2 (C-Ar), 168.2 (C=O); HRMS calcd. for $C_{17}H_{15}N_6O$ (ES+) *m*/*z* 319.1302 $[M+H]^+$, found 319.1301.

Note: Unable to visualise all carbon environments by ^{13}C NMR.

2-(3-Amino-(*N*-*tert*-Butyloxycarbonyl)phenyl)acetic acid (347)[275]

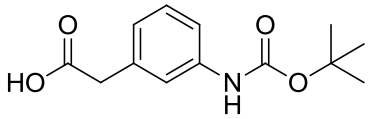

2-(3-Aminophenyl)acetic acid (1.00 g, 6.62 mmol) and di-*tert*-butyl dicarbonate (1.60 g, 7.28 mmol) were reacted in dioxane (20 ml), 1M NaOH solution (10 ml) and water (10 ml) according to **general procedure P**. The desired compound was obtained as a pale orange oil which solidified on cooling (1.58 g, 6.29 mmol, 95%). R_f 0.41 (2:3 Petrol/EtOAc); M.p. 100-102 °C; λ_{max} (EtOH/nm) 237; IR (cm^{-1}) 3301, 2981, 2159, 1694; ^{1}H NMR (500 MHz, DMSO-d_6) 1.48 (9H, s, -C(CH_3)$_3$), 3.49 (2H, s, COCH_2), 6.83-6.87 (1H, m, H-6), 7.18 (1H, dd, *J* = 7.9 and 8.0 Hz, H-5), 7.26-7.30 (1H, m, H-4), 7.41-7.44 (1H, m, H-2), 9.32 (1H, s, Ar-NH), 12.29 (1H, s, -CO_2H); ^{13}C NMR (125 MHz, DMSO-d_6) 28.1 (-C(*C*H_3)$_3$), 41.1 (CO*C*H_2), 78.9 (-*C*(CH_3)$_3$), 116.5 (C-Ar), 118.9 (C-Ar), 123.1 (C-Ar), 128.4 (C-Ar), 135.4 (C-Ar), 139.5 (C-Ar), 152.7 (*C*OC(CH_3)$_3$), 172.6 (-*C*O_2H); LRMS (ES+) *m*/*z* 252.1 $[M+H]^+$.

***tert*-Butyl 3-((2-aminoethylcarbamoyl)methyl)phenyl carbamate (348)**

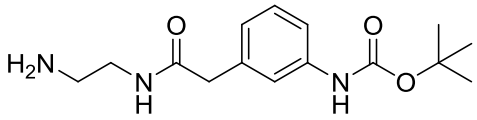

CDI (1.86 g, 11.5 mmol) and DIPEA (2.00 ml, 11.5 mmol) were added to a solution of carboxylic acid **347** (1.44 g, 5.73 mmol) in dry THF (25 ml) under nitrogen. The mixture was stirred at RT for 1.5 h, after which point it was added *via* canular to a solution of ethylenediamine (2.30 ml, 34.4 mmol) in dry THF (20 ml). The resulting suspension was stirred at RT for 18 h, after which point the solvent was removed *in vacuo*. The crude residue was purified using silica gel chromatography (7:3 DCM/MeOH) to give the desired compound as an thick colourless oil (1.48 g, 5.04 mmol, 88%). R_f 0.32 (7:3 DCM/MeOH); λ_{max} (EtOH/nm) 239; IR (cm^{-1}) 3304, 2981, 2930, 1694, 1639; ^{1}H NMR (500 MHz, DMSO-d_6) 1.48 (9H, s, -C(CH_3)$_3$), 2.57 (2H, t, *J* = 6.4 Hz, CONHCH_2CH_2), 3.04 (2H, dt, *J* = 5.9 and 6.4 Hz, CONHCH_2CH_2), 3.18 (2H, s, CH_2CO), 3.40 (2H, br, NH_2), 6.84-6.87 (1H, m, H-4), 7.15 (1H, dd, *J* = 8.0 and 8.2 Hz, H-5), 7.23-7.26 (1H, m, H-6), 7.43 (1H, br, H-2), 8.01 (1H, t, *J* = 5.9 Hz, CONH), 9.32 (1H, s, Ar-NH); ^{13}C NMR (125 MHz, DMSO-d_6) 28.1 (C(CH_3)$_3$), 42.4 (CH_2), 42.6 (CH_2), 78.9 (C(CH_3)$_3$), 118.7 (C-Ar), 122.8 (C-Ar), 128.3 (C-Ar), 139.4 (C-Ar), 152.7 (carbamate C=O), 170.0 (amide C=O); HRMS calcd. for $C_{15}H_{24}N_3O_3$ (ES+) *m*/*z* 294.1812 $[M+H]^+$, found 294.1817.

***tert*-Butyl 3-((2-(4-nitrobenzo[c][1,2,5]oxadiazol-7-ylamino)ethyl-carbamoyl)methyl) phenyl carbamate (349)**

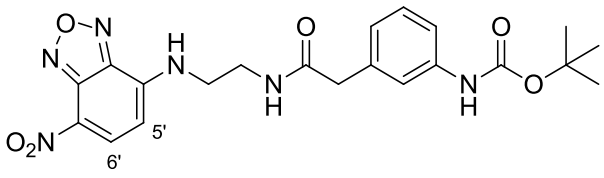

4-Chloro-7-nitrobenzofurazan (0.145 g, 0.73 mmol) in DMF (1 ml) was added dropwise to a solution of carboxylic acid **347** (0.194 g, 0.66 mmol) and triethylamine (110 µl, 0.79 mmol) in DMF (4 ml). The resultant dark red solution was stirred at RT with exclusion of light for 18 h. The solvent was removed *in vacuo* and the crude residue was purified on silica gel (19:1 DCM/MeOH) to give the desired compound as an orange solid (0.270 g, 0.59 mmol, 90%). R_f 0.38 (19:1 DCM/MeOH); M.p. 184-186 °C; λ_{max} (EtOH/nm) 241, 339; IR (cm^{-1}) 3388,

3304, 3086, 2938, 1722, 1681; ^{1}H NMR (500 MHz, DMSO-d_6) 1.46 (9H, s, -C(CH_3)$_3$), 3.32 (2H, s, CH_2CO), 3.37-3.40 (2H, m, CONHC$H_2$$CH_2$NH), 3.52-3.55 (2H, m, CONHCH$_2$CH_2NH), 6.40 (1H, d, *J* = 9.0 Hz, H-5'), 6.80-6.82 (1H, m, H-4), 7.09 (1H, dd, *J* = 8.0 and 8.0 Hz, H-5), 7.19-7.22 (1H, m, H-6), 7.42 (1H, br, H-2), 8.24 (1H, t, *J* = 5.8 Hz, CONH), 8.47 (1H, d, *J* = 9.0 Hz, H-6'), 9.27 (1H, s, Ar-NHBoc), 9.40 (1H, br, CH_2CH_2N*H*); ^{13}C NMR (125 MHz, DMSO-d_6) 28.1 (C(*C*H_3)$_3$), 30.7 (CH_2), 42.5 (CH_2), 79.0 (*C*(CH_3)$_3$), 116.4 (C-Ar), 118.8 (C-Ar), 122.7 (C-Ar), 128.2 (C-Ar), 139.4 (C-Ar), 144.8 (C-Ar), 145.3 (C-Ar), 152.7 (carbamate C=O); HRMS calcd. for $C_{21}H_{25}N_6O_6$ (ES+) *m*/*z* 457.1830 $[M+H]^+$, found 457.1830.

Note: Unable to visualise all carbon signals by NMR.

***N*-(2-(4-Nitrobenzo[c][1,2,5]oxadiazol-7-ylamino)ethyl)-2-(3-aminophenyl) acetamide (351)**

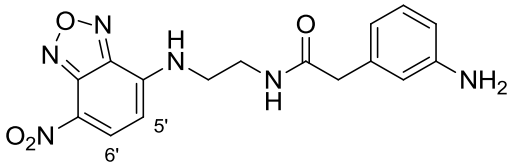

Boc-protected aniline **349** (0.154 g, 0.34 mmol) was reacted with TFA (260 µl, 3.40 mmol) in DCM (4 ml) according to **general procedure L**. Chromatography on silica (9:1 DCM/MeOH) afforded the desired compound as a dark orange solid (0.110 g, 0.31 mmol, 92%). R_f 0.43 (9:1 DCM/MeOH); M.p. 180-182 °C; λ_{max} (EtOH/nm) 210, 342; IR (cm^{-1}) 3412, 3352, 3238, 3079, 3031, 1622, 1595; ^{1}H NMR (500 MHz, DMSO-d_6) 3.22 (2H, s, CH_2CO), 3.38 (2H, dt, *J* = 5.9 and 6.2 Hz, CONHC$H_2$$CH_2$), 3.52-3.57 (2H, m, CONHCH$_2$CH_2), 4.97 (2H, s, Ar-NH_2), 6.32-6.35 (1H, m, H-4), 6.37-6.41 (2H, m, H-6/H-5'), 6.44 (1H, dd, *J* = 1.8 and 1.9 Hz, H-2), 6.85 (1H, dd, *J* = 7.7 and 7.9 Hz, H-5), 8.14 (1H, t, *J* = 5.9 Hz, CONH), 8.46 (1H, d, *J* = 8.2 Hz, H-6'), 9.42 (1H, br, CH_2CH_2N*H*); HRMS calcd. for $C_{16}H_{17}N_6O_4$ (ES+) *m*/*z* 357.1306 $[M+H]^+$, found 357.1311.

Note: Unable to visualise ^{13}C signals by NMR.

***N*-(2-(4-Nitrobenzo[c][1,2,5]oxadiazol-7-ylamino)ethyl)-2-(3-(6-(2-(triisopropylsilyl)ethynyl)-9*H*-purin-2-ylamino)phenyl)acetamide (353)**

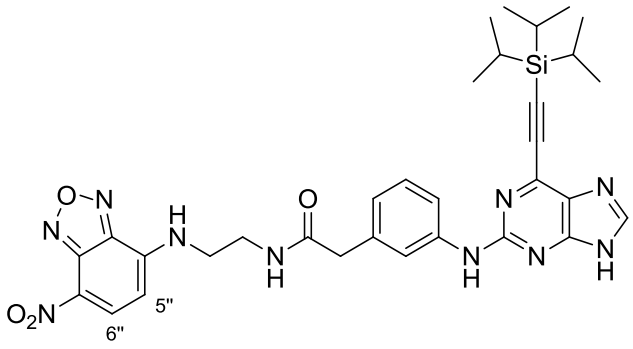

2-Fluoropurine intermediate **160** (0.100 g, 0.31 mmol), aniline **351** (0.220 g, 0.62 mmol) and TFA (120 µl, 1.57 mmol) were reacted in TFE (3 ml) according to **general procedure B**, with the reaction proceeding over 96 h. Purification *via* chromatography on silica (19:1 DCM/MeOH) afforded the desired compound as a dark orange oil (28 mg, 0.04 mmol, 14%). R_f 0.31 (19:1 DCM/MeOH); λ_{max} (EtOH/nm) 275, 339; IR (cm^{-1}) 3233, 2941, 2864, 2161, 1979, 1644, 1577; ^{1}H NMR (500 MHz, DMSO-d_6) 1.13-1.20 (21H, m, Si(CH(CH_3)$_2$)$_3$), 3.37 (2H, s, CH_2CO), 3.41 (2H, m, CONHCH_2CH_2), 3.57 (2H, m , CONHCH_2CH_2), 6.37-6.44 (2H, m, H-6'/H-5''), 6.77-6.80 (1H, m, H-4'), 7.13 (1H, dd, *J* = 7.9 and 8.0 Hz, H-5'), 7.54-7.57 (1H, m, H-2'), 7.75 (1H, d, *J* = 8.6 Hz, H-6''), 8.20-8.24 (2H, m, CONH & H-8), 8.47 (1H, br, CH_2CH_2N*H*), 9.65 (1H, s, C^2-NH), 13.07 (1H, br, H-9) ; HRMS calcd. for $C_{32}H_{39}N_{10}O_4Si$ (ES+) *m*/*z* 655.2920 $[M+H]^+$, found 655.2918.

Note: Insufficient material for ^{13}C NMR.

***N*-(2-(4-Nitrobenzo[c][1,2,5]oxadiazol-7-ylamino)ethyl)-2-(3-(6-ethynyl-9*H*-purin-2-ylamino)phenyl)acetamide (344)**

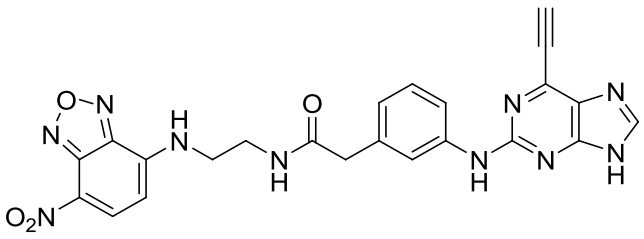

TIPS-protected purine **353** (22 mg, 0.034 mmol), KF (10 mg, 0.17 mmol) and 18-crown-6 (1 mg, 0.003 mmol) were reacted in THF (1 ml) according to **general procedure Q**. Purification *via* chromatography on silica (19:1 DCM/MeOH) afforded the desired compound

as an orange/red solid (14 mg, 0.029 mmol, 85%). R_f 0.14 (19:1 DCM/MeOH); M.p. 150-160 °C (decomposed); λ_{max} (EtOH/nm) 274; IR (cm^{-1}) 3373, 3320, 2118, 1656, 1565; ^{1}H NMR (500 MHz, DMSO-d_6) 3.35-3.45 (6H, m, CH_2CH_2/CH_2CO), 4.82 (1H, s, -C≡CH), 6.42 (1H, d, *J* = 8.9 Hz, H-5''), 6.77-6.80 (1H, m, H-6'), 7.15 (1H, dd, *J* = 7.8 and 7.9 Hz, H-5'), 7.50-7.53 (1H, m, H-2'), 7.73-7.76 (1H, m, H-4'), 8.24 (2H, m, CONH/H-8), 8.46 (1H, d, *J* = 8.9 Hz, H-6''), 9.41 (1H, br, CH_2NH), 9.63 (1H, s, C^2-NH), 13.10 (1H, s, H-9); HRMS calcd. for $C_{23}H_{19}N_{10}O_4$ (ES+) *m*/*z* 499.1585 $[M+H]^+$, found 499.1580.

Note: Insufficient material for ^{13}C NMR.

***tert*-Butyl (3-(2-((2-acetamidoethyl)amino)-2-oxoethyl)phenyl) carbamate (350)**

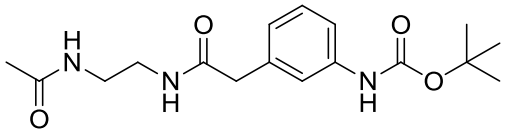

Acetic anhydride (67 µl, 0.71 mmol) was added to a solution of aminoethylcarboxamide **348** (0.188 g, 0.64 mmol) in pyridine (5 ml). The resulting solution was stirred at RT for 18 h, after which point the solvent was removed *in vacuo*. The crude residue was purified *via* chromatography on silica (19:1 DCM/MeOH) to give a colourless oil, which was triturated with petrol to give the desired compound as a white solid (0.165 g, 0.49 mmol, 77%). R_f 0.39 (19:1 DCM/MeOH); M.p. 156-158 °C; λ_{max} (EtOH/nm) 239; IR (cm^{-1}) 3317, 2976, 1688, 1643; ^{1}H NMR (500 MHz, DMSO-d_6) 1.47 (9H, s, $C(CH_3)_3$), 1.79 (3H, s, CH_3CO), 3.06-3.10 (4H, m, CH_2CH_2), 3.33 (2H, s, CH_2CO), 6.85-6.87 (1H, m, H-4), 7.15 (1H, dd, *J* = 8.0 and 8.2 Hz, H-5), 7.23-7.27 (1H, m, H-6), 7.41 (1H, br, H-2), 7.87 (1H, br, CH_2NH), 8.07 (1H, br, CH_2NH), 9.30 (1H, s, Ar-NH); ^{13}C NMR (125 MHz, DMSO-d_6) 22.6 (Ac-CH_3), 28.1 ($C(CH_3)_3$), 38.3 (CH_2), 38.4 (CH_2), 42.5 ($COCH_2$), 78.9 ($C(CH_3)_3$), 116.3 (C-Ar), 118.7 (C-Ar), 122.8 (C-Ar), 136.7 (C-Ar), 139.4 (C-Ar), 152.8 (carbamate C=O), 169.3 (amide C=O), 170.1 (amide C=O); HRMS calcd. for $C_{17}H_{26}N_3O_4$ (ES+) *m*/*z* 336.1918 $[M+H]^+$, found 336.1922.

***N*-(2-Acetamidoethyl)-2-(3-aminophenyl)acetamide (352)**

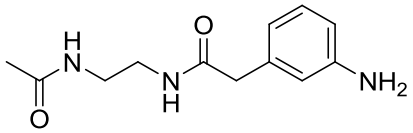

TFA (340 μl, 4.40 mmol) was added to a solution of the Boc-protected aniline **350** (0.147 g, 0.44 mmol) in DCM (4 ml). The resulting solution was stirred at RT for 18 h, after which point the solvent was removed *in vacuo* and the residue was partitioned between EtOAc (15 ml) and sat. $NaHCO_3$ solution (15 ml). Both phases were concentrated *in vacuo*, after which the residue was taken up in methanol (10 ml) and stirred at RT for 30 min. The insoluble inorganic salts were removed by filtration and the filtrate concentrated to dryness. The crude residue was purified on KP-NH silica (19:1 DCM/MeOH) to give the desired compound as an off-white solid (84 mg, 0.36 mmol, 81%). R_f 0.31 (19:1 DCM/MeOH, KP-NH); M.p. 109-112 °C; λ_{max} (EtOH/nm) 216; IR (cm^{-1}) 3421, 3295, 3094, 2988, 2938, 2029, 1633, 1548; ^{1}H NMR (500 MHz, DMSO-d_6) 1.79 (3H, s, CH_3CO), 3.06-3.09 (4H, m, CH_2CH_2), 3.22 (2H, s, CH_2CO), 4.98 (2H, s, Ar-NH_2), 6.37-6.43 (2H, m, H-4/H-6), 6.45 (1H, dd, *J* = 1.8 and 1.9 Hz, H-2), 6.91 (1H, dd, *J* = 7.6 and 7.8 Hz, H-5), 7.86 (1H, br, CH_2NH), 7.97 (1H, br, CH_2NH); ^{13}C NMR (125 MHz, DMSO-d_6) 22.6 (Ac-CH_3), 38.3 (CH_2), 38.4 (CH_2), 42.7 ($COCH_2$), 112.0 (C-Ar), 114.5 (C-Ar), 116.5 (C-Ar), 128.6 (C-Ar), 136.7 (C-Ar), 148.5 (C-Ar), 169.3 (C=O), 170.4 (C=O); HRMS calcd. for $C_{12}H_{18}N_3O_2$ (ES+) *m*/*z* 236.1394 $[M+H]^+$, found 236.1397.

***N*-(2-Acetamidoethyl)-2-(3-((6-((triisopropylsilyl)ethynyl)-9*H*-purin-2-yl)amino)phenyl)acetamide (354)**

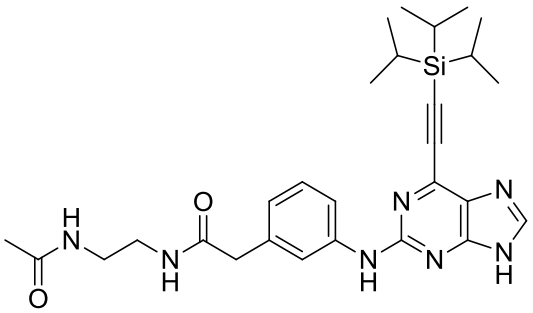

2-Fluoropurine intermediate **160** (0.140 g, 0.44 mmol), aniline **352** (0.210 g, 0.88 mmol) and TFA (175 μl, 2.26 mmol) were reacted in TFE (3 ml) according to **general procedure B**, with the reaction proceeding over 72 h. Purification by chromatography on silica (19:1

DCM/MeOH) afforded the desired compound as a yellow oil (0.118 g, 0.21 mmol, 48%). R_f 0.36 (19:1 DCM/MeOH); λ_{max} (EtOH/nm) 274, 368; IR (cm^{-1}) 3282, 2943, 2865, 2161, 1645, 1605; ^{1}H NMR (500 MHz, DMSO-d_6) 1.14-1.20 (21H, m, Si(CH(CH_3)$_2$)$_3$), 1.79 (3H, s, CH_3CO), 3.09-3.12 (4H, m, CH_2CH_2), 3.37 (2H, s, $COCH_2$), 6.83-6.86 (1H, m, H-6'), 7.20 (1H, dd, *J* = 7.8 and 7.9 Hz, H-5'), 7.53-7.56 (1H, m, H-2'), 7.76-7.79 (1H, m, H-4'), 7.88 (1H, br, CH_2N*H*), 8.06 (1H, br, CH_2N*H*), 8.24 (1H, s, H-8), 9.66 (1H, s, C^2-NH), 13.09 (1H, br, H-9); ^{13}C NMR (125 MHz, DMSO-d_6) 10.6 (Si(*C*H(CH_3)$_2$)$_3$), 18.4 (Si(CH(*C*H_3)$_2$)$_3$), 22.6 (Ac-CH_3), 38.3 (CH_2), 38.5 (CH_2), 42.7 (CO*C*H_2), 116.5 (C-Ar), 128.2 (C-Ar), 136.5 (C-Ar), 156.3 (C-Ar), 169.3 (C=O), 170.2 (C=O); HRMS calcd. for $C_{28}H_{40}N_7O_2Si$ (ES+) *m*/*z* 534.3007 $[M+H]^+$, found 534.3004.

Note: Unable to visualise all carbon signals by NMR.

***N*-(2-Acetamidoethyl)-2-(3-((6-ethynyl-9*H*-purin-2-yl)amino)phenyl)acetamide (345)**

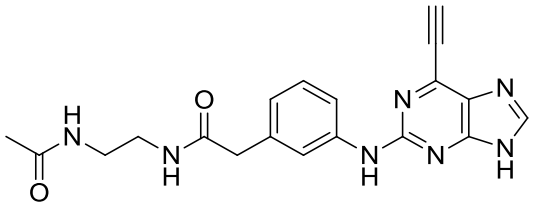

TIPS-protected purine **354** (58 mg, 0.11 mmol), KF (32 mg, 0.55 mmol) and 18-crown-6 (3 mg, 0.011 mmol) were reacted in THF (1 ml) according to **general procedure Q**. Purification *via* chromatography on silica (19:1 DCM/MeOH) afforded the desired compound as a yellow solid (28 mg, 0.074 mmol, 68%). R_f 0.22 (19:1 DCM/MeOH); M.p. 185-210 °C (decomposed); λ_{max} (EtOH/nm) 274; IR (cm^{-1}) 3265, 2113, 1646, 1604, 1577; ^{1}H NMR (500 MHz, DMSO-d_6) 1.79 (3H, s, CH_3CO), 3.08-3.12 (4H, m, CH_2CH_2), 3.37 (2H, s, CH_2CO), 4.84 (1H, s, -C≡CH), 6.83-6.86 (1H, m, H-6'), 7.21 (1H, dd, *J* = 7.9 and 8.0 Hz, H-5'), 7.51-7.54 (1H, m, H-2'), 7.75-7.78 (1H, m, H-4'), 7.91 (1H, br, CH_2N*H*), 8.09 (1H, br, CH_2N*H*), 8.28 (1H, s, H-8), 9.62 (1H, s, C^2-NH), 13.07 (1H, s, H-9); ^{13}C NMR (125 MHz, DMSO-d_6) 22.6 (Ac-CH_3), 38.3 (CH_2), 38.5 (CH_2), 42.6 (CO*C*H_2), 86.9 (C≡*C*H), 116.6 (C-Ar), 119.2 (C-Ar), 121.8 (C-Ar), 128.2 (C-Ar), 136.5 (C-Ar), 140.7 (C-Ar), 156.2 (C-Ar), 169.3 (C=O), 170.2 (C=O); HRMS calcd. for $C_{19}H_{20}N_7O_2$ (ES+) *m*/*z* 378.1673 $[M+H]^+$, found 378.1675.

Note: Unable to visualise all carbon signals by NMR.

***N*-(2-Fluoroethyl)-2-(3-nitrophenyl)acetamide (357)**

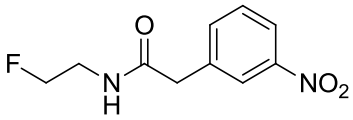

3-Nitrophenylacetic acid (0.500 g, 2.76 mmol), phosphorus trichloride (265 µl, 3.04 mmol) and 2-fluoroethylamine hydrochloride (0.686 g, 6.90 mmol) were reacted in dry MeCN (15 ml) according to **general procedure X**. Purification by chromatography on silica (4:1 Petrol/EtOAc) gave the desired compound as a pale yellow solid (0.453 g, 2.00 mmol, 72%). R_f 0.41 (4:1 Petrol/EtOAc); M.p. 116-119 °C; λ_{max} (EtOH/nm) 263; IR (cm^{-1}) 3296, 3088, 2941, 1648, 1556, 1514; ^{1}H NMR (500 MHz, DMSO-d_6) 3.38 (2H, ddt, *J* = 5.0, 5.2 and 27.9 Hz, NHCH_2), 3.64 (2H, s, $COCH_2$), 4.44 (2H, dt, *J* = 5.2 and 47.5 Hz, CH_2F), 7.62 (1H, dd, *J* = 7.8 and 8.0 Hz, H-5), 7.71-7.74 (1H, m, H-6), 8.09-8.13 (1H, m, H-4), 8.17 (1H, dd, *J* = 1.8 and 1.9 Hz, H-2), 8.46 (1H, t, *J* = 5.0 Hz, N*H*CH_2); ^{13}C NMR (125 MHz, DMSO-d_6) 41.3 ($COCH_2$), 82.4 (d, J_{CF} = 165.1 Hz, CH_2F), 121.5 (C-Ar), 123.7 (C-Ar), 129.6 (C-Ar), 136.0 (C-Ar), 138.4 (C-Ar), 147.6 (C-Ar), 169.6 (C=O); HRMS calcd. for $C_{10}H_{12}FN_2O_3$ (ES+) *m*/*z* 227.0826 $[M+H]^+$, found 227.0829.

Note: Unable to visualise all carbon environments by ^{13}C NMR – masked by solvent peak.

2-(3-Aminophenyl)-*N*-(2-fluoroethyl)acetamide (359)

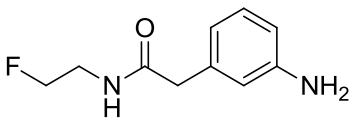

The nitro compound **357** (0.436 g, 1.93 mmol), palladium on carbon (50 mg, 10% w/w) and ammonium formate (1.21 g, 19.3 mmol) were reacted in methanol (20 ml) according to **general procedure G**. Purification by silica gel chromatography (1:1 Petrol/EtOAc) afforded the target compound as a pale red oil (0.333 g, 1.70 mmol, 88%). R_f 0.39 (1:1 Petrol/EtOAc); λ_{max} (EtOH/nm) 241, 290; IR (cm^{-1}) 3293, 3073, 2938, 1642, 1552, 1516; ^{1}H NMR (500 MHz, DMSO-d_6) 3.26 (2H, s, CH_2CO), 3.35 (2H, ddt, *J* = 5.2, 5.3 and 27.3 Hz, NHCH_2), 4.42 (2H, dt, *J* = 5.2 and 47.6 Hz, CH_2F), 4.99 (2H, s, Ar-NH_2), 6.38-6.43 (2H, m, H-4/H-6), 6.45-6.48 (1H, m, H-2), 6.92 (1H, dd, *J* = 7.6 and 7.7 Hz, H-5), 8.19 (1H, t, *J* = 5.3 Hz, N*H*CH_2); ^{13}C NMR (125 MHz, DMSO-d_6) 42.5 ($COCH_2$), 82.4 (d, J_{CF} = 164.5 Hz, NHCH_2),

112.1 (C-Ar), 114.5 (C-Ar), 116.5 (C-Ar), 128.6 (C-Ar), 136.6 (C-Ar), 148.4 (C-Ar), 170.6 (C=O); HRMS calcd. for $C_{10}H_{14}FN_2O$ (ES+) *m/z* 197.1085 $[M+H]^+$, found 197.1085.

Note: Unable to visualise all carbon environments by ^{13}C NMR – masked by solvent peak.

2-(3-Nitrophenyl)-*N*-(2,2,2-trifluoroethyl)acetamide (358)

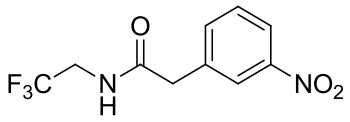

3-Nitrophenylacetic acid (0.100 g, 0.55 mmol), 2,2,2-trifluoroethylamine (110 µl, 1.38 mmol) and phosphorus trichloride (53 µl, 0.61 mmol) were reacted in dry acetonitrile (3 ml) according to **general procedure X**. Purification by silica chromatography (7:3 Petrol/EtOAc) gave the target compound as pale brown oil that solidified on cooling (0.117 g, 0.45 mmol, 81%). R_f 0.42 (7:3 Petrol/EtOAc); M.p. 134-136 °C; λ_{max} (EtOH/nm) 262; IR (cm^{-1}) 3289, 3086, 1663, 1557, 1536; ^1H NMR (500 MHz, DMSO-d_6) 3.72 (2H, s, CH_2CO), 3.94 (2H, dq, *J* = 6.4 and 9.8 Hz, CH_2CF_3), 7.63 (1H, dd, *J* = 7.9 and 8.0 Hz, H-5), 7.70-7.74 (1H, m, H-6), 8.13 (1H, ddd, *J* = 1.8, 2.1 and 8.0 Hz, H-4), 8.17 (1H, dd, *J* = 1.8 and 2.1 Hz, H-2), 8.89 (1H, t, *J* = 6.4 Hz, NH); ^{13}C NMR (125 MHz, DMSO-d_6) 40.9 (CH_2CO), 121.6 (C-Ar), 123.7 (C-Ar), 124.7 (q, J_{CF} = 279.2 Hz, CF_3), 129.7 (C-Ar), 136.0 (C-Ar), 137.9 (C-Ar), 147.6 (C-Ar), 170.2 (C=O); ^{19}F NMR (470 MHz, DMSO-d_6) -70.8; HRMS calcd. for $C_{10}H_{10}F_3N_2O_3$ (ES+) *m/z* 263.0638 $[M+H]^+$, found 263.0643.

Note: Unable to visualise all carbon environments by ^{13}C NMR – masked by solvent peak.

2-(3-Aminophenyl)-*N*-(2,2,2-trifluoroethyl)acetamide (360)

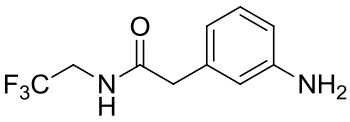

Nitro compound **358** (0.755 g, 2.88 mmol), palladium on carbon (75 mg, 10% w/w) and ammonium formate (1.81 g, 28.8 mmol) were reacted in methanol (30 ml) according to **general procedure G**. Chromatography on silica (7:3 Petrol/EtOAc) gave the target compound as a beige solid (0.602 g, 2.59 mmol, 90%). R_f 0.16 (7:3 Petrol/EtOAc); M.p. 83-85 °C; λ_{max} (EtOH/nm) 239, 291; IR (cm^{-1}) 3282, 3211, 3083, 1653, 1560; ^1H NMR (500 MHz, DMSO-d_6) 3.32 (2H, s, CH_2CO), 3.89 (2H, dq, *J* = 6.4 and 9.9 Hz, CH_2CF_3), 4.99 (2H,

s, Ar-NH_2), 6.38-6.44 (2H, m, H-4/H-6), 6.44-6.47 (1H, m, H-2), 6.92 (1H, dd, *J* = 7.8 and 7.8 Hz, H-5), 8.61 (1H, t, *J* = 6.4 Hz, CON*H*); ^{13}C NMR (125 MHz, DMSO-d_6) 42.1 (*C*H_2CO), 112.2 (C-Ar), 114.5 (C-Ar), 116.4 (C-Ar), 124.7 (q, J_{CF} = 279.4 Hz, CF_3), 128.6 (C-Ar), 136.1 (C-Ar), 148.5 (C-Ar), 171.1 (C=O); ^{19}F NMR (470 MHz, DMSO-d_6) -70.8; HRMS calcd. for $C_{10}H_{12}F_3N_2O$ (ES+) *m*/*z* 233.0896 $[M+H]^+$, found 233.0900.

Note: Unable to visualise all carbon environments by ^{13}C NMR – masked by solvent peak.

N-(2,2,2-Trifluoroethyl)-2-(3-((6-((triisopropylsilyl)ethynyl)-9*H*-purin-2-yl) amino)phenyl)acetamide (361)

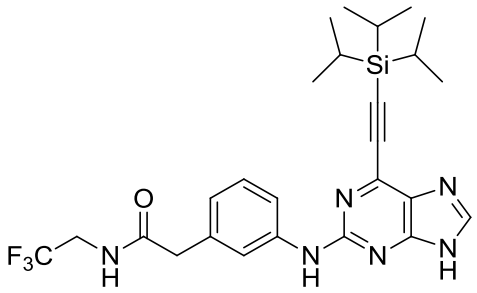

2-Fluoropurine **160** (0.250 g, 0.78 mmol), aniline **360** (0.364 g, 1.57 mmol) and TFA (150 µl, 1.96 mmol) were reacted in TFE (8 ml) according to **general procedure B** over 48 h. Chromatography on KP-NH silica (19:1 DCM/MeOH) gave the target compound as a yellow oil/gum (0.199 g, 0.37 mmol, 48%). R_f 0.29 (19:1 DCM/MeOH); λ_{max} (EtOH/nm) 276, 351; IR (cm^{-1}) 3277, 2945, 2865, 1668, 1605, 1578, 1538; ^{1}H NMR (500 MHz, DMSO-d_6) 1.13-1.22 (21H, m, Si(C*H*(CH_3)$_2$)$_3$), 3.48 (2H, s, CH_2CO), 3.92 (2H, dq, *J* = 6.4 and 9.8 Hz, C$H_2$$CF_3$), 6.83-6.86 (1H, m, H-6'), 7.21 (1H, dd, *J* = 7.8 and 7.9 Hz, H-5'), 7.58-7.60 (1H, m, H-2'), 7.75-7.78 (1H, m, H-4'), 8.24 (1H, s, H-8), 8.71 (1H, t, *J* = 6.4 Hz, CON*H*), 9.66 (1H, s, C^2-NH), 13.07 (1H, br, H-9); ^{13}C NMR (125 MHz, $CDCl_3$) 11.3 (Si(*C*H(CH_3)$_2$)$_3$), 18.7 (Si(CH(*C*H_3)$_2$)$_3$), 41.0 (q, J_{CF} = 32.8 Hz, *C*$H_2$$CF_3$), 43.5 (CO*C*$H_2$), 101.6 (C≡C-Si), 118.3 (C-Ar), 119.7 (C-Ar), 123.2 (C-Ar), 129.8 (C-Ar), 134.8 (C-Ar), 140.5 (C-Ar), 171.6 (C=O); HRMS calcd. for $C_{26}H_{34}F_3N_6OSi$ (ES+) *m*/*z* 531.2510 $[M+H]^+$, found 531.2512.

Note: Unable to visualise all carbon environments by ^{13}C NMR.

2-(3-((6-Ethynyl-9*H*-purin-2-yl)amino)phenyl)-*N*-(2,2,2-trifluoroethyl) acetamide (356)

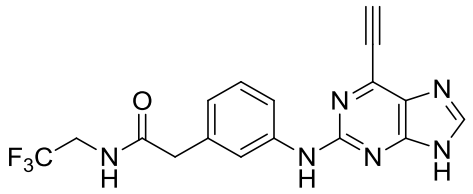

The TIPS-protected purine **361** (0.128 g, 0.24 mmol), TBAF (1M in THF, 0.29 ml, 0.29 mmol) and the TBAF scavenger bead system **231** (1.30 g, 10 x w/w) were reacted in THF (5 ml) according to **general procedure U**. Chromatography on KP-NH silica (9:1 DCM/MeOH) gave the desired compound as a yellow solid (50 mg, 0.13 mmol, 54%). R_f 0.32 (9:1 DCM/MeOH, KP-NH); M.p. 135-155 °C (decomposed); λ_{max} (EtOH/nm) 273.5, 364.0; IR (cm^{-1}) 3277, 2121, 2033, 1662; ^{1}H NMR (500 MHz, DMSO-d_6) 3.48 (2H, s, $COCH_2$), 3.93 (2H, dq, *J* = 6.3 and 9.9 Hz, CH_2CF_3), 4.84 (1H, s, C≡CH), 6.83-6.87 (1H, m, H-6'), 7.22 (1H, dd, *J* = 7.8 and 7.9 Hz, H-5'), 7.53-7.56 (1H, m, H-2'), 7.76-7.80 (1H, m, H-4'), 8.28 (1H, s, H-8), 8.74 (1H, t, *J* = 6.3 Hz, CONH), 9.64 (1H, s, C^2-NH), 13.13 (1H, br, H-9); ^{13}C NMR (125 MHz, MeOD) 41.5 (q, J_{CF} = 35.3 Hz, CH_2CF_3), 43.7 ($COCH_2$), 68.2 (C≡C), 78.7 (C≡C), 118.8 (C-Ar), 120.8 (C-Ar), 123.5 (C-Ar), 125.9 (q, J_{CF} = 277.7, CF_3), 129.9 (C-Ar), 136.7 (C-Ar), 142.1 (C-Ar), 144.5 (C-Ar), 158.4 (C-Ar), 174.6 (C=O); HRMS calcd. for $C_{17}H_{14}F_3N_6O$ (ES+) *m*/*z* 375.1176 $[M+H]^+$, found 375.1179.

Note: Unable to visualise all carbon environments by ^{13}C NMR.

***N*-(2-Fluoroethyl)-2-(3-((6-((triisopropylsilyl)ethynyl)-9*H*-purin-2-yl) amino)phenyl)acetamide (362)**

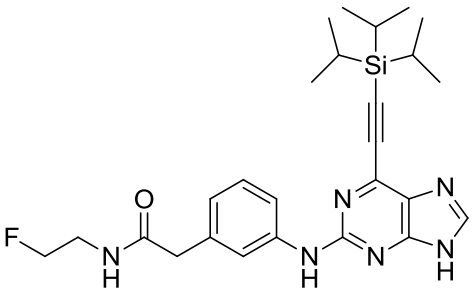

The acid **186** (0.105 g, 0.23 mmol), 2-fluoroethylamine hydrochloride (93 mg, 0.93 mmol), CDI (75 mg, 0.47 mmol) and DIPEA (120 µl, 0.70 mmol) were reacted in dry DMF (5 ml) according to **general procedure J**. Purification of silica gel (19:1 DCM/MeOH) gave the target compound as a yellow oil/gum (88 mg, 0.18 mmol, 77%). R_f 0.24 (19:1 DCM/MeOH);

λ_{max} (EtOH/nm) 276, 375; IR (cm^{-1}) 3273, 3075, 2943, 2864, 2165, 1649, 1576, 1536; ^{1}H NMR (500 MHz, DMSO-d_6) 1.13-1.23 (21H, m, Si(C*H*(C*H*$_3$)$_2$)$_3$), 3.37 (2H, ddt, *J* = 5.1, 5.2 and 27.4 Hz, NHC*H*$_2$), 4.44 (2H, dt, *J* = 5.1 and 47.2 Hz, C*H*$_2$F), 6.83-6.87 (1H, m, H-6'), 7.20 (1H, dd, *J* = 7.8 and 7.9 Hz, H-5'), 7.55-7.58 (1H, m, H-2'), 7.75-7.79 (1H, m, H-4'), 8.24 (1H, s, H-8), 8.28 (1H, t, *J* = 5.2 Hz, N*H*CH$_2$), 9.65 (1H, s, C^2-NH), 13.07 (1H, br, H-9); ^{13}C NMR (125 MHz, DMSO-d_6) 10.6 (Si(*C*H(CH$_3$)$_2$)$_3$), 18.4 (Si(CH(*C*H$_3$)$_2$)$_3$), 42.4 (CO*C*H$_2$), 82.4 (d, J_{CF} = 163.9 Hz, *C*H$_2$F), 116.6, 119.3, 128.2 (C-Ar), 132.1 (C-Ar), 136.4 (C-Ar), 155.7 (C-Ar); HRMS calcd. for $C_{26}H_{36}FN_6OSi$ (ES+) *m*/*z* 495.2698 $[M+H]^+$, found 495.2693.

Note: Unable to visualise all carbon environments by ^{13}C NMR.

2-(3-((6-Ethynyl-9*H*-purin-2-yl)amino)phenyl)-*N*-(2-fluoroethyl)acetamide (355)

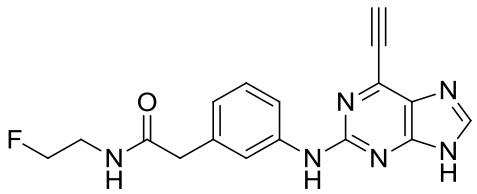

The TIPS-protected purine **362** (98 mg, 0.20 mmol), TBAF (1M in THF, 0.24 ml, 0.24 mmol) and the TBAF scavenger bead system **231** (1.00 g, 10 x w/w) were reacted in THF (5 ml) according to **general procedure U**. Silica gel chromatography (9:1 DCM/MeOH) gave the target compound as a yellow solid (33 mg, 0.10 mmol, 49%). R_f 0.39 (9:1 DCM/MeOH); M.p. 105-120 °C (decomposed); λ_{max} (EtOH/nm) 274.0, 367.5; IR (cm^{-1}) 3078, 2448, 2158, 2112, 2033, 1977, 1646; ^{1}H NMR (500 MHz, DMSO-d_6) 3.32-3.43 (4H, m, CH$_2$CO/NHCH$_2$), 4.44 (2H, dt, *J* = 5.1 and 47.3 Hz, CH$_2$F), 4.82 (1H, s, C≡CH), 6.84-6.88 (1H, m, H-6'), 7.21 (1H, dd, *J* = 7.8 and 7.9 Hz, H-5'), 7.51-7.53 (1H, m, H-2'), 7.78 (1H, dd, *J* = 1.4 and 7.9 Hz, H-4'), 8.25 (1H, s, H-8), 9.64 (1H, s, C^2-NH), 13.11 (1H, s, H-9); ^{13}C NMR (125 MHz, DMSO-d_6) 39.9 (d, J_{CF} = 20.8 Hz, NH*C*H$_2$), 42.4 (CO*C*H$_2$), 82.4 (d, J_{CF} = 165.0 Hz, CH$_2$F), 86.9 (C≡*C*H), 119.4 (C-Ar), 121.8 (C-Ar), 128.2 (C-Ar), 136.4 (C-Ar), 140.6 (C-Ar), 153.9 (C-Ar), 156.2 (C-Ar), 170.4 (C=O); HRMS calcd. for $C_{17}H_{16}FN_6O$ (ES+) *m*/*z* 339.1364 $[M+H]^+$, found 339.1369.

Note: Unable to visualise all carbon environments by ^{13}C NMR.

9-(4-Methoxybenzyl)-*N*-(pyridin-2-yl)-6-((triisopropylsilyl)ethynyl)-9*H*-purin-2-amine (372)

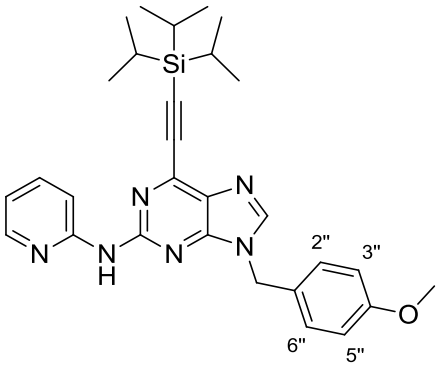

The 2-iodopurine **278** (0.199 g, 0.36 mmol), 2-aminopyridine (41 mg, 0.44 mmol), $Pd_2(dba)_3$ (37 mg, 0.04 mmol), XPhos (20 mg, 0.04 mmol) and K_2CO_3 (110 mg, 0.80 mmol) were reacted in MeCN (4 ml) according to **general procedure M**. Silica gel chromatography (7:3 Petrol/EtOAc) gave the desired compound as a pale yellow oil/gum (0.164 g, 0.32 mmol, 89%). R_f 0.39 (7:3 Petrol/EtOAc); λ_{max} (EtOH/nm) 259, 341; IR (cm^{-1}) 3174, 2943, 2864, 1732, 1594, 1572, 1540, 1515; ^{1}H NMR (500 MHz, $CDCl_3$) 1.19-1.29 (21H, m, Si(C*H*(C*H*$_3$)$_2$)$_3$), 3.81 (3H, s, OCH_3), 5.31 (2H, s, N^9-CH_2), 6.90 (2H, d, *J* = 8.4 Hz, H-3''/H-5''), 6.93-6.96 (1H, m, H-4'), 7.28 (2H, d, *J* = 8.4 Hz, H-2''/H-6''), 7.67-7.72 (1H, m, H-5'), 7.88 (1H, s, H-8), 8.24 (1H, s, C^2-NH), 8.37 (1H, ddd, *J* = 0.8, 0.9 and 4.8 Hz, H-3'), 8.44-8.48 (1H, m, H-6'); ^{13}C NMR (125 MHz, $CDCl_3$) 11.3 (Si(*C*H(CH$_3$)$_2$)$_3$), 18.7 (Si(CH(*C*H$_3$)$_2$)$_3$), 46.9 (N^9-CH_2), 55.4 (OCH_3), 101.0 (*C*≡C-Si), 101.6 (C≡*C*-Si), 112.0 (C-Ar), 114.5 (C-Ar), 117.4 (C-Ar), 127.3 (C-Ar), 129.4 (C-Ar), 130.1 (C-Ar), 137.7 (C-Ar), 142.1 (C-Ar), 143.2 (C-Ar), 148.2 (C-Ar), 152.9 (C-Ar), 153.0 (C-Ar), 155.1 (C-Ar), 159.8 (C-Ar); HRMS calcd. for $C_{29}H_{37}N_6OSi$ (ES+) *m*/*z* 513.2793 $[M+H]^+$, found 513.2778.

9-(4-Methoxybenzyl)-*N*-(pyridin-3-yl)-6-((triisopropylsilyl)ethynyl)-9*H*-purin-2-amine (373)

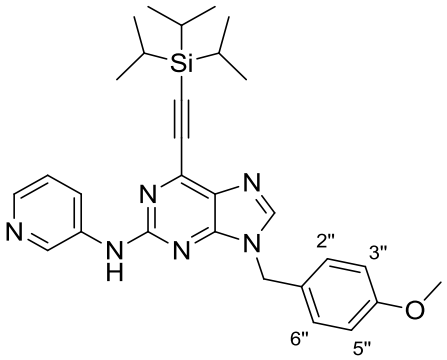

The 2-iodopurine **278** (0.208 g, 0.38 mmol), 3-aminopyridine (43 mg, 0.46 mmol), $Pd_2(dba)_3$ (37 mg, 0.04 mmol), XPhos (19 mg, 0.04 mmol) and K_2CO_3 (116 mg, 0.84 mmol) were reacted in MeCN (4 ml) according to **general procedure M**. Chromatography on silica (7:3 Petrol/EtOAc) gave the desired compound as a pale yellow oil/gum (0.112 g, 0.22 mmol, 58%). R_f 0.37 (7:3 Petrol/EtOAc); λ_{max} (EtOH/nm) 273, 344; IR (cm^{-1}) 3248, 3176, 2942, 2864, 1574, 1548, 1514; ^{1}H NMR (500 MHz, $CDCl_3$) 1.17-1.29 (21H, m, Si(C*H*(CH_3)$_2$)$_3$), 3.81 (3H, s, OCH_3), 5.29 (2H, s, N^9-CH_2), 6.90 (2H, d, *J* = 8.5 Hz, H-3''/H-5''), 7.25-7.31 (3H, m, H-2''/H-6'' & H-2'), 7.42 (1H, s, C^2-NH), 7.87 (1H, s, H-8), 8.16-8.20 (1H, s, H-4'), 8.28-8.32 (1H, m, H-6'), 8.89-8.92 (1H, m, H-2'); ^{13}C NMR (125 MHz, $CDCl_3$) 11.3 (Si(*C*H(CH_3)$_2$)$_3$), 18.7 (Si(CH(*C*H_3)$_2$)$_3$), 46.9 (N^9-CH_2), 55.4 (OCH_3), 100.8 (C≡C), 101.9 (C≡C), 114.5 (C-Ar), 123.5 (C-Ar), 125.3 (C-Ar), 127.1 (C-Ar), 129.3 (C-Ar), 130.2 (C-Ar), 136.8 (C-Ar), 140.3 (C-Ar), 142.3 (C-Ar), 142.9 (C-Ar), 143.2 (C-Ar), 152.9 (C-Ar), 155.8 (C-Ar), 159.8 (C-Ar); HRMS calcd. for $C_{29}H_{37}N_6OSi$ (ES+) *m*/*z* 513.2793 $[M+H]^+$, found 513.2786.

9-(4-Methoxybenzyl)-*N*-(pyridin-4-yl)-6-((triisopropylsilyl)ethynyl)-9*H*-purin-2-amine (374)

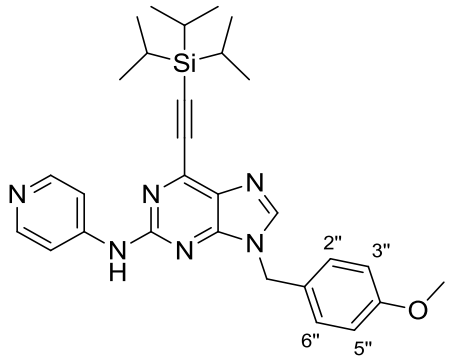

The 2-iodopurine **278** (0.209 g, 0.38 mmol), 4-aminopyridine (43 mg, 0.46 mmol), $Pd_2(dba)_3$ (37 mg, 0.04 mmol), XPhos (19 mg, 0.04 mmol) and K_2CO_3 (116 mg, 0.84 mmol) were reacted in MeCN (4 ml) according to **general procedure M**. Chromatography on silica (7:3 Petrol/EtOAc) afforded the target compound as a yellow oil/gum (0.101 g, 0.20 mmol, 53%). R_f 0.37 (7:3 Petrol/EtOAc); λ_{max} (EtOH/nm) 281, 344; IR (cm^{-1}) 3169, 2943, 2865, 1589, 1571, 1514; ^{1}H NMR (500 MHz, $CDCl_3$) 1.19-1.30 (21H, m, Si(C*H*(CH_3)$_2$)$_3$), 3.82 (3H, s, OCH_3), 5.33 (2H, s, N^9-CH_2), 6.91 (2H, d, *J* = 8.7 Hz, H-3''/H-5''), 7.29 (2H, d, *J* = 8.7 Hz, H-2''/H-6''), 7.55 (1H, s, C^2-NH), 7.62-7.65 (2H, m, H-3'/H-5'), 7.93 (1H, s, H-8), 8.46-8.50 (2H, m, H-2'/H-6'); ^{13}C NMR (125 MHz, $CDCl_3$) 11.2 (Si(*C*H(CH_3)$_2$)$_3$), 18.7 (Si(CH(*C*H_3)$_2$)$_3$), 47.1 (N^9-CH_2), 55.4 (OCH_3), 100.6 (C≡C), 102.5 (C≡C), 112.2 (C-Ar), 114.5 (C-Ar), 126.9 (C-Ar), 129.3 (C-Ar), 142.2 (C-Ar), 143.7 (C-Ar), 146.8 (C-Ar), 150.0 (C-Ar), 152.8 (C-Ar), 155.1 (C-Ar), 159.8 (C-Ar); HRMS calcd. for $C_{29}H_{37}N_6OSi$ (ES+) *m*/*z* 513.2793 $[M+H]^+$, found 513.2780.

9-(4-Methoxybenzyl)-*N*-(pyrimidin-4-yl)-6-((triisopropylsilyl)ethynyl)-9*H*-purin-2-amine (375)

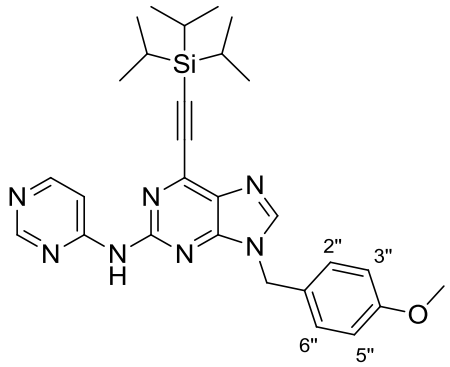

The 2-iodopurine **278** (0.206 g, 0.38 mmol), 4-aminopyrimidine (44 mg, 0.46 mmol), $Pd_2(dba)_3$ (37 mg, 0.04 mmol), XPhos (19 mg, 0.04 mmol) and K_2CO_3 (116 mg, 0.84 mmol) were reacted in MeCN (4 ml) according to **general procedure M**. Chromatography on silica (1:1 Petrol/EtOAc) gave the target compound as a yellow oil/gum (0.126 g, 0.25 mmol, 66%). R_f 0.28 (1:1 Petrol/EtOAc); λ_{max} (EtOH/nm) 276, 341; IR (cm^{-1}) 3157, 2941, 2864, 1565, 1514; ^{1}H NMR (500 MHz, $CDCl_3$) 1.17-1.30 (21H, m, Si(C*H*(CH_3)$_2$)$_3$), 3.81 (3H, s, OCH_3), 5.33 (2H, s, N^9-CH_2), 6.91 (2H, d, *J* = 8.5 Hz, H-3''/H-5''), 7.27 (2H, d, *J* = 8.5 Hz, H-2''/H-6''), 7.95 (1H, s, H-8), 8.40-8.45 (1H, m, H-6'), 8.55-8.60 (1H, m, H-5'), 8.67 (1H, s, C^2-NH), 8.92-8.95 (1H, br, H-2'); ^{13}C NMR (125 MHz, $CDCl_3$) 11.3 (Si(*C*H(CH_3)$_2$)$_3$), 18.6 (Si(CH(*C*H_3)$_2$)$_3$), 47.1 (N^9-CH_2), 55.4 (OCH_3), 100.6 (C≡C), 102.8 (C≡C), 108.4 (C-Ar), 114.6 (C-Ar), 126.8 (C-Ar), 129.3 (C-Ar), 131.0 (C-Ar), 142.0 (C-Ar), 144.1 (C-Ar), 152.8 (C-Ar), 154.0 (C-Ar), 157.2 (C-Ar), 158.3 (C-Ar), 158.4 (C-Ar), 159.9 (C-Ar); HRMS calcd. for $C_{28}H_{35}N_7OSi$ (ES+) *m*/*z* 514.2745 $[M+H]^+$, found 514.2740.

9-(4-Methoxybenzyl)-*N*-(pyrimidin-2-yl)-6-((triisopropylsilyl)ethynyl)-9*H*-purin-2-amine (376)

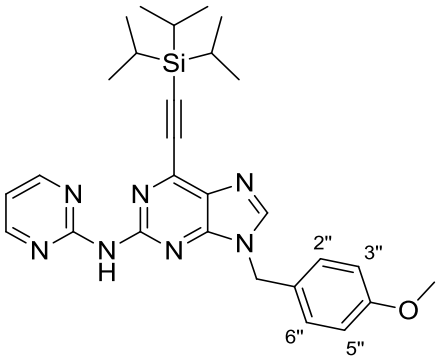

The 2-iodopurine **278** (0.208 g, 0.38 mmol), 2-aminopyrimidine (44 mg, 0.46 mmol), $Pd_2(dba)_3$ (37 mg, 0.04 mmol), XPhos (19 mg, 0.04 mmol) and K_2CO_3 (116 mg, 0.84 mmol) were reacted in MeCN (4 ml) according to **general procedure M**. Purification on silica (1:1 Petrol/EtOAc) gave the desired compound as a yellow oil/gum (95 mg, 0.18 mmol, 47%). R_f 0.30 (1:1 Petrol/EtOAc); λ_{max} (EtOH/nm) 266, 341; IR (cm^{-1}) 3241, 3170, 2943, 2865, 2360, 2337, 1711, 1571, 1514; ^{1}H NMR (500 MHz, $CDCl_3$) 1.17-1.31 (21H, m, Si(C*H*(CH_3)$_2$)$_3$), 3.81 (OCH3), 5.35 (2H, s, N^9-CH_2), 6.88 (2H, d, *J* = 8.7 Hz, H-3''/H-5''), 6.92-6.95 (1H, br, H-5'), 7.40 (2H, d, *J* = 8.7 Hz, H-2''/H-6''), 7.89 (1H, s, H-8), 8.70-8.75 (2H, m, H-4'/H-6'), 9.20 (1H, s, C^2-NH); ^{13}C NMR (125 MHz, $CDCl_3$) 11.3 (Si(*C*H(CH_3)$_2$)$_3$), 18.7 (Si(CH(*C*H_3)$_2$)$_3$), 47.1 (N^9-CH_2), 55.3 (OCH_3), 100.9 (C≡C), 101.8 (C≡C), 114.4 (C-Ar), 114.6 (C-Ar), 127.2 (C-Ar), 129.8 (C-Ar), 130.0 (C-Ar), 143.9 (C-Ar), 154.1 (C-Ar), 158.3 (C-Ar), 158.8 (C-Ar), 159.8 (C-Ar); HRMS calcd. for $C_{28}H_{35}N_7OSi$ (ES+) *m*/*z* 514.2745 $[M+H]^+$, found 514.2739.

5-Aminopyrimidine (384)[276]

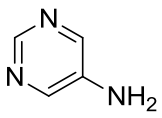

5-Amino-4,6-dichloropyrimidine (0.500 g, 3.05 mmol), ammonium formate (1.92 g, 30.5 mmol) and palladium on carbon (50 mg, 10% w/w) were reacted in methanol (30 ml) according to **general procedure G** over 1 h. Chromatography on silica (9:1 DCM/MeOH) gave the target compound as a pale yellow solid (0.239 g, 2.51 mmol, 82%). R_f 0.32 (9:1 DCM/MeOH); M.p. 160-165 °C (Lit.[276] 173-174 °C); λ_{max} (EtOH/nm) 245, 315; IR (cm^{-1})

3341, 3178, 3025, 2745, 1662, 1554; ^{1}H NMR (500 MHz, DMSO-d_6) 5.54 (2H, s, Ar-NH_2), 8.09 (2H, s, H-4/H-6), 8.35 (1H, s, H-2); ^{13}C NMR (125 MHz, DMSO-d_6) 141.4 (C-Ar), 142.9 (C-Ar), 146.7 (C-Ar); LRMS (ES+) *m*/*z* 96.1 $[M+H]^+$.

9-(4-Methoxybenzyl)-*N*-(pyrimidin-5-yl)-6-((triisopropylsilyl)ethynyl)-9*H*-purin-2-amine (377)

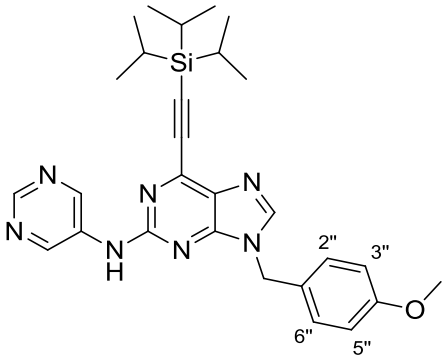

The 2-iodopurine **278** (0.220 g, 0.40 mmol), 5-aminopyrimidine **384** (46 mg, 0.48 mmol), $Pd_2(dba)_3$ (37 mg, 0.04 mmol), XPhos (19 mg, 0.04 mmol) and K_2CO_3 (122 mg, 0.89 mmol) were reacted in MeCN (4 ml) according to **general procedure M**. Silica gel chromatography (1:1 Petrol/EtOAc) gave the target compound as a yellow oil/gum (124 mg, 0.24 mmol, 60%). R_f 0.28 (1:1 Petrol/EtOAc); λ_{max} (EtOH/nm) 276, 351; IR (cm^{-1}) 3370, 3066, 2942, 2865, 1586, 1532, 1513; ^{1}H NMR (500 MHz, $CDCl_3$) 1.18-1.31 (21H, m, Si(C*H*(CH_3)$_2$)$_3$), 3.81 (OCH_3), 5.30 (2H, s, N^9-CH_2), 6.91 (2H, d, *J* = 8.8 Hz, H-3''/H-5''), 7.26 (2H, d, *J* = 8.8 Hz, H-2''/H-6''), 7.44 (1H, br, C^2-NH), 7.92 (1H, s, H-8), 8.92 (1H, s, H-2'), 9.18 (2H, s, H-4'/H-6'); ^{13}C NMR (125 MHz, $CDCl_3$) 11.3 (Si(*C*H(CH_3)$_2$)$_3$), 18.7 (Si(CH(*C*H_3)$_2$)$_3$), 47.1 (N^9-CH_2), 55.4 (OCH_3), 100.4 (C≡C), 103.0 (C≡C), 114.6 (C-Ar), 126.8 (C-Ar), 129.3 (C-Ar), 130.5 (C-Ar), 135.2 (C-Ar), 142.2 (C-Ar), 143.7 (C-Ar), 146.3 (C-Ar), 152.2 (C-Ar), 152.9 (C-Ar), 155.1 (C-Ar), 159.8 (C-Ar); HRMS calcd. for $C_{28}H_{36}N_7OSi$ (ES+) *m*/*z* 514.2745 $[M+H]^+$, found 514.2739.

***N*-(Pyridin-2-yl)-6-((triisopropylsilyl)ethynyl)-9*H*-purin-2-amine (378)**

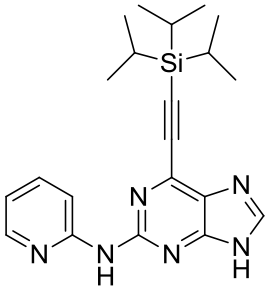

The PMB-protected purine **372** (0.143 g, 0.28 mmol) and TFA (3 ml) were reacted according to **general procedure K**. Chromatography on silica (19:1 DCM/MeOH) gave the target compound as a yellow oil (0.123 g, 0.24 mmol, 85%). R_f 0.31 (19:1 DCM/MeOH); λ_{max} (EtOH/nm) 267, 354; IR (cm^{-1}) 3258, 3120, 2942, 2864, 1592, 1572, 1541; ^{1}H NMR (500 MHz, DMSO-d_6)) 1.12-1.23 (21H, m, Si(C*H*(C*H*$_3$)$_2$)$_3$), 6.97 (1H, ddd, *J* = 0.8, 5.1 and 7.2 Hz, H-5'), 7.75 (1H, ddd, *J* = 1.2, 7.2 and 7.6 Hz, H-4'), 7.27-7.34 (3H, m, H-3'/H-6' & H-8), 9.85 (1H, s, C^2-NH), 13.22 (1H, br, H-9); ^{13}C NMR (125 MHz, DMSO-d_6) 10.6 (Si(*C*H(CH$_3$)$_2$)$_3$), 18.4 (Si(CH(*C*H$_3$)$_2$)$_3$), 98.6 (C≡*C*H), 101.8 (*C*≡CH), 112.1 (C-Ar), 117.1 (C-Ar), 129.5 (C-Ar), 137.5 (C-Ar), 139.7 (C-Ar), 143.5 (C-Ar), 147.8 (C-Ar), 153.2 (C-Ar), 153.7 (C-Ar), 155.0 (C-Ar); HRMS calcd. for $C_{21}H_{29}N_6Si$ (ES+) *m*/*z* 393.2217 $[M+H]^+$, found 393.2218.

***N*-(Pyridin-3-yl)-6-((triisopropylsilyl)ethynyl)-9*H*-purin-2-amine (379)**

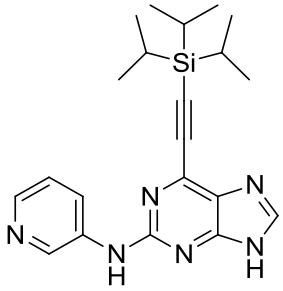

The PMB-protected purine **373** (98 mg, 0.19 mmol) and TFA (4 ml) were reacted according to **general procedure K**. Silica gel purification (19:1 DCM/MeOH) gave the target compound as a yellow oil/gum (67 mg, 0.17 mmol, 89%). R_f 0.30 (19:1 DCM/MeOH); λ_{max} (EtOH/nm) 273, 341; IR (cm^{-1}) 3123, 3067, 2942, 2865, 1590, 1574, 1541; ^{1}H NMR (500 MHz, MeOD) 1.22-1.29 (21H, m, Si(C*H*(C*H*$_3$)$_2$)$_3$), 7.38 (1H, dd, *J* = 4.7 and 8.3 Hz, H-5'), 8.14 (1H, dd, *J* = 1.2 and 4.7 Hz, H-6'), 8.23 (1H, s, H-8), 8.36-8.40 (1H, m, H-4'), 8.96-8.98

(1H, m, H-2'); ^{13}C NMR (125 MHz, MeOD) 12.5 (Si(*C*H(CH$_3$)$_2$)$_3$), 19.1 (Si(CH(*C*H$_3$)$_2$)$_3$), 100.8 (C≡C), 125.0 (C-Ar), 127.2 (C-Ar), 139.7 (C-Ar), 140.7 (C-Ar), 142.4 (C-Ar), 157.8 (C-Ar); HRMS calcd. for $C_{21}H_{29}N_6Si$ (ES+) *m*/*z* 393.2217 $[M+H]^+$, found 393.2218.

Note: Unable to visualise all carbon environments by ^{13}C NMR.

***N*-(Pyridin-4-yl)-6-((triisopropylsilyl)ethynyl)-9*H*-purin-2-amine (380)**

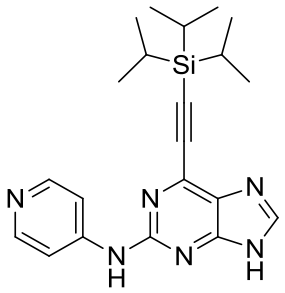

The PMB-protected purine **374** (95 mg, 0.19 mmol) and TFA (4 ml) were reacted according to **general procedure K**. Silica gel chromatography (19:1 DCM/MeOH) gave the desired compound as a yellow oil/gum (62 mg, 0.16 mmol, 84%). R_f 0.33 (19:1 DCM/MeOH); λ_{max} (EtOH/nm) 280, 347; IR (cm^{-1}) 3263, 3088, 2942, 2865, 2717, 1600, 1568; ^{1}H NMR (500 MHz, MeOD) 1.21-1.30 (21H, m, Si(C*H*(C*H$_3$*)$_2$)$_3$), 7.90 (2H, dd, *J* = 1.5 and 5.0 Hz, H-3'/H-5'), 8.30 (2H, dd, *J* = 1.5 and 5.0 Hz, H-2'/H-6'), 8.31 (1H, s, H-8); ^{13}C NMR (125 MHz, MeOD) 12.5 (Si(*C*H(CH$_3$)$_2$)$_3$), 19.1 (Si(CH(*C*H$_3$)$_2$)$_3$), 101.2 (C≡C), 102.4 (C≡C), 113.7 (C-Ar), 145.4 (C-Ar), 149.9 (C-Ar), 150.1 (C-Ar), 157.2 (C-Ar); HRMS calcd. for $C_{21}H_{29}N_6Si$ (ES+) *m*/*z* 393.2217 $[M+H]^+$, found 393.2211.

Note: Unable to visualise all carbon environments by ^{13}C NMR.

***N*-(Pyrimidin-4-yl)-6-((triisopropylsilyl)ethynyl)-9*H*-purin-2-amine (381)**

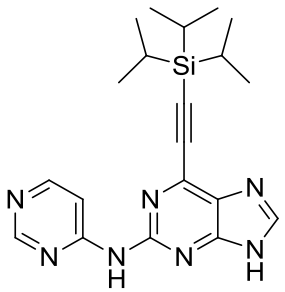

The PMB-protected purine **375** (117 mg, 0.23 mmol) and TFA (4 ml) were reacted according to **general procedure K**. Purification using chromatography on silica (19:1 DCM/MeOH)

afforded the desired compound as a yellow oil/gum (87 mg, 0.22 mmol, 96%). R_f 0.36 (19:1 DCM/MeOH); λ_{max} (EtOH/nm) 278, 340; IR (cm^{-1}) 3076, 2943, 2865, 2376, 2291, 1586, 1493; ^{1}H NMR (500 MHz, MeOD) 1.21-1.31 (21H, m, Si(C*H*(C*H*$_3$)$_2$)$_3$), 8.37 (1H, s, H-8), 8.50 (1H, d, *J* = 6.1 Hz, H-5'), 8.59 (1H, dd, *J* = 1.2 and 6.1 Hz, H-6'), 8.76 (1H, d, *J* = 1.2 Hz, H-2'); ^{13}C NMR (125 MHz, MeOD) 12.5 (Si(*C*H(CH$_3$)$_2$)$_3$), 19.1 (Si(CH(*C*H$_3$)$_2$)$_3$), 102.3 (C≡C), 109.7 (C-Ar), 146.4 (C-Ar), 157.4 (C-Ar), 158.9 (C-Ar); HRMS calcd. for $C_{20}H_{28}N_7Si$ (ES+) *m*/*z* 394.2170 $[M+H]^+$, found 394.2166.

Note: Unable to visualise all carbon environments by ^{13}C NMR.

***N*-(Pyrimidin-2-yl)-6-((triisopropylsilyl)ethynyl)-9*H*-purin-2-amine (382)**

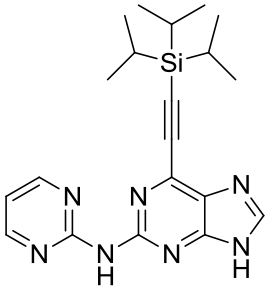

The PMB-protected purine **376** (84 mg, 0.16 mmol) and TFA (4 ml) were reacted according to **general procedure K**. Purification on silica gel (19:1 DCM/MeOH), followed by KP-NH silica (9:1 DCM/MeOH) gave the target compound as a yellow oil/gum (35 mg, 0.09 mmol, 56%). R_f 0.34 (9:1 DCM/MeOH); λ_{max} (EtOH/nm) 265, 341; IR (cm^{-1}) 3229, 3167, 2941, 2863, 1606, 1572; ^{1}H NMR (500 MHz, DMSO-d_6) 1.23-1.30 (21H, m, Si(C*H*(C*H*$_3$)$_2$)$_3$), 7.01 (1H, dd, *J* = 4.7 and 4.7 Hz, H-5'), 8.40 (1H, s, H-8), 8.56 (2H, d, *J* = 4.7 Hz, H-4'/H-6'), 10.25 (1H, s, C^2-NH), 13.42 (1H, br, H-9); ^{13}C NMR (125 MHz, DMSO-d_6) 10.6 (Si(*C*H(CH$_3$)$_2$)$_3$), 18.4 (Si(CH(*C*H$_3$)$_2$)$_3$), 98.8 (C≡C), 101.58 (C≡C), 114.6 (C-Ar), 144.7 (C-Ar), 154.0 (C-Ar), 158.0 (C-Ar), 159.2 (C-Ar); HRMS calcd. for $C_{20}H_{28}N_7Si$ (ES+) *m*/*z* 394.2170 $[M+H]^+$, found 394.2169.

Note: Unable to visualise all carbon environments by ^{13}C NMR.

***N*-(Pyrimidin-5-yl)-6-((triisopropylsilyl)ethynyl)-9*H*-purin-2-amine (383)**

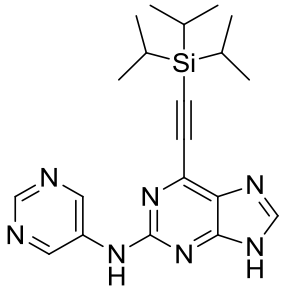

The PMB-protected purine **377** (100 mg, 0.19 mmol) and TFA (4 ml) were reacted according to **general procedure K**. Purification on silica gel (19:1 DCM/MeOH) gave the desired compound as a yellow oil/gum (66 mg, 0.17 mmol, 89%). R_f 0.34 (19:1 DCM/MeOH); λ_{max} (EtOH/nm) 276, 351; IR (cm^{-1}) 3080, 2944, 2865, 1600, 1571, 1534; ^{1}H NMR (500 MHz, MeOD) 1.21-1.29 (21H, m, Si(C*H*(C*H*$_3$)$_2$)$_3$), 8.27 (1H, br, H-8), 8.75 (1H, s, H-2'), 9.31 (2H, s, H-4'/H-6'); ^{13}C NMR (125 MHz, MeOD) 12.5 (Si(*C*H(CH$_3$)$_2$)$_3$), 19.1 (Si(CH(*C*H$_3$)$_2$)$_3$), 101.3 (C≡C), 138.3 (C-Ar), 147.2 (C-Ar), 151.4 (C-Ar), 157.2 (C-Ar); HRMS calcd. for $C_{20}H_{28}N_7Si$ (ES+) *m*/*z* 394.2170 $[M+H]^+$, found 394.2172.

Note: Unable to visualise all carbon environments by ^{13}C NMR.

6-Ethynyl-*N*-(pyridin-2-yl)-9*H*-purin-2-amine (364)

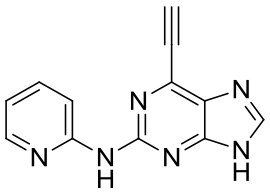

The TIPS-protected purine **378** (83 mg, 0.21 mmol), TBAF (1M in THF, 0.25 ml, 0.25 mmol) and the TBAF scavenger bead system **231** (0.80 g, 10 x w/w) were reacted in THF (5 ml) according to **general procedure U**. Chromatography on KP-NH silica (9:1 DCM/MeOH) gave the desired compound as an off-white solid (21 mg, 0.09 mmol, 43%). R_f 0.30 (9:1 DCM/MeOH, KP-NH); M.p. 240-260 °C (decomposed); λ_{max} (EtOH/nm) 252.0, 339.0; IR (cm^{-1}) 3268, 3163, 2158, 2106, 2033, 1977; ^{1}H NMR (500 MHz, DMSO-d_6) 4.90 (1H, s, C≡CH), 6.98 (1H, ddd, *J* = 0.9, 5.0 and 7.0 Hz, H-5'), 7.77 (1H, ddd, *J* = 1.9, 7.0 and 7.1 Hz, H-4'), 8.27-8.32 (2H, m, H-3'/H-6'), 8.37 (1H, s, H-8), 9.77 (1H, s, C^2-NH), 13.29 (1H, br, H-9); ^{13}C NMR (125 MHz, DMSO-d_6) 78.9 (C≡*C*H), 87.6 (*C*≡CH), 112.0 (C-Ar), 117.1 (C-

Ar), 137.6 (C-Ar), 147.8 (C-Ar), 153.2 (C-Ar), 155.0 (C-Ar); HRMS calcd. for $C_{12}H_9N_6$ (ES+) *m*/*z* 237.0883 $[M+H]^+$, found 237.0885.

Note: Unable to visualise all carbon environments by ^{13}C NMR.

6-Ethynyl-*N*-(pyridin-3-yl)-9*H*-purin-2-amine (365)

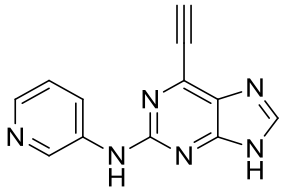

The TIPS-protected purine **379** (62 mg, 0.21 mmol), TBAF (1M in THF, 0.19 ml, 0.19 mmol) and the TBAF scavenger bead system **231** (0.60 g, 10 x w/w) were reacted in THF (5 ml) according to **general procedure U**. Chromatography on silica (9:1 DCM/MeOH) gave the desired compound as an beige solid (23 mg, 0.10 mmol, 46%). R_f 0.26 (9:1 DCM/MeOH); M.p. 220-240 °C (decomposed); λ_{max} (EtOH/nm) 270, 340; IR (cm^{-1}) 3190, 3073, 2925, 2826, 2109, 1577, 1543; ^1H NMR (500 MHz, DMSO-d_6) 4.88 (1H, s, C≡CH), 7.31-7.35 (1H, m, H-5'), 8.15 (1H, dd, *J* = 1.2 and 4.6 Hz, H-6'), 8.24 (1H, ddd, *J* = 1.2, 1.6 and 8.3 Hz, H-4'), 8.33 (1H, s, H-8), 8.94-8.96 (1H, m, H-2'), 9.88 (1H, s, C^2-NH); ^{13}C NMR (125 MHz, DMSO-d_6) 78.8 (C≡C), 87.3 (C≡C), 123.3 (C-Ar), 124.6 (C-Ar), 137.5 (C-Ar), 140.3 (C-Ar), 141.8 (C-Ar), 155.9 (C-Ar); HRMS calcd. for $C_{12}H_9N_6$ (ES+) *m*/*z* 237.0883 $[M+H]^+$, found 237.0886.

Note: Unable to visualise all carbon environments by ^{13}C NMR – insufficient material.

6-Ethynyl-*N*-(pyridin-4-yl)-9*H*-purin-2-amine (366)

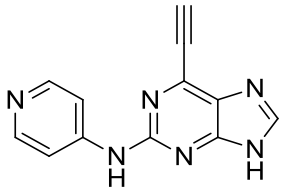

The TIPS-protected purine **380** (57 mg, 0.15 mmol), TBAF (1M in THF, 0.17 ml, 0.17 mmol) and the TBAF scavenger bead system **231** (0.60 g, 10 x w/w) were reacted in THF (5 ml) according to **general procedure U**. Chromatography on silica (9:1 DCM/MeOH) afforded the target compound as an beige solid (23 mg, 0.09 mmol, 61%). R_f 0.21 (9:1

DCM/MeOH); M.p. 240-260 °C (decomposed); λ_{max} (EtOH/nm) 282, 339; IR (cm^{-1}) 3191, 2113, 1604, 1532; ^{1}H NMR (500 MHz, DMSO-d_6) 4.93 (1H, s, C≡CH), 7.80 (2H, dd, J = 1.3 and 5.1 Hz, H-3'/H-5'), 8.36 (2H, m, H-2'/H-6'), 8.40 (1H, br, H-8), 10.21 (1H, s, C^2-NH), 13.34 (1H, br, H-9); ^{13}C NMR (125 MHz, DMSO-d_6) 78.7 (C≡C), 87.7 (C≡C), 112.0 (C-Ar), 147.2 (C-Ar), 149.8 (C-Ar), 155.3 (C-Ar); HRMS calcd. for $C_{12}H_9N_6$ (ES+) m/z 237.0883 $[M+H]^+$, found 237.0885.

Note: Unable to visualise all carbon environments by ^{13}C NMR – insufficient material.

6-Ethynyl-*N*-(pyrimidin-2-yl)-9*H*-purin-2-amine (368)

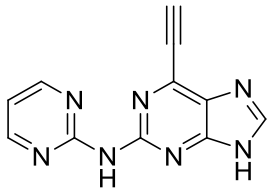

The TIPS-protected purine **382** (26 mg, 0.07 mmol), TBAF (1M in THF, 80 µl, 0.08 mmol) and the TBAF scavenger bead system **231** (0.30 g, 10 x w/w) were reacted in THF (3 ml) according to **general procedure U**. Chromatography on silica (9:1 DCM/MeOH) gave the target compound as an beige solid (9 mg, 0.04 mmol, 54%). R_f 0.24 (9:1 DCM/MeOH); M.p. 260-280 °C (decomposed); λ_{max} (EtOH/nm) 256; IR (cm^{-1}) 3248, 2991, 2112, 1608, 1572, 1546; ^{1}H NMR (500 MHz, DMSO-d_6) 4.89 (1H, s, C≡CH), 7.01 (1H, dd, J = 4.7 and 4.8 Hz, H-5'), 8.42 (1H, s, H-8), 8.57 (2H, d, J = 4.7 Hz, H-4'/H-6'), 10.23 (1H, s, C^2-NH), 13.45 (1H, br, H-9); ^{13}C NMR (125 MHz, DMSO-d_6) 87.6 (C≡C), 114.6 (C-Ar), 158.0 (C-Ar); HRMS calcd. for $C_{11}H_8N_7$ (ES+) m/z 238.0836 $[M+H]^+$, found 238.0838.

Note: Unable to visualise all carbon environments by ^{13}C NMR – insufficient material.

6-Ethynyl-*N*-(pyrimidin-5-yl)-9*H*-purin-2-amine (369)

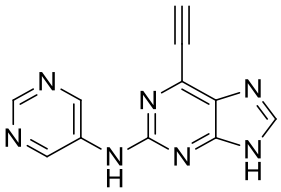

The TIPS-protected purine **383** (57 mg, 0.14 mmol), TBAF (1M in THF, 0.17 ml, 0.17 mmol) and the TBAF scavenger bead system **231** (0.60 g, 10 x w/w) were reacted in THF (5

ml) according to **general procedure U**. Chromatography on silica (9:1 DCM/MeOH) gave the desired compound as an beige solid (14 mg, 0.06 mmol, 42%). R_f 0.22 (9:1 DCM/MeOH); M.p. 250-270 °C (decomposed); λ_{max} (EtOH/nm) 255; IR (cm^{-1}) 3251, 2812, 2112, 1606, 1549; ^{1}H NMR (500 MHz, DMSO-d_6) 4.93 (1H, s, C≡CH), 8.38 (1H, s, H-8), 8.77 (1H, s, H-2'), 9.22 (2H, s, H-4'/H-6'), 10.08 (1H, s, C^2-NH), 13.30 (1H, br, H-9); ^{13}C NMR (125 MHz, DMSO-d_6) 136.2 (C-Ar), 145.9 (C-Ar), 150.9 (C-Ar), 155.3 (C-Ar); HRMS calcd. for $C_{11}H_8N_7$ (ES+) *m*/*z* 238.0836 $[M+H]^+$, found 238.0835.

5-Amino-2-fluoro-*N*-methylbenzamide (392)

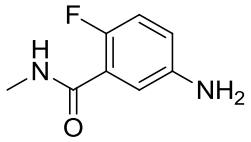

5-Amino-2-fluorobenzoic acid (0.498 g, 3.22 mmol), thionyl chloride (0.47 mmol, 6.44 mmol), methanol (30 ml) and methylamine (40% aqueous solution, 30 ml) were reacted according to **general procedure W**. Purification using silica gel chromatography (9:1 DCM/MeOH) afforded the target compound as a pale red oil (0.390 g, 2.32 mmol, 72%). R_f 0.40 (9:1 DCM/MeOH); λ_{max} (EtOH/nm) 218, 317; IR (cm^{-1}) 3338, 3240, 3060, 2942, 1637, 1535, 1491; ^{1}H NMR (500 MHz, DMSO-d_6) 2.75 (3H, d, J = 4.6 Hz, NHCH_3), 5.16 (2H, s, Ar-NH_2), 6.63 (1H, ddd, J = 3.0, 4.7 and 8.8 Hz, H-4), 6.81 (1 H, dd, J = 3.0 and 6.1 Hz, H-6), 6.92 (1H, dd, J = 8.8 and 10.6 Hz, H-3), 8.00 (1H, m, N*H*CH_3); ^{13}C NMR (125 MHz, DMSO-d_6) 26.2 (NH*C*H3), 114.0 (d, J_{CF} = 1.8 Hz, C-Ar), 116.1 (d, J_{CF} = 23.9 Hz, C-Ar), 116.6 (d, J_{CF} = 7.6 Hz, C-Ar), 123.6 (d, J_{CF} = 15.1 Hz, C-Ar), 145.1 (d, J_{CF} = 1.3 Hz, C-Ar), 151.0 (d, J_{CF} = 235.1 Hz, C-Ar), 164.5 (C=O); HRMS calcd. for $C_8H_{10}FN_2O$ (ES+) *m*/*z* 169.0772 $[M+H]^+$, found 169.0771.

2-Fluoro-*N*-methyl-5-((6-((triisopropylsilyl)ethynyl)-9*H*-purin-2-yl)amino) benzamide (393)

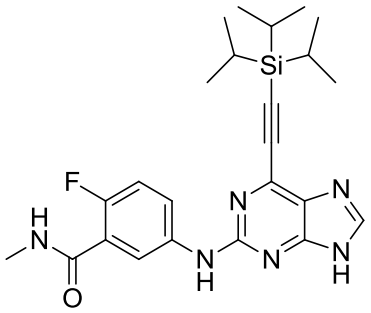

2-Fluoropurine **160** (0.240 g, 0.75 mmol), aniline **392** (0.253 g, 1.50 mmol) and TFA (145 µl, 1.88 mmol) were reacted in TFE (7 ml) according to **general procedure V**. Purification using chromatography on KP-NH silica (19:1 DCM/MeOH) gave the target compound as a yellow oil/gum (0.169 g, 0.36 mmol, 48%). R_f 0.39 (19:1 DCM/MeOH, KP-NH); λ_{max} (EtOH/nm) 274, 373; IR (cm^{-1}) 3472, 3312, 3073, 2943, 2865, 1639, 1609, 1543; ^{1}H NMR (500 MHz, DMSO-d_6) 1.13-1.20 (21H, m, Si(C*H*(CH_3)$_2$)$_3$), 2.79 (3H, d, *J* = 4.6 Hz, NHCH_3), 7.21 (1H, dd, *J* = 9.3 and 9.7 Hz, H-3'), 7.82-7.86 (1H, m, H-4'), 8.06 (1H, dd, *J* = 2.5 and 6.0 Hz, H-6'), 8.21-8.26 (2H, m, N*H*CH$_3$ & H-8), 9.86 (1H, s, C^2-NH), 13.17 (1H, br, H-9); ^{13}C NMR (125 MHz, DMSO-d_6) 10.6 (Si(*C*H(CH$_3$)$_2$)$_3$), 18.4 (Si(CH(*C*H$_3$)$_2$)$_3$), 26.2 (NH*C*H$_3$), 98.0 (*C*≡C-Si), 101.7 (C≡*C*-Si), 115.8 (d, J_{CF} = 23.6 Hz, C-Ar), 119.0 (d, J_{CF} = 2.4 Hz, C-Ar), 121.5 (C-Ar), 124.0 (d, J_{CF} = 15.9 Hz, C-Ar), 128.9 (C-Ar), 132.8 (C-Ar), 137.2 (d, J_{CF} = 2.7 Hz, C-Ar), 139.9 (C-Ar), 142.9 (C-Ar), 154.9 (d, J_{CF} = 276.9 Hz, C-Ar), 164.3 (C=O); HRMS calcd. for $C_{24}H_{32}FN_6OSi$ (ES+) *m*/*z* 467.2385 $[M+H]^+$, found 467.2382.

Note: Unable to visualise all carbon environments by ^{13}C NMR.

2-Fluoro-5-((6-ethynyl-9*H*-purin-2-yl)amino)-*N*-methylbenzamide (385)

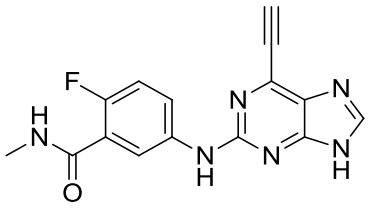

The TIPS-protected purine **393** (0.152 g, 0.33 mmol), TBAF (1M in THF, 0.39 ml, 0.39 mmol) and the TBAF scavenger bead system **231** (1.50 g, 10 x w/w) were reacted in THF (6 ml) according to **general procedure U**. Purification on silica gel (9:1 DCM/MeOH) gave the

target compound as a yellow solid (65 mg, 0.21 mmol, 63%). R_f 0.21 (9:1 DCM/MeOH); M.p. 240-260 °C (decomposed); λ_{max} (EtOH/nm) 272.0, 340.0; IR (cm^{-1}) 3306, 2544, 2112, 1637, 1614, 1582, 1552; ^{1}H NMR (500 MHz, DMSO-d_6) 2.79 (3H, d, J = 4.6 Hz, NHCH_3), 4.86 (1H, s, C≡CH), 7.23 (1H, dd, J = 9.2 and 9.8 Hz, H-3'), 7.86-7.92 (1H, m, H-4'), 7.99-8.03 (1H, m, H-6'), 8.22 (1H, q, J = 4.6 Hz, NHCH$_3$), 8.29 (1H, s, H-8), 9.82 (1H, s, C^2-NH), 13.21 (1H, br, H-9); ^{13}C NMR (125 MHz, DMSO-d_6) 26.2 (NHCH$_3$), 78.9 (C≡CH), 87.2 (C≡CH), 115.9 (d, J_{CF} = 23.6 Hz, C-Ar), 119.2 (C-Ar), 121.5 (d, J_{CF} = 6.5 Hz, C-Ar), 123.9 (d, J_{CF} = 16.3 Hz, C-Ar), 137.2 (C-Ar), 139.7 (C-Ar), 153.5 (d, J_{CF} = 243.6, Ar-CF), 156.0 (C-Ar), 164.2 (C=O); HRMS calcd. for $C_{15}H_{12}FN_6O$ (ES+) m/z 311.1051 $[M+H]^+$, found 311.1053.

Note: Unable to visualise all carbon environments by ^{13}C NMR.

Methyl 5-amino-2-chlorobenzoate (395)[277]

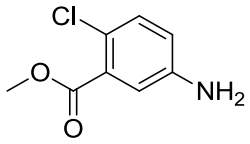

Methyl 2-chloro-5-nitrobenzoate (0.500 g, 2.32 mmol) and iron powder (1.29 g, 23.2 mmol) were reacted in acetic acid (23 ml) according to **general procedure T**. Silica gel chromatography (7:3 Petrol/EtOAc) afforded the target compound as a pale brown oil (0.332 g, 1.79 mmol, 77%). R_f 0.32 (7:3 Petrol/EtOAc); λ_{max} (EtOH/nm) 219, 256, 330; IR (cm^{-1}) 3462, 3374, 3231, 2952, 1716, 1624, 1600; ^{1}H NMR (500 MHz, DMSO-d_6) 3.81 (3H, s, OCH$_3$), 5.53 (2H, s, Ar-NH$_2$), 6.71 (1H, dd, J = 2.8 and 8.8 Hz, H-4), 6.98 (1H, d, J = 2.8 Hz, H-6), 7.15 (1H, d, J = 8.8 Hz, H-3); ^{13}C NMR (125 MHz, DMSO-d_6) 52.2 (OCH$_3$), 115.3 (C-Ar), 117.0 (C-Ar), 117.9 (C-Ar), 130.0 (C-Ar), 130.9 (C-Ar), 147.8 (C-Ar), 166.0 (C=O); LRMS (ES+) m/z 186.1 $[M+H]^+$.

5-Amino-2-chloro-*N*-methylbenzamide (396)

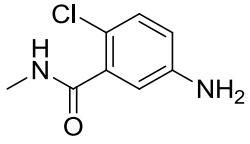

Methylamine (40% aqueous solution, 19 ml) and methyl ester **395** (0.347 g, 1.87 mmol) were reacted according to **general procedure S**. Following silica gel purification (19:1

DCM/MeOH) the desired compound was obtained as a pale red waxy solid on cooling (0.238 g, 1.29 mmol, 69%). R_f 0.43 (19:1 DCM/MeOH); M.p. 94-96 °C; λ_{max} (EtOH/nm) 251, 311; IR (cm^{-1}) 3432, 3339, 3281, 3087, 2941, 1635, 1615, 1595, 1551; ^{1}H NMR (500 MHz, DMSO-d_6) 2.71 (3H, d, J = 4.6 Hz, NHCH_3), 5.37 (2H, s, Ar-NH_2), 6.55-6.59 (2H, m, H-4/H-6), 7.05 (1H, d, J = 8.9 Hz, H-3), 8.16 (1H, q, J = 4.6 Hz, NHCH_3); ^{13}C NMR (125 MHz, DMSO-d_6) 25.8 (NHCH$_3$), 113.6 (C-Ar), 115.2 (C-Ar), 115.5 (C-Ar), 129.7 (C-Ar), 137.3 (C-Ar), 147.6 (C-Ar), 167.3 (C=O); HRMS calcd. for $C_8H_{10}ClN_2O$ (ES+) m/z 185.0476 $[M+H]^+$, found 185.0475.

2-Chloro-*N*-methyl-5-((6-((triisopropylsilyl)ethynyl)-9*H*-purin-2-yl)amino) benzamide (397)

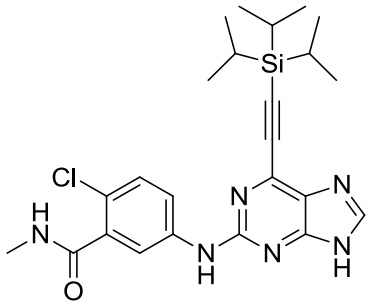

2-Fluoropurine **160** (0.202 g, 0.63 mmol), aniline **396** (0.234 g, 1.27 mmol) and TFA (122 µl, 1.58 mmol) were reacted in TFE (6 ml) according to **general procedure V**. Purification through chromatography on KP-NH silica (19:1 DCM/MeOH) gave the desired compound as a yellow oil/gum (0.106 g, 0.22 mmol, 35%). R_f 0.55 (19:1 DCM/MeOH, KP-NH); λ_{max} (EtOH/nm) 281, 370; IR (cm^{-1}) 3268, 3091, 2943, 2864, 1572, 1530; ^{1}H NMR (500 MHz, DMSO-d_6) 1.13-1.21 (21H, m, Si(CH(CH_3)$_2$)$_3$), 2.76 (3H, d, J = 4.6 Hz, NHCH_3), 7.37 (1H, d, J = 8.8 Hz, H-3'), 7.79 (1H, dd, J = 2.4 and 8.8 Hz, H-4'), 7.97 (1H, d, J = 2.4 Hz, H-6'), 8.28 (1H, s, H-8), 8.34 (1H, q, J = 4.6 Hz, NHCH_3), 9.99 (1H, s, C^2-NH), 13.22 (1H, br, H-9); ^{13}C NMR (125 MHz, DMSO-d_6) 10.6 (Si(CH(CH$_3$)$_2$)$_3$), 18.4 (Si(CH(CH$_3$)$_2$)$_3$), 24.7 (NHCH$_3$), 111.1 (C-Ar), 121.3 (C-Ar), 126.7 (C-Ar), 133.6 (C-Ar), 152.2 (C-Ar), 155.4 (C-Ar), 167.0 (C=O); HRMS calcd. for $C_{24}H_{32}ClN_6OSi$ (ES+) m/z 483.2090 $[M+H]^+$, found 483.2079.

Note: Unable to visualise all carbon environments by ^{13}C NMR.

2-Chloro-5-((6-ethynyl-9*H*-purin-2-yl)amino)-*N*-methylbenzamide (386)

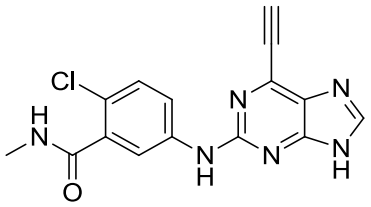

The TIPS-protected purine **397** (87 mg, 0.18 mmol), TBAF (1M in THF, 0.22 ml, 0.22 mmol) and the TBAF scavenger bead system **231** (0.90 g, 10 x w/w) were reacted in THF (4 ml) according to **general procedure U**. Chromatography on silica (9:1 DCM/MeOH) gave the target compound as a yellow solid (39 mg, 0.12 mmol, 66%). R_f 0.23 (9:1 DCM/MeOH); M.p. 180-200 °C (decomposed); λ_{max} (EtOH/nm) 278.5, 363.5; IR (cm^{-1}) 2250, 2112, 1575, 1532; ^{1}H NMR (500 MHz, DMSO-d_6) 2.77 (3H, d, J = 4.6 Hz, NHCH_3), 4.87 (1H, s, C≡CH), 7.39 (1H, d, J = 8.6 Hz, H-3'), 7.83-7.90 (2H, m, H-4'/H-6'), 8.30 (1H,br, H-8), 8.34 (1H, q, J = 4.6 Hz, N*H*CH$_3$), 9.96 (1H, s, C^2-NH), 13.25 (1H, br, H-9); ^{13}C NMR (125 MHz, DMSO-d_6) 25.9 (NHCH$_3$), 87.3 (C≡*C*H), 117.6 (C-Ar), 119.7 (C-Ar), 120.8 (C-Ar), 129.5 (C-Ar), 137.2 (C-Ar), 139.8 (C-Ar), 143.2 (C-Ar), 153.5 (C-Ar), 155.7 (C-Ar), 167.0 (C=O); HRMS calcd. for $C_{15}H_{11}ClN_6ONa$ (ES+) m/z 349.0575 $[M+Na]^+$, found 349.0578.

Note: Unable to visualise all carbon environments by ^{13}C NMR.

Methyl 5-chloro-2-(trifluoromethyl)benzoate (398)

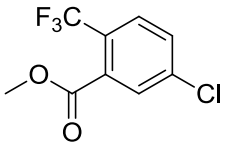

O-Methyl-*N*,*N*'-diisopropylisourea (1.16 ml, 6.41 mmol) was added to a solution of 5-chloro-2-(trifluoromethyl)benzoic acid (1.20 g, 5.34 mmol) in MeCN (20 ml). The reaction mixture was heated under microwave irradiation conditions at 120 °C for 5 min, before being filtered and the filtrate evaporated to dryness. The crude residue was purified by chromatography on silica (9:1 Petrol/EtOAc) to give the desired compound as a colourless liquid (0.911 g, 3.82 mmol, 72%). R_f 0.61 (9:1 Petrol/EtOAc); λ_{max} (EtOH/nm) 220, 274; IR (cm^{-1}) 2958, 1738, 1601, 1573; ^{1}H NMR (500 MHz, $CDCl_3$) 3.97 (3H, s, OCH_3), 7.60 (1H, dd, J = 2.0 and 8.5 Hz, H-4), 7.71 (1H, d, J = 8.5 Hz, H-3), 7.80 (1H, d, J = 2.0 Hz, H-6); ^{13}C NMR (125 MHz, $CDCl_3$) 53.1 (OCH_3), 122.9 (C-Ar), 123.0 (q, J_{CF} = 274.5 Hz, CF_3), 128.3 (q, J_{CF} = 5.4 Hz,

C-Ar), 130.5 (C-Ar), 131.3 (C-Ar), 132.6 (q, J_{CF} = 1.9 Hz, C-Ar), 138.2 (C-Ar), 165.9 (C=O); LRMS (ES+) *m*/*z* 239.1 $[M^{35}Cl+H]^+$, 241.1 $[M^{37}Cl+H]^+$.

Methyl 5-((4-methoxybenzyl)amino)-2-(trifluoromethyl)benzoate (400)

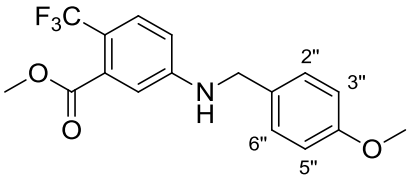

The chloro-aromatic intermediate **398** (0.480 g, 2.01 mmol), 4-methoxybenzylamine (315 µl, 2.41 mmol), palladium(II) acetate (45 mg, 0.20 mmol), 2-(dicyclohexylphosphino)3,6-dimethoxy-2′,4′,6′-triisopropyl-1,1′-biphenyl (BrettPhos) (100 mg, 0.20 mmol) and Cs_2CO_3 (0.785 g, 2.41 mmol) were suspended in THF (20 ml) in a sealed vial and the mixture was degassed for 15 min. The reaction mixture was heated at 90 °C for 1 h, before being filtered through Celite® and the filtrate concentrated *in vacuo*. Purification of the crude residue on silica (9:1 Petrol/EtOAc) afforded the target compound as a white crystalline solid on cooling (0.484 g, 1.43 mmol, 71%). R_f 0.22 (9:1 Petrol/EtOAc); M.p. 87-90 °C; λ_{max} (EtOH/nm) 270; IR (cm^{-1}) 3391, 3007, 2843, 1707, 1610, 1513; ^{1}H NMR (500 MHz, DMSO-d_6) 3.73 (3H, s, $ArOCH_3$), 3.81 (3H, s, CO_2CH_3), 4.28 (2H, d, *J* = 5.9 Hz, $NHCH_2$), 6.76 (1H, dd, *J* = 2.0 and 8.7 Hz, H-4), 6.91 (2H, d, *J* = 8.6 Hz, H-3'/H-5'), 6.93 (1H, d, *J* = 2.0 Hz, H-6), 7.21 (1H, t, *J* = 5.9 Hz, $NHCH_2$), 7.27 (2H, d, *J* = 8.6 Hz, H-2'/H-6'), 7.46 (1H, d, *J* = 8.7 Hz, H-3); ^{13}C NMR (125 MHz, DMSO-d_6) 45.2 ($NHCH_2$), 52.5 ($-CO_2CH_3$), 55.0 ($ArOCH_3$), 112.7 (q, J_{CF} = 20.3 Hz, C-Ar), 112.8 (C-Ar), 113.8 (C-Ar), 124.4 (q, J_{CF} = 271.1 Hz, CF_3), 127.9 (q, J_{CF} = 5.2 Hz, C-Ar), 128.4 (C-Ar), 130.6 (C-Ar), 131.7 (C-Ar), 151.2 (C-Ar), 158.3 (C-Ar), 167.3 (C=O); HRMS calcd. for $C_{17}H_{17}F_3NO_3$ (ES+) *m*/*z* 340.1155 $[M+H]^+$, found 340.1159.

Note: Unable to visualise all carbon environments by ^{13}C NMR.

Methyl 5-amino-2-(trifluoromethyl)benzoate (401)

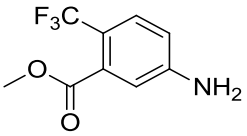

The PMB-protected aniline **400** (0.302 g, 0.89 mmol) and TFA (9 ml) were reacted according to **general procedure K**. Purification on silica gel (7:3 Petrol/EtOAc) gave the desired

compound as a pale yellow oil (0.186 g, 0.85 mmol, 96%). R_f 0.36 (7:3 Petrol/EtOAc); λ_{max} (EtOH/nm) 260, 309; IR (cm^{-1}) 3392, 3323, 3228, 2954, 1718, 1603, 1580; ^{1}H NMR (500 MHz, DMSO-d_6) 3.81 (3H, s, OCH_3), 6.11 (2H, s, Ar-NH_2), 6.75 (1H, dd, J = 2.4 and 8.7 Hz, H-4), 6.89 (1H, d, J = 2.4 Hz, H-6), 7.43 (1H, d, J = 8.7 Hz, H-3); ^{13}C NMR (125 MHz, DMSO-d_6) 52.5 (OCH_3), 113.8 (C-Ar), 114.4 (C-Ar), 128.0 (q, J_{CF} = 5.3 Hz, C-Ar), 131.7 (C-Ar), 142.5 (C-Ar), 152.0 (C-Ar), 167.2 (C=O); LRMS (ES+) m/z 220.1 $[M+H]^+$.

Note: Unable to visualise all carbon environments by ^{13}C NMR.

5-Amino-*N*-methyl-2-(trifluoromethyl)benzamide (402)

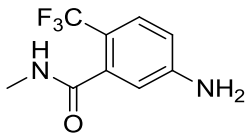

Methylamine (40% aqueous solution, 8 ml) and methyl ester **401** (0.160 g, 0.73 mmol) were reacted according to **general procedure S** over 48 hours. Purification by silica gel chromatography (9:1 DCM/MeOH) gave the target compound as an off-white solid (0.140 g, 0.64 mmol, 88%). R_f 0.39 (9:1 DCM/MeOH); M.p. 185-188 °C; λ_{max} (EtOH/nm) 256; IR (cm^{-1}) 3442, 3349, 3231, 1616, 1574, 1553; ^{1}H NMR (500 MHz, DMSO-d_6) 2.70 (3H, d, J = 4.7 Hz, NHCH_3), 5.94 (2H, s, Ar-NH_2), 6.55 (1H, d, J = 2.3 Hz, H-6), 6.63 (1H, dd, J = 2.3 and 8.6 Hz, H-4), 7.33 (1H, d, J = 8.6 Hz, H-3), 8.20 (1H, q, J = 4.7 Hz, NHCH_3); ^{13}C NMR (125 MHz, DMSO-d_6) 25.9 (NHCH$_3$), 112.0 (C-Ar), 111.8 (q, J_{CF} = 31.8 Hz, C-Ar), 112.3 (C-Ar), 112.6 (C-Ar), 124.7 (q, J_{CF} = 271.6 Hz, CF_3), 127.4 (q, J_{CF} = 5.0 Hz, C-Ar), 138.0 (q, J_{CF} = 1.8 Hz, C-Ar), 151.8 (C-Ar), 168.2 (C=O); HRMS calcd. for $C_9H_9F_3N_2ONa$ (ES+) m/z 241.0559 $[M+H]^+$, found 241.0562.

5-((9-(4-Methoxybenzyl)-6-((triisopropylsilyl)ethynyl)-9*H*-purin-2-yl)amino)-*N*-methyl-2-(trifluoromethyl)benzamide (403)

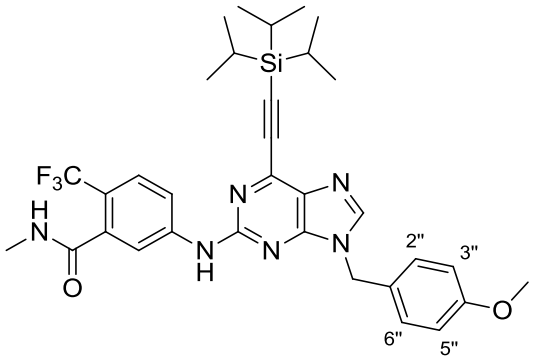

2-Iodopurine intermediate **278** (0.234 g, 0.43 mmol), aniline **402** (0.112 g, 0.51 mmol), $Pd_2(dba)_3$ (37 mg, 0.04 mmol), XPhos (19 mg, 0.04 mmol) and K_2CO_3 (0.130 g, 0.94 mmol) were reacted in MeCN (4 ml) according to **general procedure M**. Purification by silica gel chromatography (1:1 Petrol/EtOAc) gave the desired compound as a yellow oil (0.247 g, 0.39 mmol, 91%). R_f 0.44 (1:1 Petrol/EtOAc); λ_{max} (EtOH/nm) 281, 358; IR (cm^{-1}) 3287, 3092, 2943, 2865, 1656, 1576, 1536, 1514; ^{1}H NMR (500 MHz, DMSO-d_6) 1.11-1.20 (21H, m, Si(C*H*(C*H*$_3$)$_2$)$_3$), 2.75 (3H, d, *J* = 4.6 Hz, NHC*H*$_3$), 3.71 (3H, s, OCH$_3$), 5.35 (2H, s, N^9-CH$_2$), 6.92 (2H, d, *J* = 8.8 Hz, H-3''/H-5''), 7.37 (2H, d, *J* = 8.8 Hz, H-2''/H-6''), 7.66 (1H, d, *J* = 9.0 Hz, H-3'), 7.91 (1H, dd, *J* = 2.0 and 9.0 Hz, H-4'), 8.13 (1H, d, *J* = 2.0 Hz, H-6'), 8.44 (1H, q, *J* = 4.6 Hz, N*H*CH$_3$), 8.54 (1H, s, H-8), 10.40 (1H, s, C^2-NH); ^{13}C NMR (125 MHz, DMSO-d_6) 10.5 (Si(*C*H(CH$_3$)$_2$)$_3$), 18.3 (Si(CH(*C*H$_3$)$_2$)$_3$), 26.0 (NH*C*H$_3$), 46.2 (N9-*C*H$_2$), 55.0 (OCH$_3$), 99.2 (C≡*C*-Si), 101.2 (*C*≡C-Si), 114.1 (C-Ar), 116.5 (C-Ar), 117.4 (q, J_{CF} = 31.5 Hz, C-Ar), 117.5 (C-Ar), 124.2 (q, J_{CF} = 271.8 Hz, CF$_3$), 126.9 (q, J_{CF} = 5.0 Hz, C-Ar), 128.3 (C-Ar), 129.2 (C-Ar), 129.6 (C-Ar), 137.6 (q, J_{CF} = 2.4 Hz, C-Ar), 140.3 (C-Ar), 144.0 (C-Ar), 145.2 (C-Ar), 152.4 (C-Ar), 155.3 (C-Ar), 158.9 (C-Ar), 167.9 (C=O); HRMS calcd. for $C_{33}H_{40}F_3N_6O_2Si$ (ES+) *m*/*z* 637.2929 $[M+H]^+$, found 637.2926.

***N*-Methyl-2-(trifluoromethyl)-5-((6-((triisopropylsilyl)ethynyl)-9*H*-purin-2-yl)amino)benzamide (404)**

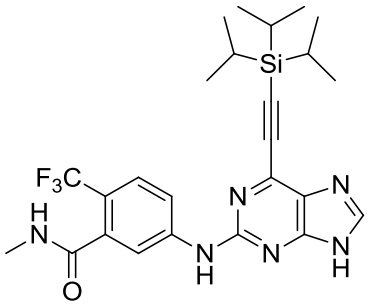

PMB-protected purine **403** (0.198 g, 0.31 mmol) and TFA (3 ml) were reacted according to **general procedure K** over 18 h. Purification using chromatography on silica (19:1 DCM/MeOH) gave the desired compound as a pale yellow oil/gum (0.148 g, 0.29 mmol, 94%). R_f 0.42 (19:1 DCM/MeOH); λ_{max} (EtOH/nm) 282, 356; IR (cm^{-1}) 3103, 2944, 2865, 1652, 1576, 1534; ^{1}H NMR (500 MHz, DMSO-d_6) 1.13-1.22 (21H, m, Si(C*H*(C*H*$_3$)$_2$)$_3$), 2.76 (3H, d, J = 4.6 Hz, NHC*H*$_3$), 7.64 (1H, d, J = 8.9 Hz, H-3'), 7.93-7.97 (1H, m, H-4'), 8.02-8.05 (1H, m, H-6'), 8.33-8.39 (2H, m, N*H*CH$_3$ & H-8), 10.27 (1H, s, C^2-NH), 13.32 (1H, br, H-9); ^{13}C NMR (125 MHz, DMSO-d_6) 10.6 (Si(*C*H(CH$_3$)$_2$)$_3$), 18.4 (Si(CH(*C*H$_3$)$_2$)$_3$), 26.0 (NH*C*H$_3$), 98.7 (C≡C), 116.2 (C-Ar), 117.3 (C-Ar), 124.2 (q, J_{CF} = 272.7 Hz, CF$_3$), 126.8 (q, J_{CF} = 5.0 Hz, C-Ar), 137.6 (C-Ar), 144.2 (C-Ar), 155.3 (C-Ar), 167.9 (C=O); HRMS calcd. for $C_{25}H_{32}F_3N_6OSi$ (ES+) m/z 517.2353 $[M+H]^+$, found 517.2349.

Note: Unable to visualise all carbon environments by ^{13}C NMR.

5-((6-Ethynyl-9*H*-purin-2-yl)amino)-*N*-methyl-2-(trifluoromethyl) benzamide (388)

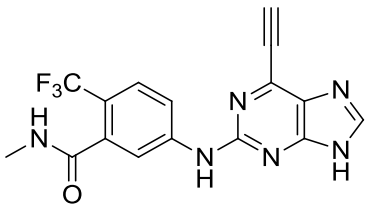

The TIPS-protected purine **404** (0.123 g, 0.24 mmol), TBAF (1M in THF, 0.29 ml, 0.29 mmol) and the TBAF scavenger bead system **231** (1.20 g, 10 x w/w) were reacted in THF (5 ml) according to **general procedure U**. Silica gel chromatography (9:1 DCM/MeOH) gave the target compound as a beige solid (54 mg, 0.15 mmol, 63%). R_f 0.18 (9:1 DCM/MeOH); M.p. 340-350 °C (decomposed); λ_{max} (EtOH/nm) 282.5, 350.0; IR (cm^{-1}) 3274, 3117, 2831,

2115, 1593, 1383; ^{1}H NMR (500 MHz, DMSO-d_6) 2.76 (3H, d, J = 4.6 z, NHCH_3), 4.93 (1H, s, C≡CH), 7.67 (1H, d, J = 8.8 Hz, H-3'), 7.92 (1H, d, J = 2.0 Hz, H-6'), 8.03 (1H, dd, J = 2.0 and 8.8 Hz, H-4'), 8.34-8.42 (2H, m, NHCH$_3$ & H-8), 10.23 (1H, s, C^2-NH), 13.37 (1H, br, H-9); ^{13}C NMR (125 MHz, DMSO-d_6) 26.0 (NHCH$_3$), 78.7 (C≡CH), 87.7 (C≡CH), 116.4 (C-Ar), 117.1 (C-Ar), 117.2 (C-Ar), 117.3 (C-Ar), 124.2 (q, J_{CF} = 271.8 Hz, C-Ar), 127.0 (q, J_{CF} = 4.7 Hz, C-Ar), 137.5 (q, J_{CF} = 2.4 Hz, C-Ar), 144.1 (C-Ar), 155.4 (C-Ar), 167.8 (C=O); HRMS calcd. for $C_{16}H_{12}F_3N_6O$ (ES+) m/z 361.1019 $[M+H]^+$, found 361.1023.

Note: Unable to visualise all carbon environments by ^{13}C NMR.

Methyl 2-methoxy-5-nitrobenzoate (405)[278]

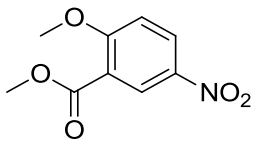

Sodium hydride dispersion in mineral oil (0.140 g, 60%, 3.48 mmol) was added to dry methanol (20 ml) sowly. Once the reaction had subsided, methyl 2-chloro-5-nitrobenzoate (0.503 g, 2.32 mmol) was added and the reaction mixture was heated at 50 °C for 4 h. The solvent was removed *in vacuo* and the resultant residue was dissolved in EtOAc (20 ml) and washed with brine (20 ml). The organic phase was dried ($MgSO_4$) and evaporated to dryness, and the crude product was purified using chromatography on silica gel (7:3 Petrol/EtOAc). The target compound was acquired as an off-white solid on cooling (0.344 g, 1.63 mmol, 70%). R_f 0.39 (7:3 Petrol/EtOAc); M.p. 99-101 °C (Lit.[278] 99-100 °C); λ_{max} (EtOH/nm) 219, 299; IR (cm^{-1}) 3391, 3088, 2959, 2849, 1703, 1609, 1585, 1512; ^{1}H NMR (500 MHz, DMSO-d_6) 3.85 (3H, s, Ar-OCH$_3$), 3.99 (3H, s, -CO$_2$CH$_3$), 7.41 (1H, d, J = 9.2 Hz, H-3), 8.44 (1H, dd, J = 3.0 and 9.2 Hz, H-4), 8.49 (1H, d, J = 3.0 Hz, H-6); ^{13}C NMR (125 MHz, DMSO-d_6) 52.5 (OCH$_3$), 57.0 (OCH$_3$), 113.5 (C-Ar), 120.2 (C-Ar), 126.4 (C-Ar), 129.0 (C-Ar), 139.9 (C-Ar), 163.0 (quat-C), 164.2 (quat-C); LRMS (ES+) m/z 212.1 $[M+H]^+$.

Methyl 5-amino-2-methoxybenzoate (406)[279]

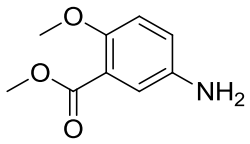

The nitro compound **405** (0.854 g, 4.04 mmol) and iron powder (2.26 g, 40.4 mmol) were reacted in acetic acid (40 ml) according to **general procedure T**. Silica gel chromatography (1:1 Petrol/EtOAc) gave the desired compound as a pale yellow oil (0.735 g, 3.88 mmol, 96%). R_f 0.37 (1:1 Petrol/EtOAc); λ_{max} (EtOH/nm) 218, 341; IR (cm^{-1}) 3428, 3360, 3237, 2950, 2836, 1712, 1628, 1500; ^{1}H NMR (500 MHz, $CDCl_3$) 3.85 (3H, s, OCH_3), 3.89 (3H, s, OCH_3), 6.84 (2H, s, Ar-NH_2), 7.16-7.20 (2H, m, H-3/H-4), 7.28-7.31 (1H, m, H-6); ^{13}C NMR (125 MHz, $CDCl_3$) 52.1 (OCH_3), 56.8 (OCH_3), 114.1 (C-Ar), 118.2 (C-Ar), 120.4 (C-Ar), 139.5 (C-Ar), 152.4 (C-Ar), 166.8 (C-Ar), 176.0 (C=O); LRMS (ES+) *m*/*z* 182.1 $[M+H]^+$.

5-Amino-2-methoxy-*N*-methylbenzamide (407)

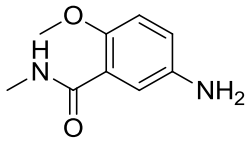

Methyl ester **406** (0.660 g, 3.64 mmol) and methylamine (40% aqueous solution, 30 ml) were reacted according to **general procedure S**. Purification by chromatography on silica (9:1 DCM/MeOH) gave the target compound as a pale yellow oil (0.480 g, 2.66 mmol, 73%). R_f 0.44 (9:1 DCM/MeOH); λ_{max} (EtOH/nm) 218, 335; IR (cm^{-1}) 3335, 3242, 2942, 2833, 1640, 1606, 1541; ^{1}H NMR (500 MHz, DMSO-d_6) 2.78 (3H, d, *J* = 4.7 Hz, NHCH_3), 3.76 (3H, s, OCH_3), 4.81 (2H, s, Ar-NH_2), 6.66 (1H, dd, *J* = 3.0 and 8.6 Hz, H-4), 6.84 (1H, d, *J* = 8.6 Hz, H-3), 7.10 (1H, d, *J* = 3.0 Hz, H-6), 8.09 (1H, q, *J* = 4.7 Hz, N*H*CH_3); ^{13}C NMR (125 MHz, DMSO-d_6) 26.2 (NH*C*H_3), 56.2 (OCH_3), 113.3 (C-Ar), 115.8 (C-Ar), 117.3 (C-Ar), 122.9 (C-Ar), 142.4 (C-Ar), 148.4 (C-Ar), 165.6 (C=O); HRMS calcd. for $C_9H_{13}N_2O_2$ (ES+) *m*/*z* 181.0972 $[M+H]^+$, found 181.0971.

2-Methoxy-*N*-methyl-5-((6-((triisopropylsilyl)ethynyl)-9*H*-purin-2-yl) amino)benzamide (408)

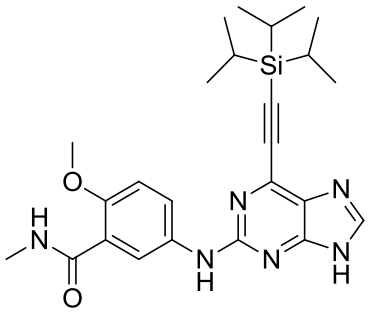

2-Fluoropurine **160** (0.196 g, 0.62 mmol), aniline **407** (0.222 g, 1.23 mmol) and TFA (120 µl, 1.54 mmol) were reacted in TFE (6 ml) according to **general procedure V**. Purification by KP-NH silica chromatography (19:1 DCM/MeOH) afforded the target compound as a yellow oil/gum (0.136 g, 0.28 mmol, 45%). R_f 0.45 (19:1 DCM/MeOH, KP-NH); λ_{max} (EtOH/nm) 240, 277, 379; IR (cm^{-1}) 3394, 3275, 3102, 2943, 2864, 1645, 1607, 1573, 1536; ^{1}H NMR (500 MHz, DMSO-d_6) 1.13-1.20 (21H, m, Si(C*H*(CH_3)$_2$)$_3$), 2.80 (3H, d, *J* = 4.5 Hz, NHCH_3), 3.85 (3H, s, OCH_3), 7.06 (1H, d, *J* = 9.1 Hz, H-3'), 7.83 (1H, dd, *J* = 2.4 and 9.1 Hz, H-4'), 8.09 (1H, d, *J* = 2.4 Hz, H-6'), 8.13 (1H, q, *J* = 4.5 Hz, N*H*CH_3), 8.21 (1H, s, H-8), 9.61 (1H, s, C^2-NH), 13.08 (1H, br, H-9); ^{13}C NMR (125 MHz, DMSO-d_6) 10.6 (Si(*C*H(CH_3)$_2$)$_3$), 18.4 (Si(CH(*C*H_3)$_2$)$_3$), 26.3 (NH*C*H_3), 56.0 (OCH3), 97.7 (*C*≡C-Si), 101.8 (C≡*C*-Si), 112.1 (C-Ar), 121.0 (C-Ar), 122.3 (C-Ar), 123.3 (C-Ar), 134.0 (C-Ar), 139.9 (C-Ar), 142.5 (C-Ar), 151.5 (C-Ar), 156.4 (C-Ar), 165.5 (C=O); HRMS calcd. for $C_{25}H_{35}N_6O_2Si$ (ES+) *m/z* 479.2585 $[M+H]^+$, found 479.2581.

Note: Unable to visualise all carbon environments by ^{13}C NMR.

2-Methoxy-5-((6-ethynyl-9*H*-purin-2-yl)amino)-*N*-methylbenzamide (387)

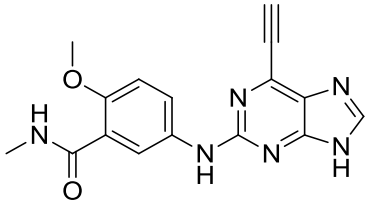

The TIPS-protected purine **408** (0.122 g, 0.25 mmol), TBAF (1M in THF, 0.31 ml, 0.31 mmol) and the TBAF scavenger bead system **231** (1.20 g, 10 x w/w) were reacted in THF (5 ml) according to **general procedure U**. Silica gel chromatography (9:1 DCM/MeOH)

afforded the desired compound as a yellow solid (49 mg, 0.15 mmol, 61%). R_f 0.27 (9:1 DCM/MeOH); M.p. 290-310 °C (decomposed); λ_{max} (EtOH/nm) 237.0, 275.0, 346.5; IR (cm^{-1}) 3364, 3167, 3010, 2104, 1636, 1608, 1540, 1492; ^{1}H NMR (500 MHz, DMSO-d_6) 2.81 (3H, d, *J* = 4.6 Hz, NHC*H*$_3$), 3.86 (3H, s, OCH_3), 4.83 (1H, s, C≡CH), 7.09 (1H, d, *J* = 9.0 Hz, H-3'), 7.87 (1H, dd, *J* = 2.8 and 9.0 Hz, H-4'), 8.06 (1H, d, *J* = 2.8 Hz, H-6'), 8.15 (1H, q, *J* = 4.6 Hz, N*H*CH_3), 8.25 (1H, s, H-8), 9.55 (1H, s, C^2-NH), 13.12 (1H, br, H-9); ^{13}C NMR (125 MHz, DMSO-d_6) 26.3 ($NHCH_3$), 55.0 (OCH_3), 79.0 (*C*≡CH), 86.9 (C≡*C*H), 112.1 (C-Ar), 121.1 (C-Ar), 122.4 (C-Ar), 123.1 (C-Ar), 133.9 (C-Ar), 151.6 (C-Ar), 156.5 (C-Ar), 165.5 (C=O); HRMS calcd. for $C_{16}H_{15}N_6O_2$ (ES+) *m*/*z* 323.1251 $[M+H]^+$, found 323.1258.

Note: Unable to visualise all carbon environments by ^{13}C NMR.

Methyl 2-cyano-5-nitrobenzoate (409)

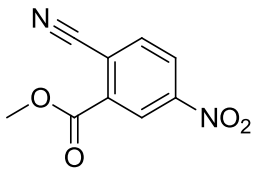

Methyl 2-chloro-5-nitrobenzoate (100 mg, 0.46 mmol), zinc cyanide (30 mg, 0.26 mmol), zinc powder (6 mg, 0.09 mmol) and bis(tri-*tert*-butylphosphino)palladium(0) (28 mg, 0.05 mmol) were suspended in DMA (3 ml) in a sealed vial and the mixture was degassed for 15 min. The reaction mixture was heated at 95 °C for 1 h, before sat. $NaHCO_3$ solution (2 ml) was added. The mixture was extracted with EtOAc (2 x 10 ml) and the combined organic extracts were washed with brine (10 ml), dried ($MgSO_4$) and evaporated to dryness. Purification of the crude residue by chromatography on silica (4:1 Petrol/EtOAc) gave the target compound as an off-white solid (90 mg, 0.44 mmol, 96%). R_f 0.34 (4:1 Petrol/EtOAc); M.p. 143-146 °C; λ_{max} (EtOH/nm) 214, 257; IR (cm^{-1}) 3114, 3051, 2964, 2868, 2235, 1725, 1606, 1533; ^{1}H NMR (500 MHz, DMSO-d_6) 3.99 (3H, s, OCH_3), 8.34 (1H, d, *J* = 8.4 Hz, H-3), 8.60 (1H, dd, *J* = 2.4 and 8.5 Hz, H-4), 8.71 (1H, d, *J* = 2.4 z, H-6); ^{13}C NMR (125 MHz, DMSO-d_6) 53.4 (OCH_3), 116.0 (quat-C), 116.9 (quat-C), 125.1 (C-Ar), 127.7 (C-Ar), 133.6 (C-Ar), 136.9 (C-Ar), 149.5 (C-Ar), 162.5 (C=O); LRMS (ES+) *m*/*z* 207.1 $[M+H]^+$.

Note: Unable to differentiate cyano ^{13}C NMR signal from aromatic carbon.

Methyl 5-amino-2-cyanobenzoate (410)

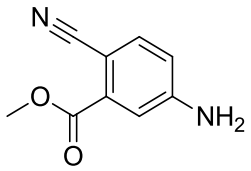

The nitro compound **409** (0.648 g, 3.14 mmol) and iron powder (1.75 g, 31.4 mmol) were reacted in acetic acid (30 ml) according to **general procedure T**. Silica gel chromatography (1:1 Petrol/EtOAc) gave the desired compound as an off-white solid (0.470 g, 2.67 mmol, 85%). R_f 0.45 (1:1 Petrol/EtOAc); M.p. 173-176 °C; λ_{max} (EtOH/nm) 233, 286, 341; IR (cm^{-1}) 3458, 3363, 3237, 2957, 2208, 1711, 1639, 1597; ^{1}H NMR (500 MHz, DMSO-d_6) 3.86 (3H, s, OCH_3), 6.45 (2H, s, Ar-NH_2), 6.80 (1H, dd, J = 2.4 and 8.4 Hz, H-4), 7.24 (1H, d, J = 2.4 Hz, H-6), 7.54 (1H, d, J = 8.4 Hz, H-3); ^{13}C NMR (125 MHz, DMSO-d_6) 95.6 (C-Ar), 115.1 (C-Ar), 116.3 (C-Ar), 119.0 (C-Ar), 132.9 (C≡N), 136.2 (C-Ar), 152.7 (C-Ar), 164.7 (C=O); HRMS calcd. for $C_9H_9N_2O_2$ (ES+) m/z 177.0659 $[M+H]^+$, found 177.0658.

(*E*)-6-Amino-2-methyl-3-(methylimino)isoindolin-1-one (413)

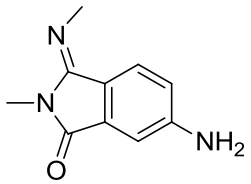

Methylamine (40% aqueous solution, 10 ml) was added to methyl ester **410** (0.163 g, 0.93 mmol) and the resultant red solution was stirred at RT for 18 h. Removal of the solvent *in vacuo*, followed by silica gel chromatography (9:1 DCM/MeOH) gave the undesired compound as a pale yellow solid (0.131 g, 0.69 mmol, 74%). R_f 0.33 (9:1 DCM/MeOH); M.p. 187-190 °C; λ_{max} (EtOH/nm) 243, 271, 356; IR (cm^{-1}) 3418, 3332, 3218, 2917, 2868, 1704, 1649, 1615; ^{1}H NMR (500 MHz, DMSO-d_6) 3.01 (3H, s, amide N-CH_3), 3.53 (3H,s, imine N-CH_3), 6.13 (2H, s, Ar-NH_2), 6.80 (1H, dd, J = 2.2 and 8.4 Hz, H-5), 6.92 (1H, d, J = 2.2 Hz, H-7), 7.77 (1H, d, J = 8.4 Hz, H-4); ^{13}C NMR (125 MHz, DMSO-d_6) 24.5 (Amide N-CH3), 37.2 (Imine N-CH3), 106.8 (C-Ar), 116.0 (C-Ar), 116.4 (C-Ar), 127.3 (C-Ar), 134.4 (C-Ar), 152.2, 152.8, 167.2 (C=O); HRMS calcd. for $C_{10}H_{12}N_3O$ (ES+) m/z 190.0975 $[M+H]^+$, found 190.0975.

Note: Unable to distinguish ^{13}C NMR signals at 152.2 and 152.8.

(*E*)-6-((9-(4-Methoxybenzyl)-6-((triisopropylsilyl)ethynyl)-9*H*-purin-2-yl) amino)-2-methyl-3-(methylimino)isoindolin-1-one (416)

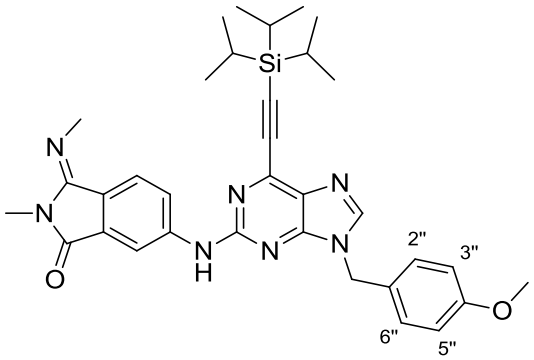

The 2-iodopurine **278** (0.310 g, 0.57 mmol), aniline **413** (0.128 g, 0.48 mmol), $Pd_2(dba)_3$ (55 mg, 0.06 mmol), XPhos (29 mg, 0.06 mmol) and K_2CO_3 (0.173 g, 1.25 mmol) were reacted in MeCN (6 ml) according to **general procedure M**. Silica gel chromatography (1:1 Petrol/EtOAc) gave the target compound as a pale yellow oil/gum (0.190 g, 0.31 mmol, 54%). R_f 0.39 (1:1 Petrol/EtOAc); λ_{max} (EtOH/nm) 281, 352; IR (cm^{-1}) 3298, 2942, 2864, 1725, 1661, 1577, 1543; ^{1}H NMR (500 MHz, DMSO-d_6) 1.12-1.22 (21H, m, Si(C*H*(C*H*$_3$)$_2$)$_3$), 3.09 (3H, s, amide N-CH_3), 3.64 (3H, s, imine N-CH_3), 3.70 (3H, s, OCH_3), 5.36 (2H, s, N^9-CH_2), 6.92 (2H, d, *J* = 8.6 Hz, H-3''/H-5''), 7.47 (2H, d, *J* = 8.6 Hz, H-2''/H-6''), 8.01-8.08 (2H, m, H-4'/H-5'), 8.48-8.52 (1H, m, H-7'), 8.54 (1H, s, H-8), 10.48 (1H, s, C^2-NH); ^{13}C NMR (125 MHz, DMSO-d_6) 10.6 (Si(*C*H(CH$_3$)$_2$)$_3$), 18.4 (Si(CH(*C*H$_3$)$_2$)$_3$), 24.7 (amide N-CH_3), 37.4 (imine N-CH_3), 42.2 (N^9-CH_2), 55.1 (OCH_3), 99.2 (C≡C), 101.2 (C≡C), 111.4 (C-Ar), 114.1 (C-Ar), 121.2 (C-Ar), 126.7 (C-Ar), 128.2 (C-Ar), 129.5 (C-Ar), 129.6 (C-Ar), 133.6 (C-Ar), 140.3 (C-Ar), 143.9 (C-Ar), 145.1 (C-Ar), 152.2, 152.4, 155.3 (C-Ar), 158.9 (C-Ar), 166.9 (C=O); HRMS calcd. for $C_{34}H_{42}N_7O_2Si$ (ES+) *m*/*z* 608.3164 $[M+H]^+$, found 608.3159.

Note: Unable to distinguish ^{13}C NMR signals at 152.2 and 152.4.

(*E*)-2-Methyl-3-(methylimino)-6-((6-((triisopropylsilyl)ethynyl)-9*H*-purin-2-yl) amino)isoindolin-1-one (417)

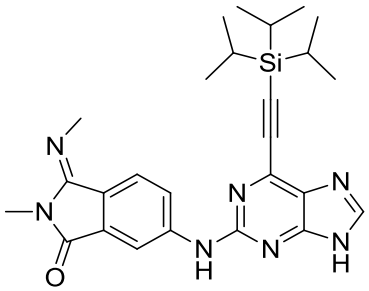

The PMB-protected purine **416** (0.144 g, 0.24 mmol) and TFA (5 ml) were reacted according to **general procedure K**. Purification on silica gel (19:1 DCM/MeOH) gave the desired compound as a yellow oil/gum (90 mg, 0.18 mmol, 75%). R_f 0.55 (19:1 DCM/MeOH); λ_{max} (EtOH/nm) 282, 370; IR (cm^{-1}) 3344, 3071, 2943, 2865, 1712, 1659, 1598, 1577, 1547; ^1H NMR (500 MHz, DMSO-d_6) 1.13-1.23 (21H, m, Si(C*H*(C*H*$_3$)$_2$)$_3$), 3.08 (3H, s, amide N-CH_3), 3.63 (3H, s, imine N-CH_3), 7.98 (1H, dd, *J* = 2.0 and 8.5 Hz, H-5'), 8.05 (1H, d, *J* = 8.5 Hz, H-4'), 8.35 (1H, br, H-8), 8.50 (1H, d, *J* = 2.0 Hz, H-7'), 10.39 (1H, s, C^2-NH), 13.39 (1H, br, H-9); ^{13}C NMR (125 MHz, DMSO-d_6) 10.6 (Si(*C*H(CH$_3$)$_2$)$_3$), 18.4 (Si(CH(*C*H$_3$)$_2$)$_3$), 24.7 (amide N-CH_3), 37.4 (imine N-CH_3), 98.6 (C≡C), 111.1 (C-Ar), 115.1 (C-Ar), 121.2 (C-Ar), 126.7 (C-Ar), 133.6 (C-Ar), 144.2 (C-Ar), 152.2 (C=N), 155.4 (C-Ar), 167.0 (C=O); HRMS calcd. for $C_{26}H_{34}N_7OSi$ (ES+) *m/z* 488.2589 $[M+H]^+$, found 488.2583.

Note: Unable to visualise all carbon environments by ^{13}C NMR.

(*E*)-6-((6-Ethynyl-9*H*-purin-2-yl)amino)-2-methyl-3-(methylimino) isoindolin-1-one (418)

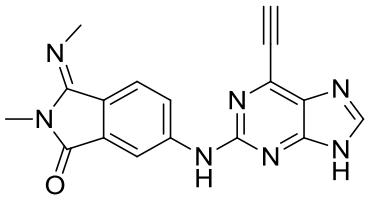

The TIPS-protected purine **417** (76 mg, 0.16 mmol), TBAF (1M in THF, 0.19 ml, 1M, 0.19 mmol) and the TBAF scavenger bead system **231** (0.80 g, 10 x w/w) were reacted in THF (4 ml) according to **general procedure U**. Silica gel chromatography (9:1 DCM/MeOH) afforded the target compound as a yellow solid (27 mg, 0.08 mmol, 53%). R_f 0.34 (9:1 DCM/MeOH); M.p. 280-300 °C (decomposed); λ_{max} (EtOH/nm) 286, 347; IR (cm^{-1}) 3253,

3062, 2957, 2922, 2700, 2116, 1720, 1653, 1606; ^{1}H NMR (500 MHz, DMSO-d_6) 3.08 (3H, s, amide N-CH_3), 3.63 (3H, s, imine N-CH_3), 4.92 (1H, s, C≡CH), 8.02 (1H, dd, *J* = 1.8 and 8.5 Hz, H-5'), 8.07 (1H, d, *J* = 8.5 Hz, H-4'), 8.39 (1H, s, H-8), 8.44 (1H, d, *J* = 1.8 Hz, H-7'), 10.34 (1H, s, C^2-NH), 13.45 (1H, br, H-9); ^{13}C NMR (125 MHz, DMSO-d_6) 24.7 (amide N-CH3), 37.4 (imine N-CH3), 78.7 (C≡C), 87.6 (C≡C), 111.2 (C-Ar), 121.0 (C-Ar), 121.2 (C-Ar), 126.8 (C-Ar), 133.6 (C-Ar), 144.1 (C-Ar), 152.2 (C=N), 155.3 (C-Ar), 167.0 (C=O); HRMS calcd. for $C_{17}H_{14}N_7O$ (ES+) *m*/*z* 332.1254 $[M+H]^+$, found 332.1255.

Note: Unable to visualise all carbon environments by ^{13}C NMR.

2-Cyano-5-nitrobenzoic acid (420)

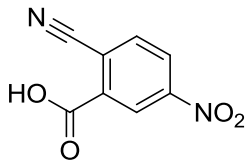

NaOH solution (2.6 ml, 1M, 2.6 mmol) was added to a suspension of the methyl ester **409** (0.502 g, 2.43 mmol) in methanol (7.5 ml). After stirring at RT for 30 min, the resultant suspension was filtered, and the filtrate diluted with water (15 ml). The filtrate was washed with EtOAc (15 ml), before being adjusted to pH 3-4 with 2M HCl. The solution was extracted with EtOAc (2 x 20 ml), and the combined organic extracts were dried (MgSO4) and concentrated *in vacuo*. The resultant solid was combined with the filtrand from the reaction mixture and dried in a vacuum oven. The target compound was obtained as an off-white solid (0.359 g, 1.87 mmol, 77%). R_f 0.22 (7:3 DCM/MeOH, 0.1% AcOH); M.p. >350 °C; λ_{max} (EtOH/nm) 261; IR (cm^{-1}) 3514, 3329, 3240, 3101, 2243, 1608, 1520; ^{1}H NMR (500 MHz, DMSO-d_6) 8.04 (1H, d, *J* = 8.4 Hz, H-3), 8.30 (1H, dd, *J* = 2.4 and 8.4 Hz, H-4), 8.67 (1H, d, *J* = 2.4 Hz, H-6); ^{13}C NMR (125 MHz, DMSO-d_6) 116.9 (quat-C), 118.0 (quat-C), 123.8 (C-Ar), 124.4 (C-Ar), 135.4 (C-Ar), 145.1 (C-Ar), 149.1 (C-Ar), 163.9 (C=O); HRMS calcd. for $C_8H_3N_2O_4$ (ES+) *m*/*z* 191.0098 $[M+H]^+$, found 191.0097.

2-Cyano-*N*,*N*-dimethyl-5-nitrobenzamide (421)

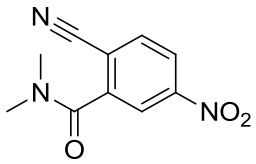

The carboxylic acid **420** (0.500 g, 2.57 mmol), dimethylamine hydrochloride (0.251 g, 3.09 mmol), EDC (0.740 g, 3.86 mmol), HOBt (0.453 g, 3.35 mmol) and DIPEA (0.54 ml, 3.09 mmol) were combined in dry DMF (30 ml) and stirred at RT under N_2 for 18 h. The solvent was removed under reduced pressure and the residue was dissolved in water (50 ml) and extracted with DCM (3 x 50 ml). The combined organic extracts were dried through a phase separator, evaporated to dryness, and the crude residue purified by chromatography on silica (1:1 Petrol/EtOAc) to give the target compound as a pale yellow solid (0.522 g, 2.38 mmol, 92%). R_f 0.42 (1:1 Petrol/EtOAc); M.p. 199-202 °C; λ_{max} (EtOH/nm) 253; IR (cm^{-1}) 3096, 3032, 2940, 2234, 1633, 1531; ^{1}H NMR (500 MHz, DMSO-d_6) 2.88 (3H, s, N-CH_3), 3.07 (3H, s, N-CH_3), 8.27 (1H, d, *J* = 9.0 Hz, H-3), 8.41-8.44 (2H, m, H-4/H-6); ^{13}C NMR (125 MHz, DMSO-d_6) 34.6 (N-CH_3), 38.3 (N-CH_3), 114.5 (C-Ar), 115.7 (C≡N), 122.3 (C-Ar), 124.4 (C-Ar), 135.3 (C-Ar), 141.9 (C-Ar), 149.8 (C-Ar), 164.8 (C=O); HRMS calcd. for $C_{10}H_{10}N_3O_3$ (ES+) *m*/*z* 220.0717 $[M+H]^+$, found 220.0714.

5-Amino-2-cyano-*N*,*N*-dimethylbenzamide (422)

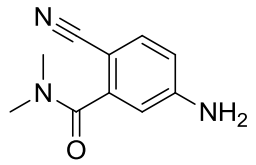

The nitro compound **421** (0.492 g, 2.24 mmol) and iron powder (1.25 g, 22.4 mmol) were reacted in acetic acid (20 ml) according to **general procedure T**. Chromatography on silica gel (19:1 DCM/MeOH) gave the desired compound as an off-white solid (0.333 g, 1.76 mmol, 79%). R_f 0.40 (19:1 DCM/MeOH); M.p. 174-176 °C; λ_{max} (EtOH/nm) 282; IR (cm^{-1}) 3389, 3345, 3222, 2208, 1659, 1592, 1561; ^{1}H NMR (500 MHz, DMSO-d_6) 2.84 (3H, s, N-CH_3), 2.99 (3H, s, N-CH_3), 6.34 (2H, br, Ar-NH_2), 6.50 (1H, d, *J* = 2.2 Hz, H-6), 6.63 (1H, dd, *J* = 2.2 and 8.6 Hz, H-4), 7.45 (1H, d, *J* = 8.6 Hz, H-3); ^{13}C NMR (125 MHz, DMSO-d_6) 34.2 (N-CH_3), 37.9 (N-CH_3), 92.7 (C-Ar), 110.8 (C-Ar), 113.4 (C-Ar), 118.7 (C≡N), 134.2

(C-Ar), 142.0 (C-Ar), 152.9 (C-Ar), 167.5 (C=O); HRMS calcd. for $C_{10}H_{12}N_3O$ (ES+) *m*/*z* 190.0975 $[M+H]^+$, found 190.0976.

2-Cyano-5-((9-(4-methoxybenzyl)-6-((triisopropylsilyl)ethynyl)-9*H*-purin-2-yl)amino)-*N*,*N*-dimethylbenzamide (423)

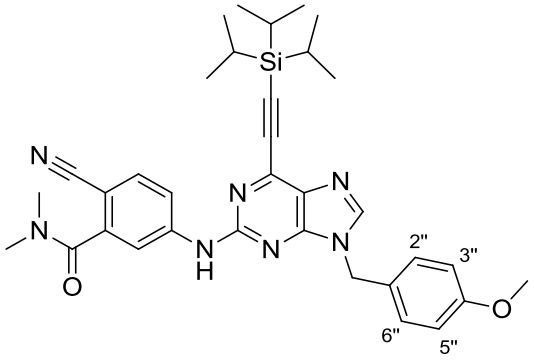

2-Iodopurine intermediate **278** (0.289 g, 0.53 mmol), aniline **422** (0.120 g, 0.63 mmol), $Pd_2(dba)_3$ (46 mg, 0.05 mmol), XPhos (24 mg, 0.05 mmol) and K_2CO_3 (0.160 g, 1.16 mmol) were reacted in MeCN (5 ml) according to **general procedure M**. Silica gel chromatography (1:1 Petrol/EtOAc) gave the desired compound as a yellow oil/gum (0.224 g, 0.37 mmol, 74%). R_f 0.40 (1:1 Petrol/EtOAc); λ_{max} (EtOH/nm) 226, 309; IR (cm^{-1}) 2942, 2864, 2221, 1635, 1586, 1514; ^{1}H NMR (500 MHz, DMSO-d_6) 1.14-1.22 (21H, m, Si(C*H*(CH_3)$_2$)$_3$), 2.89 (3H, s, N-CH_3), 3.06 (3H, s, N-CH_3), 3.72 (3H, s, OCH_3), 5.36 (2H, s, N^9-CH_2), 6.91 (2H, d, *J* = 8.7 Hz, H-3''/H-5''), 7.32 (2H, d, *J* = 8.7 Hz, H-2''/H-6''), 7.82 (1H, d, *J* = 8.6 Hz, H-3'), 7.90 (1H, dd, *J* = 2.1 and 8.6 Hz, H-4'), 8.05 (1H, d, *J* = 2.1 Hz, H-6'), 8.56 (1H, s, H-8), 10.55 (1H, s, C^2-NH); ^{13}C NMR (125 MHz, DMSO-d_6) 10.5 (Si(*C*H(CH_3)$_2$)$_3$), 18.4 (Si(CH(*C*H_3)$_2$)$_3$), 34.4 (N-CH_3), 38.2 (N-CH_3), 46.2 (N^9-CH_2), 55.1 (OCH_3), 99.3 (C≡C), 99.4 (C-Ar)), 101.1 (C≡C), 114.1 (C-Ar), 115.2 (C-Ar), 117.8 (C≡N), 118.0 (C-Ar), 128.2 (C-Ar), 129.0 (C-Ar), 129.8 (C-Ar), 133.9 (C-Ar), 140.2 (C-Ar), 141.3 (C-Ar), 144.9 (C-Ar), 145.6 (C-Ar), 152.4 (C-Ar), 154.9 (C-Ar), 158.9 (C-Ar), 167.1 (C=O); HRMS calcd. for $C_{34}H_{42}N_7O_2Si$ (ES+) *m*/*z* 608.3164 $[M+H]^+$, found 608.3160.

Appendix

Enzyme	MAPK APK2	AurA	PKCz	Rsk1	PRAK	Erk1	PKD2	CK1d	Chk1
% inhib.	6	0.078*	9	8	-3	8	3	8	11
Enzyme	ABL	FYN	LYN	Chk2	MET	LCK	SRC	GSK3β	Erk2
% inhib.	39	10	9	13	6	17	22	9	2
Enzyme	PKA	AKT2	INSR	P38α	AKT1	Msk1	Msk2	P38γ	PKD1
% inhib.	1	3	-3	-1	13	6	-6	-1	31
Enzyme	MARK 2	BMX	CSNK 1A1	PKD3	BRSK1	Nek2	PIM1	SGK2	SGK3
% inhib.	27	0.83*	5	26	12	0.088*	18	7	11
Enzyme	ARG	DCAM KL2	Rsk2	Rsk3	BRSK1	PKC-α	PKC-β1	PKC-γ	PKC-δ
% inhib.	32	-2	12	14	5	15	2	29	29
Enzyme	PKC-ε	PKC-η	PKC-θ						
% inhib.	8	17	35						

Table A1: Kinase inhibition following treatment with 1 µM **176** (NCL-00017509) for ProfilerPro® plates.

	Percentage activity remaining at 1 µM Inhibitor					
Kinase	**147**	**k_m**	**176**	**k_m**	**34**	**k_m**
MKK1	95	18	46	2	16	1
MKK2	103	4	75	8	15	0
MKK6	105	2	109	4	54	5
ERK1	102	1	105	13	79	9
ERK2	91	13	92	4	70	3
JNK1	82	6	67	10	85	10
JNK2	96	8	92	3	101	7
JNK3	89	2	111	18	91	6
p38a MAPK	110	7	103	12	106	3
p38b MAPK	85	5	94	2	86	3
p38g MAPK	99	10	100	18	97	6
p38d MAPK	96	3	129	14	105	0
ERK8	86	7	108	2	14	2

RSK1	95	15	84	5	7	0
RSK2	72	2	88	19	16	0
PDK1	87	12	63	1	35	10
PKBa	91	2	116	6	124	18
PKBb	75	27	98	4	110	23
SGK1	103	14	93	16	64	1
S6K1	98	5	102	16	25	2
PKA	90	10	108	0	100	10
ROCK 2	91	6	89	2	23	1
PRK2	103	14	99	6	16	3
PKCa	95	5	108	3	86	2
PKCγ	105	10	98	4	114	5
PKCz	104	7	104	1	94	6
GCK	78	3	71	8	14	1
MINK1	87	6	92	0	13	0
MLK1	54	24	40	11	9	2
MLK3	33	5	29	0	17	2
TAO1	115	13	101	7	95	5
ASK1	96	1	128	10	68	0
TAK1	50	0	37	4	31	16
IRAK1	83	9	92	4	33	6
IRAK4	86	6	85	3	24	1
RIPK2	89	3	93	1	44	1
OSR1	93	4	103	2	84	6
TTK	80	5	92	5	35	4
MPSK1	101	7	92	21	100	6
Src	91	7	100	5	56	10
Lck	110	16	113	1	59	5
CSK	102	12	79	7	82	2
YES1	108	7	92	6	29	3
ABL	87	8	70	16	87	21
BTK	63	11	95	8	87	10
JAK2	75	1	30	0	40	4
SYK	88	14	117	7	83	2
ZAP70	114	9	119	2	88	4
FGF-R1	97	3	74	9	84	17
HER4	61	14	87	10	126	11
IGF-1R	97	6	115	5	59	16
IR	85	17	86	1	9	0
IRR	87	3	92	5	67	1
TrkA	109	7	74	7	31	2
VEG-FR	97	22	64	5	9	1
EPH-A2	105	17	122	2	110	7
EPH-A4	106	15	107	8	105	7
EPH-B1	93	1	95	1	91	14
EPH-B2	106	13	104	15	108	9

EPH-B3	99	2	88	8	122	10
EPH-B4	104	22	108	12	118	11
BRSK1	93	17	110	8	12	3
BRSK2	95	2	103	11	12	0
MELK	93	6	115	1	10	5
NUAK1	72	26	17	3	10	3
CK1d	82	9	91	5	82	27
CK2	93	5	94	13	28	1
DYRK1A	93	2	107	11	3	0
DYRK2	90	4	112	12	6	2
DYRK3	89	6	113	4	6	1
NEK2a	4	1	11	0	9	2
NEK6	101	15	103	10	79	3
IKKb	72	13	118	10	84	1
IKKe	84	0	60	1	14	2
TBK1	91	23	51	7	10	0
PIM1	101	5	108	0	38	4
PIM2	103	15	106	7	95	13
PIM3	92	4	114	12	27	3
SRPK1	75	26	94	5	67	4
EF2K	106	12	107	6	96	4
EIF2AK3	96	6	100	7	96	8
HIPK1	105	29	57	7	32	5
HIPK2	94	8	115	6	22	4
HIPK3	99	15	107	6	29	7
CLK2	77	11	63	3	6	2
PAK2	96	9	102	6	92	19
PAK4	70	7	71	15	44	4
PAK5	93	13	84	6	103	27
PAK6	97	1	102	0	81	2
MST2	79	11	90	5	30	4
MST3	92	4			103	16
MST4	96	4	94	4	41	2
PKD1	104	18	120	13	43	4
STK33	74	9	72	10	34	7
MSK1	87	5	129	20	60	0
MNK1	91	18	110	1	116	45
MNK2	101	4	82	1	71	4
MAPKAP-K2	102	13	78	9	68	3
MAPKAP-K3	89	15	94	3	105	14
PRAK	101	15	103	8	30	5
CAMKKb	101	19	103	4	23	2
CAMK1	95	14	138	18	55	5
SmMLCK	97	15	107	1	9	0
PHK	89	9	126	6	6	2

DAPK1	93	5	85	4	13	1
CHK1	77	18	38	4	15	2
CHK2	73	10	59	4	31	0
GSK3b	87	0	100	10	30	6
CDK2-Cyclin A	83	7	96	10	46	1
PLK1	89	11	115	6	116	3
Aurora A	95	9	69	4	55	1
Aurora B	77	13	67	7	103	2
TLK1	95	5	96	0	90	9
LKB1	100	3	95	11	91	9
AMPK	83	2	60	1	6	0
MARK1	92	10	87	4	14	7
MARK2	93	12	95	3	100	4
MARK3	101	24	96	10	8	1
MARK4	90	3	89	9	27	1
TIE2	100	3	111	1	111	33
BRK	74	1	103	13	117	7
MEKK1	85	7	104	6	105	4
TTBK1	81	21	-	-	86	4
TESK1	89	15	-	-	97	0
WNK1	109	12	-	-	117	4
DDR2					107	11
CDK9-cyclin T1	79	4	-	-	106	4
SIK2	78	12	-	-	63	53
SIK3	88	0	-	-	33	5
TSSK1	79	8	-	-	16	2
CK1y2	83	0	-	-	56	11

Table A2: Kinase inhibition data for **147** (NCL-00016727) and **176** (NCL-00017509) and the literature irreversible Nek2 inhibitor **34** from the National Centre for Protein Kinase Profiling, Dundee University.

Bibliography

1. Chabner, B. A.; Roberts, T. G. Chemotherapy and the war on cancer. *Nat. Rev. Cancer* **2005**, 5, 65-72.

2. Krumbhaar, E. B.; Krumbhaar, H. D. The Blood and Bone Marrow in Yelloe Cross Gas (Mustard Gas) Poisoning. *J. Med. Res.* **1919**, 40, 497-508.

3. Gilman, e. a. The Biological Actions and Therapeutic Applications of the B-Chloroethyl Amines and Sulfides. *Science* **1946**, 103, 409-436.

4. Gilman, A. The initial clinical trial of nitrogen mustard. *Am. J. Surg.* **1963**, 105, 574-578.

5. Silverman, R. B. *The Organic Chemistry of Drug Design and Drug Action Second Edition*. Elsevier Academic Press: 2004.

6. Wills, L.; Clutterbuch, P.; Evans, B. D. F. A new factor in the production and cure of macrocytic anaemias and its relation to other haemopoietic principles curative in pernicious anaemia. *Biochem. J.* **1937**, 31, 2136-2147.

7. Li, M. C.; Hertz, R.; Bergenstal, D. M. Therapy of choriocarcinoma and related trophoblastic tumors with folic acid and purine antagonists. *N. Engl. J. Med.* **1958**, 259, 66-74.

8. Gottesman, M. M. Mechanisms of Cancer Drug Resistance. *Annu. Rev. Med.* **2002**, 53, 615-627.

9. Skipper, H. E.; Thomson, J. R.; Elion, G. B.; Hitchings, G. H. Observations on the anticancer activity of 6-mercaptopurine. *Cancer Res.* **1954**, 14, 294-298.

10. Longley, D. B.; Harkin, D. P.; Johnston, P. G. 5-Fluorouracil: Mechanisms of Action and Clinical Strategies. *Nat. Rev. Cancer* **2003**, 3, 330-338.

11. Bensch, K. G.; Malawista, S. E. Microtubule crystals: a new biophysical phenomenon induced by Vinca alkaloids. *Nature* **1968**, 218, 1176-1177.

12. He, L.; Jagtap, P. G.; Kingston, D. G. I.; Shen, H.-J.; Orr, G. A.; Horwitz, S. B. A Common Pharmacophore for Taxol and the Epothilones Based on the Biological Activity of a Taxane Molecule Lacking a C-13 Side Chain†. *Biochemistry* **2000**, 39, 3972-3978.

13. Frei, E. The effectiveness of combinations of antileukemic agents in inducing and maintaining remission in children with acute leukemia. *Blood* **1965**, 26, 642-656.

14. Devita, V. T.; Serpick, A. A.; Carbone, P. P. Combination chemotherapy in the treatment of advanced Hodgkin's disease. *Ann. Intern. Med.* **1970**, 73, 881-895.

15. Rosenberg, B.; Vancamp, L.; Krigas, T. Inhibition of cell division in Escherichia coli by electrolysis products from a platinum electrode. *Nature* **1965**, 205, 698-699.

16. Evans, B. D.; Raju, K. S.; Calvert, A. H.; Harland, S. J.; Wiltshaw, E. Phase II study of JM8, a new platinum analog, in advanced ovarian carcinoma. *Cancer Treat. Rep.* **1983**, 67, 997-1000.

17. Minocha, A.; Long, B. H. Inhibition of the DNA catenation activity of type II topoisomerase by VP16-213 and VM26. *Biochem. Biophys. Res. Commun.* **1984**, 122, 165-170.

18. Sawyers, C. Targeted cancer therapy. *Nature* **2004**, 432, 294-297.

19. Hanahan, D.; Weinberg, Robert A. Hallmarks of Cancer: The Next Generation. *Cell* **2011**, 144, 646-674.

20. Yokota, J. Tumor progression and metastasis. *Carcinogenesis* **2000**, *21*, 497-503.

21. Hanahan, D.; Weinberg, R. A. The hallmarks of cancer. *Cell* **2000**, 100, 57-70.

22. Bhowmick, N. A.; Neilson, E. G.; Moses, H. L. Stromal Fibroblasts in Cancer Initiation and Progression. *Nature* **2004**, 432, 332-337.

23. Zwick, E.; Bange, J.; Ullrich, A. Receptor tyrosine kinase signalling as a target for cancer intervention strategies. *Endocr-Relat. Cancer* **2001**, 8, 161-73.

24. Sherr, C. J. Principles of Tumor Suppression. *Cell* **2004**, 116, 235-246.

25. Evan, G.; Littlewood, T. A Matter of Life and Cell Death. *Science* **1998**, 281, 1317-1322.

26. Hollstein, M.; Sidransky, D.; Vogelstein, B.; Harris, C. C. p53 mutations in human cancers. *Science* **1991**, 253, 49-53.

27. Adams, J. M.; Cory, S. The Bcl-2 apoptotic switch in cancer development and therapy. *Oncogene* **2007**, 26, 1324-1337.

28. Hanahan, D.; Folkman, J. Patterns and emerging mechanisms of the angiogenic switch during tumorigenesis. *Cell* **1996**, 86, 353-364.

29. Carmeliet, P. VEGF as a key mediator of angiogenesis in cancer. *Oncology* **2005**, 69, 4-10.

30. Blasco, M. A. Telomeres and human disease: ageing, cancer and beyond. *Nat. Rev. Genet.* **2005**, 6, 611-622.

31. Cavallaro, U.; Christofori, G. Cell adhesion and signalling by cadherins and Ig-CAMs in cancer. *Nat. Rev. Cancer* **2004**, 4, 118-132.

32. Futreal, P. A.; Coin, L.; Marshall, M.; Down, T.; Hubbard, T.; Wooster, R.; Rahman, N.; Stratton, M. R. A census of human cancer genes. *Nat. Rev. Cancer* **2004**, 4, 177-183.

33. Nowell, P. C.; Hungerford, D. A. A minute chromosome in human chronic granulocytic leukemia. *Science* **1960**, 132.

34. Capdeville, R.; Buchdunger, E.; Zimmermann, J.; Matter, A. Glivec (STI571, imatinib), a rationally developed, targeted anticancer drug. *Nat. Rev. Drug Discov.* **2002**, 1, 493-502.

35. Druker, B. J. Efficacy and safety of a specific inhibitor of the BCR-ABL tyrosine kinase in chronic myeloid leukemia. *N. Engl. J. Med.* **2001**, 344, 1031-1037.

36. Roninson, I. B. Isolation of human mdr DNA sequences amplified in multidrug-resistant KB carcinoma cells. *Proc. Natl. Acad. Sci. USA* **1986**, 83, 4538-4542.

37. Hurwitz, H. Bevacizumab plus irinotecan, fluorouracil, and leucovorin for metastatic colorectal cancer. *N. Engl. J. Med.* **2004**, 350, 2335-2342.

38. Slamon, D. J. Use of chemotherapy plus a monoclonal antibody against HER2 for metastatic breast cancer that overexpresses HER2. *N. Engl. J. Med.* **2001**, 344, 783-792.

39. Lynch, T. J. Activating mutations in the epidermal growth factor receptor underlying responsiveness of non-small-cell lung cancer to gefitinib. *N. Engl. J. Med.* **2004**, 350, 2129-2139.

40. Paez, J. G. EGFR mutations in lung cancer: correlation with clinical response to gefitinib therapy. *Science* **2004**, 304, 1497-1500.

41. Alberts, B.; Johnson, A.; Lewis, J.; Raff, M.; Roberts, K.; Walter, P. *Molecular Biology of the Cell*. Garland Science: New York, 2008.

42. Murray, A.; Hunt, T. *The Cell Cycle*. Oxford University Press: New York, 1993.

43. Malumbres, M.; Barbacid, M. Cell cycle kinases in cancer. *Curr. Opin. Genet. Dev.* **2007**, 17, 60-65.

44. Johnson, L. Protein kinases and their therapeutic explotation. *Biochem. Soc. Trans.* **2007**, 35, 7-11.

45. Zhang, J.; Yang, P. L.; Gray, N. S. Targeting cancer with small molecule kinase inhibitors. *Nat. Rev. Cancer* **2009**, 9, 28-39.

46. Fedorov, O.; Sundström, M.; Marsden, B.; Knapp, S. Insights for the development of specific kinase inhibitors by targeted structural genomics. *Drug Discovery Today* **2007**, 12, 365-372.

47. Malumbres, M.; Barbacid, M. Cell cycle, CDKs and cancer: a changing paradigm. *Nat. Rev. Cancer* **2009**, 9, 153-166.

48. Malumbres, M.; Barbacid, M. To cycle or not to cycle: A critical decision in cancer. *Nat. Rev. Cancer* **2001**, 1, 222-231.

49. Crasta, K.; Surana, U. Disjunction of conjoined twins: Cdk1, Cdh1 and separation of centrosomes. *Cell Div.* **2006**, 1, 12.

50. Ortega, S.; Prieto, I.; Odajima, J.; Martin, A.; Dubus, P.; Sotillo, R.; Barbero, J. L.; Malumbres, M.; Barbacid, M. Cyclin-dependent kinase 2 is essential for meiosis but not for mitotic cell division in mice. *Nat. Genet.* **2003**, 35, 25-31.

51. Rane, S. G.; Dubus, P.; Mettus, R. V.; Galbreath, E. J.; Boden, G.; Reddy, E. P.; Barbacid, M. Loss of Cdk4 expression causes insulin-deficient diabetes and Cdk4 activation results in [beta]-islet cell hyperplasia. *Nat. Genet.* **1999**, 22, 44-52.

52. Malumbres, M.; Sotillo, R. o.; Santamaría, D.; Galán, J.; Cerezo, A.; Ortega, S.; Dubus, P.; Barbacid, M. Mammalian Cells Cycle without the D-Type Cyclin-Dependent Kinases Cdk4 and Cdk6. *Cell* **2004**, 118, 493-504.

53. Berthet, C.; Aleem, E.; Coppola, V.; Tessarollo, L.; Kaldis, P. Cdk2 Knockout Mice Are Viable. *Curr. Biol. : CB* **2003**, 13, 1775-1785.

54. Kærn, M.; Hunding, A. Dynamics of the Cell Cycle Engine: Cdk2-kinase and the Transition into Mitosis. *J. Theor. Biol.* **1998**, 193, 47-57.

55. Jablonska, B.; Aguirre, A.; Vandenbosch, R.; Belachew, S.; Berthet, C.; Kaldis, P.; Gallo, V. Cdk2 is critical for proliferation and self-renewal of neural progenitor cells in the adult subventricular zone. *J. Cell Biol.* **2007**, 179, 1231-1245.

56. van den Heuvel, S.; Harlow, E. Distinct Roles for Cyclin-Dependent Kinases in Cell Cycle Control. *Science* **1993**, 262, 2050-2054.

57. Harbour, J. W.; Luo, R. X.; Santi, A. D.; Postigo, A. A.; Dean, D. C. Cdk Phosphorylation Triggers Sequential Intramolecular Interactions that Progressively Block Rb Functions as Cells Move through G1. *Cell* **1999**, 98, 859-869.

58. Malumbres, M.; Barbacid, M. Is Cyclin D1-CDK4 kinase a bona fide cancer target? *Cancer Cell* **2006**, 9, 2-4.

59. Liu, Q.; Guntuku, S.; Cui, X.-S.; Matsuoka, S.; Cortez, D.; Tamai, K.; Luo, G.; Carattini-Rivera, S.; DeMayo, F.; Bradley, A.; Donehower, L. A.; Elledge, S. J. Chk1 is an essential kinase that is regulated by Atr and required for the G2/M DNA damage checkpoint. *Gen. Dev.* **2000**, 14, 1448-1459.

60. Xiao, Z.; Xue, J.; Sowin, T. J.; Zhang, H. Differential roles of checkpoint kinase 1, checkpoint kinase 2, and mitogen-activated protein kinase–activated protein kinase 2 in mediating DNA damage–induced cell cycle arrest: implications for cancer therapy. *Mol. Cancer Ther.* **2006**, 5, 1935-1943.

61. Zhou, B.-B. S.; Bartek, J. Targeting the checkpoint kinases: chemosensitization versus chemoprotection. *Nat. Rev. Cancer* **2004**, 4, 216-225.

62. www.tainano.com/chin/Molecular%20Biology%20Glossary.htm. (19th June 2012).

63. Vale, R. D.; Milligan, R. A. The Way Things Move: Looking Under the Hood of Molecular Motor Proteins. *Science* **2000**, 288, 88-95.

64. Kops, G. J. P. L.; Weaver, B. A. A.; Cleveland, D. W. On the road to cancer: aneuploidy and the mitotic checkpoint. *Nat. Rev. Cancer* **2005**, 5, 773-785.

65. Fang, G.; Yu, H.; Kirschner, M. W. Direct Binding of CDC20 Protein Family Members Activates the Anaphase-Promoting Complex in Mitosis and G1. *Mol. Cell* **1998**, 2, 163-171.

66. Malmanche, N.; Maia, A.; Sunkel, C. E. The spindle assembly checkpoint: Preventing chromosome mis-segregation during mitosis and meiosis. *FEBS Lett.* **2006**, 580, 2888-2895.

67. Evans, L.; Mitchison, T.; Kirschner, M. Influence of the centrosome on the structure of nucleated microtubules. *J. Cell Biol.* **1985**, 100, 1185-1191.

68. Doxsey, S. Re-evaluating centrosome function. *Nat. Rev. Mol. Cell Biol.* **2001**, 2, 688-698.

69. Wheatley, D. N. *The Centriole*. Elsevier academic press: 1982.

70. Haren, L.; Remy, M.-H.; Bazin, I.; Callebaut, I.; Wright, M.; Merdes, A. NEDD1-dependent recruitment of the γ-tubulin ring complex to the centrosome is necessary for centriole duplication and spindle assembly. *J. Cell Biol.* **2006**, 172, 505-515.

71. Wiese, C.; Zheng, Y. A new function for the [gamma]-tubulin ring complex as a microtubule minus-end cap. *Nat. Cell Biol.* **2000**, 2, 358-364.

72. Mogensen, M. M.; Malik, A.; Piel, M.; Bouckson-Castaing, V.; Bornens, M. Microtubule minus-end anchorage at centrosomal and non-centrosomal sites: the role of ninein. *J. Cell Sci.* **2000**, 113, 3013-3023.

73. Gromley, A. A novel centriolar protein with a centrosomal function. *Mol. Biol. Cell* **2000**, 11.

74. Sudakin, V.; Chan, G. K. T.; Yen, T. J. Checkpoint inhibition of the APC/C in HeLa cells is mediated by a complex of BUBR1, BUB3, CDC20, and MAD2. *J. Cell Biol.* **2001**, 154, 925-936.

75. Weaver, B. A. A.; Bonday, Z. Q.; Putkey, F. R.; Kops, G. J. P. L.; Silk, A. D.; Cleveland, D. W. Centromere-associated protein-E is essential for the mammalian mitotic checkpoint to prevent aneuploidy due to single chromosome loss. *J. Cell Biol.* **2003**, 162, 551-563.

76. Kienitz, A.; Vogel, C.; Morales, I.; Muller, R.; Bastians, H. Partial downregulation of MAD1 causes spindle checkpoint inactivation and aneuploidy, but does not confer resistance towards taxol. *Oncogene* **2005**, 24, 4301-4310.

77. Kops, G. J. P. L.; Foltz, D. R.; Cleveland, D. W. Lethality to human cancer cells through massive chromosome loss by inhibition of the mitotic checkpoint. *Proc. Natl Acad. Sci. USA* **2004**, 101, 8699-8704.

78. Hyman, A.; Karsenti, E. The role of nucleation in patterning microtubule networks. *J. Cell Sci.* **1998**, 111, 2077-2083.

79. Nigg, E. A. Centrosome aberrations: cause or consequence of cancer progression? *Nat. Rev. Cancer* **2002**, 2, 815-825.

80. Meraldi, P.; Lukas, J.; Fry, A. M.; Bartek, J.; Nigg, E. A. Centrosome duplication in mammalian somatic cells requires E2F and Cdk2-cyclin A. *Nat. Cell Biol.* **1999**, 1, 88-93.

81. Hinchcliffe, E. H.; Sluder, G. Two for two: Cdk2 and its role in centrosome doubling. *Oncogene* **2002**, 21, 6154-6160.

82. Jordan, M. A.; Wilson, L. Microtubules as a target for anticancer drugs. *Nat. Rev. Cancer* **2004**, 4, 253-265.

83. Jordan, M. A.; Thrower, D.; Wilson, L. Mechanism of Inhibition of Cell Proliferation by *Vinca* Alkaloids. *Cancer Res.* **1991**, 51, 2212-2222.

84. Jordan, M. A.; Toso, R. J.; Thrower, D.; Wilson, L. Mechanism of mitotic block and inhibition of cell proliferation by taxol at low concentrations. *Proc. Natl. Acad. Sci.* **1993**, 90, 9552-9556.

85. Mountzios, G.; Terpos, E.; Dimopoulos, M.-A. Aurora kinases as targets for cancer therapy. *Cancer Treat. Rev.* **2008**, 34, 175-182.

86. Chan, C. S.; Botstein, D. Isolation and characterization of chromosome-gain and increase-in-ploidy mutants in yeast. *Genetics* **1993**, 135, 677-91.

87. Carmena, M.; Earnshaw, W. C. The cellular geography of Aurora kinases. *Nat. Rev. Mol. Cell Biol.* **2003**, 4, 842-854.

88. Castro, A. APC/Fizzy-Related targets Aurora-A kinase for proteolysis. *EMBO Rep.* **2002**, 3, 457-462.

89. Castro, A. The D-Box-activating domain (DAD) is a new proteolysis signal that stimulates the silent D-Box sequence of Aurora-A. *EMBO Rep.* **2002**, 3, 1209-1214.

90. Giet, R. Drosophila Aurora A kinase is required to localize D-TACC to centrosomes and to regulate astral microtubules. *J. Cell Biol.* **2002**, 156, 437-451.

91. Hannak, E.; Kirkham, M.; Hyman, A. A.; Oegema, K. Aurora-A kinase is required for centrosome maturation in Caenorhabditis elegans. *J. Cell Biol.* **2001**, 155, 1109-1116.

92. Berdnik, D.; Knoblich, J. A. Drosophila Aurora-A is required for centrosome maturation and actin-dependent asymmetric protein localization during mitosis. *Curr. Biol.* **2002**, 12, 640-647.

93. Giet, R.; Prigent, C. The Xenopus laevis aurora/Ip11p-related kinase pEg2 participates in the stability of the bipolar mitotic spindle. *Exp. Cell Res.* **2000**, 258, 145-151.

94. Tsai, M. Y. A Ran signalling pathway mediated by the mitotic kinase Aurora A in spindle assembly. *Nat. Cell Biol.* **2003**, 5, 242-248.

95. Kufer, T. A. Human TPX2 is required for targeting Aurora-A kinase to the spindle. *J. Cell Biol.* **2002**, 158, 617-623.

96. Ainsztein, A. M.; Kandels-Lewis, S. E.; Mackay, A. M.; Earnshaw, W. C. INCENP centromere and spindle targeting: identification of essential conserved motifs and involvement of heterochromatin protein HP1. *J. Cell Biol.* **1998**, 143, 1763-1774.

97. Murata-Hori, M.; Tatsuka, M.; Wang, Y. L. Probing the dynamics and functions of Aurora B kinase in living cells during mitosis and cytokinesis. *Mol. Biol. Cell* **2002**, 13, 1099-1108.

98. Tanaka, T. U. Evidence that the Ipl1-Sli15 (Aurora kinase-INCENP) complex promotes chromosome bi-orientation by altering kinetochore-spindle pole connections. *Cell* **2002**, 108, 317-329.

99. Andrews, P. D.; Ovechkina, Y.; Morrice, N.; Wagenbach, M.; Duncan, K.; Wordeman, L.; Swedlow, J. R. Aurora B Regulates MCAK at the Mitotic Centromere. *Dev. Cell* **2004**, 6, 253-268.

100. Yanai, A.; Arama, E.; Kilfin, G.; Motro, B. ayk1, a novel mammalian gene related to Drosophila aurora centrosome separation kinase, is specifically expressed during meiosis. *Oncogene* **1997**, 14, 2943-2950.

101. Meraldi, P.; Honda, R.; Nigg, E. A. Aurora-A overexpression reveals tetraploidization as a major route to centrosome amplification in p53-/- cells. *EMBO J.* **2002**, 21, 483-492.

102. Ota, T. Increased mitotic phosphorylation of histone H3 attributable to AIM-1/Aurora-B overexpression contributes to chromosome number instability. *Cancer Res.* **2002**, 62, 5168-5177.

103. Barr, F. A.; Sillje, H. H. W.; Nigg, E. A. Polo-like kinases and the orchestration of cell division. *Nat. Rev. Mol. Cell Biol.* **2004**, 5, 429-441.

104. Taylor, S.; Peters, J.-M. Polo and Aurora kinases - lessons derived from chemical biology. *Curr. Opin. Cell Biol.* **2008**, 20, 77-84.

105. Elia, A. E. H.; Cantley, L. C.; Yaffe, M. B. Proteomic Screen Finds pSer/pThr-Binding Domain Localizing Plk1 to Mitotic Substrates. *Science* **2003**, 299, 1228-1231.

106. Elia, A. E. H.; Rellos, P.; Haire, L. F.; Chao, J. W.; Ivins, F. J.; Hoepker, K.; Mohammad, D.; Cantley, L. C.; Smerdon, S. J.; Yaffe, M. B. The Molecular Basis for Phosphodependent Substrate Targeting and Regulation of Plks by the Polo-Box Domain. *Cell* **2003**, 115, 83-95.

107. Casenghi, M.; Meraldi, P.; Weinhart, U.; Duncan, P. I.; Körner, R.; Nigg, E. A. Polo-like Kinase 1 Regulates Nlp, a Centrosome Protein Involved in Microtubule Nucleation. *Dev. Cell* **2003**, 5, 113-125.

108. Donaldson, M. M.; Tavares, A. A.; Ohkura, H.; Deak, P.; Glover, D. M. Metaphase arrest with centromere separation in polo mutants of Drosophila. *J. Cell Biol.* **2001**, 153, 663-676.

109. Arnaud, L.; Pines, J.; Nigg, E. A. GFP tagging reveals human Polo-like kinase 1 at the kinetochore/centromere region of mitotic chromosomes. *Chromosoma* **1998**, 107, 424-429.

110. Sumara, I.; Vorlaufer, E.; Stukenberg, P. T.; Kelm, O.; Redemann, N.; Nigg, E. A.; Peters, J.-M. The Dissociation of Cohesin from Chromosomes in Prophase Is Regulated by Polo-like Kinase. *Mol. Cell* **2002**, 9, 515-525.

111. Descombes, P.; Nigg, E. A. The polo-like kinase Plx1 is required for M phase exit and destruction of mitotic regulators in Xenopus egg extracts. *EMBO J.* **1998**, 17, 1328-1335.

112. Heitz, M. J.; Petersen, J.; Valovin, S.; Hagan, I. M. MTOC formation during mitotic exit in fission yeast. *J. Cell Sci.* **2001**, 114, 4521-4532.

113. Ma, S.; Charron, J.; Erikson, R. L. Role of Plk2 (Snk) in Mouse Development and Cell Proliferation. *Mol. Cell. Biol.* **2003**, 23, 6936-6943.

114. Weerdt, B. C. M. v. d.; Medema, R. H. Polo-Like Kinases: A Team in Control of the Division. *Cell Cycle* **2006**, 5, 853-864.

115. Morris, N. R. Mitotic mutants of *Aspergillus nidulans*. *Genet. Res. Camb.* **1976**, 26, 385-399.

116. O'Connell, M. J.; Krien, M. J. E.; Hunter, T. Never say never. The NIMA-related protein kinases in mitotic control. *Trends Cell Biol.* **2003**, 13, 221-228.

117. Osmani, A. H.; O'Donnell, K.; Pu, R. T.; Osmani, S. A. Activation of the nimA protein kinase plays a unique role during mitosis that cannot be bypassed by absence of the bimE checkpoint. *EMBO J.* **1991**, 10, 2669-2679.

118. Osmani, S. A.; Pu, R. T.; Morris, N. R. Mitotic induction and maintenance by overexpression of a G2-specific gene that encodes a potential protein kinase. *Cell* **1988**, 53, 237-244.

119. Pu, R. T.; Osmani, S. A. Mitotic destruction of the cell cycle regulated NIMA protein kinase of Aspergillus nidulans is required for mitotic exit. *EMBO J.* **1995**, 14, 995-1003.

120. Krien, M. J. E.; West, R. R.; John, U. P.; Koniaras, K.; McIntosh, J. R.; O'Connell, M. J. The fission yeast NIMA kinase Fin1p is required for spindle function and nuclear envelope integrity. *EMBO J.* **2002**, 21, 1713-1722.

121. Moniz, L.; Dutt, P.; Haider, N.; Stambolic, V. Nek family of kinases in cell cycle, checkpoint control and cancer. *Cell Div.* **2011**, 6, 18.

122. Heung, L. J.; Del Poeta, M. Unlocking the DEAD-box: a key to cryptococcal virulence? *J. Clin. Invest.* **2005**, 115, 593-595.

123. Peifer, M.; Berg, S.; Reynolds, A. B. A repeating amino acid motif shared by proteins with diverse cellular roles. *Cell* **1994**, 76, 789-791.

124. Dawe, H. R.; Farr, H.; Gull, K. Centriole/basal body morphogenesis and migration during ciliogenesis in animal cells. *J. Cell Sci.* **2007**, 120, 7-15.

125. Liu, S.; Lu, W.; Obara, T.; Kuida, S.; Lehoczky, J.; Dewar, K.; Drummond, I. A.; Beier, D. R. A defect in a novel Nek-family kinase causes cystic kidney disease in the mouse and in zebrafish. *Development* **2002**, 129, 5839-5846.

126. Janaswami, P. M.; Birkenmeier, E. H.; Cook, S. A.; Rowe, L. B.; Bronson, R. T.; Davisson, M. T. Identification and Genetic Mapping of a New Polycystic Kidney Disease on Mouse Chromosome 8. *Genomics* **1997**, 40, 101-107.

127. Smith, L. A.; Bukanov, N. O.; Husson, H.; Russo, R. J.; Barry, T. C.; Taylor, A. L.; Beier, D. R.; Ibraghimov-Beskrovnaya, O. Development of Polycystic Kidney Disease in Juvenile Cystic Kidney Mice: Insights into Pathogenesis, Ciliary Abnormalities, and Common Features with Human Disease. *J. Am. Soc. Nephrol.* **2006**, 17, 2821-2831.

128. O'Regan, L.; Fry, A. M. The Nek6 and Nek7 Protein Kinases Are Required for Robust Mitotic Spindle Formation and Cytokinesis. *Mol. Cell. Biol.* **2009**, 29, 3975-3990.

129. Bertran, M. T.; Sdelci, S.; Regue, L.; Avruch, J.; Caelles, C.; Roig, J. Nek9 is a Plk1-activated kinase that controls early centrosome separation through Nek6/7 and Eg5. *EMBO J.* **2011**, 30, 2634-2647.

130. Moniz, L. S.; Stambolic, V. Nek10 Mediates G2/M Cell Cycle Arrest and MEK Autoactivation in Response to UV Irradiation. *Mol. Cell. Biol.* **2011**, 31, 30-42.

131. Wu, D.; Chen, B.; Parihar, K.; He, L.; Fan, C.; Zhang, J.; Liu, L.; Gillis, A.; Bruce, A.; Kapoor, A.; Tang, D. ERK activity facilitates activation of the S-phase DNA damage checkpoint by modulating ATR function. *Oncogene* **2005**, 25, 1153-1164.

132. Melixetian, M.; Klein, D. K.; Sorensen, C. S.; Helin, K. NEK11 regulates CDC25A degradation and the IR-induced G2/M checkpoint. *Nat. Cell Biol.* **2009**, 11, 1247-1253.

133. Fry, A. M. The Nek2 protein kinase: a novel regulator of centrosome structure. *Oncogene* **2002**, 21, 6184-6194.

134. Hames, R. S.; Fry, A. M. Alternative splice variants of the human centrosome kinase Nek2 exhibit distinct patterns of expression in mitosis. *Biochem. J.* **2002**, 361, 77-85.

135. Westwood, I.; Cheary, D.-M.; Baxter, J. E.; Richards, M. W.; van Montfort, R. L. M.; Fry, A. M.; Bayliss, R. Insights into the Conformational Variability and Regulation of Human Nek2 Kinase. *J. Mol. Biol.* **2009**, 386, 476-485.

136. Rellos, P.; Ivins, F. J.; Baxter, J. E.; Pike, A.; Nott, T. J.; Parkinson, D.-M.; Das, S.; Howell, S.; Fedorov, O.; Shen, Q. Y.; Fry, A. M.; Knapp, S.; Smerdon, S. J. Structure and Regulation of the Human Nek2 Centrosomal Kinase. *J. Biol. Chem.* **2007**, 282, 6833-6842.

137. Schultz, S.; Fry, A.; Sutterlin, C.; Ried, T.; Nigg, E. Cell cycle-dependent expression of Nek2, a novel human protein kinase related to the NIMA mitotic regulator of Aspergillus nidulans. *Cell Growth Differ.* **1994**, 5, 625-635.

138. Fry, A. M.; Meraldi, P.; Nigg, E. A. A centrosomal function for the human Nek2 protein kinase, a member of the NIMA family of cell cycle regulators. *EMBO J.* **1998**, 17, 470-481.

139. Fry, A. M.; Mayor, T.; Meraldi, P.; Stierhof, Y.-D.; Tanaka, K.; Nigg, E. A. C-Nap1, a Novel Centrosomal Coiled-Coil Protein and Candidate Substrate of the Cell Cycle–regulated Protein Kinase Nek2. *J. Cell Biol.* **1998**, 141, 1563-1574.

140. Hames, R. S.; Crookes, R. E.; Straatman, K. R.; Merdes, A.; Hayes, M. J.; Faragher, A. J.; Fry, A. M. Dynamic Recruitment of Nek2 Kinase to the Centrosome Involves Microtubules, PCM-1, and Localized Proteasomal Degradation. *Mol. Biol. Cell* **2005**, 16, 1711-1724.

141. Kubo, A.; Sasaki, H.; Yuba-Kubo, A.; Tsukita, S.; Shiina, N. Centriolar satellites: molecular characterization, ATP-dependent movement toward centrioles and possible involvement in ciliogenesis. *J. Cell Biol.* **1999**, 147, 969-980.

142. Fry, A. M.; Schultz, S. J.; Bartek, J.; Nigg, E. A. Substrate Specificity and Cell Cycle Regulation of the Nek2 Protein Kinase, a Potential Human Homolog of the Mitotic Regulator NIMA of Aspergillus nidulans. *J. Biol. Cell* **1995**, 270, 12899-12905.

143. Mayor, T.; Stierhof, Y.-D.; Tanaka, K.; Fry, A. M.; Nigg, E. A. The Centrosomal Protein C-Nap1 Is Required for Cell Cycle–Regulated Centrosome Cohesion. *J. Cell Biol.* **2000**, 151, 837-846.

144. Bollen, M.; Stalmans, W. The Structure, Role, and Regulation of Type 1 Protein Phosphatases. *Crit. Rev. Biochem. Mol. Biol.* **1992**, 27, 227-281.

145. Helps, N. R.; Luo, X.; Barker, H. M.; Cohen, P. T. NIMA-related kinase 2 (Nek2), a cell-cycle-regulated protein kinase localized to centrosomes, is complexed to protein phosphatase 1. *Biochem. J.* **2000**, 349, 509-518.

146. Andreassen, P. R.; Lacroix, F. B.; Villa-Moruzzi, E.; Margolis, R. L. Differential Subcellular Localization of Protein Phosphatase-1 α, γ1, and δ Isoforms during Both Interphase and Mitosis in Mammalian Cells. *J. Cell Biol.* **1998**, 141, 1207-1215.

147. Meraldi, P.; Nigg, E. A. Centrosome cohesion is regulated by a balance of kinase and phosphatase activities. *J. Cell Sci.* **2001**, 114, 3749-3757.

148. Bahe, S.; Stierhof, Y.-D.; Wilkinson, C. J.; Leiss, F.; Nigg, E. A. Rootletin forms centriole-associated filaments and functions in centrosome cohesion. *J. Cell Biol.* **2005**, 171, 27-33.

149. Bahmanyar, S.; Kaplan, D. D.; Deluca, J. G.; Giddings, T. H.; O'Toole, E. T.; Winey, M.; Salmon, E. D.; Casey, P. J.; Nelson, W. J.; Barth, A. I. beta-Catenin is a Nek2 substrate involved in centrosome separation. *Gen. Dev.* **2008**, 22, 91-105.

150. Pan, D. Hippo signaling in organ size control. *Gen. Dev.* **2007**, 21, 886-897.

151. Mardin, B. R.; Lange, C.; Baxter, J. E.; Hardy, T.; Scholz, S. R.; Fry, A. M.; Schiebel, E. Components of the Hippo pathway cooperate with Nek2 kinase to regulate centrosome disjunction. *Nat. Cell Biol.* **2010**, 12, 1166-1176.

152. Rapley , J.; Baxter, J. E.; Blot, J.; Wattam, S. L.; Casenghi, M.; Meraldi, P.; Nigg, E. A.; Fry, A. M. Coordinate Regulation of the Mother Centriole Component Nlp by Nek2 and Plk1 Protein Kinases. *Mol. Cell. Biol.* **2005**, 25, 1309-1324.

153. Ciferri, C.; Musacchio, A.; Petrovic, A. The Ndc80 complex: Hub of kinetochore activity. *FEBS Lett.* **2007**, 581, 2862-2869.

154. Zheng, L.; Chen, Y.; Lee, W.-H. Hec1p, an Evolutionarily Conserved Coiled-Coil Protein, Modulates Chromosome Segregation through Interaction with SMC Proteins. *Mol. Cell. Biol.* **1999**, 19, 5417-5428.

155. Chen, Y.; Riley, D. J.; Zheng, L.; Chen, P.-L.; Lee, W.-H. Phosphorylation of the Mitotic Regulator Protein Hec1 by Nek2 Kinase Is Essential for Faithful Chromosome Segregation. *J. Biol. Chem.* **2002**, 277, 49408-49416.

156. Qiu, X.-L.; Li, G.; Wu, G.; Zhu, J.; Zhou, L.; Chen, P.-L.; Chamberlin, A. R.; Lee, W.-H. Synthesis and Biological Evaluation of a Series of Novel Inhibitor of Nek2/Hec1 Analogues. *J. Med. Chem.* **2009**, 52, 1757-1767.

157. Faragher, A. J.; Fry, A. M. Nek2A kinase stimulates centrosome disjunction and is required for formation of bipolar mitotic spindles. *Mol. Biol. Cell* **2003**, 14, 2876-2889.

158. Sonn, S.; Khang, I.; Kim, K.; Rhee, K. Suppression of Nek2A in mouse early embryos confirms its requirement for chromosome segregation. *J. Cell Sci.* **2004**, 117, 5557-5566.

159. Mayor, T.; Stierhof, Y. D.; Tanaka, K.; Fry, A. M.; Nigg, E. A. The centrosomal protein C-Nap1 is required for cell cycle-regulated centrosome cohesion. *J. Cell Biol.* **2000**, 151, 837-846.

160. Kaplan, D. D.; Meigs, T. E.; Kelly, P.; Casey, P. J. Identification of a Role for β-Catenin in the Establishment of a Bipolar Mitotic Spindle. *J. Biol. Chem.* **2004**, 279, 10829-10832.

161. O'Regan, L.; Blot, J.; Fry, A. Mitotic regulation by NIMA-related kinases. *Cell Div.* **2007**, 2, 25.

162. Eto, M.; Elliott, E.; Prickett, T. D.; Brautigan, D. L. Inhibitor-2 Regulates Protein Phosphatase-1 Complexed with NimA-related Kinase to Induce Centrosome Separation. *J. Biol. Chem.* **2002**, 277, 44013-44020.

163. Paintrand, M.; Moudjou, M.; Delacroix, H.; Bornens, M. Centrosome organization and centriole architecture: their sensitivity to divalent cations. *J. Struct. Biol.* **1992**, 108, 107-128.

164. Wai, D. H.; Schaefer, K. L.; Schramm, A.; al., e. Expression analysis of pediatric solid tumor cell lines using oligonucleotide microarrays. *Int. J. Oncol.* **2002**, 20, 441-451.

165. de Vos, S.; Hofmann, W. K.; Grogan, T. M.; Krug, U.; Schrage, M.; Miller, T. P.; Braun, J. G.; Wachsman, W.; Koeffler, H. P.; Said, J. W. Gene expression profile of serial samples of transformed B-cell lymphomas. *Lab. Invest.* **2003**, 83, 271-285.

166. Hayward, D. G.; Clarke, R. B.; Faragher, A. J.; Pillai, M. R.; Hagan, I. M.; Fry, A. M. The Centrosomal Kinase Nek2 Displays Elevated Levels of Protein Expression in Human Breast Cancer. *Cancer Res.* **2004**, 64, 7370-7376.

167. Ren, B.; Cam, H.; Takahashi, Y.; Volkert, T.; Terragni, J.; Young, R. A.; Dynlacht, B. D. E2F integrates cell cycle progression with DNA repair, replication, and G2/M checkpoints. *Gen. Dev.* **2002**, 16, 245-256.

168. Kokuryo, T.; Senga, T.; Yokoyama, Y.; Nagino, M.; Nimura, Y.; Hamaguchi, M. Nek2 as an Effective Target for Inhibition of Tumorigenic Growth and Peritoneal Dissemination of Cholangiocarcinoma. *Cancer Res.* **2007**, 67, 9637-9642.

169. Vieth, M.; Sutherland, J. J.; Robertson, D. H.; Campbell, R. M. Kinomics: characterizing the therapeutically validated kinase space. *Drug Discovery Today* **2005**, 10, 839-846.

170. Noble, M. E. M.; Endicott, J. A.; Johnson, L. N. Protein Kinase Inhibitors: Insights into Drug Design from Structure. *Science* **2004**, 303, 1800-1805.

171. Wakeling, A. E.; Guy, S. P.; Woodburn, J. R.; Ashton, S. E.; Curry, B. J.; Barker, A. J.; Gibson, K. H. ZD1839 (Iressa): An Orally Active Inhibitor of Epidermal Growth Factor Signaling with Potential for Cancer Therapy. *Cancer Res.* **2002**, 62, 5749-5754.

172. www.fda.gov. (13th August 2012).

173. Gan, H. K.; Seruga, B.; Knox, J. J. Sunitinib in solid tumors. *Exp. Opin. Invest. Drugs* **2009**, 18, 821-834.

174. Wilhelm, S. M.; Adnane, L.; Newell, P.; Villanueva, A.; Llovet, J. M.; Lynch, M. Preclinical overview of sorafenib, a multikinase inhibitor that targets both Raf and VEGF and PDGF receptor tyrosine kinase signaling. *Mol. Cancer Ther.* **2008**, 7, 3129-3140.

175. Weisberg, E.; Manley, P.; Mestan, J.; Cowan-Jacob, S.; Ray, A.; Griffin, J. D. AMN107 (nilotinib): a novel and selective inhibitor of *BCR-ABL*. *Br. J. Cancer* **2006**, 94, 1765-1769.

176. Allen, L. F.; Sebolt-Leopold, J.; Meyer, M. B. CI-1040 (PD184352), a targeted signal transduction inhibitor of MEK (MAPKK). *Semin. Oncol.* **2003**, 30, Supplement 16, 105-116.

177. Ohren, J. F.; al., e. Structures of human MAP kinase kinase 1 (MEK1) and MEK2 describe novel noncompetitive kinase inhibition. *Nat. Struct. Mol. Biol.* **2004**, 11, 1192-1197.

178. Adrian, F. J.; Ding, Q.; Sim, T.; Velentza, A.; Sloan, C.; Liu, Y.; Zhang, G.; Hur, W.; Ding, S.; Manley, P.; Mestan, J.; Fabbro, D.; Gray, N. S. Allosteric inhibitors of Bcr-abl-dependent cell proliferation. *Nat. Chem. Biol.* **2006**, 2, 95-102.

179. Burgi, H. B.; Dunitz, J. D.; Lehn, J. M.; Wipff, G. Stereochemistry of reaction paths at carbonyl centres. *Tetrahedron* **1974**, 30, 1563-1572.

180. Barf, T.; Kaptein, A. Irreversible Protein Kinase Inhibitors: Balancing the Benefits and Risks. *J. Med. Chem.* **2012**.

181. Cohen, M. S.; Zhang, C.; Shokat, K. M.; Taunton, J. Structural bioinformatics-based design of selective, irreversible kinase inhibitors. *Science* **2005**, 308, 1318.

182. Bell, I. M.; Stirdivant, S. M.; Ahern, J.; Culberson, J. C.; Darke, P. L.; Dinsmore, C. J.; Drakas, R. A.; Gallicchio, S. N.; Graham, S. L.; Heimbrook, D. C.; Hall, D. L.; Hua, J.; Kett, N. R.; Kim, A. S.; Kornienko, M.; Kuo, L. C.; Munshi, S. K.; Quigley, A. G.; Reid, J. C.; Trotter, B. W.; Waxman, L. H.; Williams, T. M.; Zartman, C. B. Biochemical and Structural Characterization of a Novel Class of Inhibitors of the Type 1 Insulin-like Growth Factor and Insulin Receptor Kinases. *Biochemistry* **2005**, 44, 9430-9440.

183. Norman, B. H.; Shih, C.; Toth, J. E.; Ray, J. E.; Dodge, J. A.; Johnson, D. W.; Rutherford, P. G.; Schultz, R. M.; Worzalla, J. F.; Vlahos, C. J. Studies on the Mechanism of Phosphatidylinositol 3-Kinase Inhibition by Wortmannin and Related Analogs. *J. Med. Chem.* **1996**, 39, 1106-1111.

184. Zhou, W.; Hur, W.; McDermott, U.; Dutt, A.; Xian, W.; Ficarro, S. B.; Zhang, J.; Sharma, S. V.; Brugge, J.; Meyerson, M.; Settleman, J.; Gray, N. A. A structure-guided approach to creating covalent FGFR inhibitors. *Chem. Biol.* **2010**, 17, 285.

185. Carmi, C.; Cavazzoni, A.; Vezzosi, S.; Bordi, F.; Vacondio, F.; Silva, C.; Rivara, S.; Lodola, A.; Alfieri, R. R.; La Monica, S.; Galetti, M.; Ardizzoni, A.; Petronin, P. G.; Mor, M. Novel irreversible epidermal growth factor receptor inhibitors by chemical modulation of the cysteine-trap portion. *J. Med. Chem.* **2010**, 53, 2038.

186. Schirmer, A.; Kennedy, J.; Murli, S.; Reid, R.; Santi, D. V. Targeted covalent inactivation of protein kinases by resorcyclic acid lactone polyketides. *Proc. Natl. Acad. Sci. U.S.A.* **2006**, 103, 4234.

187. Toral-Barza, L.; Zhang, W.-G.; Huang, X.; McDonald, L. A.; Salaski, E. J.; Barbieri, L. R.; Ding, W.-D.; Krishnamurthy, G.; Hu, Y. B.; Lucas, J.; Bernan, V. S.; Cai, P.; Levin, J. I.; Mansour, T. S.; Gibbons, J. J.; Abraham, R. T.; Yu, K. Discovery of lactoquinomycin and related pyranonaphthoquinones as potent and allosteric inhibitors of AKT/PKB: mechanistic involvement of AKT catalytic activation loop cysteines. *Mol. Cancer Ther.* **2007**, 6, 3028-3038.

188. Leproult, E.; Barluenga, S.; Moras, D.; Wurtz, J. M.; Winssinger, N. Cysteine mapping in conformationally distinct kinase nucleotide binding sites: application to the design of selective covalent inhibitors. *J. Med. Chem.* **2011**, 54, 1347.

189. Serafimova, I. M.; Pufall, M. A.; Krishnan, S.; Duda, K.; Cohen, M. S.; Maglathlin, R. L.; McFarland, J. M.; Miller, R. M.; Frödin, M.; Taunton, J. Reversible targeting of noncatalytic cysteines with chemically tuned electrophiles. *Nat. Chem. Biol.* **2012**, 8, 471-476.

190. Wu, G.; Qiu, X.-L.; Zhou, L.; Zhu, J.; Chamberlin, R.; Lau, J.; Chen, P.-L.; Lee, W.-H. Small Molecule Targeting the Hec1/Nek2 Mitotic Pathway Suppresses Tumor Cell Growth in Culture and in Animal. *Cancer Res.* **2008**, 68, 8393-8399.

191. Whelligan, D. K.; Solanki, S.; Taylor, D.; Thomson, D. W.; Cheung, K.-M. J.; Boxall, K.; Mas-Droux, C.; Barillari, C.; Burns, S.; Grummitt, C. G.; Collins, I.; van Montfort, R. L. M.; Aherne, G. W.; Bayliss, R.; Hoelder, S. Aminopyrazine Inhibitors Binding to an Unusual Inactive Conformation of the Mitotic Kinase Nek2: SAR and Structural Characterization. *J. Med. Chem.* **2010**, 53, 7682-7698.

192. Solanki, S.; Innocenti, P.; Mas-Droux, C.; Boxall, K.; Barillari, C.; van Montfort, R. L. M.; Aherne, G. W.; Bayliss, R.; Hoelder, S. Benzimidazole Inhibitors Induce a DFG-Out Conformation of Never in Mitosis Gene A-Related Kinase 2 (Nek2) without Binding to the Back Pocket and Reveal a Nonlinear Structure−Activity Relationship. *J. Med. Chem.* **2011**, 54, 1626-1639.

193. Innocenti, P.; Cheung, K.-M. J.; Solanki, S.; Mas-Droux, C.; Rowan, F.; Yeoh, S.; Boxall, K.; Westlake, M.; Pickard, L.; Hardy, T.; Baxter, J. E.; Aherne, G. W.; Bayliss, R.; Fry, A. M.; Hoelder, S. Design of Potent and Selective Hybrid Inhibitors of the Mitotic Kinase Nek2: Structure–Activity Relationship, Structural Biology, and Cellular Activity. *J. Med. Chem.* **2012**, 55, 3228-3241.

194. Hayward, D. G.; Newbatt, Y.; Pickard, L.; Byrne, E.; Mao, G.; Burns, S.; Sahota, N. K.; Workman, P.; Collins, I.; Aherne, W.; Fry, A. M. Identification by High-Throughput Screening of Viridin Analogs as Biochemical and Cell-Based Inhibitors of the Cell Cycle–Regulated Nek2 Kinase. *J. Biomol. Screening* **2010**, 15, 918-927.

195. Henise, J. C.; Taunton, J. Irreversible Nek2 Kinase Inhibitors with Cellular Activity. *J. Med. Chem.* **2011**, 54, 4133-4146.

196. Hayakawa, H.; Haraguchi, K.; Tanaka, H.; Miyasaka, T. Direct C-8 Lithiation of Naturally-Occurring Purine Nucleosides. A Simple Method for the Synthesis of 8-Carbon-Substituted Purine Nucleosides(Organic,Chemical). *Chem. Pharm. Bull.* **1987**, 35, 72-79.

197. Leonard, N. J.; Bryant, J. D. Regioselective electrophilic reactions on substituted purines. Predominant intermediacy of 6- or 8-purinyl carbanions. *J. Org. Chem.* **1979**, 44, 4612-4616.

198. Li, X.; Vince, R. Synthesis and biological evaluation of purine derivatives incorporating metal chelating ligands as HIV integrase inhibitors. *Bioorg. Med. Chem.* **2006**, 14, 5742-5755.

199. Pfleiderer, W. *Pyrimidines, Pteridines and Purines*. LONZA: 1986.

200. Whitfield, H. J.; Griffin, R. J.; Hardcastle, I. R.; Henderson, A.; Meneyrol, J.; Mesguiche, V.; Sayle, K. L.; Golding, B. T. Facilitation of addition-elimination reactions in pyrimidines and purines using trifluoroacetic acid in trifluoroethanol. *Chem. Commun.* **2003**, 2802-2803.

201. Sagrera, G.; Seoane, G. Acidic Rearrangement of (Benzyloxy)chalcones: A Short Synthesis of Chamanetin. *Synthesis* **2009**, 2009, 4190-4202.

202. Riley, K. E.; Merz, K. M. Effects of Fluorine Substitution on the Edge-to-Face Interaction of the Benzene Dimer. *J. Phys. Chem. B* **2005**, 109, 17752-17756.

203. Surry, D. S.; Buchwald, S. L. Dialkylbiaryl phosphines in Pd-catalyzed amination: a user's guide. *Chem. Sci.* **2011**, 2, 27-50.

204. Coxon, C. R. Design and Synthesis of Irreversible Inhibitors of Nek2 Kinase. Doctoral thesis, Newcastle University, 2010.

205. Nagatsugi, F.; Uemura, K.; Nakashima, S.; Maeda, M.; Sasaki, S. 6-Vinylated guanosine as a novel cross-linking agent and its versatile synthesis from the 6-O-tosylate by Pd(0)-catalyzed cross-coupling. *Tetrahedron Lett.* **1995**, 36, 421-424.

206. Singh, N. P.; McCoy, M. T.; Tice, R. R.; Schneider, E. L. A simple technique for quantitation of low levels of DNA damage in individual cells. *Exp. Cell Res.* **1988**, 175, 184-191.

207. Caddick, S.; Wilden, J. D.; Bush, H. D.; Judd, D. B. Synthesis of Functionalised Sulfonamides via Microwave Assisted Displacement of PFP-Sulfonates with Amines. *QSAR Comb. Sci.* **2004**, 23, 902-905.

208. Singh, J.; Petter, R. C.; Kluge, A. F. Targeted covalent drugs of the kinase family. *Curr. Opin. Chem. Biol.* **2010**, 14, 475-480.

209. Parlow, J. J.; Vazquez, M. L.; Flynn, D. L. A mixed resin bed for the quenching and purification of tetrabutylammonium fluoride mediated desilylating reactions. *Bioorg. Med. Chem. Lett.* **1998**, 8, 2391-2394.

210. Colombo, M.; Bossolo, S.; Aramini, A. ChemInform Abstract: Phosphorus Trichloride Mediated and Microwave-Assisted Synthesis of a Small Collection of Amides Bearing Strong Electron-Withdrawing Group Substituted Anilines. *ChemInform* **2009**, 40, 6541-6544.

211. Kjellberg, J.; Johansson, N. G. Characterization of N7 and N9 alkylated purine analogues by 1H and 13C nmr. *Tetrahedron* **1986**, 42, 6541-6544.

212. Harada, H.; Asano, O.; Hoshino, Y.; Yoshikawa, S.; Matsukura, M.; Kabasawa, Y.; Niijima, J.; Kotake, Y.; Watanabe, N.; Kawata, T.; Inoue, T.; Horizoe, T.; Yasuda, N.; Minami, H.; Nagata, K.; Murakami, M.; Nagaoka, J.; Kobayashi, S.; Tanaka, I.; Abe, S. 2-Alkynyl-8-aryl-9-methyladenines as Novel Adenosine Receptor Antagonists: Their Synthesis and Structure−Activity Relationships toward Hepatic Glucose Production Induced via Agonism of the A2B Receptor. *J. Med. Chem.* **2000**, 44, 170-179.

213. Dakin, H. D.; West, R. A general reaction of amino acids. *J. Biol. Chem.* **1928**, 78, 91-105.

214. Tran, K.-V.; Bickar, D. Dakin−West Synthesis of β-Aryl Ketones. *J. Org. Chem.* **2006**, 71, 6640-6643.

215. Hocek, M.; Holy, A. ChemInform Abstract: A Facile Synthesis of 6-Cyanopurine Bases. *ChemInform* **1996**, 27, 1386-1389.

216. Joern, M.; Svenja, R.; Carsten, R. Indolinone derivatives and process for their manufacture. WO2009071524 (A2) 11/06/2009, 2009.

217. Ulysse, L. G.; Yang, Q.; McLaws, M. D.; Keefe, D. K.; Guzzo, P. R.; Haney, B. P. Process Development and Pilot-Scale Synthesis of New Cyclization Conditions of Substituted Phenylacetamides to Tetrahydroisoquinoline-2-ones Using Eaton's Reagent. *Org. Proc. Res. Dev.* **2009**, 14, 225-228.

218. Zhen-Dan, S.; Karki, R. G.; Oishi, S.; Worthy, K. M.; Bindu, L. K.; Dharmawardana, P. G.; Nicklaus, M. C.; Bottaro, D. P.; Fisher, R. J.; Burke Jr, T. R. Utilization of a nitrobenzoxadiazole (NBD) fluorophore in the design of a Grb2 SH2 domain-binding peptide mimetic. *Bioorg. Med. Chem. Lett.* **2005**, 15, 1385-1388.

219. Wood, K. A.; Hoskin, P. J.; Saunders, M. I. Positron Emission Tomography in Oncology: A Review. *Clin. Oncol.* **2007**, 19, 237-255.

220. Mathias, L. J. Esterification and alkylation reactions employing isoureas. *Synthesis* **1979**, 561-576.

221. Littke, A.; Soumeillant, M.; Kaltenbach, R. F.; Cherney, R. J.; Tarby, C. M.; Kiau, S. Mild and General Methods for the Palladium-Catalyzed Cyanation of Aryl and Heteroaryl Chlorides. *Org. Lett.* **2007**, 9, 1711-1714.

222. Spiessens, L. I.; Anteunis, M. J. O. NMR Studies on Imidines. III.1H and 13C Nuclear Magnetic Resonance Study on the Tautomerism and Geometrical Isomerism of 3-Iminoisoindolinone and Some Alkylated Derivatives. Observation of E and Z Isomers About a Free Imino Grouping. *Bulletin des Sociétés Chimiques Belges* **1983**, 92, 965-993.

223. Dunn, A. D. The synthesis of pyrrolopyridines and pyridopyridazines. *J. Het. Chem.* **1984**, 21, 965-968.

224. Wrobel, J.; Dietrich, A.; Woolson, S. A.; Millen, J.; McCaleb, M.; Harrison, M. C.; Hohman, T. C.; Sredy, J.; Sullivan, D. Novel spirosuccinimides with incorporated isoindolone and benzisothiazole 1,1-dioxide moieties as aldose reductase inhibitors and antihyperglycemic agents. *J. Med. Chem.* **1992**, 35, 4613-4627.

225. Rosenthal, J.; Schuster, D. I. The Anomalous Reactivity of Fluorobenzene in Electrophilic Aromatic Substitution and Related Phenomena. *J. Chem. Educ.* **2003**, 80, 679.

226. Gossen, M.; Bujard, H. Tight control of gene expression in mammalian cells by tetracycline-responsive promoters. *Proc. Natl. Acad. Sci.* **1992**, 89, 5547-5551.

227. Fry, A. M. Personal communication (unpublished work). In 2011.

228. Rieseberg, M.; Kasper, C.; Reardon, K. F.; Scheper, T. Flow cytometry in biotechnology. *Appl. Microbiol. Biotechnol.* **2001**, 56, 350-360.

229. Tyler, R. K.; Shpiro, N.; Marquez, R.; Eyers, P. A. VX-680 Inhibits Aurora A and Aurora B Kinase Activity in Human Cells. *Cell Cycle* **2007**, 6, 2846-2854.

230. Huck, J. J.; Zhang, M.; McDonald, A.; Bowman, D.; Hoar, K. M.; Stringer, B.; Ecsedy, J.; Manfredi, M. G.; Hyer, M. L. MLN8054, an Inhibitor of Aurora A Kinase, Induces

Senescence in Human Tumor Cells Both In vitro and In vivo. *Mol. Cancer Res.* **2010**, 8, 373-384.

231. www.azooptics.com. (06/09/2012).

232. Arris, C. E.; Boyle, F. T.; Calvert, A. H.; Curtin, N. J.; Endicott, J. A.; Garman, E. F.; Gibson, A. E.; Golding, B. T.; Grant, S.; Griffin, R. J.; Jewsbury, P.; Johnson, L. N.; Lawrie, A. M.; Newell, D. R.; Noble, M. E. M.; Sausville, E. A.; Schultz, R.; Yu, W. Identification of Novel Purine and Pyrimidine Cyclin-Dependent Kinase Inhibitors with Distinct Molecular Interactions and Tumor Cell Growth Inhibition Profiles. *J. Med. Chem.* **2000**, 43, 2797-2804.

233. Gray, N. S.; Kwon, S.; Schultz, P. G. Combinatorial Synthesis of 2,9-Substituted Purines. *Tetrahedron Lett.* **1997**, 38, 1161-1164.

234. Winzeler, E.; Gray, N. S.; Han, D.; Cheng, D. Compounds and compositions as kinase inhibitors. WO2008094737 (A2), 2008.

235. Brown, D. J. Improved syntheses in the pyrimidine series. II. The preparation of 4:5-diaminopyrimidine. *J. Appl. Chem.* **1952**, 2, 239-241.

236. Smith, V. H.; Christensen, B. E. Pyrimidines. V. Dehalogenation and nuclear reduction of certain pyrimidines. *J. Org. Chem.* **1955**, 20, 829-838.

237. Taylor, E. C.; Thompson, M. J. On the Reaction of 2,4-Dichloro-5-nitropyrimidine with Amines1. *J. Org. Chem.* **1961**, 26, 5224-5226.

238. Barlin, G. B. Kinetics of reactions in heterocycles. Part IV. The reaction of chloropurines and their 9-methyl derivatives with sodium ethoxide or piperidine. *J. Chem. Soc. B: Phys. Org.* **1967**, 954-958.

239. Arca, V.; Paradisi, C.; Scorrano, G. Competition between radical and nonradical reactions of halonitrobenzenes in alkaline alcoholic solutions. *J. Org. Chem.* **1990**, 55, 3617-3621.

240. Xie, H.; Ng, D.; Savinov, S. N.; Dey, B.; Kwong, P. D.; Wyatt, R.; Smith, A. B.; Hendrickson, W. A. Structure−Activity Relationships in the Binding of Chemically Derivatized CD4 to gp120 from Human Immunodeficiency Virus. *J. Med. Chem.* **2007**, 50, 4898-4908.

241. Rarick, M. J.; Brewster, R. Q.; Dains, F. B. The Formation of Aromatic Ethers from p-Nitrofluorobenzene. *J. Am. Chem. Soc.* **1933**, 55, 1289-1290.

242. Carrigan, C. N.; Bartlett, R. D.; Esslinger, C. S.; Cybulski, K. A.; Tongcharoensirikul, P.; Bridges, R. J.; Thompson, C. M. Synthesis and in Vitro Pharmacology of Substituted Quinoline-2,4-dicarboxylic Acids as Inhibitors of Vesicular Glutamate Transport. *J. Med. Chem.* **2002**, 45, 2260-2276.

243. Niemann, C.; Mead, J. F.; Benson, A. A. The Synthesis of 3'-Fluoro-dl-thyronine and Some of its Iodinated Derivatives. *J. Am. Chem. Soc.* **1941**, 63, 609-611.

244. Chuaqui, C. Heteroaryl compounds useful as Raf kinase inhibitors. WO2010078408 (A1) 2010.

245. Renodon-Cornière, A.; Dijols, S.; Perollier, C.; Lefevre-Groboillot, D.; Boucher, J.-L.; Attias, R.; Sari, M.-A.; Stuehr, D.; Mansuy, D. N-Aryl N‘-Hydroxyguanidines, A New Class of NO-Donors after Selective Oxidation by Nitric Oxide Synthases: Structure−Activity Relationship. *J. Med. Chem.* **2001**, 45, 944-954.

246. Elliott, R. D.; Thomas, H. J.; Shaddix, S. C.; Adamson, D. J.; Brockman, R. W.; Riordan, J. M.; Montgomery, J. A. Nitrosoureido nucleosides as potential inhibitors of nucleotide biosynthesis. *J. Med. Chem.* **1988**, 31, 250-254.

247. Ellington, J. C.; Arnett, E. M. Kinetics and thermodynamics of phenolate silylation and alkylation. *J. Am. Chem. Soc.* **1988**, 110, 7778-7785.

248. Kondo, Y.; Kojima, S.; Sakamoto, T. General and Facile Synthesis of Indoles with Oxygen-Bearing Substituents at the Benzene Moiety. *J. Org. Chem.* **1997**, 62, 6507-6511.

249. Martin, M. W.; Newcomb, J.; Nunes, J. J.; McGowan, D. C.; Armistead, D. M.; Boucher, C.; Buchanan, J. L.; Buckner, W.; Chai, L.; Elbaum, D.; Epstein, L. F.; Faust, T.; Flynn, S.; Gallant, P.; Gore, A.; Gu, Y.; Hsieh, F.; Huang, X.; Lee, J. H.; Metz, D.; Middleton, S.; Mohn, D.; Morgenstern, K.; Morrison, M. J.; Novak, P. M.; Oliveira-dos-Santos, A.; Powers, D.; Rose, P.; Schneider, S.; Sell, S.; Tudor, Y.; Turci, S. M.; Welcher, A. A.; White, R. D.; Zack, D.; Zhao, H.; Zhu, L.; Zhu, X.; Ghiron, C.; Amouzegh, P.; Ermann, M.; Jenkins, J.; Johnston, D.; Napier, S.; Power, E. Novel 2-Aminopyrimidine Carbamates as Potent and Orally Active Inhibitors of Lck: Synthesis, SAR, and in Vivo Antiinflammatory Activity. *J. Med. Chem.* **2006**, 49, 4981-4991.

250. Wong, C.; Griffin, R. J.; Hardcastle, I. R.; Northen, J. S.; Wang, L.-Z.; Golding, B. T. Synthesis of sulfonamide-based kinase inhibitors from sulfonates by exploiting the abrogated SN2 reactivity of 2,2,2-trifluoroethoxysulfonates. *Org. Biomol. Chem.* **2010**, 8, 2457-2464.

251. Mu, F.; Coffing, S. L.; Riese, D. J.; Geahlen, R. L.; Verdier-Pinard, P.; Hamel, E.; Johnson, J.; Cushman, M. Design, Synthesis, and Biological Evaluation of a Series of Lavendustin A Analogues That Inhibit EGFR and Syk Tyrosine Kinases, as Well as Tubulin Polymerization. *J. Med. Chem.* **2001**, 44, 441-452.

252. Sykes, B. M.; Hay, M. P.; Bohinc-Herceg, D.; Helsby, N. A.; O'Connor, C. J.; Denny, W. A. Leaving group effects in reductively triggered fragmentation of 4-nitrobenzyl carbamates. *J. Chem. Soc. Perkin Trans. 1* **2000**, 1601-1608.

253. Sloss, M. K.; McKenna, J.; Yoon, W. H.; Norris, S.; Robinson, D.; Parnes, J.; Shelvin, G. Pyrazole pyrazine amine compounds as kinase inhibitors, composition thereof and methods of treatment therewith. WO2009089042 (A1), 2009.

254. Rekha, V. V.; Ramani, M. V.; Ratnamala, A.; Rupakalpana, V.; Subbaraju, G. V.; Satyanarayana, C.; Rao, C. S. A Simple, Efficient, Green, Cost Effective and

Chemoselective Process for the Esterification of Carboxylic Acids. *Org. Proc. Res. Dev.* **2009**, 13, 769-773.

255. Clark, C. R.; Wells, M. J. M.; Sansom, R. T.; Norris, G. N.; Dockens, R. C.; Ravis, W. R. Anticonvulsant activity of some 4-aminobenzamides. *J. Med. Chem.* **1984**, 27, 779-782.

256. Wenker, H. Alkyl- and Dialkylamides of p-Aminobenzoic Acid. *J. Am. Chem. Soc.* **1938**, 60, 1081-1081.

257. Strazzolini, P.; Giumanini, A. G.; Runcio, A.; Scuccato, M. Experiments on the Chaperon Effect in the Nitration of Aromatics†. *J. Org. Chem.* **1998**, 63, 952-958.

258. McMillan, F. H.; Kun, K. A.; McMillan, C. B.; King, J. A. Hexamethylene-1,6-bis-t-amines in Which Part of the Six Carbon Chain is also Part of a Six-membered Ring. *J. Am. Chem. Soc.* **1956**, 78, 4077-4081.

259. Campbell, R.; Peterson, C. J. N-Nitrobenzamides. I. Synthesis, Spectra, and Structure1. *J. Org. Chem.* **1963**, 28, 2294-2298.

260. Sorenson, R. J. Selective N-Arylation of Aminobenzanilides under Mild Conditions Using Triarylbismuthanes. *J. Org. Chem.* **2000**, 65, 7747-7749.

261. Jackman, L. M.; Kavanagh, T. E.; Haddon, R. C. Studies in nuclear magnetic resonance—IX. Rotational barriers in substituted N,N-dimethylbenzamides. *Org. Magn. Resonance* **1969**, 1, 109-123.

262. Mallory, F. B.; Varimbi, S. P. Furazan Oxides. III. An Unusual Type of Aromatic Substitution Reaction1,2. *J. Org. Chem.* **1963**, 28, 1656-1662.

263. dos Santos, C. l. M. G.; McCabe, T.; Watson, G. W.; Kruger, P. E.; Gunnlaugsson, T. The Recognition and Sensing of Anions through "Positive Allosteric Effects" Using Simple Urea−Amide Receptors. *J. Org. Chem.* **2008**, 73, 9235-9244.

264. Muth, C. W.; Abraham, N.; Linfield, M. L.; Wotring, R. B.; Pacofsky, E. A. Condensation Reactions of a Nitro Group. II.1 Preparation of Phenanthridine-5-oxides and Benzo(c)cinnoline-1-oxide2. *J. Org. Chem.* **1960**, 25, 736-740.

265. Baumgarten, H. E.; Creger, P. L.; Zey, R. L. Cinnolines. VI. The Structure of Neber's Lactam. A New Synthesis of 3-Cinnolinol1,2. *J. Am. Chem. Soc.* **1960**, 82, 3977-3982.

266. Shtacher, G.; Dayagi, S. Iodophenyl derivatives of .alpha.-methyl alanine and isovaline as potential oral cholecystographic agents. *J. Med. Chem.* **1972**, 15, 1174-1177.

267. Ingold, C. K.; Shaw, F. R.; Ingold, E. H. CXIX.—The nature of the alternating effect in carbon chains. Part XIV. The directive action of groups of the form –CH2·SO2·R in aromatic substitution. *J. Chem. Soc.* **1927**, 813-832.

268. Zahn, K.; Koch, H. Acid dyestuffs of the anthraquinone series. DE623883 (C), 1936.

269. RajanBabu, T. V.; Reddy, G. S.; Fukunaga, T. Nucleophilic addition of silyl enol ethers to aromatic nitro compounds: scope and mechanism of reaction. *J. Am. Chem. Soc.* **1985**, 107, 5473-5483.

270. Forbes, I. T. A short and efficient synthesis of N-substituted indol-2-ones (oxindoles). *Tetrahedron Lett.* **2001**, 42, 6943-6945.

271. Nakashima, T.; Suzuki, I. Ring Contraction of 3-Hydroxyquinolines to Oxindoles with Hydrogen Peroxide in Acetic Acid. *Chem. Pharm. Bull.* **1969**, 17, 2293-2298.

272. Shriner, R. L.; Child, R. G. The Synthesis of N-Substituted Carbamates1. *J. Am. Chem. Soc.* **1952**, 74, 549-550.

273. Späth, E.; Manjunath, B. L.; Pailer, M.; Jois, H. S. Synthese und Konstitution des Psoralens. *Berichte der deutschen chemischen Gesellschaft (A and B Series)* **1936**, *69*, 1087-1090.

274. Orton, K. J. P. CXLIII.-Benzoylation of fatty acids in the presence of ammonia. Formation of amides. *J. Chem. Soc. Trans.* **1901**, *79*, 1351-1356.

275. Maji, S. K.; Haldar, D.; Banerjee, A.; Banerjee, A. Fibril-forming model synthetic peptides containing 3-aminophenylacetic acid. *Tetrahedron* **2002**, *58*, 8695-8702.

276. Short, L. N.; Thompson, H. W. 38. Infra-red spectra of derivatives of pyrimidine. *J. Chem. Soc. (Resumed)* **1952**, 168-187.

277. Takasaki, M.; Motoyama, Y.; Higashi, K.; Yoon, S.-H.; Mochida, I.; Nagashima, H. Chemoselective Hydrogenation of Nitroarenes with Carbon Nanofiber-Supported Platinum and Palladium Nanoparticles. *Organic Lett.* **2008**, *10*, 1601-1604.

278. Huebner, C. F.; Link, K. P. Studies on 4-Hydroxycoumarin. VII. Reactions of 4-Hydroxycoumarin with Cationoid Reagents1. *J. Am. Chem. Soc.* **1945**, *67*, 99-102.

279. Chen, H.; Boiziau, J.; Parker, F.; Maroun, R.; Tocque, B.; Roques, B. P.; Garbay-Jaureguiberry, C. Synthesis and structure-activity studies of a series of [(hydroxybenzyl)amino]salicylates as inhibitors of EGF receptor-associated tyrosine kinase activity. *J. Med. Chem.* **1993**, *36*, 4094-4098.